Development of novel therapies using liposomes and poly-lactic acid nanoparticles encapsulated with dietary antioxidants for the treatment of acute kidney injury

By

Kauther Ibrahim Layas

A thesis submitted in partial fulfilment of the requirements of the University of Brighton for the degree of Doctor of Philosophy

April 2022

Abstract

Acute kidney injury (AKI) is defined as an abrupt fall in kidney function. Even with advanced technology, there is no single pharmaceutical treatment for AKI. The main mechanism behind the pathophysiology of AKI seems to be oxidative stress, although treatment with antioxidants does not provide complete amelioration of AKI. Liposomes are lipid vesicles consisting of a liquid core surrounded with one or more phospholipid bilayer. Polymeric nanoparticles on the other hand, are solid colloidal nanoparticles consisting mainly of macromolecules. Both are within the nano-sized range and it is possible to encapsulate both hydrophobic and hydrophilic drugs within them to suit targeted delivery options. The objective of the current study was to encapsulate antioxidants with different pharmacokinetic properties (α-tocopherol, curcumin, resveratrol, sinapic acid, ferulic acid and epicatechin) in liposomes and in polylactic acid (PLA) nanoparticles for the purpose of preventing or treating AKI. Liposomes were produced by the hydration of a lipid film to prepare large multilamellar vesicles, followed by membrane extrusion to form smaller unilamellar vesicles. Polymeric nanoparticles were prepared by double emulsification solvent diffusion method using PLA as the polymer. They were then characterized for their particle size, zeta-potential, surface morphology, drug loading, thermal properties, antioxidant activity, as well as for any toxicity and protection against oxidant injury caused by paraquat in renal NRK-52E cells. The liposomes were found to have a particle size of 194-260 nm and a zeta-potential of -12 to -6 mV. PLA nanoparticles were slightly larger in size ranging from 314-557 nm with a more negative charge on the surface (-37 to -23 mV). Loading efficiency varied between different antioxidants. HPLC results showed 76.1 ± 1.4%, 52.9 ± 11.1%, 12 ± 1.2%, 55.0 ± 6.5%, 20.8 ± 3.5% & 10.23 ± 1.5% encapsulation for α-tocopherol, curcumin, resveratrol, sinapic acid, ferulic acid and, epicatechin liposomes, respectively. The loading efficiency for PLA nanoparticles was 67.6 ± 7.1%, 52.4 ± 22.7%, 40.8 ± 3%, 9.5 ± 4.8%, 15.4 ± 4.7% & 5.4 ± 3.4% for the same order on encapsulated antioxidants. Images from scanning electron microscopy and light microscope showed nanoparticles to be spherical in shape. Fourier Transform-infrared spectroscopy and thermal analysis revealed that PLA nanoparticles resemble PLA structure and

properties more than the antioxidants encapsulated within them. All encapsulated liposomes found to have some antioxidant activity measured using inhibition of peroxynitrite dependent tyrosine nitration test and ABTS assay with negligible activity for blank liposomes. There was no major reduction in cell viability after 24 hours exposure to antioxidant-loaded liposomes or PLA nanoparticles, which may indicate safety of these nanoparticles. However, there was arguable significant reduction using high doses of curcumin-loaded nanoparticles. All antioxidants encapsulated within liposomes and PLA nanoparticles showed some variable protection against paraquat toxicity in NRK-52E cells. From these results, it can be concluded that liposomes and PLA nanoparticles developed in this study can provide some protective activity against oxidation in renal cells and have the potential after further investigation to be used to prevent or treat AKI.

Table of Contents

Table of Figures

List of Tables

Covid impact

This study has been conducted during the period 2018 -2021, and like any other research, has been affected by the covid-19 pandemic. There are several parts of the study that could have been done differently or in more depth but due to impact of covid-19 and the government recommendations to work from home, I have been forced to cut some experiments. I have mentioned these experiment and recommended them in future work.

Acronyms

3-NT	3-Nitrotyrosine
8-OHDG	8-Hydroxydeoxyguanosine
AA	Acetic acid
AAPH	2,2′-azobis (2-amidinopropane) hydrochloride
ABTS	2,2'-azinobis-(3-ethylbenzothiazoline-6-sulfonic acid)
AKI	Acute Kidney Injury
AKIN	Acute Kidney Injury Network
ATP	Adenosine triphosphate
BBB	Blood Brain Barrier
CAT	Catalase
CKI	Chronic Kidney Injury
CMC	Critical Micelle Concentration
CPI	Consumer Products Inventory
Cryo-TEM	Cryogenic Transmission Electron Microscopy
DASH	Dietary Approaches to Stop Hypertension
DCM	Dichloromethane
DESE	Double Emulsion/ Solvent Evaporation
DESD	Double Emulsion/ Solvent Diffusion
D.I. water	Deionised water
DLS	Dynamic Light Scattering
DMPC	Dimyristoylphosphatidylcholine
DMSO	Dimethyl sulfoxide
DNA	Deoxyribonucleic acid
DOPC	Dioleoylphosphatidylcholine
DOPE	Dioleoylphosphatidylethanolamine
DOTAP	1,2-Dioleoyl-3-trimethylammoniumpropane
DPPC	Dipalmitoylphosphatidylcholine
DSC	Differential Scanning Calorimeter
DSPC	Distearoylphosphatidylcholine
EDTA	Ethylenediaminetetraacetic acid
EE	Encapsulating Efficiency

ESD	Emulsification/Solvent Diffusion
ESE	Emulsification/Solvent Evaporation
ET	Electron Transfer
FBS	Foetal Bovine Serum
FRAP	Ferric ion Reducing Antioxidant Parameter
FT-IR	Fourier Transform-Infra Red spectroscopy
GALT	Gut-Associated Lymphoid Tissue
GFR	Glomerular Filtration Rate
GIT	Gastrointestinal Tract
GM	Growth Medium
GPx	Glutathione peroxidase
GC	Gas Chromatography
GSH	Glutathione
GSSG	Glutathione disulphide
H_2O_2	Hydrogen Peroxide
HAT	Hydrogen Atom Transfer
HIF	Hypoxia Inducible Factor
$HO^{\bullet}$	Hydroxyl Radical
$HO_2^{\bullet}$	Hydroperoxyl Radical
HPLC	High Performance Liquid Chromatography
i.m.	Intramuscular
i.p.	Intraperitoneal
i.v.	Intravenous
IC_{50}	Inhibitory Concentration
ICH	International Council for Harmonisation
ICU	Intensive care unit
IKK	IκB-kinase
IL	Interleukin
IM	Incubation Medium
IMPS	Invalid Metabolic Panaceas
LDH	Lactate dehydrogenase
LDL	Low-density Lipoprotein
LE	Loading Efficiency
LM	Light Microscopy
LOD	Limit of detection

LOQ	Limit of Quantification
LUV	Large Uni-lamellar Vesicles
MAPK	Mitogen-Activated Protein Kinase
MLV	Multi-lamellar Vesicles
MPMS	1-methoxyphenazine methosulphate
MPT	Mitochondrial Permeability Transition
MS	Mass Spectroscopy
MTT	3-[4,5-dimethylthiazol-2-yl]-2,5 diphenyl tetrazolium bromide
NADPH	reduced Nicotinamide Adenine Dinucleotide Phosphate
NF-κB	Nuclear factor kappa-light-chain-enhancer of activated B cells
NOS	Nitric Oxide Synthase
NRK-52E	Renal proximal tubular cell line
NSAID	Nonsteroidal anti-inflammatory drugs
$^1O_2$	Singlet Oxygen
O_2	Oxygen
$O_2^{\bullet-}$	Superoxide Anion
O_3	Ozone
$ONOO^-$	Peroxynitrite
OPA	Ortho-phosphoric acid
PAINS	Pan-Assay Interference Compound
PARP	Poly (ADP-ribose) polymerase
PBS	Phosphate Buffer Solution
PdI	Polydispersity Index
PEG	Polyethyleneglycol
PTN	Peroxynitrite dependent Tyrosine Nitration
PLA	Polylactic acid
PLGA	Polylactic-co-glycolic acid
PQ	Paraquat
PVA	Polyvinyl alcohol
r.t.	retention time
RIFLE	Risk Injury Failure Loss of Kidney function End-stage kidney disease
RBS	Reactive Bromine Species
RCS	Reactive Chlorine Species
RES	Reticuloendothelial System
RESOLV	Rapid Expansion of Supercritical Solution in Liquid Solvent

RESS	Rapid Expansion of Supercritical Solutions
RNA	Ribonucleic acid
RNS	Reactive Nitrogen Species
$RO_2^{\bullet}$	Peroxyl Radical
ROS	Reactive Oxygen Species
RSD	Relative Standard Deviation
s.c.	Subcutaneous
SAS	Supercritical Antisolvent
SCFs	Supercritical Fluids
SCr	Serum Creatinine
SD	Standard Deviation
SEM	Scanning Electron Microscopy
SOD	Superoxide dismutase
SUV	Small Uni-lamellar Vesicles
T_c	Melting Transition Temperature
T_g	Glass Transition Temperature
TBA	Thiobarbituric assay
TEAC	Trolox Equivalent Antioxidant Capacity
TFA	Trifluoro-acetic acid
TNF	Tumour Necrosis Factor
TRPx	Thioredoxin peroxidase
UO	Urine Output
XO	Xanthine Oxidase

Acknowledgments

I will start this acknowledgment by saying “Alhumd Allah” which is Arabic for thank you god.

During the course of my studies, I have received a great deal of provision, support and help from all the people surrounding me. I would first like to thank my supervisors, Dr. A. Pannala and Dr. C. Chatterjee, whose knowledge were priceless in the formulating of the research topic and methodology in particular. I would like to acknowledge the pharmaceutical laboratory team for their wonderful assistance and support. You supported me greatly and were always willing to help me. I also want to acknowledge the Libyan embassy for funding my studies and to thank my tutors there for their excellent cooperation and for all of the opportunities I was given to conduct my research.

I would particularly like to recognise the support I have seen from my family most particularly my children. When I made the decision to go back to my studies and pursue a PhD degree after all these years, I have been called the supermom. I want to seize the moment to reply to that and say I actually have super kids. They have shown me much patience and help throughout these four years that I cannot describe. I want to say thank you to my husband, parents, brothers and sisters for their wise counsel and sympathetic ear. You provided me with the tools and guidance that I needed to choose the right direction and successfully complete my studies. Finally, I want to show a great thank you to One World Nursery, who helped me with my youngest and provided her with a second home. I am certain that they have showed her much passion and affection that will affect her entire lifetime.

Kauther Ibrahim Layas,

The University of Brighton,

July 2021.

Declaration

I declare that the research contained in this thesis, unless otherwise formally indicated within the text, is the original work of the author. The thesis has not been previously submitted to this or any other university for a degree, and does not incorporate any material already submitted for a degree.

Kauther Ibrahim Layas,

The University of Brighton,

July 2021.

Chapter 1: Acute kidney injury and its connection to oxidative stress

One of the main functions of the kidney is to filter the blood and remove nitrogenous waste, excess fluids and excess electrolytes. Acute kidney Injury (AKI), formally known as acute renal failure, is a broad definition of a condition where the kidneys suddenly fail to function as an excretory organ (Kellum *et al*., 2011, Belloma *et al*., 2012, Naveen 2014). Even if patients survive AKI, they are most likely to suffer chronic immune or cardiovascular diseases later (Kellum *et al*., 2011, Rangaswamy & Sud, 2018) and have a higher risk of developing chronic kidney disease (CKD, chronic renal failure) (Mayer 2015, Belloma *et al*., 2012, Basile *et al*., 2003, Wald *et al*., 2009, Coca et al., 2012, Rangaswamy & Sud, 2018). Although, there are no precise studies of the burden of AKI at an economic level, it clearly contributes to extended hospital stay, excess hospital costs and increased mortality (Chertow *et al*., 2005).

This introduction will give a brief description to the definitions and classifications of AKI. It will mention the different factors involved in the pathology of this disease focusing on oxidative stress. It will also cover how antioxidants have recently been investigated as a preventative as well as a treatment option and their limitations as free drugs. The possible improvement in their bioavailability by two main novel drug delivery systems; liposomes and polymeric nanoparticles will be. Other future proposed therapies such as inflammatory mediators and genetic modifiers will be discussed briefly.

1.1 A brief introduction to the renal system

The renal system normally consists of the urinary tract; two kidneys, two ureters, bladder and urethra, in addition to the arteries, veins and nerves that enter the kidneys from the concave site at the hilum. The kidneys are located retroperitoneally, at the back of the abdominal cavity on each side of the spine. The kidney is made up of an outer cortex containing all the glomeruli and an inner medulla containing the loops of Henle, the vasa recta and end part of the collecting duct. [Figure 1.1]. The kidney is encapsulated in a surrounding fibrous capsule which is surrounded by peri-renal fat which includes the adrenal gland. (Callaghan 2017, Field 2001).

Each kidney contains almost one million nephrons, which are the main functional units of the kidneys. Individual nephron consists of a glomerulus and a tubule, leading to a collecting duct. The glomerulus is a network of capillary vessels that are surrounded by Bowman's capsule, which is the beginning of the tubule. This filters the blood, preventing large substances such as proteins and red blood cells from entering the tubules. A collection of two types of cells: smooth muscles called juxtaglomerular cells and special tubule cells called macula densa are present adjacent to the glomerulus, called juxtaglomerular apparatus. This secretes an important enzyme called renin. The filtrate will then pass through the tubule, starting from the proximal tubule, the descending and ascending loop of Henle, the distal tubule emptying into the collecting duct. It will undergo several changes in its composition to form urine. The collecting ducts will then merge together to form the renal papilla to form the renal pelvis. (Callaghan 2017, Field 2001) [Figure 1.1].

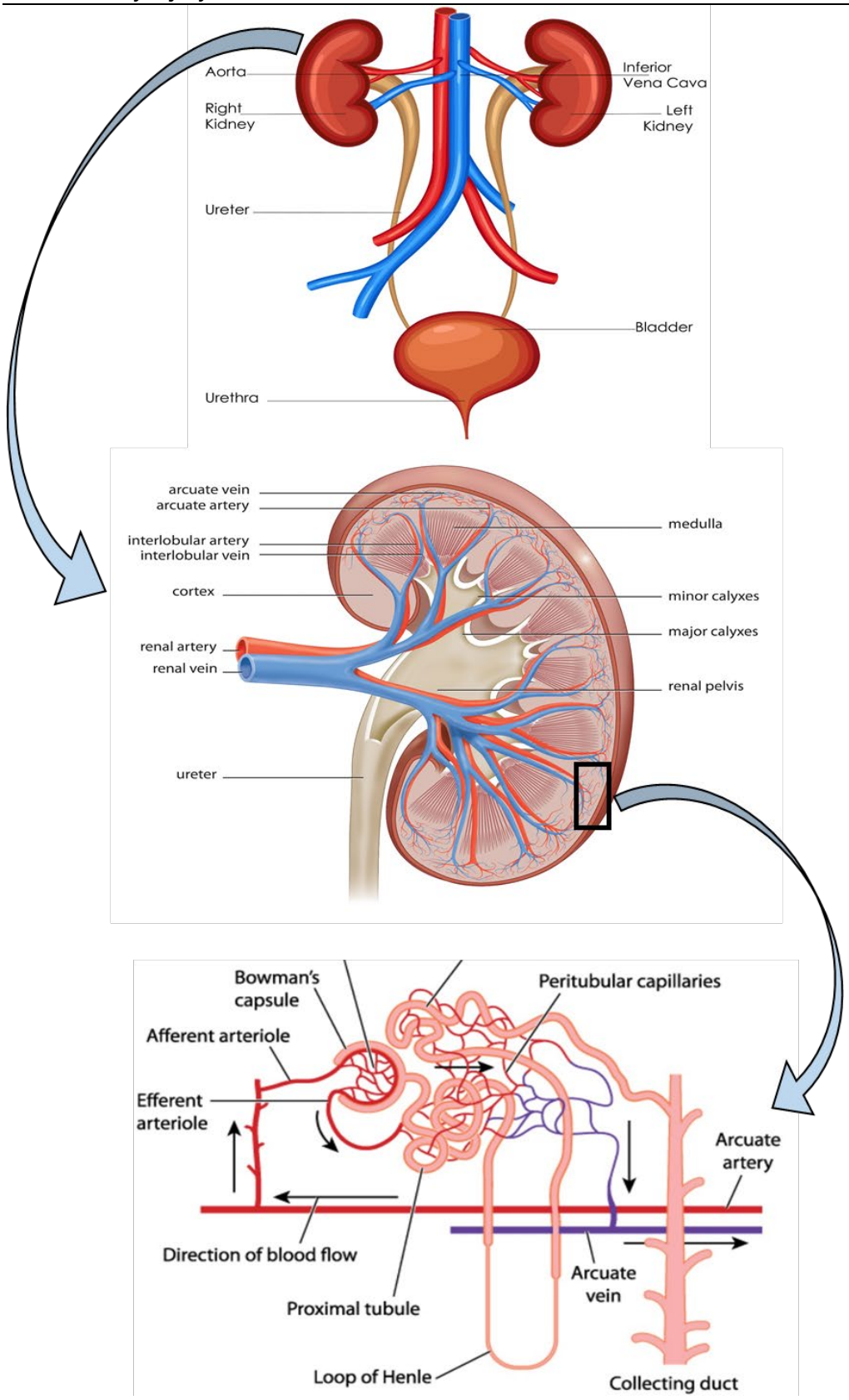

Figure 1.1: Victor illustration of the anatomy of renal system, kidney & a single nephron. (Source: ShutterStock, stock photography company with minor editing)

1.2 Physiology of kidneys

The function of the renal system is very complex, but its main function is to regulate body fluids and maintain homoeostasis. This is performed by three different steps; filtration, reabsorption and secretion. The filtrate is formed by filtering the blood entering the glomerulus from the afferent arteriole into the Bowman's capsule. This is done through three different layers of cells; first, through the endothelial cells lining the capillaries of the glomerulus, then through the glomerular basement membrane and finally through the epithelial cells of Bowman's capsule. The driving force at this point is only the pressure gradient within the glomerulus which is a combination of blood pressure and renal haemodynamics. Most of the water and solutes are then reabsorbed back into the blood circulation at different points of the tubule with different mechanisms, including simple and facilitated diffusion, active transport, symport and osmosis [Figure 1.2]. Solutes that are reabsorbed include amino acids, glucose, fructose, sodium, potassium, calcium, hydrogen carbonate and chloride ions. Urine formation also involves the secretion of non-filtered endogenous and exogenous substances from the blood into the urine along the proximal and distal tubule. Examples include ammonia which diffuses passively and hydrogen ions which diffuses actively by antiport in exchange of sodium ions (Callaghan 2017, Field *et al*., 2001). Different hormones regulate kidney function. These include antidiuretic hormone (vasopressin) and aldosterone which increase the reabsorption of water and sodium, respectively in the collecting ducts. Natriuretic peptides, on the other hand, increases sodium excretion in different parts of the nephron. Parathyroid hormone and fibroblast growth factor-23, both regulate phosphate excretion and vitamin D production. Other hormones produced by the kidneys are renin and erythropoietin (Callaghan 2017).

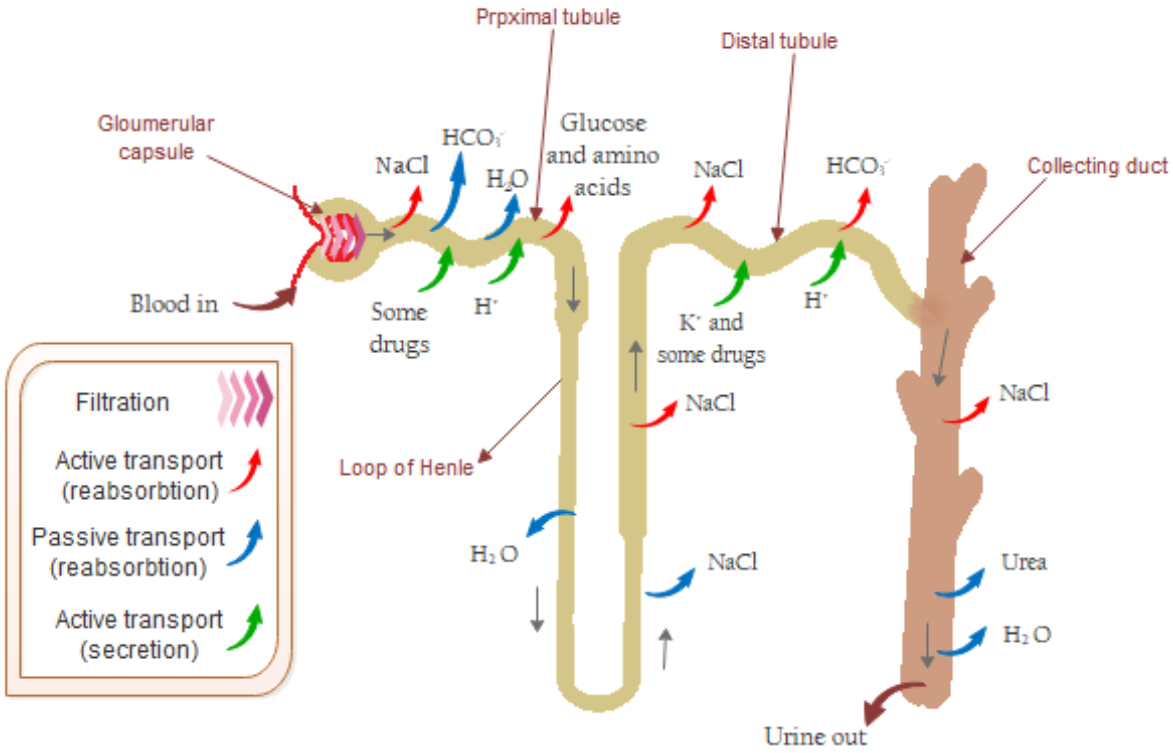

Figure 1.2: Different reabsorption and secretion mechanism at different sites of renal tubule. Adapted from Hoenig and Zeidel, 2014 (Original figure in colour)

1.3 Definitions of acute kidney injury

Although, numerous attempts have been made to define AKI with many variations described, there is no one uniform definition used worldwide. This is the main cause for lacking precise statistical studies on its epidemiology (Mendoza 2011, Mehta *et al*., 2007, Waikar & Bonventre, 2008). In 2004, the Risk Injury Failure Loss of Kidney function End-stage kidney disease (RIFLE) classification was established to define and classify AKI (Mendoza 2011, Hoste *et al*., 2006). This system was altered in 2007 to the Acute Kidney Injury Network (AKIN) classification to give more specificity and sensitivity to the concept (Mendoza 2011, Lopes & Jorge, 2013). AKI is now defined by the abrupt fall (hours to days) in kidney function, leading to a rise in serum creatinine (SCr) and/or a decrease in urine output (UO) (Mendoza 2011, Kellum *et al*., 2011, Rahman *et al*., 2012). Electrolyte disturbance may be observed, as the serum sodium and calcium ions may be decreased, and serum potassium and phosphate levels may be increased compared to normal conditions. Hypervolaemia or hypovolaemia may be present according to severity of the injury (Rahman *et al*., 2012). As shown in Table 1.1, the SCr and UO are used according to the AKIN, to classify AKI into three stages. Stage 1, where SCr increases by 150-200%, Stage 2, where SCr increases by 200-300% and stage 3, where SCr increase by over 300% (Mendoza 2011, Rahman *et al*., 2012).

Table 1.1: The AKIN classification (Adapted from Mendoza 2011)

Stage	***SCr Criteria***	***UO Criteria***
1	Increase in SCr of ≥ 0.3 mg/dl or increase to 150-200% (1.5 to 2 fold) from baseline	Less than 0.5 mL/kg/hour (for > 6 hour)
2	Increase in SCr to >200-300% (2 to 3-fold) from baseline	Less than 0.5 mL/kg/hour (for > 12 hour)
3	Increase in SCr > 300% (> 3-fold) from baseline or SCr ≥ 4.0 mg/dl with acute increase ≥ 0.5 mg/dl	Less than 0.3 mL/kg/hour (for 24 hour) or anuria (for 12 hour)

1.4 The epidemiology of acute kidney injury

As mentioned previously in section 1.3, the epidemiology of this condition is controversial. One specific study used the RIFLE classification and found the morbidity rate for AKI in hospitalized patients to be 9% (Mendoza 2011, Thakar 2013). Another specific review mentioned that the number of patients diagnosed with AKI in USA, Europe and Australia in 2010, was over one million patients (Mehta *et al*., 2015) with 2% of hospital admissions referred to dialysis (Mehta *et al*., 2015). AKI is at its highest percentage in the intensive care unit (ICU) and in seriously injured patients, where it ranges from 9% to 52% (Mayer 2015, Thaker *et al*., 2009). According to the RIFLE criteria, it may also go up to 66%. Mortality rate due to AKI seems to be quite high; around 32% of AKI patients do not survive (Mayer 2015, Rangaswamy & Sud, 2018). Several researchers indicate the reason behind its wide epidemiology is that it is a multi-organ disease with overlapping causes (Kellum *et al*., 2011), for example, the incidence of AKI after angiography ranges from 1% to 38% according to different studies and population (Mendoza 2011).

It should be mentioned that the diagnosis of AKI is increasing along with an increased awareness of its importance (Ronco *et al*., 2007, Lewington *et al*., 2013). Still there is a significant amount of missing data, especially from developing countries where AKI is becoming a major cause of patient morbidity and mortality (Mayer 2015).

1.5 Classification and aetiology of acute kidney injury

AKI is classified according to its aetiology as pre-renal (a functional response of structurally normal kidneys to hypoperfusion), intrinsic renal (involving structural damage to the renal parenchyma), or post-renal (e.g. due to urinary tract obstruction) (Chen & Busse, 2017, Rahman *et al.,* 2012).

1.5.1 Pre-renal acute kidney injury

Pre-renal AKI occurs when the primary cause of injury is external to the kidneys (excluding an obstruction in the flow of urine) leading mainly to hypoperfusion (Ronco *et al*., 2007). Hypovolaemia by excessive blood loss, diarrhoea, vomiting, burns or pancreatitis are all causes of pre-renal AKI (Rahman *et al*., 2012). A second cause is reduced cardiac output, as in myocardial infarction, stroke, trauma, sepsis and transplantation; all may lead to ischaemia and reperfusion injury leading to AKI (Mendoza 2011). Conditions affecting the main artery supplying the kidneys such as renal artery stenosis is another cause of pre-renal AKI (Yung 2013). Drugs such as, ciclosporin, tacrolimus, angiotensin-converting-enzyme inhibitors and angiotensin-receptor blockers can also cause AKI by specifically affecting renal haemodynamics. (Rahman *et al*., 2012).

1.5.2 Intrinsic acute kidney injury

Intrinsic kidney injury is when the main cause of AKI is located within the kidney, involving changes in the structure of the parenchyma renal cells (Mendoza 2011). Several diseases may affect specific parts of the kidney including glomerulonephritis affecting the glomeruli, vasculitis affecting the vessels and acute tubular necrosis affecting the interstitium (Rahman *et al*., 2012). Many medications are known to be nephrotoxic, these include radiocontrast agents, aminoglycosides, amphotericin, non-steroidal anti-inflammatory drugs (NSAIDs), β-lactam antibiotics, sulphonamides, acyclovir, methotrexate and cisplatin (Mendoza 2011, Belloma *et al*., 2012, Finlay & Jones, 2017).

1.5.3 Post-renal acute kidney injury

The main cause of post renal AKI is urinary tract obstruction. In order for an obstruction to cause damage to completely healthy kidneys, it must be bilateral or within the bladder. The blockage leads to increased intra-tubular pressure or impaired renal blood flow that may lead to diminished glomerular filtration rate (GFR) (Makris & Spanou, 2016). This may be due to an enlarged prostate gland, kidney, ureteral or bladder stones or a tumour within the kidney or bladder. (Finlay & Jones, 2017)

In all three aetiologies of AKI, oxidative stress has always been found in its pathophysiology. However, before explaining the relationship between oxidative stress and AKI, some basic definitions as free radicals, reactive oxygen species (ROS), and antioxidants will be discussed.

1.6 Reactive oxygen species and their sources

A free radical is any species capable of independent existence and contains one or more unpaired electron. They could either be cation radicals after losing an electron or anion radicals after gaining one. They can also be formed by homolytic fission, which involves breaking down a covalent bond by applying energy leading to even distribution of the two electrons of that bond. This is different from heterolytic fission, which leads to the formation of non-radical species (ions), (Gutteridge 1996, Halliwell 2012).

- A molecule can lose an electron to form a radical cation

  $A \rightarrow A^{\bullet +} + e^-$

- It can gain an electron to form a radical anion

  $A + e^- \rightarrow A^{\bullet -}$

- Homolytic fission can also form radicals

  $A\text{-}B \rightarrow A^{\bullet} + B^{\bullet}$

- Heterolytic fission forms ions

  $A\text{-}B \rightarrow A^- + B^+$

- If two radicals meet, they combine their unpaired electrons to form a covalent bond

  $A^{\bullet} + B^{\bullet} \rightarrow A\text{-}B$

- A radical can donate its unpaired electron to another molecule

  $A^{\bullet} + B \rightarrow A^+ + B^{\bullet -}$

- It can accept an electron from another molecule

$A^{\bullet} + B \rightarrow A^{-} + B^{\bullet+}$

- Or it can simply combine with another molecule

$A^{\bullet} + B \rightarrow [A\text{-}B]^{\bullet}$

Where the centre of the radical is an oxygen atom, it is called a ROS and examples include the superoxide anion ($O_2^{\bullet-}$), hydroxyl radical ($HO^{\bullet}$), hydroperoxyl radical ($HO_2^{\bullet}$) and peroxyl radical ($RO_2^{\bullet}$). However, it should be noted that not all ROS are free radicals, examples include singlet oxygen ($^1O_2$), hydrogen peroxide (H_2O_2), ozone (O_3) and hypochlorous acid (HOCl), (Ray *et al*., 2012, Chandrasekaran *et al*., 2016, Halliwell & Gutteridge, 2012).

Other reactive species include reactive nitrogen species (RNS) such as nitric oxide ($NO^{\bullet}$), dinitrogen trioxide (N_2O_3) and nitrogen dioxide ($NO_2^{\bullet}$), reactive chlorine species (RCS) such as atomic chlorine and reactive bromine species (RBS) such as atomic bromine, where the radical is centred on a nitrogen, chlorine and bromine; respectively. Peroxynitrite ($ONOO^-$) is a RNS but sometimes also regarded as a ROS, due to its diverse reaction pathway. For instance, it can directly react with CO_2 [Figure 1.4] or proteins or indirectly by generating $HO^{\bullet}$ (Chandrasekaran *et al*., 2016, Newsholme *et al*., 2016, Halliwell & Gutteridge, 2012).

$O_2^{\bullet-}$ and H_2O_2 can normally be formed in the mitochondria *via* the reduction of oxygen (O_2) within the electron transport chain by complexes I, II and III or by oxidoreductase enzymes (Vakifahmetoglu-Norberg *et al*., 2016, Chandrasekaran *et al*., 2016, Ahmad *et al*., 2017). About 0.4-4% of O_2 is converted to $O_2^{\bullet-}$ *via* normal cell respiration, mainly in the mitochondria (Preedly 2014). These ROS should normally be further reduced to H_2O by cytochrome oxidase of complex IV to overcome their harmful effects (Cadenas & Davies, 2000, Brand 2016). Another source of H_2O_2 is a direct two electron reduction of O_2 by monoamine oxidase in the outer membrane of the mitochondria (Cadenas & Davies, 2000). $HO^{\bullet}$ is an important ROS due to its high reactivity. It is generated under conditions of oxidative stress leading to oxidant injury. It is formed in the presence of copper or

iron ions from H_2O_2 in mitochondrial membrane through Fenton or Haber Weiss chemistry (Cadenas & Davies, 2000, Newsholme *et al*., 2016, Ahmad *et al*., 2017) [Figure 1.3].

Additionally, ROS can be produced intracellularly by nicotinamide adenine dinucleotide phosphate (NADPH) oxidase (mainly in the neutrophils and macrophages), cytochrome P450 and nitric oxide synthase (Ahmad *et al*., 2017). $O_2^{\bullet-}$ is also produced in small amounts under normal physiological conditions by xanthine oxidase (XO). This small amount seems to increase under certain pathological states including ischaemia and reperfusion, due to the conversion of xanthine dehydrogenase to xanthine oxidase (Ahmad *et al*., 2017).

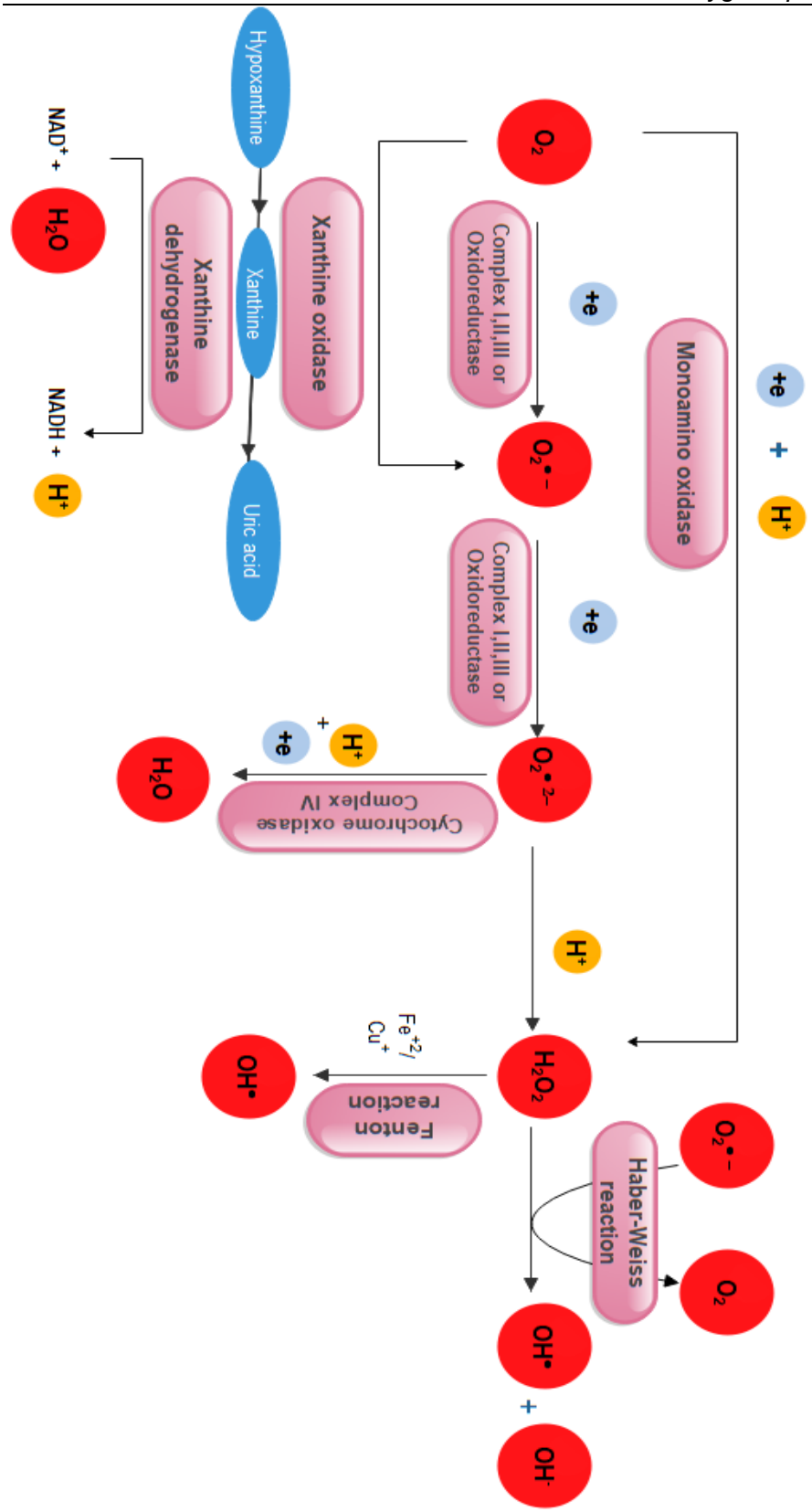

Figure 1.3**: Production of ROS in vivo.** Oxygen is converted into superoxide anion and then into peroxide via complex I, II, III, xanthine oxidase and monoamine oxidase. This can be counterbalanced by complex IV, unless transformed into hydroxyl radicals by Fenton and Haber-Weiss reactions. Adapted from Cadenas & Davies, 2000 (Original figure in colour).

Nitric oxide synthase (NOS) converts L-arginine into L-citrulline in the presence of oxygen to produce $NO^{\bullet}$ using different cofactors (Ahmad *et al*., 2017, Aicardo *et al*., 2016, Bartesaghi & Radi, 2018). Although, $NO^{\bullet}$ is selective in its reactions and usually will not cause cellular damage, but it reacts with $O_2^{\bullet-}$ to form the highly reactive $ONOO^-$, which has many harmful effects (Ahmad et al., 2017, Berlett & Stadtman, 1997, Spickett & Forma, 2015, Radi *et al*., 1991, Pannala *et al*., 1997, Pannala et al., 1998). The latter can react with biological carbon dioxide to form nitrosoperoxycarbonate ($ONOOCO_2^{\bullet}$), which decomposes to $CO_3^{\bullet-}$ and $NO_2^{\bullet}$. $NO^{\bullet}$ may also react with O_2 to form NO_2. (Spickett & Forma, 2015, Pannala *et al*., 1997). [Figure 1.4]. $NO^{\bullet}$ has an important role in regulating smooth muscle tone and platelet adhesion by the activation of guanylate cyclase (Ahmad *et al*., 2017, Aicardo *et al*., 2016, Bartesaghi & Radi, 2018).

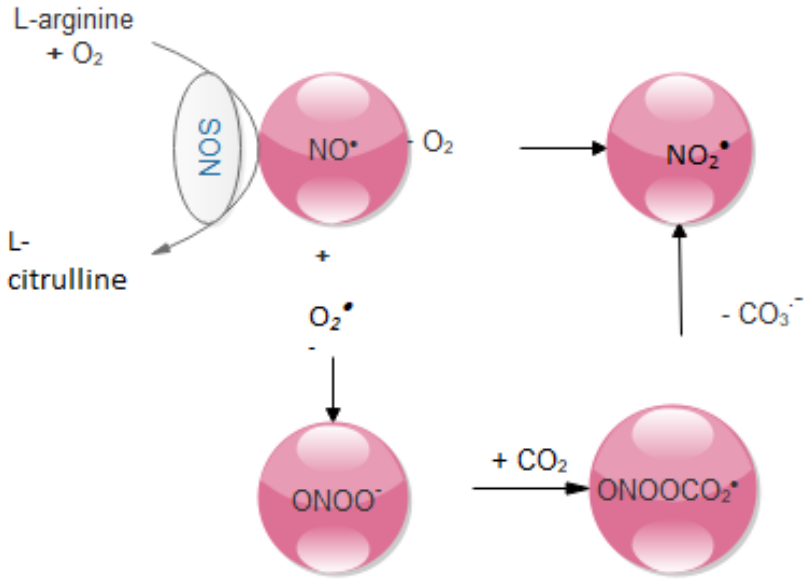

Figure 1.4: Some sources of RNS (Original figure in colour)

ROS in relatively low concentrations are believed to have important functions in regulating cellular signalling, facilitating normal growth and reproduction (Ray *et al*., 2012, Newsholme *et al*., 2016, Ahmad *et al*., 2017). Higher levels of ROS are associated with defence against infection, as they have an important role in killing pathogens. This increase can be found in lymphocytes *via* 5-lipoxygenase and in endothelial cells *via* tumour necrosis factor (TNF). TNFα, interleukin-1 (IL-1), bacterial lipopolysaccharide, and tumour promoter 4-O-

tetradecanoylphorbol-13-acetate are stimulators of cyclooxygenase-1 that may also lead to increased level of ROS during infection (Ahmad *et al.,* 2017).

ROS are highly reactive molecules with at least one unpaired electron located in their outer orbitals (Ahmad *et al*., 2017). It is a broad definition of a group of oxygen species either as free radicals or non-radical derivatives (Halliwell & Gutteridge, 2012). They increase due to the presence of inflammation, infection or ischaemia and may affect mitochondrial function, which according to recent studies, is the main cause of renal cell damage in AKI (Mendoza 2011, Chen & Busse, 2017, Ahmad *et al*., 2017). Their damaging effect can be by different mechanisms including protein oxidation, lipid peroxidation and DNA damage and often involves a combination (Mendoza 2011, Chen & Busse, 2017, Ahmad *et al*., 2017). This will be discussed in more details below. It should be mentioned that free radicals can also be sourced directly from the environment. Sources include air pollution, cigarette smoke, radiation (such as X-rays) and chemical waste (such as herbicides) (Kumar 2011). External sources increase free radicals in the body either by acting as free radicals themselves or by initiating electrons movement by introducing energy to atoms.

1.7 The general mechanisms of oxidative stress and its effect on different biomolecules

ROS, due to their high reactivity, are capable of reacting with a host of biological molecules including unsaturated fatty acids, proteins and nucleic acids to name a few. Such reactions could result subsequent events including apoptosis and necrosis (Ahmad *et al*., 2017). Several destructive reactions of ROS with different biological molecules will be discussed below.

1.7.1 Protein oxidation by reactive oxygen species

Proteins are formed mainly of polypeptide chains of amino acids. When a ROS such as $HO^{\bullet}$ reduces the carbon atom of an amino acid it forms a carbon centred free radical. This in turn is highly reactive and can further react with O_2

and other ROS to form alkylperoxyl radical intermediate, alkylperoxide, followed by formation of an alkoxyl radical, leading to the formation of a hydroxylated protein or interact with other amino acids to form new free radicals, which can undergo the same pathway. If oxygen is absent, the carbon centred free radical can cross-link with other carbon centred free radicals (Berlett & Stadtman, 1997), thus modifying its structure and function [Figure 1.5]. The peptide chain may break down at the alkoxyl radical stage by either the diamide or α-amidation pathways. The ROS may also react with the glutamyl, aspartyl, and prolyl residue in a similar method, leading to protein fragmentation (Berlett & Stadtman, 1997).

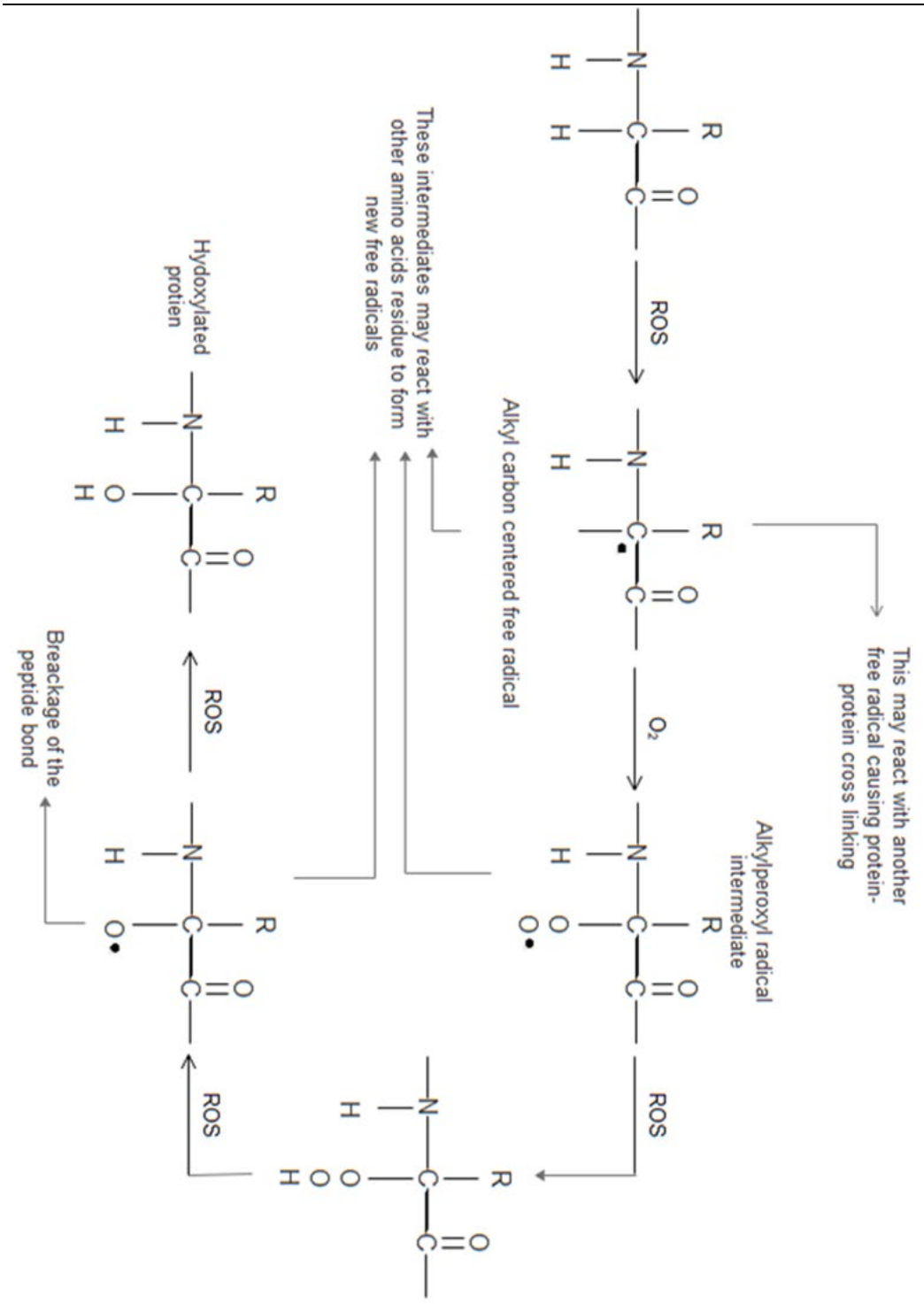

Figure 1.5: **Different effects of ROS on amino acid residue**. ROS may react with the amino acid forming a carbon centred carbonyl radical which can then form peroxyl radical and an oxyl radical. These products can lead to protein cross linking, forming new free radicals, breakage of peptide chain and hydroxylation of proteins. (Adapted from Berlett & Stadtman, 1997).

The side chains of the amino acids are also most likely to be oxidized by ROS with some more liable than others. Figures 1.6 & 1.7 below show the most sensitive amino acids and their oxidation products (Berlett & Stadtman, 1997). Sulphur containing amino acids cysteine and methionine can undergo oxidation by any ROS to form a disulphide or a methionine sulfoxide, respectively. These residues can be converted back into their reduced state by disulphide reductases and methionine sulfoxide reductases, respectively, unless they are further oxidized (Berlett & Stadtman, 1997). Tyrosine and tryptophan are aromatic amino acids that are either oxidized to 3,4-dihydroxyphenylalanine and 2-, 4-, 5-, 6-, and 7-hydroxytryptophan, respectively, or nitrated by $ONOO^-$. The nitration of these residues will obstruct enzyme activity and signal transduction pathways (Berlett & Stadtman, 1997).

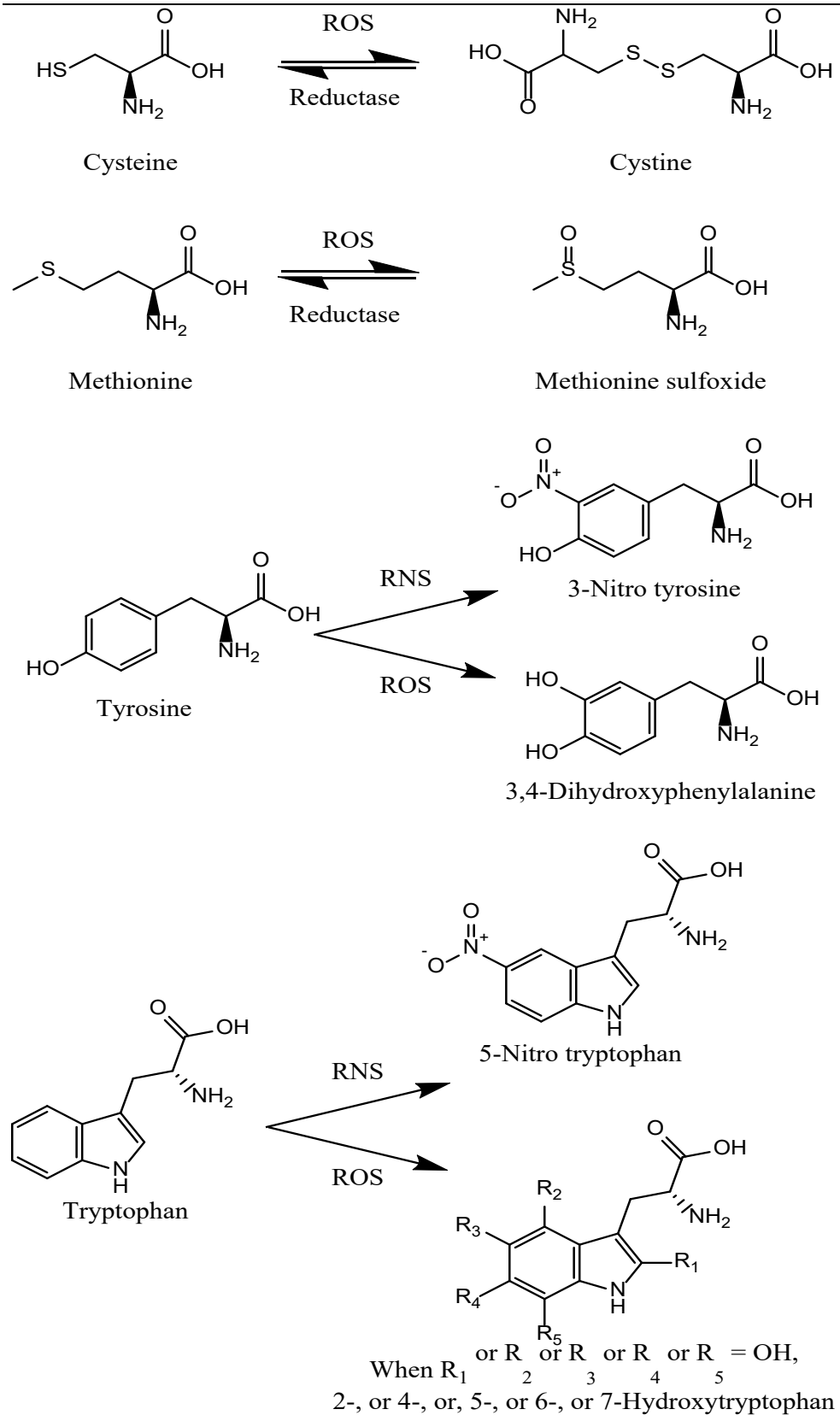

Figure 1.6: Oxidation products of aromatic and sulphur containing amino acids when exposed to ROS and RNS (Adapted from Berlett & Stadtman, 1997)

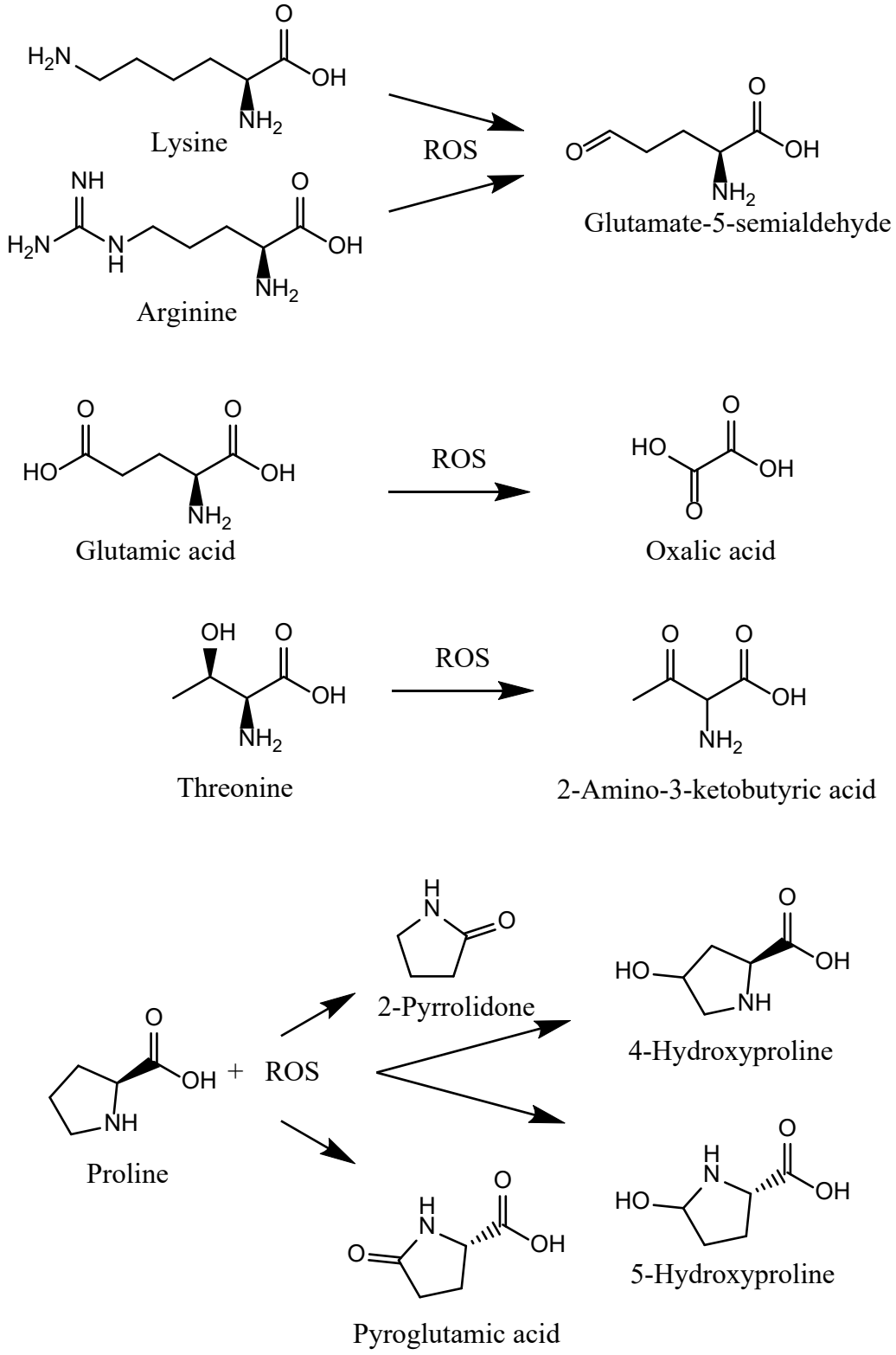

Figure 1.7: Oxidation products of some most sensitive amino acids to ROS (Adapted from Berlett & Stadtman, 1997).

1.7.2 Lipid peroxidation by reactive oxygen species

Oxidation of lipids can be mediated by enzymes or by ROS. The reaction of lipids with free radicals is more specifically called lipid peroxidation (Spickett & Forma, 2015). Polyunsaturated fatty acids are considered the most susceptible to peroxidation, due to their weak carbon-hydrogen bonds adjacent to the double bonds. The reaction of a ROS, such as $OH^{\bullet}$ with a fatty acid, leads to the abstraction of hydrogen and the formation of fatty acid radical. This usually rearranges and reacts with O_2 to form a peroxyl radical, which in turn can react with a neighbouring fatty acid to form a peroxide and a new carbonyl radical, initiating a chain reaction (Spickett & Forma, 2015). [Figure 1.8]. Products of these reactions include isoprostanes and malondialdehyde which can be used as markers of oxidative damage (Preedy 2014). The addition of hydroxyl group to phospholipids in the bilayer membrane, may increases its water permeability, reducing its barrier function and initiate apoptosis.

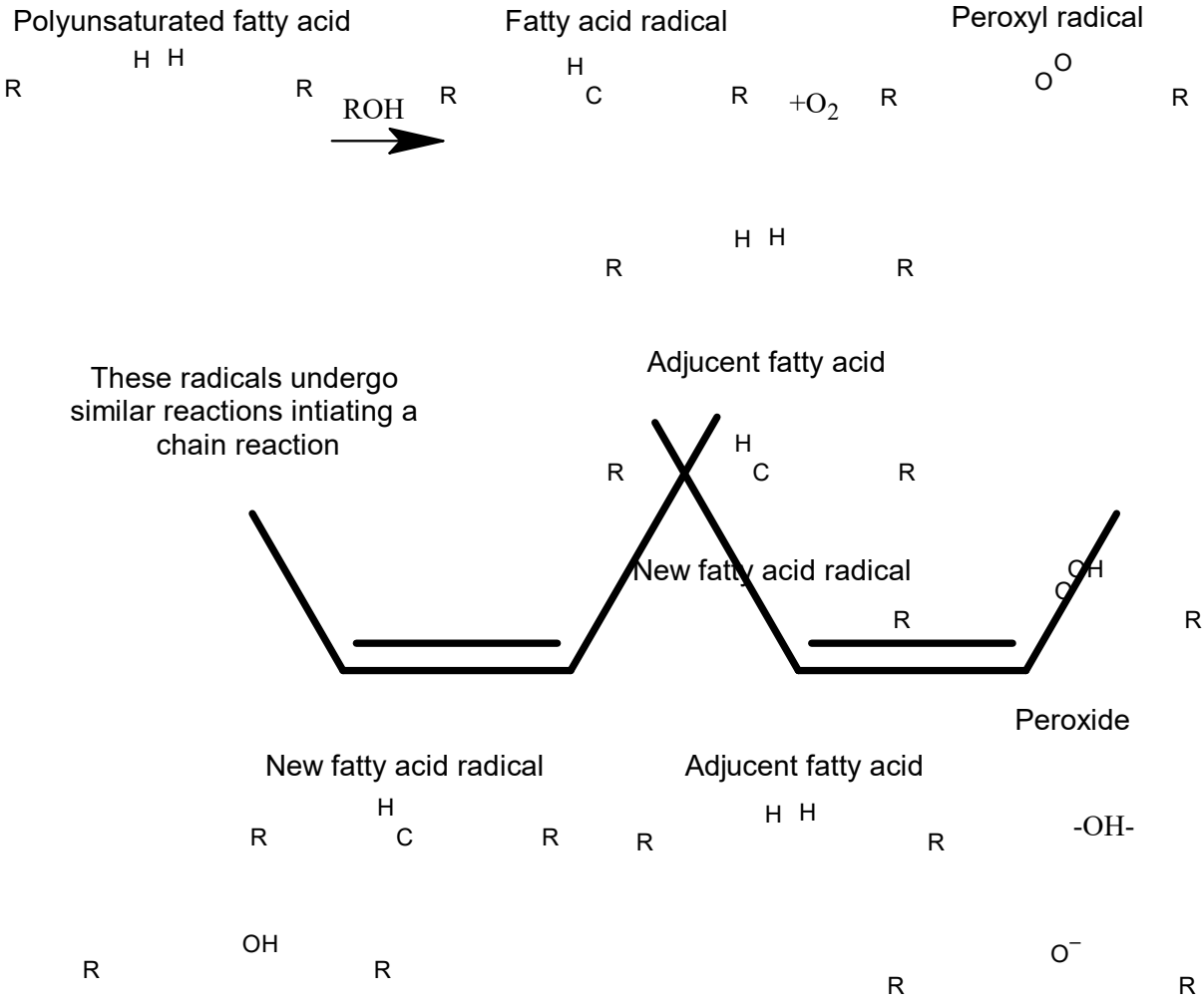

Figure 1.8: Lipid peroxidation chain reaction. (Adapted from Spickett & Forma, 2015)

1.7.3 Oxidation of nucleic acids by reactive oxygen species

Nucleic acids are the biopolymers deoxyribonucleic acid (DNA) and ribonucleic acid (RNA) comprising of the four nucleotide bases. Oxidation of nucleic acids can lead to strand breakage, abasic sites, sugar modifications and alterations to the nucleotide bases (Preedy 2014). $HO^{\bullet}$ is the major ROS responsible for oxidative stress to DNA (Baskin & Salem, 2020). It either, abstracts hydrogen from the sugar structure or adds to the π-bond of the base, forming different compounds (Baskin & Salem, 2020). Important examples of DNA base oxidation are the formation of 8-hydroxydeoxyguanosine (8-OHDG) from 2'-deoxyguanosine and 5-hydroxyuracil from uracil [Figure 1.9] (Barzilai & Yamamato, 2004). These can be repaired by base excision repair pathways. In

conditions where the nucleus is unable to correct the alteration in the DNA strand, mutations may occur. If the oxidative stress is increased, cells undergo brief growth arrest and increased level of defensive protein expression. Further increase in the stress, induces permanent growth arrest, in which cells stop multiplying (Barzilai & Yamamato, 2004).

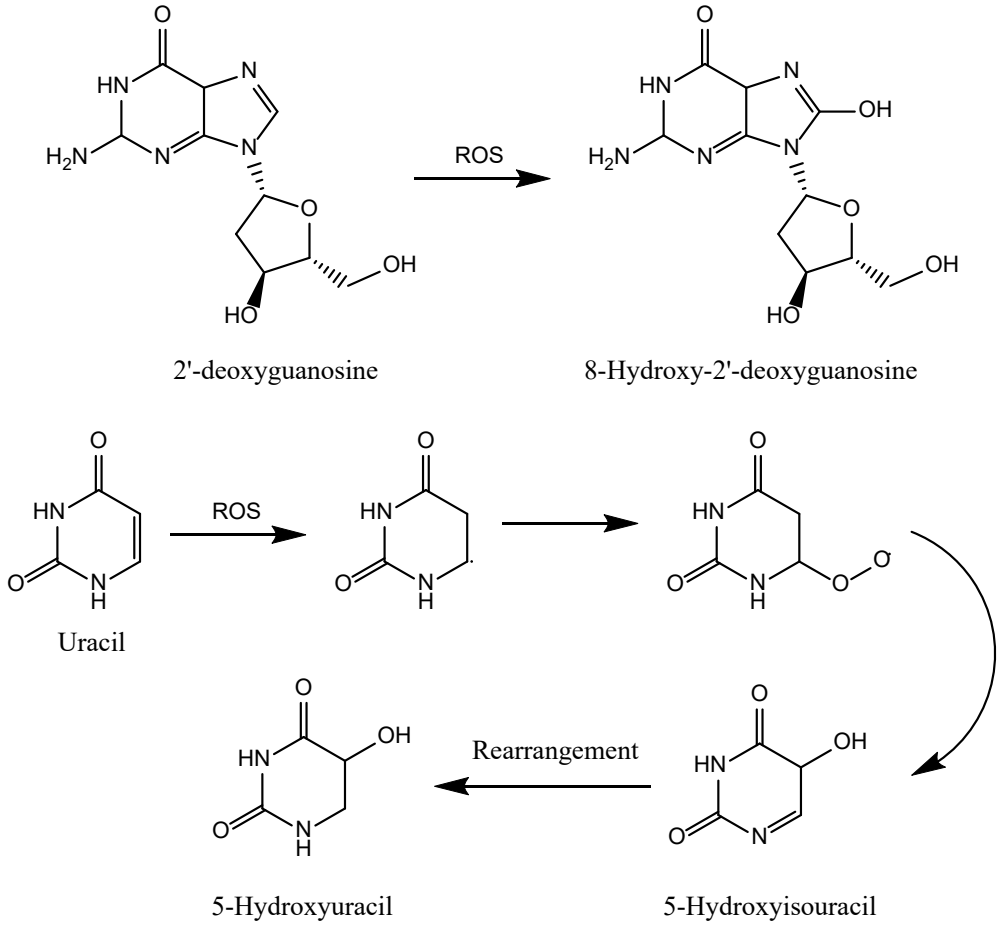

Figure 1.9: The formation of 8-hyroxy-2'-deoxyguanisine from 2'-deoxyguanosine and uracil oxidation pathway leading to the formation of 5-hydroxyuracil (Adapted from Valavanidis et al., 2009 and von Sonntag et al., 2006)

Poly (ADP-ribose) polymerase (PARP) is an enzyme present mainly in the nucleus. In addition to other function, it's mainly responsible for signalling DNA damage and repair. Over activation of this enzyme has been linked to ischaemic injury to the brain, heart and kidneys. This has been attributed to the depletion of ATP, increased expression of pro-inflammatory agents and adhesion molecules

(Devalaraja-Narashimha *et al*., 2005). There is some evidence that PARP inhibitors, such as 3-aminobenzamide and 5-aminoisoquinoline, can provide protection against the ischaemia/reperfusion injury which contributes to the development of AKI (Chatterjee *et al*., 2000; 2004).

1.8 Natural antioxidant activity in human cells

Antioxidants can be defined in general as any compound or system capable of donating an electron to a free radical to prevent its harmful effects (Surh 2005, Halliwell & Gutteridge, 2012). Cells normally detoxify the harmful effect of free radicals by different mechanisms. These can be divided into two main categories: enzymes and small molecules.

1.8.1 Enzymes with antioxidant activity

Superoxide dismutase (SOD), catalase (CAT), glutathione peroxidase (GPx) and thioredoxin peroxidase (TRPx) are enzymes that have free radical scavenging activity especially to $O_2^{\bullet-}$ radical (Newsholme *et al*., 2016). Mammalian cells, and especially renal proximal tubular cells, have three different forms of SOD; SOD1 (CuZnSOD), SOD2 (MnSOD) and extracellular SOD3 (ecSOD) (Basile *et al*., 2012). SOD1 exists mainly in the cytoplasm and lysosomes. SOD2, on the other hand, is mainly present in the mitochondria and to some extent in the cytosol. All SODs dismutate superoxide to hydrogen peroxide and oxygen. CAT exists in the peroxisomes and GPx exists in the cytosol and mitochondria. Both enzymes catalyse the decomposition of H_2O_2 to H_2O and O_2 (Ichikawa *et al*., 1994). These antioxidant enzymes play an important role in protecting the kidney against oxidative kidney injury (Ichikawa *et al*., 1994).

1.8.2 Small molecules of antioxidant nature

Ascorbic acid (vitamin C), tocopherols (vitamin E), polyphenols, carotenoids and bioflavonoids are molecules from dietary sources that act as antioxidants. Metallic nutrients such as selenium, copper, zinc, manganese and iron act as biofactors with an important role in enzyme antioxidant activity (Salmonoswicz

2014). Compounds such as vitamin C and E act by donating electrons, therefore reducing highly reactive free radicals and becoming themselves free radicals. However, the unpaired electrons in these compounds become delocalized by resonance leading to reduced activity and stability (Halliwell & Gutteridge, 2007).

It is worth noting that the defence system of antioxidants works as a network. For example, when free radicals, oxidizes lipids forming lipid radicals, this can be neutralized by α-tocopherol, which itself is oxidized to tocopheroxyl radical. Ascorbic acid donates an electron to tocopheroxyl radical forming an ascobyl radical. Glutathione (GSH) or thioredoxin$_{(red)}$ can be converted by GPx or TRPx, respectively to their oxidized forms glutathione disulphide (GSSG) or thioredoxin$_{(oxd)}$, respectively, by increasing the lifespan of ascorbic acid. The latter can then be converted back by the NADPH cycle (Baskin & Salem, 2020) [Figure 1.10].

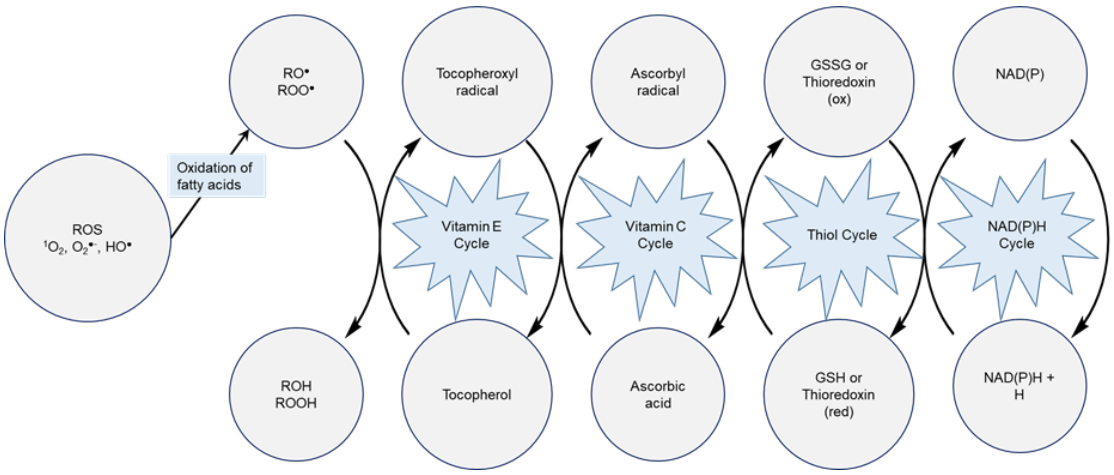

Figure 1.10: An example of antioxidants working as a network. (Adapted from Surh 2005)

1.9 Pathophysiology of acute kidney injury

It is important to understand the pathophysiology of AKI in order to determine the best treatment. The main mechanisms of developing AKI are vascular disruption leading to endothelial damage, direct reaction to an exogenous toxin, suppression of renal autoregulation and the release of inflammatory

mediators (Mendoza 2011, Ronco *et al*., 2007). A more recent study states that the pathophysiology of AKI includes inflammation, immune dysregulation, defective microcirculation and oxidative stress (Chen & Busse, 2017).

During ischaemia-reperfusion, the decreased blood flow to the kidneys leads to decreased oxygen and accumulation of metabolic products within cells. This in turn leads to reduced high-energy phosphate and imbalanced ion gradient across cell membrane. When blood is re-perfused back to the cells is when the real injury occurs. Free radicals are accumulated, which induce lipid peroxidation, polysaccharide depolymerization and DNA degradation (Mendoza 2011). The proximal tubules have been found to be most sensitive to hypoxia, ischaemia and toxic damage (Mendoza 2011, Basile *et al*., 2012). This may be due to the impairment of the mitochondrial function and proximal tubular cells contain an abundance of mitochondria by which they produce the metabolic energy required for tubular transport (Funk *et al*., 2010). Injury to the proximal tubular cells has been found to lead to AKI (Nowak *et al*., 1998).

Inflammation has a variety of contributions in developing AKI. It may lead to decreased blood flow to the cortex outer medulla affecting both function and viability of the renal tubules. This can be due to the innate as well as the adaptive immune responses, enhanced leukocyte-endothelial interactions and the generation of proinflammatory and chemotactic cytokines (Ronco *et al*., 2007). The inflammatory state due to hypoxia is also induced by several factors such as IL-1β, hypoxia inducible factor (HIF) and mitogen-activated protein kinase (MAPK) (Mendoza 2011). Moreover, the activation of NF-κB and its subsequent pathway is enhanced, which is also involved in inflammation due to oxidative stress (Sahu *et al*., 2015). ROS have been reported to be crucial in the canonical IκB-kinase (IKK) dependent NF-κB activation pathway. After the binding of the pro-inflammatory cytokines such as IL-1β and TNFα to their cellular receptors a series of different cascade reactions occur, leading to the release of NF-κB and entering the nucleus. NF-κB, then activates the transcription of several target genes such as cytokines and chemokines. This has been demonstrated by the increase in ROS levels after NF-κB inducers and the blockage of NF-κB activation after most

antioxidant treatment (Gloire *et al*., 2006, Shi *et al*., 2019). Inhibitor studies of the NF-κB activation pathway revealed diminishing in kidney injury after different inducers which suggests a role of NF-κB in the pathogenesis of AKI (Zhang & Sun 2015, Song *et al*., 2019).

In a single nephron, microcirculation impairment can also be a cause of AKI. This is due the alteration in the trans-glomerular pressure gradient leading to insufficient filtration causing cell death due to reduced adenosine triphosphate (ATP). (Chen & Busse, 2017). The reduced blood flow is more dominant in the medulla of the kidney (Karlberg et al., 1983, Bonventre & Yang, 2011). These microvascular dysfunctions including impaired microvascular permeability have an important role in AKI (Sutton 2009).

Recently, the role of oxidative stress in AKI has been studied extensively (Mendoza 2011, Chen & Busse, 2017). Experiential as well as some clinical data shows that oxidative stress is the main pathway of developing AKI in critically ill patients (Pavlakou *et al*., 2008, Busse, 2017). Oxidative stress is characterised by an increase in the production of ROS in contrast to endogenous antioxidants leading to cellular damage (Pavlakou *et al*., 2017, Ray et al., 2012, Newsholme *et al*., 2016). When the kidneys fail to compensate the increase in ROS, an imbalance in the homeostasis occurs leading to AKI (Pavlakou *et al*., 2008, Ray *et al*., 2012) [Figure 1.11].

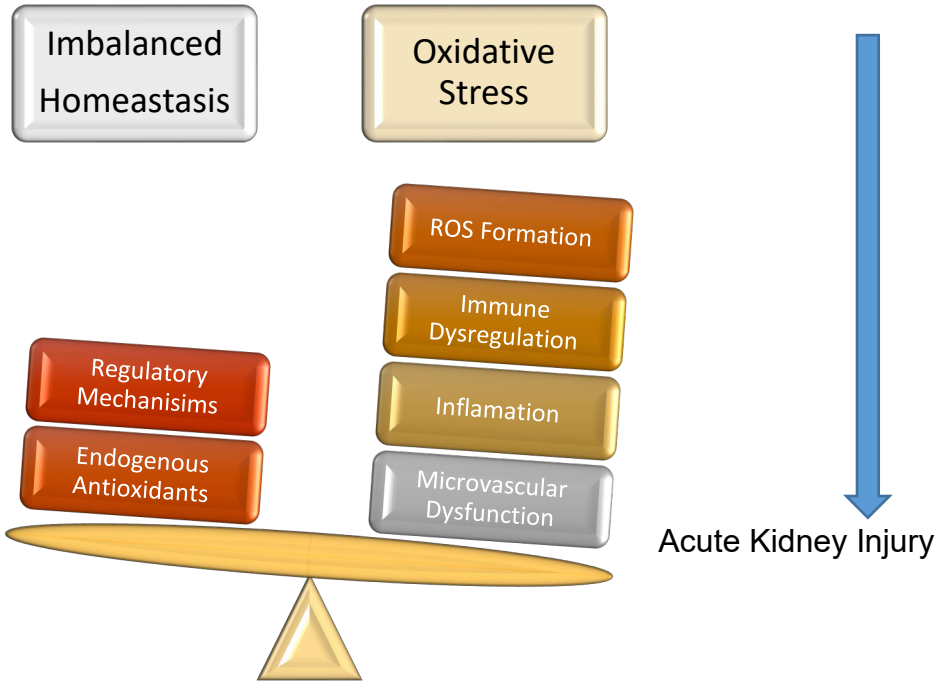

Figure 11: **AKI and oxidative stress** (Adapted from Pavlakou et al., 2008). When there is an imbalance between oxidative stress and antioxidant mechanisms in the renal cells, this may lead to AKI (Original figure in colour)

1.10 The role of oxidative stress/nitrative stress in acute kidney injury

As mentioned above (section 1.9), oxidative stress plays an important role in AKI. Whatever was the initial trigger for renal damage, the pathway leading to AKI is commonly by ischaemic and/or nephrotoxic damage caused directly to the tubules or by activation of molecular mediators. In both pathways, ROS levels are raised above normal, leading to the development or progression of AKI (Rodrigo 2009). One of the proposed mechanisms in which oxidative injury leads to cell death is by mitochondrial permeability transition (MPT) where the mitochondria are the first organelle to be affected in the cells. During cell injury, the ROS formation is increased in the mitochondria, leading to the oxidation of the dithiol groups in the membrane. This increases the permeability of the mitochondrial membrane thereby inducing MPT. The cells then undergo either apoptosis or necrosis according to ATP level (Leamasters *et al*., 1998, Kim *et al*., 2003, Kim *et al*., 2006, Takeyama *et al*., 2002). This will be discussed in more detail in section 1.11. Lipid peroxidation affects not only the mitochondrial membrane but also the lysosomal

and plasma membranes (Paller *et al*., 1984). Studies now target the mitochondria as a therapeutic approach for the treatment of AKI (Ishimoto & Inagi, 2016).

The ROS and RNS species $O_2^{\bullet -}$, H_2O_2, $HO^{\bullet}$, $NO^{\bullet}$ and $ONOO^-$ are among the most important involved in the development and progression of AKI (Basile *et al*., 2012). Post injury, the cellular damage caused by these species is worsened due to the decreased activity of some antioxidant enzymes, alteration of xanthine oxidase, defective electron transport chain and increased levels of iron that may be released from storage points. In a model of ischaemia/reperfusion in rats, the level of H_2O_2 was increased 1.5-fold after ischaemia and 4-fold after reperfusion (González-Flecha & Boveris, 1995). Cisplatin also affects the electron transport chain where mainly the complexes I and IV are inhibited thereby increasing the formation of ROS (Kruidering *et al*., 1997).

Several *in vivo* studies have shown that ischaemia and reperfusion results in reduced gene expression of antioxidant enzymes such as SOD, catalase and GPx. The oxidative stress as a result was increased, leading to renal tissue damage (Dobashi *et al*., 2000, Leach *et al*., 1998). Mice with SOD deficiency, showed a more severe AKI after ischaemia and reperfusion compared to wild mice (Yamanobe *et al*., 2007). An *in vitro* and *in vivo* study suggested that reducing iron has a significant role in AKI post cisplatin treatment. The use of a cytochrome P450 inhibitor, namely piperonyl butoxide and cimetidine either on renal tubular epithelial cell or in rats after administration of cisplatin, demonstrated the role of cytochrome P450 as a source of iron in cisplatin-induced AKI. In animal models, cisplatin increased iron in the kidney, impaired renal function and induced histological changes. On LLC-PK1 cells (porcine kidney cells), cisplatin again increased iron level and induced cytotoxicity. The effects were reversed on both models by cytochrome P450 inhibitors (Baliga *et al*., 1998).

$NO^{\bullet}$ at high concentrations induces programmed cell death in tubular epithelial cells *via* the activation of caspase-8 (Du *et al*., 2006). Pro-inflammatory cytokines released after kidney inflammation, regulate tubular epithelial cells apoptosis. This can be regulated by a caspase-8 inhibitor (Du *et al*., 2005). It is

worth mentioning that $NO^{\bullet}$ in physiological levels has an important role in cell signalling. Also, some studies have shown that if obtained from exogenous sources, it can play a protective role against renal injury after ischaemia-reperfusion (Garcia-Criado *et al*., 1998, Hegarty *et al*., 2001). Its main contribution to kidney damage is the formation of peroxynitrite which is thought to cause both lipid peroxidation as well as inhibition of DNA synthesis (Noiri *et al*., 2001). Peroxynitrite has also been linked to cisplatin-induced AKI. Due to its high reactivity, it reacts with different amino acids leading to the changes in protein structure and function. Immunohistochemical localisation showed an increase in 3-nitrotyrosine (3-NT) in the proximal tubules after cisplatin treatment. This was reduced after treatment with 5,10,15,20-tetrakis (4-sulfonatophenyl) porphyrinato iron (III) (a peroxynitrite decomposition catalyst). This proposes the role of nitrative stress in AKI (Chirino *et al*., 2004). However, a study also suggests that if is the levels of $NO^{\bullet}$ are maintained at physiological level, it can protect from kidney damage due to endotoxaemia (Wang *et al*., 2003).

1.11 The relationship between apoptosis and/or necrosis and acute kidney injury

Both apoptosis and necrosis are type of cell death. During apoptosis, cells shrink, the nucleus chromatin condenses and the plasma membrane forms blebs but remains contact forming apoptotic bodies, which are then cleared by neighbouring cells by phagocytosis. This process usually requires energy and involves activation of caspase pathway. Necrosis on the other hand, involves swelling of cells and their nucleus, disintegration of chromatin and complete lysis of organelles and cell membrane. This course normally does not require energy or involve caspases activation but triggers an inflammatory response in the surrounding tissue. Zhao *et al*., demonstrated that apoptosis is the main pathway involved in sepsis-induced AKI and that this can be attenuated by glycyrrhizic acid (Zhao *et al*., 2016). Formerly, it was believed that apoptosis is a programmed route, as opposed to necrosis which is an unplanned cell death. This clear distinction has been questioned by the consideration of what is called programmed necrosis or necroptosis, which is thought to be a regulated progression in ischaemic conditions (Linkermann *et al*., 2102). Death of proximal tubular cells by either path, leads to unregulated diffusion of water and other substances resulting

in reduced GFR. Additionally, the cellular debris can enter the nephron lumen forming aggregates that may cause tubular obstruction, increasing tubular pressure leading to further reduction in GFR and an imbalance in ion concentrations. Infiltrating leukocytes might block the surrounding capillaries impairing blood flow and aggravating local ischaemia. These progressions, in addition to immunological and inflammatory responses could lead to loss of renal function found in AKI (Havasi & Borkan, 2011). Although not clear, evidence shows that both apoptosis and necrosis are involved in AKI (Havasi & Borkan, 2011, Linkermann *et al*., 2102).

1.12 Available and future treatments for acute kidney injury

Even with advanced technology, physicians have failed to treat AKI effectively (Mayer 2015, Wu *et al*., 2017). The main reason that makes it difficult to treat AKI using a single set of pharmacological agents can be attributed to its complex pathogenesis and the fact that it is a multisystem disease (Kyung *et al*., 2007). Still renal replacement therapy is the main treatment approach for most of these patients after determining the main cause of the failure as being either pre-renal, intrinsic or post-renal (Pavlakou *et al*., 2008, Chen & Busse, 2017, Belloma *et al*., 2012, Finlay & Johns, 2017, Rahman *et al*., 2012). Clinical trials now aim to target AKI at three different points. First, before the injury occurs; as a prevention therapy, for example before surgery which may cause AKI. Second, at an early stage of AKI, which can be facilitated by detection of novel biomarkers which can reveal kidney injury before there is an actual functional change. Third, is to treat the AKI after the serum creatinine has been raised significantly (Mayer 2015).

Several anti-inflammatory mediators such as alkaline phosphatase, dipeptiylpeptidase-4 inhibitors and sphingosine 1 phosphate analogues are under clinical investigation to evaluate their efficiency in the treatment of AKI (Chen & Busse, 2017). Another group of drugs under investigation are genetic modifiers. Examples include I5NP which is an inhibitor of p53 tumour suppressor protein which can extend the time available for DNA repair and therefore improve cell recovery (Chen & Busse, 2017). New drugs as angiotensin II and adenosine antagonists are renal flow modifiers that attempt to address microcirculation

impairment at the level of the single nephron. Despite the protective results of both groups against AKI in animal models, there is limited evidence of their effectiveness in correcting GFR and UO in human clinical trials (Chen & Busse, 2017).

Several medicinal plants are known for their antioxidant activity and have been used for different degenerative diseases such as cancer, diabetes, osteoporosis, neurodegenerative and cardiovascular diseases. Examples of such compounds derived from natural origins include carotenoids and phenolics. Carotenoids are divided into two groups: (1) molecules holding oxygen, e.g. xanthophylls such as lutein and β-cryptoxanthin and (2) molecules with no oxygen, e.g. hydrocarbon carotenoids that are either cyclised such as α-carotene and β-carotene or linear, such as lycopene (Palipoch 2013). Phenolic compounds are mainly flavonoids, tannins and phenolic acids, including anthocyanidins such as pelargonidin, anthochlors such as butein, flavonones such as taxifolin, flavones such as luteolin, flavonols such as quercetin, isoflavones such as genistein, hydroxybenzoic acids such as gallic acid and hydroxycinnamic acids such as caffeic acid (Palipoch 2013, Halliwell & Gutteridge, 2007) [Figure 1.12]. These compounds are known for their antioxidant activity and may have the ability to ameliorate the renal function against oxidative stress. Such polyphenols have been shown to reduce AKI in animal models (Rodrigo 2009).

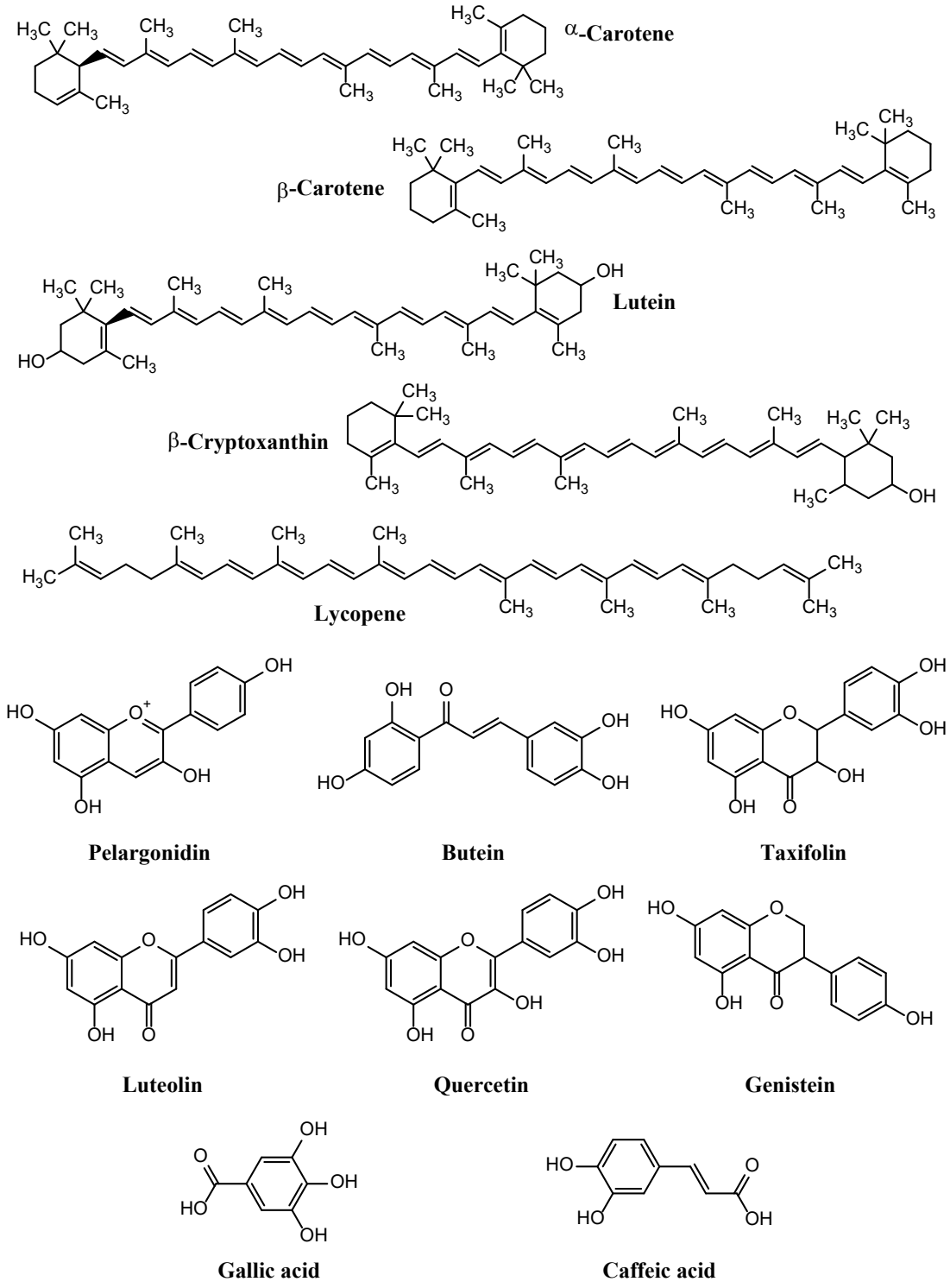

Figure 1.12: Chemical structures of xanthophylls, carotenoids and phenolic compounds

1.13 Animal studies and clinical trials on different potential treatments for acute kidney injury

Different *in vitro* and *ex vivo* studies have shown the advantages of exogenous antioxidants in renal injury, including vitamin E, vitamin C, edaravone, N-acetylcysteine, selenium, polyphenols and flavonoids such as curcumin, quercetin and resveratrol (Dennis & Witting, 2017). Tempol is an antioxidant with membrane permeable properties that acts by scavenging ROS. *In vivo* and *in vitro* studies showed possible protection of tempol against AKI induced by ischaemia/reperfusion injury (Chatterjee *et al*., 2000).

Vitamin E shows some protection against lipid peroxidation, namely the oxidation of low-density lipoprotein (LDL). Two forms of vitamin E (α-tocopherol and γ-tocopherol) have been shown to reduce LDL peroxidation induced by copper (Pannala *et al*., 1998). LDL particles carry 5-9 molecules of vitamin E, that are supposed to prevent them from being scavenged by macrophages after oxidation (Meydani 2001). This has also been demonstrated by the reduced oxidation of LDL induced by iron treatment after the administration of vitamin E (Roob *et al*., 2000). A systemic review conducted electronically using MEDLINE, EMBASE, and the Cochrane Central Register of Controlled Trials showed a potential benefit of using vitamin E plus hydration in reducing risk of contrast-induced AKI by 62% compared to hydration only. However, that review did not observe any significant effect on GFR after contrast treatment (Cho *et al*., 2017). However, a separate clinical trial did not show any benefits of using this vitamin in preventing AKI after elective cardiac surgery (Rodrigo 2009). Different mechanisms have been proposed for its “arguable” protective effect, including direct antioxidant activity by scavenging ROS, enhancing nitric oxide activity, reversing mitochondrial membrane depolarization and protecting lysosomal membrane integrity (Liu *et al*., 2015).

Troxerutin is a flavonoid found in tea, coffee and a variety of fruits and vegetables. It has been shown to have the ability to protect against AKI induced by D-galactose in mice and has both anti-inflammatory and antioxidant activity (Fan *et al*., 2008). Its mechanism of action may involve restoration of antioxidant

enzyme activity and reducing ROS formation, therefore reducing DNA damage, shown by the reduction in 8-OHDG (Liu, *et al*., 2010). Baicalein is also a natural flavonoid present in *Scutellaria baicalensis* Georgi. It has a slightly different mechanism of action, where it activates Nrf2, which has an important role in inhibiting cisplatin-induced AKI. Additionally, it inhibits MAPK activation and NF-kB (nuclear factor kappa enhancer of activated B cells) signalling pathway (Sahu *et al*., 2015).

Astaxanthin is a carotenoid derived from algae and seafood. It also has both antioxidant and anti-inflammatory activities (Augasti *et al*., 2008). Its ability to quench ROS is much higher than β-carotene, ascorbic acid and α-tocopherol. It can also reduce Fe^{3+} to Fe^{2+}. Additionally, it has a direct anti-apoptotic effect on apoptotic molecules (Gao & LI, 2018). There is significant evidence of its effect as an anticancer, antidiabetic and immune regulator. Studies also suggest its benefits in preventing oxidative stress in AKI (Augasti *et al*., 2008) mainly due to cisplatin toxicity (Gao & LI, 2018). An animal study using a severe burn rat model, showed that astaxanthin provides a dose-dependent protection against AKI (Guo *et al*., 2015). Moreover, an *in vivo* and *in vitro* study demonstrated that this carotenoid could ameliorate contrast-induced AKI (Liu *et al*., 2018).

Another group of flavonoids called proanthocyanidins oligomers are extracted mainly from red grape seeds, but are abundant in different fruit, chocolate and tea. Its antioxidant activity is fifty times higher than vitamins E and C. Studies show some evidence of potential pharmacological activity in protecting against AKI (Safa *et al*., 2010). An *in vivo* study using both acetaminophen-induced kidney damage and genomic DNA kidney injury showed that treatment with grape extract can ameliorate kidney function after injury (Bagchi *et al*., 2000). Animal studies on rats and mice showed protection against cisplatin-induced AKI (Saad *et al*., 2009, Hassan *et al*., 2014, Sayed 2009), rhabdomyolysis- induced AKI (Ulusoy *et al*., 2013), cyclosporin-induced AKI (Ulusoy *et al*., 2012) and exercise-induced AKI (Zhang et al., 2014). Furthermore, a rat study showed both biochemical and histological improvement in kidney function after contrast-induced AKI (Ozkan *et al*., 2012). Although its mechanism of action is not well confirmed, it

is believed to inhibit LDL peroxidation, protects DNA from oxidation and increases the production of $NO^{\bullet}$ by reducing its reaction with superoxide. In addition to its antioxidant activity, it also shows some anti-inflammatory activity by decreasing pro-inflammatory cytokines, e.g. IL-1, IL-12, and IL-18, TNF-α (Safa *et al*., 2010).

Probucol is a $O_2^{\bullet-}$ scavenger. It has both antioxidant activity and lipid lowering effects. *In vivo* studies showed that it has a prophylactic effect against contrast-induced AKI (Guangping *et al*., 2009, Wang *et al*., 2015), this is confirmed by a randomized controlled clinical trial in humans (Guangping *et al*., 2009, Yin *et al*., 2009, Guangping *et al*., 2013). *In vivo* investigations demonstrated that it also has protective effects against nephrotoxicity caused by gentamicin or ferric nitrilotriacetate, when given alone or in combination with vitamin E (Abdel-Naim *et al.*, 1999, Kumar *et al*., 2000, Qin *et al*., 1995). Rats which underwent bilateral ureteral obstruction showed improved kidney function when pre-treated with probucol; shown by the greater inulin and para-aminohippurate clearance, reduced level of GSSG and reduced lipid peroxidation compared to untreated rats with similar obstruction (Modi *et al*., 1990).

Gallic acid is a polyphenolic molecule, with the ability to break down the oxidation chain reaction by donating an electron. It is found in tea leaves and blackberries and is also found in high amounts in *Phyllanthus emblica*, a Thai traditional spice, in addition to vitamin C and quercetin. This plant showed some advantage in protecting against contrast-induced AKI in animals (Tasanarong *et al*., 2014). Pomegranate flower extract contains around 10% gallic acid content. *In vivo* studies demonstrated that gallic acid can ameliorate nephron damage due to gentamicin in both pomegranate extract (Sadeghi *et al*., 2015) and in pure form (Ghaznavi *et al*., 2017). Gallic acid showed protection against oxidative injury and reduced renal function in rats caused by chemotherapeutic agents such as cyclophosphamide (Olayinka *et al*., 2015), cisplatin (Akomolafe *et al*., 2014) and methotrexate (Asci *et al*., 2017). Diazinon and Lindane are pesticides that causes oxidative injury to various organs. Pre- and co-treatment with gallic acid in animal studies, showed correction of oxidative stress biomarkers in both cardiovascular, hepatic and renal systems (Ajibade *et al*., 2016, Padma *et al.,* 2011). AKI induced

by ischaemia-reperfusion (Canbek *et al*., 2011) and by sodium fluoride (Nabavi *et al*., 2013) can also be inhibited by gallic acid.

Several studies including a meta-analysis showed the advantage of using vitamin C as a prophylactic treatment for contrast induced AKI. The mechanism of action has not been determined, but it is probably due to its strong antioxidant activity (Sadat *et al*., 2013, Frei *et al*., 1989, Hamdi *et al*., 2012). Animal studies demonstrated that high doses of vitamin C has better effect than vitamin E in protecting against oxidative damage to renal cells (Rodrigo 2009). It is worth mentioning here that its effectiveness is still controversial, as some clinical trials have shown that its administration does not prevent contrast-induced AKI (Le & Chen, 2012, Brueck *et al*., 2013).

1.14 Is there a relationship between diet and acute kidney injury?

A recent investigation has shown that dietary vitamin A and E may lead to a reduced risk of AKI, with the latter having a greater benefit (Rezaei & Hemila, 2017). Studies also show that tocotrienols (antioxidants in the vitamin E family) are of greater antioxidant activity than tocopherols and are effective in preventing AKI in mice (Khan *et al*., 2010). Although α- and ɣ-tocopherols have also shown a protective role against contrast-induced AKI (Tasanarong *et al*., 2013), other studies showed that it does inhibit oxidative stress but does not reverse AKI induced by severe burns (Kim *et al*., 2011).

DASH (Dietary Approaches to Stop Hypertension) is a diet initially proposed to reduce the risk of hypertension mainly by reducing sodium intake. It recommends eating more fruit, vegetables and nuts, which could be a good source of natural antioxidants. A recent investigation has shown that those on the DASH diet have a reduced risk of developing kidney disease (Rebholz *et al*., 2016). Also due to its low sodium salt recommendations, people tend to use more spices in their food, which are usually high in antioxidants which may be a contributing factor to its benefit in reducing kidney diseases.

Green tea (*Camellia sinensis*) is consumed by many people as a hot or cold beverage, as part of their daily diet. It is rich in polyphenols with antioxidant activity, mainly epicatechin, epicatechin-3-gallate, epigallocatechin and epigallocatechin-3-gallate, with epigallocatechin-3-gallate having the highest activity. Several studies demonstrated its beneficial activity in preventing contrast- (Nasri *et al*., 2014), gentamicin- (Abdel Raheem *et al*., 2010, Veljkovic *et al*., 2016) and cyclosporin A- (Rahman *et al*., 2013, Ryu *et al*., 2011, Shin *et al*., 2012) induced AKI. It also prevented AKI in diabetic mice after cardiopulmonary bypass (Funamoto *et al*., 2014) and has been suggested for use as a prophylactic antioxidant prior to renal transplantation (Rah *et al*., 2007). It should also be mentioned that although green tea extract is a natural product, there are still not enough studies to support its clinical safety. In fact, cases of hepatoxicity have been reported after consuming concentrated green tea extract (Molinari *et al*., 2006). A case of liver failure has been reported in a 16-year-old male. It has been linked to the unsupervised use of herbal supplements specifically, green tea extract. In addition to other supplements, the subject was taking two tablets daily, which were equivalent to 400 mg epigallocatechin-3-gallate for 60 days. Biomedical analysis and radiological examination followed by extensive serological and histological tests confirmed hepatoxicity (Patel *et al*., 2013).

A meta-analysis has demonstrated some variations in the geographical epidemiology of AKI, showing that North America, Australia and Eastern Europe had a higher rate of AKI, compared to Asia and Africa. It also showed that North Africa and Central Asia had lower incidence compared to the rest of Africa and Asia, respectively (Mehta *et al*., 2015). These variations were explained by the limited reporting and resources of developing countries compared to developed countries. A different explanation could be the diet of these countries. Different spices, herbs and medicinal plants are used in greater amount in Asia and Africa, which are high in antioxidant and anti-inflammatory activity. For example, *Curcuma longa*, contains curcumin as an active ingredient, it is used as a colouring and flavouring spice in India and Africa (Kaur *et al*., 2016). *Crocus sativus* (saffron) is originally grown in Iran and used widely used in Asia and North Africa. Other plants are traditionally used for the treatment of AKI, due to their anti-inflammatory and antioxidative activity such as, *Panax ginseng*, *Nigella sativa* (black seed),

Zingiber officinale (Ginger), *Silybum marianum, Vitis vinifera* (grapes), *Punica granatum* (pomegranate), *Ginkgo biloba* and *Allium sativum* (garlic) (Boozari & Hosseinzadeh, 2017).

1.15 Improving the bioavailability of supplementary antioxidants

The role of oxidative stress in AKI, although not clear, is almost unquestionable. The real question concerns the effectiveness of antioxidants in AKI. The major drawbacks are their low solubility and permeability, instability, degradation during metabolism and for some antioxidants, their toxicity. Some of these drawbacks will be discussed in detail below for selected drugs (section 1.16). Novel drug delivery systems such as nanoparticles, liposomes, chemical modifications, coupling agents and gel-based systems may improve their bioavailability and safety profile (Ratnam *et al*., 2006, Pangeni *et al*., 2014).

Nanoparticles as the name indicates, are particles within the nano-scale usually with an average size ranging between 1 nm to 1000 nm (Soppimath *et al*., 2001). Nanotechnology has developed extensively during the recent years finding its way in medicine through novel drug delivery, either by tissue targeting or by improving drug pharmacokinetics (Faraji & Wipf, 2009). Nanoparticle is a general term that applies to different shapes, sizes and composition including inorganic, polymeric and solid lipid nanoparticles, liposomes, nanotubes, nanocrystals and dendrimers [Figure 1.13] (Faraji & Wipf, 2009). Definitions and examples will be mentioned in section 2.1.1. Polymeric nanoparticles and liposomes will be discussed in more detail below.

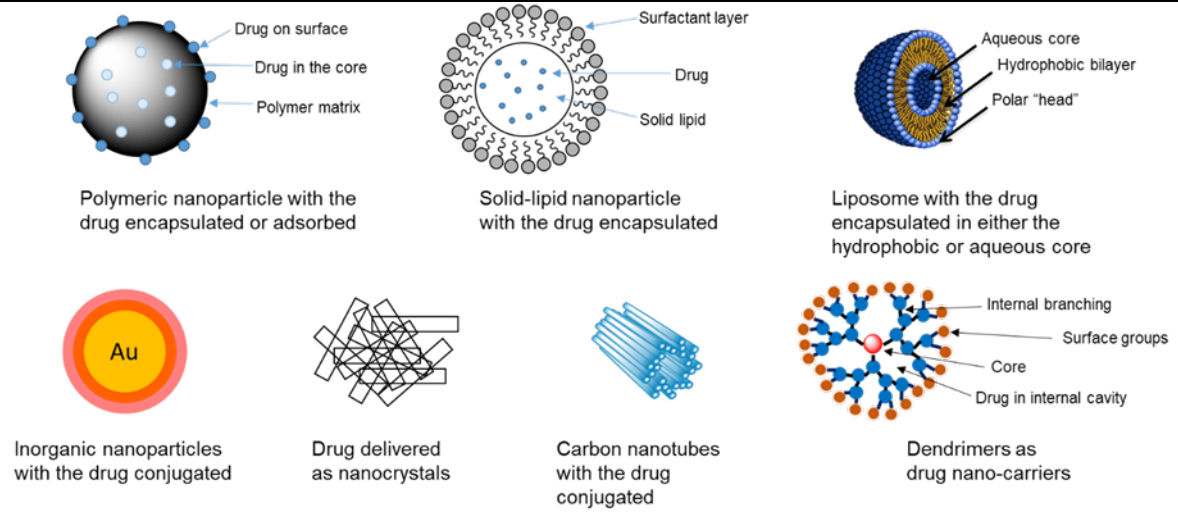

Figure 1.13: Different types of nanoparticles. Adapted from Faraji & Wipf, 2009 (Original figure in colour).

1.15.1 Polymeric nanoparticles

Polymeric nanoparticles are solid nano-scale drug carriers that can either have a matrix type structure made of a certain polymer, in which they are called nanospheres or can consist of a liquid core surrounded by a polymeric membrane where they are called nanocapsules [Figure 1.14]. In both types, drugs can either be embedded in the middle or adsorbed on the surface of the nanoparticle (Pinto Reis *et al*., 2006, Parveen *et al*., 2012, Rao & Geckeler, 2011). Biodegradable nanoparticles prepared from polymers are effective delivery systems that show many advantages over free drugs by providing excellent protection against degradation of the carried drug, hence improving its stability. They can act as good carrying devices to the site of action so fewer side effects may be observed and most importantly, they release the drug over a prolonged period giving a sustained release property (Faraji & Wipf, 2009, Pinto Reis *et al*., 2006, Parveen *et al*., 2012). Polymeric nanoparticles can be derived from many different biodegradable and biocompatible polymers such as polylactic acid (PLA), poly (D, L-glycolide), polylactic-co-glycolic acid (PLGA), polycyanoacrylate, poly (methylmethacrylate) and poly(butyl)cyanoacrylate (Faraji & Wipf, 2009). PLA is an aliphatic polyester of 2-hydroxypropionic acid. It is a biodegradable compound derived from natural sources such as starch or sugar (Lu *et al*., 2008). The advantage of using a polymer such as PLA is its degradability in the body to lactic acid, which is a

natural metabolite that can be further metabolised by Cori cycle to carbon dioxide and water [Figure 1.15]. (Silva *et al*., 2018, Buhecha *et al*., 2019).

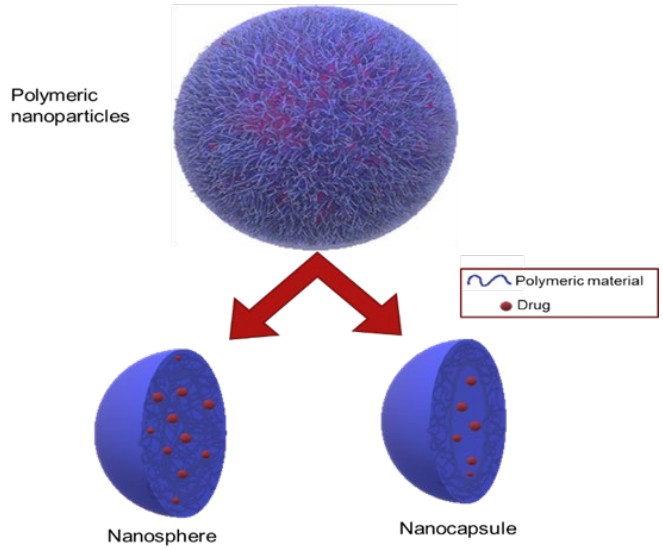

Figure 1.14: **Types of polymeric nanoparticles**. These can be either nanocapsules or nanospheres (original figure in colour)

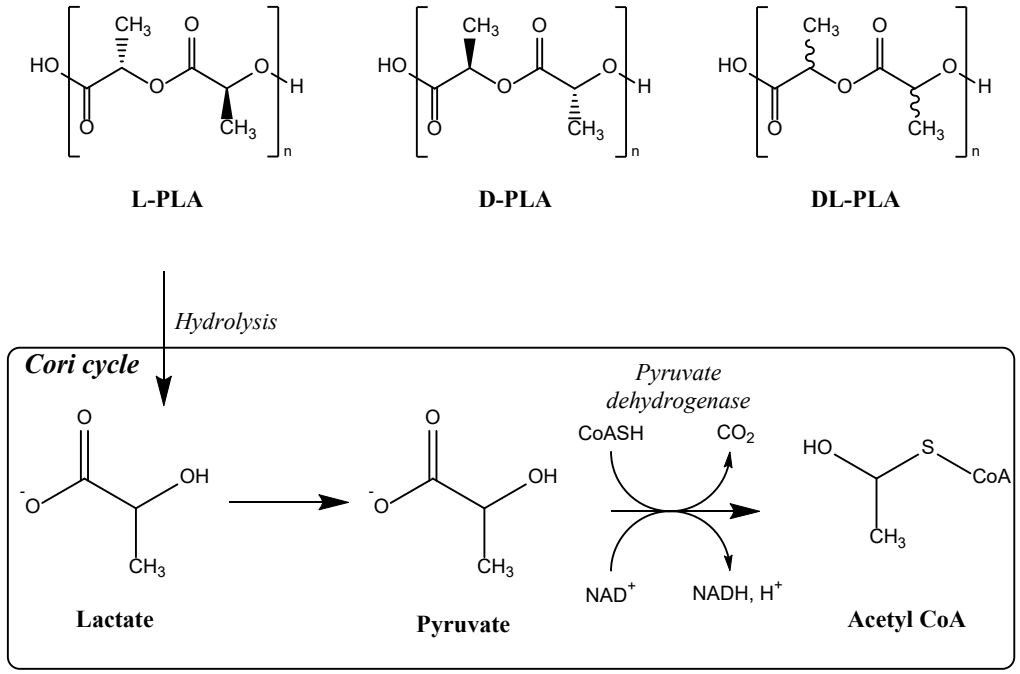

Figure 1.15: **Isomers of poly(lactic acid): l-PLA, d-PLA, dl-PLA**. The polymer hydrolyses to lactic acid in vivo, which then is metabolised in the Cori cycle (adapted from Buhecha et al., 2019)

1.15.2 Liposomes

Liposomes are vesicles within the nano to micro range. They consist of a liquid core surrounded with one or more bilayer phospholipids (Rai & Kon, 2015). It is becoming more and more possible to manipulate the composition and characteristics of the liposomes to suit targeted applications (Banerjee 2001) [Figure 1.16]. They can be used to deliver both hydrophobic and hydrophilic drugs in the lipid bilayer and aqueous core, respectively. Due to their phospholipid composition, they have the advantage of being pharmacologically inactive and are relatively safe (Sercombe *et al*., 2015). Different lipids have been used to formulate liposomes, including cholesterol, dipalmitoylphosphatidylcholine (DPPC), myristoyl-stearoylphosphatidylcholine (MSPC), dimyristoylphosphatidylcholine (DMPC), distearoylphosphatidylcholine (DSPC), dioleoylphosphatidylcholine (DOPC), dioleoylphosphatidylethanolamine (DOPE and 1,2-dioleoyl-3-trimethylammoniumpropane (DOTAP) (Bulbake *et al*., 2017, Campbell *et al*., 2000).

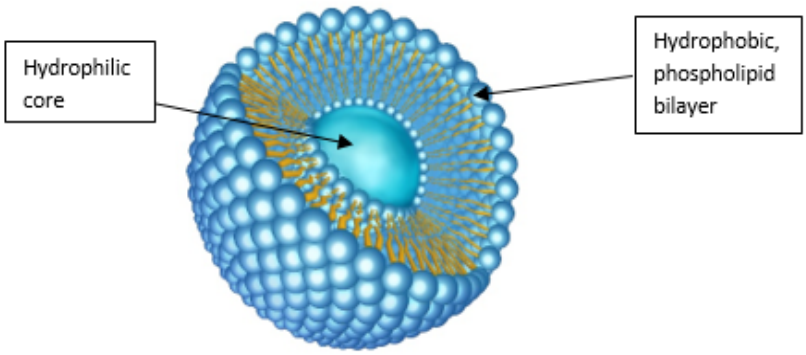

Figure 1.16: **Illustrative image showing the composition of a liposome**: consisting of a hydrophilic core surrounded with a hydrophobic phospholipid bilayer (Source: ShutterStock, stock photography company with minor editing, original figure in colour)

The use of liposomes to deliver antioxidants is an extensively researched area. Several antioxidants such as vitamin E, vitamin C (Galvao *et al*., 2016), curcumin (Alhusaini *et al*., 2018), resveratrol (Csiszár *et al*., 2016, Bonechi *et al*., 2012, Isailović *et al*., 2013), epicatechin (Fang *et al*., 2005, Fang *et al*., 2006) and

ferulic acid (Qin *et al*., 2008) have been developed as potential liposome formulations to treat different oxidative-stress related conditions such as pulmonary damage (Galvao *et al*., 2016), liver injury (Alhusaini *et al*., 2018), pathophysiological aging (Csiszár *et al*., 2016) and cancer (Fang *et al*., 2005, Fang *et al*., 2006) with varying degrees of success. The use of liposome delivery is attempted in order to improve their antioxidant activity increasing intracellular intake and prolonging their availability inside cells and therefore using less doses and reducing toxic effects. Certain antioxidants are available over the counter as dietary supplements in liposomal preparation such as resveratrol and curcumin. Their effectiveness and safety are still in need of further investigation.

1.16 Pharmacokinetics and pharmacodynamics of selected dietary antioxidants and their main drawbacks in the treatment of oxidative stress related conditions mainly AKI

As mentioned previously (section 1.15), the pharmacokinetic and pharmacodynamic properties of supplementary antioxidants are the main obstacle for their effectiveness in AKI. Below are some examples of proposed antioxidants, their sources, physicochemical properties, bioavailability, elimination and proposed mechanism of action.

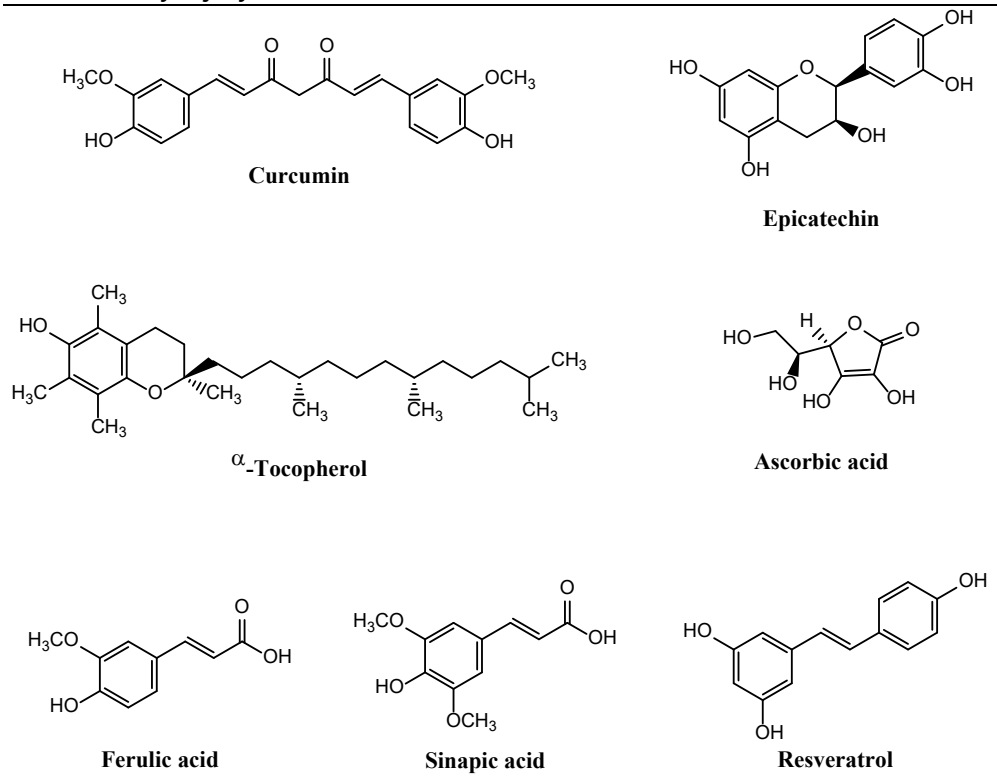

Figure 1.17: **Seven antioxidants having the potential to treat AKI** (which will be discussed in more details). Curcumin, epicatechin, α-tocopherol, ascorbic acid, ferulic acid, sinapic acid and resveratrol.

1.16.1 Vitamin C

Vitamin C (ascorbic acid) is a compound with high water solubility [Figure 1.17]. It is present in high amounts in oranges, lemons, berries, mangoes, broccoli and peppers (Halliwell & Gutteridge, 2007). Its bioavailability is almost 100% for doses up to 200 mg. This percentages declines gradually, reaching 33% with higher doses (1.25 g). It is absorbed mainly from the small intestine. It is considered not to be protein bound and therefore it is filtered into the glomerulus but reabsorbed back into the renal tubules by active transport. A 100 mg dose of oral or i.v. vitamin C results in an excretion of 25% in urine, while higher i.v. doses are 100% excreted into the urine. Elimination half-life is around 10 hours (Schwedhelm *et al*., 2003). It is mainly present as an ascorbate form at physiological pH levels. Its mechanism of action as an antioxidant is by scavenging ROS and RNS, inhibiting lipid peroxidation due to haemoglobin and regenerating α-tocopherol (Halliwell & Gutteridge, 2007).

1.16.2 Vitamin E

Vitamin E is a collective term for eight different tocopherols and tocotrienols. As α-tocopherol [Figure 1.17] is the most abundant isoform in tissues (90%), it will be the main structure discussed in detail here. α-Tocopherol is a viscous oil at room temperature, insoluble in water but soluble in ethanol and organic solvents. It is slightly yellow to amber, almost odourless, clear and darkens on exposure to air or light due to oxidation. Its melting point is 3°C and its partition coefficient (log P) =12.2 (Liu *et al*.,2015). It is a fat-soluble compound, available from natural sources in the R,R,R-stereoisomer form (Schwedhelm *et al*., 2003). Wheat-germ oil, vegetable oil, nuts, grains and green vegetables are rich in vitamin E (Halliwell & Gutteridge, 2007).

Due to its lipophilicity, its absorption depends mainly on the bile secretions. Different forms of vitamin E are transferred into the blood stream *via* the lymph in chylomicrons. Only R,R,R-α-tocopherol is transferred *via* the liver in very LDL (Schwedhelm *et al*., 2003, Halliwell & Gutteridge, 2007). Only 25-50% is absorbed from food (when the dose is less than 1 mg). Most of the drug at pharmacological doses will only be excreted *via* the faeces and only 10% will be absorbed (Baskin & Salem, 2020, Schwedhelm *et al*., 2003). Its peak plasma concentration is reached after 12-14 hours (Schwedhelm *et al*, 2003). It plays a major role in preventing lipid peroxidation by scavenging lipid peroxide radicals at a very fast rate. Furthermore, the α-tocopherol radical can react with a second peroxyl radical forming non-radical products, 8a-(lipid-dioxy)-α-tocopherones, which are hydrolyzed to α-tocopherylquinone. (Halliwell & Gutteridge, 2007).

Although, α-tocopherol was found to be a strong *in vitro* and *in vivo* antioxidant, its low hydrophilicity and high lipophilicity contributes to its limited application. Different attempts have been made to overcome its solubility, permeability and bioavailability issues by using novel drug deliveries such as liposomes, nano-emulsions and lipid nanoparticles (Niki & Abe, 2019). For example, liposomal α-tocopherol was found to have more antioxidant effects on the lungs against injuries and inflammation induced by a number of substances

including paraquat, bleomycin, and lipopolysaccharide compared to conventional α-tocopherol (Suntres 2011). As mentioned in section 1.13, there has been arguable discussions about the effectiveness of α-tocopherol on the prophylaxis treatment of AKI. However, scientists have noticed that a single dose of it, was not beneficial in preventing or reducing the severity of the disease in animal models and in human clinical trials. Combination therapy with other compounds such as vitamin C, erdosteine, N-acetylcysteine, L-arginine or selenium with α-tocopherol have shown to be more protective against AKI than α-tocopherol alone (Liu et al., 2015).

1.16.3 trans-Resveratrol

trans-Resveratrol is a stilbene antioxidant (3,5,4'-trihydroxystilbene), which means it has two phenyl groups subtitled at the two ends of an ethylene double bond (Schwedhelm *et al*., 2003) [Figure 1.17]. It is present in low concentrations in wine where it is produced by the grapes as a defence mechanism against fungi (Halliwell & Gutteridge, 2007). It is also present in blueberries, raspberries and mulberries (Holthoff *et al*., 2012). Resveratrol is a white solid powder that is insoluble in water (< 0.05 mg/ml) and soluble in organic solvents such as ethanol (50 mg/ml) with a logP = 3.10. Although it has a high absorption rate, its oral bioavailability is low (less than 1%) due to its fast metabolism in the intestine and liver (Rotches-Ribalta *et al*., 2012, Walle 2011). Its main metabolites are due to conjugation reactions to form resveratrol glucuronides and resveratrol sulphates. The activity of these metabolites requires further investigation (Wenzel 2005). Its main drawbacks are its low bioavailability, toxicity if given in high doses i.p. and instability. Further studies are needed to prove any benefit from i.v. infusion (Holthoff *et al*., 2012, Crowell *et al*., 2004).

Studies show that it has both protective as well as recovery role from sepsis-induced AKI in mice, by activation of SIRT1/3 (Holthoff *et al*., 2012, Xu *et al*., 2016, Gan *et al*., 2016). Others demonstrated that its protection and treatment is due to the prevention of inflammation caused by macrophage and endoplasmic reticulum stress-activated NF-kB pathway (Chen *et al*., 2015, Wang *et al*., 2017). Previous research has shown that its administration to ischaemia-reperfusion rat

models reduces rate of mortality (Rodrigo 2009) and that it presents potential for treatment of cisplatin-induced AKI (Hao *et al*., 2016). *In vivo* studies showed that it corrects AKI caused by arsenic trioxide by increasing its elimination and decreasing oxidative stress (Yu *et al*., 2013). A more recent study demonstrated that its mechanism is by both blocking inflammatory pathways and decreasing oxidative stress, in addition to preventing cell death *via* the Nrf2/TLR4/NF-kB pathway (Li *et al*., 2018). An ongoing clinical trial is aiming to investigate the effect of resveratrol on inflammation and oxidative stress in CKD (Ishimoto & Inagi, 2016). A prospective study of about 800 elderly subjects, did not find any influence of dietary resveratrol on different age-related diseases (Semba *et al*., 2014). Different efforts have been made in order to reduce its drawbacks such as encapsulating the drug in liposomes (Narayanan et al., 2009), solid lipid nanoparticles (where oral bioavailability increased by more than 8-fold compared to drug solution) (Pandita *et al*., 2014) and dendrimers (Chauhan 2015, Pentek *et al*., 2017). It has also been co-encapsulated with a novel NMDA receptor inhibitor (DAP5) and found to protect against ischaemia-reperfusion renal injury (Xu *et al*., 2017).

1.16.4 Curcumin

Curcumin [Figure 1.17] is a polyphenolic compound (1,7-bis (4-hydroxy- 3-methoxyphenyl) -1,6- heptadiene-3,5-dione) derived mainly from turmeric (*Curcuma longa*) (Stanic 2017). It is a yellow solid lipophilic compound with a log P value of ~3.0. It is practically insoluble in water and freely soluble in polar solvents like dimethyl sulfoxide) DMSO, methanol, ethanol, acetonitrile, chloroform and ethyl acetate. It is sparingly soluble in hydrocarbon solvents such as cyclohexane and hexane (Priyadarsini 2014).

Several studies have demonstrated the activity of curcumin to ameliorate AKI in rats (Nabavi *et al*., 2012, Hismiogullari *et al*., 2015, Fan *et al*., 2017, Ugar *et al*., 2014, Najafi *et al*., 2015, Mercantepe *et al*., 2018, Tapia *et al*., 2014, Liu *et al*., 2017, Topcu-Tarladacalisir *et al*., 2016, Kaur *et al*., 2016) while others demonstrated incomplete protection (Hammad *et al*., 2012, Vlahovic *et al*., 2007).

Its antioxidant activity is due to the ability to scavenge ROS and RNS, upregulate haem oxygenase and glutathione transferase and downregulate xanthine oxidase. In addition to its antioxidant properties, studies have shown its ability to inhibit protein kinases, downregulate pro-inflammatory proteins, cytokines, growth factors and transcription factors (Sharma *et al*., 2007, Nasr *et al*., 2016).

Despite the numerous *in vitro* and *in vivo* positive results of curcumin in preventing AKI (He *et al*., 2015), human clinical trials did not show any of its benefits (Grag *et al*., 2018). In all studies its potential as a prophylactic treatment for AKI was evident but incomplete, as the drug was administered to the animals i.p. in DMSO, orally dissolved in an oil or as a suspension. Animal and human studies have also shown that curcumin has very low oral bioavailability. This can be rationalised by its poor solubility and biodegradation through first-pass effect and intestinal metabolism. Its main degradation products include curcumin glucuronide and curcumin sulphate (Esatbeyoglu *et al*., 2012). Traces of di-, tetra- and hexa- hydrocurcumin, and hexahydrocurcuminol were found in the plasma after i.p. injection (Sharma *et al*., 2007). Different attempts have been made successfully, to improve its effectiveness such as incorporating it into liposomes (Rogers *et al*., 2011) and nanoparticles (Chen *et al*., 2017).

1.16.5 Ferulic acid and sinapic acid

Ferulic acid (4-hydroxy-3-methoxycinnamic acid) and sinapic acid (3,5-dimethoxy-4-hydroxycinnamic acid) [figure 1.17] are classified under hydroxycinnamates, which are small phenylpropanoids derived from plants. They are biosynthesised in plants from the amino acids L-tyrosine and L-phenylalanine, through the shikimic acid pathway (Herrmann & Weaver, 1999). They are available in fruits, vegetables, cereal grains and oilseed crops, so they are high in normal human diet (Nikiforovic & Abramovic, 2013). In addition to isoferulic, dihydroferulic and vanillic acids, ferulic acid is also one of the metabolic products of caffeic acid, which is present in high concentration in coffee beans (Xiao *et al*., 2009). Both ferulic and sinapic acids are available as free forms, sugar ester (glycosides) or esters of other organic compounds forms. The log P values for ferulic acid and sinapic acid were 1.42 and 1.29, respectively. They are partially soluble in water

and readily soluble in polar organic solvents such as ethanol and methanol (Galanakis *et al*., 2013).

Ferulic acid shows good absorption that can reach up to 60% after oral administration of free drug but only 1-4% of drug from daily diet. This was explained by its low bioaccessibility caused by its esterified or bound form (Anson *et al*., 2009). Its main metabolism is through conjugation with glucuronic acid, although high amount is excreted unchanged in the urine (36-43%) (Xiao *et al*., 2009). Less data is available on pure sinapic acid, but studies show that its main site of absorption is the small intestine through an active sodium gradient driven transport channel. Due to its poor solubility, its bioavailability after oral administration is very low (3%), leading to reduced bioactivity (Kern *et al*., 2003, Shakeel *et al*., 2016). It is metabolised through phase I and II in the epithelium of intestinal cells. Further study will be needed to evaluate effectiveness of its metabolites. (Chen 2015). Sinapic acid has also been found as a dimer with itself and with ferulic acid in cereals (Nikiforovic & Abramovic, 2013). Due to their phenolic structure, they show good antioxidant activity by scavenging free radicals. In addition to their anti-oxidative action, they show antimicrobial, anti-inflammatory, anticancer and anti-anxiety activity (Nikiforovic & Abramovic, 2013). Studies on cell-lines and rats showed some benefit of sinapic acid in ameliorating AKI (Ansari 2017).

1.16.6 Epicatechin

Epicatechin [Figure 1.17] as well as catechin and epigallocatechin are naturally occurring compounds in in red wine (grapes), cocoa and tea (Halliwell & Gutteridge, 2007). It has a log P value 0.11 and is sparingly soluble in water (Okumura *et al*., 2009). The oral bioavailability of epicatechin is around 4%. Although studies have showed minimal hepatic metabolism, the main reasons attributing this, was the efflux transport, low absorption and intestinal metabolism (Chen & Hsu, 2009, Lee *et al*., 2006). Efficacy has been improved in experimental studies by means of nanotechnology (Yadav *et al*., 2014). Animal studies showed some potential for this polyphenol for the treatment of AKI induced by cisplatin

(Tanabe, K, 2012, Malik *et al*., 2016) and lipopolysaccharides (Prince *et al*., 2017). Prince *et al,* however*,* suggested that this protection is *via* reaction specific for epicatechin that limits oxidant production rather than its free radical scavenging properties. This was suggested due to the very low concentrations that reaches the tissues (Prince *et al*., 2017).

1.17 Hypothesis

AKI has shown to have a vast burden on hospitalised patient, especially in ICUs. To date, there is no specific pharmacological drug used to prevent or treat AKI. Oxidative stress has a major role in the pathophysiological development of AKI. The use of dietary antioxidants such as α-tocopherol, curcumin, resveratrol, epicatechin, sinapic acid and ferulic acid can be used as a preventative and a treatment option for the injury when formulated in particular delivery systems. Antioxidants can reverse the harmful effect of ROS on renal tubular epithelial cells during oxidative injury and thereby ameliorate AKI. Their effectiveness has been challenged by their poor bioavailability at the site of action.

The hypothesis of this study is that loading dietary antioxidants with variable physicochemical properties, into novel drug delivery systems such as PLA nanoparticles and liposomes, will have an advantage over non-formulated antioxidants, in the prevention of AKI in *in vitro* model. These nanoparticles can increase penetration of poorly soluble drugs across cell membrane, increase duration of action by protection against metabolism, reduce toxicity by reducing the dose required, target specific site of action and also increase shelf life by improving stability. If these delivery systems demonstrate a superior protection against oxidative stress, they could be given as a prophylaxis treatment against AKI, to patients with high risk, for example in ICU or prior to renal transplantation.

1.18 Aims

The main aim of this study is to encapsulate antioxidants into liposomes and PLA nanoparticles and study their potential to treat or prevent AKI. In order to achieve this the following aims will be targeted:

- Encapsulated liposomes and PLA nanoparticles with six different antioxidants separately (α-tocopherol, curcumin, resveratrol, ferulic acid, sinapic acid and epicatechin)
- Characterise the produced liposomes and PLA nanoparticles for their size, surface charge, morphology and encapsulation efficiency
- Assess whether encapsulating these drugs into the delivery systems will hinder or potentiate their antioxidant activity
- Compare the toxicity profile of free and encapsulated antioxidants *in vitro* using renal epithelial (NRK-52E) cell lines
- Measure the cellular uptake of these antioxidant as free and encapsulated forms
- Study the *in vitro* activity of these antioxidant as free and encapsulated forms against the oxidative stress induced by paraquat

Chapter 2: Synthesis and characterisation of PLA nanoparticles and liposomes encapsulating different antioxidants with different physicochemical properties

2.1 An introduction to the chapter

This chapter will start with a brief introduction to nanoparticles and their types with more focus on polymeric nanoparticles and liposomes. It will answer basic questions, such as what they are, when where they first discovered, and how can they be used to improve drug delivery. It will then discuss the different methods to prepare nanoparticles and the advantages and disadvantages of each method.

The second part of this chapter will discuss in detail the selected materials and methods used to prepare and characterise selected antioxidants encapsulated into PLA nanoparticles and liposomes. All results collected followed by a comprehensive discussion and a conclusion. Antioxidants selected for investigation are α-tocopherol, curcumin, resveratrol, ferulic acid, sinapic acid and epicatechin. These antioxidants were selected for this study due to their incomplete ability to ameliorate AKI, even though they have strong antioxidant activity and are available in the daily diet. Some of the different physicochemical, pharmacokinetics and pharmacodynamics properties and attempt to improve their efficiency were described in section 1.15.

2.2 Introduction to nanoparticles

As described in chapter 1, section 1.15, nanoparticles are particles within the nano-range. They have been used extensively to manipulate different properties of different materials to suit different purposes. Nanotechnology has found its application in numerous fields replacing conventional products including cosmetics, medicines and supplements. It was also applied to countless industries such as medicine, information, communication, transport, food, sports, energy and electrical appliances. Examples include edible nanolaminates that improve packaging of food, flash memory chips for iPod nano, nanomaterial-based bio-fluids, nanofibres that filter harmful particles from the environment and polymer nanocomposites in everyday equipment like luggage, automobiles, antibacterial paint and sensors (Purohit *et al*., 2017). In 2005, the nanomaterial Consumer Products Inventory (CPI) was developed by the Woodrow Wilson International Centre for Scholars and the Project on Emerging Nanotechnologies to document the penetration of nanotechnology in the consumer market and 54 products were listed back then. The CPI was redeveloped in 2015, documenting 1814 consumer products from 662 different companies (Vance *et al*., 2015). This shows the rapid increase in the employment of nanotechnology. In medicine, nanoparticles have been utilised in the diagnosis, prevention and treatment of numerous diseases and medical conditions. Examples of their applications include drug therapy, gene therapy, biological labelling, purification of biological molecules, tissue engineering, biochips, bone replacement, anti-microbial textiles and microsurgical technology (Purohit *et al*., 2017).

Conventional medications (such as tablets, capsules, solutions, etc.) although widely used and convenient in many different ways, their activity remains restricted by the physicochemical properties of the active ingredient. Certain characteristics such as absorption, stability, taste, targeting and duration of action are not always easy to manipulate, if the drug for instance, does not possess certain solubility (Rivas *et al*., 2017). For example, paclitaxel is a very powerful chemotherapeutic agent, but due to its low hydrophilicity its formulation (known as Taxol) includes a mixture of Cremophor EL and dehydrated ethanol, which are responsible for its severe side effects. Several novel nano-drug delivery systems

have been practical to improve its physicochemical properties leading to superior patient acceptance. Abraxane® is a paclitaxel albumin-bound nanoparticle formulation that has been approved by the FDA and shown to be easier to tolerate by the patient (Ma & Mumper 2013). Encapsulating drug inside nanoparticles can have different purposes such as delayed release, targeted delivery, cover unfavourable organoleptic properties, prevent degradation in the digestive system, increase shelf-life, minimize volatilisation, reduce toxicity, control hygroscopic properties and design new dosage forms (Rivas *et al*., 2017).

2.2.1 Different types of nanoparticles

The term nanoparticle applies to different types of nanostructures. Some of which have been mentioned in section 1.15 and illustrated in figure 1.13. Inorganic nanoparticles possess unique optical, magnetic, electronic, and catalytic properties that make them distinguished from their bulk respective materials. Different molecules have been widely applied to nanomedicine using inorganic nanoparticles such as iron oxides, gold, silver, silica and quantum dots (Purohit *et al*., 2017). Nanocrystals can be formed from solutions by manipulating different thermodynamic and kinetic parameters to control nucleation and growth process. They have the advantage of catalytic properties that are usually not present in their bulk state such as gold nanoparticles (Wu *et al*., 2104). A nanotube is tube like construction in the nano-scale. As the name indicates, they are long, hollow structure with walls made from one-atom-thick sheets of carbon called graphene (Purohit *et al*., 2017). Dendrimers are hyper-branched, rounded, monodisperse, 3-D synthetic polymers in the nano-scale. They are characterised with precise size, shape and molecular weight (Purohit *et al*., 2017). Polymeric nanoparticles and liposomes have been described in chapter 1; sections 1.15.1 & 1.15.2; respectively and will be discussed further below, as they are the focus of this research.

2.2.1.1 Polymeric nanoparticles

Polymeric nanoparticles are nano-sized solid colloidal particles consisting mainly of macromolecules. One of its first application in medicine goes back to 1979 when polyalkylcyanoacrylate nanoparticles were studied as carriers for anticancer drugs (Bolhassani *et al*., 2013). The introduction of stealth protection to polymeric nanoparticles was initiated in 1994, by the use of the co-polymer, poly(lactic-co-glycolic acid)-polyethyleneglycol (PLGA-PEG). Studies continued on the control release from polymeric nanoparticles until 2005, when Abraxane was first approved by the FDA. Indeed, it enlarged the therapeutic index of paclitaxel but it did not affect its pharmacokinetic or biodistribution properties. In 2007, Genexol-PM (a paclitaxel loaded polymeric micelle) was approved by the Korean health administration for breast cancer (Caruso *et al*., 2012) and still under clinical trials for ovarian cancer (Lee *et al*., 2018). Phase I clinical trials for BIND-014 (a docetaxel encapsulated polymeric nanoparticles) started in 2011 for the treatment of prostate tumour (Kamaly *et al*., 2012). Its safety and efficacy were studied under phase II clinical trials between 2013 and 2016 and suggested that patients are likely to benefit from this treatment (Autio *et al*., 2018) [Figure 2.1]. Several formulations are already in clinical trials, whereas many others are in different phases of preclinical studies.

As mentioned previously, polymeric nanoparticles can be either nanospheres or nanocapsules. Nanospheres, as the name indicates, are usually a spherical matrix, which is completely solid in nature. They can be lipophilic in nature called lipophilic nanospheres or hydrophilic such as polyelectrolyte complexes and nanogels. Nanocapsules in contrast have a reservoir form in which a solid shell surrounds a liquid or a semisolid core. This core can be aqueous or oily in nature and so encapsulate both hydrophilic and hydrophobic drugs. For better protection against enzymatic degradation, drugs should be loaded during preparation of the nanoparticles to ensure entrapment within the carrier. Nevertheless, in situations where the drug cannot be loaded during nanoparticle preparation or it is highly sensitive to the preparation technique, it can be adsorbed on readily prepared carriers (Vauthier & Bouchemal, 2009).

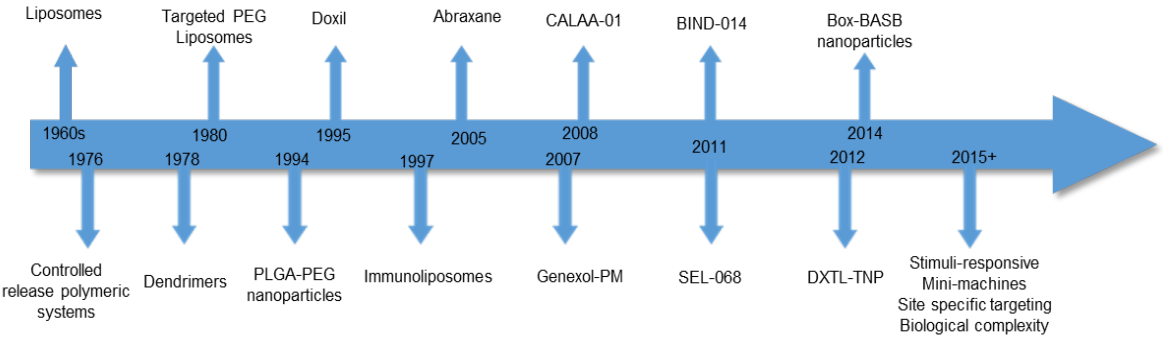

Figure 2.1: **Timeline of clinical stage nanomedicine firsts.** Liposomes, controlled release polymeric systems for macromolecules, dendrimers, targeted-PEGylated liposomes, first FDA approved liposome (DOXIL), long circulating poly(lactic-co-glycolic acid)-polyethyleneglycol(PLGA-PEG) NPs, first development of immunoliposomes, protein based drug delivery system (Abraxane; NAB Technology), polymeric micelle nanoparticles (Genexol-PM), targeted cyclodextrin-polymer hybrid nanoparticles (CALAA-01), targeted polymeric nanoparticles (BIND-014; Accurint Technology), fully integrated polymeric nanoparticle vaccines (SEL-068,tSVPt Technology). Adapted from Caruso *et al.*, 2012 (original figure in colour)

Several polymers with different characteristics are used to synthesise polymeric nanoparticles. Some are derived from natural sources such as chitosan, alginate, gelatin and albumin. Others are synthetic such as poly(epsilon-caprolactone) and poly(isobutylcyanoacrylate) (Vauthier & Bouchemal, 2009). The biodegradability of a polymer is determined by the existence of labile functional groups such as esters, orthoesters, anhydrides, carbonates, amides, urea or urethane in their backbone (Pillai & Panchagnula, 2001). Some are biodegradable such as PLA and PLGA, while others are non-biodegradable such as polymethacrylate acrylate (Rivas *et al.*, 2017). Additionally, PEG has been used as co-polymer with poly-esters such as PLA, to manipulate the nanoparticle surface charge and increase stability inside the body (Vauthier & Bouchemal, 2009).

There are many advantages of encapsulating drugs within nanoparticles. They can increase the solubility of the carried drugs or reduce their side effects through targeted delivery. Additionally, they can increase stability of their cargo in

a formulation or inside the body and therefore increase their shelf life or duration of action, respectively (Selby *et al*., 2017). Nevertheless, it is important to ensure the release of the encapsulated drug at the specified site of action and at the required rate. This depends mainly on the manipulation of different characteristics of the polymeric nanoparticles such as size, shape, surface charge, composition and amount of drug carried. For example, nanoparticles smaller than 10 nm will be cleared by the kidneys and larger than 200 nm will not pass through microcapillaries (Selby et al., 2017). The mechanisms of uptake and internalisation of nanoparticles, methods of endosomal release and how these are affected by different nanoparticle characteristics will be discussed in more detail in sections 4.3.3, 4.1.4 & 5.1.3.

2.2.1.2 Liposomes

Liposomes are sphere-like vesicles consisting of an aqueous core surrounded by one or more lipid bilayers. They should not be confused with micelles that are surrounded with a single layer. The term liposome is derived from the Greek words "*lipos* & *soma*" meaning fat and body; respectively. They were first introduced by Bangham and his colleagues in 1961 and described as swollen phospholipid systems (Cagdas *et al*., 2014). Exploration on the clinical potential of liposomes started in the 1980s, whereby they proved useful for improving the therapeutic index of their cargo, such as doxorubicin and amphotericin (Sercombe *et al*., 2015). Their main obstacle towards clinical use was the clearance by mononuclear phagocytic system (MPS), mainly in the liver and spleen. Doxil (doxorubicin encapsulating liposomes) was the first FDA approved liposomes to reach clinical approval in 1995 for AIDS related Kaposi's syndrome (Nisini *et al*, 2018). Doxil was able to escape phagocytosis due to the external coating with the hydrophilic polymer, PEG. Still this dosage form had the disadvantage of being widely bio-distributed. Active targeting was first demonstrated in 1997 by Spragg and his colleagues using antibody coupling to liposomes [Figure 2.1]. They showed that using E-selectin-targeted immunoliposomes for doxorubicin delivery showed increased activity in activated cells that express E-selectin compared to cells that were not activated. Subsequently, a number of liposomes have been developed for clinical application mainly for the treatment of cancer such as

Myocet®, DaunoXome®, Depocyt®, Mepact®, Maqibo® and Onivyde™. Additionally, Cervarix®, Inflexal®, and Epaxal® are liposomal vaccines available in the market against infection by human papilloma, influenza, and hepatitis A viruses; respectively (Nisini *et al*., 2018). Furthermore, liposomes can be administered via different routes. For example, dorzolamide liposomes for the treatment of glaucoma, administered as eye drops and liposomes carrying anti-TB drugs administered by inhalation (Nisini *et al*., 2018).

Liposomes can have an onion structure with more than one lipid bilayer called multilamellar vesicles (MLV) or have a single lipid bilayer, which are either called large unilamellar vesicles (LUV) or small unilamellar vesicles (SUV), according to their size. Furthermore, they can have more than a single vesicle within a larger bilayer, called multivesicular [Figure 2.2]. The later structure is usually not preferred due to uncontrolled release. There are several advantages for encapsulating drugs within liposomes. For instance, they can increase the efficacy, therapeutic index and stability of the encapsulated drugs. They can also reduce toxicity; help reduce exposure to sensitive tissues and may aim to avoid specific sites. They are non-toxic, biocompatible and biodegradable. Additionally, they have the flexibility to be coupled with site-specific ligands and to be administered *via* different routes. On the other hand, they possess some disadvantages as well such as, poor solubility, short half-life, drug leakage and high production cost (Akbarzadeh *et al*., 2013).

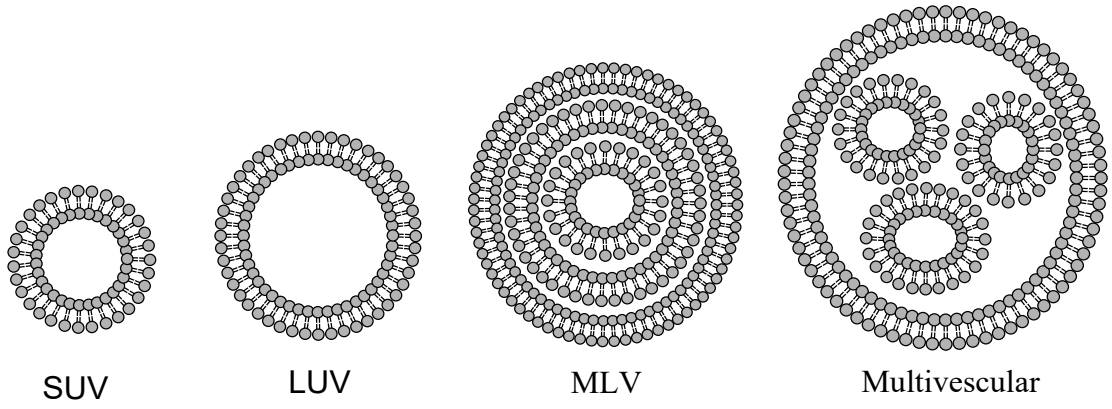

Figure 2.2: **Types of liposomes according to size and shape**. Liposomes can have a single lipid bilayer forming either SUV (usually < 100 nm) or LUV (100 – 200 nm or even bigger) or can have multilayers of bilayer lipids forming MLV. Additionally, several SUV can be surrounded by an additional lipid bilayer forming multivesicular liposomes.

Driven to improve the delivery of drugs, modifications to the lipid bilayer are under investigation, introducing a new generation of liposomes. For example, lipids containing diether linkages form archaesomes, which have more stability. Archaeosomes are liposomes with a structure made from archaeo bacterial membrane lipids including di-ether or tetra-ether. Another method of increasing their stability is the use of non-ionic surfactants and cholesterol forming niosomes or adding polaxamers or PEG to the phospholipids forming cryptosomes. Niosomes are vesicles formed from synthetic non-ionic surfactants increasing their stability. The word Cryptosome came from the Greek words ‘’Crypto’’ meaning hidden and ‘’Soma’’ meaning body, as using PEG-lated lipids instead of lipids only led to increased stability of the formed liposomes. To increase the loading efficiency or to load more than one drug, multi-bilayers from fatty acids only or adding monoesters of polyoxyethylene fatty acids, cholesterol forming vesesomes or novasomes, respectively. Additionally, genosomes and virosomes are suitable to deliver genes and antigens [Figure 2.3] (Cagdas *et al*., 2013).

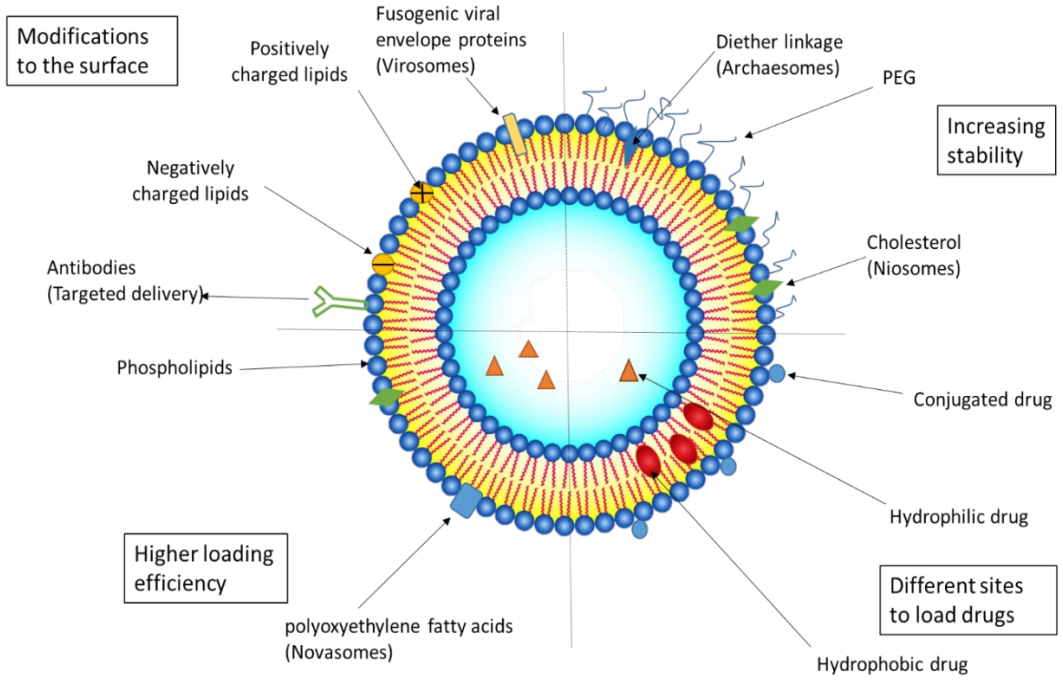

Figure 2.2.3: A liposomal structure showing sites of drug loading and different modifications to increase stability, loading efficiency, and targeting. Different modifications can be made to the surface forming virosomes, archaesomes, niosomes and novasomes. Additionally, lipids can be neutral, negatively, or positively charged. Drugs can be loaded in the centre of the liposomes or in the lipid bilayer (Adapted from Cagdas *et al*., 2013).

2.2.2 Different methods used to synthesise nanoparticles

Countless methods have been applied to synthesise nanoparticles. Among other factors, the choice depends on the type of nanoparticles, the required physical and chemical properties, application, stability, and quantity as well as the targeted site. They can be shortened into two main approaches; top-down and bottom-up. The top-down category involves using bulk or large precursors and dividing them into the desired nanoparticles such as the electronic circuit fabrication using lithography. Whereas the bottom-up category usually involves the assembly or growth of smaller precursors typically at atomic level to form nanoparticles such as semiconductor quantum dots for lasers. Both approaches can involve physical, chemical or biological methods (Purohit *et al*., 2017). Due to the wide diversity and vast subject, not all methods can be mentioned. However,

this study is mainly focused on polymeric nanoparticles and liposomes and therefore, methods used to prepare these nanoparticles will be discussed in more detail below. Furthermore, methods involving supercritical or compressed fluids can be used to prepare different types of nanoparticles and will be discussed.

2.2.2.1 Different methods used to synthesise polymeric nanoparticles

Polymeric nanoparticles have received an enormous amount of attention due to their promising delivery prospects. Different parameters can be manipulated to achieve desirable effects. As discussed previously (Sections 1.15.1 & 2.2.1.1), there are different types of polymeric nanoparticles, but the methods for their preparation are usually classified according to whether a preformed polymer is used or a polymerisation reaction is required in the formulation process. Additionally, some type can be prepared using self-assembly macromolecules or ionic gelation [Figure 2.4] (Reis *et al*., 2006, Nagavarma *et al*., 2012).

2.2.2.1.1 Methods involving polymerisation of a monomer

Methods involving polymerisation of a monomer include emulsion polymerisation, interfacial polymerisation and interfacial polycondensation. For the emulsion polymerisation, the continuous phase can be either organic or aqueous according to the monomer solubility. For example, poly(methylmethacrylate) nanoparticles have been prepared using continuous aqueous phase emulsion polymerisation to encapsulate Influenza antigen. The monomer methylmethacrylate was dissolved in aqueous solution due to its water solubility with no surfactant required (Reis *et al*., 2006). Methylcyanoacrylate was used to prepare nanoparticles to encapsulate triamcinolone, fluorescein and pilocarpine using continuous organic phase emulsion polymerisation. Here the monomer was dispersed into an organic solvent *via* a surfactant due to its insolubility in organic solvents (Reis *et al*., 2006).

Interfacial polymerisation was applied to encapsulate insulin into poly(ethylcyanoacrylate) nanoparticles. On the other hand, interfacial

polycondensation was used to encapsulate α-tocopherol into polyurethane nanoparticles. Although, polymeric nanoparticles produced by these methods have the advantage of having high encapsulating efficiency, they still show some disadvantages. For instance, most of them yield slow biodegradable or nonbiodegradable polymers with exception of alkylcyanoacrylates and poly(dialkylmethylidene malonate). Additionally, the process usually leads to residual materials such as monomers, oligomers or surfactants in the final product (Reis *et al*., 2006).

2.2.2.1.2 Methods using preformed polymers

The above disadvantages are undetected by the use of readily prepared biodegradable polymers to formulate nanoparticles. Examples of such methods include emulsification/solvent evaporation (ESE), solvent displacement, interfacial deposition, emulsification/solvent diffusion (ESD) and salting out. As the name indicates, ESE method involves two steps. First, the polymer and the drug organic solution is dispersed *via* high-energy homogenisation into an aqueous media to form an oil in water emulsion. Secondly, the solvent is evaporated leading to the precipitation of the polymeric nanoparticles with the drug dispersed within. This limits its application to lipophilic drugs and introduces difficulties in scaling up due to the high energy required for homogenisation (Reis *et al*., 2006). Although, Nagesh *et al*. have reported the possibility of applying this method on a large scale. They produced curcumin encapsulated PLGA-nanoparticles with mean particles size around 290 nm, loading efficiency over 50% and were stable for up to 6 months at room temperature (Nagesh *et al*., 2013). In addition to other polymers, this method has been applied successfully to PLA and PLGA to encapsulate different drugs such as testosterone, tetanus toxoid and cyclosporine (Reis *et al*., 2006).

In the ESD method the polymer and the drug are dissolved in a solvent which is sparingly soluble in water and then saturated with water. This solution is then added to an excess amount of water containing a surfactant to form an emulsion. This process forces the solvent to diffuse to the external phase and the polymer left as nanoparticles encapsulating the drug. This method has the

potential for scaling up due to the absence of the homogenisation step that requires high energy. Although, loading efficiency of lipophilic drugs using this technique is over 70%, hydrophilic drugs can escape to the high volume of water used, leading to reduced loading efficiency (Reis *et al*., 2006). This process has been improved by the use of double emulsion/solvent diffusion method (DESD). For example, alendronate is a hydrophilic drug that has been effectively encapsulated within PLGA nanoparticles using DESD method with high loading efficiency (Cohen-Sela *et al*., 2008). In addition, theophylline (a hydrophilic drug) was co-encapsulated with budesonide (a lipophilic drug) into PLA nanoparticles using DESD method. The nanoparticles showed acceptable loading efficiencies of both drugs (up to 24.4% & 48.2%; respectively) (Buhecha *et al*., 2019).

Solvent displacement (also called nanoprecipitation) is similar to interfacial deposition, in fact some authors use the two terms interchangeably. Both involve dissolving the polymer and the drug in a solvent that is miscible with water in the presence or absence of a surfactant. This solution is then added to water containing a surfactant while stirring. This leads to the fast diffusion of the solvent and the formation of a polymer colloidal suspension. The solvent and residual water is then removed by evaporation, ultracentrifugation or freeze drying forming the nanoparticles. The main difference between both methods is the addition of an oily compound immiscible with water to the polymer solvent. This leads to the deposition of the polymer on the interfacial phase between the oily droplets and the outer aqueous media forming nanocapsules (Reis *et al*., 2006). Due to the easy scale-up of the nanoprecipitation technique and its reproducibility, it has been applied to several drugs for mass production such as paclitaxel PLGA-encapsulated nanoparticles (Rivas *et al*., 2017). It is difficult however to apply this method to hydrophilic drugs due to their loss into the aqueous phase (Rivas *et al*., 2017).

2.2.2.1.3 Methods based on self-assembly macromolecules and ionic gelation

Another set of methods used to prepare nanoparticles rely on self-assembly of macromolecules to form nanogels or nanoplexes. Nanoplexes are obtained by mixing the positively charged polyamines with the negatively charged nucleic acids forming polyelectrolyte complexes. Examples of polyamines used are poly(ethylenimine), poly (lysine), poly(ornithine) or chitosan. Nucleic acids used can be plasmid genes, siRNA and antisense oligodeoxynucleotides that are not just part of the carrier device, but also the drug required for delivery. Nanoplexes can also be formed by mixing other oppositely charge polyelectrolytes as aliginate with polylysine and dextran sulphate with chitosan. The charge on the nanoparticles depends on the charge polyelectrolyte in excess (Vauthier & Bouchemal, 2009). Nanogels on the other hand are usually neutral and much simpler to make. They depend mainly on mixing two polymers (such as dextran and β-cyclodextrin) to form supramolecular nanoassemblies of spherical shape. The production yield can reach up to 95% with loading efficiency of 90% for hydrophobic drugs such as benzophenone and tamoxifen (Vauthier & Bouchemal, 2009). Alternatively, ionic nanogels can be prepared by a method called ionic gelation. This differs from self-assembly of nonplexes, in that a diluted gelling agent is used at a concentration below its gelling point to form a pre-gel followed by the addition of a polyelectrolyte to stabilise the nanogels. For example, calcium is added to a dilute aqueous solution of alginate to induce gelation, which is then stabilised by adding a polyamine such as polylysine. Due to their ionic nature, oligonucleotides and peptides can be loaded by means of ionic interactions (Vauthier & Bouchemal, 2009).

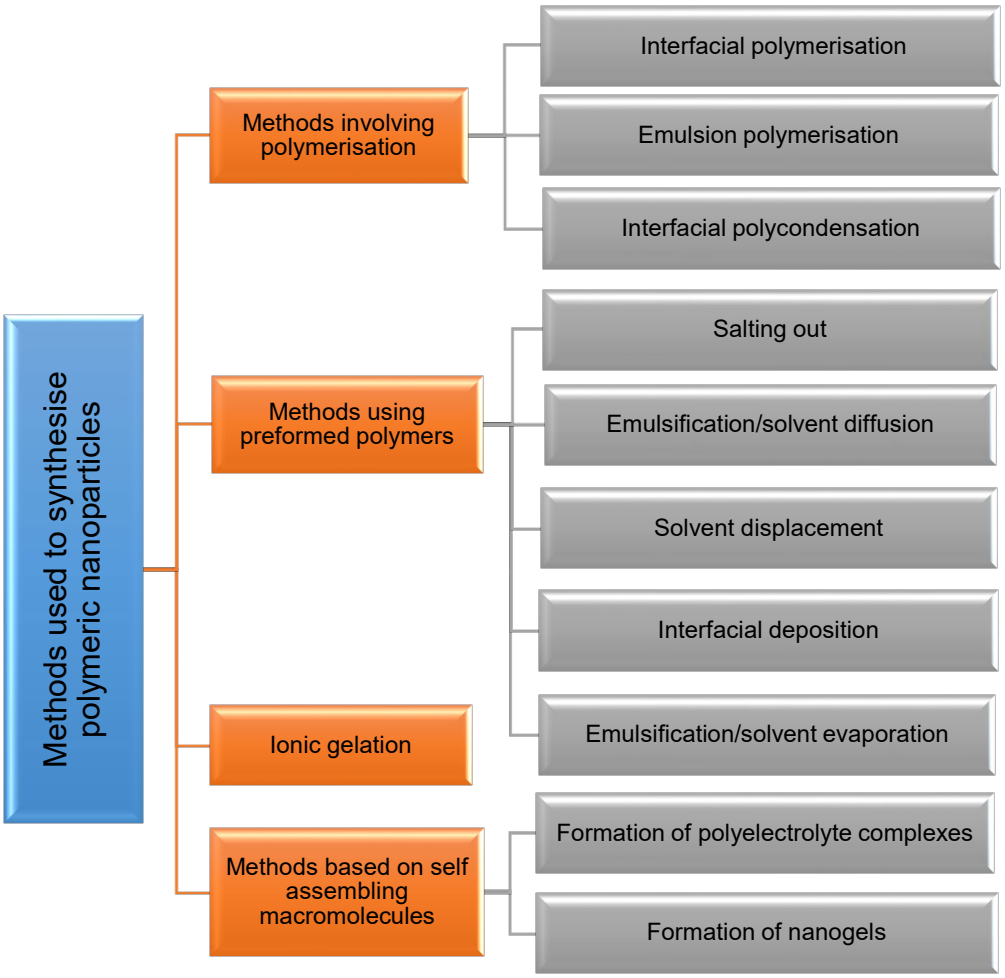

Figure 2.4: **Classification of the methods used to synthesise polymeric nanoparticles**. Methods are classified based on the precursor used in polymerisation methods from monomers, methods using preformed polymers & methods using self-assembly macromolecules and gelation agents.

2.2.2.2 Different methods used to synthesise liposomes

Since the innovation of liposomes, they have been comprehensively studied as potential drug carriers. Different methods have been applied but only a few have scaling up possibilities (Laouini *et al*., 2012). Preparing liposomes usually involves two main steps; drying lipids down after dissolving in organic solvent and then dispersing the lipids in an aqueous phase. According to whether the drug is loaded during or after liposome formation, methods are classified as passive or active loading methods; respectively [Figure 2.5]. Mechanical dispersion, solvent

dispersion and detergent removal methods are types of passive diffusion [Figure 2.6].

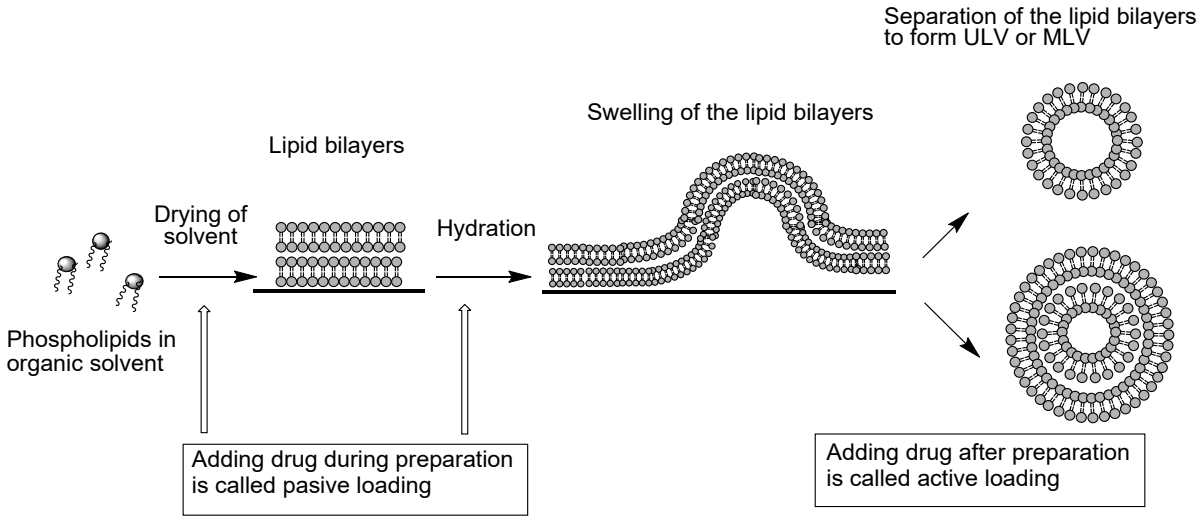

Figure 2.5: **Basic mechanism of liposome formation.** Phospholipids are dissolved in an organic solvent and subsequently dried to form a stack of bilayers. The second step is to hydrate the lipids leading to swelling of and separation into liposomes. Passive loading involves adding drug with organic or aqueous solvents during preparation. Active loading is adding the drug to already prepared liposomes.

2.2.2.2.1 Mechanical dispersion

Examples of mechanical dispersion include sonication, extrusion, freeze-thawed liposomes, lipid film hydration by hand shaking, and micro-emulsification. As mentioned previously, the lipids are dried and left as a stack of bilayers on the wall of the flask. Adding water with vigorous hand shaking will usually result in LUV or MLV. A number of factors limits the applications of these liposomes for example, their large size, wide particle size distribution, low trap volumes and inconsistency from preparation to preparation (Hope *et al*., 1993). Sonication *via* an ultra-sonic bath or probe can reduce the size of the liposomes forming SUV. Although this method is simple, its main drawbacks are the breakdown of liposomes with excessive sonication, low loading efficiency, degradation of lipids and sensitive drugs by heat production and possible contamination with metal from instruments used during synthesis. Extrusion can also be used to downsize larger

liposomes, either by passing them through a small orifice using French pressure cells or through a membrane with nano-size pores [Figure 2.6]. These have the disadvantage of low output (50 mL maximum) and the difficulty to attain high temperatures. Freeze-thawed liposomes have been shown to have low loading efficiency (20%-30%) (Akbarzadeh *et al*., 2013).

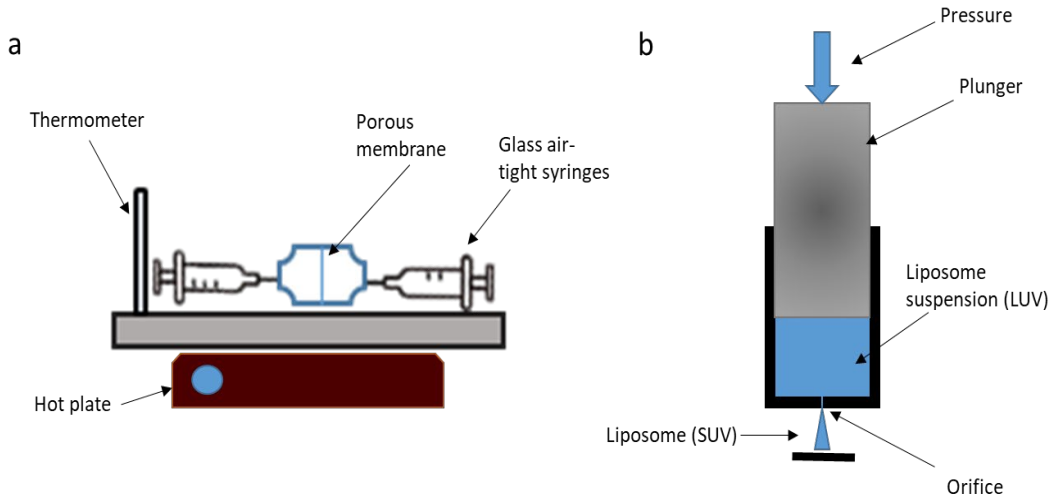

Figure 2.6: **Two apparatuses using mechanical extrusion to downsize LUV to SUV.** a: mini-extruder, depends on manually passing liposome from one side of a porous membrane to the other using air-tight syringes. Size of pores can vary from 50-500 nm. b: French pressure cell. A plunger is used to apply pressure to the liposomal suspension within a cylinder, forcing the solution to pass through a small orifice.

2.2.2.2.2 Solvent dispersion

A modification in these later methods is the reverse phase evaporation method. This permitted an increase in the aqueous space-to-lipid ratio and led increase the loading efficiency to up to 80%. Principally, reverse phase evaporation depends on the initial formation of inverted micelles from a water in oil emulsion. The emulsion is formed by short-term sonication of a two-phase system, containing phospholipids in an organic solvent such as isopropyl ether with an aqueous buffer containing the hydrophilic drug to be encapsulated. The organic phase is detached under reduced pressure, creating a viscous gel. After complete removal of the organic solvent with a rotatory evaporator the liposomes are shaped (Akbarzadeh *et al*., 2013).

2.2.2.2.3 Detergent removal methods

The final class of liposome preparation method involves the use a detergent at its critical micelle concentration (CMC) followed by the removal of the detergent by dialysis, absorption, gel chromatography or dilution. Detergents such as cholate, alkyl glycoside and triton X-100 are used to solubilise lipids at their CMC to form micelles. Upon removal or dilution of the detergent, micelles are forced to combine to form ULV. Dialysis can be achieved in dialysis bags suspended in large detergent free buffers using a device called LipoPrep, which is a version of dialysis system. Absorption is performed by shaking the micelle solution with beaded organic polystyrene adsorbers such as XAD-2 beads and Bio-beads SM2. Gel chromatography or filtration is attained by passing the micelles solution through special gel filters (such as Sephadex G-50 and Sephadex G-100) that separate the detergent by means of size exclusion. This can also be used to separate un-encapsulated drugs from liposomes for purification purposes. Finally, adding excessive buffer to the micellar solution leads to its dilution beyond its CMC and spontaneous transition to vesicles occurs (Akbarzadeh *et al*., 2013).

Loading of lipophilic drugs by passive methods is much higher (100% is often achievable) than hydrophilic drugs (< 30%) (Akbarzadeh *et al*., 2013). New methods have been developed to produce liposomes on a large scale, including heating, spray drying, freeze drying, supercritical reverse phase evaporation and crossflow injection methods (Laouini *et al*., 2012).

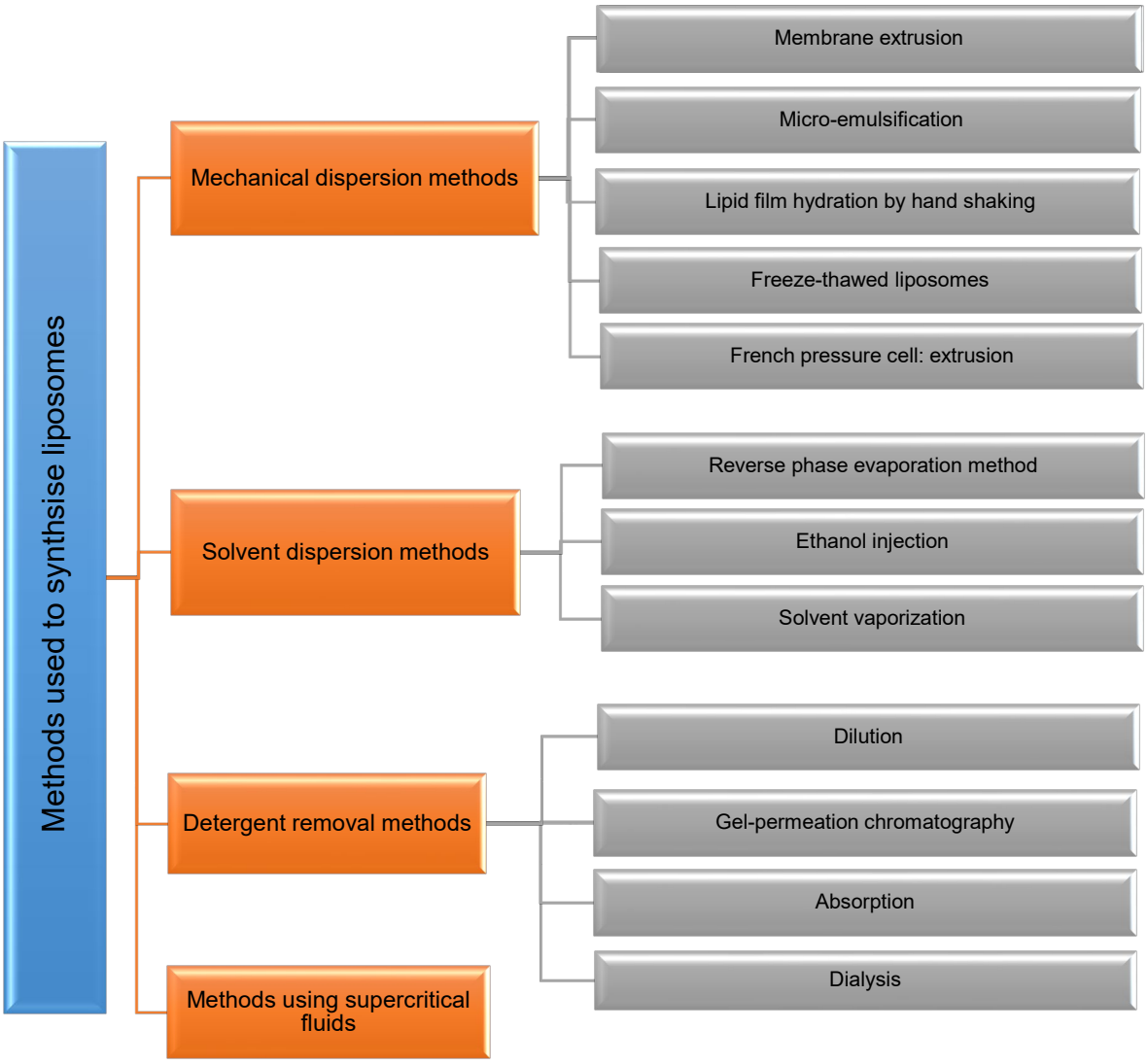

Figure 2.2.7. **Classification of the methods used to synthesise liposomes.** The passive methods used to prepare liposomes are classified into three main categories (mechanical dispersion, solvent dispersion, and detergent removal methods). Novel methods using supercritical or compressed fluids can also be applied.

2.2.2.3 Methods involving supercritical fluids (SCF) to prepare different types on nanoparticles

Although some of the above methods can be used to encapsulate both hydrophilic and lipophilic drugs, the nanoparticles formed generally have low

loading efficiency and low percentage yield. Another drawback is the remaining high solvent content and the degradation of some drugs during preparation. Novel methods based on supercritical or compressed fluids have been introduced to overcome these disadvantages, but their use is limited due to the need for expensive appliances and the necessity of high-pressure equipment (Reis *et al*., 2006, Crucho & Barros 2017).

Any matter can be present in its supercritical form if it is reserved beyond its critical temperature and critical pressure. SCF's have the advantage of being non-toxic, inert, economical, and environmentally friendly. Numerous substances such as water, nitrogen gas, xenon, nitrous oxide, ethylene, propylene, propane, ammonia, n-pentane, ethanol, and CO_2, have been attempted as SCFs. CO_2 is most commonly used in the pharmaceutical industry and classified as a safe solvent by the FDA because of its unique properties like being inert, colourless, odourless, non-toxic, non-flammable, cost effective, and recyclable. Nanoparticles that can be prepared by these methods include but not limited to polymeric nanoparticles, aerogels, microporous foams, solid lipid nanoparticles and liposomes (Chakravarty *et al*., 2019). Examples of such methods are rapid expansion of supercritical solutions (RESS) and supercritical antisolvent (SAS) methods (Chakravarty *et al*., 2019).

2.2.2.3.1 Rapid Expansion of Supercritical Solutions

This process includes using a SCF, mainly CO_2 as a solvent to solubilise a solute. The solution is then quickly depressurized by expanding it through an atomising nozzle. The depressurization leads to the reduction of the density of the SCF, which in turn reduces solute solubility and causes its precipitation. This high nucleation rate, results in a great number of nucleation sites, limiting crystal growth and produces nanoparticles with uniform size distribution. This method has the advantage of being environmentally friendly with minor operating settings, where nanoparticles are produced in a single step without solvent residues (Chakravarty *et al*., 2019). Its disadvantage, however, is the poor solubility of SCF in different solutes, the need to use co-solvents and the difficulty to optimise the method. A

small modification to this method called rapid expansion of supercritical solution in liquid vehicle (RESOLV) includes using a liquid phase to expand the SCF.

RESOLV was applied to prepare PLGA and sodium alginate nanoparticles encapsulated with fenofibrate and PLA nanoparticles encapsulated with retinyl palmitate. Both applications found that the use of a stabiliser as sodium dodecyl sulphate or Pluronic F127 is vital to produce well dispersed individual particles (Chakravarty *et al*., 2019). RESS was also applied by Frederiksen *et al*., 1997 to prepare water soluble compounds encapsulated within liposomes using ethanol as co-solvent.

2.2.2.3.2 Supercritical Antisolvent

SAS also called gas antisolvent method is based on dissolving the solute and carrier in a solvent that is miscible with the SCF (such as ethanol, acetone and DMSO). Introducing this solution to the SCF leads to supersaturation and high rate of nucleation and finally to precipitation of nanoparticles. This overcomes the disadvantage of the poor solubility power of SCF to solutes found in the RESS. On the other hand, it adds more complexity to the method and introduce the issues of residual organic solvents in the final product. Paracetamol was successfully encapsulated in PLA nano- and micro-particles using dichloromethane/acetone mixed solvents using this method (Chakravarty *et al*., 2019). There are multiple modifications to the methods involving the use of SCF that have been applied to prepare both PLA nanoparticles and liposomes but describing all methods is out of the scope of this introduction and will not be discussed further.

2.3 Aims

- To encapsulate selected antioxidants (α-tocopherol, curcumin, resveratrol, ferulic acid, sinapic acid and epicatechin) into:
    - PLA nanoparticles
    - Liposomes
- To characterize the prepared PLA nanoparticles and liposomes for their:
    - Particle size using differential light scattering (DLS) technique
    - Surface charge using zeta-potential
    - Surface morphology using light microscope and scanning electron microscope (SEM)
    - Thermal properties using differential scanning calorimetry (DSC)
    - Surface composition using Fourier transform-infra red spectroscopy (FTIR)
    - Loading and encapsulating efficiency using high performance liquid chromatography (HPLC)

2.4 Materials and methods

2.4.1 Materials and equipment details

The main equipment used for this study and their specification are listed below in table 2.1. The main materials, their purities and their sources used for this are listed below in table 2.2. Consumables were obtained from Fisher Scientific (Loughborough, Leicestershire, UK). Ultrapure water (18.2 MΩ-cm) was used throughout the study unless otherwise indicated.

Table 2.1: A list of the main equipment used in this study and its manufacture

Equipment	*Specifications and make*
Magnetic stirrer, hot plate	Laboratory hot plate - EW-04801-01 - Stuart Equipment
Homogeniser	IKA® T25 digital Ultra-Turrax®
Rotatory evaporator	IKA Rotary evaporator RV 3 V-C
Freeze drier	Benchtop, 8L, -50°C, PTFE-Coated Collector, Labconco
Light microscope	Motic™ BA210E Trinocular Compound Microscope
Mini extruder	Avanti® Polar Lipids Mini Extruder with holder/heating block, 2 gas-tight glass syringes, filter supports and polycarbonate membrane (1mL)
Malvern Zetasizer	Malvern Zetasizer Nano series, Nano-ZS90
Centrifuge	Sorvall RC-6 Plus Ultracentrifuge
sputtering coater	Quorum technologies Q150 ES sputter coater
Scanning electron microscopy	Zeiss Evo LS-15 SEM
Fourier transform-infra red spectrum	FT-IR Perkin Elmer spectrum 65 with universal ATR sampling assessor
Differential scanning calorimeter (DSC)	DSC Q2000, Mettler Toledo StarE software, UK
Lid pan press	Tzero Press (P/N 901600.90)

Table 2.2: A list of the main materials used for this study, in addition to their purities and sources.

Material	*Purity*	*Source/specifications*
(±)-α-Tocopherol	≥96%	Sigma-Aldrich Company Ltd (Poole, Dorset, UK)
trans-Resveratrol	>98%	Sigma-Aldrich Company Ltd (Poole, Dorset, UK)
Curcumin	>98%	Sigma-Aldrich Company Ltd (Poole, Dorset, UK)
Ferulic acid	≥98%	Sigma-Aldrich Company Ltd (Poole, Dorset, UK)
Sinapic acid	99%	Sigma-Aldrich Company Ltd (Poole, Dorset, UK)
-(-)Epicatechin	≥ 90%	Molekula Ltd (Munich, Bavaria, Germany)
PLA (Purasorb® PDL 02	GMP grade	Purac Biomaterials (The Netherlands)
PVA	98% hydrolysed	13,000-23,000 Sigma-Aldrich Company Ltd (Poole, Dorset, UK)
Extrusion membranes		200 nm pore polycarbonate membranes, Avanti® Polar Lipids, USA
Filter supports		10 mm, Avanti® Polar Lipids, USA
SEM specimen stub (aluminium)		AGAR Scientific, UK (12.5 mm diameter, 3.2 x 6 mm pin)
Carbon adhesive double sided		AGAR Scientific, UK (Leit Adhesive Carbon Tabs)
UV cuvettes		Disposable plastic. Fisher Scientific, UK Plastibrand (2.5-4.5 mL)
Aluminium pans		T_0 pans from TA instruments, UK
Aluminium lids		T_0 lids from TA instruments, UK
Filter membrane		Nalgene Rapid-Flow. 200nm pore size equipped with vacuum pump.
2 HPLC columns		5 µm, C18, 15 & 25 cm, 4.6 mm, Fortis Technologies Ltd, UK
NAP-25 columns		illustra™ NAP™-25 Columns, GE Healthcare,UK

2.4.2 Preparation of PLA nanoparticles encapsulated with antioxidants under investigation

The method involved in the preparation of PLA nanoparticles in this study was DESD (Buhecha *et al*., 2019), which was adopted and modified as required. As discussed in section 2.2.2.1.2, this method has the advantage of being simple and capable of encapsulating both lipophilic and hydrophilic drugs. As the purpose of this study was to encapsulate antioxidants with different solubility properties, this method was chosen to fulfil this purpose. PLA was used as the polymer for preparing the nanoparticles. PVA (98% hydrolysed, molecular weight 13,000-23,000) was used as a surfactant in the aqueous phase to stabilize the initial emulsion. Dichloromethane (DCM) and acetone were used as the organic layer. According to the solubility of the drug, it was either dissolved in the aqueous or organic phase. For each batch, 5mg drug was used for the synthesis.

Initially 2% (w/v) PVA stock solution was prepared by dissolving 2 g of PVA in 100 mL water. A magnetic stirrer was used at low speed, while heating to 70^{o}C. The solution was then filtered through 0.45 µm paper filter. In a separate beaker 200 mg PLA was dissolved in 10 mL DCM and 10 mL of the PVA solution was added. An emulsion was made by mixing using a high-speed homogeniser at 15000 rpm for 15 min. 10 mL acetone was added and further homogenised for a further 15 min at the same speed. This mixture was then transferred into an excess amount of water (100 mL) with continuous homogenising for 15 min at 15000 rpm. Any organic solvent was then removed by using a rotatory evaporator, rotating at 130 rpm, heating at 40^{o}C and vacuum pressure 70 mbar. The solution was then left overnight to ensure complete removal of organic solvents. The solution was then examined under microscope to confirm formation of nanoparticles. This solution was centrifuged at 15000 rpm and 4^{o}C for 15 min. The supernatant was separated and kept for further investigation. Pellets (containing nanoparticles) were frozen at -80^{o}C for at least one hour, after which were dried by lyophilisation. Samples were then kept in fridge for further characterisation [Figure 2.8].

Blank PLA nanoparticles were prepared using the above method to prepare sample 1, described in table 2.3. Additionally, six different antioxidants were encapsulated within different PLA nanoparticles samples and according to their solubility they were added at different steps as shown in figure 2.8. Epicatechin was dissolved in the aqueous phase at step 1, to prepare sample 7. α-Tocopherol, curcumin, ferulic acid and siapic acid were added at step 2, to the DCM to prepare samples 2, 3, 5 & 6; respectively. Finally, resveratrol was added to the acetone at step 3, to prepare sample 4. Samples are described in table 2.3. Each sample was prepared in triplicate.

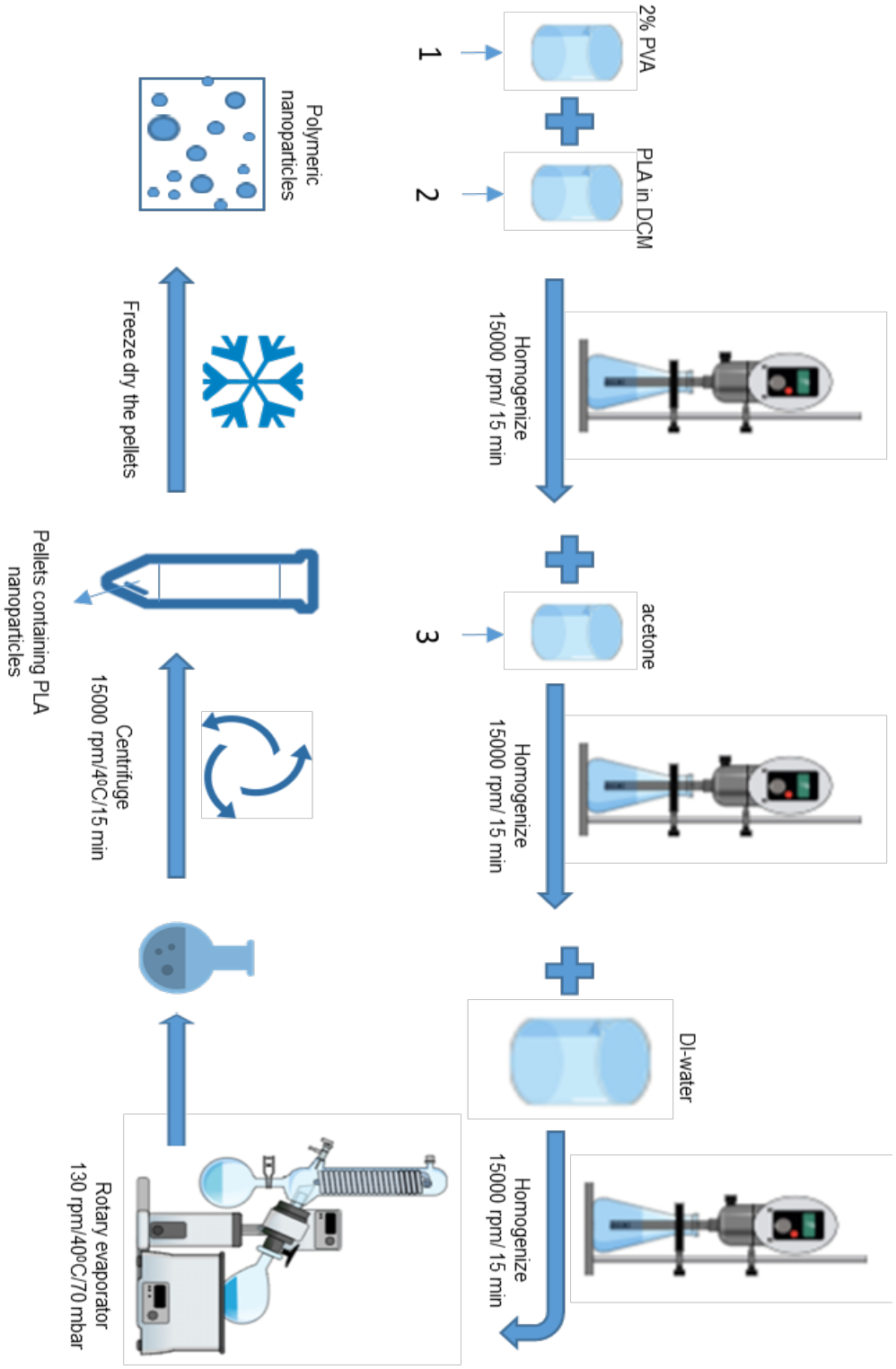

Figure 2.8: **Illustrative figure showing the different steps of PLA nanoparticle preparation.** Antioxidants were added according to their solubility to either step 1, 2 or 3 to form the six different PLA nanoparticles samples described in table 2.3.

2.4.3 Preparation of liposomes loaded with different antioxidants under investigation

The method used for the preparation of liposomes in this study was based on the hydration of lipid film to prepare large MLV, followed by membrane extrusion (Mechanical dispersion, discussed in section 2. 2. 2. 2) to form SUV [Figure 2.9]. Depending on the solubility of the drug, it was either loaded in the organic solvent dissolving the lipids or to the aqueous phase during hydration of the lipid film (Dichello *et al*., 2017). The original method was modified as required. 5 mg of drug was used for the preparation of liposomes in each batch.

DPPC solution (5 mL of 8 mg/mL in ethanol) was measured into a round bottom flask. The solvent was evaporated using a rotatory evaporator to form a uniform lipid layer around the bottom of the flask. Temperature of water bath was kept at 40^{o}C, speed of rotation was 100 rpm and pressure was reduced gradually from 700 mbar to 70 mbar. The flask was then left overnight, to ensure complete evaporation of the solvent. Subsequently, water (4 mL) was added to this film while shaking vigorously and sonicating for 10 min in an ultrasonic bath. Further 10 min of sonication was applied to ensure complete detachment of the lipid film from flask wall.

For particle size reduction of the liposomes, an Avanti mini-extruder with 200 nm pore size polycarbonate membrane and glass air-tight syringes were used. During setting up of the extruder, filter-supports were placed on both sides of the membrane to increase its lifespan. Both filter-supports and the membrane were hydrated before fixing in place and water was passed through the extruder several times to reduce product loss. The whole system was heated to 40^{o}C and the liposomal mixture was heated up to 60^{o}C to ease the passage of the lipid solution through the membrane. Each aliquot of 1 ml solution was then extruded by passing through the membrane (21X), while reducing temperature to below 41^{o}C (melting transition (T_c) of DPPC). The product was collected from opposite side, to ensure removal of insoluble un-encapsulated drug and to avoid contamination of the sample by liposomes that may have not passed through the

membrane. Due to the instability of the liposomes found during freezing and thawing, all samples of liposomes were freshly prepared and tested within two days. During this short period samples were stored in the fridge at 2-8^{o}C.

The six antioxidants under investigation (α-tocopherol, curcumin, resveratrol, ferulic acid, sinapic acid and epicatechin) were encapsulated separately into DPPC liposomes using the above method to prepare samples 9-15, described in table 2.3. With the exception of epicatechin, all antioxidants were incorporated at step 1 [figure 2.9] due to their high solubility in ethanol. Epicatechin however, was dissolved in water at step 2, due to its aqueous solubility. Additionally blank liposomes were prepared (sample 8). Each sample was prepared in triplicate.

Table 2.3: A list of the different samples prepared for this study and the different characterisation tests performed on each sample (*N* =3).

Sample number	*Description*	*Size/ charge*	*SEM*	*FT-IR*	*DSC*	*HPLC*	*Antioxidant activity*
						PLA NANOPARTICLES	
1-BP	Blank PLA nanoparticles	+	+	+	+	+	-
2-TP	α-Tocopherol PLA nanoparticles	+	+	+	+	+	-
3-CP	Curcumin PLA nanoparticles	+	+	+	+	+	-
4-RP	Resveratrol PLA nanoparticles	+	+	+	+	+	-
5-FP	Ferulic acid PLA nanoparticles	+	+	+	+	+	-
6-SP	Sinapic acid PLA nanoparticles	+	+	+	+	+	-
7-EP	Epicatechin PLA nanoparticles	+	+	+	+	+	-
							LIPOSOMES
8-BL	Blank liposomes	+	-	-	-	+	+
9-TL	α-Tocopherol liposomes	+	-	-	-	+	+
10-CL	Curcumin liposomes	+	-	-	-	+	+
11-RL	Resveratrol liposomes	+	-	-	-	+	+
12-FL	Ferulic acid liposomes	+	-	-	-	+	+
13-SL	Sinapic acid liposomes	+	-	-	-	+	+
14-EL	Epicatechin liposomes	+	-	-	-	+	+

+ & - indicates if the test has been performed or not on the corresponding sample.

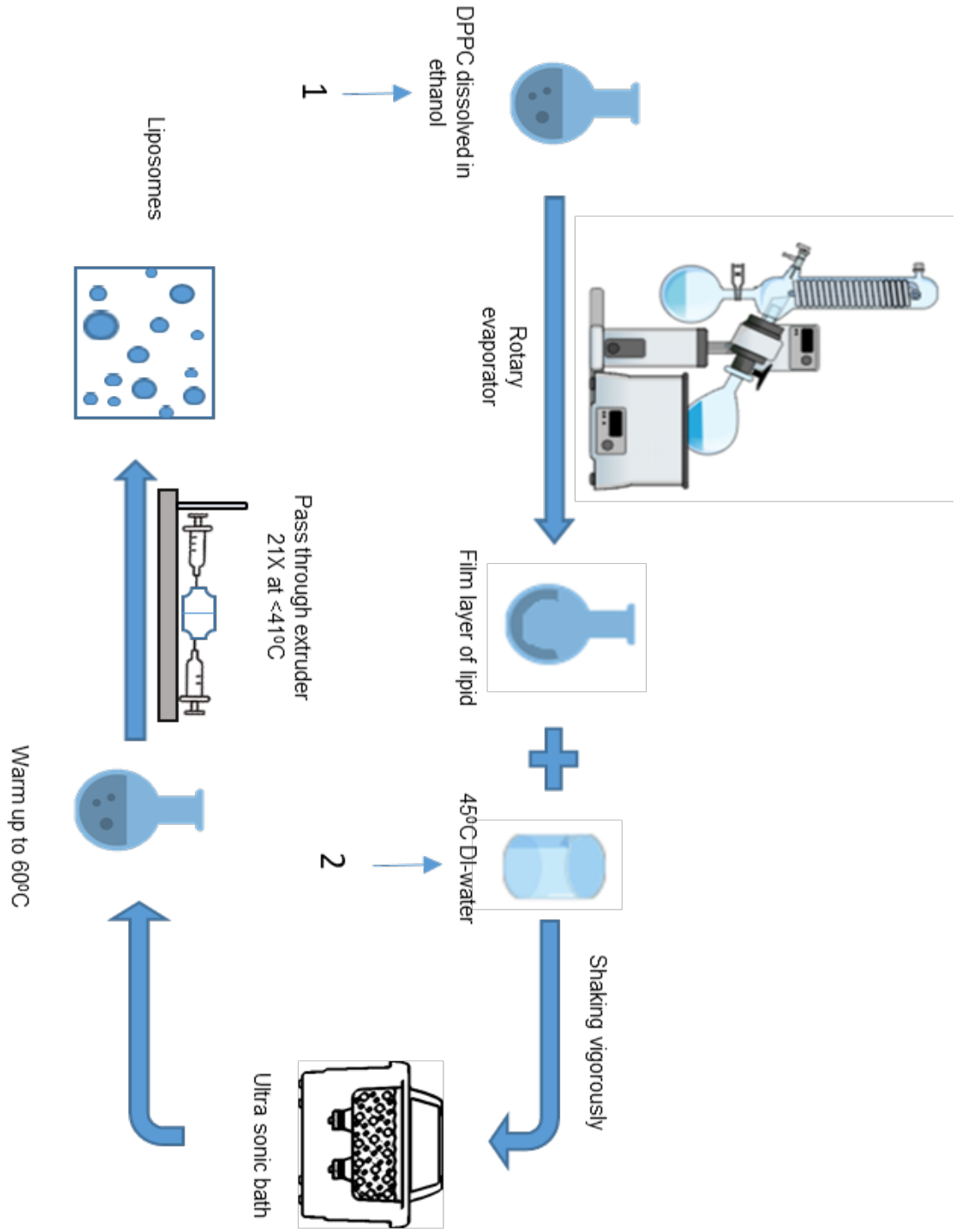

Figure 2.9**: Illustrative figure showing different steps of liposome preparation.** Antioxidants were added at step 1 or 2, according to their solubility to prepare the different samples described in table 2.3.

2.4.4 Determination of particle size for different liposomes and PLA nanoparticles using a light scattering technique

The particle size of the freeze-dried PLA nanoparticles and liposome suspensions was measured using a Malvern Zetasizer applying a dynamic light scattering (DLS) detection technique. Particles in a suspension are in a constant movement and are referred to as following Brownian motion. When light is passed through such a suspension, it diffracts at varying intensities that is based on particle size and motion. By measuring the light intensity and applying Stokes-Einstein equation (equation 2.1), particle size is then calculated.

$$D = k_B T / 6 \pi \eta r \qquad \text{Equation 2.1}$$

where;

D is the diffusion coefficient;

k_B is Boltzmann's constant;

T is the absolute temperature;

η is the dynamic viscosity;

r is the radius of the spherical particle.

All liposomal and PLA nanoparticles prepared and described in table 2.3 were analysed for their size using the following method. Approximately, 5 mg sample was suspended in 10 mL ultrapure water and sonicated for 10 min, to ensure homogenous distribution of size. A small amount was then transferred into disposable four-sided clear polystyrene cuvettes and tested for its size at 25^{o}C, with a 90^{o} angle detector. Samples were measured in triplicate and each run consisted of 30 repeats. The average, polydispersity index (PdI) and standard deviation (SD) were calculated by the zetasizer software (version 2.2). As the name indicates, PdI relates to how wide the particle size distribution is. The smaller the figure, the more uniform the particle size range. GraphPad Prism version 8. 4. 2, was used to analyse the data. Brown-Forsythe ANOVA was employed to evaluate data within each column and Dunnett’s multiple comparison

test was used to compare the particle size of encapsulated nanoparticles to blank nanoparticles. Brown-Forsythe ANOVA test was applied to compare different means of nanoparticles as it is commonly applied when there are wide variations in SD. Dunnett's test was used for comparison because it is the only *post hoc* test that allows comparison of multiple means to a control mean (Field 2009).

2.4.5 Determination of zeta-potential for different liposomes and PLA nanoparticles using electrophoretic light scattering technique

Surface charge is measured indirectly by determining the zeta-potential at the slipping plane around a particle [Figure 2.10]. A particle with a charge on the surface, leads to the attraction of ions of opposite charge nearby to the surface to form a layer called Stern layer, where they are firmly bound. The weakly attached ions form an outside layer called the diffuse layer. The potential charge at the double layer is called the zeta-potential. It is calculated indirectly by applying an electrical field, measuring the electrophoretic mobility using a light scattering technique (equation 2.2) and then applying the Henry equation (equation 2.3) (Kumar & Dixit 2017). This is a fully automated process performed by a software attached to a zetasizer (version 2.2).

$$\Delta f = {2\,\nu \sin\left(\frac{\theta}{2}\right)}/{\lambda} \qquad \text{Equation 2.2}$$

where;

Δf is the frequency shift;

ν is the particle velocity;

θ is the scattering angle;

λ is the laser wavelength.

$$UE = {2\,\varepsilon\,\zeta\,F(\mathrm{k}a)}/{3\,\eta} \qquad \text{Equation 2.3}$$

where;

UE is the measured electrophoretic mobility;

ε is the dielectric constant of the dispersant;

F(ƙa) is the Henry function;

ŋ is the viscosity;

ζ is the zeta-potential.

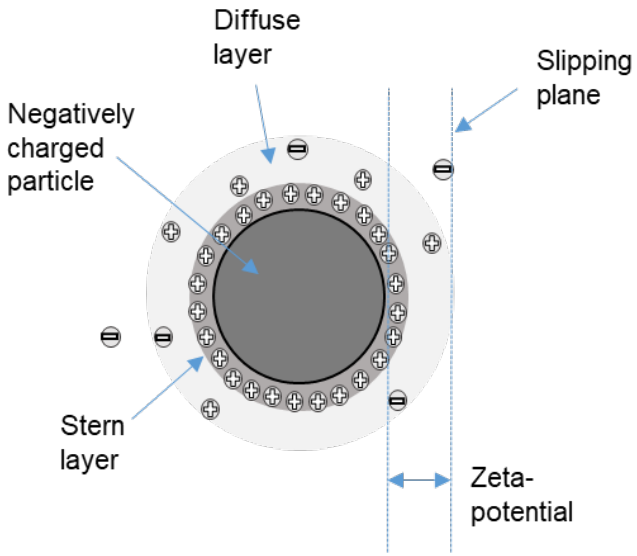

Figure 2.10: **Schematic diagram of the zeta-potential principle.** The figure shows the electrical double layer at the surface of a particle in a solution. The charge at the slipping plane is called zeta-potential (Adapted from Selvamani 2019).

Solutions of the samples listed in table 2.3 were prepared in the same manner as described in section 2.4.4. A Malvern Zetasizer Nano series was used to measure zeta-potential of the particles with a reusable folded capillary cell with gold plated electrodes. Samples were measured in triplicate with each measurement consisting of 12 runs. Results (mean zeta-potential and SD) were calculated automatically using the Zetasizer software and data was analysed in the same manner as for particle size.

Additionally, particle size analysis and zeta-potential determination using the Zetasizer were used to study the stability of liposomes suspended in a solution. The same method as above was applied on the curcumin liposomes (sample 10-CL) to analyse their particle size and zeta-potential on day 1, 2, 3, 4, 8 and 10 after the preparation of liposomes. As the aim of this step was to study the stability of liposomes synthesised and because all liposomal samples were prepared in the same method, only one sample was tested. Curcumin liposomes were used as a representative sample. Samples were stored in fridge (2-8ºC) during the entire test.

2.4.6 Studying surface morphology of nanoparticles using light microscope and scanning electron microscopy

As the name indicates, the main difference between the conventional compound light microscopy (LM) and scanning electron microscopy (SEM) is that the former uses lenses to bend light and magnify images and the latter depends on electron emission [Figure 2.11]. Electrons emitted from an electron gun pass through intensifying electromagnetic field, scanning coils and finally scans a sample in a raster pattern, which is detected by a secondary electron, backscattered electron or x-ray detector (Goldstein *et al*., 2018).

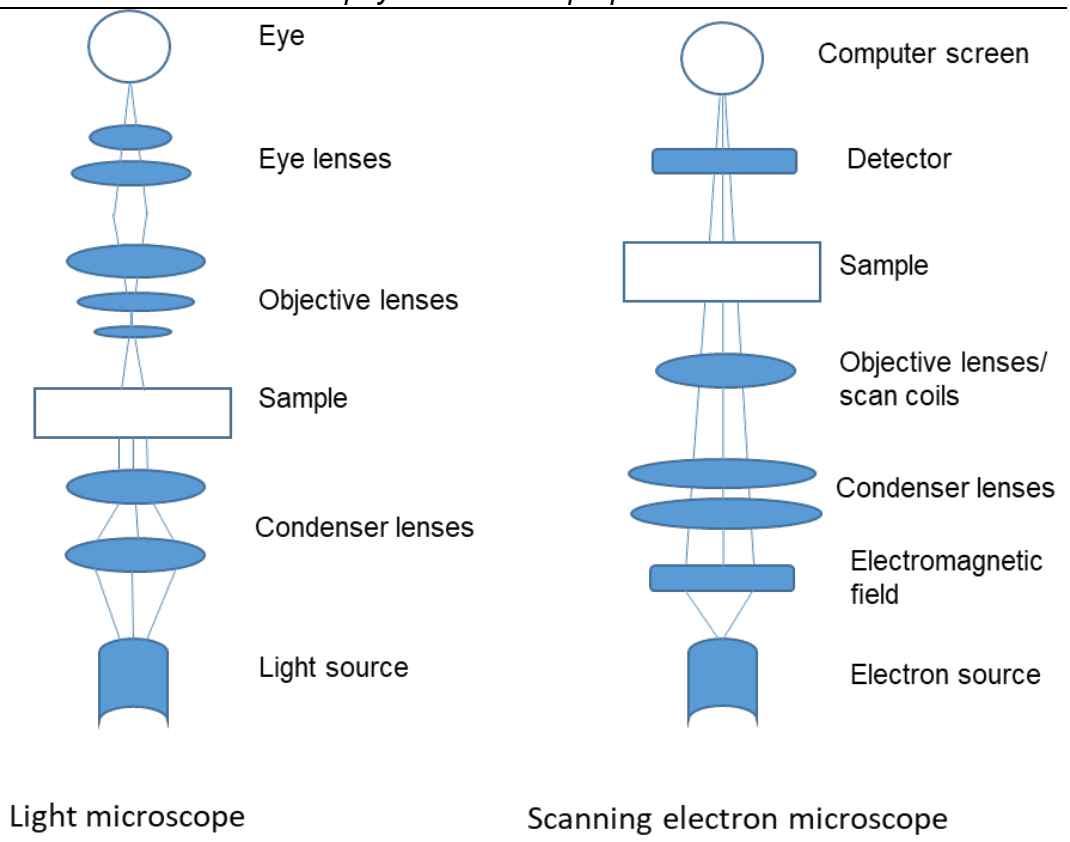

Figure 2.11: **Schematic comparison between light microscope and scanning electron microscopy.** Although, they have a completely different mechanism, there are some points of similarities such as energy source, condenser lenses, and objective lenses.

LM was used to analyse both liposomes and PLA nanoparticles in a solution form, while SEM was carried out to determine the morphology and size variation of the PLA nanoparticles in dry state. Liposomes were not analysed by SEM due to their instability when exposed to vacuum, which is necessary to either freeze dry the samples or in the coating step prior to SEM imaging. Samples for SEM (samples 1-7) were prepared by mounting the powders on 12 mm aluminium pin stubs after sticking double-sided conductive Leit-C- carbon self-adhesive mounting pads on them. Any excess powder was removed by gentle tapping and blowing air. As PLA nanoparticles are not conductive and may cause SEM image to distort or drift, samples were further coated with a platinum coat of 4-5 nm thickness using a sputtering coater. Samples were labelled with a numbering system (described in table 2.3) and inserted into a ZEISS Sigma Field Emission Gun SEM with an Everhart Thornley-Secondary Electron detector for imaging. The

accelerating voltage used ranged between 5-10 kV with a working distance around 8.5 mm. The magnification varied between images, details of which are indicated below each image (section 2.5.2).

2.4.7 Assessment of surface characteristics of the nanoparticles using Fourier transform-infra red spectroscopy for different PLA nanoparticles

Fourier transform-infra red spectroscopy (FT-IR) is an adsorption spectroscopy that utilises an electromagnetic source of radiation emitting a light with a wavelength in the infrared region. By passing through a beam splitter, this beam is split and redirected towards a fixed and a movable mirrors. The reflections are then re-joined after going through different optical paths [Figure 2.12]. An interference spectroscopy is then generated at the detector after passing through a sample. Depending on the molecular structure of the sample, a precise change in the electric dipole due to the movement of atoms to the excited state leads to stretching or bending of molecular bonds yielding a spectrum specific to that molecule. Different spectra are stored on various external databases and can be used for qualification studies (Alawam 2014).

This technique was used to detect if any drug that was not encapsulated had adhered to the particles or if there were any interactions between drug and polymer. Only PLA nanoparticles were tested (samples 1-7) due to their dry state. Samples were compared to antioxidants, PLA and PVA standards using a FT-IR Perkin Elmer spectrum 65. A Small amount (< 1 mg) freeze dried samples were mounted over the sample stage after background interference was removed. Each sample was scanned by 8 runs at a resolution of 4 cm^{-1} over a wave number region of 400-4000 cm^{-1}.

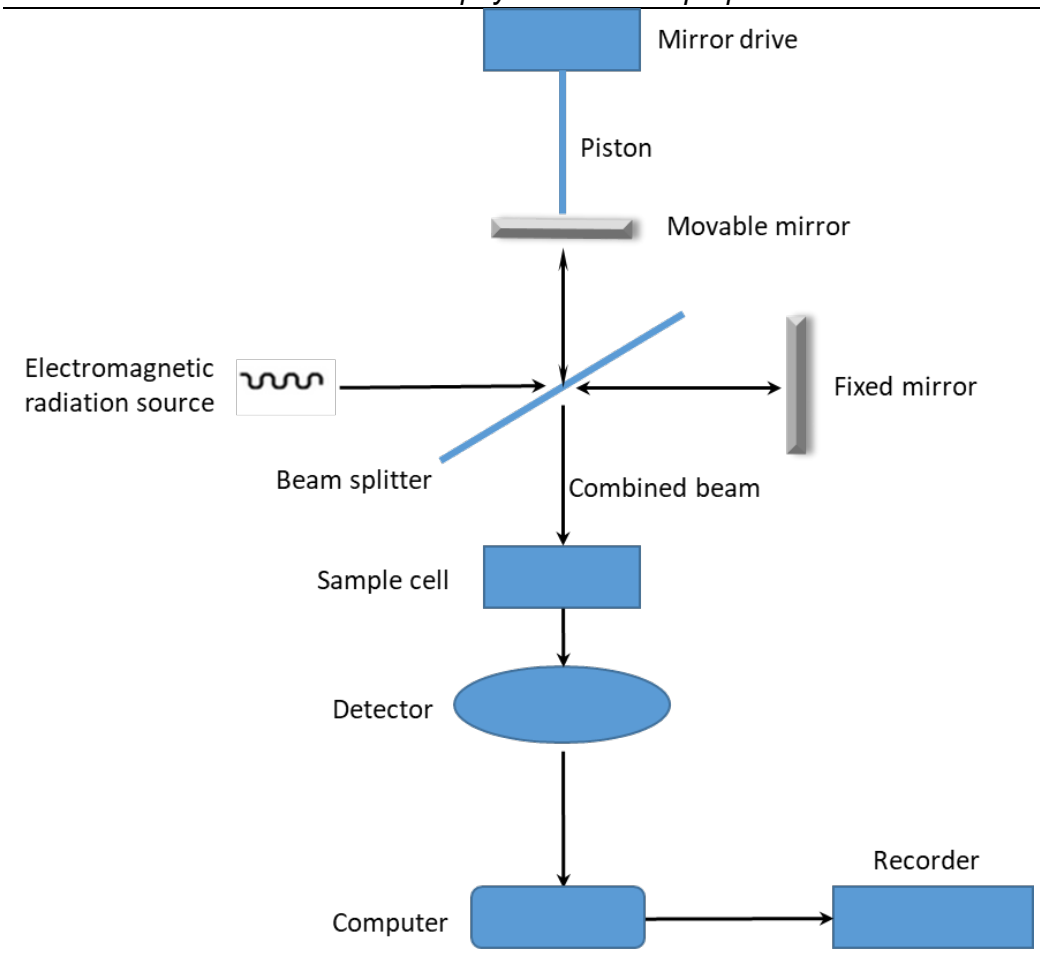

Figure 2.12: **Schematic diagram of Fourier transform-infra red spectroscopy.** An electromagnetic radiation is split and re-joined after reflecting on two mirrors. The combined beam is then detected after passing through the sample (Adapted from Rees 2010).

2.4.8 Thermal analysis of nanoparticles using differential scanning calorimeter for different PLA nanoparticles

A change in temperature leads to a change in the physical nature of a material. This change is unique to a material and it can be used as a diagnostic tool to determine its purity, for example determining the melting point of a compound. When heating a sample, the result could be either an endothermic or an exothermic reaction because of the heat flowing into or out of the material, respectively, depending on the specific characteristic of the sample. Endothermic heat flow is the result of either the heating capacity, glass transition (T_g), melting or evaporation of the material. Exothermic heat flow is a result of cooling down,

crystallization, curing or oxidation of the material. A differential scanning calorimeter (DSC) processes the difference in heat flow rate between a sample in a pan and a blank reference pan as a function of time and temperature and records its unique characteristics [Figure 2.13] (Hohne *et al*., 2003).

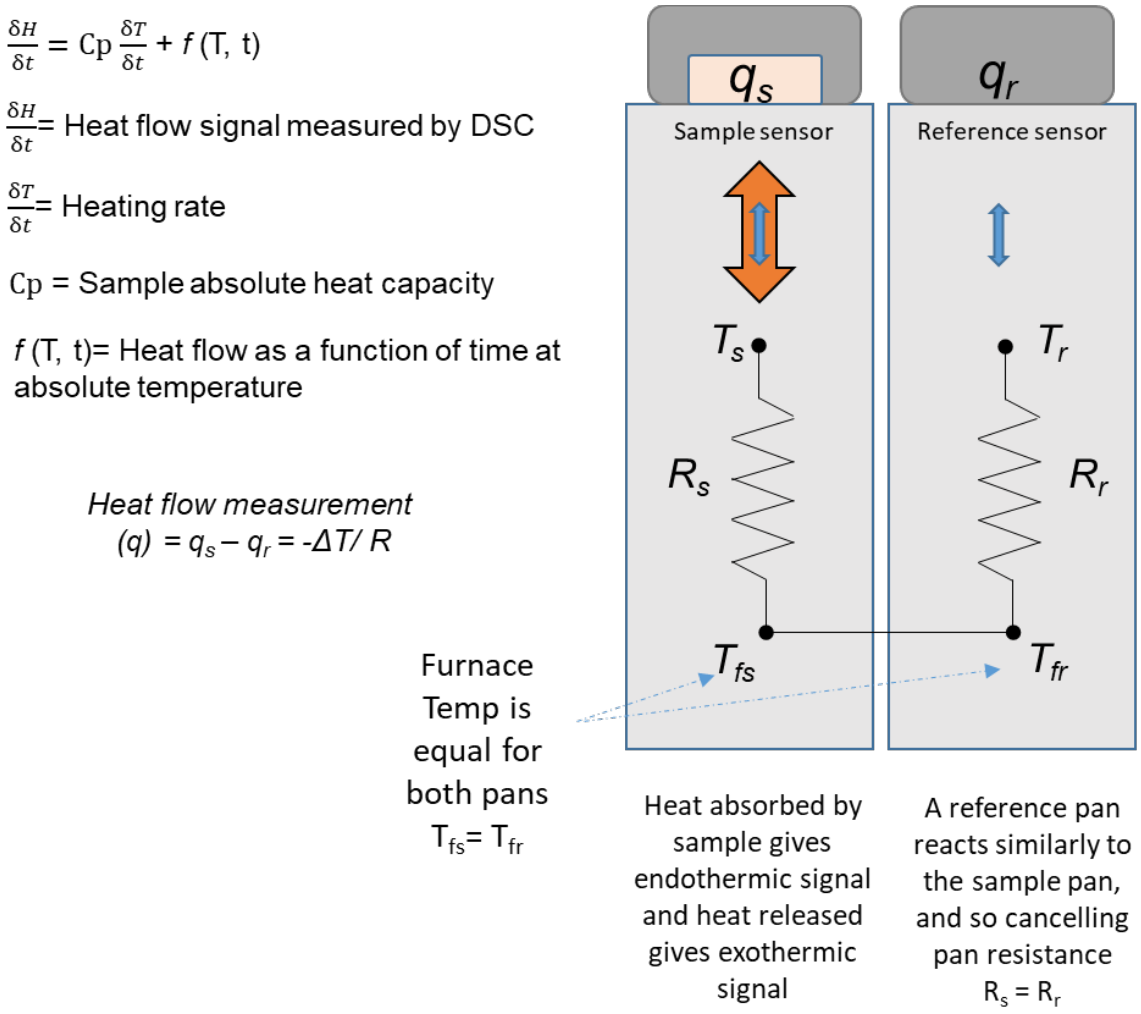

Figure 2.13. **DSC model showing how thermal properties are analysed.** The sample is either heated or cooled and the heat flow is measured as a function of time and temperature. An empty pan is used as a reference pan to cancel any heat absorption by the pan material. Both sample and reference pans are heated using the same furnace, so the heat flow reflects the sample thermal properties.

Thermal analysis of the PLA nanoparticles was studied using DSC. An accurately weighed amount (1-5 mg) of the freeze-dried PLA nanoparticle samples (samples 1-7) and PLA polymer standard, were weighed into each DSC aluminum

pan (T_0 pans). The pans were then crimp-sealed using a lid press and placed in the DSC. An empty sealed aluminum pan was used as a reference. Each sample was analysed in triplicate over the temperature range of 25-250°C at a heating rate of 10°C/min to determine the T_g of the polymer and nanoparticles.

2.4.9 Determination of the antioxidant concentration in different samples (validation of methods)

High performance liquid chromatography (HPLC) was used to determine the concentration of drugs in different samples after extraction (section 2.4.10) and to determine the amount of drug internalised during *in vivo* studies (Chapter 4). Concentrations were analysed using reversed phase HPLC using an Agilent 1220 series, equipped with Clarity-Chromatography SW, DataApex software, Agilent 1220 pump system with degasser, manual injector with a 20 µL injection loop and an Agilent 1220 UV-visible detector. For the separation of the analytes, 5 µm Fortis c18, 150 * 4.6 mm columns were used, except when analysing epicatechin a 5 µm Fortis c18, 250 * 4.6 mm column was used. HPLC parameters varied according to the compound under investigation. Details and references of the HPLC methods are shown in table 2.4. Methods were adapted as required and revalidated to conform suitability. This was explained in detail in sections 2.5.9 & 2.6.9.

HPLC mobile phases was prepared as follows: For 0.1% v/v Trifluoro-acetic acid (TFA) solution, 1 mL of TFA was dissolved in 900 mL of HPLC grade water and the volume was made up to 1000 mL, filtered through 0.45 *µ*m membrane filter and degassed using ultrasonic bath for 5 minutes. 0.1% v/v Ortho-phosphoric acid (OPA) and 2% v/v acetic acid (AA) were prepared by the same technique using 1 mL OPA and 20 mL AA; respectively. Almost all methods used isocratic system for elution, where the percentage of each mobile phase was kept constant throughout each run. The only exception was the method used for epicatechin determination, which used a gradient system to elute epicatechin. The gradient method was: at time 0.01 min 11% B; at 20 min 25% B; and 21 to 30 min 11% B.

Stock solutions (1 mg/mL) of standard antioxidants (α-tocopherol, curcumin, resveratrol, ferulic acid, sinapic acid & epicatechin) were prepared by dissolving 10 mg standards into 10 mL of the same mobile phase used for elution. Solutions with serial dilution were prepared, as needed by further dilution and each concentration was injected three times. As some methods have been adjusted, system suitability ought to be performed to evaluate the effectiveness of these methods. Calibration plots were constructed and parameters such as reproducibility; presented as the percentage relative standard deviation (%RSD), linearity (R^2) and the system sensitivity (limit of detection (LOD) and limit of quantification (LOD)) were calculated using the equations (2.4 & 2.5).

$$\boldsymbol{LOD = 3.3 \times \frac{\sigma}{slope}} \qquad \text{Equation 2.4}$$

$$\boldsymbol{LOQ = 10 \times \frac{\sigma}{slope}} \qquad \text{Equation 2.5}$$

where;

σ is the standard deviation of the response.

Defined amounts of blank PLA nanoparticles and blank liposomes (samples 1-PB & 7-BL) were dissolved in ethanol and filtered through 0.45 μM pore filters. These extracted blank samples were injected into the HPLC and analysed using the above methods. The specificity was assessed by comparing the chromatograms obtained from analysing samples containing potential interfering constituents (solvents, samples 1-PB & 7-BL) to chromatograms obtained from analysing standards. The linearity was calculated from the regression line obtained by plotting area under the peak versus concentration of standard concentrations. Precision was evaluated as repeatability during the same day by analysing three different standard samples and reported as %RSD.

Table 2.4:**The different parameters for HPLC used to calculate the measured drug concentration of different compounds under investigation in different samples**. (H_2O = Deionised water, OPA = Ortho-Phosphoric Acid, TFA = Trifluoro-acetic acid). * The gradient system used for the separation of epicatechin: at 0.01 minutes 11% B; at 20 minutes 25% B; and at 21 to 30 minutes 11% B.

Compound	Flow rate (ml/min)	Mobile phase	Run time (min)	Wavelength (nm)	Reference
α-Tocopherol	1	H_2O:methanol (2:98)	10	292	Chepda *et al*., 1999
Curcumin	1.5	0.1% v/vTFA: acetonitrile (50:50)	10	420	Jadhav *et al*., 2007
Resveratrol	1	H_2O:methanol (50:50)	8	300	Lindner *et al*., 2013
Sinapic acid	1	2% v/v AA: acetonitrile (85:15)	10	322	Elisha-lambert 2017
Ferulic acid	1	2% v/v AA: acetonitrile (85:15)	4	316	Elisha-lambert 2017
Epicatechin	1.5	0.1% OPA: acetonitrile (Gradient*)	30	280	Gottumukkala *et al*., 2014

2.4.10 Determining loading efficiency and encapsulating efficiency of different antioxidants in liposomes and PLA nanoparticles

Traditionally, the effectiveness of the method of nanoparticle preparation to encapsulate a drug is measured in two methods: loading efficiency (LE) and encapsulating efficiency (EE). The actual concentration of the drug in dry nanoparticle samples is used to calculate LE and its concentration in the supernatant is used to calculate EE, indirectly (equations below). LE only, was calculated for liposomes, as samples were not centrifuged or dried before testing. An exact weight of sample was added to an accurately measured amount of ethanol, sonicated for 15 minutes to breakdown any nanoparticle structure and filtered to extract the antioxidant within. The concentration of the antioxidants in

different samples was measured using the HPLC methods described in section 2.4.9. The peaks for different antioxidants in the samples were confirmed by comparing the retention times (r.t) and spectra of the peaks with those of standards. Each sample was tested in triplicate.

%LE for PLA nanoparticles was calculated using equations (2.6 & 2.7). This is a direct method of measuring the amount of drug loaded into the nanoparticles (Buhecha *et al*., 2019).

$$Theoretical\ Drug\ Concentration\ (DCT) = \frac{NPW \times DW}{TEW} \qquad \text{Equation 2.6}$$

where;

DCT = Theoretical drug concentration (mg)

NPW = Amount of nanoparticles powder weighed for HPLC analysis (mg)

DW = Amount of drug weighed to prepare nanoparticles (mg)

TEW = Combined weighed of drugs and polymer used in the nanoparticles (mg)

$$\%LE\ for\ polymeric\ nanoparticles = \frac{DCM(H)}{DCT} x\ 100 \qquad \text{Equation 2.7}$$

where;

DCM(H) = Drug concentration measured by HPLC (mg)

DCT = Theoretical drug concentration (mg)

EE is an indirect method of calculating the amount of drug encapsulated into the nanoparticles. It depends on measuring the concentration of drug un-encapsulated in the supernatant and then calculating the %EE using equation (2.8).

$$\%EE\ for\ polymeric\ nanoparticles = 100 - (\frac{DCM(S)}{DCT\ (S)} x\ 100) \quad \text{Equation 2.8}$$

where;

DCM(S) = Drug concentration in supernatant measured by HPLC (mg)

DCT(S) = Theoretical drug concentration in supernatant (mg)

As liposomes were not freeze dried due to their instability, accurately measured amounts of liposomes solutions were analysed using HPLC and the %LE was calculated using equation (2.9).

$$\%LE\ for\ liposomes = \frac{DCM(H)}{DCT} x\ 100 \quad \text{Equation 2.9}$$

where;

DCM(H) = Drug concentration measured by HPLC (mg)

DCT = Theoretical drug concentration (mg)

This method assumes that any unloaded drug is removed during the extrusion step by filtration due to their insolubility in the aqueous medium. This is not the case for epicatechin, as it is a water-soluble compound. For this reason, epicatechin was measured directly after extrusion and after passing through NAP-25 columns. These are disposable columns pre-packed with Sephadex™ G-25 resin and are used for the purpose of purification and desalting by gel filtration. Larger particles (in this case liposomes are excluded first and smaller molecules are entrapped in the matrix pores and so, eluted last (Ruysschaert ***et al***.,2005). Results were analysed using GraphPad Prism version 8.4.2. Bonferroni's multiple comparison test was applied to compare the %LE and %EE of PLA nanoparticles and to compare %LE of PLA nanoparticles to %LE of liposomes for each encapsulated drug. Bonferroni's test is the most popular *post hoc* test and the easiest way to compare data with multiple variables but small number of comparisons (Field 2009).

2.5 Results

2.5.1 Preparation of PLA nanoparticles encapsulated with antioxidants under investigation

As described in section 2.4.2 and in table 2.3, seven different PLA samples were prepared, one blank and six encapsulated with six different antioxidants (α-tocopherol, curcumin, resveratrol, ferulic acid, sinapic acid & epicatechin). Samples 2-TP, 3-CP, 5-FP & 6-SP, were prepared by adding the drug to the organic phase (DCM) in addition to the PLA. Sample 4-RP, resveratrol-loaded PLA nanoparticles, however, was prepared by adding the resveratrol to the co-solvent, acetone. Sample 7-EP, epicatechin-loaded PLA nanoparticles was prepared by dissolving the drug into the aqueous phase, the PVA solution. Sample 1 was a blank sample.

The addition of the organic phase to the aqueous phase containing the PVA while homogenising at high speed led to the formation of an emulsion. This was further stabilised by the addition of acetone and homogenising. Adding excess amount of water led to the formation of solid nanoparticles suspended in water. These were detected at this point with a LM (images not taken). The next step was removing the organic solvents using rotatory evaporator and leaving the suspensions overnight on a magnetic stirrer. Samples were then centrifuged to separate the nanoparticles from the water phase. Pellets were freeze dried producing a fluffy powder that was attached unfirmly to the bottom of the sample tubes. The supernatants were mostly clear and transparent for all samples except for sample 3-CP (curcumin PLA nanoparticles), which had a more yellowish colour. All supernatants were kept to determine EE. All dry sample were white in colour except for sample 3-CP, which was yellow due to the yellow colour of curcumin. Each batch produced from 100 -140 mg dry nanoparticle powder.

2.5.2 Preparation of liposomes encapsulated with antioxidants under investigation

As described in section 2.4.3 and table 2.3, seven different liposomal samples (8-14) were prepared, one blank and six encapsulated with six different

antioxidants (α-tocopherol, curcumin, resveratrol, ferulic acid, sinapic acid & epicatechin). All samples started with the preparation of the lipid solution by dissolving DPPC in ethanol. The antioxidants for preparing samples 9-13 were added to the lipid solution prior to drying. Epicatechin, however, did not dissolve thoroughly in ethanol and was therefore added to aqueous phase after drying the lipids. Drying the lipids using the rotatory evaporator led to the formation of a lipid film on the bottom wall of the round bottom flask. Adding the aqueous phase while shaking vigorously and sonicating over an ultrasonic bath led to the detachment of the lipid layer into the aqueous phase. At this point, the solutions were cloudy and whitish in colour except for sample 10-CL, which was yellowish due to the presence of curcumin. The extrusion step was performed producing more clear solutions. Except for samples 8-BL & 14-EL, all samples showed a residue deposited on the permeable membrane. Although, this method is simple, the product volume was less than 2 mL for each batch. Attempts were made to freeze dry samples, but LM as well as SEM showed that liposomal structure collapsed when applying vacuum pressure (images not shown).

2.5.3 Particle size and size distribution of different liposomes and PLA nanoparticles

All blank and drug loaded liposomes and PLA nanoparticles (samples 1-14) were measured for their particle size and particle size distribution using a light scattering technique. Results are shown in table 2.5. Selected reports copied from the zetasizer software for few tested samples are attached in appendix I. Liposomes have shown smaller particle size (183.8–260.8 nm) compared to PLA nanoparticles (314.4–556.9 nm). The PdI observed for liposomes (0.006-0.259) was less than that observed for PLA nanoparticles (0.206-1), indicating a more monodisperse system for liposomes. Most drug loaded PLA nanoparticles did not show significant difference in size compared to blank nanoparticles. The only exception was α-tocopherol-loaded PLA nanoparticles, which showed an average size of 556.9 ± 127.5 nm compared to blank PLA nanoparticles with an average of 345 ± 98.7 nm. Sinapic acid and curcumin PLA nanoparticles showed the smallest average particle size (314.4 ± 42.28 and 319.5 ± 80.29 nm; respectively). Epicatechin, sinapic acid and α-tocopherol liposomes showed the smallest

average particle size (183.8 ± 80.1, 184.8 ± 83.3 and 184.2 ± 39.85 nm; respectively). These results were not linked to any specific properties of the encapsulated antioxidants and might be explained by variable processing techniques that could be reduced by more precise processing during synthesis.

Data analysis using one-way ANOVA showed no significant difference between particles sizes measured for liposomes, $F_{(6,11)} = 0.286$, $p = 0.931$ and a significant difference between PLA nanoparticles, $F_{(6,9)} = 3.537$, $p = 0.042$. Brown-Forsythe ANOVA test was applied to compare different means of nanoparticles because of the variation in SD. Nevertheless, the *post hoc* Dunnett's test showed that multiple comparisons to blank were insignificantly different for both PLA nanoparticles and liposomes and all adjusted p values were > 0.05.

Table 2.5: Summary of the particle size measured by zetasizer of PLA nanoparticles and liposomes encapsulated with different compounds [mean ± SD, N = 3, p > 0.05] *vs* blank using Brown-Forsythe ANOVA test and Dunnett's multiple comparisons test

	PLA nanoparticles		*Liposomes*	
	Particle size (nm)	PdI	Particle size (nm)	PdI
Blank	345.0 ± 98.7	1	194.9 ± 114.0	0.256
α-Tocopherol	556.9 ± 127.5	0.241	184.2 ± 39.9	0.006
Curcumin	319.5 ± 80.3	0.206	210.4 ± 60.2	0.051
Resveratrol	457.9 ± 56.1	1	197.4 ± 102.4	0.222
Sinapic acid	314.4 ± 42.3	1	184.8 ± 83.3	0.229
Ferulic acid	355.8 ± 47.3	1	260.8 ± 116.2	0.259
Epicatechin	350.9 ± 87.4	1	183.8 ± 80.1	0.235

2.5.4 Surface charge of different liposomes and PLA nanoparticles

The Zeta-potential was measured for all samples (1-15) using the Zetasizer to study their surface charge. PLA nanoparticles showed a more negative zeta-potential on the surface of the particles (-21.6 to -38.0 mV) compared to the liposomes (-7.9 to -12.1 mV). Results are shown in table 2.6. For the purpose of demonstration only, a single report is copied from the zetasizer software for a single sample and attached in appendix II. Resveratrol PLA nanoparticles showed the lowest negative charge (-21.6 ± 10.4 mV) and the blank PLA nanoparticles showed the highest negative charge (-38.0 ± 3.85 mV) within the PLA nanoparticles tested (samples 1-7). However, within the liposomal samples tested (samples 8-14), resveratrol liposomes showed the lowest negative charge (-7.86 ± 6.36 mV) and sinapic acid liposomes showed the highest negative charge (-12.1 ± 4.97 mV). No significant difference was detected when analysing zeta-potential data using Brown-Forsythe ANOVA test, $F_{(6,9)} = 2.271$, $p = 0.126$ for PLA nanoparticles and $F_{(6, 12)} = 0.325$, $p = 0.912$ for liposomes.

Table 2.6 Summary of the zeta-potential of PLA nanoparticles and liposomes encapsulated with different compounds [mean ± SD, N = 3]

	Zeta-potential (mV)	
	PLA nanoparticles	Liposomes
Blank	-38.0 ± 3.85	-10.9 ± 3.45
α-Tocopherol	-37.6 ± 5.54	-11.9 ± 4.46
Curcumin	-30.5 ± 7.27	-11.6 ± 3.97
Resveratrol	-21.6 ± 10.40	-7.9 ± 6.36
Sinapic acid	-37.0 ± 3.80	-12.1 ± 4.97
Ferulic acid	-32.7 ± 5.29	-11.9 ± 4.40
Epicatechin	-32.9 ± 7.54	-11.3 ± 3.93

2.5.5 Studying the stability of curcumin loaded liposomes

A representative liposomal sample (10-CL) was selected to study the stability of liposomes over a period of 10 days. The sample was analysed for its particle size, size distribution and surface charge on days 1, 2, 3, 4, 8 and 10 from preparation. Results are shown in table 2.7. Two single reports from size analysis: a report from day 1 and a report from day 10 are attached in appendix II for the purpose of illustration. On day one, particle size showed an average of 132.8 ± 79.18 nm. This figure increased insignificantly on day 2 (147.4 ± 91.77 nm). Interestingly, from day 3, the particle size distribution graph showed two peaks instead of one single peak. The first peak had an average particle size comparable to the average size on day 1 and 2, ranging between 105.3 – 189.1 nm. However, the second peak showed very large particle size, ranging from 4640 – 5224 nm. As shown in the table, each peak is represented with the mean ± SD, in addition to percentage volume (%V). The %V shows the percentage of the total volume tested (≈1 mL) that is within that range. The %V for the first peak kept decreasing from 100% on day 1 to 49.5% on day 3 until 4.8% on day10, while the %V for the second peak kept increasing from 0% on day 1 to 50.5% on day 3 until 95.2% on day 10. Additionally PdI kept increasing each day rising from 0.160 on day 1 to 0.227 on day 10. No significant change in the zeta-potential was noticed within the days tested, ranging between -10.3 and -12.6 mV.

Furthermore, physical examination of the sample was performed each day of analysis. On day 1, the sample was yellowish, transparent and no evidence of precipitation was observed. No obvious change was noticed on the second day. Starting from the third day, a yellowish precipitate was detected on the bottom of the tube, which increased each day. This was thought to be released curcumin. After day 10, a change in the colour and viscosity of the sample was observed. This resembled the growth of fungus, which led to discontinuation of the stability study.

Table 2.7: Size distribution and zeta-potential of curcumin loaded liposomes from day one of preparation until day ten. [mean ± SD, N = 3]. Peaks are represented as mean ± SD (%V)

Day	*Peak 1 (nm)*	*Peak 2 (nm)*	*PdI*	*Zeta-potential (mV)*
1	132.8 ± 79.18 (100%)	-	0.160	-12.6 ± 3.92
2	147.4± 91.77 (100%)	-	0.172	-10.74 ± 3.65
3	153.9 ± 68.99 (49.5%)	5063 ± 820.0 (50.5%)	0.202	-11.99 ± 3.06
4	164.2 ± 54.24 (39.3%)	5224 ± 742.6 (60.7)	0.219	-11.7 ± 4.22
8	105.3 ± 50.54 (28.9%)	4859 ± 116.0 (71.1%)	0.212	-10.3 ± 4.32
10	189.1 ± 95.0 (4.8%)	4640 ± 142.9 (95.2%)	0.227	-11.5 ± 3.21

2.5.6 Studying surface morphology using LM and SEM for different liposomes and PLA nanoparticles

As indicated in the methods section, liposomes (samples 8-14) were only characterised for their morphology using LM [Figures 2.14]. PLA nanoparticles (samples 1-8) were examined using LM before drying. All samples showed spherical particles suspended in solution, although, images were not clear enough to show exact morphology due to instrument limitation. However, liposomal samples (samples 8-14) showed some evident of that the type of liposomes were a mixture of SUV and LUV. Sizes were estimated using a micrometre graticule. Liposomal samples showed sizes before the extrusion step in the micron range and dropped to below 300 nm when extruded. PLA nanoparticle samples showed larger particles (400-700 nm).

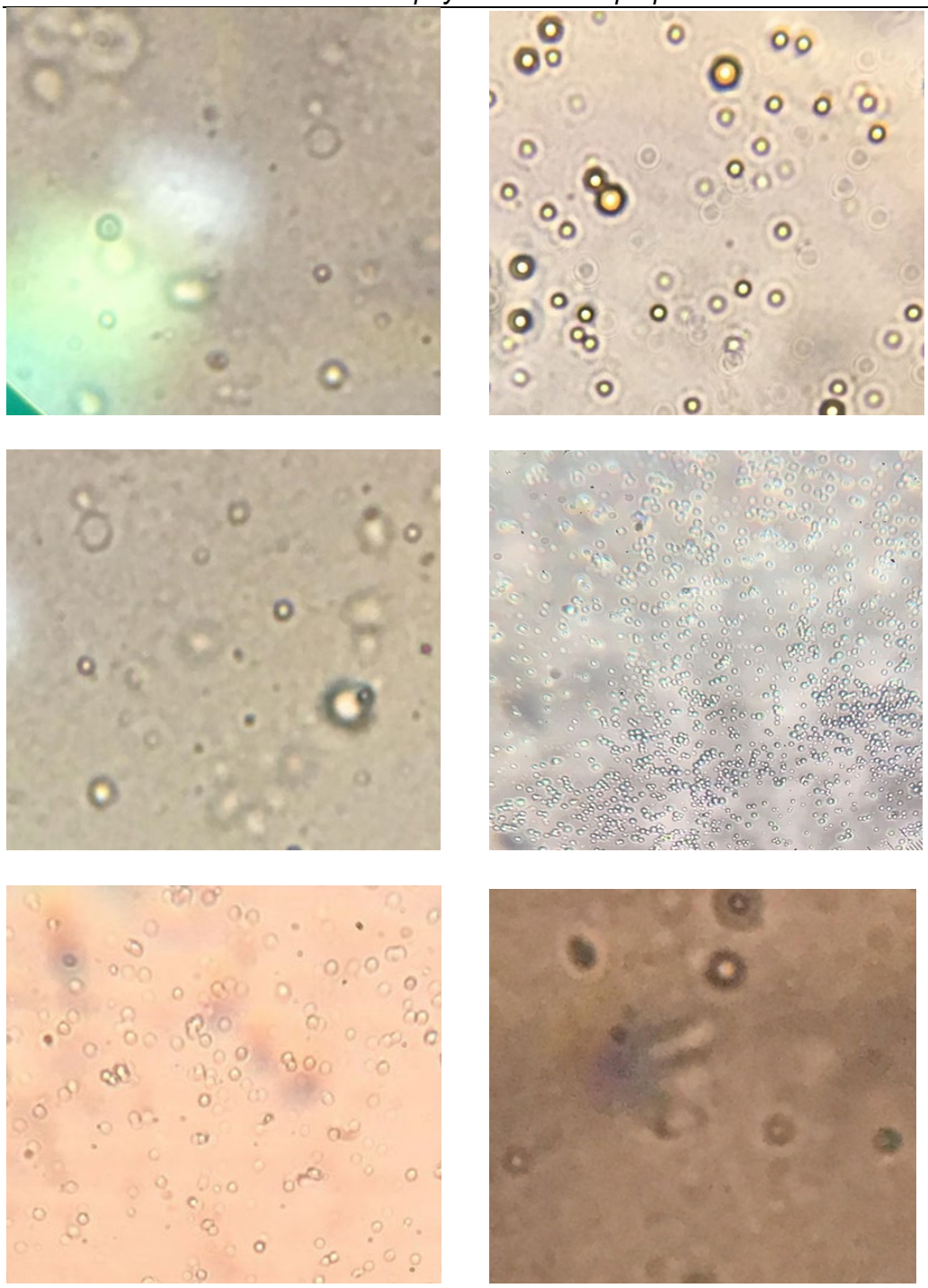

Figure 2.14: **Microscopic examination of liposomes *via* light microscope using 40X maginfication lens.** a: α-Tocopherol, b: curcumin, c: resveratrol, d: ferulic acid, e: sinapic acid and f: epicatechin encapsulated liposomes. All samples showed spherical shaped particle, but imaged not clear enogh due to instrument limitation (original figure in colour).

Selected SEM images for blank PLA nanoparticles and for PLA nanoparticles encapsulated with different antioxidants (samples 1-7) are shown below in figures 2.15 & 2.16. Overall, the images show that PLA nanoparticles are spherical in shape with a wide size distribution range. A Smart TIFF software from Carl Zeiss SMT, was used to analyse the images and measure the diameter of several particles. The majority of the particle sizes were consistent with results obtained from zetasizer with the exceptions of several huge particles that were in the micron range. Noticed from figure 2.16, that α-tocopherol PLA nanoparticles (figure 2.16.a) were larger than other nanoparticles when compared visually or *via* Smart TIFF software. The SEM images show no drug crystals other than the spherical nanoparticles.

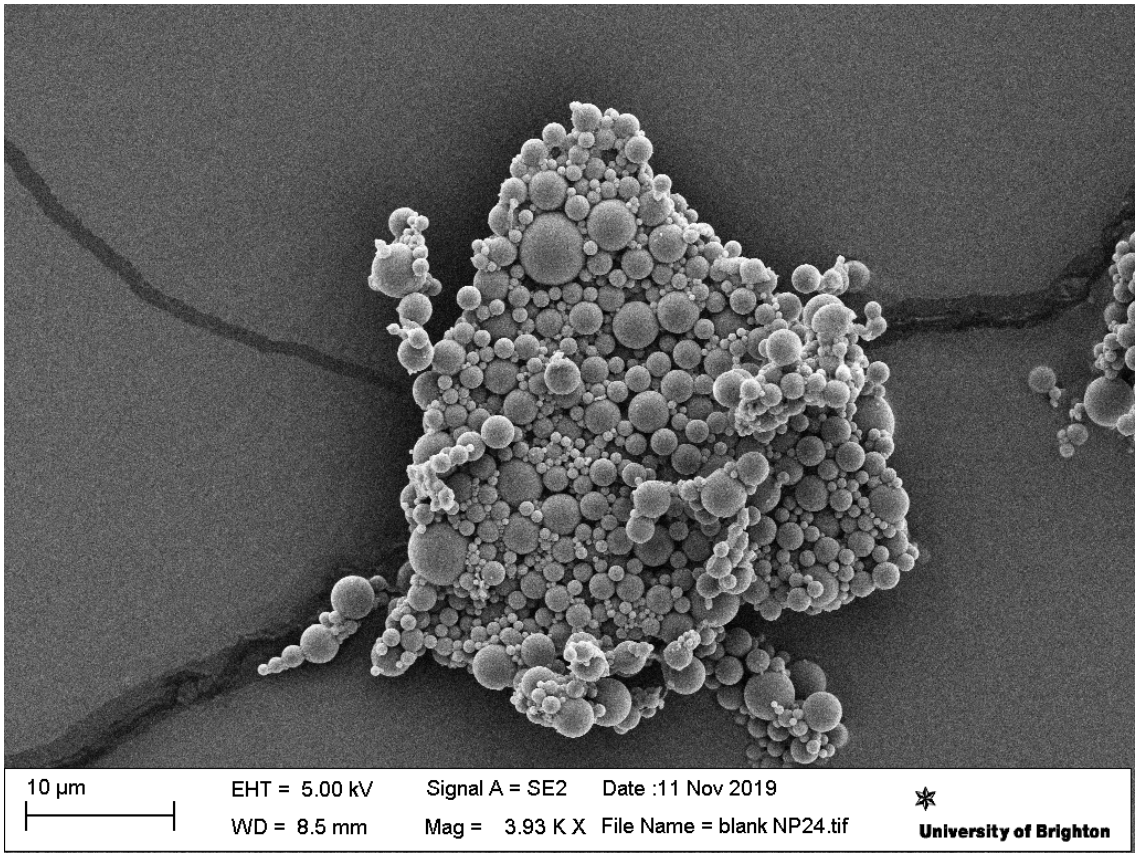

Figure 2.15*:* **SEM images for blank PLA nanoparticles.** The accelerating voltage used was 5 kV with a working distance from 8.5 mm. Nanoparticle are spherical in shape with smooth surface and variable size.

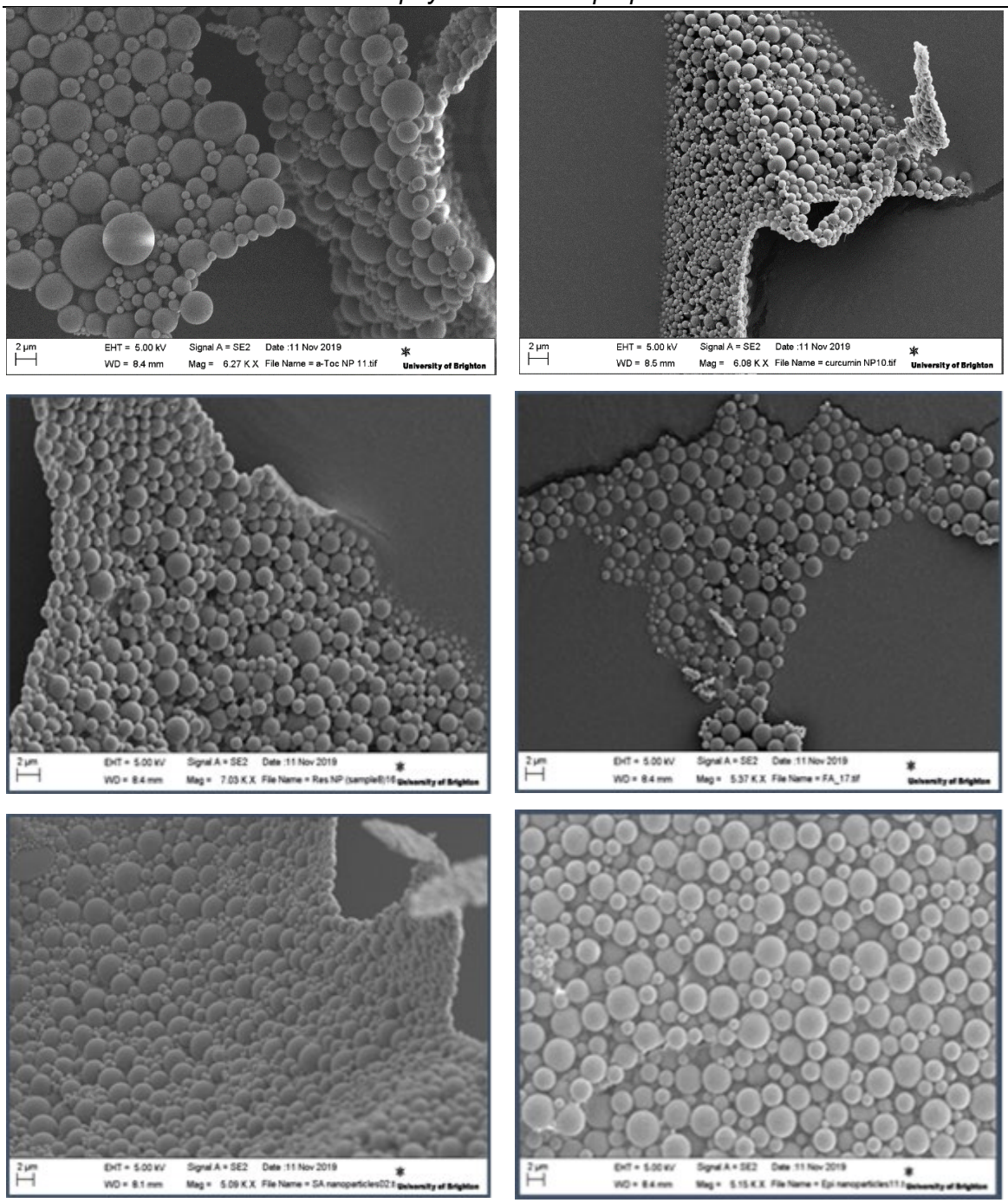

Figure 2.16: **SEM images for drug-loaded PLA nanoparticles**. The accelerating voltage used was 5 kV with a working distance from 8.1-8.5 mm. a: α-Tocopherol, b: curcumin, c: resveratrol, d: ferulic acid, e: sinapic acid and f: epicatechin-loaded PLA nanoparticles. All nanoparticles have a smooth spherical shape and are comparable in size (400-600 nm), except for image a, where the increase in size is noticed (800-2000 nm).

2.5.7 Assessment of Surface Characteristics of the Nanoparticles using FT-IR Spectroscopy

This test was performed on the freeze-dried PLA nanoparticle samples (1-7) and PLA, PVA, α-tocopherol, curcumin, resveratrol, ferulic acid, sinapic acid & epicatechin standards. The FT-IR spectra for samples 1-7 compared to the spectrum of PLA crystals are shown below [Figures 2.17- 2.23]. Full reports containing complete spectra compared to pure drug spectra are attached in appendix III. PLA is a poly-ester and so, a C=O ester sharp peak is observed around 1750 cm^{-1}. In addition, a C-O stretch is noticed in the region of 1100 – 1400 cm^{-1}. C-H and 0-H bond stretches are seen around 3000 $cm^{-1}$and 3500 cm^{-1}; respectively. These characteristic bands of PLA were noticed in both pure PLA crystals and PLA nanoparticles. FT-IR spectrum of pure α-tocopherol showed C=O, C=C and C-H formation around 1200, 1650 and 2900 cm^{-1} respectively. FT-IR spectrum of pure curcumin revealed the presence of C-H vibration, C-O-C peak, C-O (enol) peak, aromatic C=C stretch and 0-H peak around, 900, 1030, 1290, 1500, 3500 cm^{-1} respectively. Pure resveratrol FT-IR spectrum presented peaks due to the C=C (*trans*-olefinic), C-O, C=C (aromatic) and O-H bonds around 960, 1100, 1590 and 3300 cm^{-1} respectively. Peaks due to C=C aromatic ring, C-H bond stretching and –OH stretching were noticed in FT-IR spectrum of pure ferulic acid and sinapic acid around 1500, 2250 and 3500 cm^{-1}; respectively. Finally, FT-IR spectrum of epicatechin showed bands around 1100, 1500 and 3500 cm^{-1} representing C-O-C, aromatic C=C and O-H bonds. Interestingly, these characteristic peaks were covered or overlapped in the spectra produced from the drug loaded PLA nanoparticles.

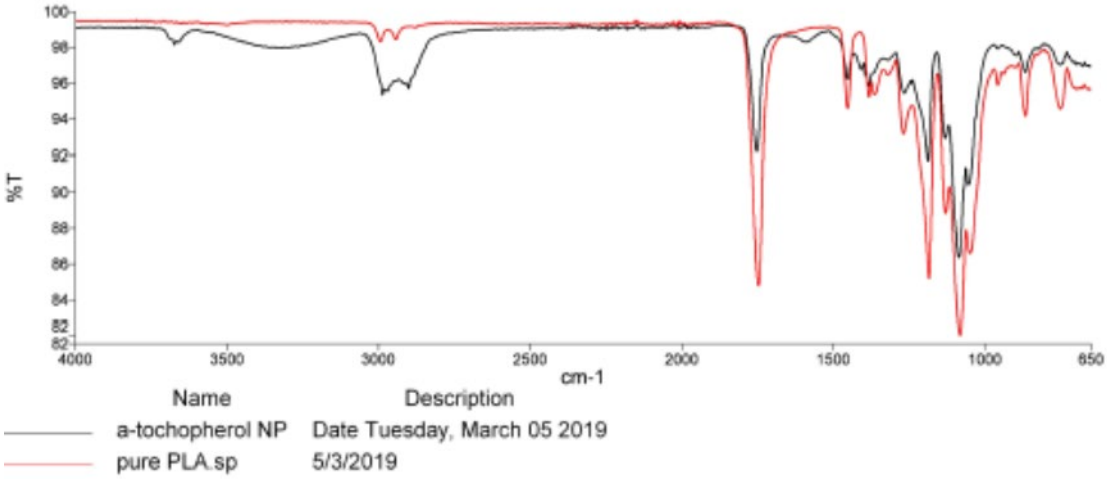

Figure 2.17: **FT-IR spectrum for α-tocopherol-loaded PLA nanoparticles (in black) and PLA (in red).** The C=O of the PLA appears in both spectrums at 1750 cm^{-1}. The bands at 865 cm^{-1} and 751 cm^{-1} and a mountainous triplet peak at 1131, 1088, and 1044 cm^{-1}, corresponding to C-O vibration in –CO-O- group in polymer chains are characteristic of the PLA, and no shift is observed. An O-H stretching appears as medium sharp at 3700 cm^{-1} and strong broad between 3550-3200 cm^{-1} in the α-tocopherol-loaded nanoparticle spectrum (original figure in colour).

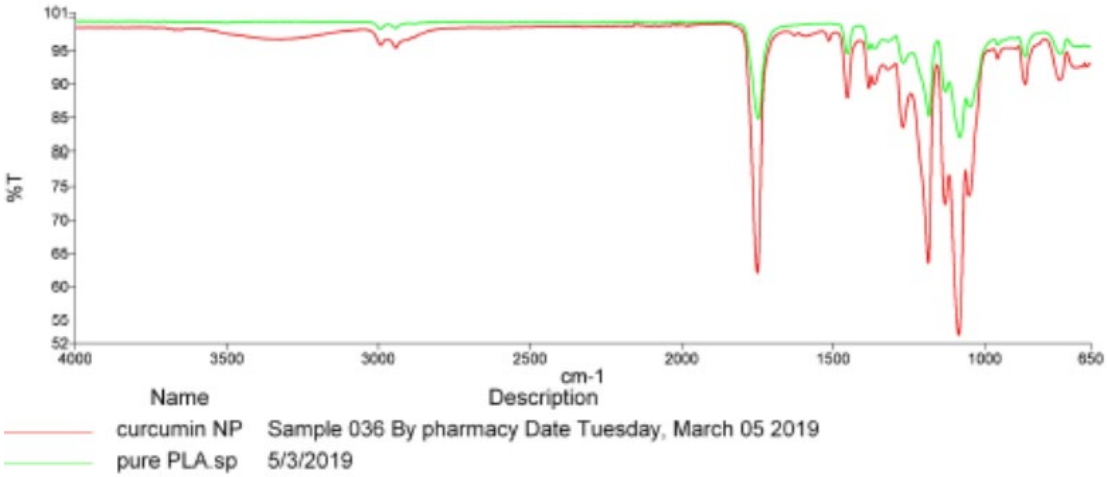

Figure 2.18: **FT-IR spectrum for curcumin-loaded nanoparticles (in red) and PLA (in green).** The distinguishing peaks of PLA appear in both spectra. No characteristic peaks of curcumin observed in curcumin-loaded PLA nanoparticles. A broad O-H stretching appears between 3550-3200 cm^{-1} in the curcumin-loaded nanoparticle spectrum (original figure in colour).

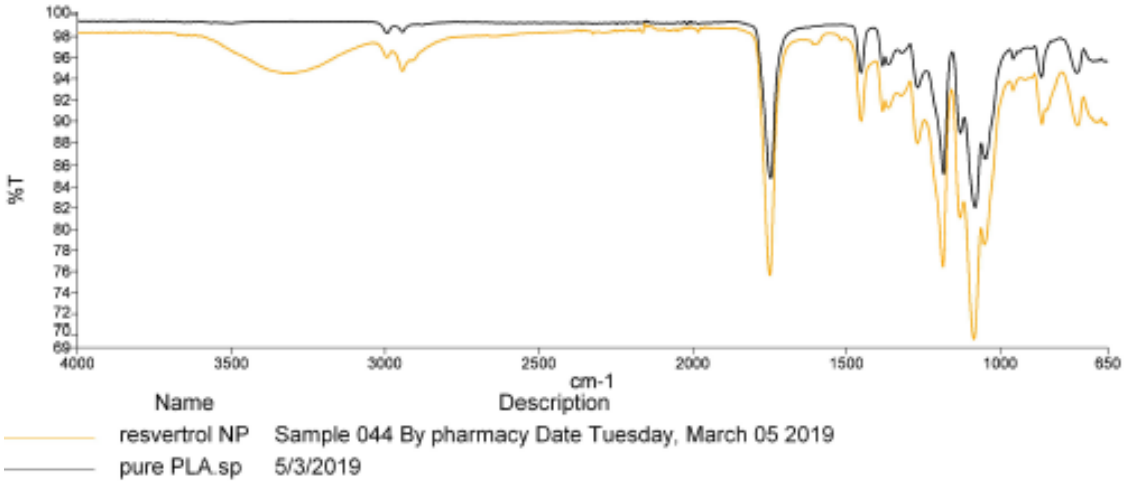

Figure 2.19: **FT-IR spectrum of resveratrol-loaded PLA nanoparticles (in yellow) and PLA (in black).** The distinguishing peaks of PLA appear in both spectra. A broad O-H stretching appears between 3550-3200 cm^{-1} in the resveratrol-loaded nanoparticle spectrum. No characteristic peaks of resveratrol observed in resveratrol-loaded PLA nanoparticles (original figure in colour).

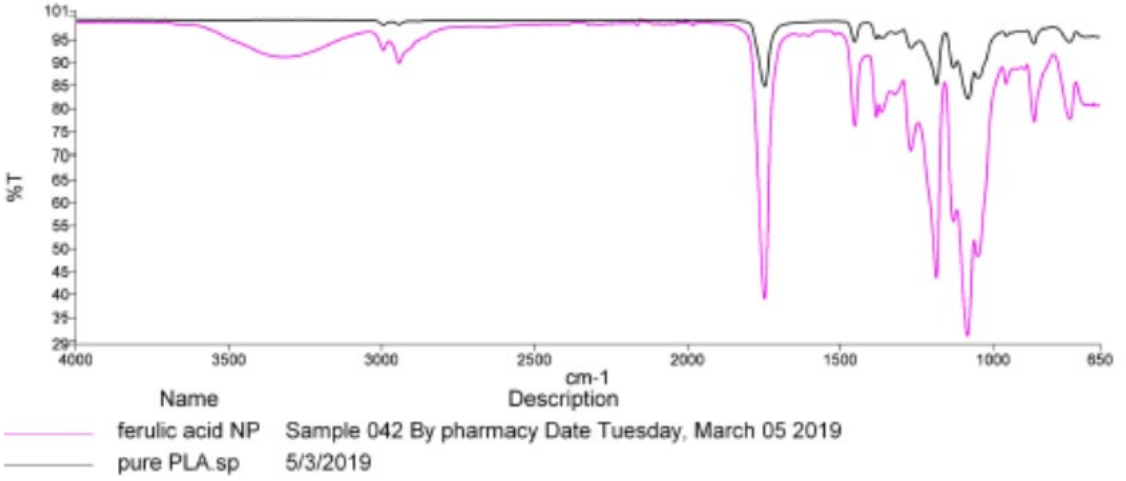

Figure 2.20: **FT-IR spectrum of ferulic acid-loaded PLA nanoparticles (in purple) and PLA (in black).** The distinguishing peaks of PLA appear in both spectra. A broad O-H stretching appears between 3550-3200 cm^{-1} in the ferulic acid-loaded nanoparticle spectrum. The unique peaks of ferulic acid are overlapped in ferulic acid-loaded PLA nanoparticles and cannot be distinguished (original figure in colour).

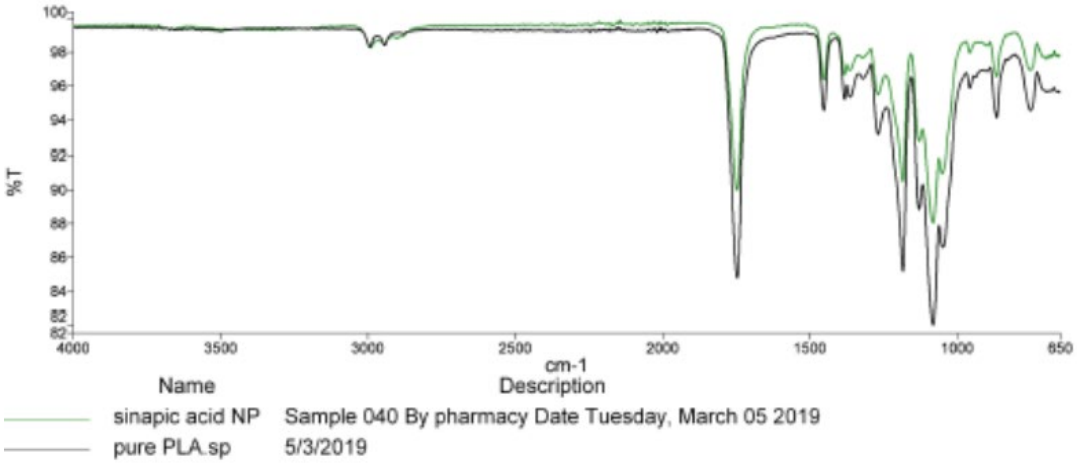

Figure 2.21: **FT-IR spectrum of sinapic acid-loaded PLA nanoparticles (in green) and PLA (in black).** The distinguishing peaks of PLA appear in both spectra. No clear peaks for sinapic acid or any other functional groups other than the functional groups of PLA in the sinapic acid-loaded PLA nanoparticles (original figure in colour)

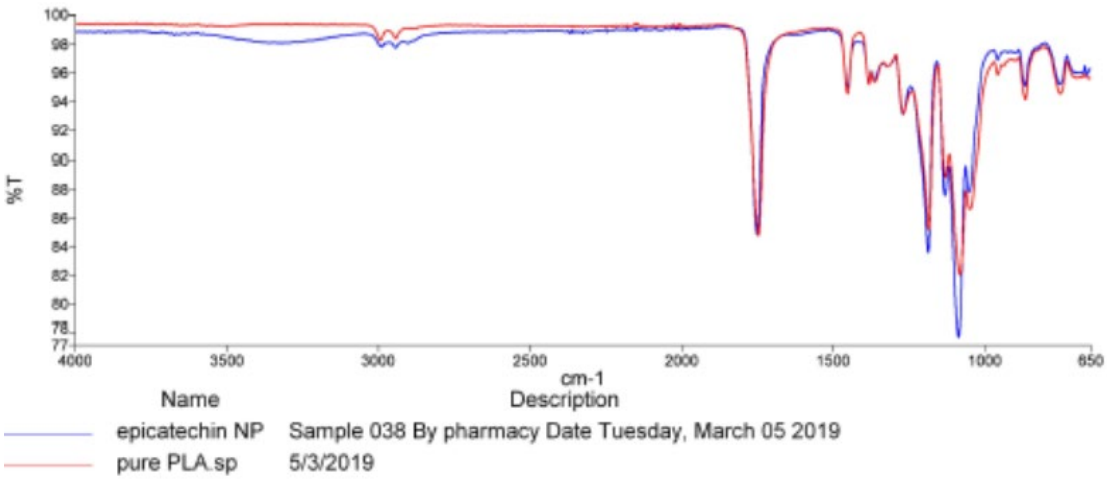

Figure 2.22**: FT-IR spectrum of epicatechin-loaded PLA nanoparticles (in blue) and PLA (in red).** The distinguishing peaks of PLA appear in both spectra. A broad O-H stretching appears between 3500-3200 cm^{-1} in the epicatechin-loaded nanoparticle spectrum. The unique peaks of epicatechin are not detected in the epicatechin-loaded PLA nanoparticles (original figure in colour).

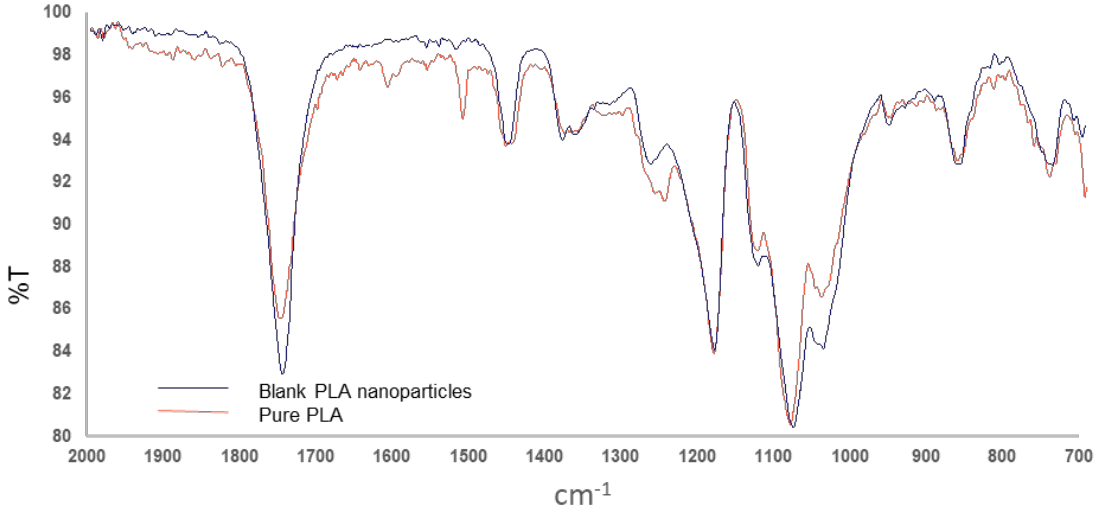

Figure 2.23: **FT-IR spectrum of blank PLA nanoparticles compared to PLA.** Both spectra are almost identical and show distinguishing peaks of PLA (original figure in colour).

FT-IR software (PerkinElmer Spectrum version 10.03.07) was used to compare the spectra. Spectra from samples 1-7 were compared with the corresponding spectrum of pure PLA, PVA and standard drugs. The FTIR software calculated a correlation factor automatically, which describes the similarity of the nanoparticle's spectrum to pure compound's spectrum. Results are summarised in table 2.8. The correlation factors of all PLA nanoparticles were much higher when compared to pure PLA than PVA or encapsulated drug.

Table 2.8: Summary of correlation between PLA nanoparticles to pure PLA, PVA and drug encapsulated with in nanoparticles

Drug encapsulated	*Correlation to PLA*	*Correlation to PVA*	*Correlation to drug encapsulated*
Blank	0.8998	0.1028	-
Curcumin	0.9211	0.1199	0.0076
Sinapic acid	0.9947	0.1517	0.0289
Ferulic acid	0.9764	0.1417	0.0332
Resveratrol	0.9737	0.1782	0.0319
α-Tocopherol	0.8452	0.3121	0.1188
Epicatechin	0.9183	0.1537	0.0701

2.5.8 Thermal analysis of drug-loaded PLA nanoparticles

A DSC measures the difference in heat flow rate between a sample and inert reference as a function of time and temperature producing a graph called thermogram. All PLA nanoparticles (samples 1-7) were tested for their thermal behaviour using DSC. Due to the water content of liposomes, it was not practical to analyse them *via* this method. The thermograms presented in this study is a function of the heat flow per gram sample and the temperature applied. Thermograms of PLA standard followed by the thermograms of the synthesised PLA nanoparticles are shown in figures 2.23 to 2.30. Thermograms were analysed using the software TRIOS v5.0.0.44608. Glass Transition (T_g) is a reversible change of an amorphous or partially crystalline material to a viscous or rubbery condition. T_g is seen as a step change in heat flow, not a peak in heat flow. As seen in all thermograms, T_g can be calculated at three positions of the step change; half height, half width and at the inflection point (most commonly used). In this discussion and for the purpose of consistency, T_g will refer to the glass transition temperature calculated at the inflection point. In the thermograms, an (I) follows this figure.

The thermogram for PLA standard showed a T_g at 46°C [Figure 2.23]. The thermograms for the blank, α-Tocopherol, curcumin, resveratrol, ferulic acid, sinapic acid and epicatechin-loaded PLA nanoparticles also revealed the presence of this step change at 45, 46, 45, 40, 44, 44 and 45°C; respectively. Additionally, α- Tocopherol PLA nanoparticles showed a wide endothermic peak between 70-150ºC [figure 2.25]. Curcumin PLA nanoparticles showed a small endothermic peak around 210ºC [Figure 2.26]. Sinapic and ferulic acids PLA nanoparticles gave an additional sharp endothermic peak at around 180°C [Figures 2.28 & 2.29]. However, there was no extra peaks for epicatechin and resveratrol PLA nanoparticles [Figure 2.27 & 2.30].

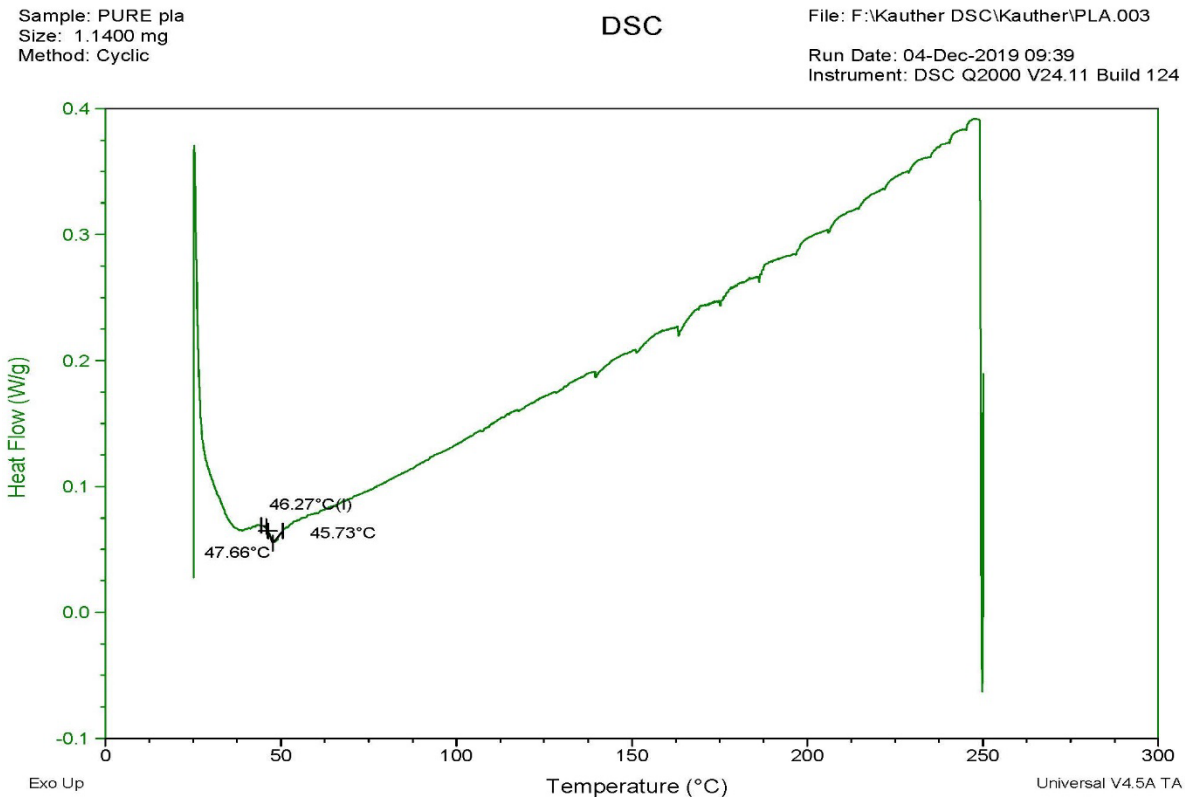

Figure 2.24: **A thermogram of PLA standard**. All thermograms was produced after heating from 25-250ºC at an increasing rate of 10ºC/min. This shows T_g at 46.27ºC.

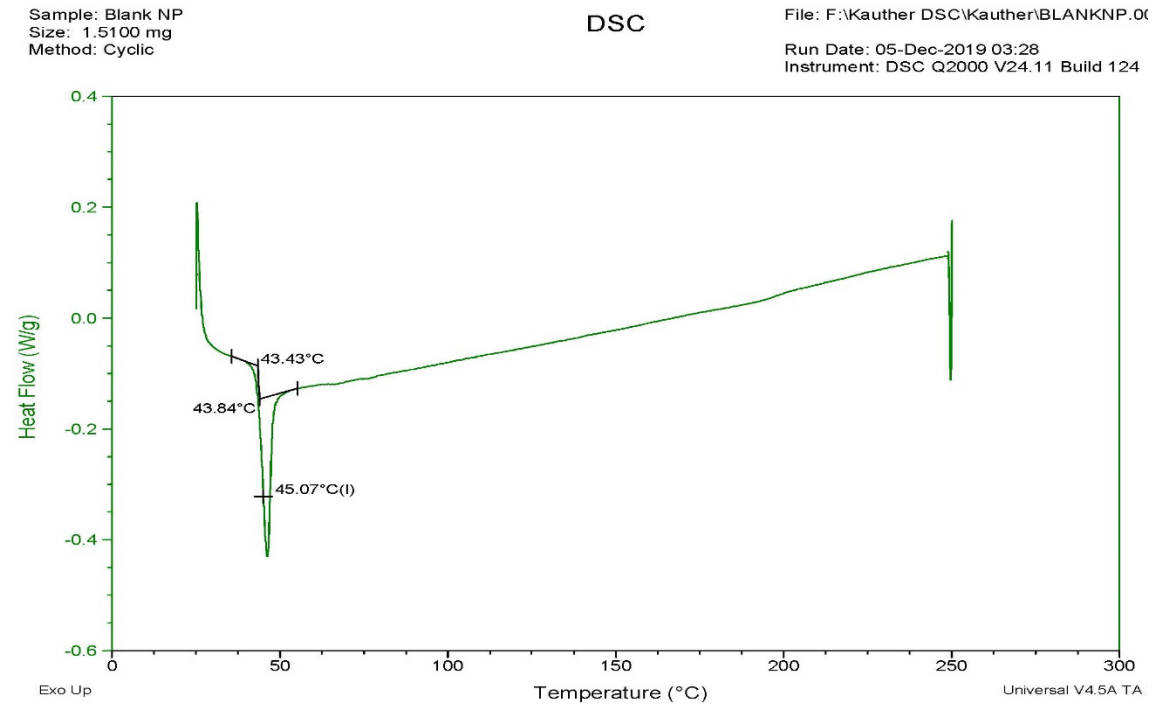

Figure 2.25**: A thermogram of blank PLA nanoparticles.** A T_g is shown at 45.07ºC**.**

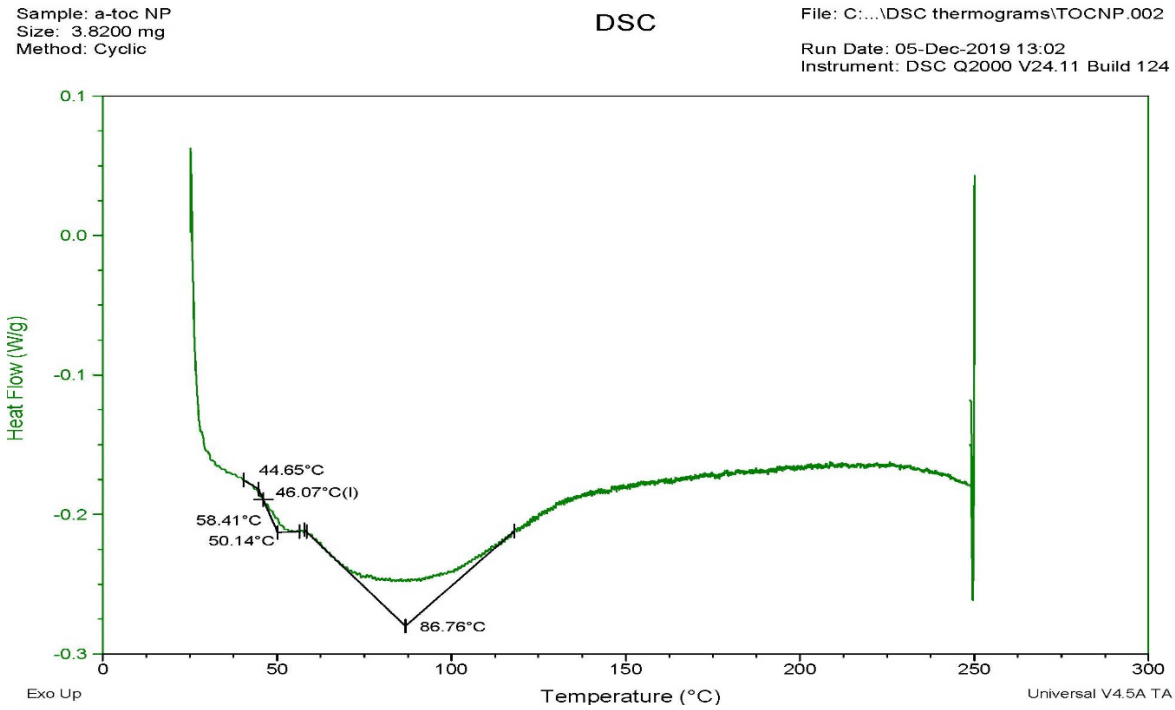

Figure 2.26**: A thermogram for α-tocopherol PLA nanoparticles**. A T_g is seen at 46.07ºC and an additional wide endothermic peak between 60 & 125ºC.

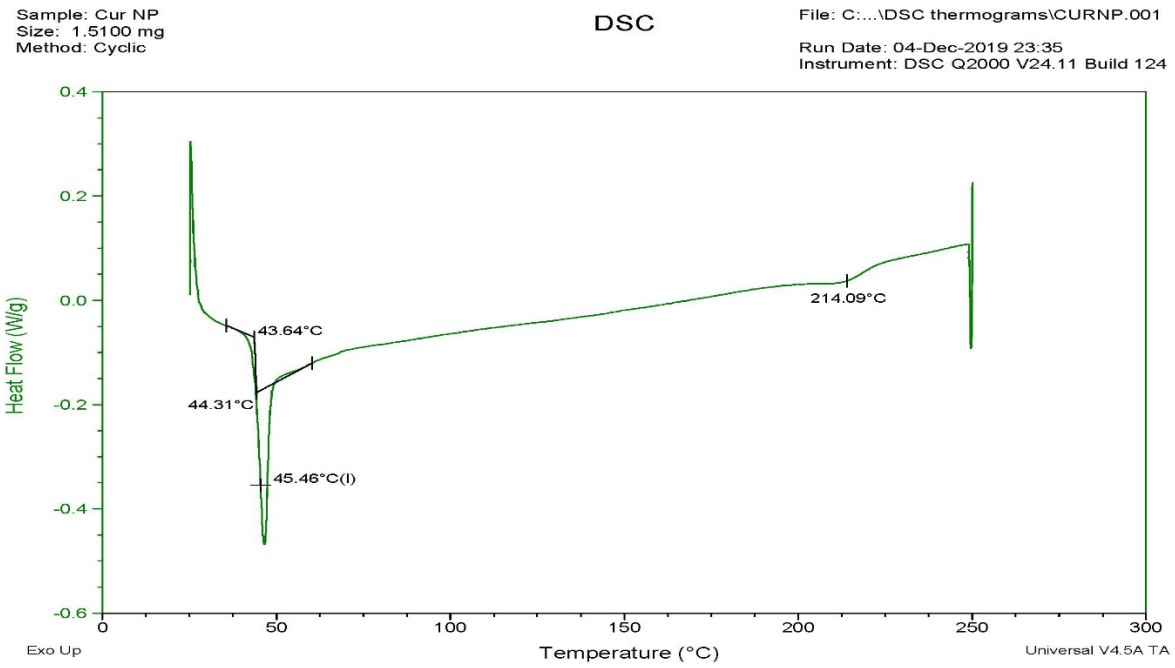

Figure 2.27: **A thermogram for curcumin PLA nanoparticles**. A T_g can be seen at 45.46ºC and a small endothermic peak is observed between 210 & 220ºC.

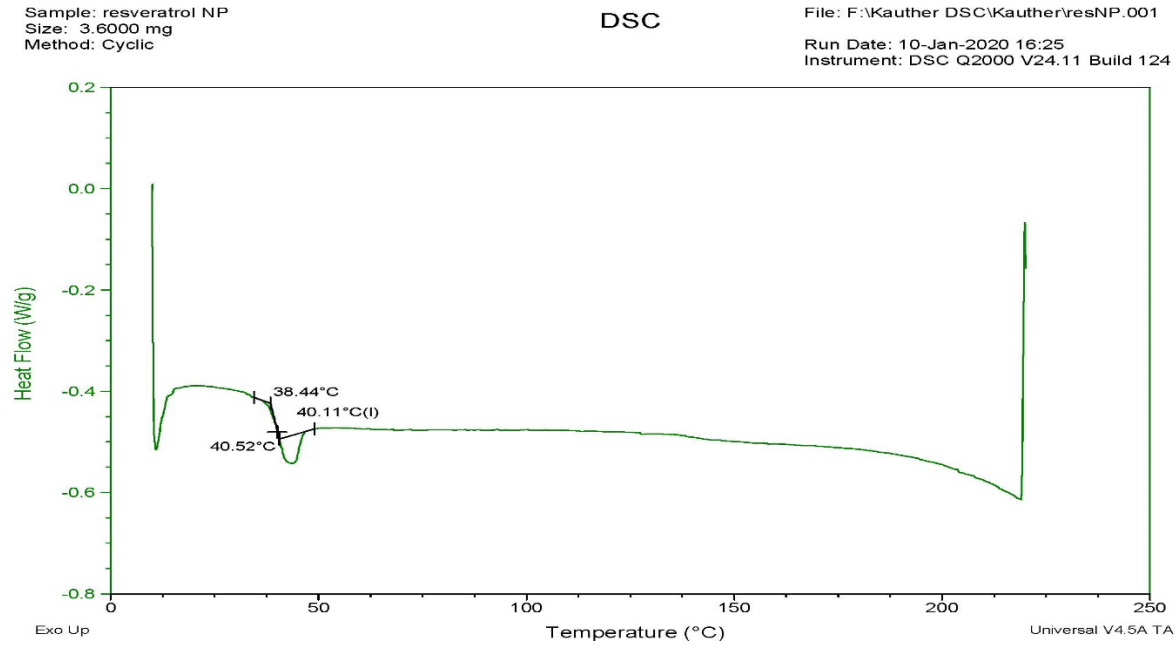

Figure 2.28**: A thermogram for resveratrol PLA nanoparticles**. Only a T_g is observed at 40.11ºC with no other peaks.

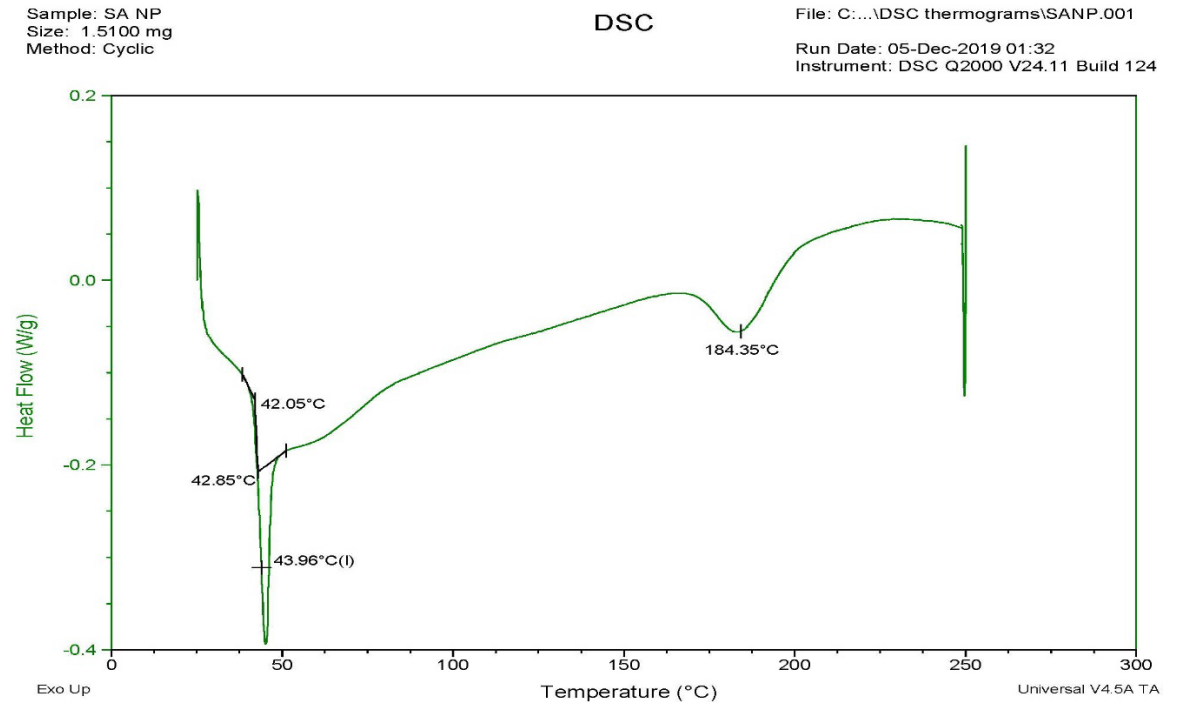

Figure 2.29: **A thermogram for sinapic acid PLA nanoparticles**. A T_g at 43.96ºC and an endothermic peak at 184.35ºC.

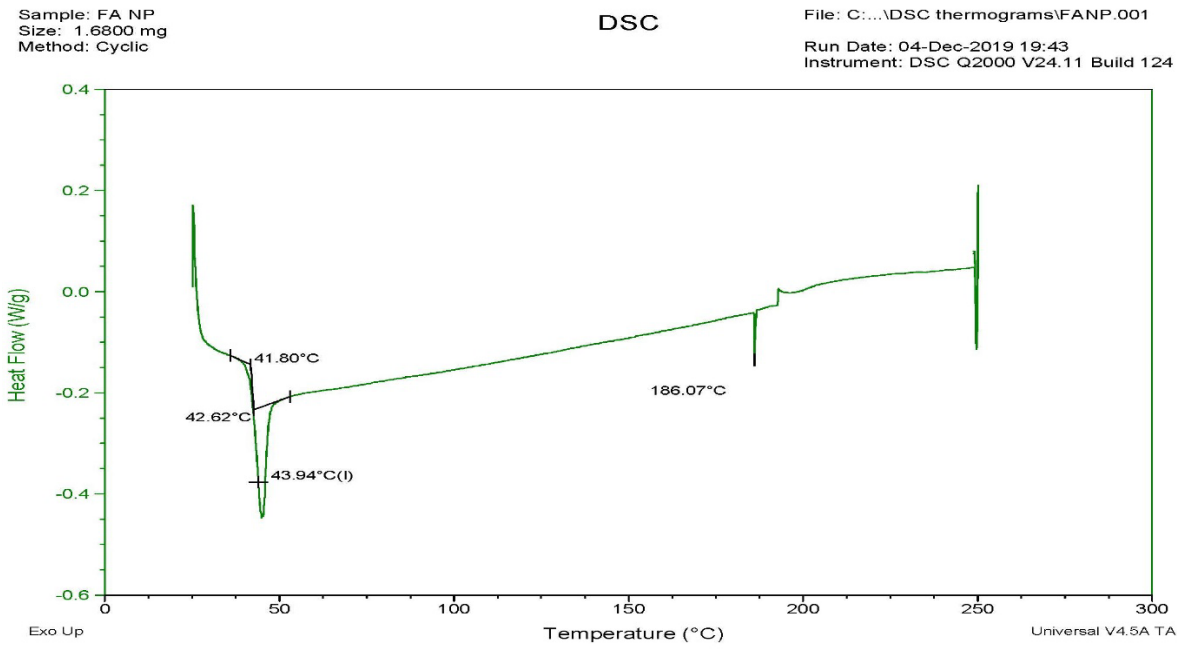

Figure 2.30: **A thermogram for ferulic acid PLA nanoparticles. A** T_g is observed at 43.94ºC and an endothermic peak at 186.07˚C.

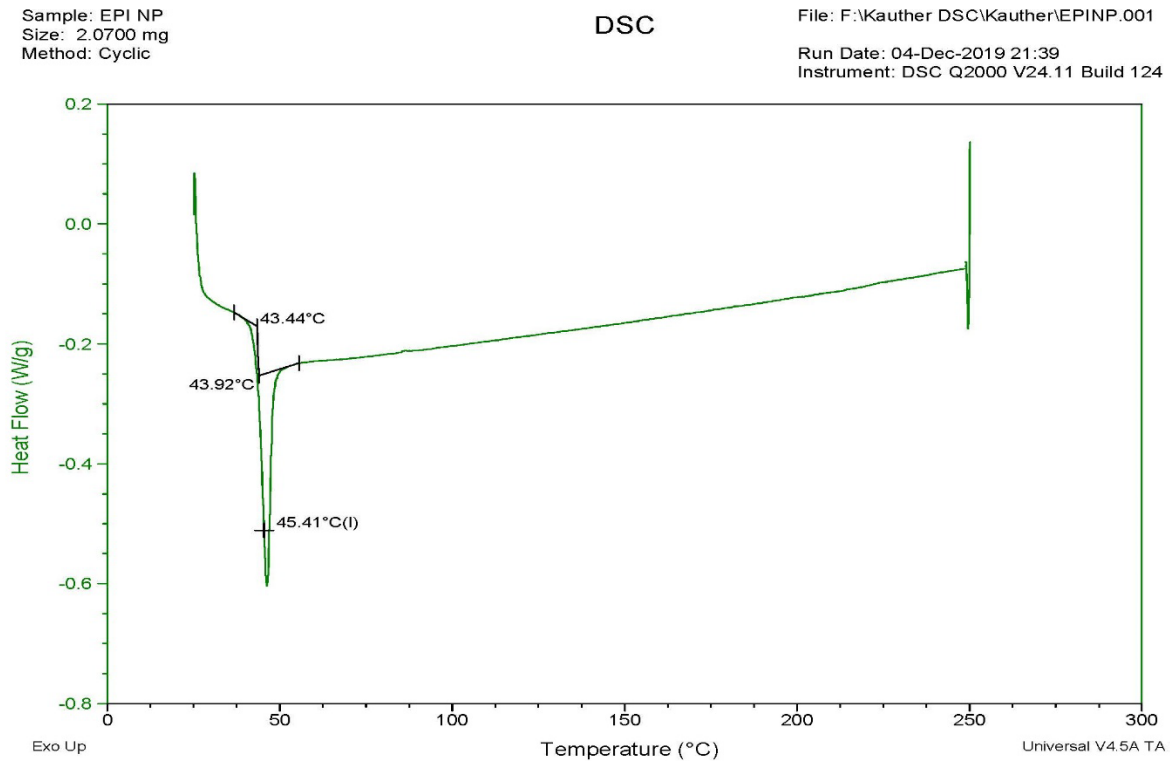

Figure 2.31: **A thermogram for epicatechin PLA nanoparticles.** A T_g is observed at 45.41ºC with no additional peak.

2.5.9 Determination of the drug concentration in different samples using high performance liquid chromatography (Analytical method validation)

To determine the concentration of antioxidants in the samples prepared, six different HPLC methods were adapted (table 2.4) and applied. In order to determine the suitability of these methods, calibration plots [Figure 2.31] were constructed after injecting serial dilutions of standards of each antioxidant to be tested (α-Tocopherol, curcumin, resveratrol, ferulic acid, sinapic acid and epicatechin). The calibration plots here are relationships between known standard concentrations injected into the HPLC (X value) and the areas under the peak calculated from HPLC chromatograms, produced by the HPLC software (Y value). These calibration plots were then used to calculate the R^2, %RSD, LOD and LOQ. The range of standard concentrations used and the different parameters calculated are listed in table 2.9. A representative sample of the HPLC chromatograms are shown in appendix IV. All chromatographs showed good peaks for the antioxidant under investigation.

The first method used to analyse α-tocopherol had a total run time of 10 min and α-tocopherol standard eluted at around 7.7 min. There were no other interfering peaks (Appendix IV, a). The linear regression and correlation coefficient were y = 7.2165x - 5.215 and R^2 = 0.9997. The %RSD for all variables was less than 9% and the LOD & LOQ were 0.25 & 0.75 µg/mL; respectively, which were low enough for the samples analysed. Due to the wide range of concentrations for the unknown observed later on, a wide range of standard concentrations were analysed and used to construct the calibration plot (0.1-100 µg/mL) [Figure 2.31.a]. Extracted blank samples did not show any interfering peaks in the chromatograph. The second method adapted was for curcumin, also had a total run time of 10 min. When injected into the HPLC curcumin standard showed three consecutive peaks at around 6, 7 & 8 min, excluding the solvent front. The last peak was identified as curcumin and was used for calculations and for plotting the calibration plot [Figure 2.31.b]. The linear regression and correlation coefficient were y = 11.39x + 0.1667 and R^2 = 0.9903. The %RSD was less than 2.1% for all standard concentrations and the LOD and LOQ were 4.90 & 1.62 µg/mL; respectively. The blank samples (samples 1-BP & 7-BL) showed peaks that eluted early on during the run between 1-3 min. These were well separated from the standard drug peaks (appendix IV, b).

The third method, used for the analysis of resveratrol had a total run time of 8 min. Resveratrol standard eluted just after 6 min with a single sharp peak at 6.8 min in the chromatograph (Appendix IV, c). From the calibration plot [Figure 2.31.c], the linear regression and correlation coefficient were calculated as y = 118.69x - 36.482 and R^2 = 0.9941. The %RSD was less than 5.8% for all standard concentrations and the LOD and LOQ were 3.52 & 1.16 µg/mL; respectively. No interfering peaks were observed from blank samples. However, the HPLC method used for the analysis of ferulic acid had a much shorter run time (4 min). Ferulic acid eluted at 2.4 min as a sharp peak followed by a very small peak at 2.7 min. The first sharp peak was used for plotting the calibration plot that showed good linear regression and correlation coefficient of y = 98.487x - 7.2878 and R^2 = 0.9988 [Figure 2.31.d]. All concentrations showed a %RSD less than 5%, the LOD was 1.27 µg/mL and the LOQ was 0.42 µg/mL. Similarly, the chromatograph from sinapic acid analysis, showed a sharp peak followed by a smaller peak. Although,

very similar parameters were used for ferulic acid and sinapic acid the run time for sinapic acid was longer (10 min) and eluted at 7.8 min. All concentrations of sinapic acid standard showed %RSD less than 3%. The method was relatively less sensitive than the method used for ferulic acid noticed by the higher LOD and LOQ (2.74 and 0.90 µg/mL; respectively). The calibration plot [Figure 2.31.e] showed linear regression and correlation coefficient of y = 88.322x - 9.5325 and R^2 = 0.9964.The three methods used for resveratrol, ferulic acid and sinapic acid analysis were used in the range from 0.1-10 µg/mL. Finally, the method used for the analysis of epicatechin had the longest run time of 30 min. This was the only method that used a gradient analysis to elute the antioxidant. Epicatechin eluted at 16 min represented by a very sharp peak. A second sharp peak eluted in all the chromatographs at 22 min with several minor peaks throughout the run. The calibration plot [Figure 2.31.e] showed a good linear regression and a correlation coefficient of y = 4.5561x - 15.189 and R^2 = 0.9997 (Equal to the R^2 of the calibration plot of α-tocopherol standard). Although, the method showed the lowest %RSD for all standard concentrations (≤ 0.74%), it was the least sensitive method (LOD = 13.81 µg/mL and LOQ = 41.84 µg/mL). The range of standard concentrations used were between 5-500 µg/mL.

Table 2.9: The different system suitability parameters calculated for each of standards under investigation using the different adapted HPLC methods

Standard	*R^2*	*%RSD*	*LOD (µg/mL)*	*LOQ (µg/mL)*	*Range (µg/mL)*
α-Tocopherol	0.9997	≤ 8.92	0.25	0.75	0.1-100
Curcumin	0.9903	≤ 2.02	4.90	1.62	1-10
Resveratrol	0.9941	≤ 5.77	3.52	1.16	0.1-10
Ferulic acid	0.9988	≤ 4.81	1.27	0.42	0.1-10
Sinapic acid	0.9964	≤ 2.87	2.74	0.90	0.1-10
Epicatechin	0.9997	≤ 0.74	13.81	41.84	5-500

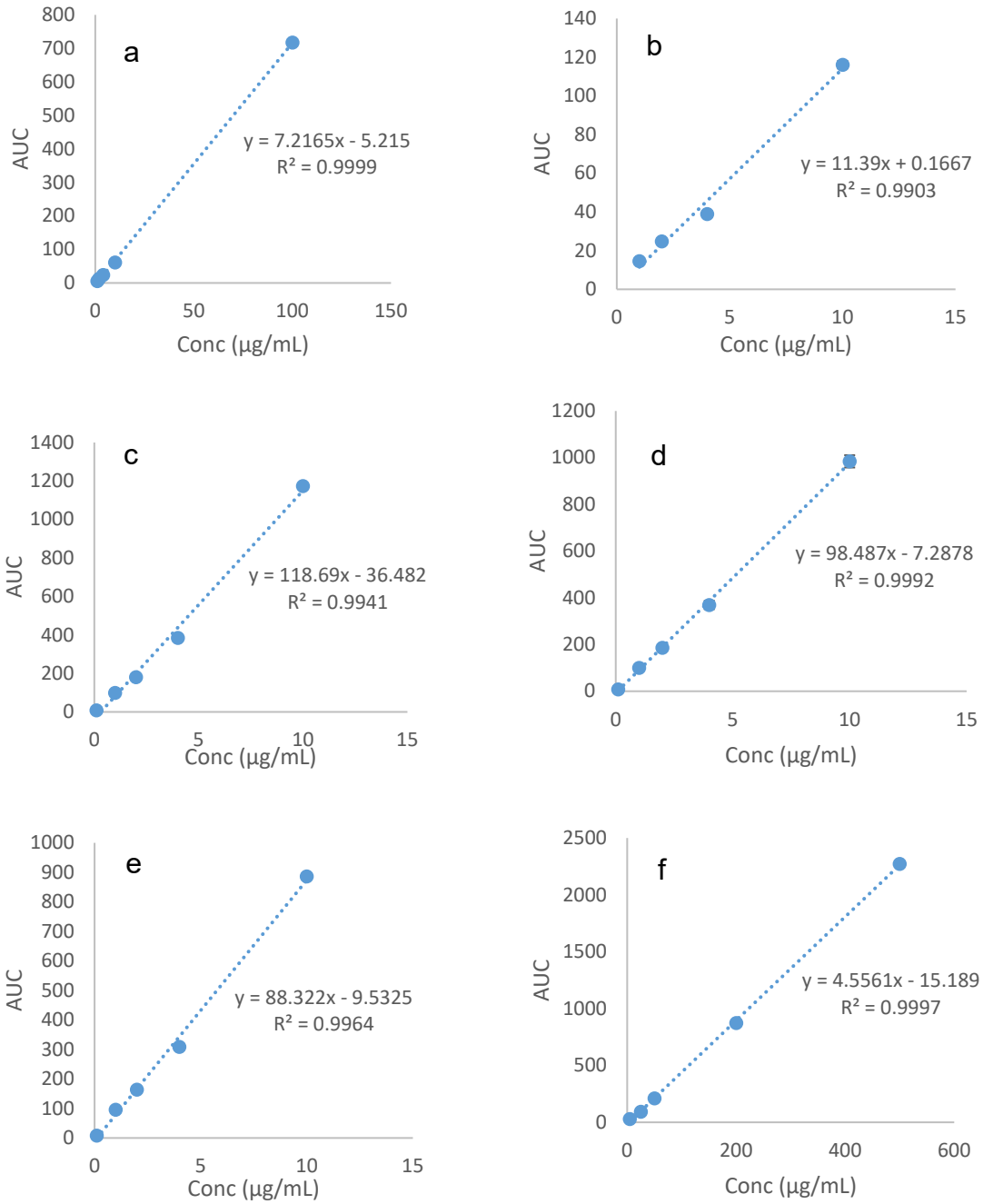

Figure 2.32**: Calibration plots for six different antioxidants under investigation using HPLC.** a: α-Tocopherol, b: curcumin, c: resveratrol, d: ferulic acid, e: sinapic acid and f: epicatechin encapsulated PLA nanoparticles. [*N* = 3, mean ± SD]

2.5.10 Determination of the drug loading efficiency and encapsulating efficiency of the different antioxidants in liposomes and PLA nanoparticles

2.5.10.1 Determination of the drug loading efficiency and encapsulating efficiency of the different antioxidants in PLA nanoparticles

After adapting and optimising the HPLC methods described in section 2.4.9, they were used to measure the concentration of the antioxidants in different nanoparticles. To calculate the %LE of antioxidants in PLA nanoparticles, antioxidant concentration in dry nanoparticles was measured after extracting the antioxidant into a solution. To calculate the %EE of antioxidants in PLA nanoparticles, the actual concentration of antioxidants in the supernatants was measured. The calculated %LE and %EE for all drug loaded PLA nanoparticles are shown in table 2.10. As shown, the %LE ranged from 5-70% and for the %EE ranged between 18-98% for the different antioxidants investigated. The orders of %LE from the highest to the lowest was ᾱ-tocopherol (67.63 ± 7.15%) > curcumin (52.35 ± 22.65%) > resveratrol (40.81 ± 29.14%) > ferulic acid (15.42 ± 4.66%) > sinapic acid (9.48 ± 4.75%) > epicatechin (5.35 ± 3.35%). %EE showed just about the same order, with exception of %EE of resveratrol (88.89 ± 0.98%) being higher than %EE of curcumin (73.8 ± 1.22%) with ᾱ-tocopherol showing the highest %EE (98.1 ± 0.54%) and epicatechin showing the lowest %EE (18.09 ± 1.95%).

It can be observed that the %EE for all drugs was higher than %LE. This can be expected, as some drug can be lost during preparation. Although, there was quite a significant difference between the two figures for resveratrol. This was attributed to the poor solubility of resveratrol in the solvent used for preparation. This low solubility led to most of drug precipitating out and lost during preparation. Data analysis, using two-way ANOVA revealed, the difference was significant $F_{(5, 24)} = 42.19$, $p < 0.001$. Bonferroni's *post hoc* multiple comparisons test showed that the significant difference was for α-tocopherol ($X_{24} = 30.47$, $p = 0.02$) and resveratrol ($X_{24} = 48.08$, $p < 0.001$), whilst the others were insignificant. The %EE is an indirect method to study how efficient has the drug being encapsulated. However, the %LE is a direct method to study the efficiency of the synthetic method to load the antioxidant into the nanoparticles and is also an indication of how uniformly the drug is distributed between nanoparticles. This may explain the

higher SD for %LE compared to %EE, which is clear with curcumin and resveratrol PLA nanoparticles.

2.5.10.2 Determination of the drug loading efficiency of the different antioxidants in liposomes

Only the %LE for all drug loaded liposomes were measured and are shown in table 2.7. The orders of %LE from the highest to the lowest was α-tocopherol (76.10 ± 1.39%) > sinapic acid (55.00 ± 6.53%) > curcumin (52.90 ± 11.11%) > ferulic acid (20.78 ± 3.45%) > resveratrol (12.04 ± 1.23%) > epicatechin (10.23 ± 1.54%). Epicatechin (a hydrophilic compound) showed a quite high %LE for liposomes when analysed directly after extrusion (98.2 ± 1.31 %). This appeared to be a false result, as both free (solubilised) and encapsulated drug could pass through the membrane filter during the extrusion step. Thus, the test was repeated after passing the produced liposomal solution through PD-10 column. This was performed to remove any free drug from the solution. The recalculated %LE for epicatechin liposomes was 10.23 ± 1.54%.

The %LE for liposomes was higher than PLA nanoparticles for most drugs except for resveratrol. Data analysis, using two-way ANOVA revealed, the difference was significant $F_{(5, 24)} = 24.19$, $p < 0.001$. Bonferroni's *post hoc* multiple comparisons test showed that the significant difference was for resveratrol ($X_{24} = -28.77$, $p = 0.037$) and sinapic acid ($X_{24} = 45.52$, $p < 0.001$), whilst the others were insignificant. Resveratrol liposomes were the only liposomal sample under investigation to show a %LE lower than the corresponding PLA nanoparticles.

Table 2.10: Summary of the loading efficiency and encapsulating efficiency for nanoparticles under investigation [N = 3, *p < 0.05, ***p < 0.001] *vs*. LE of PLA nanoparticles using two-way AVOVA, followed by Bonferroni's *post hoc* test.

	PLA nanoparticles		*Liposomes*
Drug	LE ± SD (%)	EE ± SD (%)	LE ± SD (%)
α-Tocopherol	67.63 ± 7.15	98.10 ± 0.54	76.10 ± 1.39
Curcumin	52.35 ± 22.65	73.8 ± 1.22	52.90 ± 11.11
Resveratrol	40.81 ± 29.14	88.89 ± 0.98***	12.04 ± 1.23*
Sinapic acid	9.48 ± 4.75	34.54 ± 1.09	55.00 ± 6.53***
Ferulic acid	15.42 ± 4.66	27.69 ± 2.02	20.78 ± 3.45
Epicatechin	5.35 ± 3.35	18.09 ± 1.95	10.23 ± 1.54

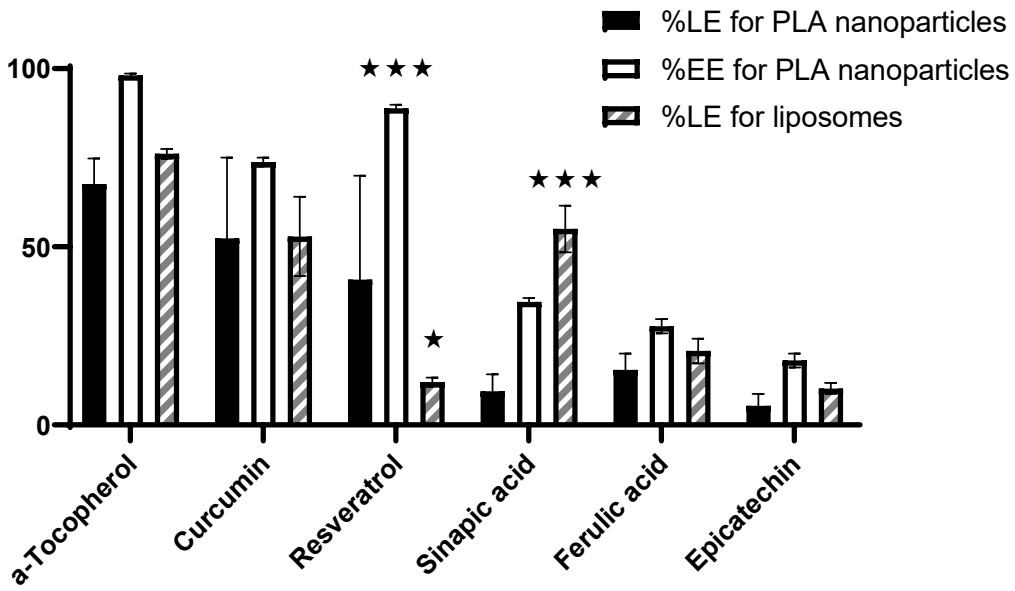

Figure 2.33: A graph representation of the loading efficiency and encapsulating efficiency for nanoparticles under investigation [*N* = 3, **p* < 0.05, ****p* < 0.001] vs. %LE of PLA nanoparticles using one-way AVOVA.

2.6 Discussion

2.6.1 Preparation of antioxidant encapsulated PLA nanoparticles

Seven different PLA samples were prepared, one blank and six encapsulated with six different antioxidants with different solubility properties (α-tocopherol, curcumin, resveratrol, ferulic acid, sinapic acid & epicatechin). The method selected for this study was DESD. As discussed above in section 2.2.2.1.2, this method has been used to encapsulate both hydrophilic and lipophilic drugs, as the use of the double emulsion system reduces the escape of hydrophilic drugs to the aqueous phase. A comparative study between DESD and DESE has been applied to alendronate-loaded PLGA nanoparticles and showed that the DESD method produces smaller particle sizes and increased %LE (Cohen-Sela *et al*.,2009). Nanoparticles produced by diffusion methods have better properties than evaporation methods (Palamoor & Jablonski, 2014). In this study, PLA was used as the nanoparticle polymer, due to its biocompatible and biodegradable properties. In addition, 2% PVA was used for its good surfactant properties. A surfactant is added in this method as an emulsifying agent and to prevent the aggregation of organic phase droplets. This method was adapted from Buhecha *et al*, 2019, where it was used to successfully encapsulate theophylline (a hydrophilic drug) and budesonide (a lipophilic drug) into PLA –nanoparticles, using the same concentration of drug, polymer and surfactant.

Samples 2-TP, 3-CP, 5-FP & 6-SP, were prepared by adding 5 mg drug to organic phase (DCM) in addition to the PLA. This was due to lipophilicity of the compounds to be encapsulated (discussed in section 1.16). Sample 4-RP on the other hand, was prepared by adding resveratrol to the co-solvent acetone. This was due to its low solubility in DCM. However, others have managed to prepare resveratrol loaded-PLA and PLA-PEG nanoparticles *via* single-emulsion solvent evaporation technique using DCM as a solvent and 1%PVA as a surfactant (Lindner *et al*., 2013). It should be noted that in the later study, the only characterisation study on the produced nanoparticles was size and %EE. Examples of additional published methods used to encapsulate resveratrol into nanoparticles include simple desolvation to form resveratrol-loaded albumin nanoparticles (Geng *et al*., 2017) and coacervation process to form resveratrol-

loaded casein nanoparticles (Penalva *et al*., 2018). Sample 7-EP was prepared by dissolving the drug into the aqueous phase, the PVA solution. Once more, this was due to its good solubility in water (discussed in section 1.16.6). Different studies prepared epicatechin-loaded albumin nanoparticles using desolvation technique (Ghosh *et al*., 2016, Yadav *et al*., 2014).

PLA can be dissolved in either DCM or ethylacetate. Both solvents can be easily removed by rotary evaporation after nanoparticle formation. Although, ethylacetate is less toxic than DCM, studies have shown that it produces larger particle size (Rachmawati *et al*., 2016). The addition of the organic phase to the aqueous phase containing PVA (as a surfactant) while homogenising at high speed (15000 rpm) led to the formation of an emulsion. This speed was previously applied by Buhecha *et al*. and was hence adapted for this study. Other studies applied sonication to form the initial emulsion system (Cohen-Sela *et al*., 2009, Palamoor & Jablonski, 2014). Some drugs are sensitive to sonication, as it leads to generation of heat within the sample and showed reduced stability even after 2 min. For this reason, homogenisation was preferred as a method of mixing (Palamoor & Jablonski, 2014). The initial emulsion was further stabilised by the addition of acetone and homogenisation. An optimisation study for DESD and DESE methods showed that the DCM with acetone, as co-solvent is the ideal organic phase to encapsulate vancomycin hydrochloride (Palamoor & Jablonski, 2014). Adding excess amount of water led to force the organic phase to escape leading to the formation of solid nanoparticles suspended in water. These were detected at this point with a LM (images not taken). At this point, the success of the method was determined by visual examination of the suspension. Separation of the organic phase or appearance of PLA aggregates was considered unsuccessful encapsulation.

The next step was removing the organic solvents using rotatory evaporator. Leaving the suspensions overnight on a magnetic stirrer ensured the removal of any residual solvent. Buhecha *et al., 2019* compared the two techniques of solvent removal and found that using a rotatory evaporator and applying a negative pressure produced nanoparticles with smaller particle size compared to overnight

stirring. This can be attributed to Ostwald ripening, where smaller particles dissolute over time and the dissolved material re-depose on the surface of larger particles (Liu & Hu, 2020). Samples were then centrifuged to separate the nanoparticles from the water phase. The method started with 205 mg solid material (200 mg polymer and 5 mg drug) and each batch produced from 100-150mg of dry powder containing nanoparticles. This is almost equivalent to 49-73% percentage yield. Material could have been lost during preparation and/or adhered to glassware used.

α-Tocopherol has been previously encapsulated in polymeric nanoparticles *via* an emulsion evaporation method using PLGA as a polymer and PVA or sodium dodecyl sulphate as a surfactant (Zigoneanu *et al*., 2008). Additionally, PLA and PLGA nanoparticles were prepared *via* a nanoprecipitation method using acetone as a solvent (Varga *et al*., 2019). Curcumin, however, has been loaded in various polymeric nanoparticles using different but similar methods. For example, Rachmawati *et al*., managed to optimize the encapsulation of 5% curcumin within PLA nanoparticles *via* emulsification-solvent evaporation method using DCM as a solvent and vitamin E polyethylene glycol succinate as a surfactant (Rachmawati *et al*., 2016). Others used PEG-PLA as a polymer using the same method with different solvents (ethylacetate or ethanol) and surfactants (ethyl-trimethylammoniumbromide or 1% PVA) (El-Naggar *et al*., 2019, Thong *et al*.,2014, Liang *et al*., 2016). Ferulic acid has also been encapsulated within different polymeric nanoparticles in previous studies using different methods such as nanoprecipitation and PLGA as polymer (Bairagi *et al*., 2018) and ionic gelation and chitosan as polymer (Panwar *et al*., 2016). Ionic gelation was also used to prepare sinapic acid loaded chitosan-nanoparticles (Balagangadharan *et al*., 2019).

2.6.2 Preparation of antioxidant encapsulated liposomes

Seven different liposomal samples (8-14) were prepared, one blank and six encapsulated with six different antioxidants (α-tocopherol, curcumin, resveratrol, ferulic acid, sinapic acid & epicatechin). The method applied to prepare the liposomes in this study is a passive loading technique, where the drugs were

added during preparation (described in section 2.2.2.2). Mechanical dispersion using an extruder was used to downsize the formed liposomes. This method was adapted from Dichello *et al*., 2017. Phospholipids are abundant in the human cells and so, have the advantage of being biocompatible. Their known amphiphilic structure provides an additional advantage of self-assembly to supramolecular structure such as liposomes in aqueous media (Li *et al*., 2015).

DPPC is a synthetic phospholipid that has shown to form more stable paclitaxel-liposomes than DSPC and DMPC (Campbell *et al*., 2000). DPPC was used to form the lipid bilayer structure of the liposomes. All samples started with the preparation of the lipid solution. The original method used chloroform to dissolve DPPC. Chloroform is considered a harmful, toxic and a carcinogenic solvent and therefore, it was replaced with ethanol. The antioxidants for samples 9-13 were added to the lipid solution prior to drying, due to the lipophilic nature and good solubility of these compounds in ethanol. Epicatechin, however, did not dissolve thoroughly in ethanol and so, was added to the aqueous phase after drying the lipid. Drying the lipids and adding the aqueous phase while shaking vigorously and sonicating over an ultrasonic bath led to the detachment of the lipid layer forming MLV liposomes suspended in the aqueous phase (mechanism described in section 2.2.2.2). The extrusion step was performed to reduce the size of these liposomes to form SUV. A membrane with a pore size of 200nm was selected. A comparative study to optimise the different parameters of extrusion, showed that membranes with pore size less than 200nm forms liposomes slightly bigger than the nominal pore size (Ong *et al*., 2016). Nevertheless, it has been recommended that filter pore size should be ≥ 200 nm, to extrude liposomes comfortably by a manual extruder. This is a limitation of manual extruders caused by the backpressure of the filter and the amount of pressure that can be applied (Hope *et al*., 1993). The solution was initially heated up to 60ºC and passed through the extruder until just below 41ºC (T_c of DPPC). T_c is the temperature at which lipids transit from gel to liquid crystalline state (Li *et al*., 2015). For this reason, heating the solution eased the passage of lipids through the membrane. Previous studies showed that increasing the temperature of the initial solution does not affect size and polydispersity of final liposomes (Ong *et al*., 2016). The same study demonstrated that increasing the number of cycles of passing through

the extruder reduces the size and polydispersity of the product until a certain number of cycles where it levels off. For this reason, the number of passage cycles was maintained to 21 cycles for each batch. Due to the instability of liposomes found by LM, SEM & zetasizer, all samples were made freshly prior to further characterisation and tests that require samples to be dry such as SEM, FT-IR and DSC were not performed on liposome samples.

Previous research has investigated to enhance the bioavailability of different antioxidants using liposomes. For example, α-tocopherol was encapsulated within DPPC and cholesterol liposomes to enhance the uptake and subcellular distribution in lungs (Suntres *et al*, 1993). Additionally, it was encapsulated within niosomes using Span 60 and Tween 80 as non-ionic surfactants to increase its stability and provides a sustained release profile (Basiri *et al*., 2017). Several methods have been used to encapsulate curcumin into liposomes, including film-hydrating method, freeze–thawing method, injection method and reversed-phase evaporation method with variable improved application against cancer compared to un-encapsulated curcumin (Feng *et al*., 2017). Thin film method followed by sonication or extrusion is considered the most studied method for the production of resveratrol liposomes. This method is limited by its difficulty to be applied on large scale. The use of Proliposomes (Spontaneous formation of liposomes upon addition of aqueous phase) however, was studied for resveratrol liposome production designed for industrial scale (Isailovic *et al*., 2013). Again, ferulic acid liposomes were prepared, characterised and evaluated in earlier studies using different methods, different lipids and surfactants (Qin *et al*., 2008, Pamunuwa *et al*., 2015). Liposomes were also used to enhance transdermal delivery of catechins (catechin, epicatechin and epigallocatechin-3-gallate) by incorporating anionic surfactants and ethanol in the method of preparation (Fang *et al*., 2006). Furthermore, Tea polyphenols (aqueous solution) and α-tocopherol (lipophilic solution) were co-encapsulated with liposomes by reverse-phase evaporation method (Ma *et al*., 2009).

2.6.3 Particle size and size distribution of different liposomes and PLA nanoparticles

The particle size distribution, PdI and surface charge of nanoparticles are highly critical characteristics to be studied when creating pharmaceutical products. These aspects of nanocarriers can affect the bulk characteristics, drug performance, processability, stability and appearance of the final product. When formulating nanoparticle-based systems, a consistent and reproducible analysis method of their mean diameter, heterogeneity and charge is crucial (Danaei *et al*., 2018). Various methods of determining the size of nanoparticles are available including microscopy, diffraction and scattering techniques, hydrodynamic techniques, coulter counter, flow cytometry and optical density method (Danaei *et al*., 2018). Numerous studies have applied light scattering techniques to measure the particle size, particle size distribution and surface charge (Ong *et al*., 2016, Cohen-Sela *et al*.,2009, Buhecha *et al*, 2019, Isailovic *et al*., 2013). These have the advantages of being non-invasive and give good statistical informative results (Danaei *et al*., 2018). For this reason, these techniques have been applied in this study (discussed in previous sections 2.4.4 and 2.4.5)

In the current study, liposomes have shown smaller particle size (180-261 nm) in comparison to PLA nanoparticles (300-600 nm). Different factors have been reported that can affect the size of the nanoparticles, such as polymer or lipid concentration, the organic solvent, temperature, ionic strength and method of preparation (Oliveira *et al*., 2013, Kulkarni & Singh 1995). Although, Cohen *et al*., have managed to produce PLA nanoparticles with smaller particle size (100- 150 nm) using DESD method, some variation was noticed in their method. First, they applied sonication instead of homogenisation to form the initial emulsion, which could introduce more energy and form smaller emulsion droplets to start with. Secondly, they only used a rotatory evaporator (reduced pressure) to remove the organic solvent. In the present study, an additional step was added, where the solution was left overnight over a magnetic stirrer to ensure complete removal of organic solvent. This could explain the larger particle size of PLA nanoparticles formed. Similarly, this was observed by Buhecha *et al.* and attributed to Ostwald ripening (discussed in section 2.6.1). Additionally, Merlin *et al*. applied DESE

method to prepare ferulic acid-loaded PLGA nanoparticles and showed an average particle size 483 nm using DLS (Merlin *et al*., 2102). Anais *et al*., 2009 tested the different variables that might affect the characteristics of PLA nanoparticles. They focused on studying emulsification diffusion method. They showed that increasing the stirring rate from 8,000 rpm to 24,000 rpm could decrease the mean particle size from 554 nm to 276 nm. However, they showed that this caused reduction in the encapsulation efficiency by 20%. They also showed the effect of polymer concentration. They found that using 3% PLA instead of 0.5% reduced the mean particle size from 626 nm to 302 nm. Additionally, they showed that using smaller diffusion volume produces a higher disperse system in terms of particle size (Anais *et al*., 2009). Rachmawati *et al.,* 2016 also encapsulated curcumin into PLA nanoparticles. They managed to prepare smaller nanoparticles (around 247 nm) using ESE method and DCM as the organic solvent than the curcumin-loaded PLA nanoparticles prepared in this study (319.5 ± 80.29 nm). However, their SEM images, FT-IR spectrum and their surface zeta-potential (-7.88 mV) indicate the adsorption of curcumin on the surface rather than encapsulated inside the particles (Rachmawati *et al*., 2016).

On the other hand, the extrusion step in liposome preparation was the main reason for the smaller particle size noticed in the results. The filter membrane pore size used for extrusion was 200nm, which was close to the diameter of the particle size of liposomes. Previous studies produced liposomes using extrusion method with similar particle size range (150-270 nm) (Isailovic *et al*., 2013). Varga *et al*., although used a different method to produce PLA nanoparticles, revealed that the concentration of PLA in the organic phase effects the particle size produced. They showed that when using 1.25 mg/mL PLA, nanoparticles where 120 nm in diameter and when PLA concentration was increased to 10 mg/mL, nanoparticles diameter increased to 200 nm (Varga *et al*., 2019). The concentration of PLA in this study was 20 mg/mL, which may explain the large mean particle size of PLA nanoparticles produced.

Alongside particle size, the PdI must also be taken into consideration, as it is an indication of the particle size distribution in the suspension. When PdI is equal to 0, this means the entire particles are in monodisperse system and when it's equal to 1, the system is completely heterodisperse. It can be noticed from the results that liposomes were closer to a monodisperse system, while PLA nanoparticles were closer to a heterodisperse system. This was explained by the extrusion step applied for liposomes. As for PLA nanoparticles, there was no separation step. When using lipid-based transporters, such as liposome and nanoliposome preparations, a PDI of 0.3 and below is thought to be acceptable and indicates a homogenous population of nanoparticles (Danaei *et al*., 2018). In this concept, all liposomal samples (8-14) have an acceptable PdI. The homogeneity of PLA nanoparticles, however, may need some method or step of refinement.

The optimum size of nanoparticles required for optimum drug delivery to any specific organ is not actually something set and depends entirely on trial and error. Although, there has been reports stating that, the smaller the nanoparticles, the slower they are cleared from the body (Ostro & Cullis, 1989, Alexis *et al*., 2008). However, there has been a study on the effect of particle size on the distribution of gold PEGylated nanoparticles after i.v. injection. This showed that the optimum particle size to target the blood capillaries and support tissue (mesangium) of the kidneys is ≈75 ± 25 nm (Choi *et al*., 2011). Furthermore, a separate study found that the larger (350-400 nm) PEG-PGLA nanoparticles are localised 5-7 more with the kidneys (proximal tubules selectively) than any other organ after i.v. injection (Williams *et al*., 2018). Future studies can be performed to optimize particle size after completing all characterization properties and delivery capability.

2.6.4 Surface charge of different liposomes and PLA nanoparticles

Zeta-potential relates to the surface charge on the nanoparticles causing either repulsion or attraction between neighbouring particles and so reflects stability of a suspension. The higher negative charge of the PLA nanoparticles

compared to liposomes was explained by the use PLA (negative charge of the carboxylic acid) for the polymeric nanoparticles and DPPC (a zwitterionic lipid) for the liposomes. This rationalised the fact that PLA nanoparticles were more stable than liposomes, due to the repulsion effect between particles. This negative zeta-potential of PLA nanoparticles was also reported in previous work. For example, quercetin-loaded PLA nanoparticles prepared *via* solvent evaporation method using a plant extract as surfactants showed a zeta-potential -50 ± 0.6 mV (Kumari *et al*., 2012). In a separate study, blank PLA nanoparticles prepared using ESE method also showed comparative zeta-potential (-36.18 mV). However, the addition of curcumin to the organic phase, in an attempt to encapsulate it into the nanoparticles led to a more neutral surface charge (-7.88 to -1.12 mV). This was explained by the masking effect of curcumin to the carboxylic groups, indicating that the drug was adsorbed on the surface rather than inside the nanoparticles (Rachmawati *et al*., 2016). The small negative zeta-potential of liposomes was also reported elsewhere. Apparently, DPPC liposomes can show positive, negative or even neutral zeta-potential. The zwitterionic molecules of DPPC can reorient their polar heads according to the ionic strength of the solution. At a low ionic concentration, the choline groups are located below the phosphate group leading to negative zeta-potential. Whereas, at a higher ionic concentration the situation is reversed. The zero zeta-potential occurs when the polar heads are oriented parallel to the liposome surface (Chibowski & Szczes, 2016). This justification and the fact that liposomes where prepared by deionised water explained the small negative zeta-potential observed in this study.

Over-all, nanoparticles with a zeta-potential magnitude over ±30 mV will theoretically have a good stability and those with a zeta-potential less than ±5 mV will ultimately coagulate by means of different attraction forces between particles, such as van der Waals, hydrophobic interactions, and hydrogen bonding (Kumar & Dixit, 2017). It has been documented that positively charged particles are absorbed faster by cells due to their attraction to the anionic cellular membrane, but they are also known to be more toxic due to the disruption of the cell wall (Clogston & Patri, 2011). Although, liposomes might show instability due to their small surface charge, this can be an advantage with respect to drug release. Reports showed that neutrally charged liposomes could easily release about 65-

70% of their cargo within 24 hours, in comparison to charged liposomes that release only 25-30%. This was interpreted by the fact that charged lipids lead to a tighter molecular packing of the lipid bilayer, leading to reduced rate of drug release (Katragadda *et al*., 1999). The zeta-potential can be altered as required for drug delivery by different processes, for example by the addition of varying concentration of a stabilizer or by manipulating the surface using positively charged mediators. In this study, no modification has been made to the nanoparticles or to the method of preparation. The purpose was to study and compare the characteristic of nanoparticles loaded with different antioxidants using the same preparation method and then manipulation of surface charge can be performed in future work.

2.6.5 Studying the stability of curcumin loaded liposomes

It is important for any particulate drug delivery system to preserve their size, size distribution and charge upon storage. Liposomes made out of DPPC only have shown in previous studies to be instable and therefore, usually combined with a fraction of cholesterol to increase rigidity (Anderson & Omri, 2008) or with a charged lipid such as dimethyl dioctadecyl ammonium bromide to prevent aggregation (Manosroi *et al*., 2008). Since, in the current method liposomes were composed of DPPC only, it was essential to study their short-term stability. Sample (10-CL), curcumin loaded liposomes, was selected for this study. The particle size, size distribution and zeta-potential were measured on days 1, 2, 3, 4, 8 and 10. After day 10, a significant change in the colour and consistency was noticed, which led to the discontinuation of the test.

On the first and second days, mean particle size (132 ± 79.18 and 147.7 ± 91.77 nm) was comparable to all the liposomal samples prepared in this study, although, a slight insignificant increase in size was noticed on the second day. The actual size distribution curve on these first days was represented as one single sharp peak. Additionally, the PdI was less than 0.2. These two markers are indicators that the population of particles were monodisperse. From day 3, a second peak appeared in the particle size distribution graph. Representing the

population as a bimodal distribution with two discrete peaks at 100 to 190 nm and 4600 to over 5200 nm. This has been attributed to aggregation (flocculation) or fusion (coalescence). Aggregation is the creation of larger units of liposomal material by combining smaller liposomes. In theory, this can be reversed by applying agitation, sonication or changing the temperature. Coalescence, however, is an irreversible process; it is the adhesion of the aggregated liposomes to form a new colloidal structure. These physical instability processes are an indication of an unstable system (Yadav *et al*., 2011).

As expected, liposomes have demonstrated to be physically unstable. This has also been shown in other studies of liposomes formulated from pure DPPC. For example, results from a study on the influence of cyclodextrines on the stability of liposomes showed that both size and PdI increase upon short-term storage (7 days) of DPPC only liposomes (Puskas & Csempesz, 2007). This aggregation or fusion upon storage has also been reported with other neutral liposomes such as DSPC liposomes but not with positively or negatively charged liposomes. The stability of charged liposomes was interpreted by the electrostatic repulsive forces that prevented aggregation (Katragadda *et al*., 1999). As mentioned above, different approaches can be made to increase the stability of liposomes, but none have been applied in this study. For this reason, liposomal samples (samples 8-14) were made freshly for each consequent test.

2.6.6 Studying surface morphology using LM and SEM for different liposomes and PLA nanoparticles

Figures from LM of liposome samples showed spherical shaped particles. It can also be noticed in figure 2.9.d. the yellow pigmentation of the particles. This was mainly due to the yellow colour of curcumin. The images appeared to show that the liposomes were a mixture of LUV and SUV. The size estimation for liposomes was conducted using a graticule (150-300 nm). Previous studies have also used optical microscopic to study the shape and type of liposomes (Yasmin *et al*., 2014, Degim *et al*., 2010). Both these studies showed that the liposomes made by thin film hydration method formed MLV. Even though, their method was similar to the current method applied, they did not apply any downsizing step after the

hydration of lipids. This may explain why their liposomes were larger. Similar images have been posted by Nguyen *et al*., 2016. They showed that curcumin-loaded liposomes made from DOPE formed liposomes in the micro-range and when using sonication as a downsizing technique they produced liposomes < 100 nm in size (Nguyen *et al*.,2016). The images from LM for liposomes, however, were not clear and do not give a clear morphology of the liposomes, due to the limitation of the instrument. It was not possible to use SEM on liposomal samples due to the fragile state of liposomes. A review article on the different techniques to characterise the morphology of liposomes explained the different reasons behind this drawback. It mentioned that freeze-drying liposomes leads to loss of structure and formation of lumps and crystal material. It also stated that applying high negative pressure during imaging could also disrupt its construction. As a final point, the review concluded that SEM is not commonly used on liposomes due to the need for fixation or drying prior to imaging (Robson *et al*., 2018). Ideally, liposomes should either be stabilised by cryo-protective agent and freeze dried for SEM imaging or examined with an SEM equipped with a liquid nitrogen chamber used to give more clear images to analyse their morphology. Other researchers used cryogenic transmission electron microscopy (cryo-TEM) to study the morphology of liposomes without disturbing their native form (Manosroi *et al*., 2008, Dichello *et al*., 2017). These can be performed in future work.

The morphology of PLA nanoparticles (samples 1-7) was studied using SEM. The shape of the nanoparticle in the SEM images, were spherical, smooth surface with variable size. It cannot be concluded using only SEM, whether PLA nanoparticles are nanospheres or nanocapsules. The size of the PLA nanoparticles using the TIFF software (350-800 nm) was comparable to those obtained from the zetasizer. α-Tocopherol-loaded PLA nanoparticles showed larger particles with several giant ones (up to 2000 nm) noticed in figure 2.16.a. This was also consistent in the results obtained from the zetasizer, where α-tocopherol-loaded PLA nanoparticles were slightly larger than all other samples. The absence of any residual drug crystals in the SEM images, indicate that no washing step was necessary after the centrifugation step. SEM is widely used for the characterisation of the surface and shape of nanoparticles. For example, it has been used in an optimisation study to compare blank particles to curcumin-loaded

PLA nanoparticles (Rachmawati *et al*., 2016). They too found that both blank and loaded particles were spherical. Additionally, blank PLA nanoparticles prepared by DESE method were also found by SEM imaging to be smooth and spherical (Moorkoth & Nampoothir, 2014). SEM was also used to study the morphology of sinapic acid-loaded chitosan nanoparticles (Balagangadharan *et al*. 2019) and spray-dried solid dispersions containing ferulic acid (Nadal *et al*, 2016).

2.6.7 Assessment of Surface Characteristics of the Nanoparticles using FT-IR Spectroscopy

FT-IR was used to confirm the composition of the PLA nanoparticles by identifying and comparing different functional groups. The blank and drug-loaded PLA nanoparticles, PLA crystals, pure drugs used and pure PVA were analysed over the wavenumber range 400 to 4000 cm^{-1}. The correlation factor calculated by the computer software attached to the FT-IR, showed that the spectrum of the drug loaded-PLA nanoparticles was highly similar to the spectrum obtained from PLA. This shows that the PLA is not altered by the preparation method. Another assumption can be taken from these results, is that the drug is encapsulated inside the particles and not adsorbed on the surface. An alternative explanation is that the ratio of drug to PLA is too small to be detected by the instrument.

Various researchers have used FT-IR to determine the interaction between the polymer and the encapsulant. For example, Varga *et al*., 2019 used this technique, to characterise the structure of α-tocopherol-loaded PLA nanoparticle. They showed that α-tocopherol sensitive bands appeared at 1150 and 1000 cm^{-1}. These are only visible in pure α-tocopherol (appendix III. a) and cannot be seen in the α-tocopherol-loaded nanoparticles in the current study. They also mentioned that he carbonyl (C=O) group of the PLA should appear at around 1750 cm^{-1}. Obviously, this only appeared in the pure PLA and drug-loaded PLA nanoparticle spectra. The bands at 865 cm^{-1} and 751 cm^{-1} are characteristic of the PLA, and no shift is detected (Varga *et al*., 2019). This was also noticed in this study, indicating no change in PLA structure [Figure 2.16].

Another study used FT-IR to study nanoparticle structure was Rachmawati *et al*., 2016. They used it to confirm that curcumin was bound to PLA *via* a hydrogen bond in curcumin-loaded PLA nanoparticles. In their study, they noticed several shifts in the curcumin and PLA specific peaks. For example, they reported that sharp peaks at 1601 and 1427 cm^{-1} due to stretching vibration of C=C of the benzene ring and olefinic bending vibration of C-H bound to the benzene ring in pure curcumin spectrum shifted when compared to curcumin-loaded PLA nanoparticles. However, in the present study, these peaks were only observed in pure curcumin spectrum and were absent in curcumin-loaded PLA nanoparticles (Appendix III. b). Moreover, the peaks at 1272 cm^{-1} and 854 cm^{-1}, representing the vibration of C-O in –C-OCH3 of phenyl ring of curcumin, were absent in curcumin-loaded PLA nanoparticle spectrum. Additionally, the bands at 865 cm^{-1} and 751 cm^{-1}, the mountainous triplet peak at 1131, 1088, and 1044 cm^{-1}, corresponding to C-O vibration in –CO-O- and the sharp C=O peak at 1750 cm^{-1} are characteristic of the PLA, and no shift is observed in this study [Figure 2.17].

A different study compared pure resveratrol to resveratrol-loaded PLGA nanoparticles *via* FT-IR (Miele *et al*., 2019). This study showed that resveratrol is presented in FT-IR spectrum as bands at 3200, 1605, 1584, 964 and 829 cm^{-1} due to O-H stretching, C-C aromatic double bond, C-C olefinic stretching, trans olefinic bond and bending vibration of C-H in the aromatic ring; respectively. Even though, these characteristic bands were clear in the pure resveratrol spectrum during the present study, it was not possible to distinguish them in the resveratrol-loaded PLA nanoparticle spectrum [Figure 2.18]. Both pure ferulic acid and pure sinapic acid spectrums showed similar peaks (appendix III. d & e). For example, in both spectra an aromatic C=O stretching appeared around 1650 cm^{-1} and an aromatic C=C stretching vibration appeared between 1430 and 1630 cm^{-1}. This similarity was linked to of their similar chemical structure [Figure 1.17]. These characteristic peaks were reported in previous work for pure ferulic acid (Nadal *et al*, 2016) and for pure sinapic acid (Balagangadharan *et al*., 2019) and were not detected in the drug-loaded PLA nanoparticle spectra during the current study [Figures 2.19 & 2.20].

Finally, the FT-IR spectrum of pure epicatechin showed characteristic peaks of its structure. For example, a peak at 1520 cm^{-1} shows the aromatic C=C group, and the peaks at 1140 cm^{-1} and 1015 cm^{-1} represent of the C–O–C group. These peaks have been confirmed in other research for pure epicatechin (Perez-Ruiz *et al*., 2018), but are not detected in epicatechin-loaded PLA nanoparticle spectrum in this study [Figure 2.21]. In all drug loaded PLA nanoparticle FT-IR spectra produced in this study (except sinapic acid-loaded PLA nanoparticles), a strong broad O-H stretching appears between 3550-3200 cm^{-1}. As all antioxidants under investigation [Figure 1. 17], and PLA [Figure 1.15] do not contain an aliphatic O-H group in their structure this could indicate the presence of residual PVA.

2.6.8 Thermal analysis of drug-loaded PLA nanoparticles

The thermal response of the drug loaded PLA nanoparticle (samples 2-7) were compared to PLA standard and to blank nanoparticles (sample 1-BP) in order to determine any similarities and differences due to interactions between the components. An endothermic response as a step change was observed in all thermographs in the range 40-46ºC, including PLA standard representing the T_g of PLA. This could indicate that the glass transition phase of the PLA was not influenced by the preparation procedure. This T_g of PLA was also reported in previous studies (Buhecha *et al*., 2019). However, in some thermograms there were additional peaks. For example, there was an additional wide endothermic peak observed in the α-tocopherol-loaded PLA nanoparticles thermogram [Figure 2.13]. This could be explained by the oxidation of the drug. It has been documented that α-tocopherol is highly oxidized at high temperature to a number of products including α-tocored and dimers that may be formed by a combination of tocopheroxyl radicals. (Niki & Abe, 2019) [Figure 2.32].

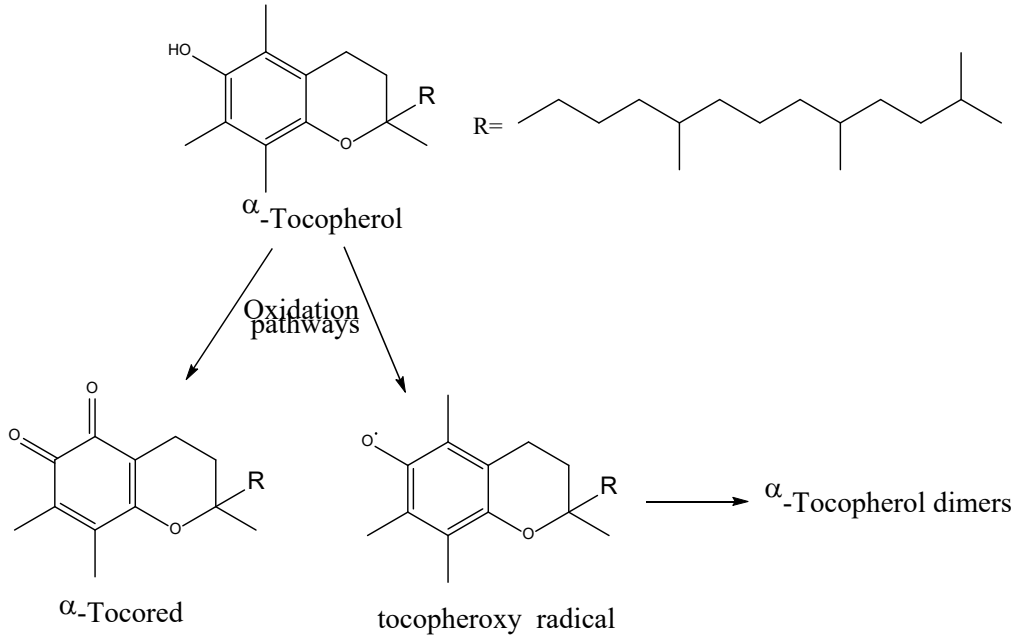

Figure 2.34: **Oxidation products of α-tocopherol produced.** Heating α-tocopherol results in the formation of α-tocored and dimers formed by a recombination of tocopheroxyl radicals.

Although, the melting point of curcumin was reported in a previous work at 180ºC with a thermal decomposition occurring at two steps 205-441ºC and 441-630ºC (Fugita *et al*., 2012). In the current study however, there was only a small endothermic peak around 210ºC, and no peak at 180ºC in the thermogram produced from the curcumin loaded PLA nanoparticles [Figure 2.14]. The absence of curcumin melting peak in a curcumin-loaded nanoparticles has been reported previously. It was explained by the interaction of curcumin inside the nanoparticles, suggesting that curcumin was in an amorphous form for that reason (RachmawatI *et al*., 2016). Ideally, samples would have been heated to a higher temperature, but due to the instrument limitation, the heating range was set between 25 -250ºC. In this study, the endothermic peak around 210ºC could be due to the beginning of curcumin decomposition as explained by Fugita *et al*., although this peak was not observed in the work proposed by Rachmawati *et al*., 2016.

An endothermic response has been observed in the thermogram of sinapic acid loaded PLA nanoparticles at 184ºC [Figure 2.16], which is slightly below the

reported melting point of pure sinapic acid at 204ºC (Nechipadappu & Trivedi, 2018). This could mean that the melting point of sinapic acid as a starting material has been influenced by polymer or by the processing method. Furthermore, the melting point of ferulic acid reported at 171ºC (Yang *et al*., 2015) was slightly below the noticed melting point in the thermogram obtained from ferulic acid loaded PLA nanoparticles at 186ºC [Figure 2.17]. No extra endothermic peak representing the melting point of resveratrol [Figure 2.15] and epicatechin [Figure 2.18] were observed with the drug-loaded PLA nanoparticles. This was a drawback due to the selected heating range which was below the melting points of the drugs.

2.6.9 Determination of the drug concentration in different samples using high performance liquid chromatography (analytical method validation)

The aim of analytical method validation is to determine that it is suitable for its planned purpose. The International Council for Harmonisation (ICH) has set up guidance on how to validate analytical procedures, ICH Topic Q2 (R1). It states that for any new assay developed to measure the content or potency of a substance, five characteristics should be considered. These analytical procedure characteristics are accuracy, precision, specificity, linearity and range. The guidelines define each characteristic and indicates the methodology of how to calculate them. As all the methods applied in the current study are in fact adapted from previously validated assays, they only required revalidation. The ICH guidelines notes that the degree of revalidation depends on the nature and degree of variation. The accuracy of an analytical method expresses the closeness of the found value to the expected value. The accuracy may be concluded once precision, linearity and specificity have been recognized. For this reason, it was not calculated in this study.

The precision of an analytical method expresses the closeness of multiple measurements of the same homogenous sample. For a new method validation, it should be recognised by three measurements: repeatability (same day), intermediate precision (within the same laboratory) and reproducibility (between laboratories). Because in this study, methods were adapted and simply

revalidated, only repeatability was calculated and was expressed as %RSD. All %RSD measurements were below %10, which is considered an acceptable limit for low concentration. Higher concentrations showed %RSD less than 2% for all methods. Previous methods showed comparable results. For instance, a method developed to measure α-tocopherol in human erythrocytes showed a determination precision between 5.2% and 6.1% (Solichova *et al*., 2003). Other studies showed lower %RSD, nevertheless determinations were made at higher concentrations. For example, the method developed and validated to measure the concentration of resveratrol in polymeric nanoparticles showed a maximum %RSD = 1.5%. Still, the lowest concentration analysed for precision in that study was 10 µg/mL (Lindner et al., 2013). In the current method used for the determination of resveratrol, that was the highest concentration used for the determination of precision, which showed %RSD = 0.1%. This concluded our methods to show acceptable repeatability.

The linearity represented as coefficient of determination; R squared value (R^2), shows how proportional the results are to the concentration of standard in the calibration plot. The closer it is to one, the more linear and so, can be more reliable in predicting the unknown (Moosavi & Ghassabian, 2018). In this study, all the R^2 values were between 0.9903 – 0.9997, which are within the acceptable limit of 1±0.03. These figures were comparable to the original developed methods. For example, the original methods developed and validated for the determination of resveratrol and epicatechin showed R^2 equal to 0.9999 and 0.9980; respectively (Lindner *et al*., 2013, Gottumkkala *et al*., 2014). In the present study, these methods were adapted and revalidated showing R^2 equal to 0.9941 and 0.9997 for resveratrol and epicatechin respectively. This demonstrates that the current methods to be linear and therefore reliable.

Specificity is the ability of an analytical method to measure the analyte in the presence of expected impurities or excipients. This was achieved by analysing solvents and blank nanoparticles (samples 1-BP & 7-BL) in the same manner as the drugs. Once more, Lindner *et al.,* and others used the same approach to demonstrate specificity and selectivity. This proves our methods are specific for

the analyte as no interference was noticed from any impurities. Finally, according to the ICH, the range is the interval between the highest and lowest concentration of analyte in the test sample for which precision, accuracy and linearity has been established. The range can vary according to the test samples. In Gottumkkala *et al*., 2014, the range of epicatechin was 100-600 µg/mL, while in the method under examination the range of epicatechin concentration was 5-500 µg/mL. In the current study, validation characteristics were all established within the range of drug concentrations under investigation.

At this point, according to the ICH guidelines revalidation was established and the methods were considered suitable for the analysis of drugs under investigation. Nevertheless, LOQ and LOD were calculated to accomplish further confidence. Modifications to a method can change these limits. For instance, the slight modification in the method developed by Gottumkkala *et al*. increased the LOD and LOQ from 0.036 & 0.45 µg/mL for the original method to 13.81 & 41.84 µg/mL in the current method used for analysis of epicatechin. However, the calculated drug concentration should be above the LOQ, and this was practised in the current study.

2.6.10 Determination of the drug loading efficiency and encapsulating efficiency of the different antioxidants in PLA nanoparticles

The %LE measured and calculated using HPLC showed that %LE of α-tocopherol PLA nanoparticles and liposomes was the highest compared to other drug loaded nanoparticles. The lowest %LE was noticed for epicatechin PLA nanoparticles and liposomes. This was linked to the lipophilicity of the drugs. α-Tocopherol being the most lipophilic with a log P 10.5 and epicatechin the most hydrophilic with a log P 1.02. The physicochemical properties of all antioxidants under investigation were discussed in detail in section 1.16.

Most %LE calculated in this study was noticed elsewhere, but some can still be improved. For example, the high %LE of α-tocopherol in PLA nanoparticles was similarly reported in another study. Vagra *et al*. applied nanoprecipitation method

using acetone and Pluronic F127 as surfactant to prepare α-tocopherol-loaded nanoparticles. They optimised the preparation method to reach a %LE of 66.15% in PLA nanoparticles, which is comparable to the %LE of sample 2-TP (67.63 ± 7.15%). In their publication, they mentioned that using different types of PLGA as polymer can increase the %LE to 75.7% and 87.69% (Vagra et al., 2019). Additionally, the %LE calculated in the current study for sample 3-CP (52.35 ± 22.65%) was also similar to the %LE calculated in the previous study by Rachmawati *et al*. (59.31 ± 3.87%). As discussed earlier, they optimised preparation parameters using ESE method to produce curcumin-loaded PLA nanoparticles using DCM as solvent. They showed that using 5% drug produces nanoparticles with %LE (89.42 ± 1.04%) higher than nanoparticles produced by using 2% drug, which is close to %drug used in the current study (2.44%). Furthermore, Lindner *et al*. calculated %EE for resveratrol-loaded PLA nanoparticles indirectly using the same analytical method applied in this study. Although they applied single-ESE to prepare the nanoparticles, the %EE (82.47 ± 5.8%) was close to the %EE calculated for sample 4-RP in the current study (88.89 ± 0.98%).

No previous studies on the encapsulation of ferulic acid, sinapic acid and epicatechin in PLA nanoparticles could be found in the published literature. However similar studies showed variable results. For instance, the %LE of epicatechin in lecithin–chitosan nanoparticles prepared by molecular self-assembly was 3.42 ± 0.85% (Perez-Ruiz et al., 2018), which was close to the current study. Others such as Yadav *et al*. and Ghosh *et al*. showed %EE of epicatechin to be much higher (54.5 % & 72%; respectively) in albumin nanoparticles prepared by desolvation (Yadav *et al*., 2014, Ghosh *et al*., 2016). Likewise, the encapsulation of ferulic acid in different nanocarriers was described with variable results. Panwar *et al*., 2016 reported that the %EE of ferulic acid in chitosan nanoparticles depends on the initial drug concentration and increased from 14.71% to 56.45% when increasing drug concentration from 0.0264 to 0.1056 mg/mL (Panwar *et al*., 2016). Merlin *et al*., 2012 however managed to prepare ferulic acid-loaded PLGA nanoparticles using DESE method with %EE equal to 76% (Merlin *et al*., 2012). Finally, the %EE of sinapic acid in chitosan

nanoparticles was stated to be 58.8–62.3% after applying ionic gelation for nanoparticle preparation (Balagangadharan *et al*., 2019).

2.6.11 Determination of the drug loading efficiency and encapsulating efficiency of the different antioxidants in liposomes

As described with PLA nanoparticles, the %LE of liposomes was noticed in some previous publications to be close to the obtained results in this study. For example, The %LE of α-tocopherol in liposomes prepared *via* ethanol injection was 78.47% (Taouzinet *et al*., 2020), which was very close to the calculated %LE in the current study (76.10%). Additionally, the encapsulation of curcumin in liposomes prepared by thin-film hydration followed by extrusion was measured as %EE by Campani et al., 2020. They showed that %EE using 10%w/w of curcumin produced liposomes with %EE equal to 43.0 ± 5.6%, which were comparable to the current results (Campani *et al*., 2020). Furthermore, %LE of resveratrol in DPPC/cholesterol liposomes was found to be around 3%. The low %LE of resveratrol in DPPC liposomes was explained by its intermediate log P. Basically, the hydroxyl groups of resveratrol may interact with polar DPPC heads on the surface of liposomes and therefore reduce its entrapment (Soo *et al*., 2015). This may also explain the low %LE reported for resveratrol liposomes in the current study.

Even though, some %LE were reported in earlier studies to be comparable to the current study, others have managed to produce much different results. For instance, ferulic acid was encapsulated *via* calcium gradient method into liposomes with a %EE around 80% (Qin *et al*., 2007). This was much higher than the results obtained the current study for ferulic acid liposomes (20.78 ± 3.45%). The high entrapment efficiency was explained by the different methodology. Additionally, epicatechin showed %EE around 63% using thin film hydration method followed by extrusion for liposomal preparation (Fanf *et al*., 2006). It should be noted however, that even though the method of preparation in the last study was similar to the current study, the lipid composition was quite different. They used egg phosphatidylcholine (4% w/v), cholesterol (1% w/v) and diacetylphosphate (0.25% w/v) for the lipid bilayer instead of DPPC. This might

explain the higher %EE achieved. Another interesting point is that the %LE for PLA nanoparticles was within the following descending order α-tocopherol, curcumin, resveratrol, ferulic acid, sinapic acid and epicatechin. This followed the lipophilicity order of these drugs, with α-tocopherol having the highest log P and epicatechin the lowest (described in table 3.3). This was consistence with the results obtained from Buhecha *et al*., 2019. They showed that using the same method described in this study the %LE for the hydrophilic drug, theophylline, was lower than the lipophilic drug, budesonide (Buhecha *et al*., 2019).

2.7 Conclusion

From this study, it can be concluded that all the antioxidants selected; α-tocopherol, resveratrol, curcumin, sinapic acid, ferulic acid and epicatechin were successfully encapsulated in both PLA nanoparticles and liposomes. These nanoparticles showed variable characteristic properties such as size, surface charge and loading efficiency. Future results can be performed to optimize these properties, but first further tests will be carried out to study their *in vitro* and *in vivo* activity. Chapter 3 will describe the antioxidant activity of all drugs under investigation in free and liposomal form. Chapter 4 and 5 will discuss the *in vivo* studies of all nanoparticle preparations.

Chapter 3: Comparing the antioxidant activity of the free drugs to the drug-loaded liposomes

3.1 An introduction to the chapter

In the previous chapter, different method used to prepare PLA nanoparticles and liposomes were discussed followed by preparation and characterisation of PLA nanoparticles and liposomes loaded with different antioxidants. The main aim of these encapsulations was to improve the physicochemical properties of the antioxidants under investigation and therefore improving their antioxidant activity. This chapter will start by a brief discussion to different assays used to assess antioxidant activity and then will cover the antioxidant activity of the drug-loaded liposomes, using two different chemical reactions. PLA nanoparticles were not tested by these chemical assays, due to the entrapment of drugs inside the nanoparticles and being not available for immediate reaction. The chemical reactions used for testing the liposomal products were the peroxynitrite dependent tyrosine nitration (PTN) test and the trolox equivalent antioxidant capacity assay (TEAC). The methods and results of these two tests will be discussed in detail.

3.2 Antioxidant activity assays

3.2.1 The significance of antioxidant activity assays

Oxidative stress has been linked to many diseases such as cancer, liver diseases, Alzheimer's disease, aging, arthritis, inflammation, diabetes, Parkinson's disease, atherosclerosis, and AIDS (Moon & Shibamoto, 2009). Numerous antioxidants have shown some potential in the prevention and/or treatment of these diseases. Examples such vitamin E, Vitamin C, resveratrol and curcumin have been discussed in detail in chapter 1. Hence, there was a need to develop *in vitro* assays to determine and compare the antioxidant activity of potential natural and synthetic antioxidants. Different assays have been applied on natural extracts to study their potential activity. For example, thiobarbituric assay (TBA) was used to evaluate the antioxidant capacity of extracts from *Cornus capitat, Glycyrrhiza glabra, Morinada elliptica roots, Thymus zygis, Rubus chamaemorus* and *Camellia sinensis*. TEAC assay was applied to study the antioxidants of phenolic compounds in red wine, balsamic vinegar, guava leaves and in a variety of Indian and Chinese medicinal plants (Moon & Shibamoto, 2009).

3.2.2 The diversity of antioxidant activity mechanism

Although, antioxidant in general means to protect from oxidation damage, they act in very different ways. As described in section 1.8, antioxidants can be defined as any compound or system capable of donating an electron to a free radical to prevent its harmful effects. Huang *et al*. used a broader and more specific definition to describe antioxidant "antioxidants are enzymes or other organic substances, such as vitamin E or β-carotene that are capable of counteracting the damaging effects of oxidation in animal tissues" (Huang *et al*., 2005). He also described dietary antioxidants as "substances in foods that significantly decreases the adverse effects of reactive species, such as ROS and RNS, on normal physiological function in humans". They can include radical chain reaction inhibitors, metal chelators, oxidative enzyme inhibitors and antioxidant enzyme cofactors (Huang *et al*., 2005).

Radical chain reaction inhibitors or sometimes referred to as primary antioxidants (AH) can react with a highly reactive alkyl radical ($R^{\bullet}$) and transfer a hydrogen atom to it, forming stable organic derivatives (RH) and an antioxidant radical ($A^{\bullet}$) that is more stable and less likely to propagate the oxidation reaction. Alternatively, can donate a single electron to a free radical forming a more stable anion (R^{-}) and cation (AH^{+}). These antioxidants usually contain a phenolic structure in their compound (Sehwag & Das, 2013).

$R^{\bullet} + AH \rightarrow RH + A^{\bullet}$ (Hydrogen donors)

$R^{\bullet} + AH \rightarrow R^{-} + AH^{+}$ (Electron donors)

On the other hand, Metal chelators prevent oxidation by forming stable complexes with metal ions and thereby preventing the catalytic effect of metals (described in section 1.6). Examples include citric acid, malic acid, ethylenediaminetetraacetic acid and phosphates. Other antioxidants act either by inhibiting the action of oxidative enzymes (such as NSAIDs which inhibit cyclooxygenase) or by enhancing the action of antioxidant enzymes (such as selenium which is a cofactor for glutathione peroxidase). Nevertheless, some antioxidants act as oxygen scavengers or reducing agents such as ascorbic acid and erythorbic acid or even by deactivating singlet oxygen such as β-carotene and lutein (Sehwag & Das, 2013, Huang *et al*., 2005).

3.2.3 Antioxidant capacity assays

As argued above, antioxidants act by very different mechanisms. This makes studying and comparing their activity *via* a single assay rather impossible and unrealistic. Various *in vitro* methods have been proposed and applied to evaluate the antioxidant activity of numerous natural and chemical substances. Depending on the chemistry behind the assay, Huang *et al.* has divided the analysis methods into two categories: hydrogen atom transfer (HAT) assays and single electron transfer (ET) [Figure 3.1] (Huang *et al*., 2005). HAT assays depend on the ability of antioxidants to scavenge free radicals, namely peroxyl radicals (by donating a hydrogen atom) leading to the protection of a biomolecule. Both the antioxidant under investigation and the biomolecule will compete to react with the

free radical. Measuring the inhibition in the reaction of biomolecule with free radical in the presence and absence of antioxidant will give some kind of meaningful way to compare results. These include oxygen radical absorbance capacity, total radical trapping antioxidant parameter, TBA, β-carotene and Crocin bleaching assays, inhibited oxygen uptake, inhibition of linoleic oxidation, inhibition of tyrosine nitration and inhibition of LDL oxidation (Huang *et al*., 2005, Xiao *et al.,* 2020).

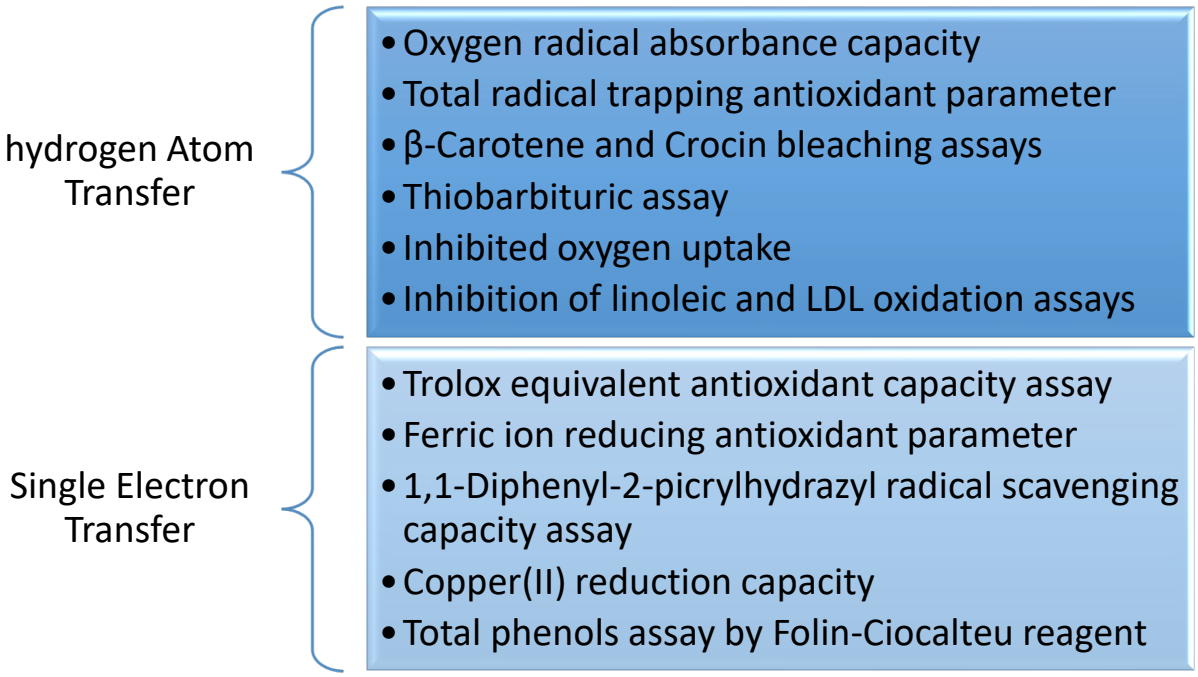

Figure 3.1: **Antioxidant activity assays classification.** These are classified into HAT and ET. Some examples are shown in the figure**.**

Conversely, ET assays depend on the reaction of antioxidant with an oxidizing agent (that changes in colour when reduced) instead of a free radical. The reduction in the colour is an estimation of the antioxidant capacity. These include TEAC, ferric ion reducing antioxidant parameter (FRAP), 1,1-Diphenyl-2-picrylhydrazyl radical scavenging capacity assay (DPPH), copper(II) reduction capacity and total phenols assay by Folin-Ciocalteu reagent (Huang *et al*., 2005, Xiao *et al.,* 2020). Other assays may include total oxidants scavenging capacity, inhibition of Briggs-Rauscher oscillation reaction, chemiluminescence and

electrochemiluminescence. $O_2^{\bullet -}$, H_2O_2, $HO^{\bullet}$, $ONOO^-$, $^1O_2$ are ROS that can be measured to assess the oxidant scavenging capacity of different antioxidants (Huang *et al*., 2005). Moon & Shibamoto divided antioxidant activity assays differently. They grouped the assays in to two groups depending on whether the method is associated with lipid peroxidation or associated with electron and radical scavenging. Assays associated with lipid peroxidation included TBA, malonaldehyde-HPLC assay, malonaldehyde-gas chromatography (GC), conjugated diene assay and β-carotene bleaching assay. Assays associated with electron and radical scavenging included DPPH, TEAC, FRAP, ferrous oxidation−xylenol orange assay, ferric thiocyanate assay and aldehyde/carboxylic acid assay (Moon & Shibamoto, 2009).

3.2.4 Factors to consider when selecting an antioxidant activity assay

No single assay is applicable to all antioxidants and therefore, consideration should be taken when choosing a method to apply. First, equipment and material should be available or easily obtained. Secondly, it should be governed by a chemical reaction and a source of free radical that is biologically relevant. Ideally, it should also be simple, have a defined endpoint, reproducible, precise and selective. Another factor is the solubility of the antioxidant to be tested. Finally, it should not be time consuming (Prior *et al*.,2005). Most of the assays mentioned above rely on the measurement of a product spectrophotometry. Although, this has the advantage of having a simple and reasonably fast outcome, results can be misleading if materials exhibit wavelengths similar to the test compound. For this reason, combing a separation step such as in malonaldehyde-HPLC and malonaldehyde-GC assays can have an advantage. Still, chromatography can show the disadvantage of being time-consuming (Moon & Shibamoto, 2009). It is then good practice to have at least two methods to study the antioxidant activity. One fast and simple to give a general idea on the test compounds and a second one that can be applied for more accurate results. In this study, two assays will be discussed and the pros and cons of each will be mentioned in more details.

3.2.4.1 TEAC assay

2,2'-azinobis-(3-ethylbenzothiazoline-6-sulfonic acid) (ABTS) is a chemical compound that can be oxidized to form a relatively stable radical cation ($ABTS^{\bullet+}$), which has a dark blue colour [Figure 3.2]. The ability to scavenge this radical has been used to evaluate the antioxidant activity of different compounds and food products. To quantify the results and ease of comparison, the decolourisation in the presence of the antioxidants is compared to the decolourisation in the presence of trolox as a standard giving a TEAC value (Re *et al*., 1999).

Formerly, ferrylmyoglobin (formed from the reaction of metmyoglobin with hydrogen peroxide) was used to oxidise ABTS. This faced a major drawback, as antioxidants can react with oxidising agent and generate misleading results. Different upgrades have been applied to the method to improve the assay. For instance, a quantification step of the produced radical was performed before the addition of antioxidants. This removed, to some extent, the interference from the oxidising agents. Additionally, different oxidising agents were used to form the coloured radical such as manganese dioxide and potassium persulphate. However, using a chemical agent to oxidise ABTS is time consuming (up to 16 hours) and so, others used enzymes such as metmyoglobin, haemoglobin, or horseradish peroxidases to catalyse the reaction. Furthermore, the absorption was measured at different wavelengths 415 and 734 nm to increase selectivity (Prior *et al*., 2005).

This method has the advantage of first, being simple and robust as spectrophotometric measurement is applied. Second, can be applied to both lipophilic and hydrophobic compounds. Finally, can be applied over a wide pH range. (Re *et al*., 1999, Xiao *et al*., 2020). However, it does not relate directly to any physiological radical source, as ABTS is not found in human cells. Moreover, the endpoint is usually measured at 4 or 6 min, this may be too soon for antioxidants with slow reaction leading to mistaken results (Prior *et al*., 2005).

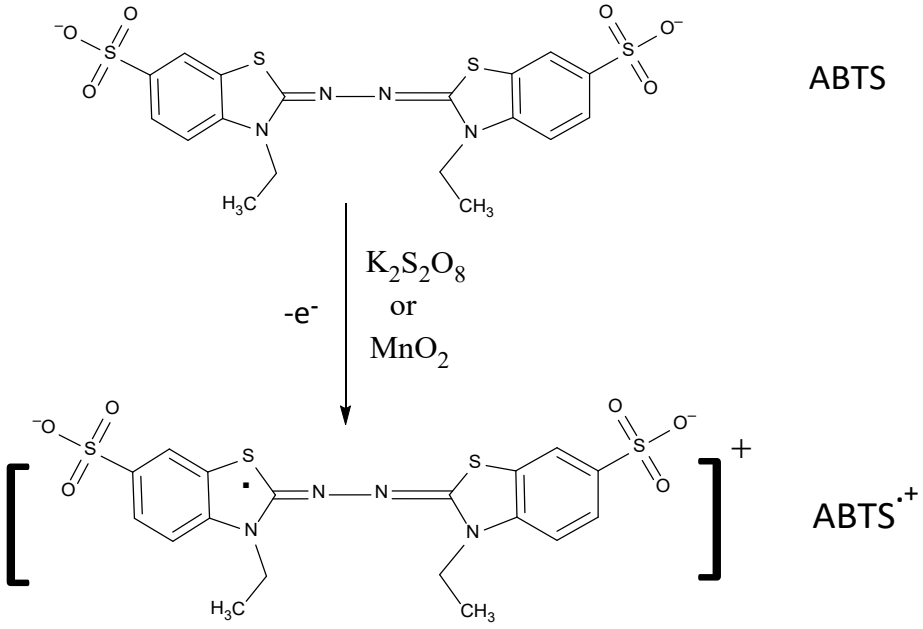

Figure 3.2**: Mechanism of TEAC assay.** Formation of ABTS radical cation (Dark blue colour) by the oxidation of ABTS with potassium persulphate or manganese dioxide.

3.2.4.2 Peroxynitrite assay

Peroxynitrite is a RNS that is be produced *in vivo* by the interaction of superoxide and nitic oxide and transformed to peroxynitrous acid at physiological pH (detailed in section 1.6). When present at low concentration, it has a valuable purpose in the stimulation of red blood cell metabolism enhancing tyrosine phosphorylation and lactate production. Conversely, when present in high concentration it obstructs tyrosine phosphorylation and glycolysis (Cruz & Fardilha, 2016). It causes oxidative damage due to lipid peroxidation, amino acid oxidation, and DNA damage. Furthermore, it has the potential for further oxidant injury *via* generation of hydroxyl radical (Whiteman *et al*., 1995, Pannala *et al* 1998).

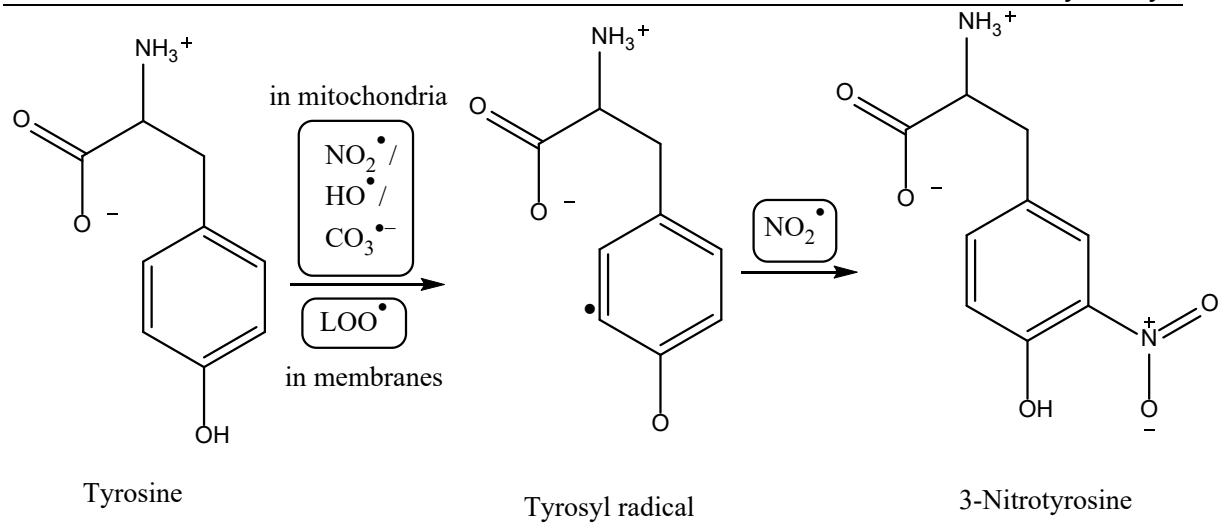

Figure 3.3: **Peroxynitrite dependent tyrosine nitration.** Two step mechanism of tyrosine nitration using free radicals sourced from peroxynitrite.

The formation of 3-NT is thought to be a two-phase process [Figure 3.3]. Initially, the amino acid tyrosine is oxidised by losing one hydrogen to form a tyrosyl radical. This step can be executed by $CO_3^{\bullet -}$, $HO^{\bullet}$, $NO_2^{\bullet}$ in the mitochondria or lipid peroxyl radicals ($LOO^{\bullet}$) in membranes. As shown in figure 1.4, $CO_3^{\bullet -}$ and $NO_2^{\bullet}$ are formed from peroxynitrite. Additionally, peroxynitrite can undergo haemolytic fission to form $HO^{\bullet}$ and $NO_2^{\bullet}$ and all these reactive species can initiate a free radical chain reaction in lipids forming $LOO^{\bullet}$. Although, 3-NT has been linked to oxidative stress due to peroxynitrite, it should be noted that there are other sources of 3-NT. For example, the peroxidases enzyme can catalyse the reaction of nitrite and tyrosine using H_2O_2 to form 3-NT (Cruz & Fardilha, 2016). Although, the actual mechanism is not clear, it readily oxidises the amino acid tyrosine to form 3-NT. The ability to inhibit 3-NT formation is used to assess antioxidant activity (Whiteman *et al*., 1995, Pannala *et al* 1998).

The concentration of 3-NT can be measured by various methods. The simplest method is direct spectrophotometry measurement at 430nm. As discussed, this can give false results if assay components absorb at similar wavelengths interfering with the assay. This can be avoided by using HPLC or GC/MS. However, this can be time consuming and requires experience and instrumentation. Immunohistochemistry technique is another method of detection

that relies on the use of antibodies to detect 3-NT. Although, these are relatively simple and had been applied in diverse biological samples, they do not show precise quantification and assay kits can be quite expensive. There are also proposed chemical reactions to form coloured complexes that can be measured at higher wavelengths. These can be easier to apply but quantification is debateable, as 3-NT is not measured directly (Gupta & Devaraju, 2014). An additional disadvantage of PTN assay is that it can only be applied to hydrophilic antioxidants, as the reaction requires an aqueous medium.

3.3 Aims

- To compare the antioxidant activity of free drugs under investigation to drug-loaded liposomes prepared in chapter 2
- To study the antioxidant activity of the different drug-loaded liposomes prepared in chapter 2 using PTN assay

3.4 Materials and methods

3.4.1 Materials and equipment details

Antioxidants under investigation are α-tocopherol, curcumin, resveratrol, ferulic acid, sinapic acid and epicatechin (details described in previous chapter). L-Tyrosine (≥ 98%), 3-NT (crystalline form), ABTS, trolox (6-hydroxy-2,5,7,8-tetramethychroman-2-carboxylic acid), Sodium nitrite (≥ 97%) and potassium persulphate were purchased from Sigma-Aldrich Company Ltd (Poole, Dorset, UK). Other consumables were purchased from Fisher Scientific (Loughborough, Leicestershire, UK). The equipment used are mostly described in chapter two with some additional instrument detailed in table 3.1.

Table 3.3.1: Details of some additional instruments used in this chapter

EQUIPMENT	SPECIFICATIONS
UV-visible spectrophotometer	PerkinElmer UV-visible spectrophotometer with single cell holder (Lambda 265)
HPLC	Agilent technology with: • Quaternary pump 1260 infinity • Auto-injector 1260 infinity • Column holder 1290 infinity • Auto-sampler 1260 infinity • Diode array detector • Chem Station software (Open LAB CDS) • 5 µm, C18, 25 cm, 4.6 mm HPLC column from Fortis Technologies Ltd, UK

3.4.2 Methods

3.4.2.1 TEAC assay

The method applied in this study was improved by Re *et al*., 1999. They described a method of direct formation of the ABTS radical cation through the reaction of ABTS with potassium persulphate followed by its spectrophotometric

quantification. The reagents react stoichiometrically at 1:0.5, generating ABTS radical cation by incomplete oxidation. This solution is stable for two days at room temperature in the dark. The percentage of decolourisation in the presence of antioxidant is an indication of the antioxidant activity (Re *et al*., 1999).

A stock solution of 7 mM ABTS and a 2.45 mM (final concentration) potassium persulfate was prepared as followed. 38.4 mg ABTS was accurately weighed and transferred to a 10 mL volumetric flask and around 7 mL water was added. 6.6 mg of potassium persulphate was added, and volume made up with water. The solution was kept in a dark place for a minimum of 12 hours and used within 2 days. The solution was then diluted in either ethanol or water (according to the solubility of antioxidant to be tested) to give an absorbance of 0.7 ± 0.02 at 734 nm. This was used as a baseline for further calculations. 30 µL of standard trolox (0-20 µM, final concentration) was added to 2.97 mL of ABTS radical cation solution and the absorbance was recorded after exactly 6 min at 734 nm. The test was repeated using different concentrations of antioxidant loaded liposomes diluted in water (samples 8-14) and free antioxidants, diluted in either ethanol (α-Tocopherol, curcumin, resveratrol, ferulic acid and sinapic acid) or water (Epicatechin) according to their solubility. Stock solutions of free antioxidants and liposomal samples were made such that, after the addition of 30 µL of their dilution to a total of 3 mL $ABTS^{\cdot+}$ solution, an inhibition of 20-80% in the absorbance, compared to blank absorbance was obtained. The percentage decolourisation was calculated and plotted against the concentration of antioxidant/trolox used. TEAC value was calculated by dividing the slope from the antioxidant or sample plot against the slope from trolox. Appropriate blanks were used before all readings.

3.4.2.2 PTN assay

This test involved two main steps: First, preparing peroxynitrite and measuring its concentration and second, performing the assay by the reaction of peroxynitrite with L-tyrosine in the presence and absence of samples and measuring the amount of 3-NT formed. The extent of inhibition of 3-NT formation is used as an indication of the antioxidant activity of the samples.

3.4.2.2.1 Peroxynitrite synthesis

The method for synthesising peroxynitrite is described in detail by Pannala *et al.* (Pannala *et al.*, 1997). It involves mixing 20 mL of acidified hydrogen peroxide (1 M in 0.5 M HCl) and 20 mL of 200 mM sodium nitrite, simultaneously into 40 mL of 1.5 M potassium hydroxide [Figure 3.4] using Y-shaped tube over ice-bath, while stirring vigorously [Figure 3.5]. Concentration of peroxynitrite was calculated by measuring the absorbance at 302 nm using a UV-spectrophotometer and applying Beer's-Lambert's Law (equation 3.1), where its molar absorptivity was 1670 mol^{-1} cm^{-1}. It is stable for up to one week at -20ºC, but in this study, only freshly prepared peroxynitrite was used.

$$A = abc \qquad \text{Equation 3.1}$$

where;

A = measured absorbance

a = molar absorptivity (1670 mol^{-1} cm^{-1})

b = path length (1 cm)

c = unknown concentration

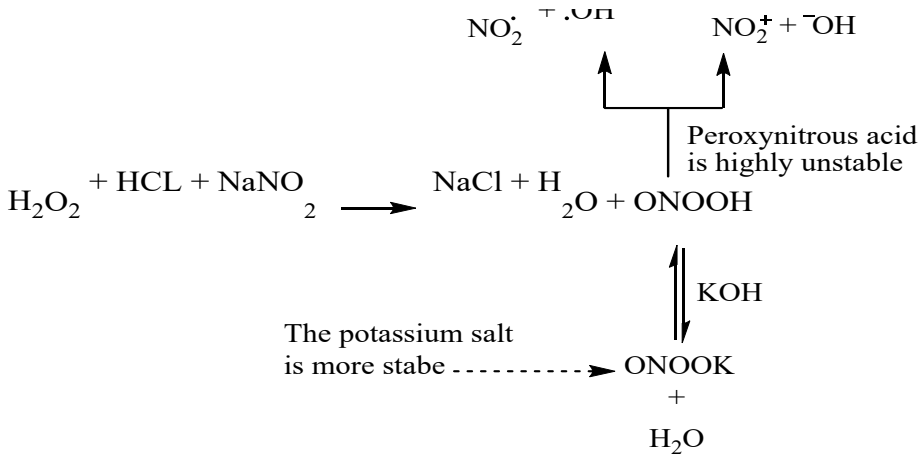

Figure 3.4: **Formation of peroxynitrite.** The reaction of acidified hydrogen peroxide with sodium nitrite yields peroxynitrous acid, which is more stable in basic conditions.

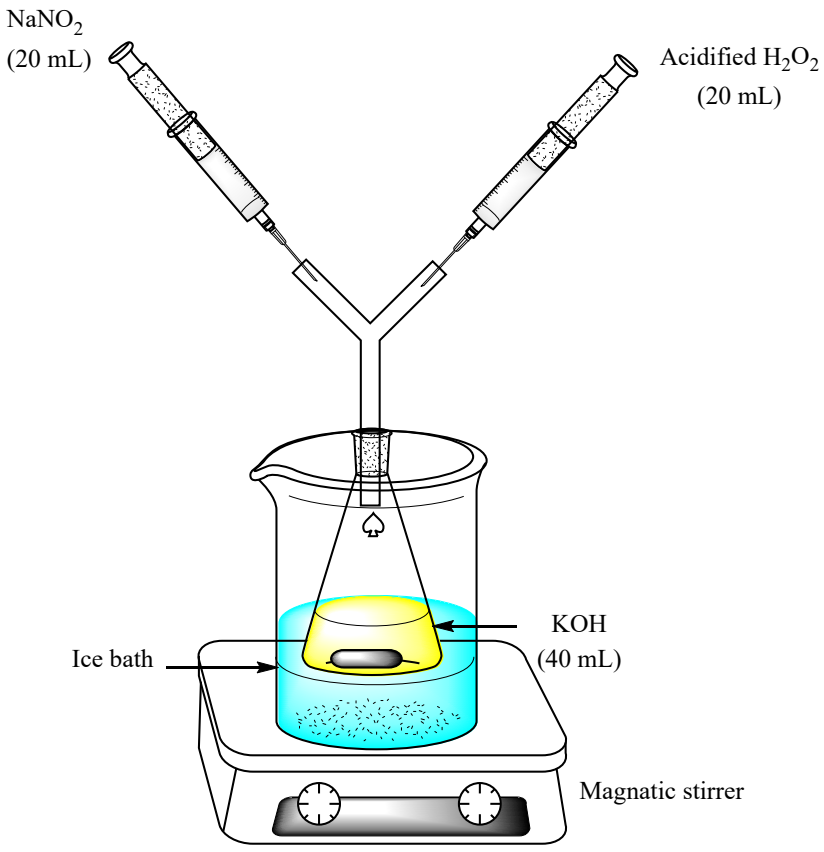

Figure 3.5: **Peroxynitrite formation.** Acidified hydrogen peroxide is added simultaneously with sodium nitrite to potassium hydroxide over an ice bath while stirring with a magnetic stirrer (original figure in colour)

3.4.2.3 Tyrosine nitration assay

Measurement of 3-NT formation was made by HPLC using Fortis C_{18}, 5 µm column (25 cm x 4.6 mm) on an Agilent 1260 system with a Quaternary pump, an auto-injector, auto-sampler and a diode array detector. The system was equipped with a Chem Station software. The mobile phase was 50 mM phosphate buffer, pH7: acetonitrile at a ratio of 95:5 (v/v), at 1 ml/min flow rate. The method was adapted from Pannala *et al*., 1997. Calibration plots were constructed using standard 3-NT and L-tyrosine (1-100 µM), monitored at 350 nm and 220 nm; respectively. System suitability was confirmed by calculating revalidation parameters as described in section 2.6.9. Different concentrations of peroxynitrite solutions (0.05-1 mM) diluted in 0.1 M NaOH were added to L-tyrosine solution (100 µM final concentration) in 0.2 mM phosphate buffer and the concentration of 3-NT formed was determined using HPLC.

The assay was carried out by adding 50 µL of freshly prepared peroxynitrite (500 µM) to a solution of 0.1 mM L-tyrosine mixed with different concentrations of liposomes containing antioxidants (samples 8-14) in 0.2 M phosphate buffer, pH7 to make up a volume of 1 mL. The assay was repeated with only L-tyrosine to estimate the level of 3-NT formation (Pannala *et al*., 1997). The % inhibition in 3-NT formation was then plotted against concentration of the antioxidant in the liposomal. Blank liposomes were also tested and the % inhibition was plotted against concentration of liposomes added (%v/v).

3.5 Results

3.5.1 TEAC assay

The assay was carried out by the interaction of different pure antioxidants and antioxidants encapsulated in liposomes with the ABTS radical cation. For testing the free lipophilic antioxidants, the radical solution was diluted in ethanol to obtain an absorbance of 0.7 ± 0.02 at 734 nm and for testing the free hydrophilic antioxidant and all liposomes (samples 8-14), the radical solution was diluted in deionized water to give the same absorbance. Stock solutions of pure antioxidants and antioxidants encapsulated into liposomes were made such that, after the addition of 30 µL of dilutions to 2.97 mL $ABTS^{\bullet+}$ solution, an inhibition of 20%-80% in the absorbance, compared to baseline absorbance at 734 nm was obtained. Absorbance was measured after exactly 6 min of initial mixing and the extent of decolourisation was calculated as percentage inhibition in absorbance. This was plotted against the concentration of antioxidant used either as free or liposome encapsulated form. The extent in the decolourisation of the $ABTS^{\bullet+}$ by increasing concentrations of trolox (0-20µM) was calculated as the percentage inhibition in the absorbance measured at 734 nm. A linear relationship was obtained when plotting the percentage inhibition against increasing concentrations of trolox [Figure 3.6].

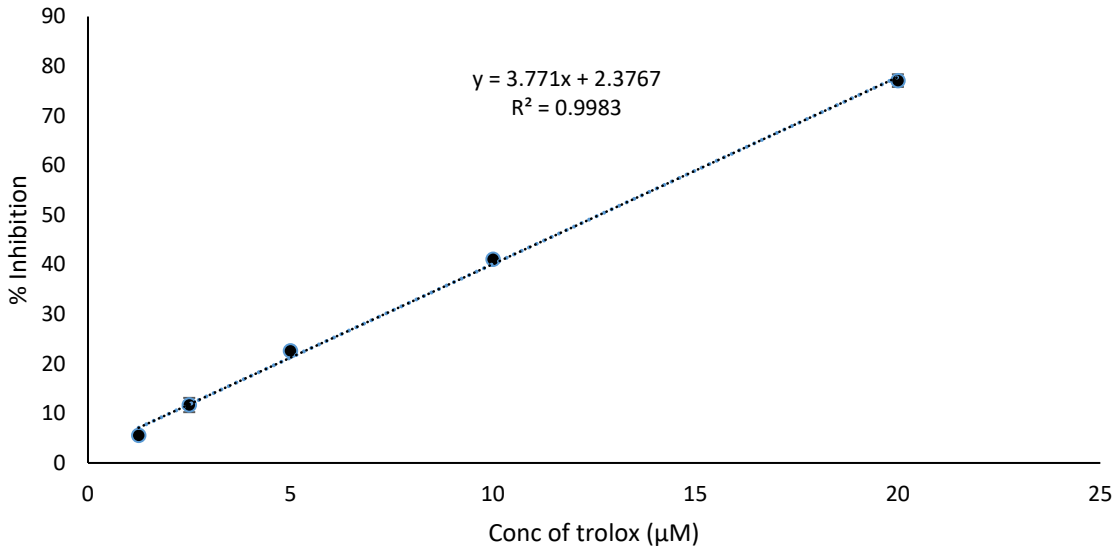

Figure 3.6: Percentage ABTS$^{\bullet+}$ decolourisation against the concentration of trolox used (mean ± SD, *N* = 3).

The extent in the decolourisation of the ABTS$^{\bullet+}$ by different free and encapsulated antioxidants in liposomes was calculated as the percentage inhibition in the absorbance and plotted as a function of the concentration of each antioxidant used. Results from free antioxidants are shown on the left column of figures 3.7 & 3.8, while results from antioxidant-loaded liposomes are shown on the right column of the same figures.

To simplify comparisons, the TEAC value was calculated for both, free and encapsulated, forms of antioxidants and for blank liposomes. There were small differences between free drug and liposomal form. These results suggest that although antioxidants might be encapsulated, they are still available for reaction. Although, not clear at this point where the reaction occurs. Blank liposomes were found to have insignificant activity with a TEAC value of 0.034. The TEAC value for free and liposomal antioxidants is shown in table 3.2 and plotted as a bar chart for ease of comparison [Figure 3.9]. Values for free antioxidants in descending order were: resveratrol (1.36 ± 0.05) > ferulic acid (1.22 ± 0.04) ≈ sinapic acid (1.23 ± 0.03) > α-tocopherol (0.90 ± 0.09) ≈ epicatechin (0.89 ± 0.01) ≈ curcumin (0.81 ± 0.02). Values for antioxidant-loaded liposomes in descending order were: resveratrol (1.16 ± 0.03) ≈ ferulic acid (1.15 ± 0.10) > curcumin (0.88 ± 0.04) >

sinapic acid (0.74 ± 0.01) > α-tocopherol (0.62 ± 0.03) > epicatechin (0.56 ± 0.01). Most liposomal forms of drugs showed a slight reduction in TEAC values, maintaining their order of antioxidant activity. The only exception was curcumin, which showed an insignificant increase in its TEAC value when loaded into liposomes.

Data analysis using two-way ANOVA showed significant difference between TEAC values of free drugs and TEAC values of drug-loaded liposomes, $F_{(1,24)} = 189.9$, $p < 0.001$. Furthermore, the *post hoc* Bonferroni's comparisons test showed that multiple comparisons of free to encapsulated antioxidants were significantly different for α-tocopherol ($X_{24} = 0.28$, $p < 0.001$), resveratrol ($X_{24} = 0.20$, $p < 0.001$), sinapic acid ($X_{24} = 0.49$, $p < 0.001$), and epicatechin ($X_{24} = 0.33$, $p < 0.001$), whilst the others were insignificant. Bonferroni's multiple comparisons test is commonly applied when SD values are small.

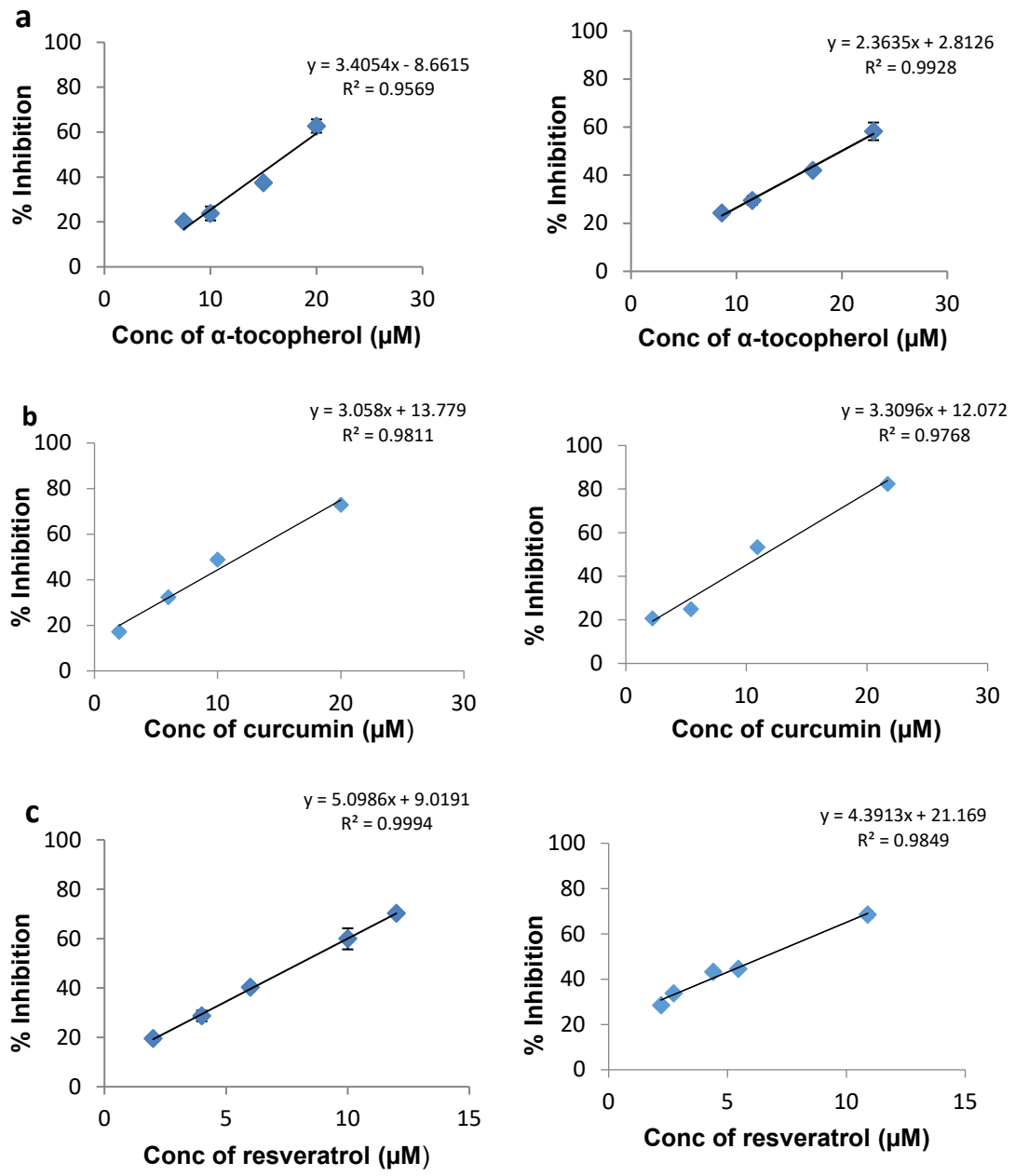

Figure 3.7: The effect of increased concentration of free antioxidants (left column) and antioxidants-loaded liposomes (right column) on the percentage inhibition in the absorbance of $ABTS^{\bullet+}$, (a) α-tocopherol, (b) curcumin, (c) resveratrol, (mean ± SD, *N* = 3).

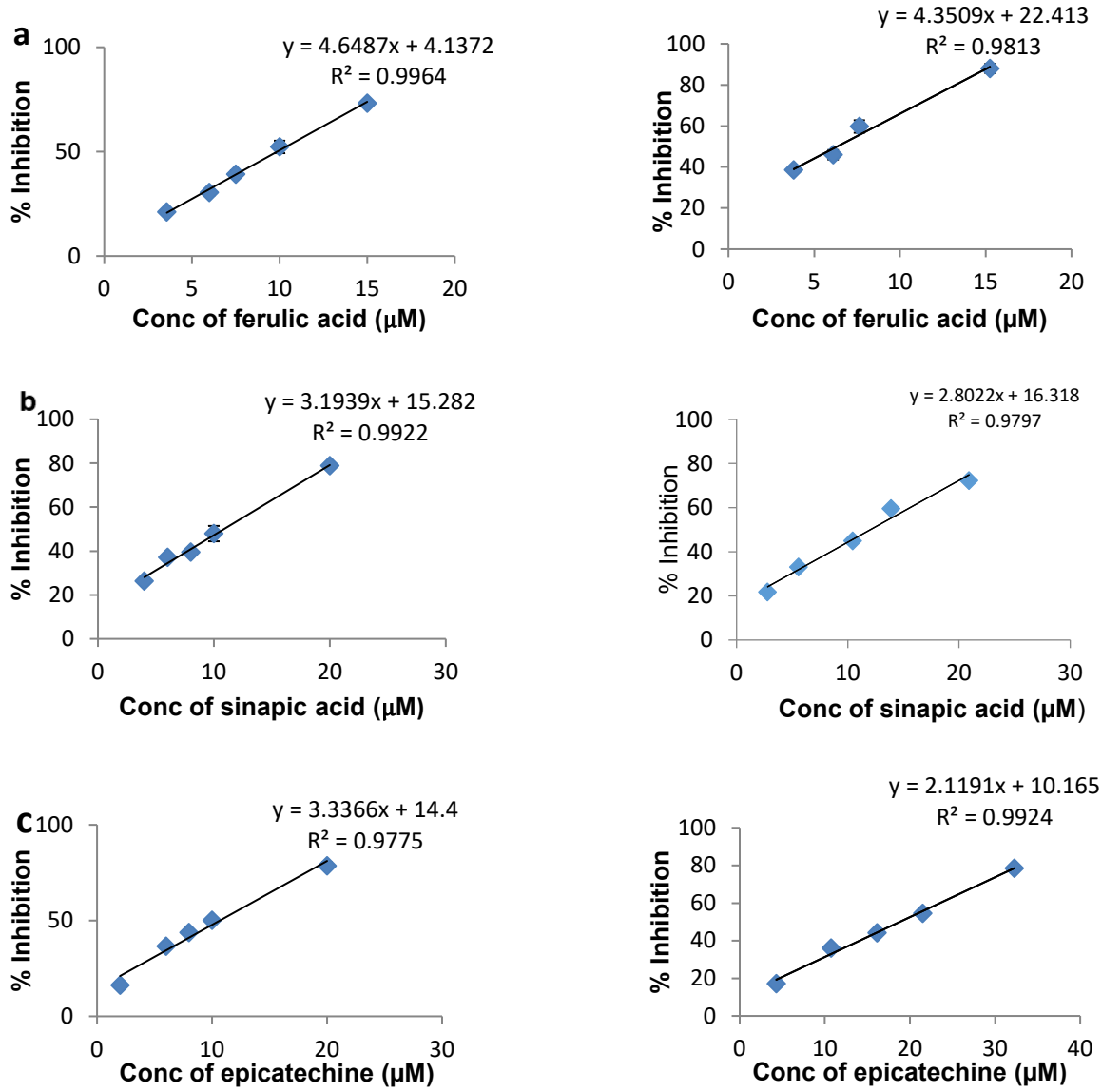

Figure 3.8: The effect of increased concentration of free antioxidants (left column) and antioxidants-loaded liposomes (right column) on the percentage inhibition in the absorbance of $ABTS^{\bullet+}$, (a) ferulic acid, (b) sinapic acid, (c) epicatechin, (mean ± SD, *N* = 3).

Table 3.2: TEAC values for pure and liposomal antioxidants using ABTS$^{\bullet+}$ assay (mean ± SD, N = 3, *** p < 0.001) when comparing two columns.

Drug	*free drug*	*liposomal form*
Blank	-	0.03 ± 0.01
α-Tocopherol	0.90 ± 0.09	0.62 ± 0.02***
Curcumin	0.81 ± 0.02	0.88 ± 0.04
Resveratrol	1.36 ± 0.05	1.16 ± 0.03***
Ferulic acid	1.22 ± 0.04	1.15 ± 0.10
Sinapic acid	1.23 ± 0.03	0.74 ± 0.01***
Epicatechin	0.89 ± 0.01	0.56 ± 0.01***

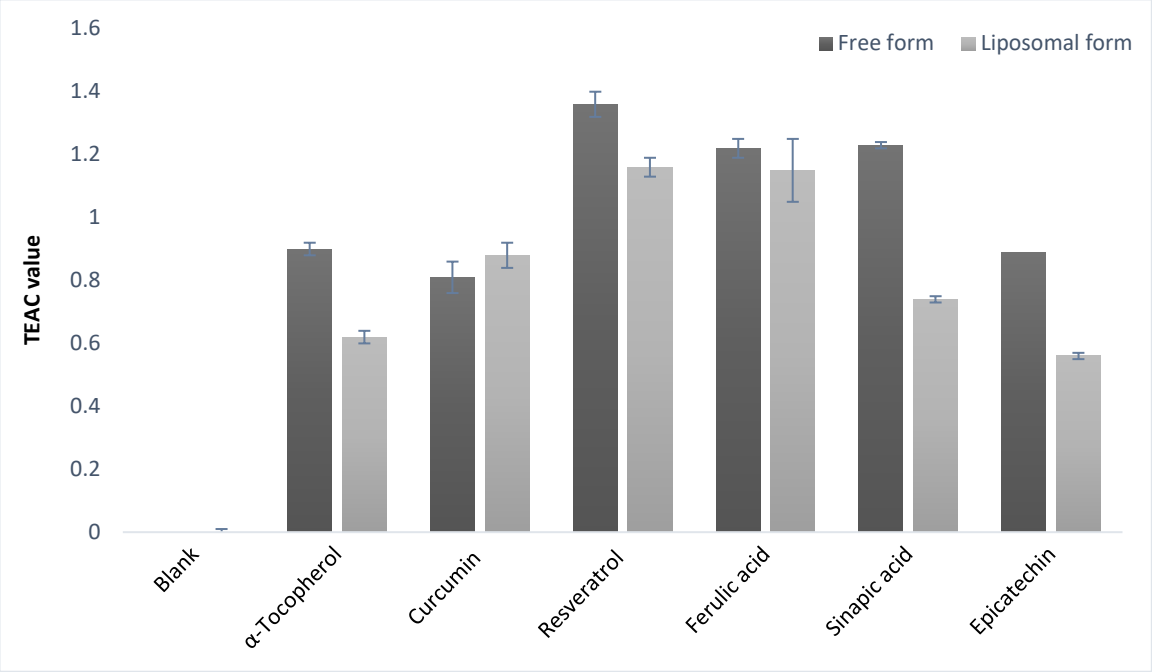

Figure 3.9: TEAC values of free antioxidants and liposomes (samples 8-14) calculated from ABTS radical assay (Mean ± SD, N = 3).

3.5.2 PTN assay

Peroxynitrite was prepared freshly and its concentration was measured on the day of the assay ranging between 20-60 mM. The addition of the two components of the reaction produced a bright yellow colour, which was kept in ice during the assay. The inhibition in peroxynitrite mediated tyrosine nitration by different liposomal antioxidants was tested as measured by the reduction in 3-NT formation. For this reason a suitable method for the detection and quantification of 3-NT was required. The method was adapted from Pannala *et al*., 1998. Good separation between L-tyrosine and 3-NT was observed in the HPLC chromatograms, where they eluted at 4.2 & 6.9 min; respectively [Figure 3.10]. The calibration plots of 3-NT and L-tyrosine are shown in figure 3.11. Linear relationship between the concentration of 3-NT and AUC was observed as measured by HPLC, with a linearity of R^2 = 0.9872 and %RSD < 0.5% for all concentrations. Likewise, the relationship between the concentration of L-tyrosine and the detected AUC was linear (R^2 = 0.9874) and reproducible (%RSD < 2). No interference was noticed when injecting liposome samples (8-14) and solvents used, indicating selectivity of the method. The product generated from the reaction of peroxynitrite with L-tyrosine was identical to standard 3-NT as indicated by elution time and spectral properties. This determines the method as suitable for the quantification of 3-NT (with a LOD = 14.34 μM & LOQ = 47.8 μM).

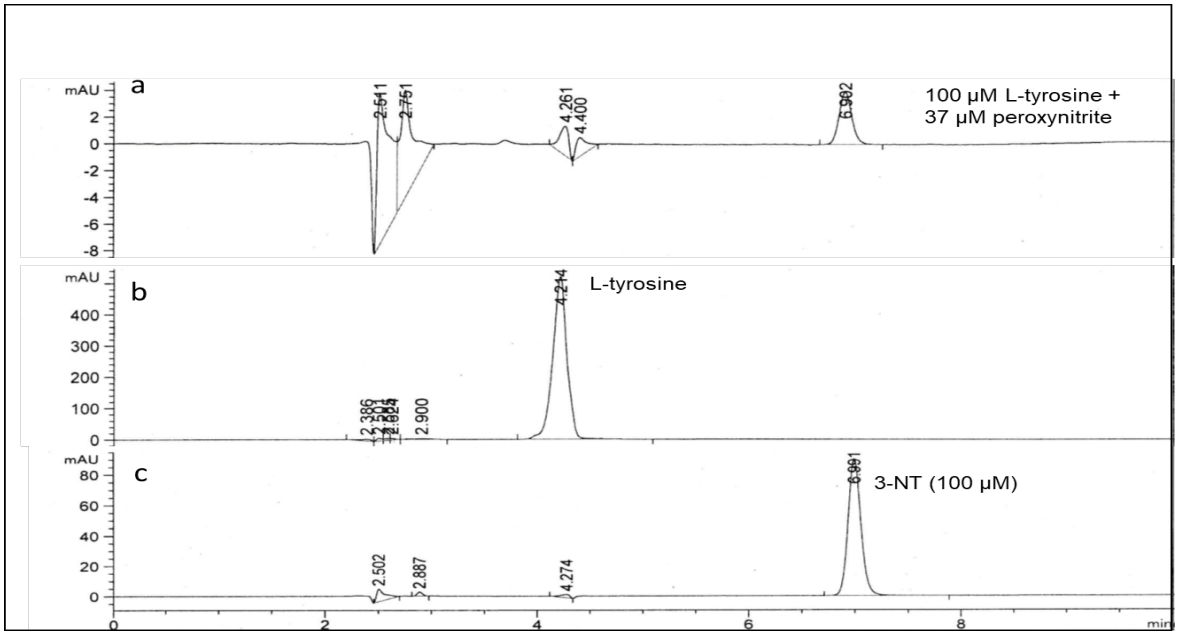

Figure 3.10: HPLC chromatographs using 95:5 50 mM PBS, pH 7: acetonitrile. (a) Nitration product of 100 µM L-tyrosine using 37 µM peroxynitrite, monitored at 350 nm. **(b)** 1mM L-tyrosine, monitored at 220 nm. **(c)** 100 µM 3-NT, monitored at 350 nm.

The concentration of L-tyrosine and 3-NT measured by HPLC after adding different concentrations of peroxynitrite solutions (0.05 – 2.67 mM) to L-tyrosine solution (100 µM) were plotted as a stacked column bar chart against the concentration of peroxynitrite added [Figure 3.12]. As observed from the chart, the increase in peroxynitrite concentration led to increased 3-NT formation along with decreased L-tyrosine. The overall recovery of both reacted and unreacted tyrosine was almost 100% with all concentrations of peroxynitrite, except for the highest concentration (2.67 mM) where it was just above 80%. Even at this high concentration, no evidence of any other products was noticed.

In this experiment, a final concentration of 500 µM peroxynitrite was used throughout the assay. 100 µL of L-tyrosine (100 µM) was incubated with increased volumes of liposomal samples (sample 8-14) in 0.2 M phosphate buffer, pH7 to make up a volume of 2950 µL (100, 200, 300, 400 & 500 µL). The assay was carried out by adding 50 µL of freshly prepared peroxynitrite (500 µM) to the

previous solutions. The assay was repeated with only L-tyrosine to estimate the level of 3-NT formation. The percentage inhibition in the formation of 3-NT due to the addition of different antioxidant-loaded liposomes was plotted against the actual concentration of drugs inside the liposomes used (calculated using the %LE determined in chapter 2). Each test was repeated in triplicate (except for samples 12-FL & 14-EL, were only tested twice due to instrument failure). Results obtained are shown below [Figure 3.13-18]. Blank liposome sample was also tested and minor inhibition was observed (<15%) that did not increase with increased volume of blank sample [Figure 3.19].

α-Tocopherol liposomes, showed an almost linear relationship between % inhibition and concentration used, but the maximum % inhibition did not exceed 75%, even with highest concentrations used [Figure 3.13]. Curcumin liposomes also showed some form of linear relationship, but low concentration did not show any protection and the highest concentrations only showed a maximum inhibition of less than 80% [Figure 3.14]. Resveratrol liposomes showed the highest % inhibition, with over 65% even with the lowest concentrations and 100% inhibition with the higher ones [Figure 3.15]. Sinapic acid liposomes, on the other hand showed an almost nonlinear relationship, although increase in concentration was followed by an increase in percentage inhibition [Figure 3.16]. Ferulic acid liposomes also showed protection but not with lower concentration and did not reach 100% inhibition [Figure 3.17]. Finally, epicatechin liposomes showed very good protection, starting from around 20% and reaching 100% with high concentrations [Figure 3.18].

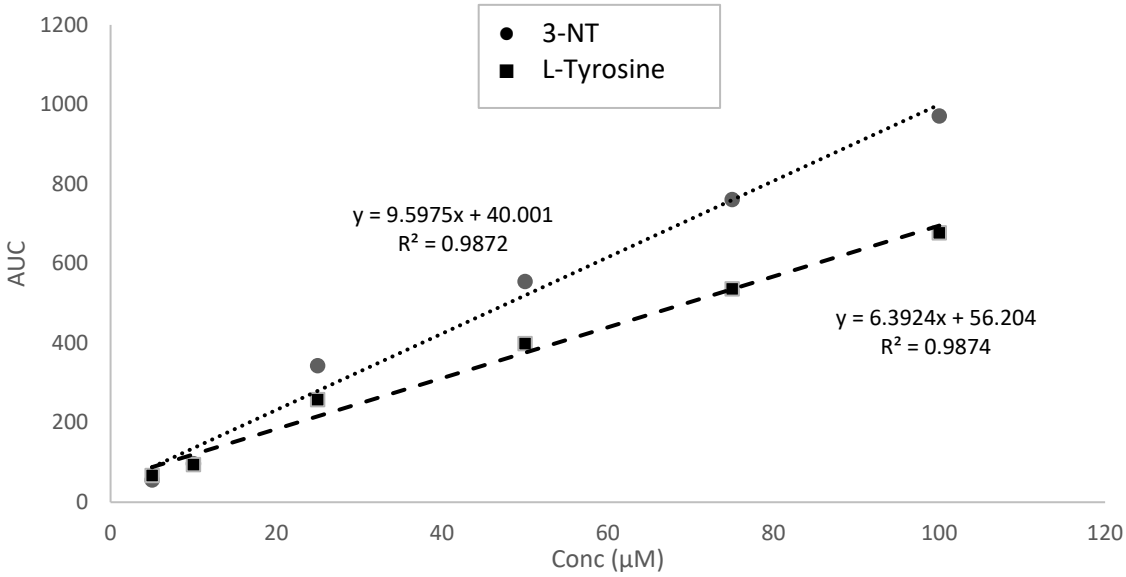

Figure 3.11: **Calibration plot of standard L-tyrosine (5-100 µM) and 3-NT (5-100 µM).** The plot is the relationship between the AUC calculated from the HPLC chromatograph and the concentration of standards injected (mean ± SD, *N* = 3). L-Tyrosine was monitored 350 nm and 3-NT was monitored at 220 nm.

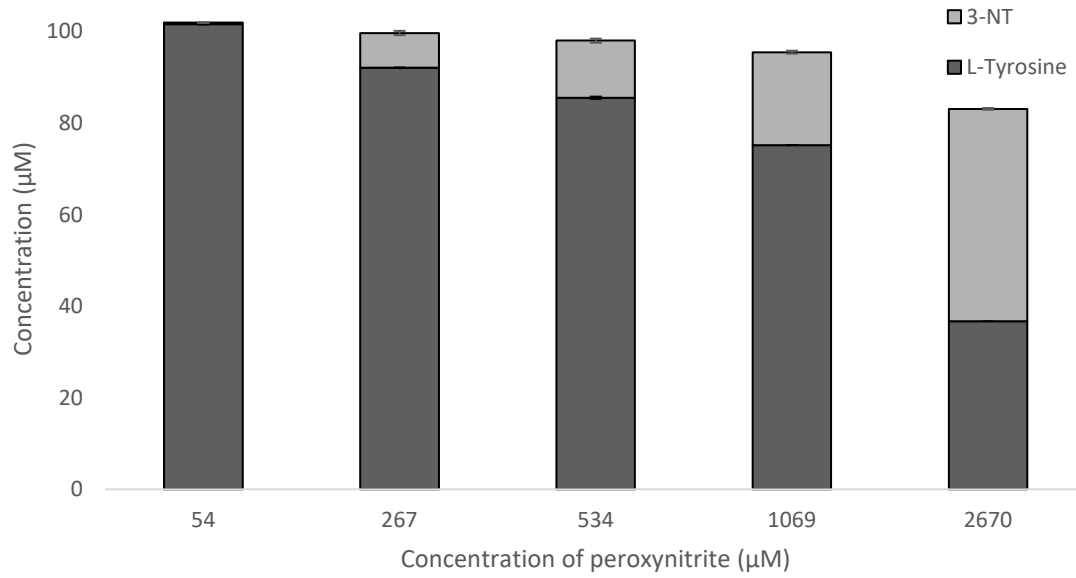

Figure 3.12: **The extent of tyrosine nitration using increased concentration of peroxynitrite** (mean ± SD, *N* = 3). Tyrosine nitration was quantified by measuring the amount of unreacted L-tyrosine and amount of 3-NT formed using HPLC.

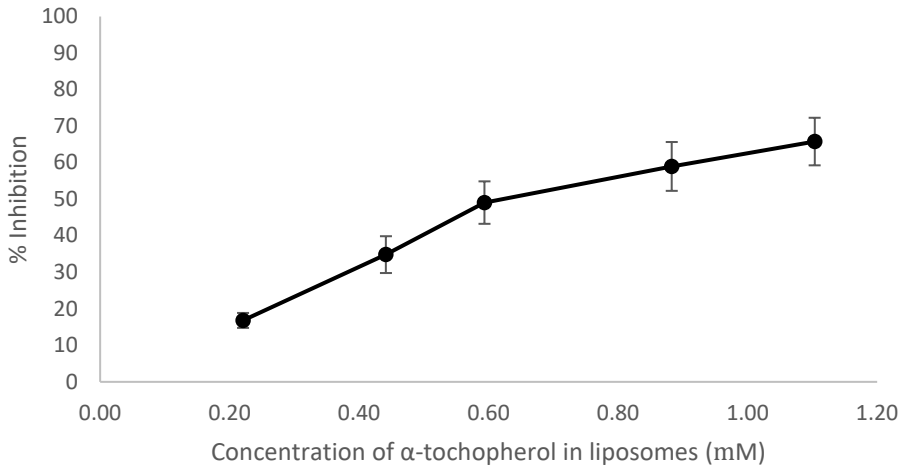

Figure 3.13: The effect of increased concentrations of α-tocopherol-loaded liposomes on the percentage inhibition of 3-NT formation in PTN assay (mean ± SD, *N* = 3).

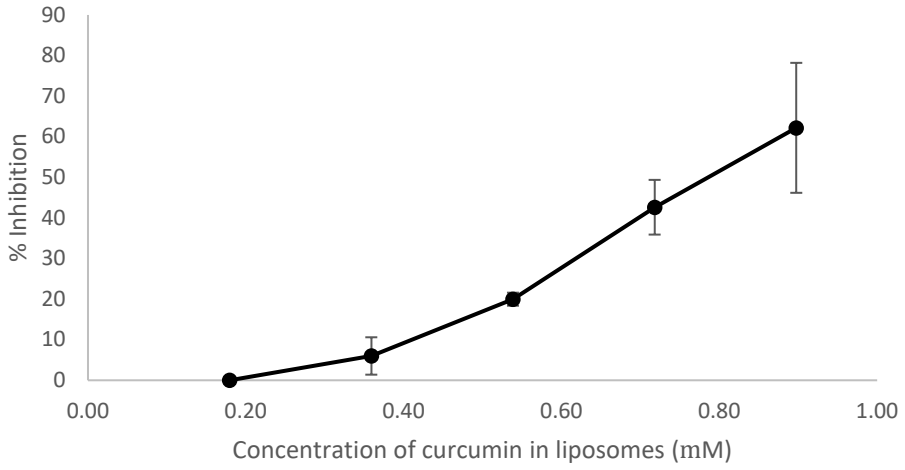

Figure 3.14: The effect of increased concentrations of curcumin-loaded liposomes on the percentage inhibition of 3-NT formation in PTN assay (mean ± SD, *N* = 3).

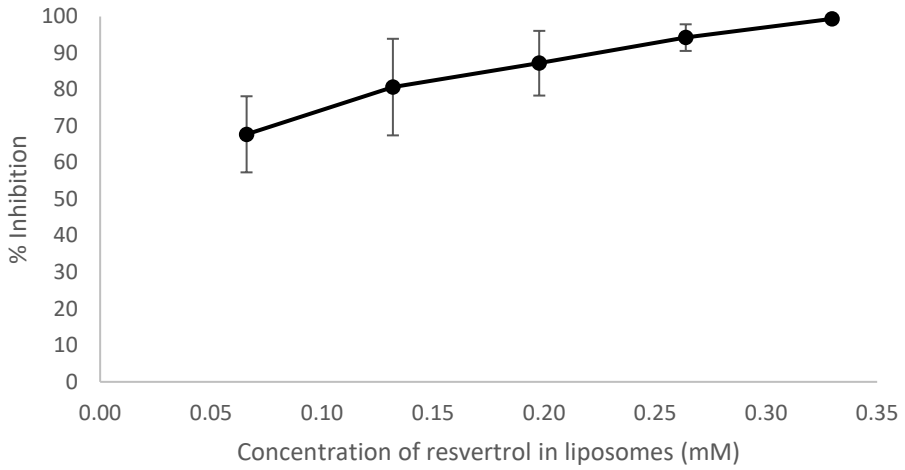

Figure 3.15 : The effect of increased concentrations of resveratrol-loaded liposomes on the percentage inhibition of 3-NT formation in PTN assay (mean ± SD, *N* = 3).

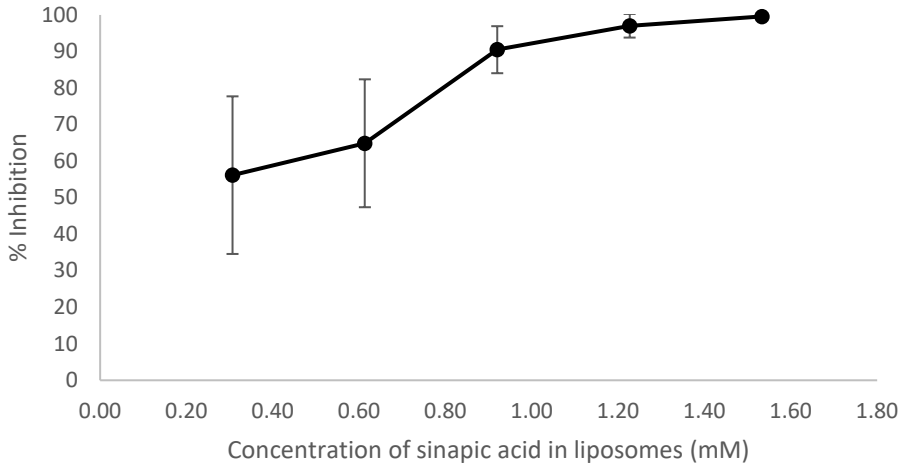

Figure 3.16: The effect of increased concentrations of sinapic acid-loaded liposomes on the percentage inhibition of 3-NT formation in PTN assay (mean ± SD, *N* = 3).

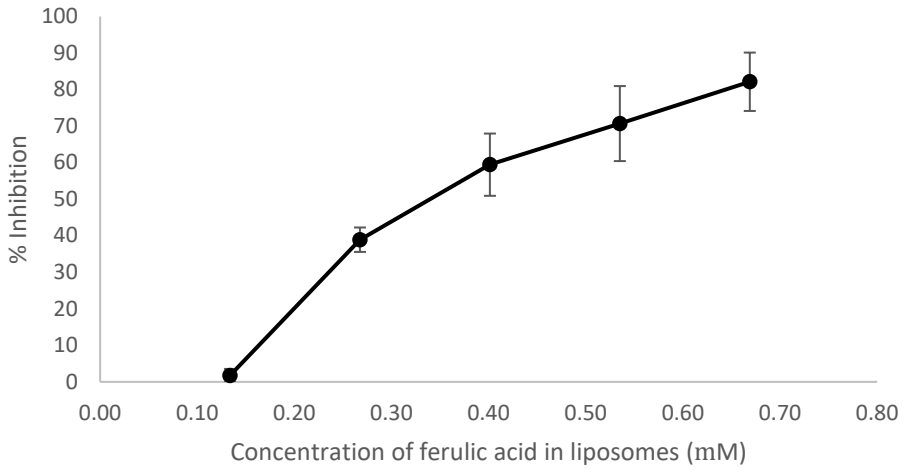

Figure 3.17: The effect of increased concentrations of ferulic acid-loaded liposomes on the percentage inhibition of 3-NT formation in PTN assay (mean ± SD, *N* = 2).

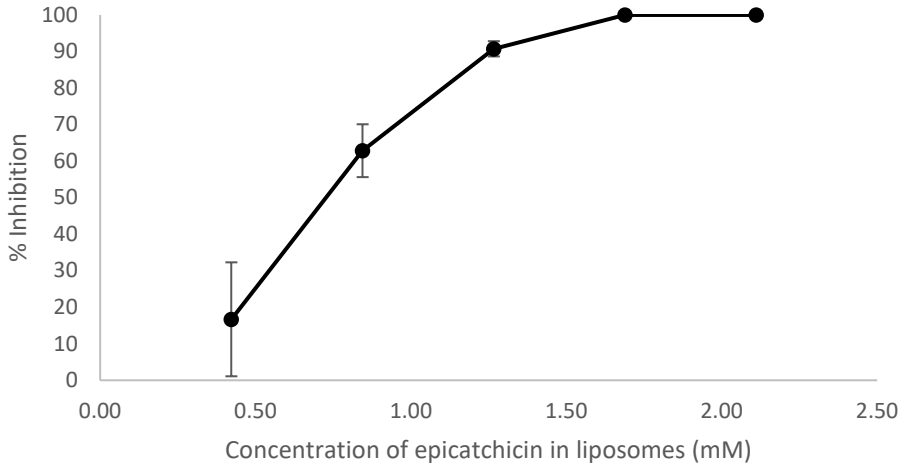

Figure 3.18: The effect of increased concentrations of epicatechin-loaded liposomes on the percentage inhibition of 3-NT formation in PTN assay (mean ± SD, *N* = 2).

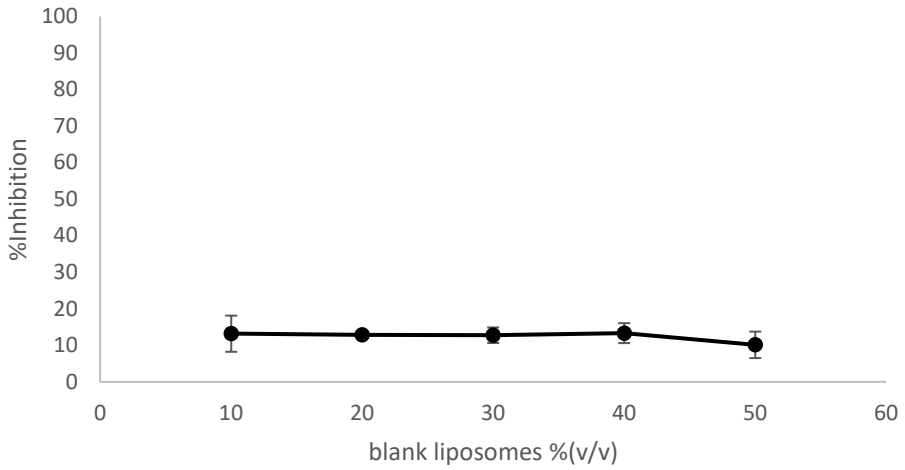

Figure 3.19: The effect of increased concentrations of blank liposomes on the percentage inhibition of 3-NT formation in PTN assay (mean ± SD, *N* = 3).

In this assay, the liposomal samples were freshly prepared and extruded on the day of analysis. Increased volumes of sample solution (0, 100, 200, 300, 400, 500 µL) was then incubated with fixed volume of L-tyrosine until peroxynitrite was prepared and quantified. The concentration of 3-NT was then determined to calculate the percentage inhibition. This was followed by the determination of the concentration of antioxidants within the volume of sample used, taking into account the %LE of each sample (results from chapter 2). The process was performed to fix the volume of sample analysed between the different antioxidants and reduce the effect of sample size on the results. However, this made comparing results between the different antioxidant-loaded liposomes rather difficult due to the variable %LE and therefore variable drug concentrations tested. For this reason, an estimated % inhibition in 3-NT formation using 0.5 mM of each antioxidant to be tested was plotted as a bar chart [Figure 3.20]. Comparing results this way showed that antioxidant activity of samples (9-14) at 0.5 mM was in the following descending order: Resveratrol > ferulic acid ≈ sinapic acid > α-tocopherol ≈ epicatechin > curcumin-loaded liposomes. This order was very similar to the order of antioxidant activity obtained from TEAC assay except for curcumin. Most importantly is that with all antioxidant-loaded liposomal samples, using higher concentrations led to a clear increase in the %inhibition in tyrosine nitration.

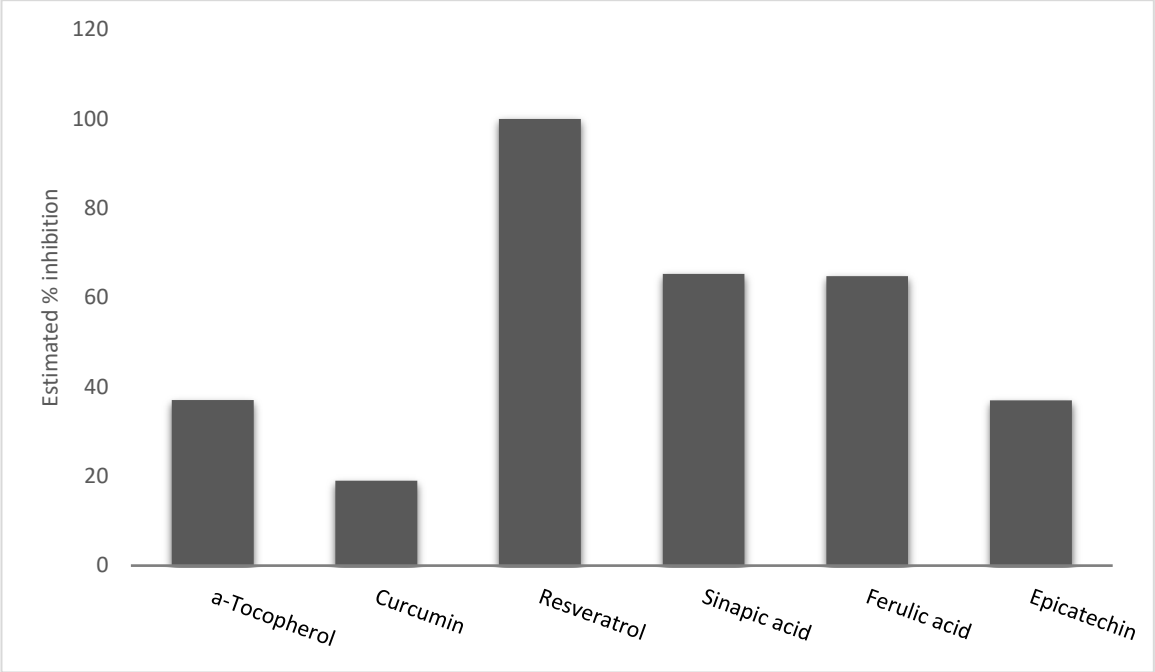

Figure 3.20: Estimated %inhibition in 3-NT formation in PTN assay due to the addition of 0.5 mM of different antioxidants-loaded liposomes.

3.6 Discussion

The antioxidants selected for this study (α-tocopherol, curcumin, resveratrol, ferulic acid, sinapic acid and epicatechin) are all natural antioxidants available in the daily diet with variable physicochemical properties (discussed in section 1.16 and summarised in table 3.1) and somewhat diverse but similar mechanism of antioxidant activity. For example, α-tocopherol loses a proton from the –OH group of the phenol ring to free radicals forming tocoperoxyl radical. Curcumin has two proposed antioxidant mechanisms of action [Figure 3.20]. The first proposed mechanism results in the formation of phenoxyl radical (similar to α-tocopherol), which can either start with the transfer of electron to the free radical forming a radical cation followed by a proton loss, or by the direct hydrogen loss (A). The second proposed mechanism is by forming a carbon-centred radical by hydrogen transfer at the diketone moiety (B). Laser flash photolysis, structure activity relationship and density functional theory studies, all confirmed that the phenolic OH is the major site of action. However, the diketone group was found to be important in the chelation of transitional metals involved in redox reactions such as iron and copper (Adhikari *et al*., 2006).

Table 3.3: Summary of the solubility of the compound under investigation in water and ethanol and their partition coefficient between octanol and water (log P)

Drug	*Solubility in H_2O*	*Solubility in ethanol*	*Log P*	*reference*
α-Tocopherol	insoluble	soluble	12.2	Liu *et al*.,2015
Curcumin	insoluble	soluble	3.29	Del Prado-Audelo *et al*., 2019
Resveratrol	insoluble	soluble	3.10	Rotches-Ribalta *et al*., 2012
Ferulic acid	Partially soluble	soluble	1.42	Galanakis *et al*., 2013
Sinapic aid	Partially soluble	soluble	1.29	Galanakis *et al*., 2013
Epicatechin	soluble	insoluble	0.11	Okumura *et al*., 2009

Similarly, resveratrol can react in different pathways when scavenging free radicals but all three pathways [Figure 3.21] form a potential phenoxyl radical. The 4'-radical was shown to be more dominant as it has a more extensive resonance system and so is a more stable radical (Xu *et al*., 2007). Additionally, ferulic acid, sinapic acid and epicatechin [Figure 3.22] form stable phenoxyl radicals when reacting with free radicals and can act by chelating metals (Zdunska *et al*., 2018, Chen 2015, Choe 2020). Moreover, ferulic acid inhibits oxidative enzymes such as xanthine oxidase and cyclooxygenase (Zdunska *et al*., 2018). To conclude, the major antioxidant mechanism of the compounds under investigation is to scavenge free radicals by donating a proton and forming a phenoxyl radical.

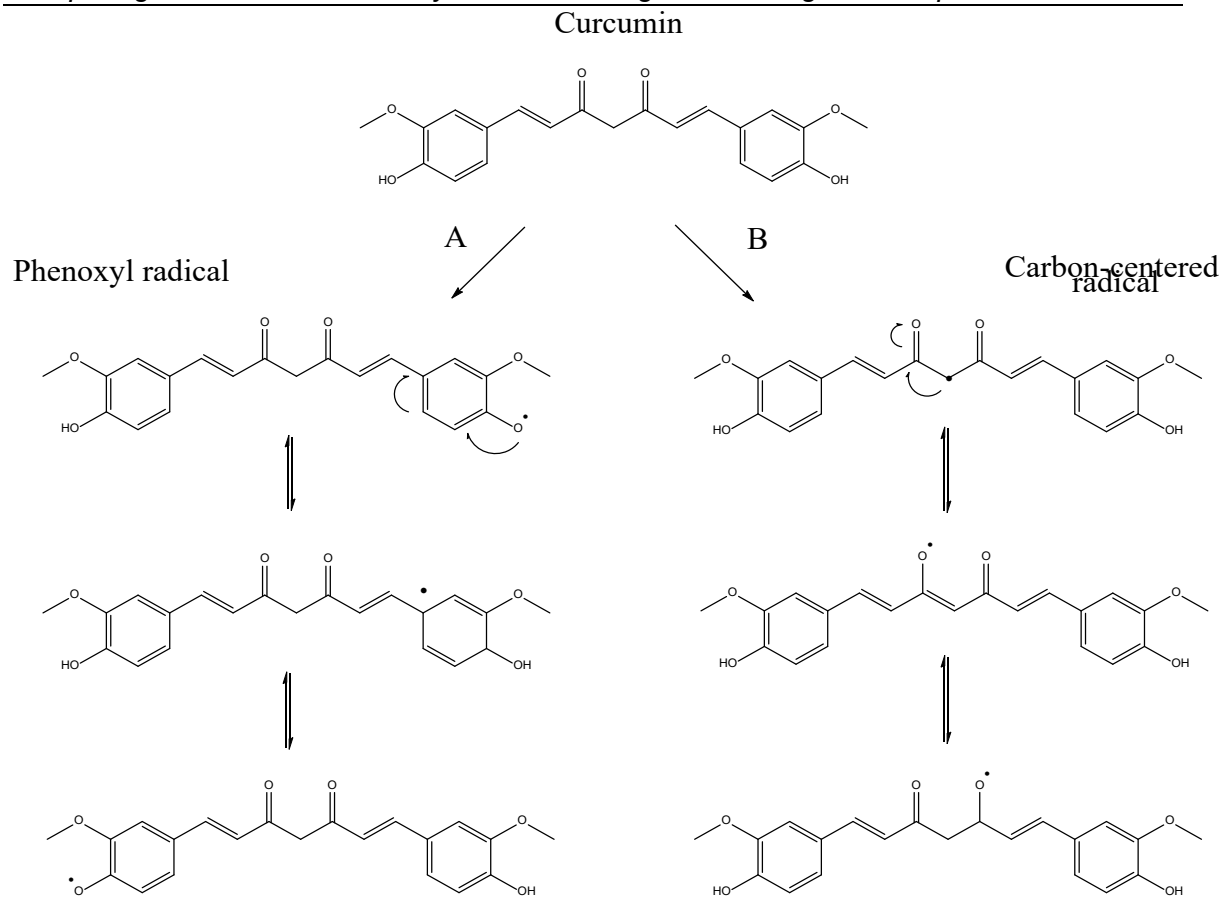

Figure 3.21**: Reaction pathway of curcumin with oxidizing radicals. (A)** A phenoxyl radical is formed by either initial electron transfer to the free radical forming radical cation, followed by proton loss to produce a phenoxyl radical or by direct hydrogen abstraction (Mostly supported by different authors). **(B)** Hydrogen atom transfer from the CH_2 group in the heptadienone link (extensively challenged).

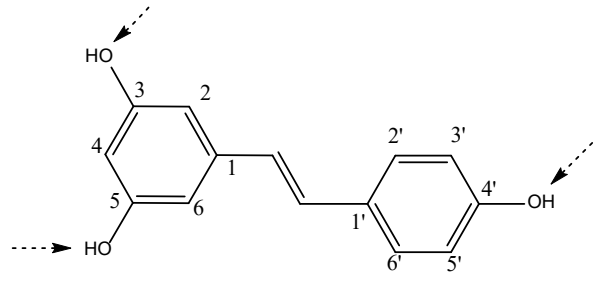

Figure 3.22: Chemical structure of trans-resveratrol showing three potential hydroxyl phenol groups that can act as H-atom donors when reacting with a free radical. Different studies confirmed that 4' phenoxyl radical is the dominant product (Xu *et al*., 2007).

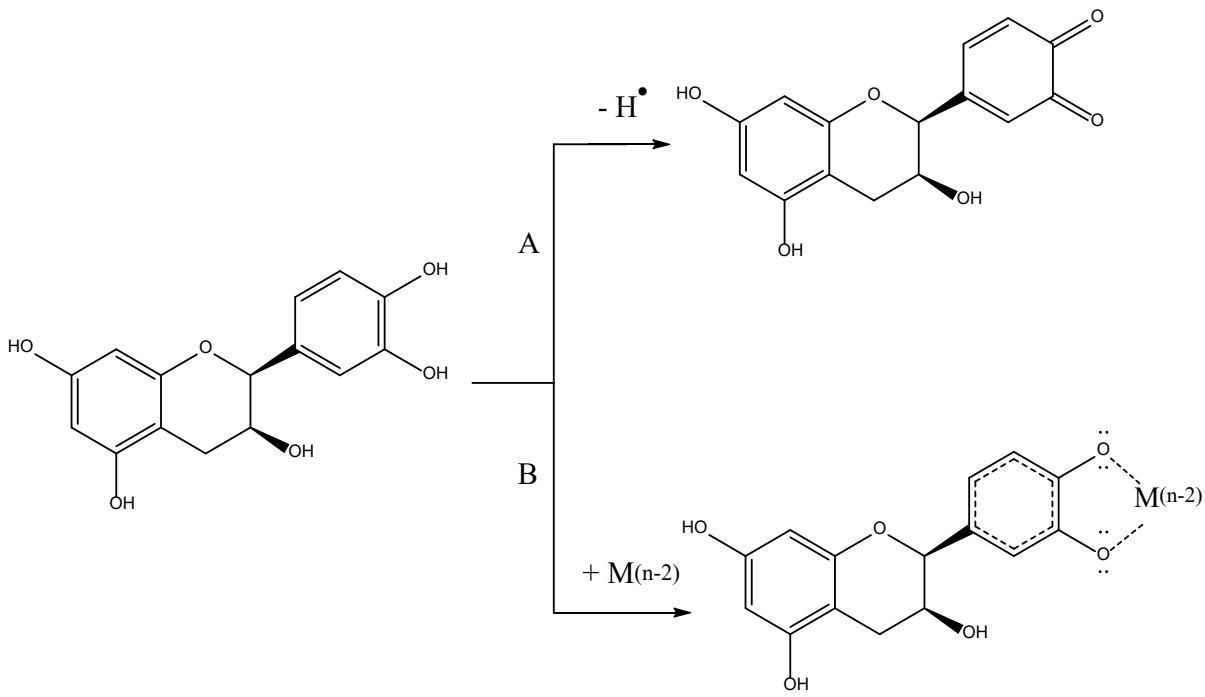

Figure 3.23: **Proposed antioxidant pathway of epicatechin. (A)** The first pathway involves proton donation from the –OH group of the phenolic ring to the free radical. The produced phenoxyl radical is stabilised by intramolecular hydrogen bonds and the by resonance phenomena. **(B)** The second pathway includes chelating metals that are prooxidants and preventing further oxidation. M = Fe or Cu (Choe 2020).

Even with the well-known antioxidant activity of these compounds, their application is limited by their physicochemical properties (discussed in chapter 1). To overcome these limitations and improve bioavailability, antioxidants were encapsulated into PLA nanoparticles and liposomes. PLA nanoparticles have a solid structure and according to results from FT-IR, DSC and SEM in chapter 2, drugs were found to be encapsulated within and not on the surface. For this reason, any attempt to study their *in vitro* antioxidant activity, should be performed after a relatively long incubation period. This was to ensure drug is released from the nanoparticles into solution and therefore, available for reaction. For instance, Linder and his co-workers, pre-incubated resveratrol-loaded nanoparticles in a buffer solution with constant agitation and tested solution using $ABTS^{\bullet+}$ assay up to 72 hours (Linder *et al*., 2013). Ideally, drug release study should have been performed prior to this experiment, in order to determine the appropriate sampling

intervals. Due to time limitation, *in vitro* antioxidant assay was not performed in this study on PLA nanoparticles.

However, liposomes have a more flexible structure, as they are lipid vesicles. Due to their vulnerability against freeze drying, no characterisation studies on their surface composition were made in chapter 2. It was not clear at this point whether the drugs are available for immediate reaction or not. For this reason, *in vitro* antioxidant activity studies were attempted after a short period of incubation. As discussed above, all antioxidants studied here have the ability to scavenge free radicals. The simple spectroscopic TEAC assay was performed due to its ability to assess this mechanism of action. Additionally it can be applied to both hydrophilic and hydrophobic compounds. As there was no separation step performed prior to this test, a second and more specific assay was required. PTN assay was applied, due to the separation *via* HPLC and for the fact that peroxynitrite is biologically relevant. The later assay was only completed on liposomal samples and not free drugs, due to the lipophilic nature of most free compounds.

3.6.1 TEAC assay

Different studies have applied the TEAC assay on the various antioxidants including the ones under investigation. Furthermore, different researchers report values in different ways. For example, some authors described the results as percentage reduction in the ABTS radical cation concentration at specific concentration of antioxidant such as Mandade *et al*., 2011. They showed that using 60 µg/mL α-tocopherol (among other antioxidants) resulted in 73.33% reduction in ABTS radical cation concentration. However, Huyut and co-workers, reported that the percentage decolourisation in ABTS radical cation using only 10 µg/mL of trolox and α-tocopherol (83.72% and 70.63%; respectively) (Huyut *et al*., 2017). Others reported results as TEAC values (Pannala *et al*., 2001, Re *et al*., 1999).

In the current study, the percentage decolourisation was plotted against the concertation of antioxidant used and its slope was determined. This slope was then divided by the slope produced by standard trolox concentration to calculate TEAC value. It can be noticed from figure 3.7.a, that using 20 µM α-tocopherol (≈ 8.6 µg/mL) showed a % decolourisation of over 60%. Although, concentrations were quite different and results were presented in different ways, it can be observed that these results were comparable to the reported results by Huyut *et al*. and Mandade *et al*. The TEAC value calculated for α-tocopherol in the current study was 0.90 ± 0.09, indicating that its activity is less than standard trolox. This was also reported by Huyut *et al*. However, Re *et al*. and Berg *et al.* reported the TEAC value for α-tocopherol to be 0.97 ± 0.02 & 0.97 ± 0.01; respectively, indicating an activity to be approximately equal to trolox (Re *et al*., 1999, Berg *et al*., 1999). These results were thought to be more realistic for two reasons: First, the SD are much smaller, representing a more precise measurement. Secondly, trolox is known as a hydrophilic analogue to α-tocopherol due to its structure similarity and identical antioxidant moiety [Figure 3.23] and therefore their antioxidant activity was expected to be similar.

Nevertheless, it has been noticed that the TEAC value calculated by the same method for the same antioxidants by different researchers can give different

figures. For example, the TEAC value reported for ferulic acid by Re *et al*. and by Apak *et al*. was 1.9 and 2.16; respectively. In the current study it was found to be 1.22 ± 0.04. All measurements were made by the same method and after the same interval (6 min). However, the method is still used to assess the antioxidant activity of several compounds and natural derivatives (Apak *et al*., 2007, Pannala *et al*., 2001, Re *et al*., 1999). Resveratrol, ferulic acid and sinapic acid as free drugs showed the highest TEAC values. This high activity compared to trolox was also noticed in a previous study (Kim *et al*., 2016, Re *et al*., 1999).

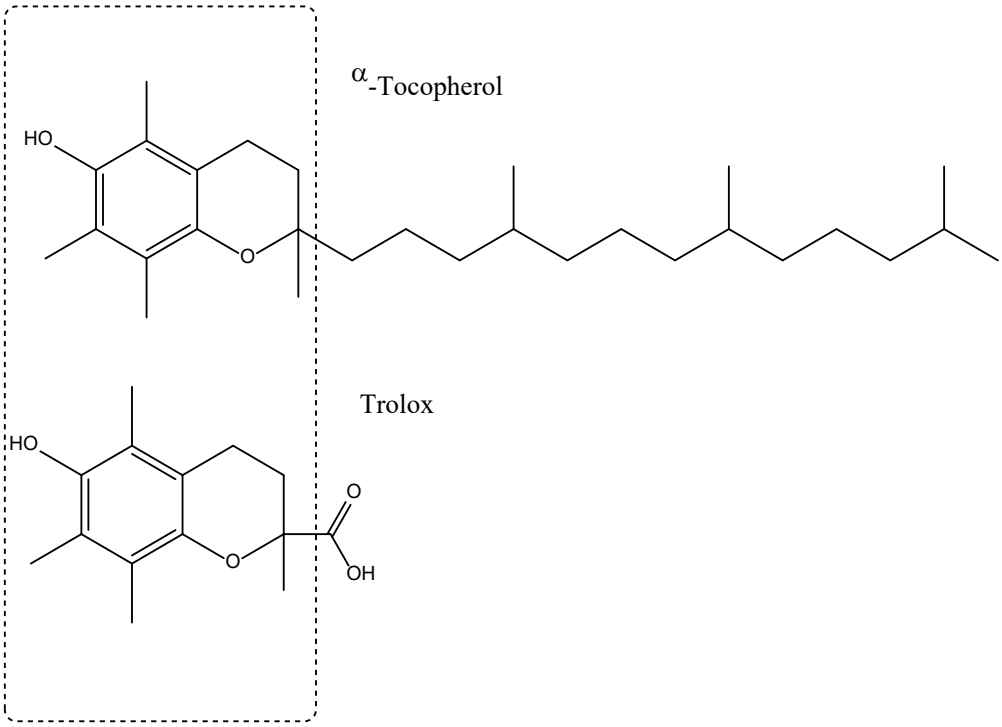

Figure 3.24**: Chemical structure of α-tocopherol and trolox.** The two structures are very similar and the hydroxyl group responsible for donating a proton to the free radical are in identical positions.

The TEAC assay has been used in other studies to evaluate the *in vitro* antioxidant activity of drug-loaded liposomes. For example, Propolis-loaded liposomes has shown to increase the % decolourisation of ABTS radical cation in a dose dependent manner (Aylin *et al*., 2020). This linear relationship was observed for all liposomal and non-liposomal samples tested in the current study. This indicates that the antioxidant activity of the tested compounds is preserved,

albeit in some cases decreased. It also gives an indication that a portion of the drug is available for immediate reaction.

3.6.2 PTN assay

Peroxynitrite mediated tyrosine nitration (PTN) assay has the advantage of being more selective due to the separation step by HPLC; however, it can only be applied to hydrophilic samples. The use of liposomes has been used to increase the solubility of lipophilic compound in water. For example, encapsulating α-tocopherol into liposomes enhanced its water solubility and improved its activity in the preservation of spermatozoa during cryopreservation (Taouzinet *et al*., 2020). Moreover, the use of liposomes enabled the dissolution of curcumin in water to produce a concentration of around 490 µg/mL (Chen *et al*., 2015). For this reason, it was possible to apply this assay to blank and antioxidant-loaded liposomes (samples 8-14).

An additional advantage of this method is the biological relevance of peroxynitrite (discussed in sections 1.6 & 3.1.2.4). The reaction of peroxynitrite with some dietary antioxidants has been discussed in the literature. For instance, the major product of its reaction with α-tocopherol has been reported to be α-tocopheroquinone. This can follow one- or two-step electron donation [Figure 3.25]. The formation of the tocopheroxyl radical is less likely to occur (Pannala *et al*., 1998). Furthermore, the reaction of peroxynitrite with hydroxycinnamates has also been studied. It has been reported that the reaction depended on the type of the functional group on the aromatic ring and the position of the hydroxyl groups. For example, ferulic acid contains an electron donating methoxy group at 3-position (accounting for greater phenoxyl radical stability) and a hydroxyl group at 4- position (accounting for 5- position activation forming a nitrated product) (Pannala *et al*., 1998). The diverse mechanism of the two assays, as shown by the dissimilar reactions to the radicals, can explain the slight difference in the order of antioxidant activity noticed in the results of the two assays.

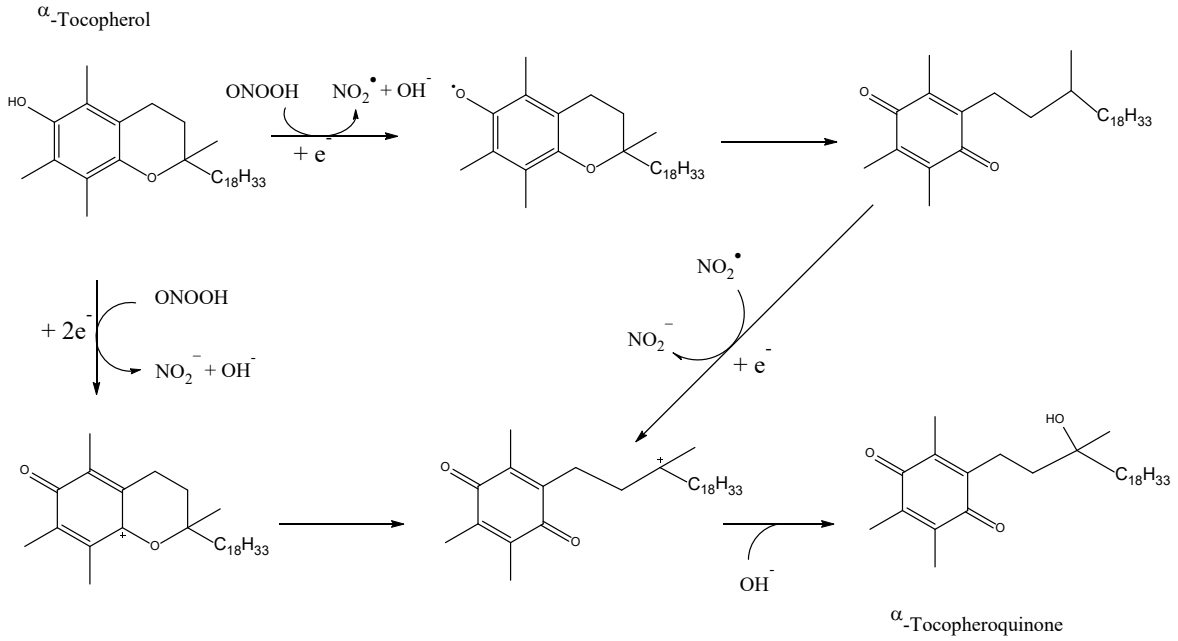

Figure 3.25: **The reaction of peroxynitrite with α-tocopherol.** The reaction can follow one-step two electron donation or two-step single electron donation to form α-tocopheroquinone (adapted from Pannala *et al*., 1998).

The assay has been previously applied to some water soluble and partially soluble antioxidants such as hydroxycinnamates (coumaric acid, caffeic acid, chlorogenic acid and ferulic acid) (Pannala *et al*., 1998) and catechin polyphenols (catechin, epicatechin, epigallocatechin and their gallic esters) (Pannala *et al*., 1997). They showed that using increased concentrations of antioxidants led to increased inhibition in tyrosine nitration. This observation was consistent with all antioxidant-loaded liposomes tested within this study (samples 9-14). However, the extent of inhibition maybe less. For example, Pannala *et al*. reported that 50 μM ferulic acid was required to inhibit 3-NT formation by 55.7 ± 8.6% (Pannala *et al*., 1997). In the current study, 400 μM ferulic acid loaded in liposomes was required to reduce 3-NT formation by 59.44 ± 8.52%. Furthermore, 100 μM epicatechin prevented tyrosine nitration by 100% (Pannala *et al*., 1997). However, in the current study this complete prevention of tyrosine nitration was only observed when using 1.7 mM epicatechin in liposomal form. This means that more drug is required to reach similar percentage inhibition, indicating less antioxidant activity. Blank liposomes showed minor inhibition in 3-NT formation, which did not increase with increased concentration.

The reduction in antioxidant activity for the liposomal drugs compared to free drug was also noticed in most of the results from the TEAC assay, except for curcumin which showed insignificant increase. This reduction was somewhat expected and could be explained by the possible encapsulation of the drugs within the liposomes. Another explanation is that the drug has been degraded or modified during the formulation procedure and its activity diminished. This justification can be eliminated, as loading efficiency studies proved otherwise. Ideally, release study should be performed at specific intervals combined with an antioxidant activity test at the same intervals. This was performed on rosmarinic acid-loaded liposomes in a separate study. They used DPPH assay to determine the antioxidant activity of the liposomes at specific intervals between 30 min and 24 hours. They showed that rosmarinic acid-loaded liposomes scavenged the DPPH radical by 41± 0.23% at 30 min and by 89 ± 0.15% at 24 hours (Yucel & Seker-Karatoprak, 2017). This shows that a portion and not the total drug is available for reaction after 30 min incubation and this portion increased after further incubation. This may explain the reduction in antioxidant activity using liposomal forms of drugs tested in this study.

The aim of encapsulating drugs in nanoparticles was to improve their physicochemical properties and therefore, improve their bioavailability. As discussed in chapter one and two, they may increase their solubility, increase absorption, increase stability, decrease toxicity, decrease elimination etc. In other words, their advantages are mainly detected in in biological systems. For this reason, *in vitro* studies were essential. The next two chapters will discuss toxicity, internalisation and activity studies on renal tubular epithelial cell lines (NRK-52E).

3.7 Conclusion

Results from the TEAC and PTN assay indicated that all drug-loaded liposomes showed antioxidant activity. This increased with increasing concentration of drugs and this indicated availability of at least a portion of the drugs for activity. The results determined by PTN assay showed that antioxidant activity was within the following descending order: Resveratrol > ferulic acid ≈ sinapic acid > α-tocopherol ≈ epicatechin > curcumin-loaded liposomes. Blank liposomes showed almost negligible activity, which did not change with increasing concentration of liposomes. There were slight differences in the order of activity using TEAC assay, which was in the descending order: resveratrol ≈ ferulic acid > curcumin > sinapic acid > α-tocopherol ≈ epicatechin. This was explained by the different mechanism of the two assays. TEAC values of free drug compared to drug-loaded liposomes were slightly reduced for most samples. This was explained by the encapsulation of the drugs within liposomes. The next two chapters will discuss toxicity, internalisation and activity studies on NRK-52E.

Chapter 4: Toxicity and internalisation studies of antioxidant-loaded nanoparticles on NRK-52E cell lines

4.1 An introduction to the chapter

In chapter two, PLA nanoparticles and liposomes loaded with different antioxidants under investigation were prepared and characterised. Antioxidant activity of the drug-loaded liposomes was measured using TEAC and PTN assays and reported in chapter three. The limitations of these assays were also discussed and the need for more relevant tests to ensure safety and efficiency. Chapter four will discuss the different routes of nanoparticle administration, the mechanisms of nanoparticles internalisation into cells and the factors affecting the fate of nanoparticles in the body. In order to study the toxicity and internalisation of antioxidants in pure form and encapsulated in both liposomes and PLA nanoparticles, *in vitro* tests were performed using renal proximal tubular (NRK-52E) cell-line. The materials, methods, results and a discussion of the *in vitro* tests used to study the toxicity and internalisation of the delivery systems developed in this research will be detailed in this chapter.

4.1.1 Routes of nanoparticle administration

Different routes have been studied and investigated to administer nanocarriers into systemic circulation. These include but not limited to oral, pulmonary, i.v. and transdermal delivery. As with conventional drug forms, all these routes have advantages and disadvantages. For example, although the oral route is non-invasive, the gut mucosa can act as an obstacle to absorption. Additionally, within the circulation, the first pass metabolism is another major obstacle. Nanoparticles have been used to administer drugs locally to the skin, eyes and lungs. Some of these routes will be discussed in detail below [Figure 4.1].

4.1.2 The oral route of administration

Nanoparticles can be absorbed after oral administration from the gastrointestinal tract (GIT) mainly through the M-cells of the Peyer's patches in the gut-associated lymphoid tissue (GALT) or to a lesser extent through the normal gut enterocytes (Florence 2005, Hagens *et al*., 2007). The M-cells are enterocytes with no microvilli, lack the thick mucus layer, and so have been adapted to enable absorption of microorganisms and larger particles as part of the innate immune system (Florence 2005, Bergin & Witzmann, 2013). Particles smaller than 100 nm can enter through endocytosis. Larger particles pass through the M-cells *via* transcytosis. Additionally, particles may enter the body *via* persorption, were they pass paracellularly into the lymph vessels and eventually blood vessels (Matteis 2017, Kadian 2018). It was reported that the reason behind enhanced absorption of nanoparticles compared to free drug is that some nanoparticles adhere to the mucosa increasing contact time (Kadian 2018). Once the nanoparticles pass the enterocytes, they enter the lymph nodes to lymph vessels and possibly navigate to the blood circulation and finally to the tissues. However, a study on mice using radio-labelled poly(methyl methacrylate) nanoparticles showed that only 10-15% is absorbed after oral administration *via* the intestine (Kreuter 1990). Another factor to consider during studying oral administration is the potential interaction with the gut flora. It has not been fully understood if unabsorbed nanoparticles can alter

normal flora. Nevertheless, the effect of an underlying condition such as increased gram-negative growth may enhance or hinder the absorption. These considerations will need to be fully determined and studied, as there is not much data covering these points. Examples of nanoparticles studied for oral administration are antitubercular drugs-loaded lectin-functionalized nanoparticles, insulin-loaded VB12-dextran nanoparticles, rapamycin-loaded nanoparticles (Kadian 2018) and citrate-capped zinc oxide nanoparticles (Beek *et al*., 2012).

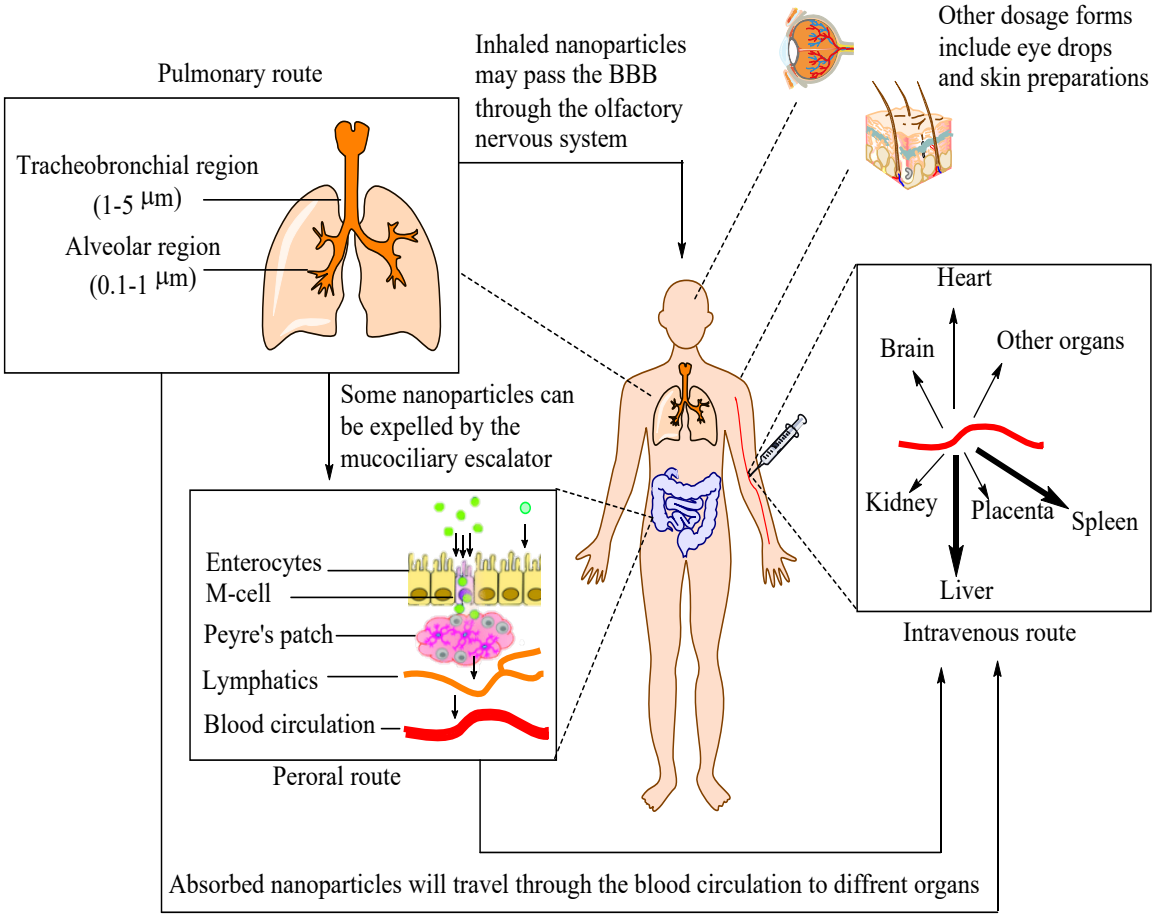

Figure 4.1: **The main routes of nanoparticle administration.** a. The oral route, were the absorption takes place through the enterocytes primarily *via* the M-cells. b. The pulmonary route, mainly for local action, but nanoparticles may be absorbed to the systemic circulation, expelled through the mucociliary escalator or pass the BBB *via* the olfactory nervous system. c. parenteral administration, mainly through the i.v. route leading to various body organs and tissues. d. Local drug application such as eye drops and skin preparations (original figure in colour)

4.1.2.1 The pulmonary route of administration

Administering conventional drugs directly to the lungs *via* the pulmonary route for local action can have the advantages of reduced therapeutic dose, rapid onset of action and reduced systemic toxicity. These advantages can also be the case for nanocarriers. For example, inhaled antitubercular-loaded PLGA nanoparticles have shown improved bioavailability and increased duration of action compared to free drugs (Kadian 2018). This was also the case with amikacin-loaded solid lipid nanoparticles, as they showed less kidney toxicity and a more sustained release, reducing dose frequency (Kadian 2018). Paclitaxel-loaded polymeric nanoparticles also showed reduced side effect for the treatment of lung cancer (Kadian 2018). Additionally, theophylline and budesonide-loaded PLA nanoparticles have been studied for a sustained release after inhalation for the treatment of COPD (Buhecha *et al*., 2019). Furthermore, a separate study compared three different routes of administration of anti-inflammatory-loaded nanoparticles to target lung inflammation. This study showed intratracheal administration to be superior to i.v. and i.p. administration in terms of lowering effective dose and reducing accumulation in liver and lymph nodes (Wang *et al*., 2021).

After inhalation, particles over 1 µm will mainly remain in the tracheobronchial region, where they can stay and act locally or be expelled by coughing (Matteis 2017). Around 80% of nanoparticles with particle size less than 100 nm will deposit in the respiratory tract at the alveolar region with low but detectable amount absorbed into blood circulation. This low amount can increase in damaged epithelial cells (Matteis 2017, Hagens *et al*., 2007). Once absorbed, nanoparticles can be distributed in different organs such as liver, heart, kidney, spleen and brain. This has been confirmed with radiolabelled nanoparticles in animal studies and in some human studies (Hagens *et al*., 2007). Heparin-loaded chitosan nanoparticles have shown promising systemic delivery after pulmonary administration (Kadian 2018). In addition to the probable absorption of nanoparticles through the respiratory system to the blood, inhaled particles may find its way directly to the brain *via* the olfactory nervous system (Hagens *et al*., 2007). This route has been studied for the delivery of nanoparticles directly to the

brain using intranasal deliver avoiding the blood brain barrier. Examples of such applications are rivastigmine-loaded chitosan nanoparticles and bromocriptine-loaded chitosan nanoparticles for the treatment and prevention of Alzheimer's disease and Parkinson's disease; respectively (Kadian 2018). Another important path to consider when studying pulmonary administration is that inhaled nanoparticles can find their way to the digestive system *via* the mucociliary escalator (Hagens *et al*., 2007).

4.1.2.2 The parenteral route of administration

The parenteral route, mainly i.v., has the main advantage of bypassing all the absorption barriers, as the nanoparticles are injected directly into the blood stream. Fasehee *et al*. compared the administration of disulfiram-loaded PEG-PLGA nanoparticles *via* i.v. and i.p. routes. They showed that i.v. administration is beneficial in suppressing tumour growth compared to the i.p. route due to the absorption barrier of the peritoneal cavity (Fasehee *et al*., 2016). Still, there are factors to consider. For example, the nanoparticles need to be stable enough in the blood compartment and not cause local or systemic toxicity. Additionally, the nanoparticles will need to find its way through the blood stream to the targeted tissue. The fate of nanoparticles is mostly to the liver and spleen after being taken up by the reticuloendothelial system (RES) (Jawahar & Meyyanathan, 2012, Park *et al*., 2018). A single study compared the distribution of cerium oxide nanoparticles in animals after oral and i.v. administration. Although the particle size of nanoparticles in that study ranged between 69.2 and 98.1 nm, oral absorption to the tissues was negligible and cerium was detected mostly in faeces. In contrast, high levels of cerium was detected in all tissues after i.v. administration, although mainly in spleen and liver (Park *et al*., 2018). Interestingly, in a separate study, PEG-PLGA nanoparticles of larger particle size (approximately 400 nm) were found to deposit mainly in the kidneys regardless of their surface charge after i.v. injection (Williams *et al*., 2015). It was hypothesized that transcytosis across the peritubular capillary endothelium is the main pathway to the tubules. The same study showed that after oral administration all the dose was excreted with faeces with minimal systemic absorption (Williams *et al*., 2018). It is also worth mentioning that the first i.v. administered nanoparticle medicine to be approved by the FDA in 2006 was Abraxane®, which is a paclitaxel protein-

bound particle drug used in the treatment breast cancer (Chenthamara *et al*., 2019).

4.1.2.3 Other routes of administration

In addition to the routes discussed above, there are other routes that have been utilised to administer nanoparticles locally to the desired site of action such as to the skin and to the eyes. For example, titanium dioxide and zinc oxide nanoparticles are added to sunscreens to absorb UV light. Studies on transdermal absorption have been controversial, with some studies showing penetration of metal oxides to the dermis and others not even passing the epidermis. Reports have shown that applying mechanical flexion to the skin can induce penetration of nanoparticles to the dermis. This suggests potential entry into the systemic circulation, but still there is not enough concluding data available (Hagens *et al*., 2007). Additionally, the use of caffeic acid-loaded liposomes have shown improved skin penetration over free drug (Katuwavila *et al*., 2016). Examples of nanoparticles intended for ocular drug delivery include cyclosporine A-loaded nanoparticles, brimonidine tartrate-loaded chitosan nanoparticles and pilocarpine HCl-loaded nanoparticles. These nanoparticles have shown advantages over traditional eye drops such as enhanced ocular retention, improved bioavailability, significant sustained effect and the potential of rapid permeation through the excised cornea (Kadian 2018).

4.1.3 Internalisation of nanoparticles into cells

In order for drug-loaded nanoparticles to produce their therapeutic effect, they need to reach their site of action in the body and release their cargo at that site. During this journey, nanoparticles will possibly pass through at least one of the biological barriers such as the gut epithelium, blood vessel endothelium and/or the membrane of its target cells. For this reason, nanoparticles must be able to enter the cells and release its load. Two different mechanisms have been proposed for internalisation of nanoparticles into cells; phagocytosis and endocytosis. Endocytosis can be subdivided in to clathrin-mediated endocytosis, caveolae-mediated endocytosis, macropinocytosis and other clathrin- and

caveolae-independent endocytosis (Hillaireau & Couvreur, 2009) [Figure 4.2]. It is important to understand the mechanism of nanoparticle internalisation as it could help to elucidate the fate of nanoparticles. For example, caveolin-mediated endocytosis is usually involved in transcytosis, where nanoparticles enter from one end of the cell and exit from the other. This is useful when absorbing nanoparticles through the gut after oral absorption, especially for endosomes that are not fused with lysosomes (Manzanares & Cena, 2020).

4.1.3.1 Phagocytosis

Phagocytosis occurs mainly in macrophages, monocytes, neutrophils and dendritic cells and to a lesser extent in fibroblasts, epithelial and endothelial cells as part of a defence mechanism. It basically involves three steps: opsonisation, adhesion and ingestion. Opsonisation is the process of labelling any alien elements (nanoparticles) using special proteins in the blood circulation called opsonins such as immunoglobulins, complement components, laminin, fibronectin, C-reactive protein and type-I collagen. The tagged particles then adhere to the cell surface *via* interaction with specific receptors such as Fc receptors or complement receptors. This triggers a series of events leading to the formation of actin that is responsible for the extension cell membrane forming a pseudopodia. This then surrounds and engulfs the nanoparticle forming a phagosome that is translocated into the cell cytoplasm. It will then fuse with a lysosome forming a phagolysosome [Figure 4.2]. The pH of this newly formed body is then reduced by the action of the proton pump ATPase on its cell membrane and filled with enzymes such as esterases and cathepsins. Depending on the characteristics of the nanoparticle these enzymes then help break down the nanoparticle and release its content (Hillaireau & Couvreur, 2009). This mechanism is rarely used for delivering drugs into cells, as the fate of nanoparticles cargo is usually degraded by lysosomal enzymes (Manzanares & Cena, 2020).

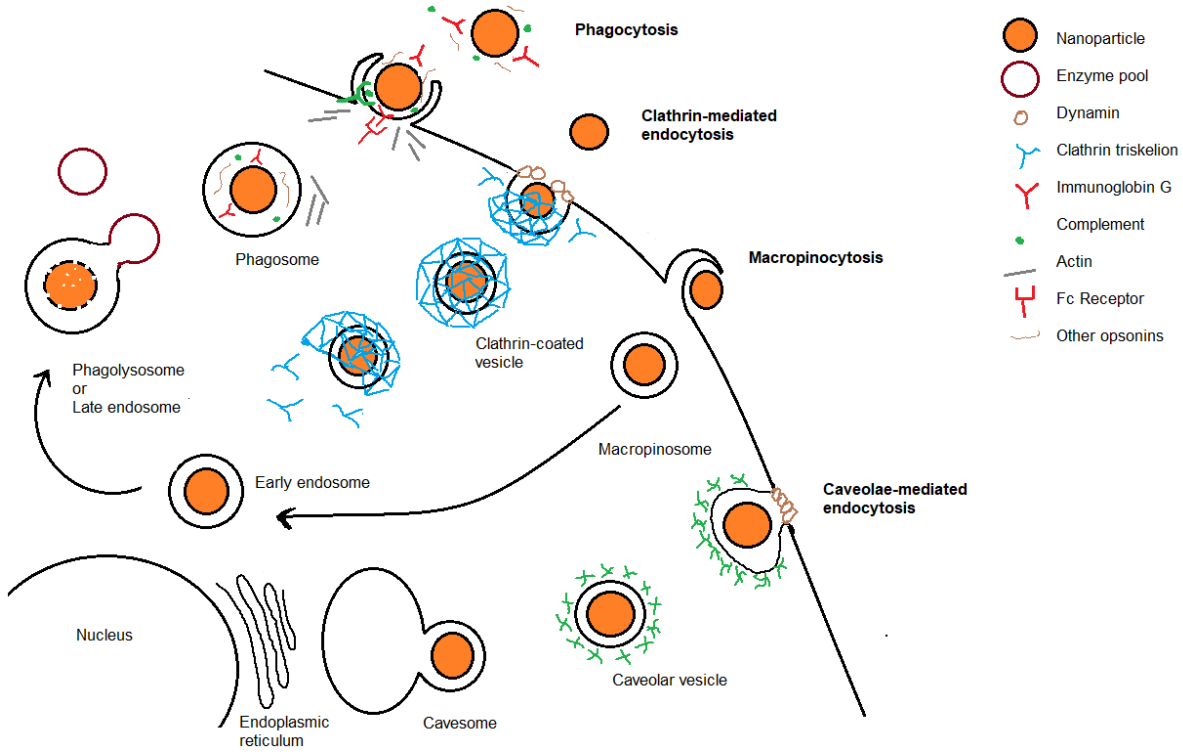

Figure 4.2: **Nanoparticles enter the cells by phagocytosis or pinocytosis (endocytosis)**. Phagocytosis: starts with particle opsonisation then adhesion and ingestion to form a phagosome, which fuse with a lysosome to form a phagolysosome. Pinocytosis can be divided into: A. Clathrin-mediated endocytosis, were the assembly of clathrin triskelion into a basket shape lattice leads to the deformation of cell membrane forming a coated vesicle that is released inside the cell when uncoated. B. Macropincytosis, which forms macropinosomes that may eventually fuse with the lysosome or be recycled back to surface. C. Caveolae-mediated pinocytosis, were the caveolin dimer deforms the cell membrane to a caveolar vesicle surrounding the particle and is then delivered to a cavesome with no lysosome activity involved (Adapted from Hillaireau & Couvreur, 2009, original figure in colour)

4.1.3.2 Pinocytosis

As opposed to phagocytosis, pinocytosis or occasionally called endocytosis occurs in all cells and not dominated by specific cells and is involved in the entrance of fluids and generally smaller nanoparticles (Manzanares & Cena, 2020, Hillaireau & Couvreur, 2009).

4.1.3.2.1 Clathrin-mediated endocytosis

Clathrins consist of tri-legged constructions called triskelions that form a polyhedral framework just below the cell membrane, facilitating the formation of a pit-like structure with a diameter around 150 nm. These pits then continue to deepen utilising GTPase until they close around a nanoparticle forming a vesicle coated with clathrin. This is then decoated forming initially, an early endosome (internal pH ≈ 6) then a late endosome (internal pH ≈ 5) that fuses with a prelysosomal vesicles (holding hydrolase) leading to nanoparticle degradation and cargo release. These events can be receptor dependent (utilising specific ligand-receptor interaction) or receptor independent (utilising non-specific electrostatic and hydrophobic interactions) [Figure 4.2] (Hillaireau & Couvreur, 2009).

4.1.3.2.2 Caveolae-mediated endocytosis

Caveolin is a dimeric protein augmented with cholesterol and sphingolipids forming invaginations in the cell membrane with a diameter of 50-100 nm called caveolae. These mediate the endocytosis and transcytosis of different proteins and viruses and can be used to deliver nanoparticles. This mechanism is similar to the clathrin-mediated endocytosis but is a more regulated process that is initiated by specific ligand-receptor interaction and does not involve any lysosomal enzyme activity. This occurs mainly in the endothelial cells and to a less instant in the smooth muscle cells and fibroblasts. [Figure 4.2] (Hillaireau & Couvreur, 2009).

4.1.3.2.3 Macropinocytosis

This pathway is more similar to phagocytosis but with no selectivity. Projections made by actin in the cell membrane collapse over extracellular fluid like a wave forming intracellular vacuoles (1-5 μm) called macropinosomes. However, it does not require any special ligands and usually shrink after a reduction in their pH. They also might ultimately fuse with lysosomes or another part of cell membrane for recycling [Figure 4.2] (Hillaireau & Couvreur, 2009, Manzanares & Cena, 2020).

4.1.3.2.4 Other clathrin- and caveolae-independent endocytosis

In addition to the above pathways, nanoparticles can enter the cells *via* different clathrin- and caveolae- independent endocytosis such as the use of microdomains rich in cholesterol named rafts (Hillaireau & Couvreur, 2009). Various mechanisms have been recently reviewed that depend on different enzymes or molecules such as Rho GTPase, ADP-ribosylation factor 6 and flotillin dependent endocytosis. However, these are still in need for further understanding (Zhao & Stenzel, 2018) and are not utilised significantly to transfer nanoparticles (Manzanares & Cena, 2020).

4.1.4 Factors affecting absorption and distribution of nanoparticles to tissues and organs

Figure 4.3 summarises the different nanoparticles characteristics that can determine their journey and final fate inside the body. Due to wide variety and the diverse behaviour of nanoparticles, as well as the different results obtained from *in vitro* and *in vivo* studies, it is difficult to assume their pharmacokinetic performance. Nevertheless, these factors can be used to estimate an approximate behaviour.

4.1.4.1 Particle size

The size of nanoparticles is one of the main factors affecting its penetration through tissue barriers. Studies showed that optimum absorption after oral administration (around 30%) occurs when particles are between 50 and 100 nm (Hagens *et al*., 2007, Florence 2005). Any particle over 1000 nm will be trapped in the Peyer's patch (Florence 2005). So, generally, the larger the particle the lesser the absorption. However, this is not always the case. For instance, it has been reported that larger anionic polyamidoamine dendrimers deposit at higher levels into cells compared to smaller dendrimers (Bergin & Witzmann, 2013). The size of the nanoparticle will affect the method of cell internalisation. Generally, particles larger than 500 nm enter cells *via* phagocytosis. Nanoparticles less than 200 nm usually involves clathrin-mediated endocytosis and particles up to 500 nm are

predominantly internalised *via* caveolae-mediated endocytosis (Hillaireau & Couvreur, 2009). However, pathways such as micropinocytosis are independent of particle size and can internalise nanoparticles from 0.2 nm up to 5 μm (Zhao & Stenzel, 2018).

Nevertheless, nanoparticles over 100 nm in the blood will be detected and cleared *via* the reticuloendothelial system in the liver, spleen, lung and any particles less than 5 nm will be excreted *via* the urine (Chenthamara *et al*., 2019). Another important consideration is the possible binding of nanoparticles with proteins forming protein corona that led to an increase in particle size (Manzanares & Cena, 2020). Furthermore, in some circumstances such as in cancerous tissues, cells become leakier due to the enhanced permeability and retention effect and nanoparticles with mean particle size up to 220 nm can pass the cell membrane and target the tumour cells (Fasehee *et al*., 2016, Tan & Ho, 2018). Particle size can also affect skin penetration. For example, studies showed that particles around 4 nm can pass intact skin, while particles around 45 nm can only penetrate damaged skin (Matteis 2017).

4.1.4.2 Surface charge

The charge on the surface of nanoparticles measured as surface zeta-potential can also affect absorption and distribution. Studies have shown that neutrally and positively charged nanoparticles can penetrate the mucus barrier covering the GIT more easily (Bergin & Witzmann, 2013). Equally, the toxicity level of cationic nanoparticles has been reviewed to be higher than anionic nanoparticles causing haemolysis and clotting (Chenthamara *et al*., 2019). Furthermore, neutral nanoparticles can be unstable due to the formation of aggregates leading to larger particles that are absorbed less. Another disadvantage of neutral nanoparticles is their lower affinity to bind to cell receptors due to reduced electrostatic forces (Hillaireau & Couvreur, 2009). It is known that cell membranes possess a negatively charged surface, which increases the adhesion of positively charged nanoparticles and favouring rates of internalisation compared to negatively charged nanoparticles (Hillaireau & Couvreur, 2009). Finally, negatively charged liposomes (prepared from negatively charged lipids

such as (phosphatidylserine, phosphatidic acid and phosphatidylglycerol) have shown to be recognised and cleared more rapidly by the RES (Li *et al*., 2014).

4.1.4.3 Shape and flexibility

A characteristic factor that may affect the fate of nanoparticles is their shape and rigidity. It is through that rigid spherical shape that nanoparticles are favoured by macrophages. For instance, a single study showed that polyacrylamide nanoparticles with soft flexible structure did not stimulate actin formation and therefore did not promote phagocytosis. This was opposite to the more rigid polymeric nanoparticles with comparable surface characteristics. However, this is not the case for liposomes. It was reported that liposomes with a rigid structure (due to the addition of cholesterol to fatty acids during preparation) are less likely to be opsonised and therefore escape phagocytosis (Hillaireau & Couvreur, 2009). Another review stated that rigid nanoparticles are more prone to be internalised *via* clathrin-mediated endocytosis as opposed to flexible nanoparticles that are enter cells through macropinocytosis (Manzanares & Cena, 2020).

As mentioned above nanoparticles with particle size over 100 nm will be detected and cleared by the macrophages and accumulate mainly in the liver and spleen. However, it was reported that ammonium functionalised carbon nanotubes were effectively used to deliver small interfering RNA (siRNA) with an approximate length of 300 nm to kidney cells in AKI animal models. Over 22% of the injected dose was transported into proximal tubular calls *via* clathrin-mediated endocytic uptake mechanism with the majority of the dose eliminated in the urine (Alidori *et al*., 2016) indicating that the shape of the nanoparticles clearly effects its fate. Another example of the influence of shape, is reported with cylinder shaped nanoparticles. It was noticed that elongated nanoparticles such as cylindrical latex nanoparticles, polystyrene ellipsoids, polystyrene worms and self-assembled rods can escape phagocytosis and therefore, enhancing circulation time. However, this comes with the drawback of reduced cellular uptake (Zhao & Stenzel, 2018). Still,

the optimum shape for effective delivery has been controversial and in need for further study (Manzanares & Cena, 2020)

4.1.4.4 Composition and nature of material

Another important feature to consider is the nature of the material used to prepare the nanoparticles. Most studies showed the major sites of nanoparticle accumulation after reaching systemic circulation are the liver and the spleen (Baek *et al*., 2012). This was rationalised by the increased macrophages in these organs, indicating cell entry *via* phagocytosis. This increase is mainly reported with hydrophobic nanoparticles such as PLA and PLGA nanoparticles and was rationalised by the increased van der Waals interactions between opsonins and nanoparticle surface leading to increased phagocytosis (Hillaireau & Couvreur, 2009). However, a study on the absorption, distribution and excretion of zinc oxide nanoparticles after oral administration showed that they were mainly accumulated in the liver, lungs and kidneys but not in the spleen. This indicated a different method of cell entry, probably involving the formation of Zn0-S bonds that were found abundant (using powder x-ray diffraction and transmission electron microscopy) in this study at sites of accumulation (Baek *et al*., 2012). Furthermore, albumin nanoparticles are capable of selective targeting to podocytes of Bowman's capsule (due to increased albumin's natural receptors: neonatal Fc receptors) and to breast, lung, liver and gastric cancers (due to overexpression of a special extracellular matrix glycoprotein with high protein binding affinity) (Tan & Ho, 2018).

4.1.4.5 Surface coating and targeting

In addition to the size, shape, charge and type of nanoparticles, they can be engineered or coated to display certain characteristics such as increased stability, reduced aggregation, longer duration of action, enhanced cell adhesion or even active targeting. For example, using PEGylated polymers such as PEG-PLA and PEG-PLGA can reduce liver accumulation and prolong systemic circulation. Targeting can be achieved *via* different means such as the addition of folate to target cancer cells with overexpressed folate receptors (Fasehee *et al*., 2016).

Transferrin receptors are also overexpressed in tumour cells. This has been used to target these cells by coating nanoparticles with transferrin to increase cellular uptake (Hillaireau & Couvreur, 2009). For the purpose of increased absorption, nanoparticles can be coated with lectins, invasin or internalin fragments leading to increased cell membrane adhesion. However, these adjustments produced variable and unclear outcomes and are in need of further study (Florence 2005).

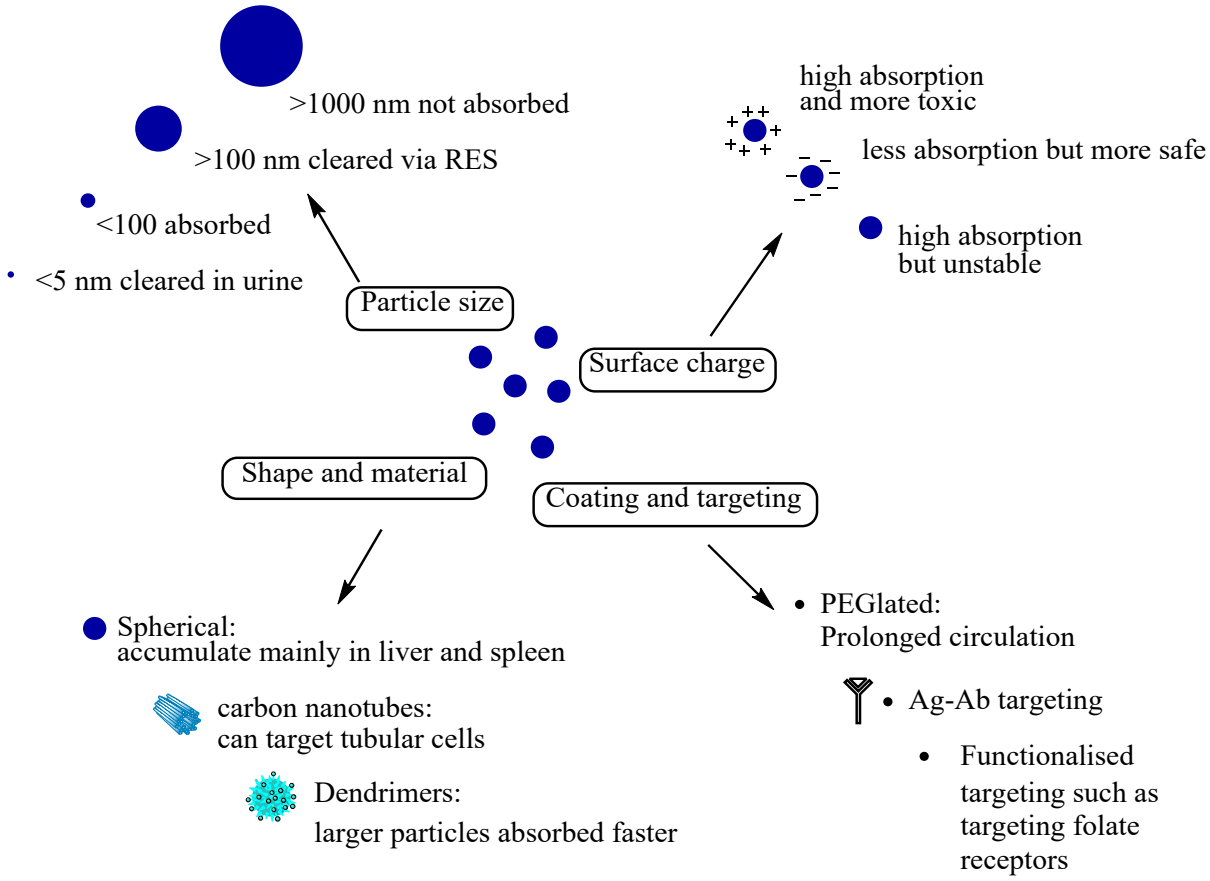

Figure 4.3: **Different nanoparticle characteristics that may affect absorption, distribution and elimination.** The mean particle size, surface charge, shape, type and coating material can determine the fate of nanoparticles after entering the body (original figure in colour)

4.1.5 Toxicity of nanoparticles

As described above, nanoparticles as drug carriers have been proven to find their way into the circulation and then to various organs. Furthermore, inorganic nanomaterials are used in different industrial products such as food,

paints and cosmetics, which can then enter the body by ingestion, inhalation or dermal penetration (Matteis 2017). Due to the different pharmacokinetic properties of nanoparticles compared to free drugs, it is reasonable to consider differences in their toxicity profile. For example, carbon nanotubes are known to cause platelet aggregation unlike C-60 fullerenes, which are their main components (Chenthamara *et al*., 2019). Additionally, results from *in vitro* cytotoxicity studies are different from *in vivo* studies. For example, Quantum dot nanocrystals (2.2 nm, positively charged) used in imaging and targeting studies were found to be cytotoxic in *in vitro* studies. This was not observed in *in vivo* studies (Hagens *et al*., 2007). It was reported that the main cause of nanotoxicity is the induction of the inflammatory system, the rise in ROS level and the disturbance of homeostasis. This is caused by nanoparticles such as amorphous titanium oxide and silver nanoparticles (Chenthamara *et al*., 2019, Matteis 2017). The higher toxicity profile of cationic nanoparticles was attributed to the increased attraction to the negatively charged proteins in the blood stream forming protein corona. These induce inflammatory responses such as cytokines release. Additionally, smaller gold nanoparticles (4 nm) induce ROS production and IL-8 secretion more than larger ones (70 nm) (Matteis 2017).

4.1.6 NRK-52E cell lines

As discussed above, different cells internalise nanoparticles *via* different pathways. The NRK-52E cell line was originally cloned from normal rat kidney proximal tubular cells and maintain their distinct morphology and function throughout culture. They were used in the current study, as the main aim was to improve the efficiency of selected antioxidants for the prevention or treatment of AKI. Furthermore, the proximal tubule is main part of the kidney that is affected in AKI (discussed in section 1.9).

4.1.7 Cell viability test

The MTT (3-[4,5-dimethylthiazol-2-yl]-2,5 diphenyl tetrazolium bromide) formazan conversion assay was used to assess cell viability in this study (Mossmann 1983, Abe & Matsuki 2000). The rationale is based on MTT being

reduced inside the mitochondria of living cells into purple formazan crystals by an oxidoreductase enzymatic reaction utilizing NADH or NADPH [Figure 4.4] (Mossmann 1983). More recent data has shown that this reaction also occurs outside the mitochondria but still within the cell and so can be used as an indication of cell viability (Fotakis & Timbrell, 2006). The reduction in this reaction (measured by the intensity of the produced formazan crystals) is used as an indication of cell damage (Abe & Matsuki, 2000).

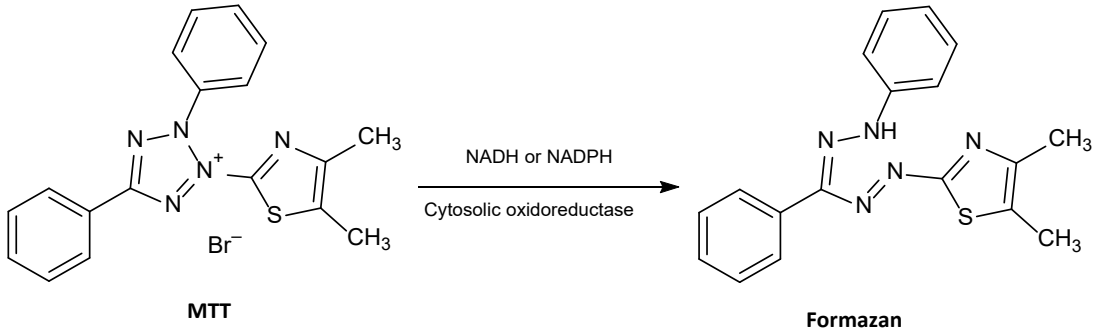

Figure 4.4: Reduction of MTT by NADPH/NADH oxidoreductase to MTT formazan

4.1.8 Determination of cell death using membrane integrity assay

The lactate dehydrogenase (LDH) assay was adapted from that described by Abe & Matsuki, 2000, to test the integrity of cell membrane. Its main principle depends on the release of LDH produced intracellularly into the surrounding medium after cell membrane damage. Although, different methods are available to measure the level of LDH released, in this study it mainly depends on the reduction of β-NAD to NADH by the formation of pyruvate from lactate in the presence of LDH. MTT is then transformed into formazan (measured colourimetrically) by NADH in the presence of 1-methoxyphenazine methosulphate (MPMS) [Figure 4.5]. Triton-X100 is added to remove any cell debris and to solubilise formazan formed (Abe & Matsuki, 2000).

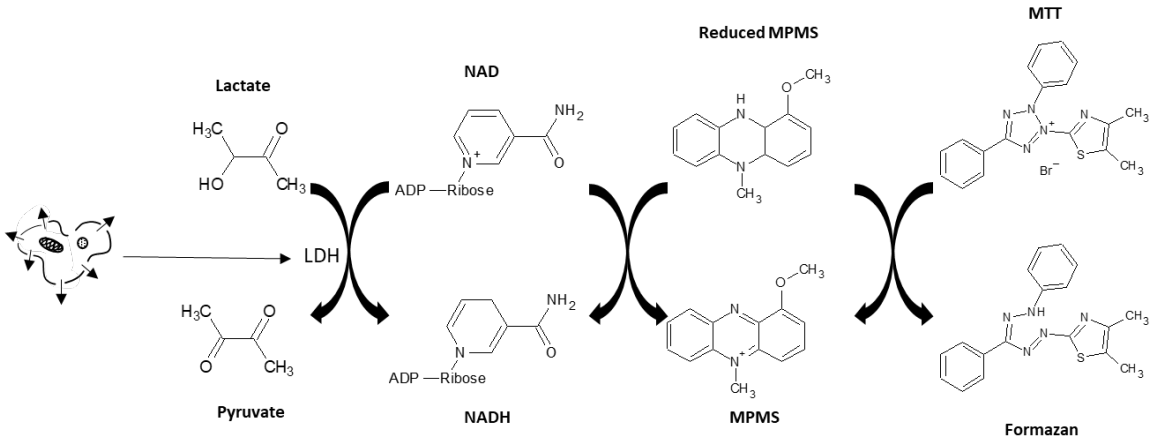

Figure 4.5: **The main reaction mechanism for LDH assay**. When cells are damaged, LDH is released into the supernatant. This enzyme is the rate limiting step of formazan formation (purple colour) from MTT (yellow colour), giving an applicable method of quantification (Adapted from Abe & Matsuki, 2000).

4.2 Aims

- To passage and culture NRK-52E cells in order to maintain a sustainable number of viable cells to perform all *in vitro* studies
- To determine the concentration of drugs internalised into NRK-52E cells using free and encapsulated forms prepared in chapter two
- To determine the safety and/or toxicity of free and encapsulated forms of antioxidants prepared in chapter two

4.3 Materials and methods

4.3.1 Materials and equipment

The antioxidants under investigation were: curcumin, resveratrol, epicatechin, α-tocopherol, ferulic acid and sinapic acid (details described in section 2.3.1). The NRK-52E cell line was purchased from ECACC (Porton Down, Wiltshire, UK). All other solvents, chemicals, cell culture supplements and sterile consumables were purchased from Fisher Scientific Ltd (Loughborough, Leicestershire, UK). The equipment used in this chapter are summarised in table 4.1.

Table 4.1: Details of the equipment used in the studies described in chapter 5

EQUIPMENT	SPECIFICATIONS
Incubator	Galaxy 170S, New Brunswick
96-Well plate reader uv-visible spectrophotometer	ASYS UVM340 Hitech GmbH equipped with DigiRead software version 1.3.0.0
HPLC	Detailed in section 2.3.1

4.3.2 Methods

4.3.2.1 Cell culture technique

NRK-52E cells were obtained at passage 15 and used within passage 16-26. The Dulbecco's modified Eagle's medium was used as growth medium after adding 5% foetal bovine serum (FBS), 1% non-essential amino acids and 0.5% penicillin-streptomycin mixture. This mixture was recommended by ECACC as the ideal growth medium (GM) for growing the NRK-52E cell line. Cells were either grown in 75 cm^2 polystyrene canted neck flasks with a standard growth surface for adherent cells or 24-well flat base standard cell culture plates – these will be referred to as flasks and plates; respectively throughout this study.

In order to split cells into flasks or plates for further testing, cells were sub-cultured at 70-90% confluence with cell seeding at 1-3 X 10,000 cells/cm^2. Initially,

the cells were detached from the flask and collected into tubes. 10 mL trypsin (0.25%) plus ethylenediaminetetraacetic acid (EDTA) was added to cells and incubated for 5 min to detach the cells from the flasks. 10 mL GM was then added in order to neutralise the trypsin. The cell suspension was then collected in 50 mL centrifuge tubes and centrifuged at 500 G for 5 min. The supernatant was removed, and pellets were then re-suspended into 50 mL GM. This suspension was either divided into four flasks or three 24-well plates and one flask (according to experiment requirement or for continuous cell culture). Cells were maintained in an incubator at 37ºC in a humidified 5% CO_2 atmosphere and GM was changed 12 hours after seeding and then every 48-72 hours. Experiments were all performed after cells reached confluence. Incubation medium (IM) containing same ingredients as GM but without FBS was added and was used to pre-incubate cells with either antioxidants samples or/and PQ.

4.3.2.2 Internalisation studies

4.3.2.2.1 Internalisation procedure and extraction method

Internalisation studies were performed on NRK-52E cells. The aim was to determine and compare the percentage of drugs internalised into the cells after 24 hours exposure to drug solutions, drug-loaded PLA nanoparticles and drug-loaded liposomes. For each antioxidant, three different samples were prepared: free antioxidant solution, antioxidant-loaded liposomes and antioxidant-loaded PLA nanoparticles. Free antioxidant solutions were prepared by dissolving 5 mg of standard drug in 4 mL ethanol or DI-water (according to drug solubility), then diluted by a dilution factor of 1:20 in IM. Freshly prepared liposomes were diluted by the same dilution factor (1:20) in IM, immediately after extrusion. PLA nanoparticles samples were prepared by suspending an accurately weighed number of freeze-dried nanoparticles (equivalent to 2.5 mg of drug) in 2 mL in DI-water. Again, this was diluted by a dilution factor of 1:20 in IM. Theoretically, 62.5 µM drug concentration was prepared for each sample. The %LE was taken into account during final concentration to calculate the actual drug concentration in each sample.

Cells were grown to full confluence in 75 cm^2 flasks. Flasks were dosed with the solutions prepared above separately. The cells were then kept in an incubator at 37ºC in a humidified 5% CO_2 atmosphere. After 24 hours, cells were removed from incubator and the excess dosing IM was removed by aspiration. Cells were then washed with phosphate buffer solution (PB), pH 7.4 twice to ensure removal of any IM. Cells were then detached from the flask and collected into tubes as stated in section 4.3.2.1. The supernatant was removed and the cell pellets were then re-suspended in a measured volume of extracting solution (40: 40: 20 methanol: acetonitrile: DI-water). The amount of antioxidant in the collected solutions was then measured by HPLC.

4.3.2.2.2 Measurement of antioxidants in extracted solutions

The HPLC methods described in section 2.4.9 and summarised in table 2.4 were used to determine the amount of antioxidants in the solutions extracted above, with few modifications. First, a guard column was used before the main column to prevent blockage. Secondly, samples were spiked with known concentration of respective standard antioxidant. A blank extract spiked with the same concentration was taken into account during calculation to minimise interference and increase sensitivity. Finally, calibration plots were reconstructed using serial dilutions of standard antioxidants (0.1-10 µg/mL). Analytical parameters such as R^2, LOD and LOQ were recalculated. After determining the concentration of drug in the extruded solutions (recovered concentration), the %internalisation was calculated from the following formula:

$$\% \, Internalisation = {Recovered\ concentration}/{Concentration\ of\ drug\ in\ sample} * 100$$

4.3.2.3 Testing the toxicity of antioxidant solutions, the antioxidant-loaded liposomes and PLA nanoparticles

The safety of free antioxidants under investigation (α-tocopherol, curcumin, resveratrol, sinapic acid, ferulic acid and epicatechin) and their novel delivery

systems (PLA nanoparticles and liposomes prepared in chapter 2) were tested on NRK-52E cells. Free antioxidants were initially dissolved in either ethanol (or in DI-water in the case of epicatechin), then diluted in IM (0, 3.13, 6.25, 15.63, 31.25, 62.5 µg/mL). NRK-52E cells were grown on 24-well plates to 80-90% confluence. The GM was removed and 500 µL of the increased concentrations of different antioxidants were added and incubated in an incubator at 37°C in a humidified 5% CO_2 atmosphere for 24 hours. The cells were then inspected under LM and tested using MTT and LDH assay, detailed below. Liposomes and PLA nanoparticles were tested in the same manner, but all preparations were diluted in IM only with no ethanol used. Sonication was used to aid uniformity.

4.3.2.3.1 Cell viability test (MTT assay)

Cells at this point, either treated or not will have been grown on 24-well plates. 0.2 mg/mL MTT solution was prepared in IM and kept warm in water bath at temperature 37°C. 500 µL of this solution was added to each well, after removal of test medium. The plates were then incubated in an incubator at 37°C in a humidified 5% CO_2 atmosphere. After one-hour incubation, the solution was removed and the formazan crystals were dissolved by adding 125 µL DMSO to each well. Then, duplicates of 50 µL from each well was transferred into 96-well plate and analysed using a multi-well plate UV-visible spectrophotometer at wavelength 540 nm. %Cell viability was then calculated using the formula below:

$$\%\, Cell\, Viability = {Absorbance\ of\ treated\ cells}/{Absorbance\ of\ control\ cells} * 100$$

4.3.2.3.2 Determination of cell death using membrane integrity assay (LDH assay)

Cells used for this test were grown on 24-well plates to full confluent. 125 µL Triton X-100 (0.1%) was added to an untreated well and cells were scratched using a plastic tip to ensure complete release of intracellular LDH. This was considered as 100% LDH cell content for calculations. After 5 min, duplicates of 50

µL of supernatants (either treated or untreated) were transferred into 96-well plates. 50 µL LDH substrate (2.5 mg/mL lithium lactate, 2.5 mg/mL β-NAD, 600 µM MTT, 100 µM MPMS, 1 M pH8.2 Tris-HCl and 0.1% Triton X-100) was added and incubated for 15 min at room temperature in the dark. The formed formazan was measured colourimetrically at 540 nm using a UV-Visible multiplate reader. The LDH released from test cells was calculated as a percentage compared to Triton X-100 treated cells, using the following formula:

$$\%\ LDH = {Absorbance\ from\ test\ cells}/{Absorbance\ from\ Triton\ X-100\ treated\ cells} * 100$$

To ease evaluation and comparison, results from LDH assay were represented as, the %increase in LDH release from cells treated with PQ compared to untreated cells (referred to in this study as %increase in LDH release) rather than %LDH released. This was calculated using the following formula:

$$\%Increase\ in\ LDH\ release = \frac{\%LDH\ from\ PQ\ treated\ cells - \%LDH\ from\ untreated\ cells}{\%LDH\ from\ untreated\ cells} * 100$$

4.4 Results

4.4.1 Revalidation of the HPLC methods

The amount of drug internalised into the cells was measured after incubating NRK-52E cells with a known amount of different antioxidant formulations (free form liposomal form and loaded into PLA nanoparticles) separately, for 24 hours. Measurements of antioxidant concentrations in the solutions extracted from these cells were made by HPLC. The same methods used to measure %LE and %EE were revalidated to ensure they are suitable for this purpose. There was an insignificant difference in the r.t of the antioxidants after introducing the guard column. For example, the r.t. for α- tocopherol, curcumin, resveratrol, ferulic acid, sinapic acid and epicatechin in the original method (full reports in Appendix IV) was 7.7 ,8.1, 2.8, 2.3, 2.3 and 16.1 min; respectively, which was approximate to the r.t. for the current method (7.9, 8.0, 2.6, 2.1, 2.3 and 16.2 min; respectively). Although additional peaks were observed in the chromatograms when injecting the blank solutions and the extruded samples, none were interfering with the analytes under investigation. This indicates that the methods used were selective for the drugs under investigation [Figure 4.6]. The concentration of drug recovered in the extruded sample was less than the LOD and LOQ. This issue was resolved by spiking the sample and a blank solution with a known concentration of standard solution and calculating the difference. The %RSD was less than 2% for all measurements and the linear regression measured by the R^2 was 0.99 for all calibration plots in the range between (0.1-10 µg/mL). These parameters indicate the methods were suitable for the measurement of the concentration of drugs internalised in the cells.

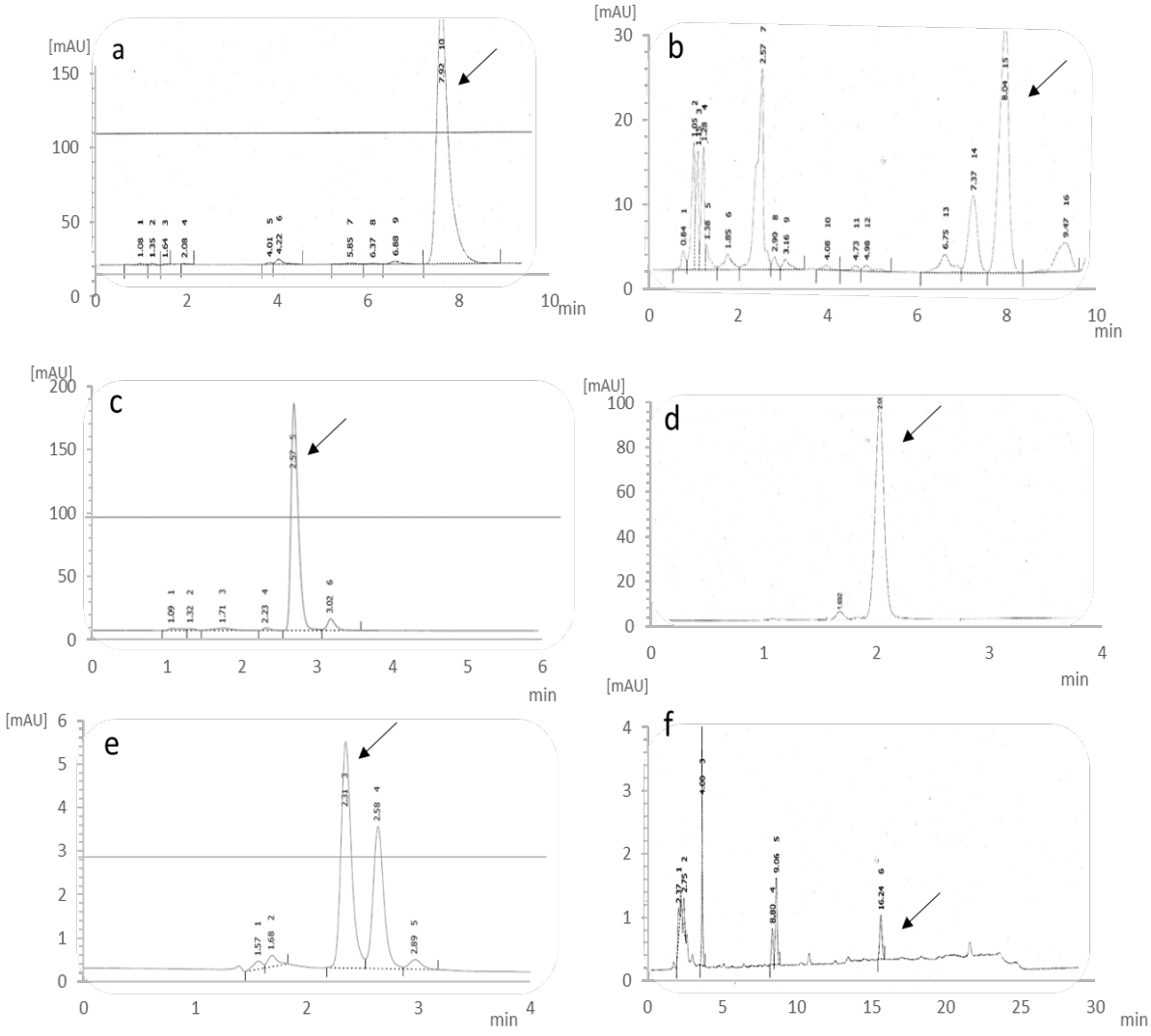

Figure 4.6: **HPLC chromatographs of internalisation studies for the different antioxidants under investigation (r.t):** a. α-Tocopherol (7.9 min), b. curcumin (8.1 min), c. resveratrol (2.6 min), d. ferulic acid (2.1 min), e. sinapic acid (2.3 min) and f. epicatechin (16.2 min). Extracted solutions (after 24-hour incubation of different antioxidant samples on NRK-52E cells) were analysed with same methods described in section 2.4.9. No peaks interfered with the r.t. of the analytes (indicated by the arrows).

4.4.2 Internalisation studies

The above methods were used to measure the amount of drugs internalised into cells. Results are summarised in table 4.1. Overall, liposomal samples showed higher %internalisation for all drugs compared to free drugs and drug-loaded PLA nanoparticle samples, ranging between 0.79 – 27.05%. This increase

was more evident for epicatechin, curcumin and ferulic acid-loaded liposomes showing %internalisation of 27.05 ± 1.07%, 24.98 ± 0.22% and 20.99 ± 1.06%; respectively compared to the free form of these drugs having %internalisation of 4.18 ± 0.03%, 4.22 ± 0.02% and 7.93 ± 0.07%; respectively. Sinapic acid and resveratrol-loaded liposomes still showed an increase in %internalisation (8.35 ± 0.01% and 5.95 ± 0.09%; respectively) compared to their free form but was less noticeable (4.75 ± 0.01% and 0.53 ± 0.09%; respectively). In contrast, α-tocopherol-loaded liposomes showed insignificant increase in the %internalisation (0.79 ± 0.01%) compared to its free form (0.63 ± 0.03%).

However, drug-loaded nanoparticles showed variable results. For instance, epicatechin and curcumin-loaded PLA nanoparticles showed %internalisation of 36.29 ± 0.09% and 25.44 ± 0.10%; respectively which were higher than their free and liposomal form. Conversely, the %internalisation of ferulic acid and sinapic acid-PLA nanoparticles (3.81 ± 0.04% and 0.76 ± 0.05%; respectively) were lower than their respective free and liposomal forms. However, resveratrol and α-tocopherol-loaded PLA nanoparticles did not show any significant change compared to their free form.

Data analysed using two-way ANOVA showed significant differences when comparing drug-loaded liposomes and PLA nanoparticles to their free forms ($F_{(5, 18)} = 3016$, $p < 0.001$). Applying Dunnett's *post hoc* multiple comparisons test, showed that the significant difference was for curcumin-loaded PLA nanoparticles and liposomes ($X_{18} = -21.22$ & -20.76; respectively, $p < 0.001$), ferulic acid-loaded PLA nanoparticles and liposomes ($X_{18} = 4.120$ & -13.06; respectively, $p < 0.001$), sinapic acid-loaded PLA nanoparticles and liposomes ($X_{18} = 3.990$ & -3.600; respectively, $p < 0.001$), epicatechin-loaded PLA nanoparticles and liposomes ($X_{18} = -32.11$ & -22.87; respectively, $p < 0.001$) and resveratrol-loaded liposomes ($X_{18} = -5.420$, $p < 0.001$). In contrast, α-tocopherol-loaded PLA nanoparticles and liposomes and resveratrol-loaded PLA nanoparticles were insignificant.

To summarise, both PLA nanoparticles and liposomes increased the internalisation of curcumin and epicatechin. Resveratrol, ferulic acid and sinapic acid internalisation was only improved using liposomes. Finally, no significant effect was recorded using either PLA nanoparticles or liposomes as nanocarriers for α-tocopherol.

Table 4.2: Summary of %internalisation for different antioxidant formulations under investigation. (mean ± SD, $N = 2$, ***$p < 0.001$) *vs*. free form using two-way ANOVA, followed by Dunnett's multiple comparisons test.

Drug	*Free form*	*PLA nanoparticles*	*Liposomes*
α-Tocopherol	0.63 ± 0.03	0.51 ± 0.01	0.79 ± 0.01
Curcumin	4.22 ± 0.02	25.44 ± 0.10***	24.98 ± 0.22***
Resveratrol	0.53 ± 0.09	0.93 ± 0.03	5.95 ± 0.09 ***
Ferulic acid	7.93 ± 0.07	3.81 ± 0.04***	20.99 ± 1.06***
Sinapic acid	4.75 ± 0.01	0.76 ± 0.05***	8.35 ± 0.01***
Epicatechin	4.18 ± 0.03	36.29 ± 0.09***	27.05 ± 1.07***

4.4.3 Toxicity studies

Before testing the efficiency of the liposomes and PLA nanoparticles developed in this study, toxicity studies were performed to ensure safety of these samples. Different concentrations of all samples prepared (Samples 1-14), in addition to serial dilutions of free antioxidants were incubated separately with NRK-52E cells for 24 hours. Their effect on the cells was measured by two means MTT and LDH assay, in addition to visual inspection using LM. Figures 4.7- 4.12 show the results from both assays. The effects were variable among samples, mostly dose independent.

For instance, results from MTT showed a slight reduction in cell viability at all concentrations of α-tocopherol-loaded liposomes and PLA nanoparticles (ranging between 80.38% to 89.71% and 62.74% to 82.56%; respectively) which were dose independent [Figure 4.7]. The free form of α-tocopherol (solution) showed an interesting pattern, with an insignificant decrease (95.80 ± 8.44%) in

cell viability using 3.14 μg/mL, followed by a minor and insignificant rise in MTT formation (109.5 ± 8.53%) using 6.25 μg/mL. This was followed by a dose-dependent decrease in %viability (97.75 ± 7.54%, 89.06 ± 10.18% & 82.53 ± 9.22%; respectively) using concentrations 15.63, 31.25 and 62.5 μg/mL. These results were consistent with the results from LDH assay, although the variable increase in LDH release was insignificant. The %increase in LDH release ranged from 3.32 ± 1.04% to 6.64 ± 0.54% for α-tocopherol-loaded liposomes and from 4.11 ± 0.25% to 9.15 ± 0.82% for α-tocopherol-loaded PLA nanoparticles, which were also dose independent. The only increase in LDH release (3.72 ± 3.51% & 8.71 ± 2.38%) was noticed from α-tocopherol solution was when using high concentrations (31.25 and 62.5 μg/mL; respectively).

Data analysis using ordinary two-way ANOVA showed significant difference in the results from MTT and LDH assays for all α-tocopherol forms and therefore was followed by Bonferroni's *post hoc* multiple comparisons test. This was applied to all the results from the toxicity studies. The analysis showed $F_{(5, 60)} = 2.72$, $p = 0.028$ for α-tocopherol-loaded liposomes. Bonferroni's test showed that all its concentrations to cause significant reduction in MTT compared to blank with variable *p* values. Blank *vs* 2.38 μg/mL showed $X_{60} = 18.50$, $p < 0.001$, blank *vs* 4.76 μg/mL showed $X_{60} = 10.29$, $p = 0.024$, blank *vs* 11.89 μg/mL showed $X_{60} = 12.99$, $p = 0.002$, blank *vs* 23.78 μg/mL showed $X_{60} = 10.53$, $p = 0.020$ and blank *vs* 47.56 μg/mL showed $X_{60} = 19.62$, $p < 0.001$. No significant change in the results from LDH assay when applying Bonferroni's test.

The PLA nanoparticles showed a significant difference in its results $F_{(5, 60)} = 6.91$, $p < 0.001$. Applying Bonferroni's test to compare individual results from 2.12, 4.23, 10.58, 21.17 and 42.33 μg/mL to blank showed significant difference ($p < 0.001$) in all results from MTT with mean differences (X_{60}) of 21.07, 17.07, 21.44, 28.09 and 37.26%; respectively and no significant difference from LDH assay. Furthermore, the free form of α-tocopherol also showed a significant difference in its results $F_{(5, 60)} = 2.87$, $p = 0.022$). However, applying Bonferroni's test to compare results to blank, showed the only difference to be significant is for 31.25 μg/mL using ($X_{60} = 10.94$, $p = 0.032$) and 62.5 μg/mL ($X_{60} = 17.47$, $p < 0.001$) from

the MTT results. No significant difference was observed from the rest of concentrations using MTT assay and from all concentrations using LDH assay.

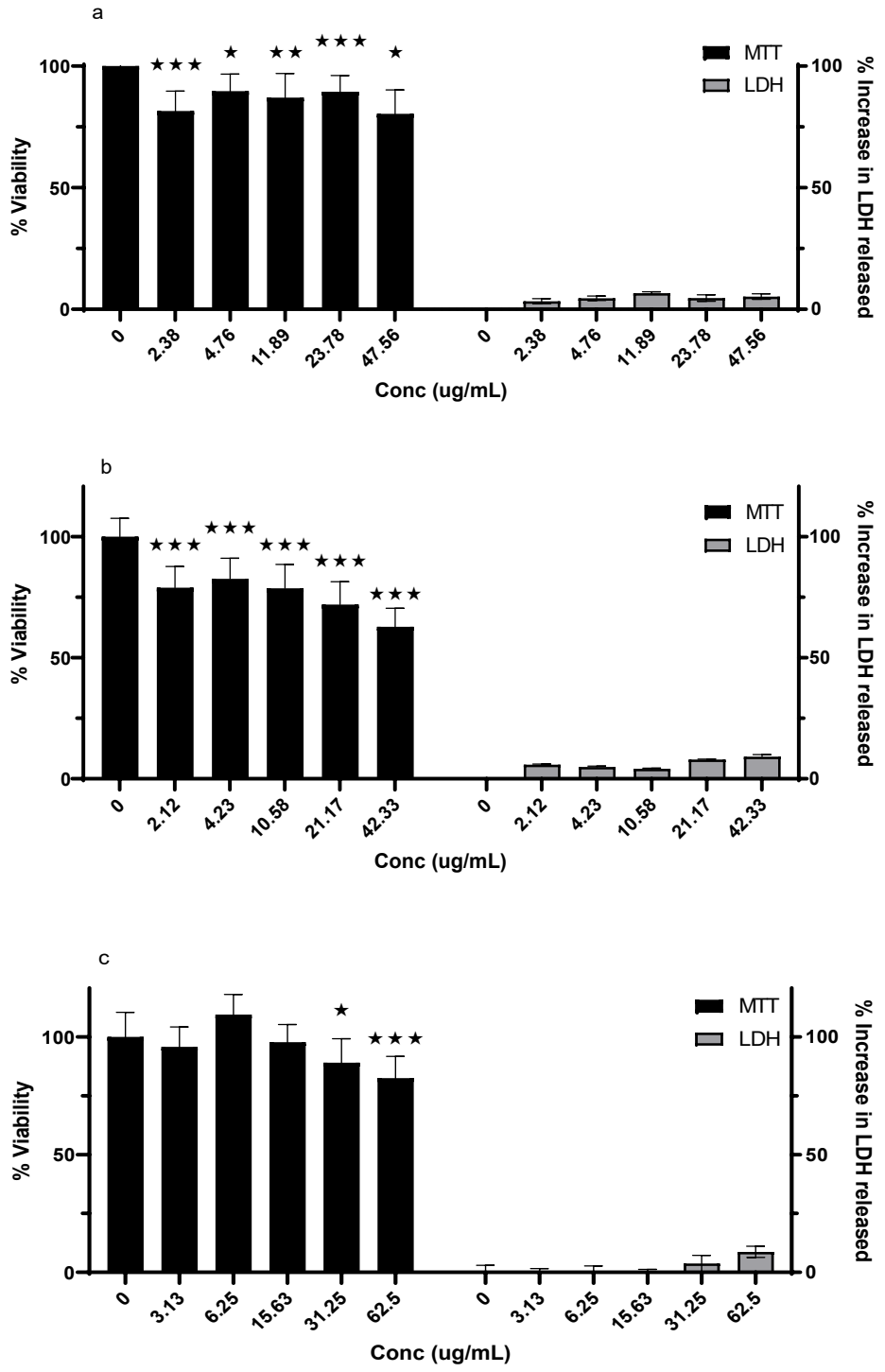

Figure 4.7: The effect of increased concentration of α-tocopherol in three different forms on NRK-52E cells measured using two different assays: MTT and LDH. a. α-tocopherol-loaded liposomes. b. α-tocopherol-loaded PLA nanoparticles. c. α-tocopherol solution. (mean ± SD, $N = 6$, * $p < 0.05$, ** $p < 0.01$, *** $p < 0.001$ *vs* blank [0 µg/mL]). Data analysed using ordinary two-way ANOVA, followed by Bonferroni's multiple comparisons test.

However, this was not the case with curcumin. As no significant change in neither MTT formation nor in LDH release was noticed using low concentrations of all curcumin samples. As opposed to using high doses, which showed significant effect on cells. For example, using 26.12 μg/mL curcumin-loaded liposomes led to a reduction in cell viability to 86.96 ± 6.01%. This was consistent with the observed increase in LDH releases using the same concentration (63.06 ± 6.35% increase in LDH release). However, there was a quite significant increase in LDH release observed (21.15 ± 3.20% & 28.11 ± 3.20%), even when using a slightly lower concentration (6.53 & 13.06 μg/mL).

Additionally, using high concentrations of curcumin-loaded PLA nanoparticles (8.35 & 18.56 μg/mL) led to a higher reduction in cell viability than liposomes, measured by MTT (74.79 ± 24.49% & 72.83 ± 22.58%; respectively) [Figure 4.8]. Although, the SD were quite high, that may indicate loss of precision, the loss in cell viability was confirmed by the increase in LDH release using the same concentrations (92.19 ± 9.92% & 92.19 ± 9.34%; respectively). However, using high concentrations of curcumin solution (free form), also led to a significant reduction in cell viability (51.22 ± 12.03% & 25.94 ± 15.88%) which was confirmed by the increase in LDH release (28.10 ± 5.56% & 26.16 ± 3.32%) using the same concentrations (31.25 & 62.5 μg/mL; respectively). However, these concentrations were much higher than the curcumin concentration in the PLA nanoparticles also causing a significant reduction. It should be pointed out, that using 15.63 μg/mL curcumin in solution showed only an insignificant reduction in cell viability (91.60 ± 12.21%) confirmed by insignificant increase in LDH release (8.38 ± 0.56%), indicating that the PLA nanoparticle form of curcumin had a more harmful effect using comparable concentrations.

Data analysis showed significant difference for curcumin-loaded liposomes $F_{(5, 60)} = 24.48$, $p < 0.001$, curcumin-loaded PLA nanoparticles $F_{(5, 60)} = 23.24$, $p < 0.001$ and curcumin solution $F_{(5, 60)} = 11.99$, $p < 0.001$. Bonferroni's test showed that 26.12 μg/mL curcumin in liposomal form caused significant reduction in MTT compared to blank ($X_{60} = 13.04$, $p = 0.012$), with no significant difference using lower concentrations. However, LDH results were quite different, with significant

difference ($p < 0.001$) when comparing results using concentrations 6.53, 13.06 & 26.12 μg/mL to blank, X_{60} = 21.15, 28.11 & 63.06; respectively. Furthermore, 8.35 & 18.56 μg/mL curcumin in PLA nanoparticles showed significant difference in MTT results compared to blank (X_{60} = 25.21, $p = 0.008$ & X_{60} = 27.17, $p = 0.004$; respectively) and no significant change using lower concentrations. Applying the *post hoc* test showed that significant difference using concentrations 6.28 μg/mL (X_{60} = 25.82, $p = 0.007$), 8.35 μg/mL (X_{60} = 95.2, $p < 0.001$), and 18.56 μg/mL (X_{60} = 92.19, $p < 0.001$). Once more, two concentrations of the free form of curcumin showed significant difference when compared to blank. First, 31.25 μg/mL curcumin showed X_{60} = 48.78, $p < 0.001$ from the MTT assay and X_{60} = 28.10, $p < 0.001$ from the LDH assay. Secondly, 62.5 μg/mL curcumin showed X_{60} = 74.06, $p < 0.001$ from the MTT assay and X_{60} = 26.16, $p < 0.001$ from the LDH assay. There was no significant change in the results from the MTT and LDH assays using lower concentrations, when applying Bonferroni's test.

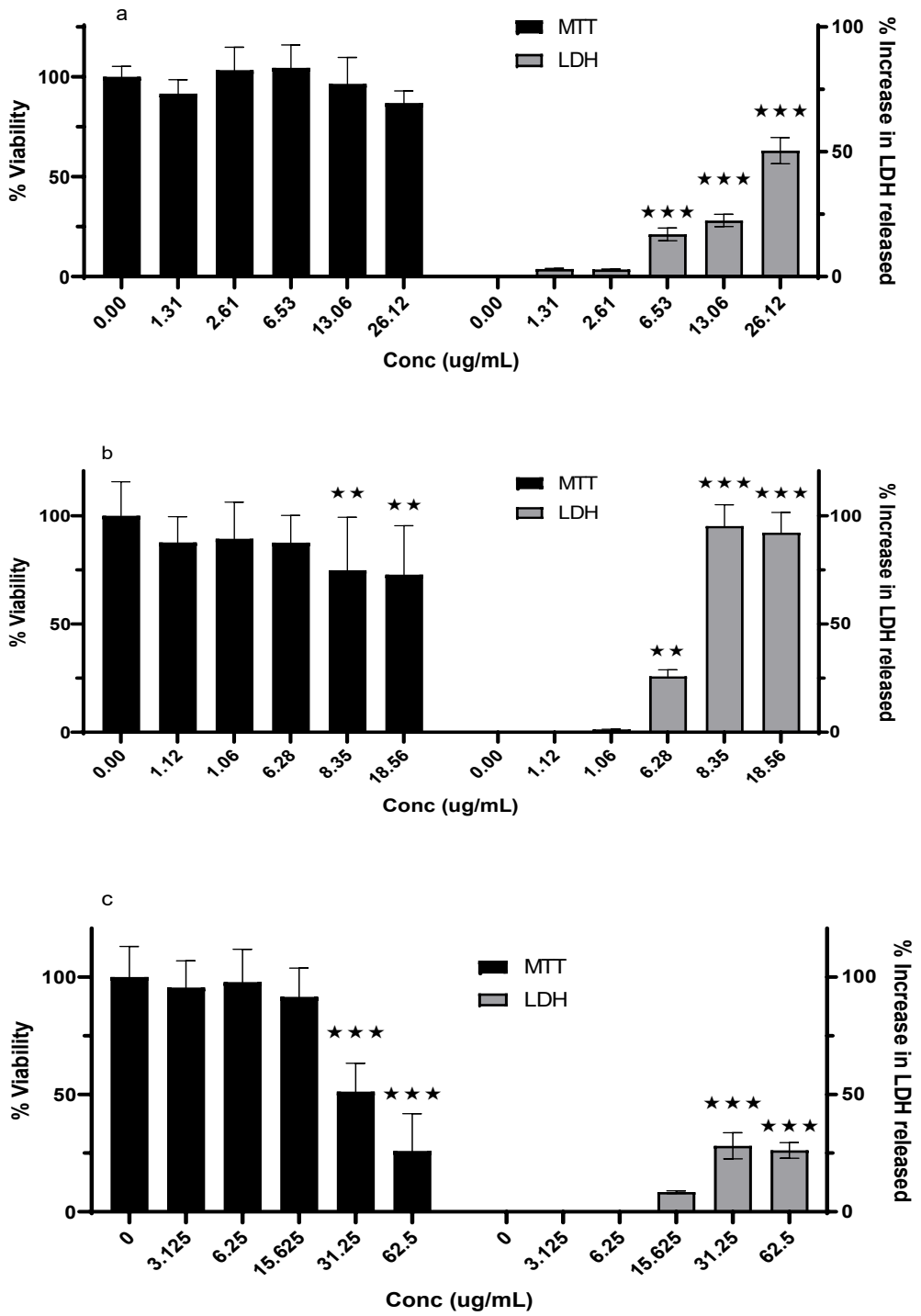

Figure 4.8: The effect of increased concentration of curcumin in three different forms on NRK-52E cells measured using two different assays: MTT and LDH. a. curcumin-loaded liposomes. b. curcumin-loaded PLA nanoparticles. c. curcumin solution. (mean ± SD, $N = 6$, ** $p < 0.01$, *** $p < 0.001$ *vs* blank [0 µg/mL]). Data analysed using ordinary two-way ANOVA, followed by Bonferroni's multiple comparisons test.

The results from the resveratrol samples (liposomes and PLA nanoparticles) also showed some inconsistency between MTT and LDH. The %viability decreased from 90.50% to 77.58% using resveratrol-loaded liposomes (1.72 – 34.38 μg/mL) in a dose-dependent manner [Figure 4.9]. The %viability also decreased from 91.22% to 62.47% using resveratrol-loaded PLA nanoparticles although, the resveratrol concentration was much lower (0.36 – 7.29 μg/mL). No significant increase in LDH release was observed using liposomes (0 – 1.38%) or PLA nanoparticles (0 – 7.82%). On the other hand, there was a noticeable rise in the %increase in LDH release (14.05 ± 2.26% & 56.36 ± 8.34%) using high concentrations of resveratrol solution (31.25 & 62.5 μg/mL; respectively). This was consistent with the reduction in %viability measured from the MTT assay (81.70 ± 12.47% & 75.48 ± 12.58%; respectively) using the same concentrations. Interestingly, using low concentrations of resveratrol solution (3.13 & 6.25 μg/mL) led to small increase in %viability (112.94 ± 10.25% & 104.79 ± 12.62%; respectively).

Data analysis showed no significant difference in the data collected from resveratrol-loaded liposomes, $F_{(5, 60)} = 1.82$, $p = 0.123$. However, Bonferroni's test showed that at concentrations of 8.59, 17.19 & 34.38 μg/mL resveratrol in liposomal form caused a quite significant reduction in MTT compared to blank [($X_{60} = 21.73$, $p = 0.011$), ($X_{60} = 22.74$, $p = 0.007$) & ($X_{60} = 22.42$, $p = 0.008$); respectively]. The lower concentrations did not cause any significant differences in %viability. No significant difference was observed in the LDH data using all concentrations. Resveratrol-loaded PLA nanoparticles showed significant difference using two-way ANOVA, $F_{(5, 60)} = 7.64$, $p < 0.001$. Bonferroni's multiple comparisons test showed the significant difference to be using concentrations 1.81 μg/mL ($X_{60} = 23.58$, $p = 0.001$), 3.63 μg/mL ($X_{60} = 39.45$, $p < 0.001$) & 7.29 μg/mL ($X_{60} = 37.53$, $p < 0.001$) compared to blank. Finally, data from resveratrol solution also showed significant difference when analysing using two-way ANOVA, $F_{(5, 60)} = 8.13$, $p < 0.001$. Bonferroni's test showed significant difference in MTT data using concentrations 3.16 μg/mL ($X_{60} = -12.94$, $p = 0.04$), 31.25 μg/mL ($X_{60} = 18.30$, $p = 0.002$) & 62.5 μg/mL ($X_{60} = 24.52$, $p < 0.001$) and in LDH data using concentrations 31.25 μg/mL ($X_{60} = 14.05$, $p = 0.022$) & 62.5 μg/mL ($X_{60} = 56.36$, $p < 0.001$). There were no significant differences in the other results.

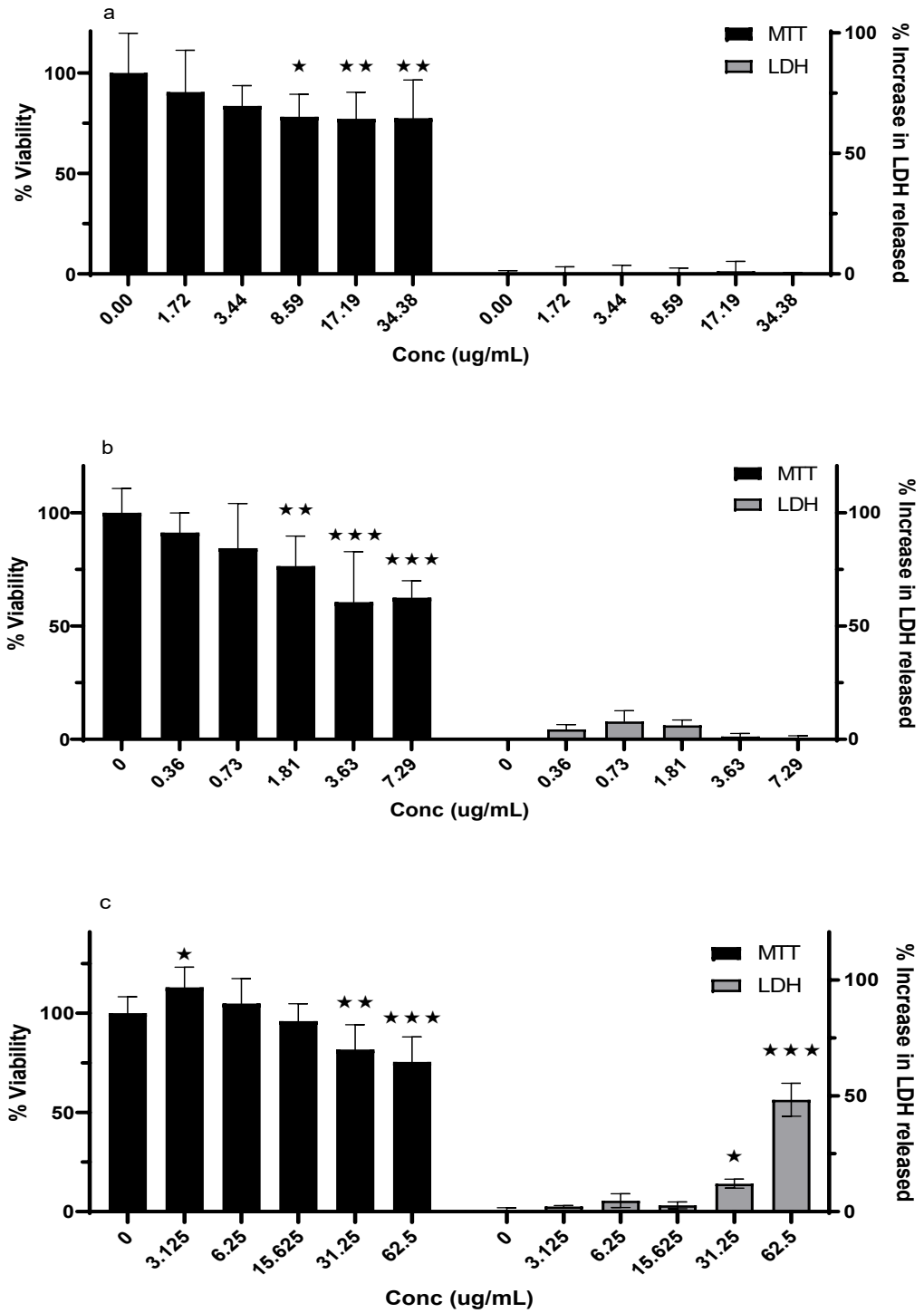

Figure 4.9: The effect of increased concentration of resveratrol in three different forms on NRK-52E cells measured using two different assays: MTT and LDH. a. resveratrol-loaded liposomes. b. resveratrol-loaded PLA nanoparticles. c. resveratrol solution. (mean ± SD, $N = 6$, * $p < 0.05$, ** $p < 0.01$, *** $p < 0.001$ *vs* blank[0 µg/mL]). Data analysed using ordinary two-way ANOVA, followed by Bonferroni's multiple comparisons test.

Although, the above antioxidants (α-tocopherol, curcumin and resveratrol) showed variable harmful effect on cells in some of their forms and concentrations, this was not observed with ferulic acid, sinapic acid and epicatechin forms. For instance, ferulic acid-loaded liposomes caused minor reductions in %viability (82.61 – 88.69%) and minor variations in %increase in LDH release (1.33 – 7.33%) which was not concentration dependent. Contradictory to this, ferulic acid-loaded PLA nanoparticles caused a minor increase in %viability (108.38 ± 9.53%, 104.69 ± 10.21%, 102.11 ± 12.31% & 104.87 ± 15.08%) using concentrations 0.65, 1.30, 3.24 & 12.97 μg/mL; respectively. Using 6.48 μg/mL led to insignificant reduction in %viability (96.23 ± 12.30%). The change in %increase in LDH was also minor (0.16 – 3.86%). Negligible variations in %viability using ferulic acid solution (93.24 – 99.92%) and also in %increase in LDH release (5.47 – 9.83%), which were also concentration independent [Figure 4.10].

Even less variation was observed using sinapic acid-loaded liposomes, were %viability ranged between 91.61 – 94.40% and %increase in LDH release ranged between 0 – 2.91%. Similar to ferulic acid-loaded PLA nanoparticles, sinapic acid-loaded nanoparticles also caused slight but insignificant variation in %viability (95.34 – 107.67%) and in %increase in LDH release (1.99 – 9.83%). Furthermore, there were insignificant changes in %viability (91.85 – 101.15%) and %increase in LDH release (1.83 – 5.59%) using the sinapic acid solution [Figure 4.11]. Similarly, epicatechin-loaded liposomes did not cause substantial effect on cells, were %viability ranged between 91.19 – 97.24% and %increase in LDH release ranged between 0.39 – 6.69%. Similar to ferulic acid and sinapic acid, the PLA form of epicatechin caused a minor insignificant increase in %viability (99.32 – 106.76%) with minimal variation in %increase in LDH release (1.24 – 6.05%). To finish, epicatechin solution (free form) caused insignificant change in %viability (92.56 – 100.49%) and in %increase in LDH release (1.92 – 9.44%) [Figure 4.12].

Data analysis using two-way ANOVA showed insignificant difference in all three forms of ferulic acid, sinapic acid and epicatechin as following: Ferulic acid-loaded liposomes $F_{(5, 60)} = 1.01$, $p = 0.422$, ferulic acid-loaded PLA nanoparticles $F_{(5, 60)} = 0.90$, $p = 0.487$, ferulic acid solution $F_{(5, 60)} = 0.40$, $p = 0.844$, sinapic acid-

loaded liposomes $F_{(5, 60)} = 1.02$, $p = 0.415$, sinapic acid-loaded PLA nanoparticles $F_{(5, 60)} = 0.83$, $p = 0.536$, sinapic acid solution $F_{(5, 60)} = 1.02$, $p = 0.412$, epicatechin-loaded liposomes $F_{(5, 60)} = 0.41$, $p = 0.838$, epicatechin-loaded PLA nanoparticles $F_{(5, 60)} = 1.86$, $p = 0.114$ and epicatechin solution $F_{(5, 60)} = 0.48$, $p = 0.792$.

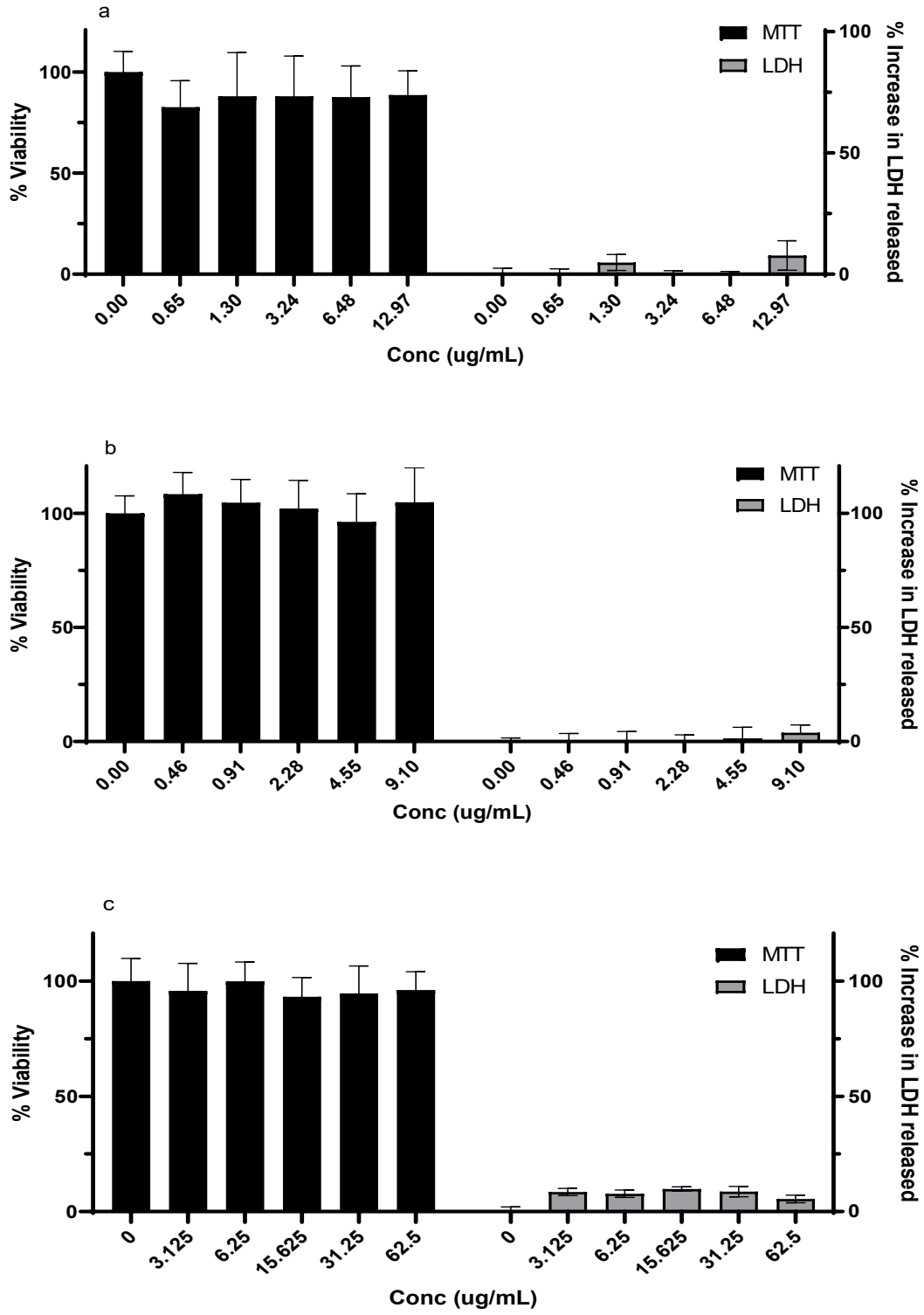

Figure 4.10: The effect of increased concentration of ferulic acid in three different forms on NRK-52E cells measured using two different assays: MTT and LDH. a. ferulic acid-loaded liposomes. b. ferulic acid-loaded PLA nanoparticles. c. ferulic acid solution. (mean ± SD, *N* = 6). Data analysed using ordinary two-way ANOVA, no significant difference was found between results.

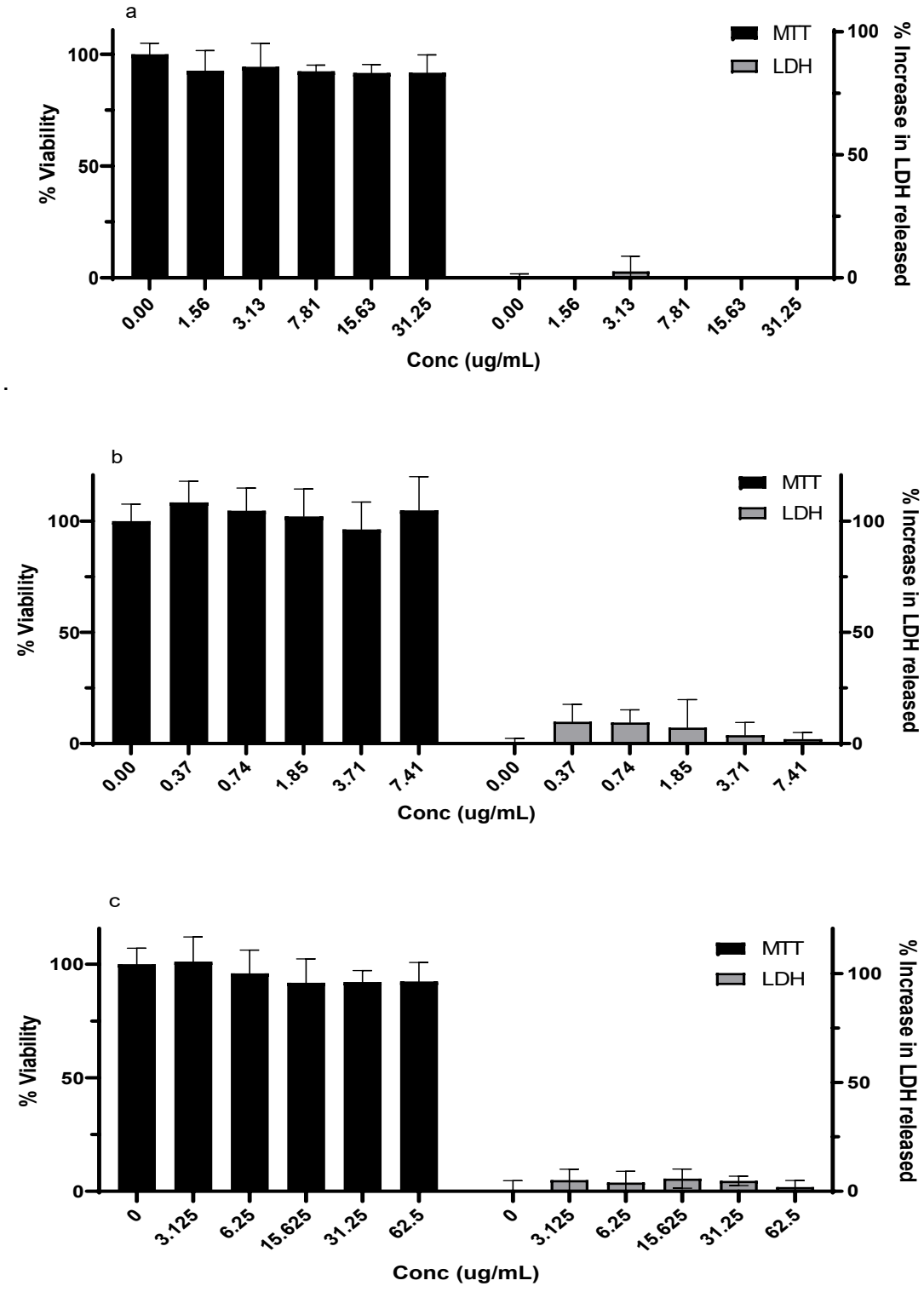

Figure 4.11: The effect of increased concentration of sinapic acid in three different forms on NRK-52E cells measured using two different assays: MTT and LDH. a. sinapic acid-loaded liposomes. b. sinapic acid-loaded PLA nanoparticles. c. sinapic acid solution. (mean ± SD, *N* = 6). Data analysed using ordinary two-way ANOVA, no significant difference was found between results.

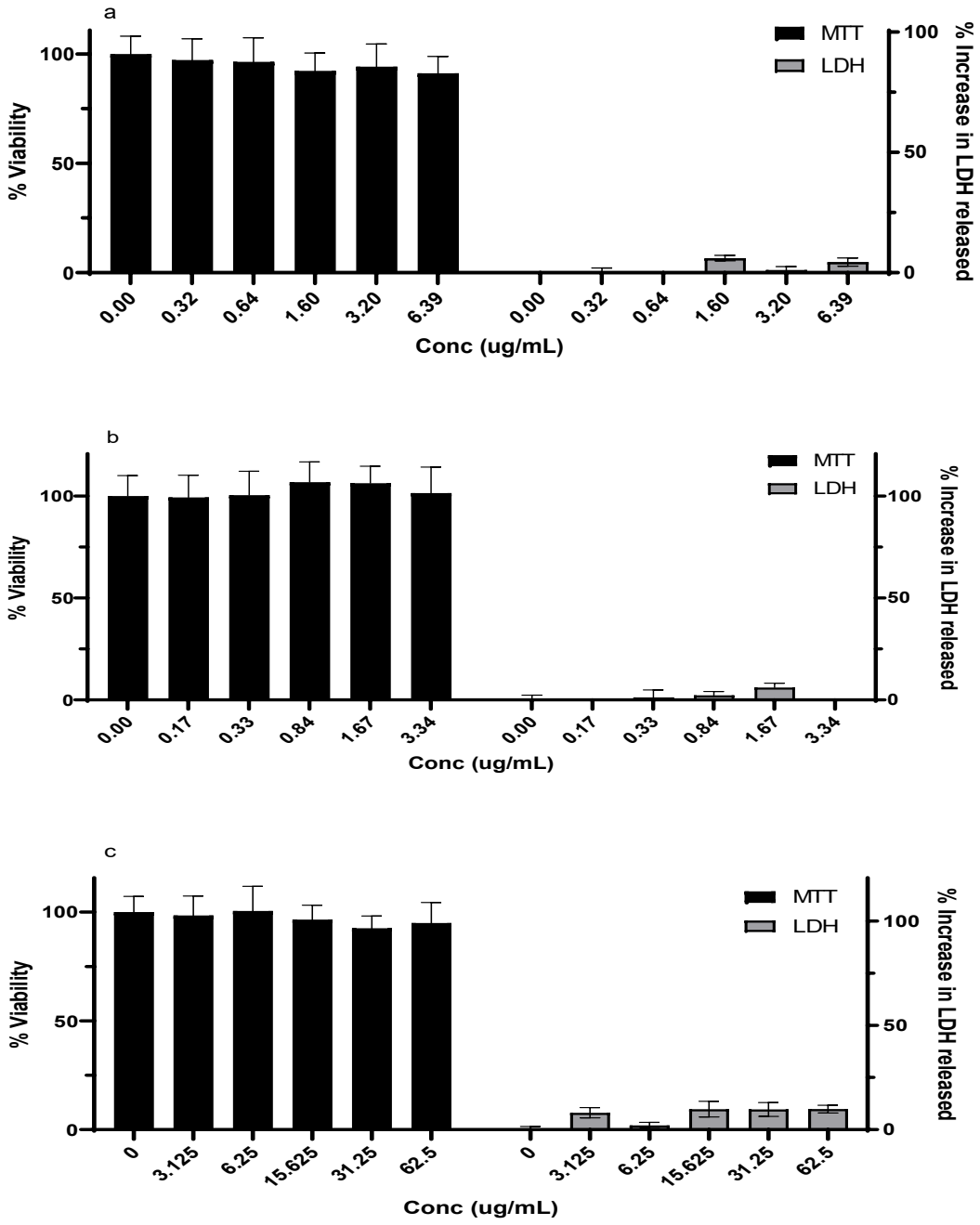

Figure 4.12: The effect of increased concentration of epicatechin in three different forms on NRK-52E cells measured using two different assays: MTT and LDH. a. epicatechin-loaded liposomes. b. epicatechin-loaded PLA nanoparticles. c. epicatechin solution. (mean ± SD, *N* = 6). Data analysed using ordinary two-way ANOVA, no significant difference was found between results.

Overall, no major reduction in cell viability was noticed using all samples under investigation, with the exception of the following: that high doses of α-tocopherol-loaded PLA nanoparticles led to a reduction in cell viability to ≥ 62% and ≤ 10% increase in LDH release. High doses of curcumin-loaded liposomes although, did not affect %viability, it increased %LDH up to 63% and high doses of curcumin-loaded PLA nanoparticles led to a reduction in the %viability to ≥ 72% and an excessive increase in %LDH release up to 95%. Resveratrol-loaded liposomes and PLA nanoparticles led to a reduction in viability to ≥77% & ≥ 60%; respectively with no increase in LDH release. The free forms of antioxidants showed approximately the same pattern where only the following showed significant change: high doses of α-tocopherol solution reduced cell viability to a minimum of 82% and increased %LDH release to no more than 9%. High doses of curcumin solution led to a drop in cell viability to 25% and a rise in %increase in LDH up to 28%. High doses of resveratrol solution reduced cell viability down to 75% and increased %LDH to 56%. No significant effect was reported using ferulic acid, sinapic acid and epicatechin as free or encapsulated forms within the tested range of concentration.

Microscopic examination of cells revealed no significant change in cell shape using most antioxidant preparations (data not shown). The only exception was the use high doses of free curcumin and free resveratrol. This was mostly consistent with the results from the MTT and LDH assay. Although, the high rise in LDH release reported using high dose of curcumin-loaded liposomes and PLA nanoparticles was not as evident under the microscope as expected.

4.5 Discussion

4.5.1 Internalisation studies

In the current studies, tubular epithelial NRK-52E cells have been used as the proximal tubule is the main target in AKI. The internalisation studies have been performed to study the amount of drug entering the cells using the three forms under investigation (liposomes, PLA nanoparticles and free form). A definite amount of each form was incubated with the NRK-52E cells for 24 hours and then cells collected, washed and lysed in an extraction solvent. The amount of drug in the extraction solvent was measured using HPLC and used to calculate the %internalisation. Although, this method is not entirely accurate, it remains a simple and a rapid method to use. The lack of accuracy originates from two mainly reasons. First, the amount extracted represents not only the drug inside the cells, but also the drug adsorbed on the cell membrane. Second, a portion of, or the entire amount of drug entering the cell may be metabolised prior to analysis. The slight modifications in the HPLC methods did not affect accuracy and precision. Furthermore, the extraction solvents did not affect selectivity. Therefore, these methods were applied to measure concentration of drug entering the cells.

Despite these drawbacks, the method was used to give an estimation of the amount of drug entering the cell, in order to provide a means of comparison. Yan *et al*. applied a similar method to compare the cellular uptake of different curcumin forms (solutions, liposomes, nanoemulsion and polymer micelles) by intestinal Caco-2 cells (Yan *et al*., 2019). As expected, they showed that using nanopreparations improved cellular uptake (1.73 ± 0.01%, 2.16 ± 0.23%, 3.96 ± 0.31% and 2.31 ± 0.32%; respectively using 40 μg/mL curcumin after a maximum of 1 hour). In the current study, the %internalisation for curcumin solution (4.22 ± 0.02%) was also improved using PLA nanoparticles (25.44 ± 0.10% and liposomes (24.98 ± 0.22%) after 24 hours. Others have also showed that curcumin internalisation is improved using nanoparticles such as curcumin-loaded PEG-PLGA on neuronal cells (Paka & Rammassay, 2017), curcumin-loaded PLGA nanoparticles conjugated with P-glycoprotein on KB-V1 and KB-3-1 cells (Punfa *et al*., 2016) and curcumin-loaded PLGA on CAL27-cancer cells

(Chang *et al*., 2013). Although, the latter used fluorescence microscope to quantify internalisation rather than of HPLC.

Measuring the cellular uptake using HPLC following cell digestion, was also used by Alqahtani *et al*., 2015 to compare α-tocopherol-loaded PLGA and PLGA coated with chitosan nanoparticles (mean diameter, zeta-potential 131 ± 4.8 nm, -5.6 ± 2.4 mV and 174 ± 6.3 nm, 8.3 ± 1.5 mV; respectively) to α-tocopherol micelles (used to represent free form). They showed that using PLGA coated with chitosan nanoparticles showed improved cellular uptake of over micelles by 2.5-fold. However, using naked PLGA nanoparticles insignificantly reduced cellular uptake. This was consistent with our results using PLA nanoparticles. In their study, Caco-2 cells were incubated for 0, 0.5, 1 and 2 hours, with no increase in absorption after 2 hours (Alqahtani *et al*., 2015). Another justification of the low cellular uptake of α-tocopherol using all three forms could be its degradation during the assay. From the onset of preparation, going through incubation into cells, extractions and finally analysis using HPLC, α-tocopherol could have been oxidised by atmospheric oxygen and degraded (as discussed in chapter 2).

Different attempts have been employed to improve the cellular uptake of resveratrol. For example, the resveratrol internalisation into Caco-2 cells was increased from 3.5% as free form to 5-7% as resveratrol-loaded chitosan (CS) and γ-poly (glutamic acid) nanocapsules (Jeon *et al*., 2016). Another attempt by Min *et al*. was encapsulating resveratrol in modified forms of trimethyl chitosan. They used the confocal microscopy to quantify the intensity of fluorescence as indicator of cellular uptake. They reported that the intensity of encapsulated forms of resveratrol ranged between 58.2 and 76.6 (a. u.), as opposed to free form which only resulted in low fluorescence (22.3 ± 2.5) (Min *et al*., 2018). In the current study and as expected, very low %internalisation of resveratrol (0.53 ± 0.09%) was calculated using its free form. This was rationalised by its low level of aqueous solubility and stability. However, the %internalisation increased insignificantly by 1.8-fold using PLA nanoparticles and significantly by 11 folds using liposomes.

The %internalisation of both sinapic acid and ferulic acid increased significantly using liposomes, as opposed to PLA nanoparticles which was surprisingly reduced. There has been very little research regarding the *in vitro* cellular uptake of sinapic acid and ferulic acid-loaded nanoparticles. However, Bondi *et al*. measured the ability of solid lipid nanoparticles to deliver ferulic acid into cells by a different means. They quantified the percentage of ROS produced intracellularly after incubation of LAN5 cells with a ROS generator (positive control). They then showed that the inhibition in ROS generation after pre incubation with ferulic acid-loaded solid lipid nanoparticles was more evident than that with its free form, suggesting that solid lipid nanoparticles are good carriers of ferulic acid into cells. Additionally, a separate study showed that the inhibitory concentrations (IC_{50}) of free and encapsulated form of sinapic acid against T47D human breast cancer cells were 646.4 μM and 84.74 μM; respectively (Abdel Rahman *et al*., 2018). This might be an indication of increased cellular uptake. Furthermore, caffeic acid-loaded liposomes (which have a similar structure to ferulic acid and sinapic acid) have showed to have increased skin permeation (41.8%) compared to its free form (5.3%) in an *ex vivo* skin permeability study (Katuwavila *et al*., 2016). This was consistent with the increase in ferulic acid and sinapic acid cellular uptake reported in the current study using their liposomal form. The possible reasons for their low %internalisation when encapsulated in PLA nanoparticles, are the low %LE, large mean particle size and relatively high zeta-potential.

Epicatechin is one of the main polyphenols in green tea and in common with other catechins in green tea, it has low bioavailability. Encapsulating epicatechin into liposomes and PLA nanoparticles has increased the %internalisation significantly in this study. In a separate study, tea catechins also showed increased permeability across Caco-2 cells using tea catechins-loaded nanoparticles prepared from chitosan and an edible polypeptide (24%) as compared to their free form (less than 6%) (Tang *et al*., 2012), which was consistent with our study. Additionally, epigallocatechin gallate (another main polyphenol in green tea) was encapsulated in egg phosphatidylcholine liposomes showing a 20-fold increase in drug deposition in basal cell carcinomas. This was

contributed to the increased stability of the drug in the encapsulated form (Fang ***et al***., 2005).

The internalisation test in this study is simple but has its limitations. It only shows the amount of drug internalised into the cells but does not show the mechanism of how it enters the cells. Other studies have proposed different methods to understand how nanoparticles are taken up by cells. For example, the internalisation of α-tocopherol and γ-tocotrienol-loaded PLGA nanoparticles was reduced by 10-fold when incubating cells under 4ºC as compared to 37ºC degree. This indicates an energy dependent mechanism of entry such as endocytosis (Alqahtani ***et al***., 2015). *In vitro* models have been used to correlate to *in vivo* studies but definitely have their limitations which can be attributed to reduced survival of isolated cells, interrupted metabolic capability, disrupted cell-to-cell interaction, disordered tissue topology and lack of whole organ communication (Bergin & Witzmann, 2013). However, they still remain the main tool for the study of safety and efficiency of newly developed medication, prior to animal studies.

Cell lines are frequently used as an alternative to primary cells to study different biological processes. They are cost effective, easy to handle, offer a limitless supply and avoid ethical worries related to the use of animal and human material. However, caution must be taken when analysing the results, as cell lines do not always precisely imitate the primary cell. In order to support the outcomes, key control tests using primary cells should always be repeated (Kaur & Dufour, 2012).

4.5.2 Toxicity studies

To study the toxicity of our novel delivery systems, increased concentration of all antioxidant samples prepared in this study (samples 1-14) and their free forms were incubated separately with NRK-52E cells. After 24-hour incubation, cells were examined under the microscope and tested using the MTT and LDH assays. Usually in toxicity tests, the concentration is increased until full cell death is recorded, in order to calculate IC_{50}. In the current test however, cells were still

viable even with the highest concentrations. For this reason, a more accurate name for these studies is biocompatibility tests.

At the first glance, it could be noticed from the results obtained from α-tocopherol [figure 4.10] that there is significant difference in the %viability from MTT assay but not from the LDH assay. Both tests have been used as an indication of cell viability. However, in the MTT assay, MTT is converted to formazan in living cells by means of their redox activity and so, represent viability. On the other hand, in the LDH assay, the amount of LDH released form the cells into the surrounding medium after damage to cell membrane is measured and so more precisely represents cell death (Abe & Matsuki, 2000). This might explain the increased sensitivity of the MTT assay compared to the LDH assay reported in the current and previous studies (Fotakis & Timbrell, 2006). However, in the current study, no noticeable effect was observed during microscopic examination, indicating minimal harmful effect of all three forms of α-tocopherol. As opposed to other forms of vitamin E, α-tocopherol has been reported previously to be not cytotoxic, which is consistent with the current study (McCormick & Parker, 2004).

In most of the toxicity tests performed in the current study, there was no significant difference between free and encapsulated drugs. This, and the absence of microscopic changes, indicate the safe use of both liposomes and PLA nanoparticles in delivering drugs into cells. This was consistent with results obtained from He *et al*. who showed that using free ferulic acid or ferulic acid-loaded PEG-diphenylalanine nanoparticles did not reduce the viability of Raw264.7 and HUVEC cells even at high doses up to 200 μg/mL (He *et al*., 2021). Moreover, and consistent with the current study, the use of sinapic acid showed negligible cytotoxicity even at concentrations up to 500 μM (≈ 112 μg/mL) & 2000 μM (≈ 448 μg/mL) over Chinese hamster lung fibroblasts (V79) and human cervical carcinoma (HeLa) cells; respectively. Whether these high concentrations, disturb NRK-52E cell viability or not, will require further investigation. This is because each cell line responds differently to different environments and chemicals.

However, this was not the case with resveratrol. Using high concentrations of free and encapsulated forms of resveratrol produced a significant reduction in cell viability as measured by the MTT assay. However, only high concentrations of free resveratrol showed significant increase in cell death as measured by LDH assay and microscopic examination. This could be explained by the increased sensitivity of the MTT assay explained above. Nevertheless, the reduction in %viability using liposomes did not exceed 77% using concentrations 8.59, 17.19 & 34.38 μg/mL. This was in contrast to the free form, which after the initial increase in viability using concentrations 3.13 & 6.25 μg/mL, showed a concentration dependent reduction reaching around 75% using 62.5 μg/mL. Most of these results are consistent with the results obtained by Kristl *et al*., 2009 who showed that using low dose of free resveratrol (10 μM) produced a slight increase in the metabolic activity of human-derived renal epithelial cells. Moreover, they showed that using a higher dose (100 μM) showed a significant reduction in cell metabolism. Furthermore, they reported the protective effect of using the liposomal form of resveratrol, even at a high dose (100 μM) (Kristl *et al*., 2009). The use of nanoparticles has been reported by several authors to reduce toxicity. For example, Batool *et al*. managed to increase the cellular uptake and reduce the toxicity of *Bistorta amplexicaulis* extract against HUVEC cells by using DPPC and cholesterol liposomes (Batool *et al*., 2021).

Similar to resveratrol, using high doses of curcumin showed significant reduction in cell viability. This was consistent with previous reported results by Moustapha *et al*. They showed that using 25 μM (≈ 9.2 μg/mL) curcumin induced cell death by 50% to human hepatoma-derived (Huh-7) cells. According to their study, this was equivalent to 1.25 μM (0.46 μg/mL) intracellular concentration (Moustapha *et al*., 2015). Unexpected and inconsistent with literature were the results obtained using curcumin-loaded liposomes and PLA nanoparticles. The augmentation in the LDH release in the LDH assay was not consistent with minimal reduction in the %viability obtained from the MTT assay or with microscopic examination. The possible explanation is the interference of the yellow colour of curcumin in the LDH assay. During the LDH assay, a measured amount of the medium is withdrawn and the LDH substrate mixture is added. This differs from the MTT assay where all excess medium is removed and the MTT

solution is added to the clean cells. The increased solubility of curcumin in the medium using liposomes and PLA nanoparticles may explain its interference in the LDH assay results from these encapsulated forms and not in the free form. To overcome this dilemma, control cell wells incubated with the same concentration of each form should be taken into account during calculations.

In some cases such as in cancer cells, cytotoxicity is the preferable outcome and can also be achieved by the use of antioxidants and their nanocarriers. For example, free ferulic acid and ferulic acid-loaded PLGA nanoparticles coated with chitosan both showed promising antitumour activity. After a period of 48 hours, the cell viability of B16-F10 was reduced to 46% and 37% using 60 μg/mL free and nanoparticle encapsulated form of ferulic acid; respectively. Furthermore, these forms showed promising cytotoxic activity over Hela cells with a maximum inhibition of 69% and 52%; respectively, after a period of 48 hours using 30 μg/mL (which was not concentration dependent). This antitumour activity is thought to be mainly due to the antioxidant activity of ferulic acid, as excessive ROS can cause DNA damage and carcinogenesis (Lima *et al*., 2018). Additionally, curcumin-loaded PLGA nanoparticles conjugated with P-glycoprotein also showed improved cytotoxicity against KB-V1 and KB-3-1 (cervical cancer cell lines) over free curcumin (Punfa *et al*., 2012).

4.6 Conclusion

In conclusion, liposomes showed significant increase in cellular uptake to all antioxidants under investigation, except α-tocopherol, which was minimally increased after encapsulation. This was justified by the breakdown of α-tocopherol during analysis. Curcumin and epicatechin cellular uptake were increased significantly also using PLA nanoparticles. However, resveratrol was increase was marginal using PLA nanoparticles. Furthermore, the cellular uptake of α-tocopherol, sinapic acid and ferulic acid decreased when encapsulated in PLA nanoparticles.

Toxicity studies, or more accurately biocompatibility studies, showed that the use of α-tocopherol, ferulic acid, sinapic acid and epicatechin are relatively safe to use within the studied range of concentration in all three forms (free, liposomal and PLA nanoparticles). Free resveratrol and curcumin showed slight cytotoxicity at high concentrations, which was reduced using encapsulated forms.

Chapter 5: *In vitro* activity studies of antioxidant-loaded liposomes and PLA nanoparticles on the NRK-52E cell line

5.1 Introduction

In the previous chapter, we tested the toxicity and the internalisation of PLA nanoparticles and liposomes loaded with different antioxidants. This chapter will focus on the efficiency of these delivery systems. In chapter one (sections 1.9, 1.10 & 1.11) the pathophysiology of AKI and its relationship to oxidation was described, which showed that oxidative stress is the main pathway of AKI development. For this reason, methods of analysing oxidative stress on cells were essential. This chapter will discuss how oxidative stress can be induced and analysed *in vitro*. It will then focus on the different mechanisms and factors affecting drug release from nanoparticles. Finally, it will describe the materials, methods, results and discussions used to study the *in vitro* activity of the antioxidants under investigation as free form and encapsulated in both liposomes and PLA nanoparticles. The renal NRK-52E cell line was also used in these studies, as the proximal tubule is the primary structure involved in the development of AKI.

5.1.1 Inducing oxidative stress *in vitro*

To assess the potential of existing or newly developed antioxidants on cell lines, different inducers of oxidative stress have been explored. This can be achieved by adding any chemical that stimulates the release of ROS or direct addition ROS such as H_2O_2 (Lushchak 2014). Examples of chemical inducers that have been applied in previous studies include gentamicin (Mohammed *et al*., 2018, Acharya *et al*., 2013, Abdel-Raheem *et al*., 2010, Abdel-Naim *et al*., 1999), cisplatin (Ansari 2017, Akomolafe *et al*., 2014, Kruidering *et al*., 1997), copper sulphate (Alhusaini *et al*., 2018), mercuric chloride (Augusti *et al*., 2008), d-galactose (Liu *et al*., 2010), sodium fluoride (Nabavi *et al*., 2013), 2,2′-azobis (2-amidinopropane) hydrochloride (AAPH) (Banerjee *et al*., 2008) and Paraquat (PQ) (Schmuck *et al*., 2002).

5.1.1.1 Paraquat as a chemical inducer of oxidative stress

PQ is a chemical compound widely used in agriculture as a herbicide. Its chemical name is N, N'-dimethyl-4,4'-bipyridinium dichloride and is highly water soluble (Kimbrough 1974). It has also been reported as a highly toxic compound to both animals and humans. The primary organs affected by paraquat toxicity are the lungs and kidneys. PQ accumulates in the lungs by active transport in the Clara and alveolar epithelial cells. It accumulates in the kidney, as renal excretion is its main excretion mechanism but this is compromised by damage to proximal tubular cells. The main reason for its toxicity is the generation of ROS, such as $O_2^{\bullet-}$, H_2O_2 and $HO^{\cdot}$, leading to oxidation of cellular NADPH and peroxidation of polyunsaturated fatty acids (Suntres 2002). It produces its damage through a process called redox cycling, where it is initially reduced by different enzymes such as cytochrome P-450 reductase, complex I, XO and nitric oxide synthase to $PQ^{\cdot+}$ and then re-oxidised to its original state in the presence of O_2 by generating $O_2^{\bullet-}$. The latter then produces different ROS as discussed in section 1.6 (Dinis-Oliveira *et al*., 2008) [Figure 5.1]. For this reason, it was chosen as an oxidative stress inducing agent which was used to model AKI on a renal cell line (NRK-52E cells).

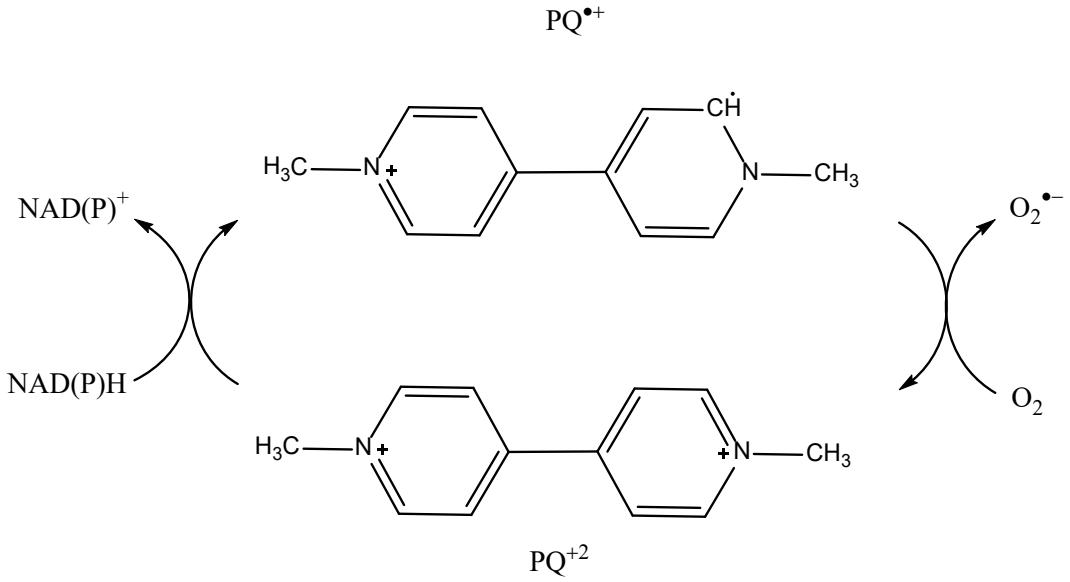

Figure 5.1**: The redox cycle of paraquat.** Initially it is reduced to its radical form ($PQ^{\bullet+}$) by different enzymes then re-oxidised to its original form (PQ^{2+}), producing superoxide from oxygen. Adapted from Dinis-Oliveira *et al*., 2008.

5.1.2 Evaluation of oxidative stress *in vitro*

In order to study the safety and efficacy of samples under investigation against oxidative stress, it was necessary to assess the impact of oxidative stress on NRK-52E cells. There are different means of measuring oxidative stress including direct measurement of ROS produced, measuring the resulting damage to biomolecules or measuring antioxidant levels. Although direct measurement of ROS produced is thought to be the most promising, it is extremely difficult due to their high reactivity and instability. Examples of such methods include fluorogenic probes to measure free radicals or spectrophotometric procedures to measure derivatives of reactive oxygen metabolites. On the other hand, measuring the subsequent effect of these ROS on biomolecules such as lipids, proteins and DNA is considered a more reliable approach; although several oxidative stress biomarkers are complex and expensive to analyse and may be subject to further oxidative stress during isolation. The 2,4-dinitrophenylhydrazine method, 2D gel electrophoresis and western blot are examples of methods used to measure protein carbonyl (as a marker of oxidative stress). Malondialdehyde is one of the commonly measured biomarkers of lipid peroxidation and 8-OHDG produced by DNA modification, is a major biomarker of DNA oxidative stress (discussed in

section 1.7.3). Also discussed in section 1.8, are the important antioxidant defence mechanisms naturally available in the biological systems, either being enzymatic such as SOD, CAT and GPx or small molecules such as vitamin E and vitamin C. Different methods are available to measure their levels individually in biological systems (Katerji 2019). In this study, cell viability and cell death were measured to assess oxidative stress level in NRK-52E cells to give a general idea of effectiveness of samples under investigation. Details of these methods are described in chapter 4. These methods are indirect measurements but still practical and inexpensive methods of measuring ROS generation and produce a generalised indication of protection against oxidative stress.

5.1.3 Drug release from nanoparticles

To determine when and how nanoparticles would be needed to be administered to the cells to assess efficacy, the mechanism of drug release was investigated. One of the main aims of encapsulating drugs into nanoparticles is to have a sustained or controlled drug release. There are different methods by which drugs can be released from their carriers. Lee & Yeo, 2015 divided these methods into four categories: diffusion-controlled release, solvent-controlled release, degradation-controlled release and stimuli-controlled release [Figure 5.2]. Diffusion-controlled release of drug can usually be found in nanoparticles that consist of a core surrounded by a barrier such as liposomes or nanocapsules. The rate-controlling factor in this mechanism is the concentration of drug inside the nanoparticle, in which drug is released across the membrane barrier into the surroundings. It is worth noting that nanospheres can also release their cargo *via* this mechanism. However, because they are attracted to the outer polymeric membrane, drug is initially released at a high rate followed by a slow release rate. Solvent-controlled release mainly depends on the surrounding solvent entering the particle, which can then affect the drug release. The solvent can enter the nanoparticle *via* osmosis where water diffuses from a low drug concentration to a high drug concentration, or *via* swelling where glassy hydrophilic polymers swell and release the drug when in contact with fluids. In the degradation-controlled release mechanisms, the drug is released after hydrolytic or enzymatic cleavage of bonds such as amides and esters in the polymer that makes up the barrier or matrix. Depending on the type of polymer and size of particle it can erupt in one

step as bulk degradation releasing the entire cargo at once or wear down from surface to core resulting in a more gradual release. Finally, stimuli-controlled release is a mechanism that depends on external factors to trigger drug release such as temperature, pH, ionic strength, ultrasonic waves and electric or magnetic fields. These mechanisms are mainly used to target specific sites (Lee & Yeo, 2015).

In the current study, neither the rate nor the mechanism of drug release from the nanoparticles under investigation were studied. However, both liposomes and PLA nanoparticles have been used to encapsulate drugs for the purpose of improving pharmacokinetic properties and ultimately enhance bioavailability.

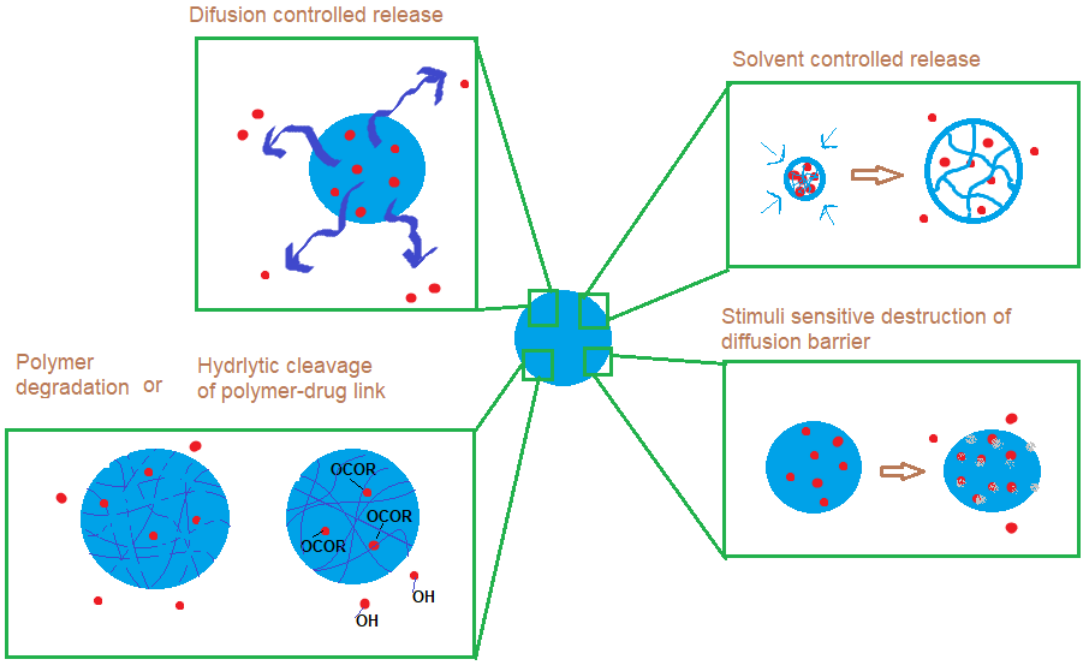

Figure 5.2: **Drug release mechanisms from nanoparticles.** A drug entrapped in nanoparticles can be released into the surrounding environment by different mechanisms: Diffusion-controlled release, solvent-controlled release in which water may enter the nanoparticles *via* osmosis, degradation-controlled release *via* hydrolytic or enzymatic degradation and stimuli-controlled release *via* temperature, pH, ionic, ultrasonic or magnetic external factor (Adapted from Lee & Yeo, 2015, original figure in colour).

5.2 Aims

- To determine the range of PQ concentration, that can be further used to induce oxidative stress and damage in NRK-52E cells.
- To determine the efficiency of free and encapsulated forms of the different antioxidants prepared in chapter two against oxidative stress induced in NRK-52E cells by PQ.

5.3 Materials and methods

5.3.1 Materials and equipment

Materials and equipment used in this chapter are described in the previous chapter (section 4.3.1). Paraquat was purchased from Sigma-Alrich.

5.3.2 Methods

5.3.2.1 Cell culture technique

NRK-52E cells were obtained at passage 15 and used within passage 16-26. Cells were maintained using the same techniques described in section 4.3.2.1.

5.3.2.2 Paraquat mediated AKI in NRK-52E cells

PQ was used to induce injury to NRK-52E cells *in vitro*, to mimic the oxidant injury produced on renal tubular epithelial cells during AKI (Elisha-Lambert 2017). NRK-52E cells were grown on 24-well plates to 80-90% confluence. The GM was removed and 500 µL of different concentrations of PQ (0-1 mM and 0-10 mM) prepared in IM was added. The cells were then incubated in an incubator at 37°C in a humidified 5% CO_2 atmosphere for 24 hours. The cells were then inspected under light microscope and tested using MTT and LDH assay. Tests were repeated in replicates of six.

5.3.2.3 Pre-incubation of NRK-52E cells with antioxidants and antioxidants preparations

To compare the effectiveness of free antioxidants and their novel delivery systems under investigation (PLA nanoparticles and liposomes), they were tested for their ability to protect cells from PQ induced oxidative stress. All preparations were prepared and diluted to make 6.25 & 62.5 µg/mL theoretical drug concentration, regardless of their %LE and %internalisation. This was to ensure all other variables such as PLA, PVA and lipid concentrations were kept constant. The calculations, however, were made according to actual concentration of drug

inside each preparation (considering the %LE as calculated in chapter 2, table 2.10).

Free drug solutions were prepared by dissolving a known amount of each drug in ethanol (or DI-water in the case of epicatechin) and then diluting with IM to make up two concentrations, 6.25 and 62.5 µg/mL. Drug- loaded liposomes were prepared fresh (as described in section 2.4.3) and diluted in IM after extrusion to achieve the same two theoretical concentrations. Similarly, the same theoretical concentrations of drug-loaded PLA nanoparticles were prepared. PLA nanoparticles were previously prepared, freeze-dried and stored in fridge (as described in section 2.4.2) and on the day of testing, they were re-suspended in IM. NRK-52E cells were grown on 24-well plates, to 80-90% confluence. The GM was removed and 500 µL of the two different concentrations of each antioxidant preparation prepared in IM were added to the cells, separately. After 24 hours of incubation at 37°C in a humidified 5% CO_2 atmosphere, the medium was removed and 500 µL of PQ was added at increasing concentrations (0, 0.2, 0.4, 0.6, 0.8, 1 mM). Cells were then tested after a further 24-hour incubation in the same conditions using the MTT and LDH assays (described in sections 4.3.2.3.1 & 4.3.2.3.2; respectively). All tests were repeated in replicates of six.

5.4 Results

5.4.1 Paraquat dose response

PQ was used to induce oxidative damage in NRK-52E cells. In order to determine the appropriate range of concentrations to be used for the drug studies, increasing concentrations of PQ (0-10 mM) were added to cells and incubated for 24 hours. Results from microscopic examination, LDH and MTT assays (data not shown) indicated that cells demonstrated no sign of viability above 1 mM. For this reason, further tests used PQ in the concentration range of 0–1 mM.

Images from microscopic examination of increasing concentrations of PQ (0, 0.2, 0.4, 0.6, 0.8 and 1 mM) are shown in figure 5.3. Untreated cells (0 mM PQ) demonstrated a flat monolayer morphology. No significance change in the morphology of the cells was detected using 0.2 mM PQ compared to 0 mM PQ. At 0.4 mM PQ cells started to shrink losing their normal shape and the nuclei appeared more condense (marked with arrows in [Figure 5.2.c], however, cells continued to appear stretched in their confluent monolayer. Addition of 0.6 mM PQ, led to a significant number of floating dead cells with increased extracellular space. These changes were abundant and involved almost 100% of the cells using 0.8 and 1 mM PQ, indicating complete cell death.

The relationship between the concentration of PQ was plotted against %LDH released and cell viability, obtained from LDH and MTT assays, respectively [Figure 5.4]. No considerable difference in the %LDH released from cells subject to 0.2 mM PQ was measured compared to untreated cells. There was, however, a significant increase in the %LDH with increased PQ concentration from 0.4 to 0.8 mM stabilised between 0.8 & 1 mM. These results correlate to the observations taken from microscopic examination, indicating that cell membrane starts to lose its integrity at 0.4 mM and cells undergo complete necrosis at 0.8 mM. MTT results showed an inverse response with percentage viability decreasing with increased concentration of PQ between 0.2 & 0.8 mM. There was also a slight increase in cell viability using 0.2 mM PQ compared to untreated cells.

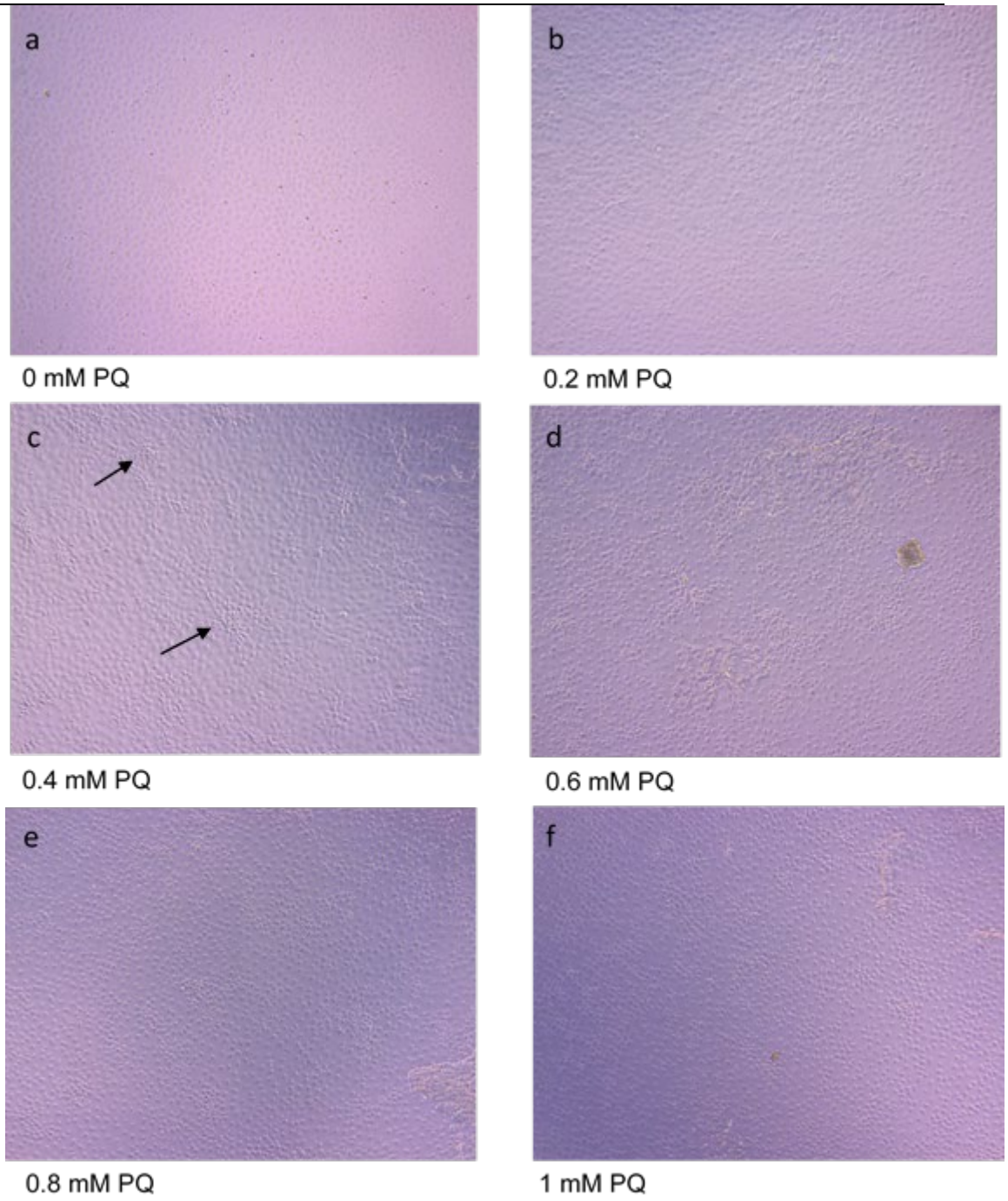

Figure 5.3: Microscopic examination showing the effect of increased concentrations of PQ (0–1 mM) on NRK-52E cells after 24-hour incubation period (original figure in colour)

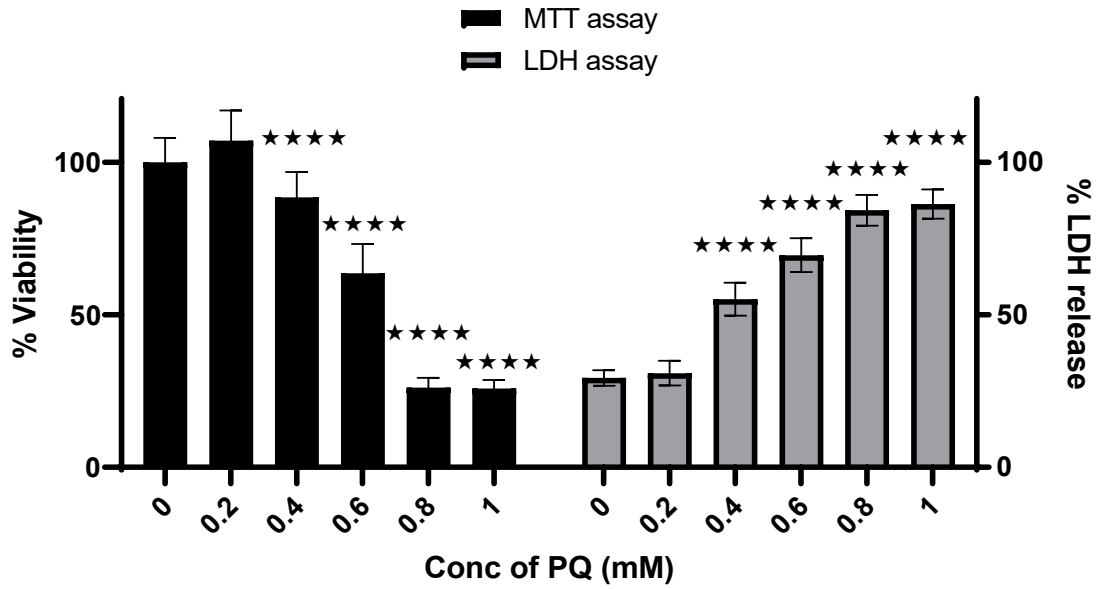

Figure 5.4: **PQ dose response graph**. The effect of increased concentrations of PQ on %viability of, and %LDH released by, NRK-52E cells, mean ± SD, $N = 6$, $p < 0.001$ (using ordinary one-way ANOVA), **** $p < 0.0001$ compared to untreated cells (0 mM PQ) (using Bonferroni's *post hoc* test).

Data analysis using ordinary one-way ANOVA showed significant effect from the PQ concentration on data, $F(5,30) = 136.5$, $p < 0.001$ for MTT assay and $F(5,30) = 175.0$, $p < 0.001$ for LDH assay. Applying Bonferroni's *post hoc* test to compare means of treated cells to untreated cells, showed significant differences for concentrations 0.4, 0.6, 0.8 and 1 mM PQ compared to 0 mM PQ for both LDH and MTT assays. No significant difference was observed when comparing 0.2 mM PQ to untreated cell. The significant effect of PQ on both MTT and LDH results was observed in all further graphs, and so will not be mentioned again to reduce repetition.

5.4.2 Effect of pre-incubation with antioxidant solution and antioxidant encapsulated in PLA nanoparticles and liposomes.

The oxidative damage observed from PQ above, was challenged by the intervention with antioxidant solutions, PLA nanoparticles and liposomes. Cells

were pre-incubated for 24 hours with these antioxidant preparations and then treated with increased concentration of PQ (0-1 mM). Cells were then tested using both LDH and MTT assays.

5.4.2.1 Effect of pre-incubation with α-tocopherol-loaded liposomes, PLA nanoparticles and antioxidant solution

α-Tocopherol solution was prepared initially by dissolving a known amount of α-tocopherol standard in ethanol and then diluting with IM to make up two concentrations, 6.25 and 62.5 µg/mL. α-Tocopherol- loaded liposomes were prepared freshly and diluted in IM after extrusion to theoretically, make-up to the same two concentrations. The same theoretical concentrations of α-tocopherol-loaded PLA nanoparticles solutions were prepared in IM. After a period of 24 hours pre-incubation with the above solutions, the media was removed, and increased concentrations of PQ (0-1 mM) were added separately to different cell wells and re-incubated. After a period of 24 hour the MTT and LDH assays were performed. Considering the %LE of each preparation, the actual concentration of α-tocopherol in the samples was calculated. Each sample was given a code to ease discussion [Table 5.1].

Table 5.1: The actual concentration of α-tocopherol in each sample and its given code

Drug	*Form*	*Theoretical conc (µg/mL)*	*%LE*	*Actual conc (µg/mL)*	*code*
α-Tocopherol	liposomes	6.25	76.10%	4.76	TL-1
α-Tocopherol	liposomes	62.5	76.10%	47.56	TL-2
α-Tocopherol	PLA nanoparticles	6.25	67.63%	4.23	TP-1
α-Tocopherol	PLA nanoparticles	62.5	67.63%	42.27	TP-2
α-Tocopherol	solution	6.25	NA	6.25	TS-1
α-Tocopherol	solution	62.5	NA	62.5	TS-2

5.4.2.1.1 Pre-incubation with α-tocopherol-loaded liposomes

As previously shown in section 5.4.1, the increase in PQ concentration led to a reduction in %viability and an increase in %LDH released from cells. The pre-incubation with TL-1 & TL-2 led to slight reductions in cell viability (83.27 ± 8.07% & 82.29 ± 9.08%; respectively) compared to adding 0.2 mM PQ only (102.49 ± 8.71%). However, these samples (TL-1 & TL-2) ameliorated the reduction in cell viability caused by higher concentrations of PQ (0.4 and 0.6 mM PQ). Complete death of cells (< 10%) observed using 0.8 mM PQ which was only slightly affected using TL-1 (13.39 ± 3.24%) but not by TL-2. No beneficial effect was recorded using both concentrations of α-tocopherol-loaded liposomes when 1 mM PQ was used (cell viability < 10%) [Figure 5.5]. Similarly, the increase in PQ concentration led to an increase in LDH release, which was ameliorated using both concentrations of α-tocopherol-loaded liposomes (TL-1 & TL-2). Furthermore, pre-incubation with TL-2 led to a reduction in the %increase in LDH release below the baseline. Indicating that the %LDH released from cells treated with TL-2 plus 0.2 mM PQ was less than that released from untreated cells. Even with 1 mM PQ, pre-incubation with α-tocopherol-loaded liposomes reduced the increase in LDH release to around 50% using both samples [Figure 5.6].

Data analysis for the MTT results using two-way ANOVA showed significant effect from α-tocopherol concentration on the data $F_{(2, 90)} = 26.85$, $p < 0.0001$. Bonferroni's *post hoc* multiple comparisons test showed significant difference between cells treated with 0.2, 0.4 and 0.6 mM PQ and pre-incubated with TL-1 (X_{90} = -19.22, 67.84 and 26.74; respectively, $p < 0.0001$) or TL-2 (X_{90} = -20.20, 50.95 and 15.75; respectively, $p < 0.001$) compared to cells treated with the same concentration of PQ only. All other results showed no significant difference. Furthermore, the same analysis was applied to the LDH results and similarly showed significant effect from α-tocopherol concentration on the data $F_{(2, 75)}$ = 402.1, $p < 0.0001$. Bonferroni's test showed significant difference for all results obtained from cells treated with TL-1 sample plus PQ compared to those treated with PQ only, with X_{75} = 11.11, $p < 0.001$ using 0.2 mM PQ and $X_{75} > 40$, $p <$ 0.0001 using all other PQ concentrations.

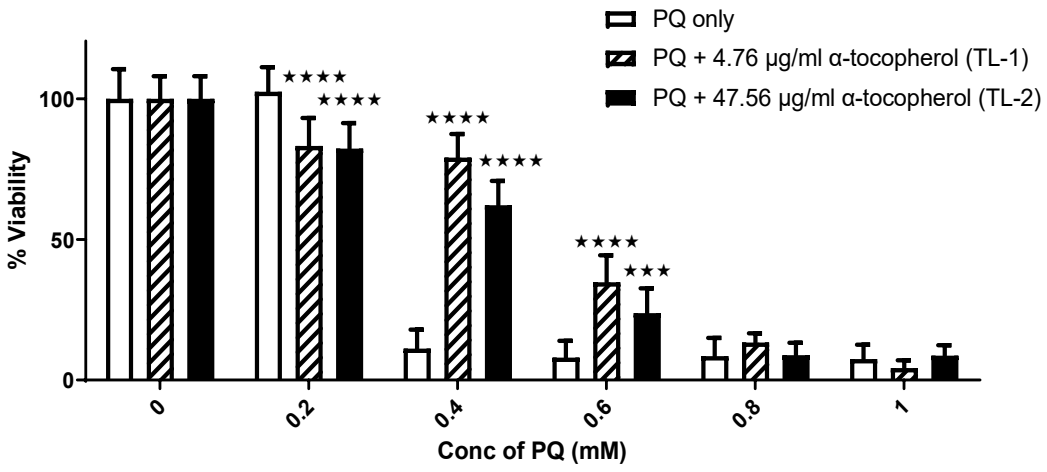

Figure 5.5: **The effect of two diffrent conc of α-tocopherol-loaded lipososmes plus PQ compared to PQ only on %viability of cells using MTT assay.** Mean ± SD, $N = 6$, $p < 0.0001$ (using two-way ANOVA), *** $p < 0.001$, **** $p < 0.0001$ compared to PQ only (using Bonferroni's *post hoc* test).

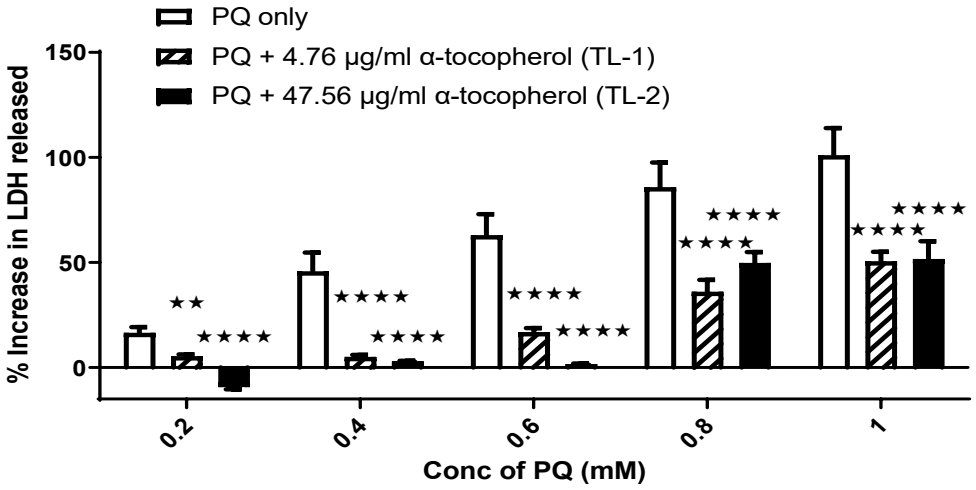

Figure 5.6: **The effect of two different concentrations of α-tocopherol-loaded liposomes plus PQ compared to PQ only on %increase in LDH release from cells**. Mean ± SD, *N* = 6, *p* < 0.0001 (using two-way ANOVA), ** *p* < 0.01, **** p < 0.0001 compared to PQ only (using Bonferroni's *post hoc* test).

5.4.2.1.2 Pre-incubation with α-tocopherol-loaded PLA nanoparticles

Comparable but less obvious results were recorded when pre-incubating cells with α-tocopherol-PLA nanoparticles. However, a small decease in cell viability (72.73 ± 10.02%) using 0.2 mM PQ, can be observed that was considerably raised to 80.84 ± 7.48% & 85.93 ± 9.85% using samples TP-1 & TP-2; respectively. The use of PQ in concentrations 0.4 – 1 mM led to a complete drop in cell viability (4.09 – 6.54%) that slightly raised with pre-incubation with TP-1 (8.35 – 20.12%) and more noticeably with TP-2 (12.98 – 36.35%) [Figure 5.7]. As with the MTT assay, the results from the LDH assay showed a dose-dependent increase in LDH release using increased concentration of PQ (0.2 -1 mM). This was remarkably ameliorated using both concentrations of α-tocopherol-loaded PLA nanoparticles with even better protection using TP-2 [Figure 5.8]. The pre-incubation with TL-1 & TL-2 showed better protection than TP-1 & TP-2 after treating with 0.4 and 0.6 mM PQ, as indicated by MTT and LDH assay.

Data analysis using two-way ANOVA showed significance effect α-tocopherol concentration on the results from MTT assay ($F_{(2, 90)} = 30.65$, *p* <

0.0001) and from LDH assay ($F_{(2, 75)} = 560.7$, $p < 0.0001$). Applying Bonferroni's multiple comparisons test to the MTT data, showed that the significant difference was for three main results: 0.2 mM PQ plus TP-2 compared to 0.2 mM PQ only ($X_{90} = 13.20$, $p = 0.007$), 0.4 mM PQ plus TP-1 compared to 0.4 mM PQ only ($X_{90} = 14.45$, $p = 0.002$) and 0.4 mM PQ plus TP-2 compared to 0.4 mM PQ only ($X_{90} = 30.68$, $p < 0.0001$). However, applying the same test to the LDH data, showed significant difference in all results compared to PQ only, with $X_{75} > 22$ and $p < 0.0001$ for all.

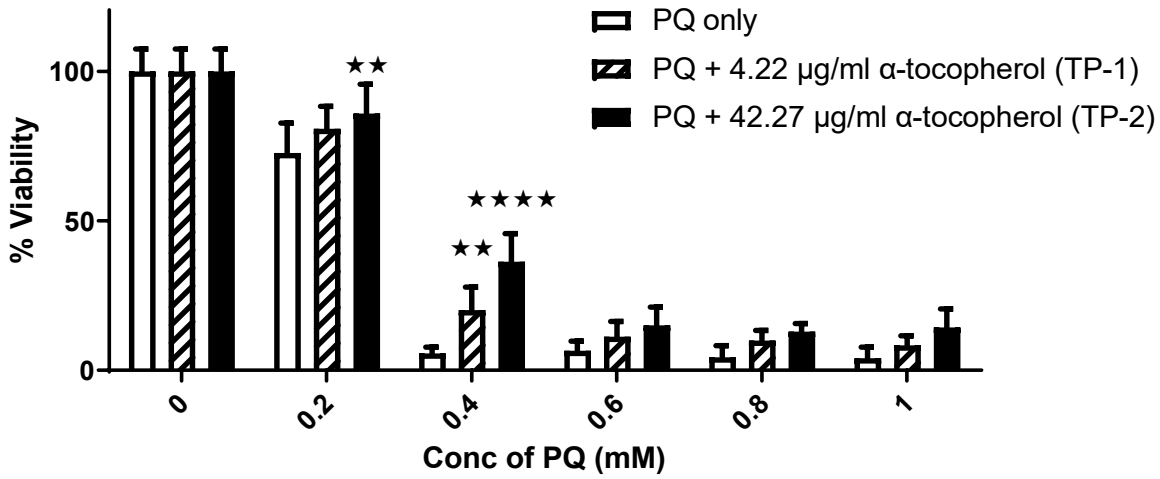

Figure 5.7: **The effect of two diffrent conc of α-tocopherol-loaded PLA nanoparticles plus PQ compared to PQ only on %viability of cells using MTT assay.** Mean ± SD, $N = 6$, $p < 0.0001$ (using two-way ANOVA), ** $p < 0.01$, **** $p < 0.0001$ compared to PQ only (using Bonferroni's *post hoc* test).

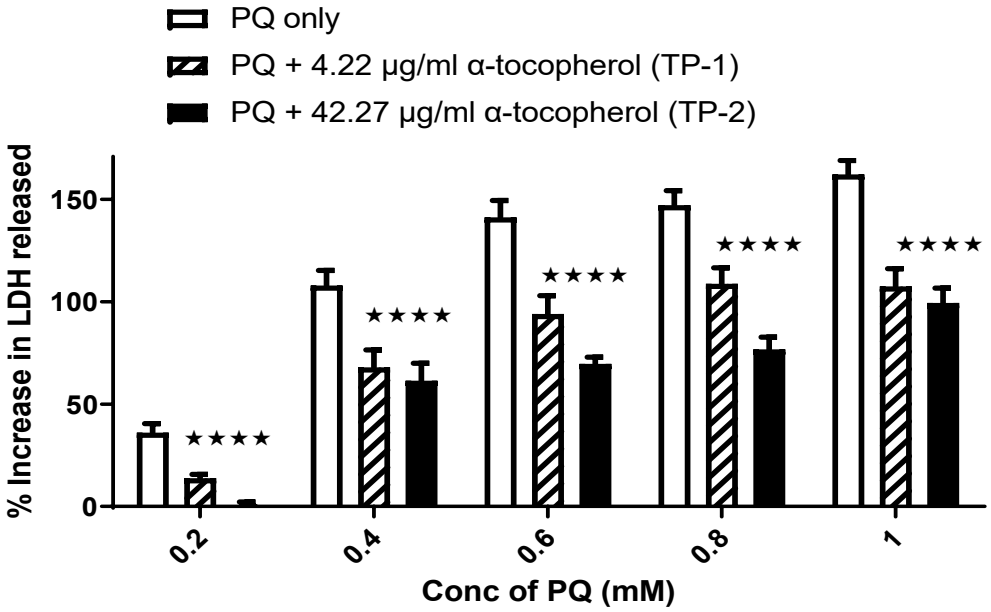

Figure 5.8: **The effect of two different concentrations of α-tocopherol-loaded PLA nanoparticles plus PQ compared to PQ only on the %increase in LDH release from cells**. Mean ± SD, *N* = 6, *p* < 0.0001 (using two-way ANOVA), **** *p* < 0.0001 for both TP-1 & TP-2 compared to PQ only (using Bonferroni's *post hoc* test).

5.4.2.1.3 Pre-incubation with α-tocopherol solution

In a similar way, the pre-incubation with α-tocopherol solution showed protection against the harmful effects of PQ [Figure 5.9 & 5.10]. The use of TS-1, although not significant, led to a rise in the %viability, to 105.10 ± 10.17%. Conversely, the pre-incubation with TS-2 led to a non-significant decrease in %viability to 87.76 ± 8.80%. This was consistent with the results from LDH assay, which showed that %increase in LDH release from 5.92 ± 1.36% using 0.2 mM to 20.98 ± 4.63%. Although, the use of TS-1 & TS-2 showed good amelioration to the reduction in the %viability caused by 0.4 mM, this protection was more evident with TL-1 & TL-2. The use of higher concentration of α-tocopherol solution (TS-2) showed better protection against 0.6, 0.8, 1 mM PQ than TS-1, as indicated from the MTT and LDH results.

Data analysis using two-way ANOVA showed significance from the α-tocopherol concentration variable on the data from MTT ($F_{(2, 90)} = 21.58$, $p < 0.0001$). Further analysis using Bonferroni's test showed the significant difference was evident only in 0.4 mM PQ plus TS-1 compared to PQ only ($X_{90} = 47.56$, $p < 0.0001$), 0.4 mM PQ plus TS-2 compared to PQ only ($X_{90} = 44.23$, $p < 0.0001$) and 0.6 mM PQ plus TS-2 compared to PQ only ($X_{90} = 24.14$, $p < 0.0001$). Similarly, significant results were obtained from the LDH data $F_{(2,75)} = 334.4$, $p < 0.0001$ using two-way ANOVA test. However, almost all concentrations of PQ plus both TS-1 & TS-2 showed significant results when compared to PQ only ($X \geq 15.06$, $p < 0.0001$ for all). The only exception was the use of 0.2 mM PQ plus TS-1 compared to PQ only, which showed non-significant difference.

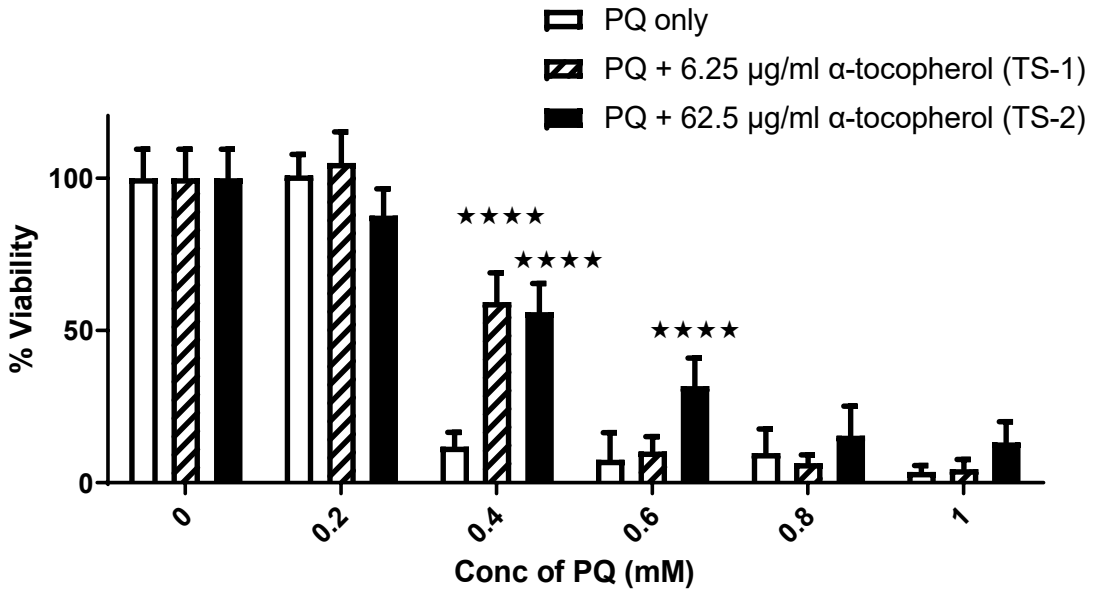

Figure 5.9: **The effect of two diffrent conc of α-tocopherol solution plus PQ compared to PQ only on %viability of cells using MTT assay.** Mean ± SD, $N = 6$, $p < 0.0001$ (using two-way ANOVA), **** $p < 0.0001$ compared to PQ only (using Bonferroni's *post hoc* test).

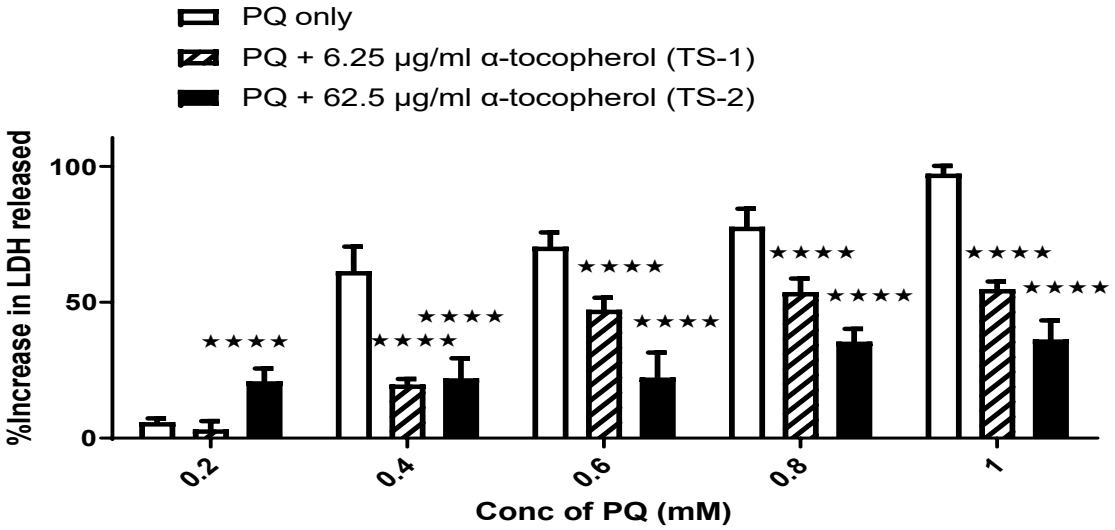

Figure 5.10: **The effect of two different concentrations of α-tocopherol solution plus PQ compared to PQ only on the %increase in LDH release from cells**. Mean ± SD, *N* = 6, *p* < 0.0001 (using two-way ANOVA), **** p < 0.0001 compared to PQ only (using Bonferroni's *post hoc* test).

5.4.2.2 Effect of pre-incubation with curcumin-loaded liposomes, PLA nanoparticles and solution

Curcumin solution, PLA nanoparticles and liposomes were prepared in the same manner as α-tocopherol preparations (section 5.4.2.2.1). However, considering the %LE of curcumin in its novel formulations, the sample concentrations were lower compared to α-tocopherol preparations [Table 5.2].

Table 5.2 : The concentration of curcumin in each sample and its given code

Drug	*Form*	*Theoretical conc (µg/mL)*	*%LE*	*Actual conc (µg/mL)*	*code*
Curcumin	liposomes	6.25	52.90%	3.31	CL-1
Curcumin	liposomes	62.5	52.90%	33.06	CL-2
Curcumin	PLA nanoparticles	6.25	52.35%	3.27	CP-1
Curcumin	PLA nanoparticles	62.5	52.35%	32.72	CP-2
Curcumin	solution	6.25	NA	6.25	CS-1
Curcumin	solution	62.5	NA	62.5	CS-2

5.4.2.2.1 Effect of pre-incubation with curcumin-loaded liposomes

As with α-tocopherol, the destructive effect of PQ on the cells was challenged by pre-incubating cells with curcumin in its novel formulations. Unpredictably, curcumin-loaded liposomes further reduced the viability of the cells. The %viability using 0.2 mM PQ was reduced from 100.69 ± 7.95% to 89.66 ± 7.34% & 11.44 ± 1.71% when pre-incubating with CL-1 & CL-2; respectively. Additionally, the %viability using 0.4 mM PQ was also reduced from 75.16 ± 7.54% to 58.3 ± 8.73% and 11.97 ± 2.03% when pre-incubating with the same samples; respectively. No significant change was observed using pre-incubation of either CL-1 or CL-2 after treatment with ≥ 0.6 mM PQ [Figure 5.11]. This was mostly consistent with the results from LDH assay. The %increase in LDH release due to 0.4 mM PQ treatment (56.03 ± 8.39%) was further increased to 107.71 ± 7.33% & 100.44 ± 3.41% using pre-incubation with CL-1 & CL-2; respectively. The %increase in LDH release also increased after treating with 0.2 mM PQ from 15.53 ± 6.51% to 111.34 ± 5.88% when pre-incubating with CL-2. However, a significant reduction in the %increase in the LDH release was noticed when pre-incubating with CL-1 (2.56 ± 1.66%). No substantial protection was noticed using curcumin-loaded liposomes after treatment with ≥ 0.6 mM PQ, although, there

were small reductions in %increases in LDH release using both CL-1 & CL-2 [Figure 5.12].

Data analysis showed significant effect of curcumin concentration on the data from both MTT assay ($F_{(2, 90)} = 140.3$, $p < 0.0001$) and LDH assay ($F_{(2, 75)} = 127.90$, $p < 0.0001$) using two-way ANOVA. Applying Bonferroni's test to compare individual results from MTT assay to PQ only showed significant diferences between cells treated with 0.2 & 0.4 mM PQ and pre incubated with CL-1 ($X_{90} = 11.30$ & 16.86; respectively, $p < 0.01$) or with CL-2 ($X_{90} = 89.52$ & 63.19; respectively, $p < 0.0001$). Applying the same test to the LDH results showed significant diffrence between most results from cells pre-incubated with CL-1 or CL-2 and PQ only treated cells, were $X_{75} > 10$ and $p < 0.01$. No significant difference was observed when comparing pre-incubation with CL-2 plus 0.6 mM PQ to PQ only and when comparing pre-incubation with either CL-1 or CL-2 plus 1mM PQ to PQ only.

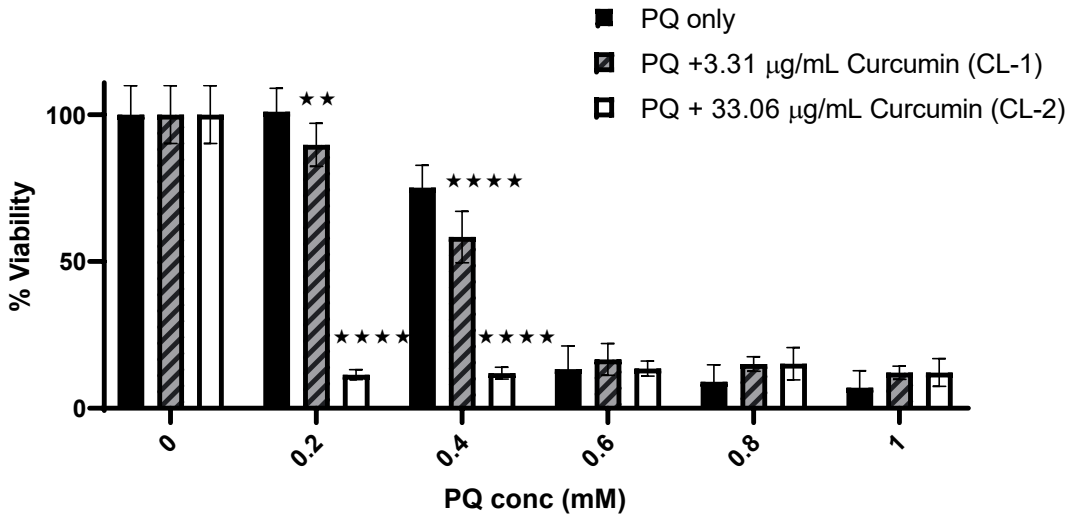

Figure 5.11: **The effect of two different concentrations of curcumin-loaded liposomes plus PQ compared to PQ only on %viability of cells using the MTT assay.** Mean ± SD, $N = 6$, $p < 0.0001$ (using two-way ANOVA), $^{**}p < 0.01$, $^{****}p < 0.0001$ compared to PQ only (using Bonferroni's *post hoc* test).

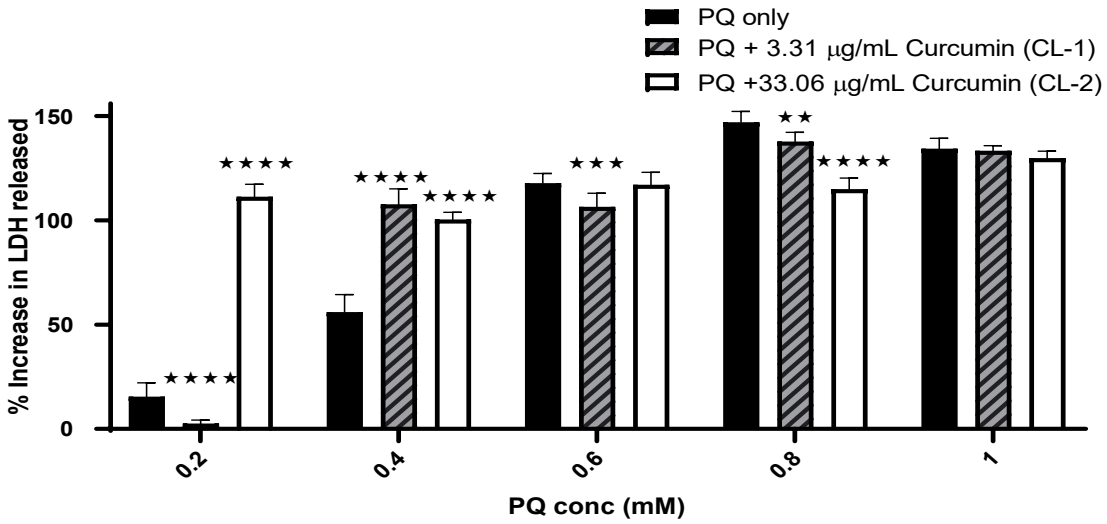

Figure 5.12: **The effect of two different concentrations of curcumin-loaded liposomes plus PQ compared to PQ only on the %increase in LDH release from cells**. Mean ± SD, *N* = 6, $p < 0.0001$ (using two-way ANOVA), ** $p < 0.01$, *** $p < 0.001$, **** $p < 0.0001$ compared to PQ only (using Bonferroni's *post hoc* test).

5.4.2.2.2 Effect of pre-incubation with curcumin-loaded PLA nanoparticles

The use of curcumin-loaded PLA nanoparticles showed results comparable with curcumin-loaded liposomes, with some exceptions. Pre-incubation with CP-1 and CP-2 led to a reduction in cell viability from 99.57 ± 7.02% using 0.2 mM PQ only to 79.13 ± 8.58% and 33.17 ± 8.8%; respectively. Furthermore, pre-incubating with CP-2 reduced the %viability from 41.28 ± 7.58% using 0.4 mM PQ to 20.33 ± 6.58%. In contrast, the %viability increased to 67.11 ± 8.92% when pre-incubating with CP-1. Pre-incubating with both CP-1 & CP-2 led to slight inconsequential increases in the %viability after treatment with 0.6, 0.8 and 1 mM PQ [Figure 5.13]. As previously shown, the increase in PQ concentration led to a gradual increase in LDH release. This increase was not ameliorated when pre-incubating with CP-1 until treating with 0.8 and 1 mM PQ. Pre-incubating with CP-2 led to complete cell death, regardless of the PQ concentration, as indicated with %increase in LDH release which was over 120% after treatment with PQ [Figure 5.14].

Analysing data using two-way ANOVA showed significance effect from curcumin concentration on both MTT data ($F_{(2, 90)} = 44.15$, $p < 0.0001$) and LDH

data ($F_{(2, 75)}$ = 577.1, p < 0.0001). Using Bonferroni's *post hoc* test to further analyse the MTT results showed significance difference in the following: 0.2 mM PQ only *vs*. PQ + CP-1 (X_{90} = 20.44, p < 0.0001), 0.2 mM PQ only *vs*. PQ + CP-2 (X_{90} = 66.40, p < 0.0001), 0.4 mM PQ only *vs*. PQ + CP-1 (X_{90} = -25.83, p < 0.0001), 0.4 mM PQ only *vs*. PQ + CP-2 (X_{90} = 20.95, p < 0.0001), 0.8 mM PQ only *vs*. PQ + CP-2 (X_{90} = -9.73, p = 0.0173) and 1 mM PQ only *vs*. PQ + CP-2 (X_{90} = -11.70, p = 0.0035). No significant difference was observed using all other concentrations. Applying the same test on LDH data, showed significant diffrences between most results from PQ only *vs*. pre-incubation with CP-1 & CP-2, except for 0.2 mM PQ only *vs*. PQ + CP-1 and 0.6 mM PQ only *vs*. PQ + CP-1, which showed non-significant differences.

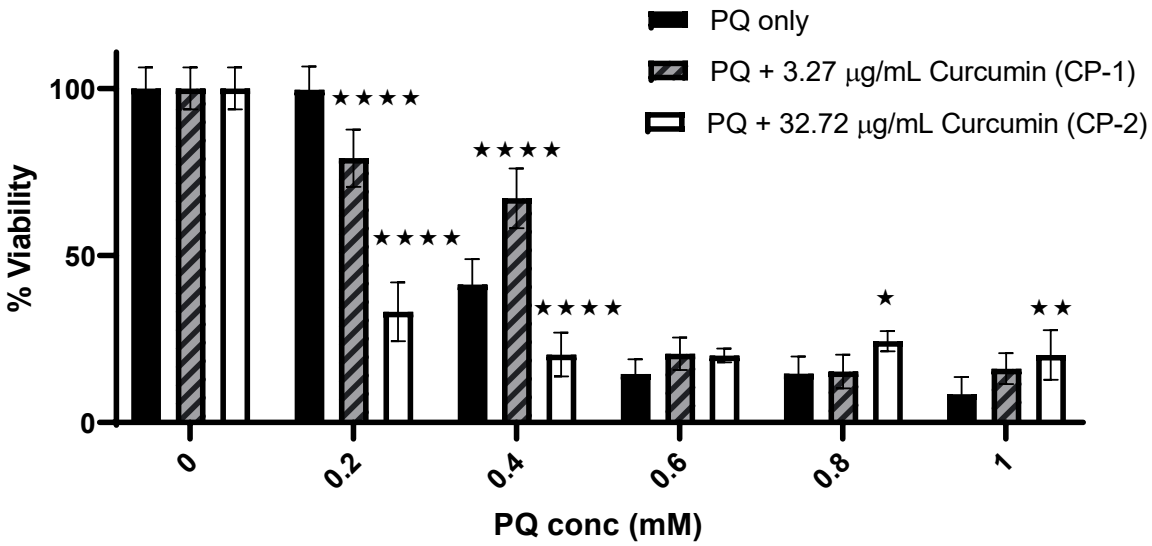

Figure 5.13**: The effect of two different concentrations of curcumin-loaded PLA nanoparticles plus PQ compared to PQ only on %viability of cells using MTT assay.** Mean ± SD, N = 6, p < 0.0001 (using two-way ANOVA), *p < 0.05, **p < 0.01, **** p < 0.0001 compared to PQ only (using Bonferroni's *post hoc* test).

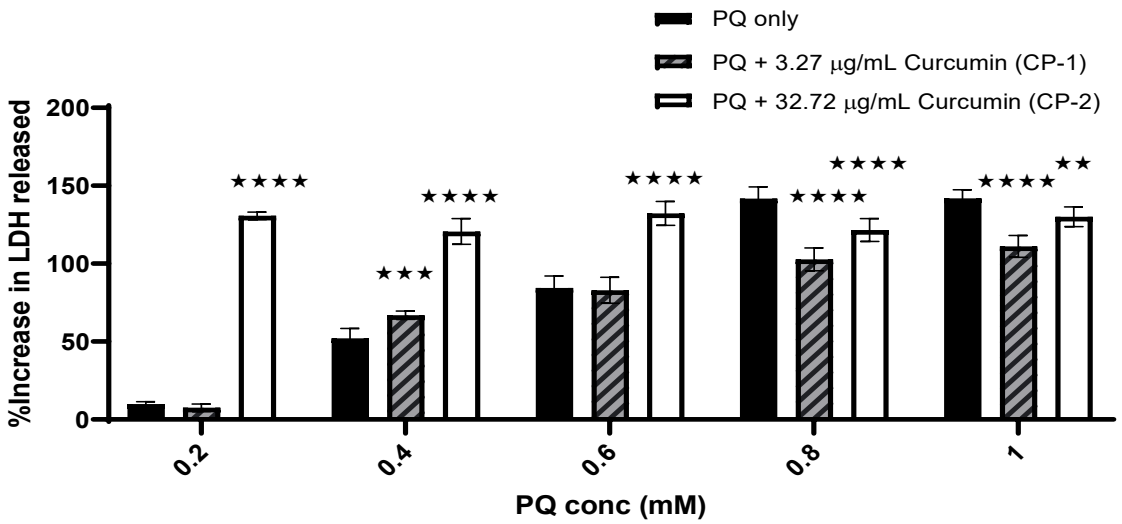

Figure 5.14: **The effect of two different concentrations of curcumin-loaded PLA nanoparticles plus PQ compared to PQ only on the %increase in LDH release from cells**. Mean ± SD, $N = 6$, $p < 0.0001$ (using two-way ANOVA), ** $p < 0.01$, *** $p < 0.001$, **** $p < 0.0001$ compared to PQ only (using Bonferroni's *post hoc* test).

5.4.2.2.3 Effect of pre-incubation with curcumin solution

The pre-incubation of curcumin solution (un-encapsulated form) prior to the treatment with PQ, showed comparable but a less harmful effect than its encapsulated form. As discussed previously, low doses of PQ (0.2 mM) led to a slight increase in %viability (107.14 ± 9.61%), which was further increased by pre-incubation with CS-1 to 115.11 ± 6.03% (unlike CL-1 & CP-1). However, pre-incubation with CS-2 led a plunge in the %viability (30.34 ± 5.38%), as observed with CL-2 & CP-2. Pre-incubation with CS-1 & CS-2, led to a reduction in %viability from 72.99 ± 10.00% (using 0.4 mM PQ) to 61.33 ± 8.13% & 25.17 ± 7.29%; respectively, as observed when pre-incubating with CL-1 & CL-2. Although, no considerable effect was noticed when pre-incubating with CS-1 after the treatment with ≥ 0.6 mM PQ, there was however, a minor increase in %viability when pre-incubating with CS-2 [Figure 5.15]. The data from the LDH assay showed no notable effect from pre-incubation with CS-1 at all PQ concentrations. Conversely, variable effect was observed when pre-incubating with CS-2. Initially, the %increase in LDH increased from 5.47 ± 0.17% (using 0.2 mM PQ only) to 21.8 ± 1.57% when pre-incubating with CS-2, followed by no effect on the treatment with

0.4 mM PQ. However, the protection effect of pre-incubating with CS-2 on the treatment with PQ (≥ 0.6 mM) was noteworthy. The %increase in LDH release was lowered from 75.19 ± 8.63% (using 0.6 mM PQ) to 31.43 ± 4.02%, from 84.11 ± 6.51% (using 0.8 mM PQ) to 41.17 ± 4.05% and from 112.69 ± 8.95% (using 1 mM PQ) to 30.67 ± 2.51%, when pre-incubating with CS-2 [Figure 5.16]. This protection was not noted with curcumin in its encapsulated forms.

Again, data analysis using two-way ANOVA showed significance effect from curcumin concentration on the results from MTT assay ($F_{(2, 90)} = 36.61$, $p < 0.0001$) and from the LDH assay ($F_{(2, 75)} = 267.5$, $p < 0.0001$). Applying the Bonferroni's *post hoc* test to compare the MTT results showed significant difference between the following results: 0.2 mM PQ only *vs*. PQ + CS-2 ($X_{90} = 76.80$, $p < 0.0001$), 0.4 mM PQ only *vs*. PQ + CS-1 ($X_{90} = 11.66$, $p = 0.0295$), 0.4 mM PQ only *vs*. PQ + CS-2 ($X_{90} = 47.82$, $p < 0.0001$) and 1 mM PQ only *vs*. PQ + CS-2. No significant differences were noted for the rest of the results. Applying the same test to the LDH results showed a significant difference in the following: 0.2 mM PQ only *vs.* PQ + CS-2 ($X_{75} = -16.33$, $p < 0.0001$), 0.6 mM PQ only *vs*. PQ + CS-2 ($X_{75} = 43.76$, $p < 0.0001$), 0.8 mM PQ only *vs*. PQ + CS-2 ($X_{75} = 42.94$, $p < 0.0001$), 1 mM PQ only *vs*. PQ + CS-1 ($X_{75} = 9,44$, $p = 0.0101$) and 1 mM PQ only *vs*. PQ + CS-2 ($X_{75} = 82.02$, $p < 0.0001$). No significant differences were noticed in all other results.

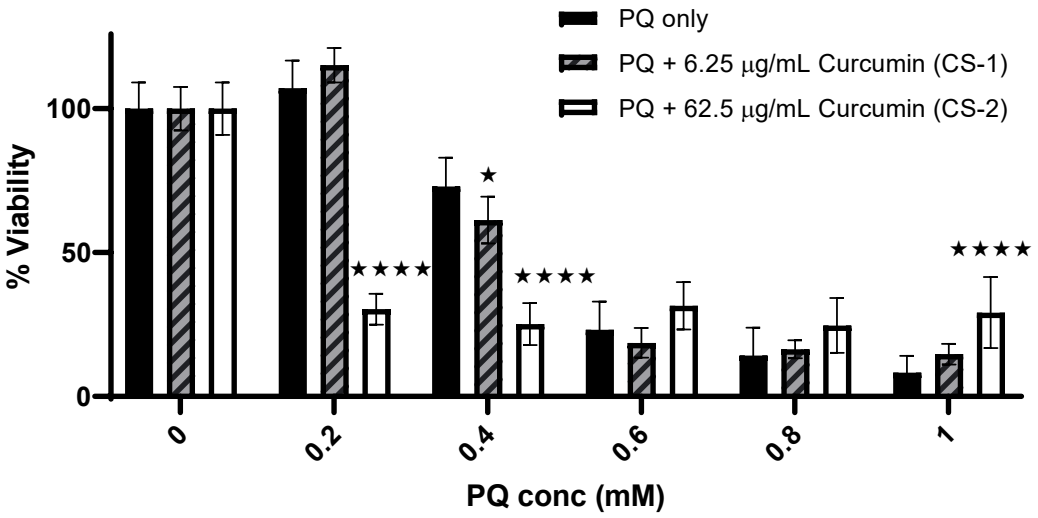

Figure 5.15: **The effect of two different concentrations of curcumin solution plus PQ compared to PQ only on %viability of cells using MTT assay.** Mean ± SD, $N = 6$, $p < 0.0001$ (using two-way ANOVA), * $p < 0.05$, **** $p < 0.0001$ compared to PQ only (using Bonferroni's *post hoc* test).

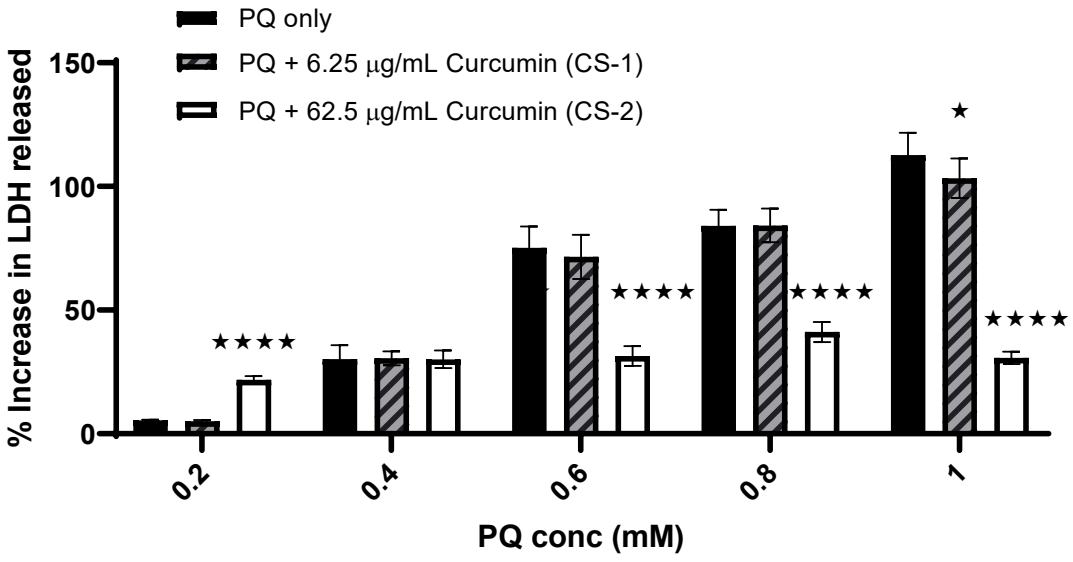

Figure 5.16: **The effect of two different concentrations of curcumin solution plus PQ compared to PQ only on the %increase in LDH release from cells**. Mean ± SD, $r = 6$, $p < 0.0001$ (using two-way ANOVA), * $p < 0.05$, **** $p < 0.0001$ compared to PQ only (using Bonferroni's *post hoc* test).

5.4.2.3 Effect of pre-incubation with resveratrol-loaded liposomes, PLA nanoparticles and solution

Resveratrol was also prepared as free (solution) and encapsulated forms in liposomes and PLA nanoparticles in the same manner as α-tocopherol (section 5.4.2.1). Details of the calculated concentrations within each sample, when considering the %LE are shown in table 5.3.

Table 5.3: The concentration of resveratrol in each sample and its given code

Drug	*Form*	*Theoretical conc (µg/mL)*	*%LE*	*Actual conc (µg/mL)*	*code*
Resveratrol	Liposomes	6.25	12.04%	0.75	RL-1
Resveratrol	Liposomes	62.5	12.04%	7.53	RL-2
Resveratrol	PLA nanoparticles	6.25	40.81%	2.55	RP-1
Resveratrol	PLA nanoparticles	62.5	40.81%	25.51	RP-2
Resveratrol	solution	6.25	NA	6.25	RS-1
Resveratrol	solution	62.5	NA	62.5	RS-2

5.4.2.3.1 Effect of pre-incubation with resveratrol-loaded liposomes

It has been observed that the harmful effect of PQ starts to be significantly noticed from 0.4 mM. This harmful effect has been challenged using two concentrations of resveratrol-loaded liposomes. The %viability increased from 51.5 ± 10% using 0.4 mM PQ only to 76.74 ± 5.94% and 73.08 ± 11.49% after pre-incubating with RL-1 and RL-2; respectively. RL-1 continued to show protection even at higher concentration of PQ, although not as significant at 0.8 and 1 mM PQ. No significant effects were observed after pre-incubation with RL-2 using PQ concentrations ≥ 0.6 mM [Figure 5.17]. However, the results from the LDH assay showed more protection from the pre-incubation of RL-2. The %increase in LDH release was lowered from 46.81 ± 5.38%, 120.57 ± 7.91%, 162.09 ± 10.59%,

161.84 ± 6.96% and 159.09 ± 4.18% (using 0.2, 0.4, 0.6, 0.8 and 1 mM PQ only; respectively) to 13.23 ± 2.19%, 100.66 ± 4.23%, 122.37 ± 11.43, 136.12 ± 3.09% and 123.79 ± 4.33%; respectively after pre-incubating with RL-2 [Figure 5.18].

As with previous results, data was analysed using two-way ANOVA showed a significance effect of resveratrol concentration on both MTT ($F_{(2, 90)} = 10.08$, $p < 0.0001$) and LDH results ($F_{(2, 75)} = 239.7$, $p < 0.0001$). Using Bonferroni's test on the MTT results showed significant difference between 0.4 mM PQ only compared to pre-incubation with RL-1 ($X_{90} = 25.24$, $p < 0.0001$) and with RL-2 ($X_{90} = 21.58$, $p < 0.0001$) and between 0.6 mM PQ only and pre-incubating with RL-1 ($X_{90} = 14.56$, $p = 0.0043$). No significant difference was noted when comparing all other results. However, using the same test on the LDH results showed significant differences mainly after pre-incubating with RL-2 with $X_{75} > 25$, $p < 0.0001$ for all PQ concentrations compared to PQ only. Additionally, 0.8 mM PQ only, compared to 0.8 mM PQ pre-incubated with RL-1 showed a small significant difference ($X_{75} = -10.92$, $p = 0.0116$). No significant difference was noted between the rest of the results.

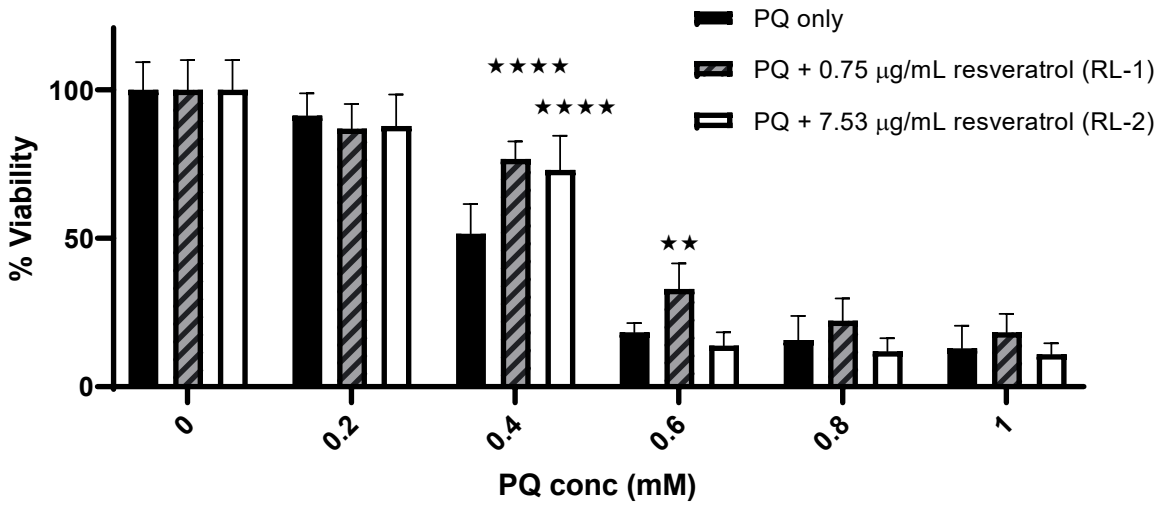

Figure 5.17: **The effect of two different concentrations of resveratrol-loaded lipososme plus PQ compared to PQ only on %viability of cells using MTT assay.** Mean ± SD, $N = 6$, $p < 0.0001$ (using two-way ANOVA), ** $p < 0.01$, **** $p < 0.0001$ compared to PQ only (using Bonferroni's *post hoc* test).

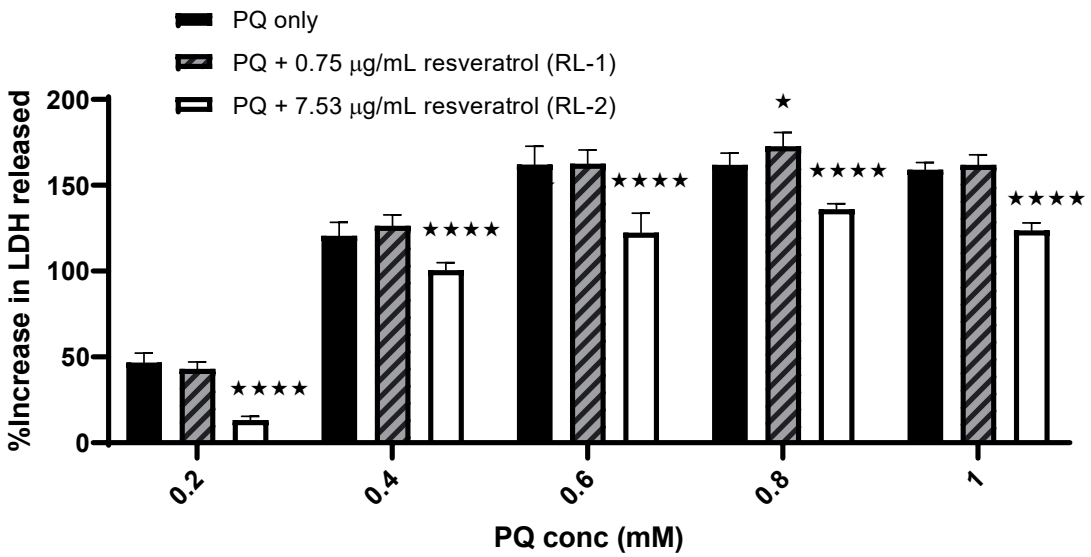

Figure 5.18: **The effect of two different concentrations of resveratrol-loaded liposomes plus PQ compared to PQ only on the %increase in LDH release from cells**. Mean ± SD, *N* = 6, *p* < 0.0001 (using two-way ANOVA), * *p* < 0.05, **** *p* < 0.0001 compared to PQ only (using Bonferroni's *post hoc* test).

5.4.2.3.2 Effect of pre-incubation with resveratrol-loaded PLA nanoparticles

The effect of PQ was also challenged using pre-incubation with resveratrol-loaded PLA nanoparticles. As with resveratrol-loaded liposomes, an increase in the %viability was noticed from 19.69 ± 6.19% using 0.4 mM PQ only to 53.29 ± 7.27% and 51.05 ± 9.97% when pre-incubating with RP-1 and RP-2; respectively. However, a slight reduction in %viability was noticed after pre-incubating with RP-2 and treating with 0.2 mM PQ (not noticed with RP-1). There was no effect on the %viability using either RP-1 or RP-2 after treating with higher concentrations of PQ (≥ 0.6 mM) [Figure 5.19]. In contrast to the effect of liposomes, pre-incubating with both strengths of resveratrol-loaded PLA nanoparticles showed protection in the LDH assay, although more evident with RP-2 [Figure 5.20].

Data analysis using two-way ANOVA showed significance effect from resveratrol concentration on the MTT results ($F_{(2, 90)} = 5.402$, $p = 0061$) with significant difference detected using Bonferroni's test between the following: 0.2

mM PQ only *vs*. PQ + RP-2 (X_{90} = 14.88, p = 0.0035), 0.4 mM PQ + RP-1 *vs.* PQ only (X_{90} = 33.60, p < 0.0001) and 0.4 mM PQ + RP-2 *vs.* PQ only (X_{90} = 31.36, p < 0.0001). No significant difference was noted in the rest of the MTT results. Applying the same analysis tests to the LDH data also showed a significant effect from resveratrol concentration on the results ($F_{(2, 75)}$ = 162.6, p < 0.0001) with significant differences between 0.4 mM PQ only *vs*. PQ + RP-1 (X_{75} = 45.88, p < 0.0001) and 0.8 mM PQ only *vs*. PQ + RP-1 (X_{75} = 16.59, p = 0.0005). Additionally, significant effects were observed between all PQ only concentrations *vs*. pre-incubation with RP-2 (X_{75} ≥ 21.45, p < 0.0001). No significant difference was noted in other results.

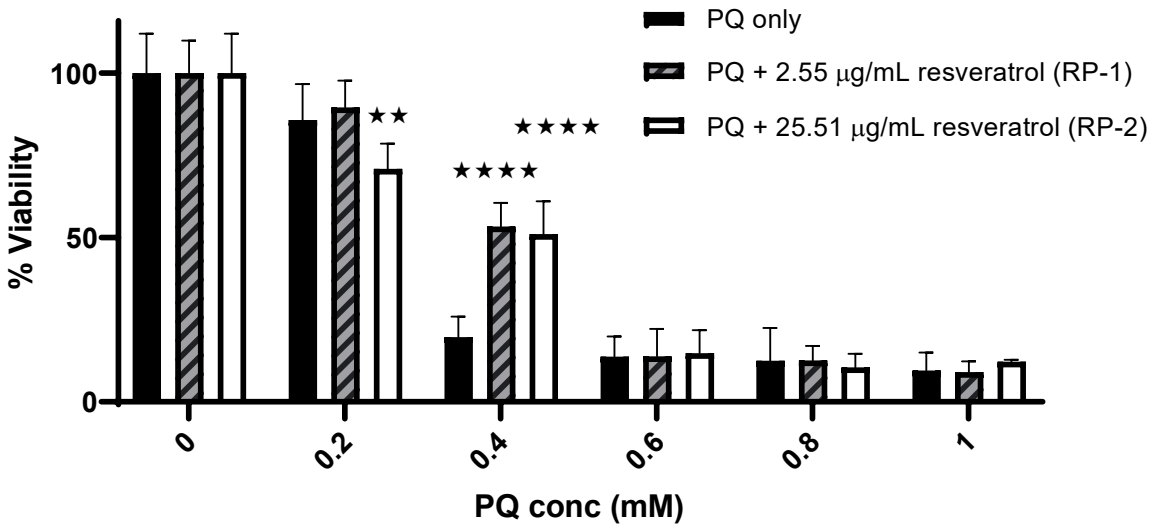

Figure 5.19: **The effect of two different concentrations of resveratrol-loaded PLA nanoparticles plus PQ compared to PQ only on %viability of cells using MTT assay.** Mean ± SD, N = 6, p < 0.0001 (using two-way ANOVA), ** p < 0.01, **** p < 0.0001 compared to PQ only (using Bonferroni's *post hoc* test).

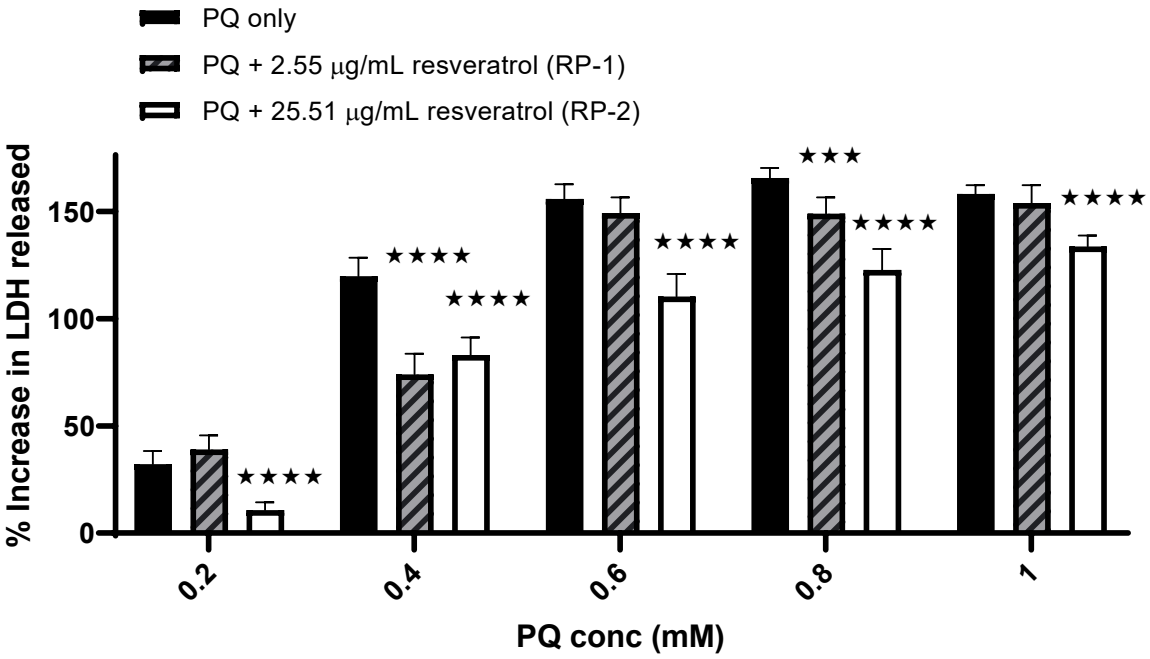

Figure 5.20: **The effect of two different concentrations of resveratrol-loaded PLA nanoparticles plus PQ compared to PQ only on the %increase in LDH release from cells**. Mean ± SD, $N = 6$, $p < 0.0001$ (using two-way ANOVA), *** $p < 0.001$, **** $p < 0.0001$ compared to PQ only (using Bonferroni's *post hoc* test).

5.4.2.3.3 Effect of pre-incubation with resveratrol solution

Slightly different results were obtained when the cells were pre-incubated with resveratrol solution (un-encapsulated form) prior to treatment with PQ. Initially, the %viability was reduced from 104.05 ± 12.37% (using 0.2 mM PQ) to 91.49 ± 11.95 and 69.32 ± 6.4% when pre-incubating with RS-1 & RS-2; respectively. This was followed by a rise in %viability from 28.74 ± 5.37% (using 0.6 mM PQ) to 63.43 ± 12.82% and 51.22 ± 11.76% when pre-incubating with RS-1 & RS-2; respectively. No obvious effect was noted from pre-incubation with these sample on the %viability caused by ≥ 0.6 mM PQ [Figure 5.21]. The harmful effect of RS-2 was also noticed in the LDH assay results using 0.2 mM PQ, although not noted with RS-1 with the %increase in LDH release leaping from 24.11 ± 7.75% using 0.2 mM PQ only to 104.83 ± 9.83% when pre-incubating with RS-2. A smaller increase from 59.13 ± 13.72% (using 0.4 mM PQ only) to 67.47 ± 7.02% was also observed when pre-incubating with same sample. Trivial reductions were also noted in the %increase in the LDH release caused by PQ

when pre-incubating with RS-2. No major effect was observed using RS-1 in the LDH results [Figure 5.22].

Data analysis using previously applied tests showed significant effect from resveratrol concentration on both MTT data ($F_{(2, 90)} = 3.992$, $p = 0.0218$) and LDH data ($F_{(2, 75)} = 17.06$, $p < 0.0001$) and significant differences between the following: 0.2 mM PQ only *vs*. PQ + RS-1 ($X_{90} = 12.56$, $p = 0.0262$), 0.2 mM PQ only *vs*. PQ + RS-2 ($X_{90} = 34.73$, $p < 0.0001$), 0.4 mM PQ only *vs*. PQ + RS-1 ($X_{90} = -34.69$, $p < 0.0001$) & 0.4 mM PQ only *vs*. PQ + RS-2 ($X_{90} = -22.48$, $p < 0.0001$) in the MTT results and 0.2 mM PQ only *vs*. PQ + RS-2 ($X_{75} = -80.72$, $p < 0.0001$) & 0.8 mM PQ only *vs*. PQ + RS-2 ($X_{75} = 14.56$, $p = 0.0172$) in the LDH results. No significant differences were noted between the other results

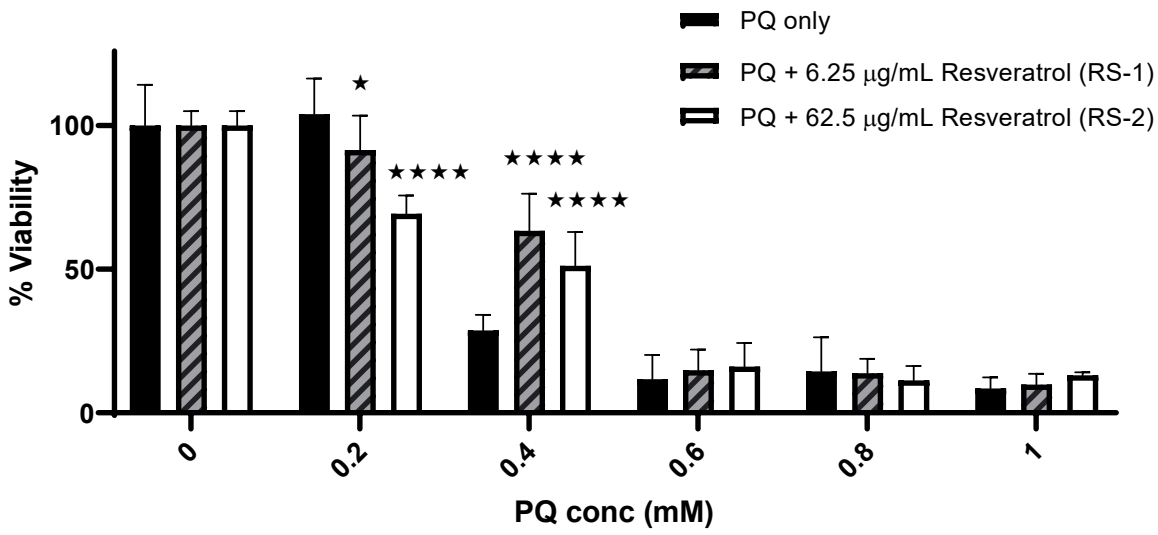

Figure 5.21: **The effect of two different concentrations of resveratrol solution plus PQ compared to PQ only on %viability of cells using MTT assay.** Mean ± SD, $N = 6$, $p < 0.0001$ (using two-way ANOVA), ** $p < 0.01$, **** $p < 0.0001$ compared to PQ only (using Bonferroni's *post hoc* test).

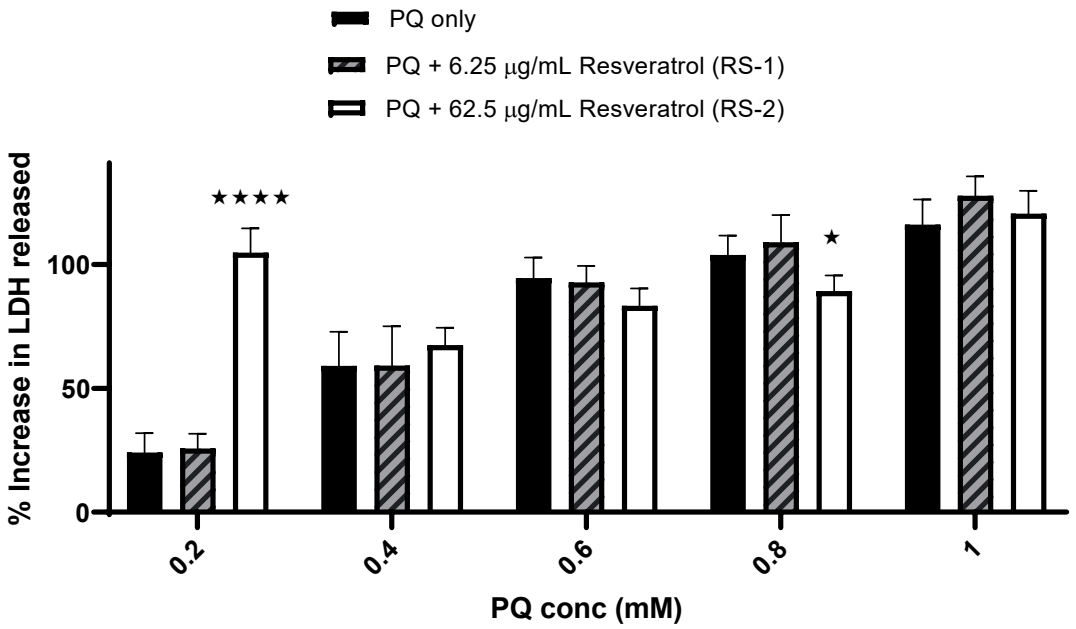

Figure 5.22: **The effect of two different concentrations of resveratrol solution plus PQ compared to PQ only on the %increase in LDH release from cells**. Mean ± SD, $N = 6$, $p < 0.0001$ (using two-way ANOVA), * $p < 0.05$, **** $p < 0.0001$ compared to PQ only (using Bonferroni's *post hoc* test).

5.4.2.4 Effect of pre-incubation with ferulic acid solution, PLA nanoparticles and liposomes

As with previously tested samples, ferulic acid was prepared in two concentrations in three different forms: ferulic acid-loaded liposomes (FL-1 & FL-2), ferulic acid-loaded PLA nanoparticles (FP-1 & FP-2) and ferulic acid solution (FS-1 & FS-2). These samples were prepared in the same manner as α-tocopherol samples. The concentration of FA in each sample was calculated and shown in table 5.4.

Table 5.4: The concentration of ferulic acid in each sample and its given code

Drug	*Form*	*Theoretical conc (µg/mL)*	*%LE*	*Actual conc (µg/mL)*	*code*
Ferulic acid	Liposomes	6.25	20.78%	1.30	FL-1
Ferulic acid	Liposomes	62.5	20.78%	12.99	FL-2
Ferulic acid	PLA nanoparticles	6.25	15.48%	0.97	FP-1
Ferulic acid	PLA nanoparticles	62.5	15.48%	9.68	FP-2
Ferulic acid	Solution	6.25	NA	6.25	FS-1
Ferulic acid	Solution	62.5	NA	62.5	FS-2

5.4.2.4.1 Effect of pre-incubation with ferulic acid-loaded liposomes

To test the ability of ferulic acid-loaded liposomes to ameliorate the harmful effect of PQ on NRK-52E cells, cells were pre-incubated with FL-1 & FL-2 for 24 hours prior to treatment with 0 – 1 mM PQ. After further 24 hours, the cells were tested using the MTT and LDH assays. At 0.2 mM PQ, the %viability of the cells rose from 79.43 ± 10.65% using PQ only to 92.51 ± 10.15% & 84.4 ± 9.43% when pre-incubating with FL-1 & FL-2; respectively. A more prominent protection was shown when using FL-2 at 0.4 mM PQ, were the %viability rose from 22.78 ± 9.64% using PQ only to 28.67 ± 6.61% & 53.05 ± 10.17% when pre-incubating with FL-1 & FL-2; respectively. No evident protection was observed in the MTT results at higher concentrations of PQ [Figure 5.23]. However, the LDH assay results showed particularly good protection of both FL-1 & FL-2 against the harmful effect of PQ, even at 1 mM. It was also noticed that more protection was observed using FL-2 than FL-1, indicating that this was concentration dependent [Figure 5.24].

Data analysis showed significance effect from ferulic acid concentration on the MTT results using two-way ANOVA ($F_{(2, 90)} = 9.599$, $p = 0.0002$) and significant differences using Bonferroni's test between 0.2 mM PQ only and PQ +

FL-1 (X_{90} = -13.08, p = 0.0089) and between 0.4 mM PQ only and PQ + FL-2 (X_{90} = -30.27, p < 0.0001). There were no significant differences between all the other MTT results. The LDH data also showed significance effect from ferulic acid concentration using two-way ANOVA ($F_{(2, 75)}$ = 209.3, p < 0.0001) and significant differences using Bonferroni's test between all results from PQ only *vs*. pre-incubation with FL-1 & FL-2 (X_{75} > 20, p < 0.0001 at all PQ concentrations, except 0.6 mM PQ only *vs*. PQ + FL-1 which showed X_{75} = 12.99, p = 0.0041).

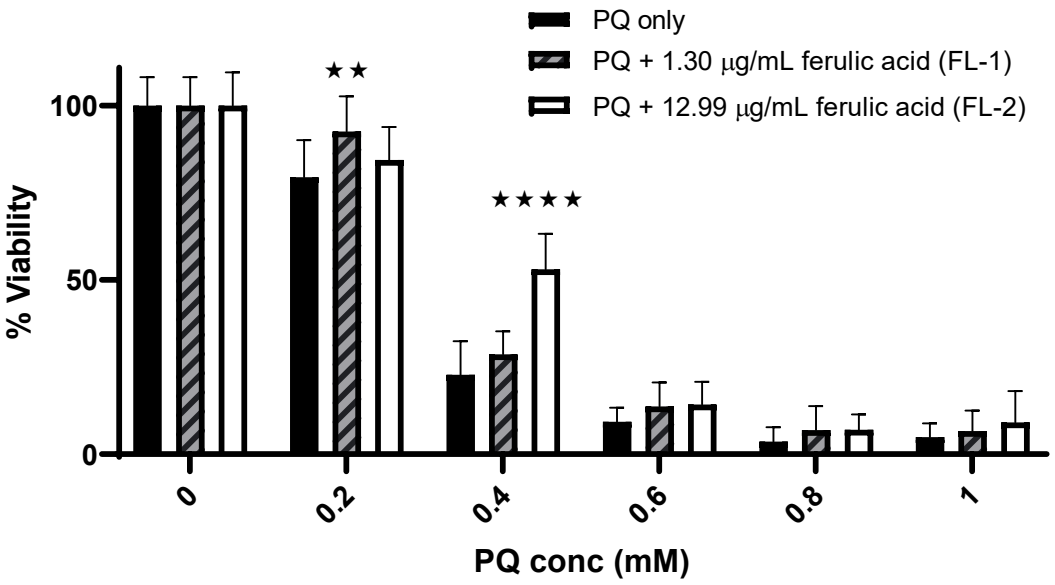

Figure 5.23: **The effect of two different concentrations of ferulic acid-loaded liposomes plus PQ compared to PQ only on %viability of cells using MTT assay.** Mean ± SD, N = 6, p < 0.0001 (using two-way ANOVA), ** p < 0.01, **** p < 0.0001 compared to PQ only (using Bonferroni's *post hoc* test).

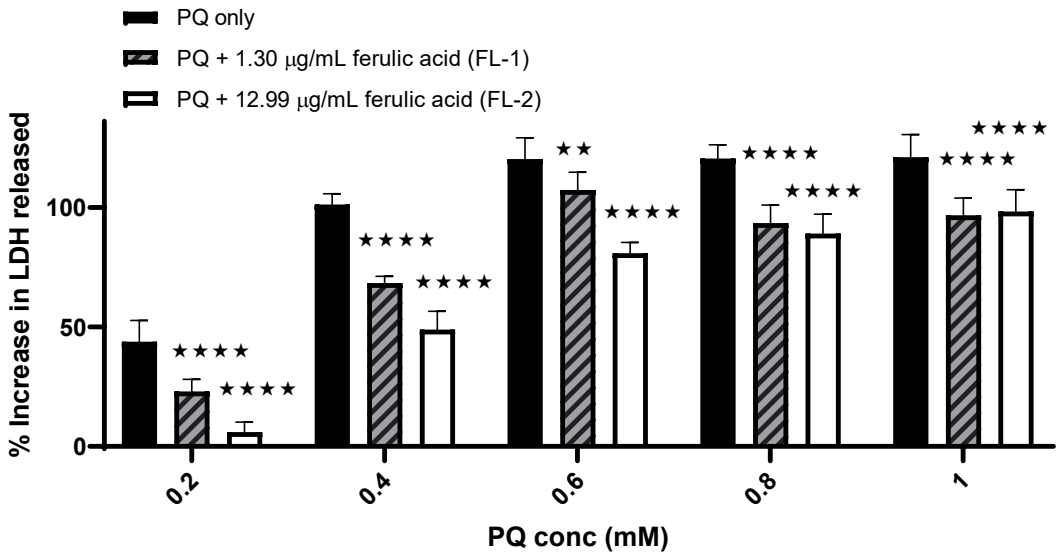

Figure 5.24: **The effect of two different concentrations of ferulic acid-loaded liposomes plus PQ compared to PQ only on the %increase in LDH release from cells**. Mean ± SD, *N* = 6, $p < 0.0001$ (using two-way ANOVA), ** $p < 0.01$, **** $p < 0.0001$ compared to PQ only (using Bonferroni's *post hoc* test).

5.4.2.4.2 Effect of pre-incubation with ferulic acid-loaded PLA nanoparticles

Furthermore, ferulic acid PLA nanoparticles were also tested for their ability to prevent PQ toxicity. MTT assay showed protection from both FP-1 & FP-2 at all PQ concentrations, which was more pronounced at 0.4 & 0.6 mM, where the %viability increased from 20.96 ± 10.23% using 0.4 mM only to 42.56 ± 11.07% & 75.15 ± 9.71% when pre-incubating with FP-1 & FP-2; respectively and from 12.41 ± 3.59% using 0.6 mM PQ to 26.71 ± 9.83% & 36.00 ± 9.66% when pre-incubating with the same samples; respectively [Figure 5.25]. Although, the protection of FL-2 was also obvious in the LDH results, no protection was observed when pre-incubating with FL-1 in the LDH results. Moreover, there was slight increase in the %increase in the LDH release after pre-incubation with FL-1, which was more noticeable at 0.8 and 1 mM PQ [Figure 5.26]. Both liposomes and PLA nanoparticles showed good protection against the harmful effect of PQ, however, the LDH data suggests better activity from the ferulic acid-loaded liposomes.

Analysing data using the same tests mentioned above showed significance effect from ferulic acid concentration on the MTT data ($F_{(2, 90)} = 40.30$, $p < 0.0001$) and significant differences between the following results: 0.4 mM PQ only *vs*. PQ + FP-1 ($X_{90} = -21.60$, $p < 0.0001$), 0.4 mM PQ only *vs*. PQ + FP-2 ($X_{90} = -54.19$, $p < 0.0001$), 0.6 mM PQ only *vs*. PQ + FP-1 ($X_{90} = -14.30$, $p = 0.0061$) and 0.6 mM PQ only *vs.* PQ + FP-2 ($X_{90} = -23.59$, $p < 0.0001$). No significant differences were observed between all the other results. Furthermore, the analysis tests showed significance effect from ferulic acid concentration on the LDH results ($F_{(2, 75)} = 196.5$, $p < 0.0001$) and significant differences between results from PQ only *vs*. pre-incubation with FP-2 at all PQ concentrations ($X_{75} \geq 21.03$, $p < 0.0001$). However, only significant differences were noted between 0.8 and 1 mM PQ only compared to pre-incubation with FP-1 ($X_{75} = -10.92$, $p = 0.0186$ & $X_{75} = -17.04$, $p = 0.0002$; respectively) with no significant differences using lower PQ concentrations.

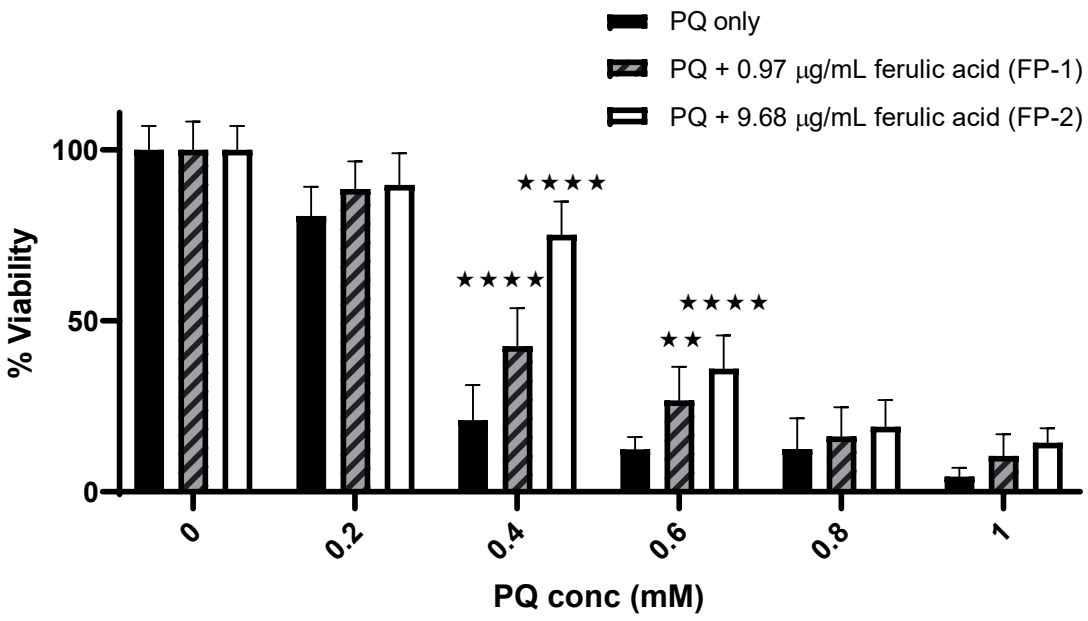

Figure 5.25: **The effect of two different concentrations of ferulic acid-loaded PLA nanoparticles plus PQ compared to PQ only on %viability of cells using MTT assay.** Mean ± SD, $N = 6$, $p < 0.0001$ (using two-way ANOVA), ** $p < 0.01$, **** $p < 0.0001$ compared to PQ only (using Bonferroni's *post hoc* test).

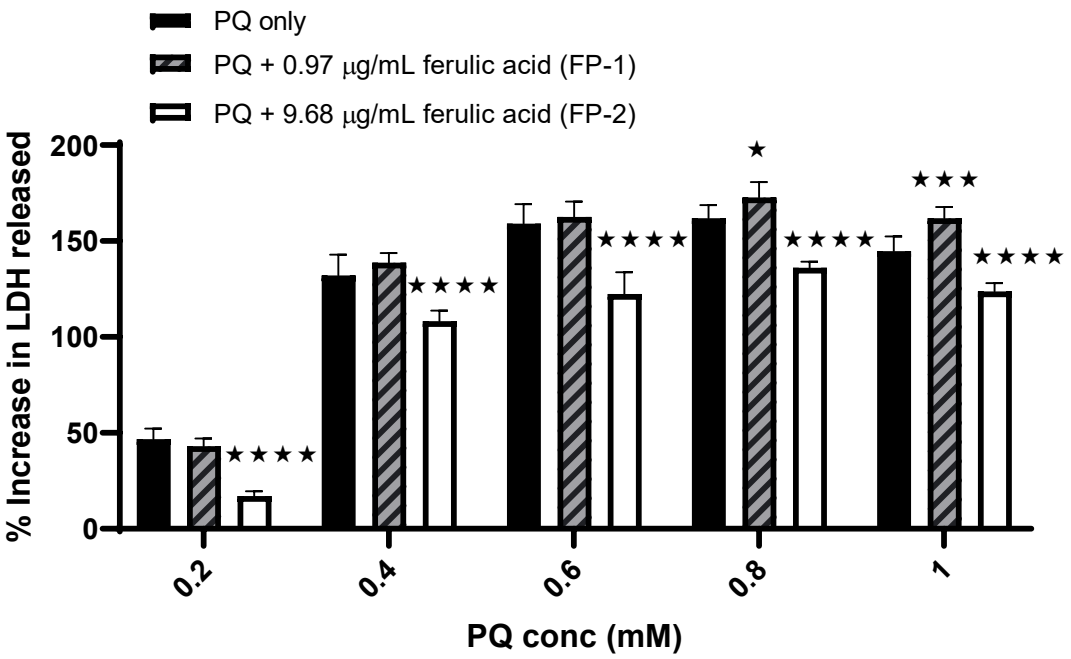

Figure 5.26: **The effect of two different concentrations of ferulic acid-loaded PLA nanoparticles plus PQ compared to PQ only on the %increase in LDH release from cells**. Mean ± SD, $N = 6$, $p < 0.0001$ (using two-way ANOVA), * $p < 0.05$, *** $p < 0.001$, **** $p < 0.0001$ compared to PQ only (using Bonferroni's *post hoc* test).

5.4.2.4.3 Effect of pre-incubation with ferulic acid solution

To assess whether the encapsulation of ferulic acid into nanoparticles had any impact on its activity, ferulic acid (like other antioxidants) was also tested in its free form (solution). Looking at the MTT results, ferulic acid showed good protection against PQ damage, mainly at concentrations 0.4 & 0.6 mM. The %viability boosted from 23.69 ± 6.55% & 18.19 ± 9.37 using 0.4 and 0.6 mM PQ only; respectively, to 54.42 ± 8.11% & 30.75 ± 9.85%; respectively when pre-incubating with FS-1 and to 53.38 ± 9.59% & 39.42 ± 9.14%; respectively when pre-incubating with FS-2. There was also some protection at 0.8 and 1 mM PQ, although less evident [Figure 5.27]. The protection of FS-2 at 0.4 and 0.6 mM PQ was also noticeable in the LDH results, which was to a lesser extent at 0.8 & 1 mM PQ. However, no protection was noticed when pre-incubating with FS-1 [Figure 5.28]. The data suggests the possible potential of ferulic acid in protecting against the harmful effect of PQ in its free form. However, comparing the results from the

LDH assay shows the benefits from encapsulating ferulic acid into nanoparticles mainly liposomes.

Analysing data as previously prescribed showed significance effect from ferulic acid concentration on the MTT results ($F_{(2, 90)} = 21.63$, $p < 0.0001$) with significant different between the following: 0.4 mM PQ only *vs*. PQ + FS-1 ($X_{90} = -30.73$, $p < 0.0001$), 0.4 mM PQ only *vs*. PQ + FS-2 ($X_{90} = -29.69$, $p < 0.0001$), 0.6 mM PQ only *vs*. PQ + FS-1 ($X_{90} = -30.73$, $p = 0.0163$), 0.6 mM PQ only *vs*. PQ + FS-2 ($X_{90} = -21.23$, $p < 0.0001$) and 0.8 mM PQ only *vs*. PQ + FS-2 ($X_{90} = -13.76$, $p = 0.0063$). Additionally, there was significance effect from ferulic acid concentration on the LDH data ($F_{(2, 75)} = 45.40$, $p < 0.0001$) with significant differences between the following: 0.4 mM PQ only *vs.* PQ + FS-2 ($X_{75} = 30.84$, $p < 0.0001$), 0.6 mM PQ only *vs.* PQ + FS-1 ($X_{75} = -22.38$, $p < 0.0003$), 0.6 mM PQ only *vs.* PQ + FS-2 ($X_{75} = 40.78$, $p < 0.0001$) and 1 mM PQ only *vs.* PQ + FS-2 ($X_{75} = 15.15$, $p < 0.0001$). No significant differences were observed between all other results and PQ only.

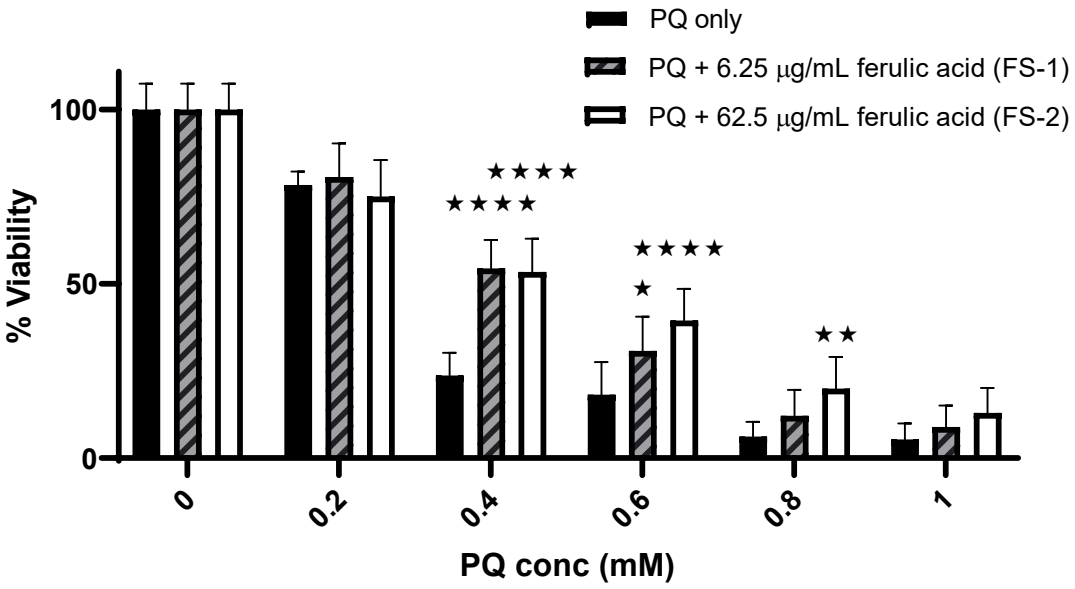

Figure 5.27: **The effect of two different concentrations of ferulic acid solution plus PQ compared to PQ only on %viability of cells using MTT assay.** Mean ± SD, $N = 6$, $p < 0.0001$ (using two-way ANOVA), * $p < 0.05$, ** $p < 0.01$, **** $p < 0.0001$ compared to PQ only (using Bonferroni's *post hoc* test).

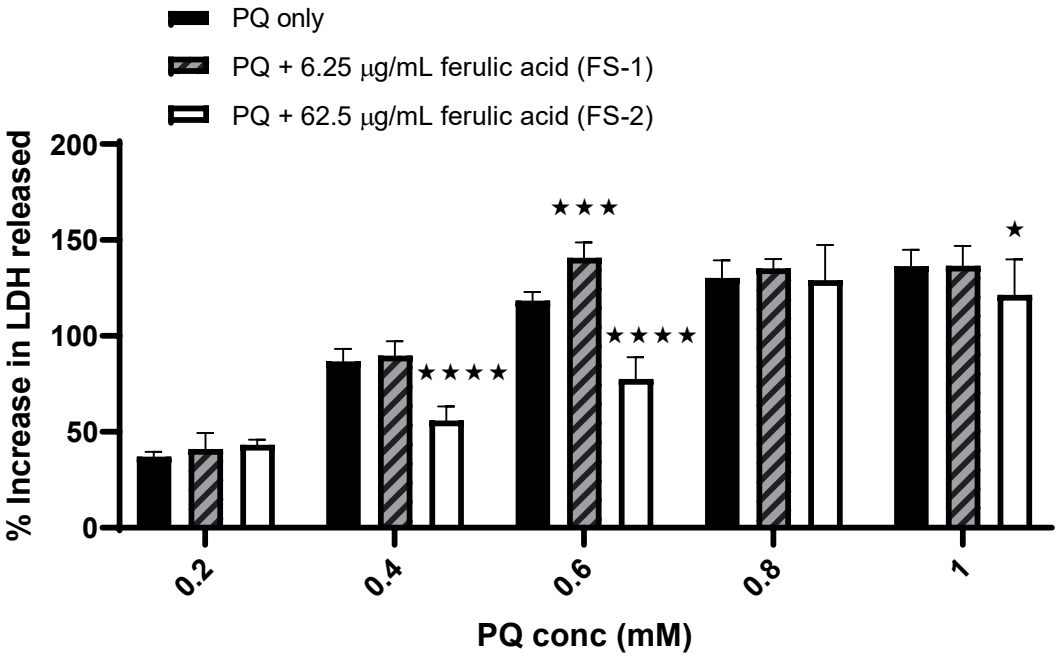

Figure 5.28: **The effect of two different concentrations of ferulic acid solution plus PQ compared to PQ only on the %increase in LDH release from cells**. Mean ± SD, *N* = 6, $p < 0.0001$ (using two-way ANOVA), * $p < 0.05$, *** $p < 0.001$, **** $p < 0.0001$ compared to PQ only (using Bonferroni's *post hoc* test).

5.4.2.5 Effect of pre-incubation with sinapic acid solution, PLA nanoparticles and liposomes

As previously for the other antioxidants under investigation, sinapic acid was prepared in three different formulations (liposomes, PLA nanoparticles and solution), each in two samples with different strengths. Each sample was prepared as with α-tocopherol and tested for its ability to protect against the harmful effect of PQ. The concentration of sinapic acid in each sample (according to the %LE) was calculated and indicated in table 5.5.

Table 5.5: The concentration of sinapic acid in each sample and its given code

Drug	*Form*	*Theoretical conc (µg/mL)*	*%LE*	*Actual conc (µg/mL)*	*code*
Sinapic acid	Liposomes	6.25	55.00%	3.44	SL-1
Sinapic acid	Liposomes	62.5	55.00%	34.38	SL-2
Sinapic acid	PLA nanoparticles	6.25	9.48%	0.59	SP-1
Sinapic acid	PLA nanoparticles	62.5	9.48%	5.93	SP-2
Sinapic acid	solution	6.25	NA	6.25	SS-1
Sinapic acid	solution	62.5	NA	62.5	SS-2

5.4.2.5.1 Effect of pre-incubation with sinapic acid-loaded liposomes

Sinapic acid-loaded liposomes were prepared in two strengths (SL-1 & SL-2) and tested using both MTT and LDH assay for their ability to reduce the harmful effect of PQ on NRK-52E cells. No substantial effect was noticed in the MTT results from pre-incubation with either SL-1 or SL-2 after treatment with 0.2 mM PQ, although, there was a slight increase in %viability when pre-incubating with SL-1. However, there was substantial reduction in the %viability after treating cells with 0.4 mM PQ (53.39 ± 10.41%), that was unexpectedly, worsened using pre-incubation with SL-1 (37.27 ± 7.59%) and SL-2 (24.31 ± 6.10%). There were also further reductions in cell viability using pre-incubation with SL-2 after treatment with 0.6, 0.8 and 1 mM PQ, but the reductions were insignificant [Figure 5.29]. Some of these results were confirmed using the LDH assay. As there was quite an increase in LDH release after treating with 0.2 mM PQ (43.08 ± 5.83%) compared to untreated cells, this was efficiently reduced to 13.61 ± 6.13% and 16.5 ± 9.9% after pre-incubation with SL-1 & SL-2; respectively. However, the effects of treatment with ≥ 0.4 mM PQ could not be ameliorated neither with SL-1 nor SL-2.

Furthermore, the detrimental effect was shown after pre-incubation with SL-2, mainly at 0.4 and 0.6 mM PQ [Figure 5.30].

Data analysis using two-way ANOVA followed by Bonferroni's *post hoc* test showed significance effect from sinapic acid concentration on the %viability in the MTT data ($F_{(2, 90)} = 9.198$, $p = 0.0002$) with significant different between 0.4 mM PQ only *vs*. pre-incubation with SL-1 ($X_{90} = 16.12$, $p = 0.0015$) and *vs*. pre-incubation with SL-2 ($X_{90} = 29.08$, $p < 0.0001$). No significant differences were noted between the other concentrations. However, using the same analysis tests showed no significant effect from sinapic acid concentration on the %increase in the LDH release ($F_{(2, 75)} = 1.646$, $p = 0.1997$). Although, the interaction between the two independent variables (PQ and sinapic acid concentrations) was considered significant $F_{(8, 75)} = 13.03$, $p < 0.0001$). Bonferroni's test showed significant differences between the following: 0.2 mM PQ only *vs*. PQ + SL-1 ($X_{75} = 29.47$, $p < 0.0001$), 0.2 mM PQ only *vs*. PQ + SL-2 ($X_{75} = 26.58$, $p < 0.0001$), 0.4 mM PQ only *vs*. PQ + SL-2 ($X_{75} = -26.18$, $p < 0.0001$) and 0.6 mM PQ only *vs*. PQ + SL-2 ($X_{75} = -19.76$, $p = 0.0004$). There were no significant differences observed between all the other concentrations.

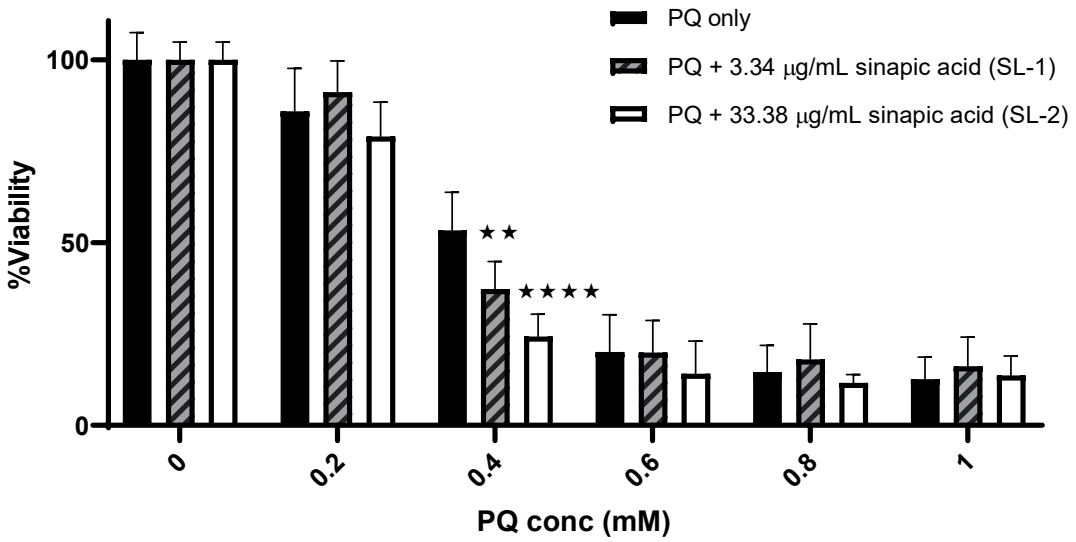

Figure 5.29: **The effect of two different concentration of sinapic acid-loaded liposomes plus PQ compared to PQ only on %viability of cells using MTT assay.** Mean ± SD, *N* = 6, $p < 0.0001$ (using two-way ANOVA), ** $p < 0.01$, **** $p < 0.0001$ compared to PQ only (using Bonferroni's *post hoc* test).

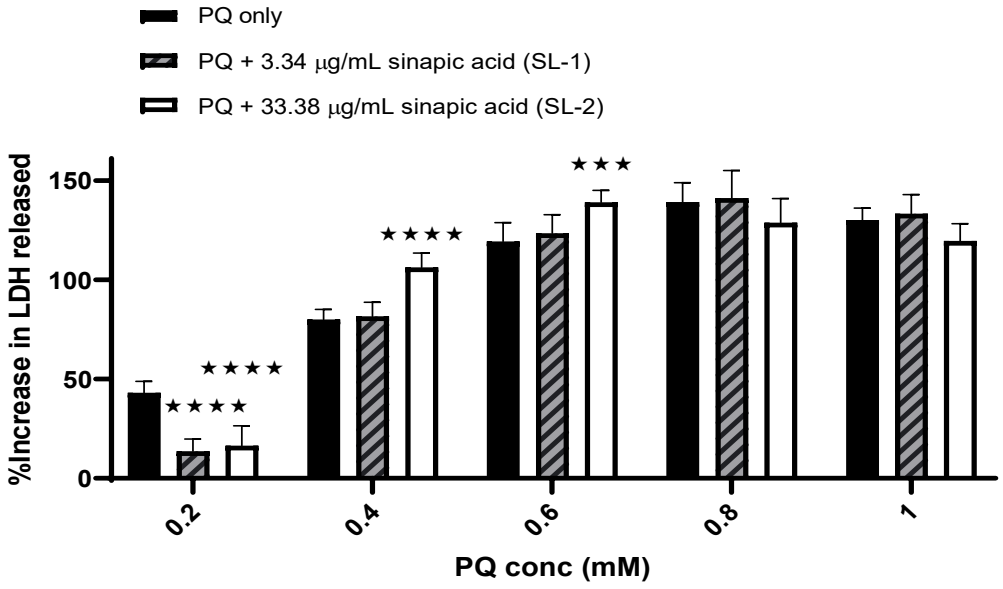

Figure 5.30: **The effect of two different concentrations of sinapic acid-loaded liposomes plus PQ compared to PQ only on the %increase in LDH release from cells**. Mean ± SD, *N* = 6, $p < 0.0001$ (using two-way ANOVA), *** $p < 0.001$, **** $p < 0.0001$ compared to PQ only (using Bonferroni's *post hoc* test).

5.4.2.5.2 Effect of pre-incubation with sinapic acid-loaded PLA nanoparticles

As previously described, the effect of pre-incubation with sinapic acid-loaded liposomes on the demonstrated harmful effect of PQ was studied using two different concentrations (SP-1 & SP-2). No significant protection from both concentrations of sinapic acid was observed in the MTT results. Although, there was a slight increase in %viability from 89.69 ± 10.22%, using 0.2 mM PQ only to 95.04 ± 9.58% and 93.99 ± 9.37% when pre-incubating with SP-1 & SP-2; respectively. In addition to small increase that was noticed from 48.94 ± 10.45% using 0.4 mM PQ only to 59.52 ± 10.65% when pre-incubating with SP-2, with no increase noticed using SP-1 [Figure 5.31]. Similar results were obtained from the LDH assay, with no dramatic effect from nanoparticles, where a slight reduction in the %increase in LDH release was noticed from 43.83 ± 8.91% using 0.2 mM PQ only to 28.00 ± 2.15% and 37.53 ± 9.93% when pre-incubating with SP-1 & SP-2; respectively. However, there was only a slight protective effect was noticed at 0.4 mM PQ using SP-1 where the %increase in LDH release was reduced from 101.19 ± 8.91% to 89.25 ± 8.37%, with no protection after pre-incubating with SP-2 (101.12 ± 8.87%). Furthermore, there was an additional increase in the %increase in the LDH release when pre-incubating using these nanoparticles, which was more noticeable using SP-2 at 0.8 and 1 mM PQ [Figure 5.32].

Analysing the MTT data using two-way ANOVA showed no significant effect from the sinapic acid concentration ($F_{(2, 90)} = 2.173$, $p = 0.1198$) or from the interaction of the two independent variables (PQ and sinapic acid concentrations) $F_{(10, 90)} = 0.8074$, $p = 0.6220$. For this reason, no *post hoc* tests were necessary. The same test was applied on the LDH data, showing significant effect from the sinapic acid concentration on the results ($F_{(2, 75)} = 11.41$, $p < 0.0001$). Bonferroni's *post hoc* test showed significant differences in the following results: 0.2 mM PQ only *vs*. PQ + SP-1 ($X_{75} = 15.83$, $p = 0.0018$), 0.4 mM PQ only *vs*. PQ + SP-1 ($X_{75} = 11.94$, $p = 0.0018$), 0.8 mM PQ only *vs*. PQ + SP-2 ($X_{75} = -12.36$, $p = 0.0169$) and 1 mM PQ only *vs*. PQ + SP-2 ($X_{75} = -15.84$, $p = 0.0018$). No significant differences were noted between all of the other results.

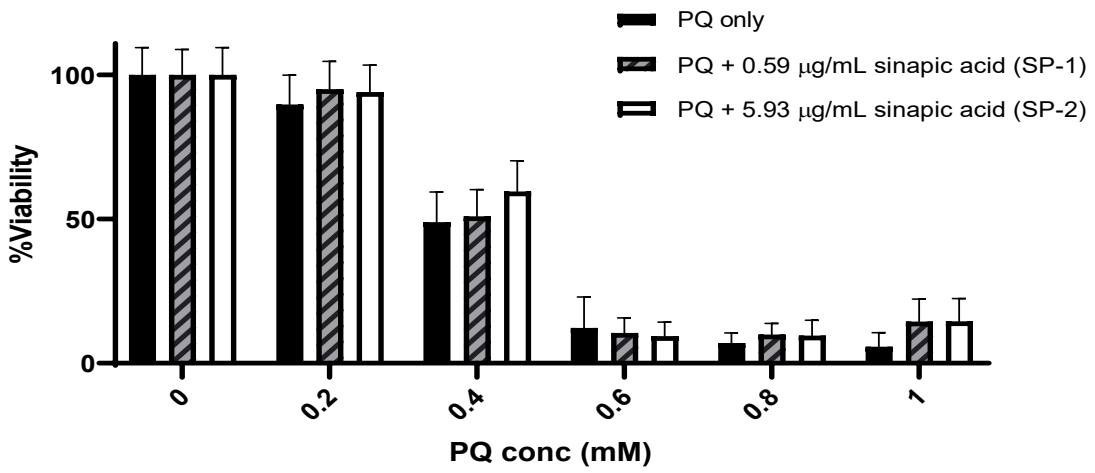

Figure 5.31: **The effect of two different concentrations of sinapic acid-loaded PLA nanoparticles plus PQ compared to PQ only on %viability of cells using MTT assay.** Mean ± SD, $N = 6$, $p < 0.0001$ (using two-way ANOVA), no signifiacant differences were detected when comparing to PQ only (using Bonferroni's *post hoc* test).

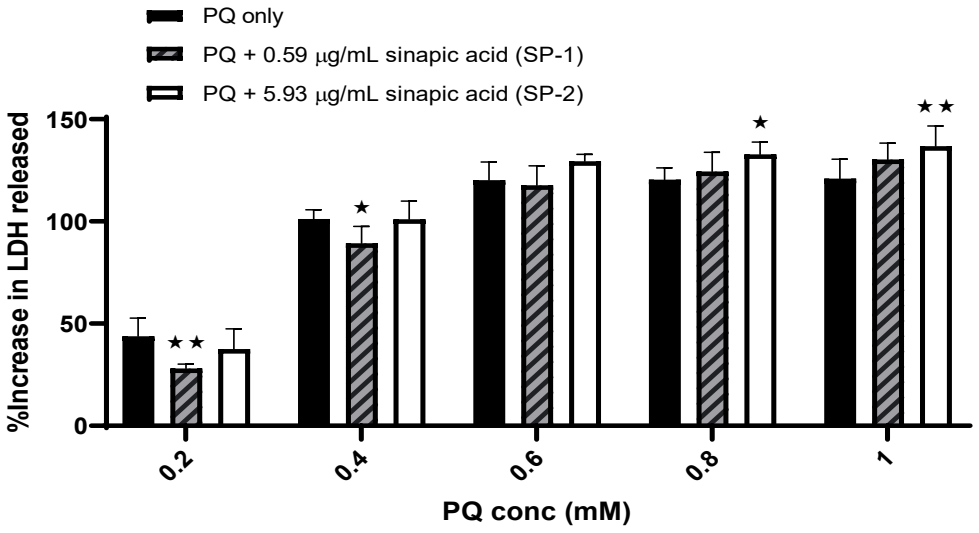

Figure 5.32: **The effect of two different concentrations of sinapic acid-loaded PLA nanoparticles plus PQ compared to PQ only on the %increase in LDH release from cells**. Mean ± SD, $N = 6$, $p < 0.0001$ (using two-way ANOVA), * $p < 0.05$, ** $p < 0.01$ compared to PQ only (using Bonferroni's *post hoc* test).

5.4.2.5.3 Effect of pre-incubation with sinapic acid solution

For the purpose of comparison, free form of sinapic acid (solution) was also tested in the same method as it's liposomal and PLA nanoparticle forms. Two concentrations of sinapic acid solution (SS-1 & SS-2) were prepared and tested as for previous antioxidant solutions. MTT results showed considerable protection against the harmful effect of PQ when pre-incubating with SS-1 and even more protection when pre-incubating with SS-2. For example, the %viability rose from 55.83 ± 10.34%, 25.98 ± 10.41%, 9.33 ± 5.77% and 9.16 ± 6.82% using 0.4, 0.6, 0.8 and 1 mM PQ only; respectively to 89.17 ± 7.82%, 67.26 ± 9.71%, 33.45 ± 10.04% and 24.66 ± 8.86%; respectively when pre-incubating with SS-2 [Figure 5.33]. This protection was also evident in the LDH results, mainly at higher concentrations of PQ. For example, the %increase in the LDH release was reduced from 118.58 ± 9.09% using 0.8 mM PQ only to 78.79 ± 6.45% & 85.31 ± 11.37% when pre-incubating with SS-1 & SS-2; respectively. Additionally, the %increase in the LDH release was reduced from 127.73 ± 8.97% using 1 mM to 101.55 ± 7.44% and 113.85 ± 4.29% when pre-incubating with SS-1 & SS-2; respectively [Figure 5.34]. Unlike ferulic acid, these results showed that, there was no benefit of encapsulating sinapic acid in either liposomes nor in PLA nanoparticles.

Data analysis to the MTT results using two-ANOVA showed significant effect from the sinapic acid concentration on the results ($F_{(2, 90)} = 58.58$, $p < 0.0001$). Bonferroni's multiple comparisons test showed significant differences between the following: 0.4 mM PQ only *vs*. PQ + SS-2 ($X_{90} = -33.34$, $p < 0.0001$), 0.6 mM PQ only *vs*. PQ + SS-1 ($X_{90} = -24.49$, $p < 0.0001$), 0.6 mM PQ only *vs*. PQ + SS-2 ($X_{90} = -41.28$, $p < 0.0001$), 0.8 mM PQ only *vs*. PQ + SS-2 ($X_{90} = -24.12$, $p < 0.0001$) and 1 mM PQ only *vs*. PQ + SS-2 ($X_{90} = -24.49$, $p = 0.0032$). No significant differences were noted in the rest of the results. Analysing the LDH data in the same manor also showed significant effect from the sinapic acid concentration on the results ($F_{(2, 75)} = 15.52$, $p < 0.0001$). The *post hoc* test showed significant differences between 0.8 mM PQ only *vs*. pre-incubation with SS-1 ($X_{75} = 39.79$, $p < 0.0001$) and *vs*. SS-2 ($X_{75} = 33.27$, $p < 0.0001$). In addition to a significant difference between 1 mM PQ only *vs*. pre-incubation with SS-1 (X_{75}

= 29.18, $p < 0.0001$) and *vs*. SS-2 (X_{75} = 13.88, $p = 0.0080$). No significant differences were noted at lower PQ concentrations.

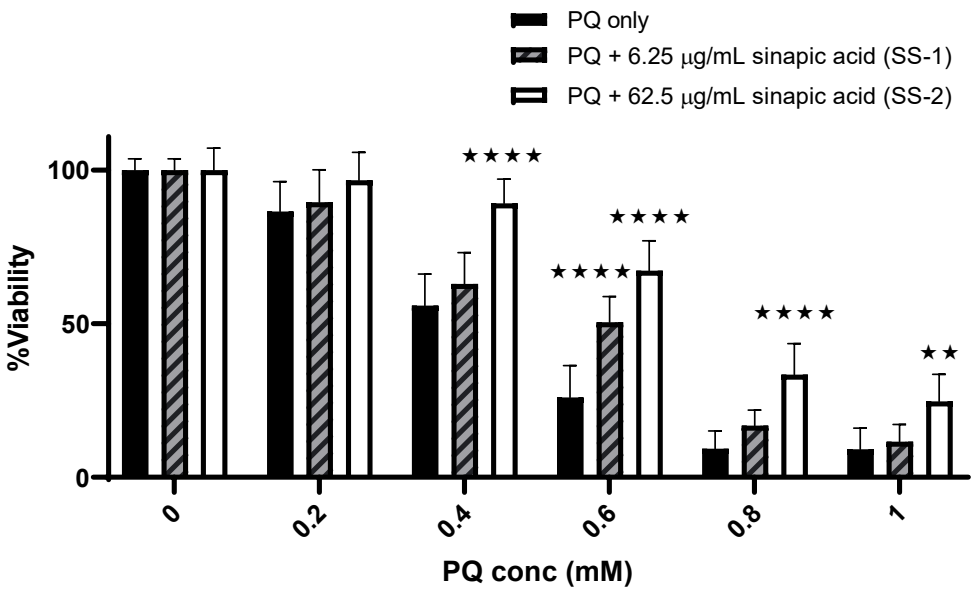

Figure 5.33: **The effect of two different concentrations of sinapic acid solution plus PQ compared to PQ only on %viability of cells using MTT assay.** Mean ± SD, *N*= 6, $p < 0.0001$ (using two-way ANOVA), ** $p < 0.01$, **** $p < 0.0001$ compared to PQ only (using Bonferroni's *post hoc* test).

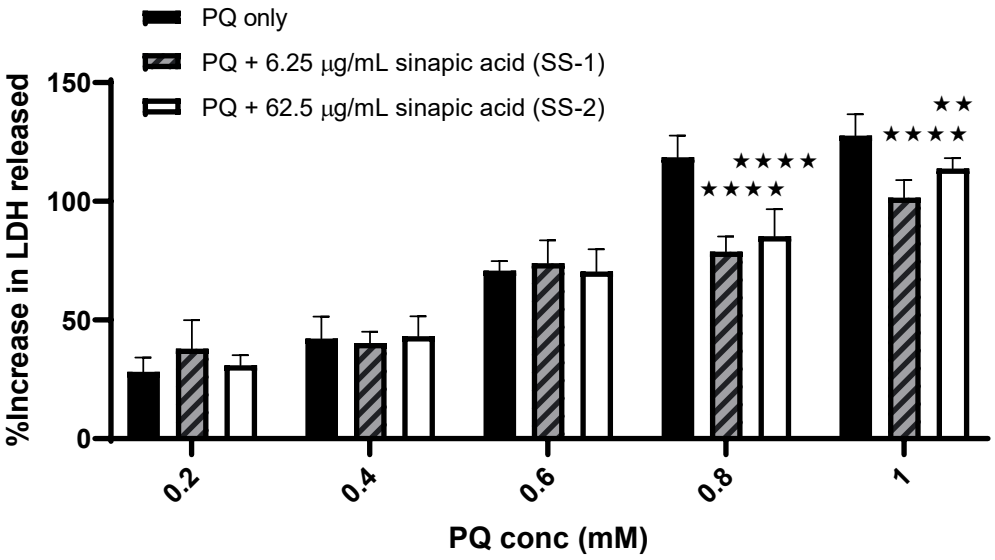

Figure 5.34: **The effect of two different concentrations of sinapic acid solution plus PQ compared to PQ only on the %increase in LDH release from cells**. Mean ± SD, $N = 6$, $p < 0.0001$ (using two-way ANOVA), ** $p < 0.01$, **** $p < 0.0001$ compared to PQ only (using Bonferroni's *post hoc* test).

5.4.2.6 Effect of pre-incubation with epicatechin solution, PLA nanoparticles and liposomes

Epicatechin solution, PLA nanoparticles and liposomes were prepared in the same manner as all other antioxidants preparations under investigation, with exception that deionized water was used to dissolve the epicatechin and then further diluted in IM, to represent its free form. As previously described, each sample was prepared in two strengths and tested for its ability to protect cell against PQ oxidation using two assays; MTT and LDH. The calculated concentrations of epicatechin in each sample are shown in table 5.6.

Table 5.6: The concentration of epicatechin in each sample and its given code

Drug	*Form*	*Theoretical conc (µg/mL)*	*%LE*	*Actual conc (µg/mL)*	*code*
Epicatechin	liposomes	6.25	10.23%	0.64	EL-1
Epicatechin	liposomes	62.5	10.23%	6.39	EL-2
Epicatechin	PLA nanoparticles	6.25	5.35%	0.33	EP-1
Epicatechin	PLA nanoparticles	62.5	5.35%	3.34	EP-2
Epicatechin	solution	6.25	NA	6.25	ES-1
Epicatechin	solution	62.5	NA	62.5	ES-2

5.4.2.6.1 Effect of pre-incubation with epicatechin-loaded liposomes

Once more, the harmful effect of PQ on NRK-52E cells was challenged using two concentrations of epicatechin-loaded liposomes (EL-1 & EL-2). Liposomes were prepared as previously described in chapter 2. Cells were pre-incubated with these liposomes for 24 hours and then with increased concentrations of PQ for a further 24-hour period after which, cells were tested using MTT and LDH assays. Remarkable, effect was observed from these liposomes on the viability of the cells. For example, pre-incubation with EL-1 & EL-2 increased the viability of cells from 88.41 ± 4.7% when treating with 0.2 mM PQ to 111.12 ± 9.63% and 101.03 ± 10.23%; respectively. The protective effect was even observed even at the highest concentration of PQ, where the %viability increased from 6.10 ± 2.08% when treated with 1 mM PQ to 17.41 ± 9.99% and 18.8 ± 7.59% after pre-incubating with EL-1 & EL-2; respectively [Figure 5.35]. These results were confirmed using the LDH assay, for example, the %increase in the LDH release was reduced from 10.87 ± 1.51% after treating with 0.2 mM PQ to 2.28 ± 1.10% and -2.63 ± 3.16% when pre-incubating with EL-1 & EL-2; respectively. As with the MTT results, the protective effect was observed up to the highest concentration of PQ (1 mM), where the %increase in the LDH release was

reduced from 218.04 ± 4.62% to 191.2 ± 3.22% & 173.11 ± 3.98% when pre-incubating with EL-1 & EL-2; respectively [Figure 5.36].

Data analysis to the MTT data, using two-way ANOVA showed significant effect from the concentration of epicatechin on the %viability ($F_{(2, 90)} = 43.07$, $p < 0.0001$). Bonferroni's *post hoc* test showed significant differences between the %viability of cells treated with PQ only *vs*. cells treated with PQ plus pre-incubation with both EL-1 & EL-2 at most PQ concentrations tested ($X_{90} > -11$, $p < 0.05$). The only exception was 0.4 mM PQ only *vs*. PQ + EL-2, which showed no significant difference. Analysing the LDH data using the same tests also showed a significant effect of the epicatechin concentration on the results ($F_{(2, 75)} = 186.8$, $p < 0.0001$) with significant differences between all cells treated with PQ only and those treated with PQ plus pre-incubation with EL-1 & EL-2 ($X_{75} > 8.59$, $p < 0.05$).

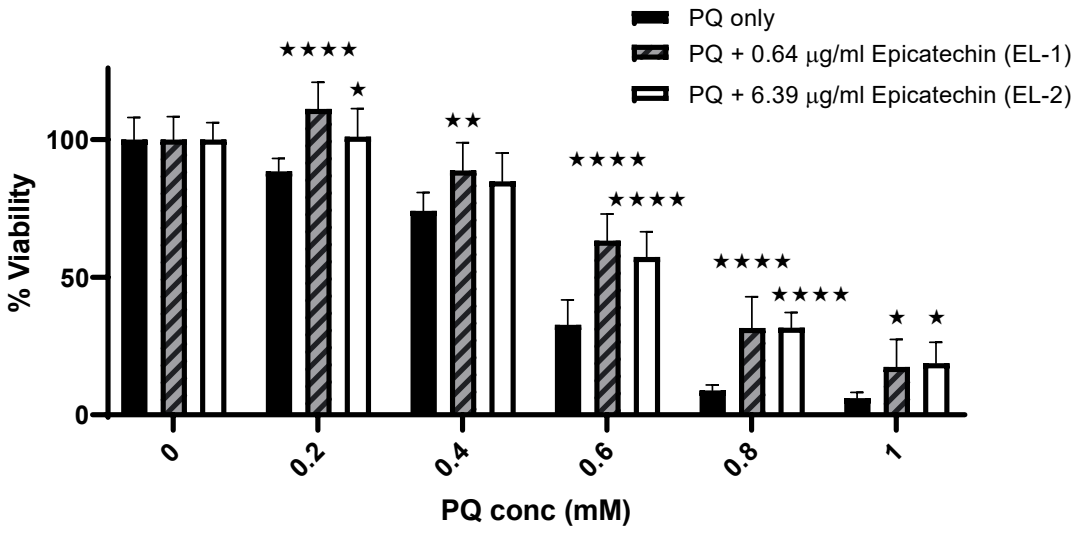

Figure 5.35: **The effect of two different concentrations of epicatechin-loaded lipososmes plus PQ compared to PQ only on %viability of cells using MTT assay.** Mean ± SD, $N = 6$, $p < 0.0001$ (using two-way ANOVA), * $p < 0.05$, ** $p < 0.01$, **** $p < 0.0001$ compared to PQ only (using Bonferroni's *post hoc* test).

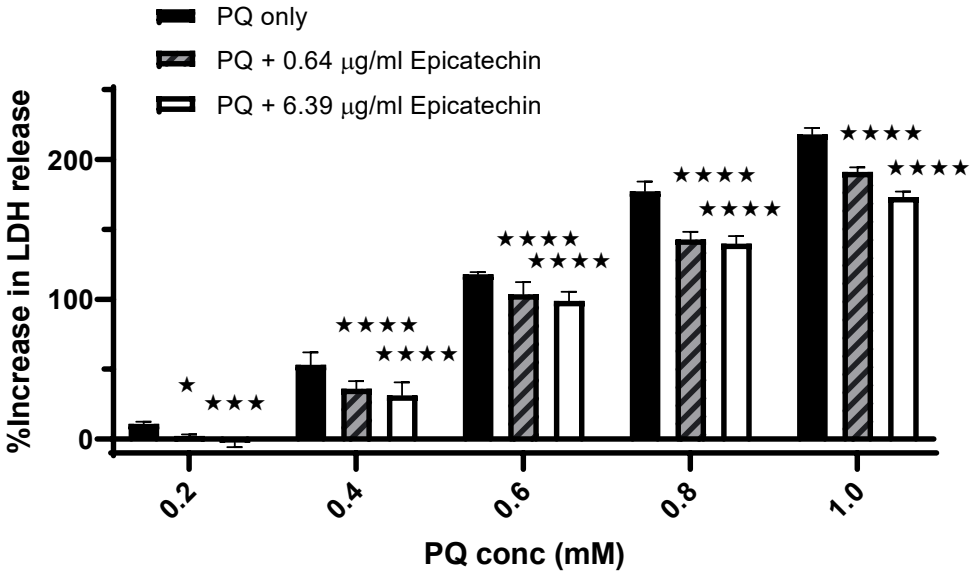

Figure 5.36: **The effect of two different concentrations of epicatechin-loaded liposomes plus PQ compared to PQ only on the %increase in LDH release from cells**. Mean ± SD, $N = 6$, $p < 0.0001$ (using two-way ANOVA), * $p < 0.05$, **** $p < 0.0001$ compared to PQ only (using Bonferroni's *post hoc* test).

5.4.2.6.2 Effect of pre-incubation with epicatechin-loaded PLA nanoparticles

In the same way as liposomes, epicatechin-loaded PLA nanoparticles were tested for their activity. Although not as effective, a good protection was still observed in the MTT and LDH results. The highest protection was observed at 0.4 and 0.6 mM PQ, where the %viability increased from 79.94 ± 6.82% & 32.85 ± 8.88%; respectively after treating with PQ only to 99.83 ± 7.36% & 53.1 ± 9.64; respectively when pre-incubating with EP-1 and to 93.17 ± 9.98% & 48.9 ± 10.46%; respectively when pre-incubating with EP-2 [Figure 5.37]. The protective effect in the LDH results was also observable at all PQ concentrations. For example, the %increase in the LDH release after treating with 0.2 mM PQ (17.87 ± 4.08%), almost returned to zero when pre-incubating with EP-1 (5.44 ± 1.66%) & EP-2 (3.49 ± 2.5%). Even at a high PQ concentration (1mM), the %increase in the LDH release was reduced from 200.54 ± 4.88% to 187.71 ± 9.97% & 191.17 ± 8.97% when pre-incubating with EP-1 & EP-2; respectively [Figure 5.38].

Analysing the MTT data showed significant effect from the concentration of epicatechin on the %viability ($F_{(2, 90)} = 15.17$, $p < 0.0001$). Using Bonferroni's *post hoc* test showed significant differences between the following: 0.4 mM PQ only *vs*. PQ + EP-1 ($X_{90} = -19.89$, $p < 0.0001$), 0.4 mM PQ only *vs*. PQ + EP-2 ($X_{90} = -13.23$, $p = 0.0107$), 0.6 mM PQ only *vs*. PQ + EP-1 ($X_{90} = -2025$, $p < 0.0001$) and 0.6 mM PQ only *vs*. PQ + EP-2 ($X_{90} = -19.89$, $p = 0.0016$). No significant differences were noted between all other results. Applying the same analysis tests on the LDH data, also showed significant effect from the concentration of epicatechin on the results ($F_{(2, 75)} = 80.11$, $p < 0.0001$) with significant differences between all cells treated with PQ only and cells pre-incubated with either EP-1 or EP-2 ($X_{75} > 7.8$, $p < 0.05$).

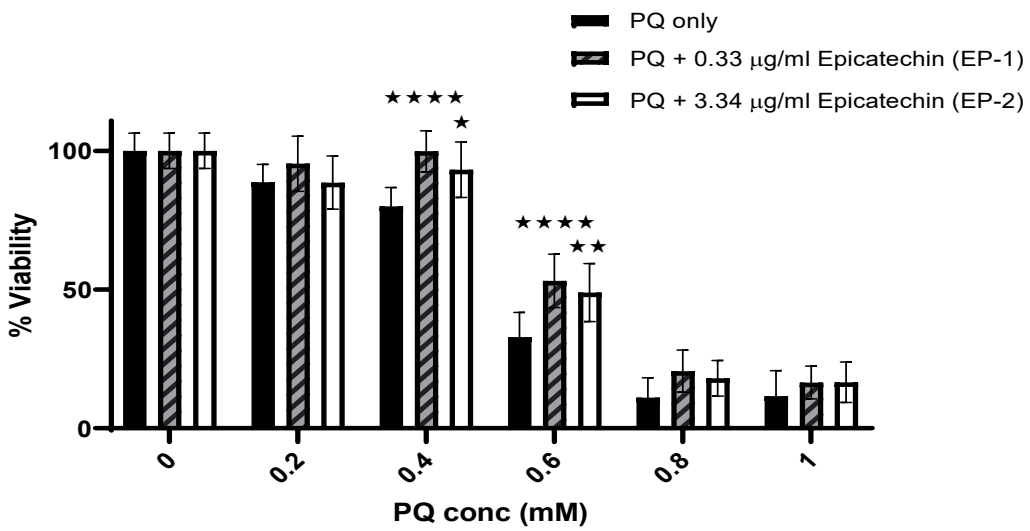

Figure 5.37: **The effect of two different concentrations of epicatechin-loaded PLA nanoparticles plus PQ compared to PQ only on %viability of cells using MTT assay.** Mean ± SD, $N = 6$, $p < 0.0001$ (using two-way ANOVA), * $p < 0.05$, ** $p < 0.01$, **** $p < 0.0001$ compared to PQ only (using Bonferroni's *post hoc* test).

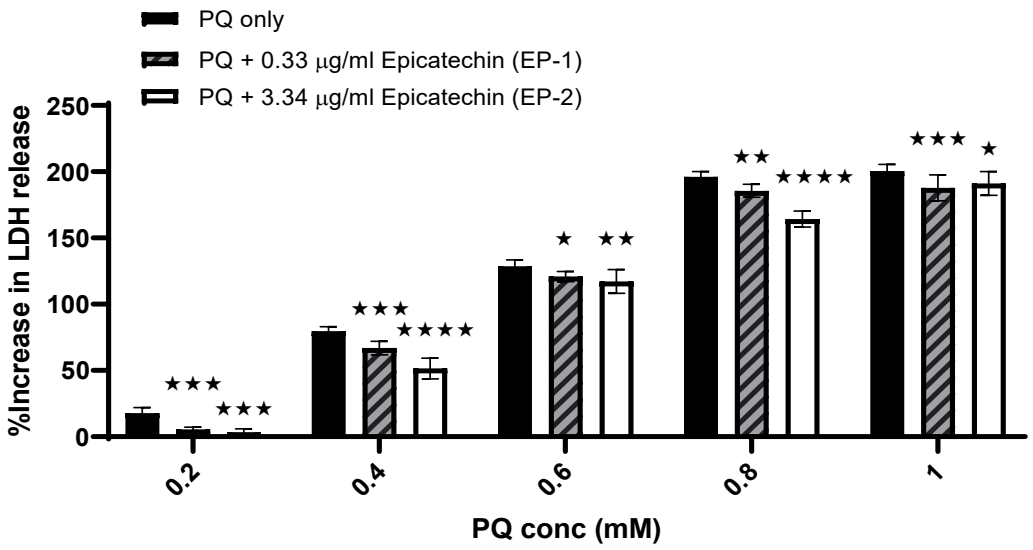

Figure 5.38: **The effect of two different concentrations of epicatechin-loaded PLA nanoparticles plus PQ compared to PQ only on the %increase in LDH release from cells**. Mean ± SD, $N = 6$, $p < 0.0001$ (using two-way ANOVA), * $p < 0.05$, ** $p < 0.01$, *** $p < 0.001$, **** $p < 0.0001$ compared to PQ only (using Bonferroni's *post hoc* test).

5.4.2.6.3 Effect of pre-incubation with epicatechin solution

To check whether the encapsulation of epicatechin into either liposomes or PLA nanoparticles had any influence on its activity, epicatechin solution (as free from) was tested in the same way as its encapsulated forms. The MTT results showed some protection from epicatechin against PQ. This was mostly evident at 0.4 mM PQ, were the %viability increased from 77.17 ± 9.45% to 96.20 ± 5.39% & 88.43 ± 4.59% after pre-incubating with ES-1 & ES-2; respectively [Figure 5.39]. Looking at the results from the LDH assay [Figure 5.40], the protection was only evedent using ES-2 at PQ concentartions ≥ 0.4 mM. However, there was a significant increases in the LDH release after pre-incubation with ES-2 at 0.2 mM PQ. No noticible effect from pre-incubating cells with ES-1 at all PQ concentrations tested as detected. The results indicate the benefits of encapsulating epicatechin into nanoparticles, mainly liposomes.

Data analysis to the MTT results, using two-way ANOVA showed significant effect from the concentation of epicatechin on the %viability ($F_{(2, 90)} = 8.250$, $p = 0.0005$). Bonferroni's test showed significat differnces between 0.4 mM PQ only *vs*. PQ + ES-1 ($X_{90} = -19.03$, $p = 0.0003$), between 0.4 mM PQ only *vs*. PQ + ES-2 ($X_{90} = -11.26$, $p = 0.0420$) and between 0.6 mM PQ only *vs*. PQ + ES-1 ($X_{90} = -11.84$, $p = 0.0312$). No significant differences were noticed between all other results. Applying the same tests also showed significant effect from the concentartion of epicatechin on the results ($F_{(2, 75)} = 475.2$, $p < 0.0001$) with significant differences only after treating with ES-2 ($X_{75} = -13.97$, $p = 0.0038$ at 0.2 mM PQ and $X_{75} > 18$, $p > 0.001$ at ≥ 0.4 mM PQ).

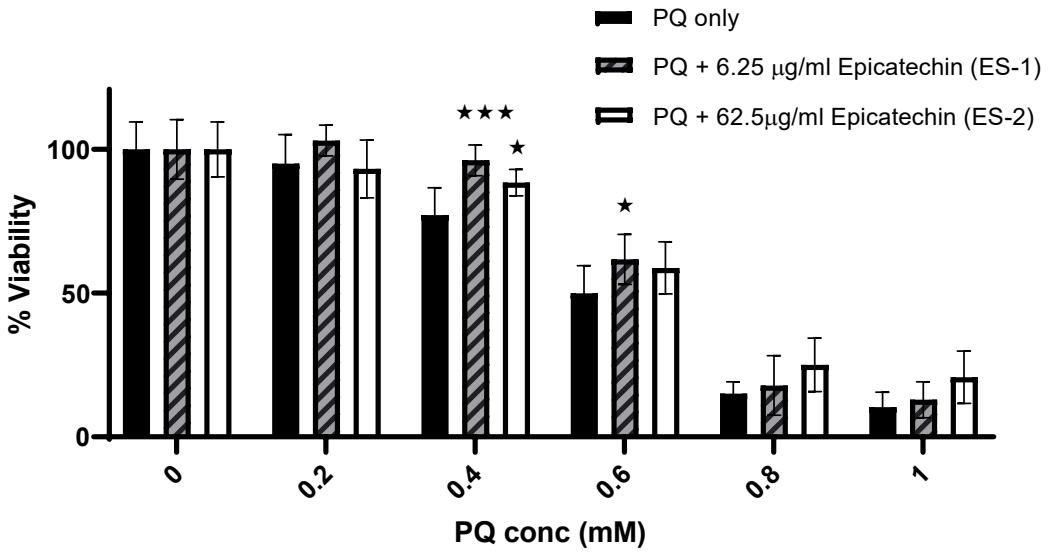

Figure 5.39: **The effect of two different concentrations of epicatechin solution plus PQ compared to PQ only on %viability of cells using MTT assay.** Mean ± SD, $N = 6$, $p < 0.0001$ (using two-way ANOVA), * $p < 0.05$, *** $p < 0.001$ compared to PQ only (using Bonferroni's *post hoc* test).

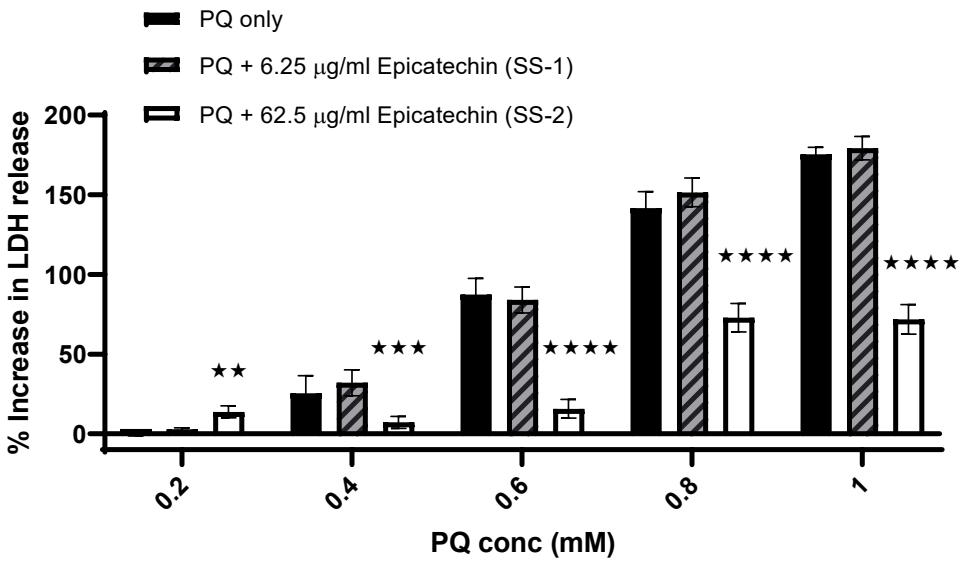

Figure 5.40: **The effect of two different concentrations of epicatechin solution plus PQ compared to PQ only on the %increase in LDH release from cells**. Mean ± SD, $r = 6$, $p < 0.0001$ (using two-way ANOVA), ** $p < 0.01$, *** $p < 0.001$, **** $p < 0.0001$ compared to PQ only (using Bonferroni's *post hoc* test)

5.5 Discussion

5.5.1 Paraquat dose response

The slight increase in the cell viability using low concentration of PQ (0.2 μM), measured by the MTT assay has been reported elsewhere. This has been attributed to the increased antioxidant activity of cells as part of cellular defence strategy and increased resistance to stress (Lushchak, V, 2014). Although, this was not consistent in all graphs, figure 5.6 & 5.16, for example, showed that the %viability was slightly reduced after treating with 0.2 mM PQ. However, this has also been reported elsewhere, and has been attributed to cell-to-cell variability. Different researchers including Dixit *et al*., found that identical cells, even in the same environment can sometimes react differently to external stimuli. Somehow, although not fully understood why, the genetic material of identical cells can produce different levels of proteins (such as G-proteins and regulators of G-protein signalling) and therefore react differently to stimuli such as drugs or toxins (Dixit *et al*., 2014).

After that minor increase in %viability, PQ caused a dose dependent reduction in cell viability which was confirmed by the increase in the LDH release (an indication of cell membrane damage). This is consistent with previous studies (Bus et al., 1976, Carmines et al., 1981). Several studies have proposed the mechanism by which PQ induces cell toxicity. Bus *et al*. demonstrated that the redox cycle of PQ that releases ROS, is the main cause of its harmful effect where ROS cause lipid peroxidation in the membrane leading to leakage and death (Bus *et al*., 1976). Carmines *et al*., showed the possibility of macromolecular synthesis inhibition as a mechanism of cell toxicity (Carmines *et al*., 1981). Additionally, it has been mentioned that PQ obstructs the activity of mitochondrial complexes I and III, thus distressing the electron transfer chain and inhibiting the synthesis of NADPH leading to an increased generation of ROS (Qian *et al*., 2019).

5.5.2 Effect of pre-incubation with antioxidant and antioxidant novel delivery systems on PQ toxicity

Although, the mechanism of PQ toxicity is not fully understood, it clearly involves the redox cycle leading to oxidative damage. Therefore, it was selected to induce oxidative stress to NRK-52E cells to represent AKI. For this reason, it is also reasonable to assume that antioxidants will reduce its toxicity (Suntres 2002). The use of nanoparticles has been proposed in many studies to improve the antioxidant activity of many dietary antioxidants, including the ones under investigation in this research. The harmful effect of PQ on cells has been challenged by pre-incubating cells with antioxidant-loaded nanoparticles under investigation (prepared and characterised in chapter 2). Due to the nature of nanoparticles and the time needed for drugs to be released from delivery systems, pre-incubation was applied rather than co-incubation with PQ. Additionally, to reveal whether the encapsulation of these antioxidants into nanoparticles had any influence on their activity, free antioxidants were also tested. The activity test mainly involved the pre-incubation of cells with the sample (at two different concentrations) for 24 hours, then treating with PQ (0 – 1 mM) for a further 24-hour period. Cells were then tested using both the MTT assay (for cell viability) and LDH assay (for cell death). Different antioxidants have been proposed and studied for their activity against PQ, taking into account its oxidative damage, for example, naringin, sylimarin, edaravone, *Bathysa cuspidata* extracts, alpha-lipoic acid, pirfenidone, lysine acetylsalicylate, selenium, quercetin, C-phycocyanin, bacosides and ascorbic acid (Ayala *et al*., 2014).

5.5.2.1 Effect of pre-incubation with α-tocopherol solution and α-tocopherol-loaded liposomes and PLA nanoparticles.

The activity of α-tocopherol solution against PQ on NRK-52E cells has been described in section 5.4.2.1.3. It was clear from both MTT and LDH assays that both concentrations (TS-1 & TS-2) had beneficial effect in protecting cells from the harmful effect of PQ at concentrations ≥ 0.4 mM. The potential protective effect of α-tocopherol as an antioxidant against the toxicity of PQ has been reported in a number of previous *in vitro* and *in vivo* studies (Kim *et al*., 1998, Suntres 2002, Fahim *et al*., 2013). For example, the *in vitro* study by Kim *et al*., 1998 showed that

0.1 μM α-tocopherol solution can show some protection to human keratinocytes against 0.2 mM PQ toxicity measured using neutral red uptake assay. However, this study showed no protection from higher concentration of α-tocopherol. Additionally, no protection was observed against PQ induced skin irritation to guinea pig using α-tocopherol solution in the same study (Kim *et al*., 1998). However, in the current study, at 0.2 mM PQ, only TS-1 showed some benefit from pre-incubating the cells, as opposed to TS-2, which showed further damage to cells in both MTT and LDH results. This was slightly consistent with the results obtained from Kim *et al*., 1998. This slight harmful outcome was also noticed in chapter 4, in the toxicity studies, with high doses of α-tocopherol solution (section 4.4.3). The possible explanation of this harmful effect is the pro-oxidant activity of certain antioxidants such as polyphenols, carotenoids and α-tocopherol at high concentrations in certain environments (Pesrson *et al*., 2006, Halliwell 2008, Palozza 2004, Poljsak & Raspor, 2007, Solter *et al*., 2019). The mechanism of the pro-oxidant effect of α-tocopherol is not yet fully understood but could be linked to the formation of the α-tocophoryl radical that is not fully scavenged using other antioxidants.

Indeed, there was some protection from pre-incubation with α-tocopherol in its free form however, better protection was observed using α-tocopherol-loaded liposomes. Additionally, high concentration of α-tocopherol in liposomal form did not cause any harmful effect even at low PQ concentration. Encapsulating α-tocopherol into PLA nanoparticles did not show superior protection against PQ when compared to its solution form. However, it did not cause any harmful effect to the cells at low concertation of PQ. Additionally, it should be considered the concentration of α-tocopherol in TP-1 and TP-2 is lower than TS-1 and TS-2; respectively due to the %LE of α-tocopherol in PLA nanoparticles. The benefits could be more noticeable if using same concentration of drug. The benefit of encapsulating α-tocopherol into nanoparticles such as liposomes has been documented elsewhere. For example, α-tocopherol-loaded liposomes relieved the progression of PQ induced damage to rat lungs (Suntres & Shek, 2008). Another example is the encapsulation of α-tocopherol in PLGA nanoparticles and in PLGA-Chitosan nanoparticles, which showed improved cellular uptake, antioxidant and antiproliferative activity (Alqahtani *et al*., 2015). In the later study, ESE method was used to form PLGA nanoparticles, where chitosan solution was added at the

end to form chitosan-coated PLGA nanoparticles. They incorporated an additional microfluidisation step to downsize their nanoparticles to 131 ± 4.8 and 174 ± 6.3 nm; respectively. This may explain their increased cellular uptake (Alqahtani *et al*., 2015).

5.5.2.2 Effect of pre-incubation with curcumin solution and curcumin-loaded liposomes and PLA nanoparticles

The MTT and LDH results after pre-incubating with different curcumin formulations and treating with PQ were somehow conflict-ridden. For instance, high concentration of curcumin solution demonstrated an enhanced harmful effect when treating with low concentration of PQ. However, the same concentration of curcumin showed attenuation of the effect of PQ at higher concentrations. These controversial results were also observed using curcumin-loaded liposomes and PLA nanoparticles which was, however, more detrimental than the unencapsulated form. The debatable results were also observed in other studies. For example, in a study by Nikdad *et al*. showed that 100 mg/kg curcumin and 100 mg/kg nano-curcumin reduced the oxidative stress induced by 5 mg/kg PQ on liver mitochondria of Wistar rats, with nanocurcumin being more effective. Here, the activity of curcumin was measured by MTT, FRAP assay, TBA assay, CAT and SOD activity assays (Nikdad *et al*., 2020). Another study however, showed that 10 nM curcumin increases cell death (using rat mesencephalon-derived cell line) in cells treated with 0.1, 0.25 and 0.5 mM PQ. The study also showed that significant cell death was observed using curcumin only at concentrations higher than 10 μM. (Ortiz-Ortiz *et al*., 2009). Moreover, a separate study indicated that whether curcumin acts as an antioxidant or pro-oxidant depends on its concentration (Banerjee *et al*., 2008). This study measured the haemolysis, TBA assay, potassium ion loss and GSH concentration as indicators of RBC cells viability and AAPH to induce oxidative stress. Curcumin inhibited haemolysis by AAPH at IC_{50} of 43 ± 5 μM and did induce haemolysis even at 50 μM. Additionally, this high concentration of curcumin did not lead to lipid peroxidation as measured by the TBA assay. In fact, it protected the cell membrane from lipid peroxidation caused by AAPH at IC_{50} of 23.2 ± 2.5 μM. Contrary, potassium loss was increased using all concentrations of curcumin. However, the reduction in GSH concentration

caused by AAPH was corrected using 10 μM curcumin and further reduced using higher concentrations of curcumin (Banerjee *et al*., 2008).

However, a review article by Nelson *et al*., 2017 describing the properties of curcumin has provided an interesting point of view in which curcumin has been classified as a pan-assay interference compound (PAINS) and an invalid metabolic panacea (IMPS) and doubts most publications describing its activity. PAINS are compounds that give false positive results mainly be interfering with the assay and IMPS are mainly ambiguous or poor lead compounds found in natural products (Nelson *et al*., 2017). It should be noted that the possible interference from curcumin in the results was not taken into account when performing the tests in this study. It was assumed that because curcumin was pre-incubated with the cells and washed off prior to PQ treatment and testing that there will be no interference. However, looking at the results from the LDH assay, mainly from curcumin-loaded liposomes and PLA nanoparticles shows that unexpected high %increase in LDH release. This could be explained by interference in the absorbance measurements. During the LDH assay, a known amount of medium was withdrawn and the LDH substrate was added to it followed by absorbance reading. Encapsulating curcumin into liposomes or PLA nanoparticles increased its solubility and could explain why readings were much higher. To overcome this possibility, the media from cells treated with same concentrations of curcumin samples should be measured for absorbance and used as blank or control in calculations. This can be repeated and applied in future work.

5.5.2.3 Effect of pre-incubation with resveratrol solution and resveratrol-loaded liposomes and PLA nanoparticles

In this current study, there was some protection against PQ observed after pre-incubation with resveratrol solutions. This was an expected result, due to its known antioxidant activity and was also shown in previous reports (He *et al*., 2012, Benjamin *et al*., 2018). However, at a low concentration of PQ, the resveratrol solution showed enhanced harmful effects on the cells, which was more evident with higher concentrations of resveratrol. This harmful effect of high doses of resveratrol solution is discussed in section 4.5.2. However, the encapsulated

forms of resveratrol (liposomes and PLA nanoparticles) did not show any detrimental effect on the cells. This could be attributed to the reduction in the toxicity of resveratrol due to its encapsulation, or to the lower concentration of resveratrol in liposomes and PLA nanoparticles. The fact that 7.5 μg/mL resveratrol in its liposomal form and 25 μg/mL in its PLA nanoparticle form showed less harmful effect and more beneficial effect than 6.25 μg/mL supports the possible protection to the cells from resveratrol. Shi *et al.* have also reported the improved antioxidant activity of resveratrol in its nanoparticle form and showed that the encapsulation of resveratrol into zien/sodium hyaluronate nanoparticles improves its *in vitro* antioxidant and antitumour activities (Shi *et al*., 2021). Furthermore, the encapsulation of resveratrol into β-lactoglobulin nanoparticles also showed improved *in vitro* antioxidant activity against H_2O_2 treatment in human type-2 alveolar epithelial cells compared to its native form (Kim *et al*., 2016).

5.5.2.4 Effect of pre-incubation with ferulic acid and sinapic acid formulations

Both ferulic and sinapic acid solutions also showed some protection against PQ toxicity, although to a different extent. This is most probably linked to their antioxidant activity shown in chapter 3. The *in vitro* and *in vivo* antioxidant activity of these hydroxycinnamates has been reported in previous studies (Benjamin *et al*., 2018, Chen 2016, Nithya 2017). The encapsulation of ferulic acid and sinapic acid into nanoparticles showed a slight improvement in their activity against PQ and this was more noticeable using liposomes mainly in the LDH data. Although, this was evident for sinapic acid-loaded nanoparticles at low concentration of PQ, at higher PQ the unencapsulated form showed better protection. This might be linked to the reduced antioxidant activity of sinapic acid-loaded liposomes measured using the TEAC assay. Encapsulation of ferulic acid into solid lipid nanoparticles has also been shown to enhance delivery to neuroblastoma cells and increase cell viability after treatment with recombinant β-amyloid peptide (an oxidative stress inducer) (Picone *et al*., 2009). The incorporation of ferulic acid into liposomes prepared *via* calcium acetate gradient method was also proven to show increased protection against oxidative stress induced by t-butyl hydroperoxide on U937 cells (pro-monocytic human myeloid leukaemia cell lines) (Qin *et al*., 2008).

Additionally, chitosan nanoparticles have increased the possibility of using sinapic acid in bone generation mainly by improving their bioavailability. Sinapic acid-loaded chitosan nanoparticles were combined with polycarbonate fibres and showed accelerated bone formation in calvarial bone defect model rats. This was attributed to improved physicochemical properties (Balagangadharan *et al*., 2019).

5.5.2.5 Effect of pre-incubation with epicatechin solution and epicatechin-loaded liposomes and PLA nanoparticles

Epicatechin is an antioxidant with good water solubility and so, to assess its activity as an unencapsulated form it was dissolved in water forming a clear solution. At a high concentration, it showed relatively good protection against PQ toxicity. The protection of epicatechin was reported in other studies. For example, the amelioration of PQ toxicity in rat peritoneal exudated macrophage by epicatechin was reported by Ki & Cho, 1995, in addition to seven other flavonoids (chatichin, flayone, chrysin, apigenin, quercetin, morin and biochanin A) (Ki & Cho, 1995). Additionally, 1% green tea extract mixed with feed, which is rich in epicatechin and other catechins, also showed reduced oxidative stress and endothelin-1 expression (an indicator of pulmonary fibrosis) caused by 0.3 mg/kg PQ on the lungs of male Sprague–Dawley rats (Kim *et al*., 2006). Although, the encapsulation of epicatechin in liposomes and PLA nanoparticles was quite low, there was considerable improved protection provided by these forms as observed in both MTT and LDH assays. This could be explained by increased stability and/or enhanced internalisation and in-line with the protection previously reported by Yadav *et al*. Who showed that the encapsulation of catechin and epicatechin into albumin nanoparticles improves bioavailability, increases stability and enhances their antioxidant activity against A549 cells (adenocarcinomic human alveolar basal epithelial cell lines). They used the desolvation method to synthesise the nanoparticles with very small mean particle sizes (45 ± 5 nm and 48 ± 5 nm respectively) and relatively high %EE (60.5 and 54.5 % respectively) which may explain the increased activity compared to the current study (Yadav *et al*., 2014).

5.6 Conclusion

Dietary antioxidants under investigation (α-tocopherol, curcumin, resveratrol, ferulic acid, sinapic acid and epicatechin) in their free form all showed some protection but to a variable extent against the oxidative stress caused by PQ. However, this activity was limited either due to pharmacokinetic properties or due to toxicity. The encapsulation of these antioxidants into liposomes or PLA nanoparticles may be used to overcome these limitations.

Chapter 6: General Discussion and Future Work

6.1 Introduction

This chapter will outline and summarise the aims and the methods of the current study with a thorough discussion of the results. It will summarise, analyse and critically discuss the results for each antioxidant and its delivery system. The main aim is to link the results in an attempt to find clarification and explanation of the observations to the overall hypothesis and aims. It will also describe the limitations of this work and finally, refer to proposed future work.

6.2 Outline

As discussed in chapter 1, one of the leading functions of the kidneys is to filter the blood and remove nitrogenous waste, excess fluids and excess electrolytes. When the renal system suddenly fails to perform its main functions due to an internal or external cause, the condition is called AKI. Even with advanced medicine, there is currently no remedy available to treat AKI and management relies principally on renal replacement therapy, after action taken to relieve the aetiology of the condition. It is clear however, that the pathophysiology of AKI involves oxidative stress to renal cells, mainly the tubular epithelial cells, and they are also considered to be one of the many cell types within the kidney sensitive to oxidative injury.

Natural antioxidants include enzymes and smaller molecules. Oxidative stress occurs when the generation of ROS exceeds the natural antioxidant system. There have been numerous investigations on the possibility to ameliorate AKI through treatment with exogenous antioxidants. Dietary antioxidants have shown promising activity but usually failed when tested *in vivo* or during clinical trials with their major drawback being linked to their pharmacokinetic properties and poor bioavailability. Nanotechnology can be used to overcome the associated limitations such as solubility, stability or toxicity.

Nanoparticles have been used in many fields including medicine. Theoretically, by manipulating the characteristics of nanoparticles, they can be used as delivery systems to transport the desired amount of drug, to the desired site of action, in the desired amount of time and for the desired period of time. There are different types of nanoparticles such as polymeric nanoparticles, liposomes, dendrimers, solid lipid nanoparticles etc. Each can be made by a variety of methods using different material depending on a number of factors such as the properties of the drug, the intended use, the required characteristics, feasibility and the cost.

In this study, six dietary antioxidants, with diverse physical properties that hinder their potential as possible treatments for AKI, have been selected to

improve their bioavailability. These antioxidants are α-tocopherol, curcumin, resveratrol, ferulic acid, sinapic acid and epicatechin and have been used in this study to enhance their physicochemical properties, improve delivery and ultimately increase activity for the benefit of treating AKI more successfully. These antioxidants have been encapsulated into both liposomes and PLA nanoparticles. The characteristics of these nanoparticles have been described in chapter 2, followed by their antioxidant activity in chapter 3. Chapters 4 & 5 presented the *in vitro* tests performed on NRK-52E cells to evaluate their delivery potential, toxicity and activity against PQ induced oxidative stress. An outline of the work performed in this study is shown in figure 6.1.

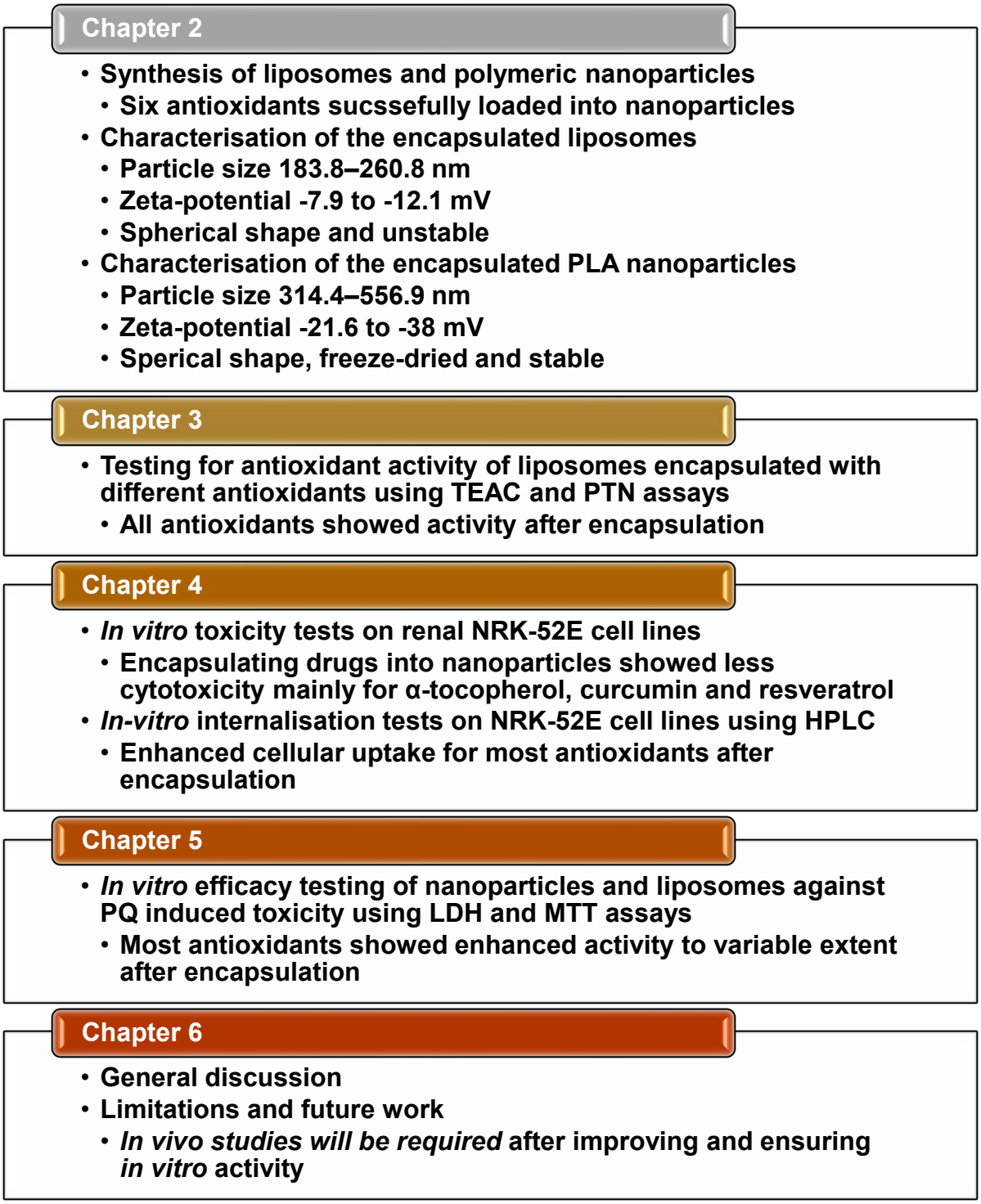

Figure 6.1: A general outline of the work performed in this study with the main outcome of each chapter.

6.3 Antioxidants under investigation and a discussion of the results obtained from their encapsulation into novel delivery systems

6.3.1 α-Tocopherol

α-tocopherol is a strong natural antioxidant available in the human body. It exerts it action mainly by scavenging lipid peroxide radicals and forming a more stable α-tocopherol radical, which can further react with another peroxyl radical. It is insoluble in water, soluble in ethanol and liable to oxidation when exposed to light and/or air. Its bioavailability is hindered by its poor absorption caused by its high lipophilicity. Studies on the ability of this antioxidant to alleviate AKI showed some benefit (Tasanarong *et al*., 2013) while others showed its limitation to reverse the injury (Kim *et al*., 2011). Efforts have been made to overcome its limitations by using novel drug delivery systems such as liposomes, nano-emulsions and lipid nanoparticles (Niki & Abe, 2019).

In this study, α-tocopherol was encapsulated into liposomes and PLA nanoparticles, in an attempt to improve its physicochemical properties. Liposomes were made using thin lipid film rehydration method followed by extrusion to lower their mean particle size and PdI and filter out any unencapsulated drug. PLA nanoparticles were prepared by DESE method and then freeze dried. The final liposomes had an average particle size of 184.2 ± 39.85 nm and a zeta-potential of -11.9 ± 4.46 mV. Microscopic examination showed spherical shaped particles, although the LM had its limitation on image quality. The PLA nanoparticles had an average particle size of 556.9 ± 127.5 nm and a zeta-potential of -37.6 ± 5.54 mV. These results were comparable to the results obtained by Anais *et al*., 2009 who synthesised α-tocopherol-loaded PLA nanoparticles using emulsification diffusion method with particle size ranging between 500-700 nm and a zeta-potential ranging between −27.5 to −24.3 mV, depending on variables like drug concentration, stirring rate, polymer concentration and volume of aqueous diffusion phase (Anais *et al*., 2009). The large particle size of the PLA nanoparticles in this study was confirmed using SEM, which also showed spherical shaped particles. The %LE of α-tocopherol into liposomes was 76.10 ± 1.39%, and into PLA nanoparticles was 67.63 ± 7.15%, which were both fairly high. Antioxidant activity of liposomes was shown to be preserved in both TEAC and

PTN assays. Encapsulating the drug into liposomes or in PLA nanoparticles did not enhance the %internalisation into cells, although the results might have been misleading due to the possible breakdown of the drug prior to analysis using HPLC. The toxicity studies showed a slight reduction in %viability that was not observed in the LDH assay results. However, activity study showed beneficial effect of encapsulation over free form, which was more pronounced using liposomes. This could be explained by the smaller particle size and/or the more neutral surface charge of liposomes (as discussed in sections 4.1.3.1 & 4.1.3.2).

In this study, the TEAC and PTN assays were used to study the antioxidant activity of the encapsulated drugs. Other authors used different antioxidant activity tests to study the effect of nanoparticle encapsulation on dietary antioxidants. For example, Alqahtani and his colleagues showed that the use of PLGA and PLGA coated with chitosan improves the antioxidant activity of α-tocopherol and γ-tocotrienol. They measured the inhibition in cholesterol oxidation to 7-ketocholesterol using an HPLC method and showed that using the encapsulated forms of α-tocopherol and γ-tocotrienol increased their antioxidant activity by approximately 4-fold, compared to their free forms after 48 hours (Alqahtani *et al*., 2015). Coating nanoparticles with chitosan has shown advantages over naked nanoparticles in increasing internalisation and activity. As mentioned previously, PLGA nanoparticles showed improved antioxidant activity of α-tocopherol and γ-tocotrienol. Moreover, coating these nanoparticles with chitosan showed increased *in vitro* cellular uptake by 3-fold. This has been attributed to the positive zeta-potential of chitosan coated PLGA nanoparticles, which causes electrostatic attraction to the negatively charged cell membrane (Alqahtani *et al*., 2015).

6.3.2 Curcumin

Curcumin is a phenolic compound that has been used as a traditional remedy and as a spice in many different countries. Studies have shown its potential as antioxidant, anti-inflammatory, anti-diabetes, anti-carcinogenic and anti-angiogenesis. Nevertheless, low bioavailability, poor pharmacokinetics, insolubility in water and low stability at pH ≥ 7 are factors that reduces its potential *in vivo*. The use of nanoparticles such PLGA nanoparticles have demonstrated the

possible improvement of its cellular uptake and antitumour activity (Punfa *et al*., 2012). In the current study, the same methods described above were used to encapsulate curcumin in both liposomes and PLA nanoparticles. The mean particle size was 210.4 ± 60.24 & 319.5 ± 80.29 nm for liposomes and PLA nanoparticles; respectively and the zeta-potential was -7.86 ± 6.36 & -30.5 ± 7.27 mV, respectively.

Stability studies showed signs of aggregation and precipitation after the third day of liposomal preparation. When freeze-dried, the liposomes raptured and lost their shape. Therefore, the liposomes were freshly prepared for any further testing. In addition to other factors, the choice of lipids can affect the stability of liposomes. These will be further discussed below in section 6.4.2. Images from LM showed spherical shaped liposomes, which were comparable to the images obtained by Nguyen *et al*., 2016. Images from SEM also showed spherical shaped PLA nanoparticles. Rachmawati *et al*., 2016 also used SEM to study the morphology of curcumin-loaded PLA nanoparticles. Although, their blank PLA nanoparticle images were comparable to the images in the current study showing spherical particles with smooth surface, the images of the curcumin-loaded PLA nanoparticles were less clear and showed traces of crystals on the surface of the particles. In addition to their results from surface zeta-potential, FT-IR and DSC, their images indicated that the drug is more probably adsorbed on the surface (Rachmawati *et al*., 2016). In the current study however, results indicate that the drug is most likely to be encapsulated inside the nanoparticles.

The antioxidant activity tests (TEAC and PTN assays) showed that the liposomes preserved curcumin antioxidant activity. However, this was not shown in the *in vitro* test. Curcumin in its free form, mainly at high doses, showed harmful effects to the cells using the LDH and MTT assay. This was consistent with the results obtained from the activity against low PQ concentration although in the presence of high doses of PQ, it showed some amelioration of PQ toxicity. These mixed results were also noted by other researchers and were attributed to its dual effect; pro-oxidant and antioxidant activity, which is dose dependent. For example, (2,2′-azobis (2-amidinopropane) hydrochloride) is an oxidant that causes oxidative

damage to RBC through lipid peroxidation (measured by TBA), haemolysis (measured by haemoglobin absorbance) and potassium ion loss (measured by flame photometry). Curcumin was able to reverse the lipid peroxidation and haemolysis effect at IC_{50} around 23 and 45 μM, respectively. However, at these concentrations it also induced potassium loss. Additionally, at concentrations less than 10 μM it prevented GSH oxidation, while at higher concentrations it caused GSH depletion (Banerjee *et al*., 2008). Another study showed that although curcumin has strong anti-inflammatory and antioxidant activity, it causes oxidative damage to the DNA in the presence of Cu(II) due to the formation of ROS (Ahsan *et al*., 1999). This could explain the toxicity of high concentrations of curcumin found in this study. Encapsulating curcumin into liposomes and PLA nanoparticles led to significantly increased %internalisation, explaining the significant increase in the pro-oxidant effect. The pro-oxidant effect of curcumin-loaded liposomes on RBC was also found to be dose-dependent in a separate study (> 10 μg/mL) (Storka *et al*., 2013). However, the possible interference of curcumin in the results should not be excluded and tests should be repeated taking into account this possibility.

6.3.3 Resveratrol

As discussed in section 1.16.3, resveratrol is stilbene antioxidant present in grapes and different berries in low concentrations. It is known for its antioxidant, anticancer, anti-inflammatory and oestrogenic activities (Wenzel & Somoza, 2005, Xu *et al*., 2007). The main obstacles restricting the efficiency of resveratrol as antioxidant is its low solubility, instability, low bioavailability, rapid metabolism and toxicity. These can be amended by the use of various nanoparticles (Shaito *et al*., 2020, Pangeni *et al*., 2014). For instance, resveratrol-loaded chitosan and γ-poly(glutamic acid) nanocapsules have been shown to increase the solubility by 3.2-4.2 fold and intensify the stability against UV-light (Jeon et al., 2016). The %LE of resveratrol in liposomes can be improved (> 92%) by incorporation of long chain free fatty acids in the lipid layer such as stearic acid. Furthermore, coating liposomes with chitosan helps improve its stability and reduces the release rate (Yang *et al*., 2017, Park *et al*., 2014).

This study attempted to encapsulate resveratrol in liposomes and in PLA nanoparticles. The mean particle size for liposomes and PLA nanoparticles were respectively 197.4 ± 102.4 and 457.9 ± 56.1 nm and their surface zeta-potentials were -7.86 ± 6.36 and -21.6 ± 10.4 mV; respectively. LM and SEM images showed both types of nanoparticles to be spherical in shape. %LE efficiency for liposomes (12.04 ± 1.23%) was quite low compared to PLA nanoparticles (40.81 ± 29.14%). However, the %internalisation for liposomes (5.95 ± 0.09%) was around 11 times higher than free resveratrol compared to PLA nanoparticles (0.93 ± 0.03%) which was only around two-fold higher. Again, several factors may have caused this effect, such as the smaller particle size and/or the more neutral charge.

Jeon *et al*., 2016 have reported the increased cellular uptake by the use of encapsulation of resveratrol into nanoparticles. Encapsulating resveratrol into chitosan and γ-poly (glutamic acid) nanocapsules using ionic gelation showed increased cellular uptake by Caco-2 cells from 3.5% to around 6%. This was explained by the increased stability and solubility of encapsulated resveratrol compared to its free form (Jeon *et al*., 2016). During the toxicity tests in the current study, both liposomes and PLA nanoparticle forms of resveratrol showed less harmful effect on the cells than its free form mainly in the LDH assay. Furthermore, the benefit of encapsulation was also clear in the activity tests against PQ on the NRK-52E cell. Resveratrol has recently been reported for its hormetic dose–response effect. This means that it has a dual action: cytoprotective at low doses and cytotoxic at high doses although the exact biological active concentration is yet to be determined (Shaito *et al*., 2020). The use of high doses of resveratrol was found to cause renal toxicity in *in vivo* studies where administration of doses higher than 300 mg/kg to rats *via* gavage led to signs of renal toxicity such as reduced weight, increased BUN and creatinine level (Crowell *et al*., 2004). The advantages of encapsulating resveratrol into nanoparticles such as increased stability, enhanced antioxidant activity, improved internalisation and decreased toxicity has been discussed thoroughly with several examples and possible advantages by Chung *et al*., 2020. They debated the efficiency of resveratrol, its limitations and possible improvements. It is difficult to deliver resveratrol at an effective dose without reaching cytotoxic levels. Ideally, encapsulating resveratrol helps delivering the drug and allow slow release to achieve optimum activity

without toxic levels being reached. Examples of some nanoparticles with promising improved resveratrol activity include transferrin-modified PEG-LA nanoparticles used for glioma, chitosan nanoparticles used for Alzheimer's and diabetes disease, zinc-pectinate nanoparticles used for gastric complications, casein nanoparticles for cardiac failure and solid lipid nanoparticles for insulin resistance (Chung *et al*., 2020).

6.3.4 Ferulic acid

Ferulic acid is a hydroxycinnamate derived in plants through the shikimic pathway. Due its low bioaccessibility, it is poorly absorbed from the daily diet although a reasonable amount is absorbed when in free form (discussed in section 1.16.5). It is a strong antioxidant, antimicrobial, anti-inflammatory and anticancer drug, however, it suffers from low stability and low water solubility. In order to overcome these limitations, ferulic acid was also encapsulated into liposomes and PLA nanoparticles. The mean particle sizes were found to be respectively 260.8 ± 116.2 and 355.8 ± 47.26 nm and their surface zeta-potentials were found to be-11.9 ± 4.40 and -32.7 ± 5.29 mV; respectively. LM and SEM were used to study the surface morphology of the liposomes and PLA nanoparticles and both were found spherical in shape. %LE of ferulic acid were comparable; 20.78 ± 3.45% for liposomes and 15.42 ± 4.66% for PLA nanoparticles.

Antioxidant activity tests found that encapsulating ferulic acid into liposomes preserved its activity as a ROS scavenger. Encapsulating ferulic acid into liposomes increased its %internalisation into NRK-52E cells from 7.93 ± 0.07% to 20.99 ± 1.06%, although, encapsulating it into PLA nanoparticles decreased it to 3.81 ± 0.04%. However, this did not affect the *in vitro* activity against PQ induced toxicity significantly. Indeed unencapsulated ferulic acid showed some protection to the cells against PQ; however this was noticeably enhanced when encapsulated into liposomes. This can be explained by the increased internalisation. Although, %LE and %internalisation of ferulic acid using PLA nanoparticles were relatively low, making the concentration taken up by the cells low, the *in vitro* activity was quite high. This may be explained by the increased solubility and/or stability of ferulic acid in nanoparticles. These results were consistent with the results

obtained from other researchers, showing the benefits of encapsulating ferulic acid into nanoparticles such as solid lipid nanoparticles (Gupta *et al*., 2020), PEG-diphenylalanine nanoparticles (He *et al*., 2021), PLGA nanoparticles (Merlin *et al*., 2012) and chitosan-coated PLGA nanoparticles (Lima *et al*., 2018).

6.3.5 Sinapic acid

Sinapic acid is also a hydroxycinnamate with an additional methoxy group, making it marginally more hydrophilic than ferulic acid. Likewise, its activities such as antioxidant and anti-inflammatory activities are hindered by its poor aqueous solubility. In the attempt to improve its pharmacokinetic properties, similar to previous antioxidants, it was encapsulated into both liposomes and PLA nanoparticles. The mean particle size was measured to be 184.8 ± 83.3 nm and 314.4 ± 42.28 nm and the surface zeta-potentials were -12.1 ± 4.97 mV and -37 ± 3.80 mV; respectively. The %LE of ferulic acid was 55.00 ± 6.53% and 9.48 ± 4.75% in liposomes and PLA nanoparticles; respectively, with spherical shape particles for both.

Encapsulating sinapic acid into liposomes showed a slightly reduced antioxidant activity as shown by the TEAC values but still preserved activity that was somehow equal or higher than ferulic acid-loaded liposomes using the PTN assay. However, as with ferulic acid, encapsulating into liposomes increased %internalisation into NRK-52E cells by almost two-fold compared to unencapsulated sinapic acid, while PLA nanoparticles reduced it significantly. All three forms did not affect cell viability and membrane integrity as shown in the MTT and LDH assays; respectively. The safety of sinapic acid has been discussed in a review article, where its toxicity profile was described to be considerably low (Chen 2015). *In vitro* activity tests against PQ, might have shown slight benefit of encapsulated sinapic acid at low PQ concentration. However, unencapsulated sinapic acid was found to be more effective at higher PQ concentrations. The reduced antioxidant activity of sinapic acid in liposomal form has also been reported by Martinovic *et al*., 2019. However, others have shown the benefits of encapsulating sinapic acid into nanoparticles such as chitosan nanoparticles

(Balagangadharan *et al*., 2019). Further studies will be required to uncover possible advantage of encapsulating sinapic acid into nanoparticles.

6.3.6 Epicatechin

Epicatechin is a flavonoid that is also available from natural sources with low bioavailability. Although, it has some water solubility, its activity is hindered due to low absorption and rapid metabolism. Similar to other antioxidants under investigation it was encapsulated into liposomes and PLA nanoparticles to improve its pharmacokinetic properties. The mean particle size of liposomes was 183.8 ± 80.1 nm and for PLA nanoparticles it was 350.9 ± 87.4 nm. Their surface zeta-potentials were -11.3 ± 3.93 and -32.9 ± 7.54 mV; respectively. The encapsulation of epicatechin was found to be the lowest among all the antioxidants under investigation in both liposomes (%LE = 10.23 ± 1.54%) and PLA nanoparticles (%LE = 5.35 ± 3.35%, %EE = 18.09 ± 1.95%). This was attributed to its hydrophilicity, as it has been reported that encapsulating hydrophilic compound is more difficult in nanoparticles (Buhecha *et al*., 2019). These results were comparable to the results obtained by Perez-Ruiz *et al*., 2018. They produced epicatechin-loaded lecithin–chitosan nanoparticles using molecular self-assembly, with %LE equal to 3.42 ± 0.85%. However, there are other studies that managed to produce nanoparticles with higher %LE for epicatechin such as Ghosh *et al*., 2016. Here, epicatechin and morin (another flavonoid) were encapsulated within albumin nanoparticles enhancing their solubility and anticancer activity. They used the desolvation method for preparing nanoparticles with %EE of around 88% for morin and 72% for epicatechin (Ghosh *et al*., 2016).

Encapsulation of epicatechin into both liposomes and PLA nanoparticles improved the %internalisation remarkably from 4.18 ± 0.03% to 27.05 ± 1.07% and 36.29 ± 0.09%; respectively. The toxicity test found all three forms to be harmful to the NRK-52E cells within the concentration ranges tested. Examining the *in vitro* activity results showed that the same concentration of epicatechin in the liposomal form showed more protection against PQ than epicatechin in its free form. Furthermore, a lower epicatechin concentration was used in the PLA nanoparticle form and still found to be more protective. This can be explained by the increased

cellular uptake and was consistent with the results noted by Perez-Ruiz *et al*., 2018 who showed cytotoxic activity against breast cancer cell lines increased by four-fold using the nanoencapsulated form of epicatechin (Perez-Ruiz *et al*., 2018). Additionally, the increased antioxidant and cytotoxic activities of epicatechin was also improved using albumin nanoparticles which was attributed to the enhanced solubility which led to increased cellular uptake (Ghosh *et al*., 2016).

6.4 Limitations

6.4.1 Synthesis method

In this study, the DESE method was used to prepare the PLA nanoparticles. This method is considered relatively simple and can be used to encapsulate both hydrophilic and lipophilic drugs. However, it did produce large particle sizes that may have hindered the absorption. It has been chosen as it has the advantage of having been optimised previously by the research group and antioxidants tested have variable solubility (Buhecha *et al*., 2019). The solvent evaporation method is also a simple process but produces much larger particles even at high stirring rates. Another method that may have been used is the nanoprecipitation method. This method has been used to encapsulate α-tocopherol in PLA nanoparticles and produce mean particle size around 150 nm. However, it was not selected as it can only be applied to lipophilic drugs and cannot be used for epicatechin (Anais *et al*., 2009). Different methods, along with their advantages and limitations, have been discussed in section 2.2.2.

On the other hand, to prepare liposomes for this study, the DPPC lipid rehydration method was used followed by extrusion for downsizing. Generally, liposomes were produced with acceptable mean particle sizes and relatively good LE and activity. The advantage of extrusion over other methods of downsizing is the production of optimum liposomes concerning their homogeneity (Chatterjee & Banerjee, 2002). This was also observed in the current study, as the PDI was considered quite low compared to PLA nanoparticles. A study performed by Ong *et al*., 2016 compared the different methods used to downsize liposomes made using unsaturated soybean phosphatidylcholine (extrusion, freeze-thawing, sonication and homogenization). The study showed that extrusion was the optimum method due to its reproducibility and homogeneity among all the methods assessed (Ong *et al*., 2016). The main drawbacks behind this method are that it takes a relatively long time and difficult to scale up. However, some other studies applied sonication for downsizing the liposomes. Applying sonication for 5-10 min can produce small liposomes with mean diameter < 50 nm, depending on the type of lipid (Chatterjee & Banerjee, 2002). The latter produces smaller liposomes but less %LE. Additionally, a separation step will be required to remove any

undissolved free drug. In this study, no separation step was added except when producing epicatechin-loaded liposomes (due to its solubility in water).

6.4.2 Choice of material

In addition to the synthetic method, the choice of building material making the nanoparticle also affects its characteristics. To prepare liposomes, natural lipids (such as egg or soybean phosphatidylcholines) or synthetic lipids (such as DPPC or DMPC) can be used. Although, synthetic lipids are more expensive, they have the advantage of higher purity and increased stability. The choice of lipid also effects the surface charge of the prepared liposomes. This is important, as the surface charge effects not only the stability of liposomes but also their fate in the blood circulation. For example, negatively charged liposomes are cleared much faster by the RES (as discussed in detail in sections 2.6.4 & 4.1.3.3). In this study, DPPC lipid was used to synthesise the liposomes for its high purity and zwitterionic nature. This choice of lipid however, led to a reduced stability in the liposomal product. It is possible to formulate liposomes with phospholipids only, for example, Nguyen *et al.,* 2016 formed liposomes using DOPE only. However, as with the DPPC liposomes, their structure was easily destroyed on storage. They showed that adding cholesterol to their lipid phase led to a more rigid bilayer forming liposomes that could be stored for up to nine months at 4ºC. (Nguyen *et al.,* 2016). Another method of increasing circulating time of liposomes is the incorporation of PEG-phospholipid. For example, PEGylated DSPE are commonly used in various drug delivery systems due to the steric barrier of PEG which stabilises the final liposomal product. Doxil® (anticancer formulation containing doxorubicin-loaded liposomes) is an example of an FDA approved drug that utilises this feature (Li *et al*., 2015).

Polymeric nanoparticles were prepared using PLA in the current study. It has many advantages (such as biodegradability, biocompatibility and nontoxic properties) and has been used extensively to prepare both microparticles and nanoparticles (Lee *et al*., 2016). However, PLA nanoparticles still possess some disadvantages such as uptake by RES due to its negative surface charge (Lee *et al*., 2016). To overcome this, PEG-PLA has been used successfully in different

studies such as for systemic delivery of small interfering polo-like kinase 1 (where it showed increased anticancer activity in a murine xenograft model) and to enhance siRNA cellular uptake (where it improved gene-specific knockdown in the adult zebrafish hearts) (Lee *et al*., 2016). Another disadvantage of PLA is that the produced nanoparticles have relatively low %LE, low reproducibility, wide size distribution, high initial burst and presence of residual organic solvent (Lee *et al*., 2016). Some of these have been noticed in the current study such as the high PdI and SD, representing homogeneity and reproducibility; respectively.

Other polymeric materials have been used for the production of nanoparticles from synthetic and natural sources with different advantages and disadvantages. For example, PLGA is a synthetic polyester widely used for controlled drug delivery. It mainly has the same advantages and disadvantage as PLA, although PLGA was shown to have a slower degradation rate (Martins *et al*., 2018). Natural polymers can be sourced from plants, animals and microorganisms. They have the advantage of being inexpensive, biodegradable, biocompatible and relatively nontoxic. Examples of polymers from animal origins include albumin, gelatin, hyaluronic acid, and chitosan. These have been widely applied in nanomedicine especially as nanocarriers of anticancer drugs. Their main disadvantage is that they may be immunogenic and usually require chemical modification before they can be used. Abraxane® is a paclitaxel-loaded albumin nanoparticles formulation approved for i.v. administration for the treatment of cancer. Cellulose, starch, soy protein and zien are polymers from plant origins which are abundant in nature and cause less immunogenic issues. Due to their hydrophilic nature they can escape opsonisation and can be exploited for the encapsulation and controlled release of hydrophobic drugs. Polyhydroxyalkanoates such as poly(hydroxybutyrate), are examples of polymers produced from microbiological origins. In addition to their natural polymer's advantages, they show good thermoplasticity and so can be sterilised safely at the final stage of production (Gagliardi *et al*., 2021).

6.4.3 Studying the surface morphology

In the current study, LM was used to examine the surface morphology of liposomes. This only gave a general idea of the shape of the particles due to the limitations of the instrument. The reason for using this technique and not SEM was the fragility of the liposomes prepared by DPPC lipids only. To overcome this stability issue, researchers have used cryo-SEM. The later instrument freezes samples instantly and then images can be taken while under vacuum. Wang *et al*., 2012, used this technique to study the morphology and the controlled release of drugs from cationic liposomes. Another method to overcome this issue is to increase the stability of the liposomes by incorporating cholesterol in the lipid phase (Wang *et al*., 2012) or coating with a protective layer such as chitosan (Park *et al*., 2014) or N-(2-hydroxypropyl)methacrylamide polymer (Zaborova *et al*., 2018) in order to use SEM to study the morphology.

6.4.4 *In vitro* studies

In vitro models have been used to correlate to *in vivo* studies but definitely have their limitations. However, they still remain the main course of studying safety and efficiency of newly developed medication, prior to animal studies. In the current studies, NRK-52E cells have been used to correlate to the tubular epithelial cells, as they are the main target in AKI. Cell lines are frequently used as an alternative to primary cells to study different biological processes as they are cost effective, easy to handle, offer a limitless supply and avoid ethical worries related to the use of animal and human material. However, caution must be taken when analysing the results as cell lines do not always precisely imitate the primary cell. In order to support the outcomes, key control tests using primary cells should always be repeated (Kaur & Dufour, 2012). Furthermore*, in vivo* studies will definitely give a more prospective potential for these novel delivery systems.

6.5 Future work

Future results can be performed to optimize these characteristic properties of nanoparticles such as reducing particle size, minimizing particle size variation, modifying zeta-potential, improving loading efficiency. Liposomes will need to be stabilised, in order to prevent breakdown during freeze-drying, SEM examination will need to be performed on liposomes and stability studies on both forms using all encapsulated drugs. Release study of antioxidants from nanoparticles and liposomes into different media needs to be investigated in order to understand the dissolution profile. This work will give further information on the pharmacokinetic profile of the encapsulated drugs.

Furthermore, antioxidant activity tests will need to be performed on all three forms: PLA nanoparticles, liposomes and free drugs. Additionally, *in vitro* antioxidant activity using cell culture techniques might give more information on their activity compared to the tests applied in this study. Regarding the toxicity studies, higher concentrations of encapsulated antioxidants will need to be investigated in order to calculate IC_{50}. Moreover, other oxidants such as hydrogen peroxide or gentamicin rather than just PQ can be used to investigate efficacy. New biomarkers will need to be used that are more relevant to AKI. Finally, *in vitro* models have been used to correlate to *in vivo* studies but definitely have their limitations. For this reason, *in vivo* studies must be performed to determine efficacy.

Diverse models have been used to represent AKI. The reason behind this diversity is the different aetiology of AKI (described in section 1.5). Table 6.1 describes some of these models and their representing cause. Any of these models can be used in future studies following the current study as oxidative stress is involved in all classes of AKI regardless of the initial cause. Previous studies have applied some of these models to study the efficiency of the antioxidants under investigation. For example, a study by Stojiljkovic *et al*., 2018 used 100 mg/kg gentamicin for 8 days to induce AKI in Wistar rats and showed that co-administration with 100 mg/kg α-tocopherol led to attenuation of oxidative stress observed in the histopathological and biochemical assays (Stojiljkovic *et al*.,

2018). Another study by Wu *et al*., 2017 used 10 ml/kg glycerol i.m. to induce AKI in rats and administered 200 mg/kg/day curcumin orally for 3 days. They used different biochemical tests such sCr, BUN, SOD, MDA, creatine kinase, KIM-1, TNF-α, IL-6 levels, immunohistochemical staining and Western blot (to assess oxidative stress) and *in situ* TUNEL apoptosis fluorescence staining (to assess cell apoptosis) showing the ability of curcumin to ameliorate rhabdomyolysis-induced AKI (Wu *et al*., 2017).

In addition to the experiments detailed in this thesis, different tests were planned to be made. However, due to the impact of covid-19 they were cutdown. These include:

- SEM studies on freeze dried liposomes
- Release studied from nanoparticles
- *In vivo* study using a model of PQ-mediated AKI using biomarkers for kidney function (SCr & UO) and injury (β-NAG and KIM-1). The ability of the encapsulated nanoparticle to attenuate the harmful effect of increased concentrations of PQ (i.p.) on Wistar rats will need to be determined. This model has been used previously by Prabal Chatterjee (Chatterjee *et al*., 2000) and Ben Elisha-Lambert (Elisha-Lambert 2017).

Table 6.1: Different animal models with mimicking cause and administration dose (Adapted from Singh *et al*., 2012).

Animal model	*Mimicking cause*	*Dose & Administration route*
Glycerol-induced AKI	rhabdomyolysis	Single dose, 8-10 ml/kg i.m.
ischaemia-reperfusion-induced AKI	haemodynamic changes	Clamping one or both renal arteries for a certain period
Gentamicin-induced AKI	renal failure due to clinical administration of gentamicin	Multiple doses for 4-10 days, 40-200 mg/kg i.p.
cisplatin-induced AKI	renal failure due to clinical administration of cisplatin	Single dose, 5–40 mg/kg i.p.
NSAID-induced AKI (such as acetaminophen)	renal failure due to clinical administration of NSAIDs	Single dose, 375–3000 mg/kg i.p.
ifosfamide-induced AKI	renal failure due to clinical administration of ifosfamide	Multiple doses for 1-5 days, 50–1100 mg/kg i.p.
Uranium-induced AKI	occupational hazard	Single dose 0.5–20 mg/kg i.v.
Potassium dichromate-induced AKI	occupational hazard	Single dose 15 mg/kg, s.c.
S-(1,2-dichlorovinyl)-L-cysteine-induced-AKI	contaminated water	Single dose 5–30 mg/kg, i.p.
sepsis-induced AKI	infection	Ligation of cecum and punctured three time or administration of LPS
radiocontrast-induced AKI (such as Diatrizoate)	radiocontrast media	Single dose, 2–10 ml/kg, i.v.

6.6 Conclusion

From this study, it can be concluded that all the antioxidants selected; α-tocopherol, resveratrol, curcumin, sinapic acid, ferulic acid and epicatechin were successfully encapsulated in both PLA nanoparticles and liposomes. These nanoparticles showed variable but acceptable characteristic properties such as size, surface charge and loading efficiency. Results from the TEAC and PTN assay indicated that all drug-loaded liposomes showed antioxidant activity. This activity increased with increasing concentration of drugs. Hence, indicate availability of the antioxidants for reaction. The results from the PTN assay showed that antioxidant activity followed in descending order: resveratrol > ferulic acid ≈ sinapic acid > α-tocopherol ≈ epicatechin > curcumin-loaded liposomes. Blank liposomes showed almost negligible activity, which did not change with increasing concentration of liposomes. There were slight differences in the order of activity using TEAC assay, which was, in the descending order: resveratrol ≈ ferulic acid > curcumin > sinapic acid > α-tocopherol ≈ epicatechin. This was explained by the different mechanism of the two assays. TEAC values of free drug compared to drug-loaded liposomes were slightly reduced for most samples. This can be attributed to the encapsulation of the drugs within liposomes.

Internalisation tests showed sufficient amount of drug entering the cells using both liposomes and PLA nanoparticles. This was consistent with the results from antioxidant activity, indicating that the drugs are available for action. Although, results from toxicity study showed effects of some form on cell viability, the effect was not dramatic and cells were still viable with high doses. Efficacy studies showed variable benefits of using both forms of nanoparticles to encapsulate antioxidants against PQ toxicity. Overall, it can be concluded from this study that the novel drug delivery systems; liposome and PLA nanoparticles have the potential to improve the efficacy of antioxidants with poor bioavailability (such as α-tocopherol, curcumin, resveratrol, ferulic acid, sinapic acid and epicatechin) in the treatment of AKI. Unquestionably, further studies will be required to demonstrate and evidence this potential.

References

Abdel-Naim, A, Abdel-Wahab, M, Atteia, F. (1999) Protective effects of vitamin E probucol against gentamicin-induced nephrotoxicity in rats. *Pharmacological Research.* 40(2): 183-187

https://doi.org/10.1006/phrs.1999.0494

Abdel-Raheem, T, EL-Sherbeny, A, Taye, A. (2010) Green tea ameliorates renal oxidative damage induced by gentamicin in rats. *Pakistan Journal of Pharmaceutical Sciences.* 1: 21–28

Abdel Rahman, G, El-Azab, S, El Bolok, A, El-Gayar, S, Mohamed, A. (2018) Anticancer potentials of free and nanocapsulated sinapic acid on human squamous cell carcinoma cell line: *In vitro* study. *Journal of Medical Sciences*.18: 134-142

https://dx.doi.org/10.3923/jms.2018.134.142

Abe, K, Matsuki, N. (2000) Measurement of cellular 3-(4,5-dimethylthiazol-2-yl)-2,5-diphenyltetrazolium bromide (MTT) reduction activity and lactate dehydrogenase release using MTT. *Neuroscientific Research*. 38(4): 325-329

https://doi.org/10.1016/s0168-0102(00)00188-7

Achaya, C, Thakar, H, Vajpeyee, S. (2013) A study of oxidative stress in gentamicin induced nephrotoxicity and effect of antioxidant vitamin C in Wistar rats. *National Journal of Physiology Pharmacy and Pharmacology.* 3(1): 14-20

http://dx.doi.org/10.5455/njppp.2013.3.14-20

Adhikari, S, Priyadarsini, K, Mukherjee, T. (2006) Physico-chemical studies on the evaluation of the antioxidant activity of herbal extracts and active principles of some Indian medicinal plants. *Recent Advances in Indian Herbal Drug Research*.40: 174–183

https://doi.org/10.3164/jcbn.40.174

Ahmad, G., Almasry, M., Dhillon, S., Abuayyash, M, Kothandaraman, N, Cakar, Z. (2017) Overview and sources of reactive oxygen Species (ROS) in the reproductive system. In: Agarwal A, Sharma, R, Gupta, S, Harlev, A, Ahmed, G,

Plessis, S, Esteves, S, Wang, S, Durairajanayagam, D. (eds) Oxidative stress in human reproduction. *Springer, Cham*. 1-16. Online ISBN: 978-3-319-48427-3

https://doi.org/10.1007/978-3-319-48427-3_1

Ahsan, H, Parveen, N, Khan, N, Hadi, S. (1999) Pro-oxidant, anti-oxidant and cleavage activities on DNA of curcumin and its derivatives demethoxycurcumin and bisdemethoxycurcumin. *Chemico-Biological Interactions*. 121(2): 161-175

https://doi.org/10.1016/S0009-2797(99)00096-4

Aicardo, A, Martinez, DM, Campolo, N, Bartesaghi, S, Radi, R. (2016) Biochemistry of nitric oxide and peroxynitrite: sources, targets and biological implications. In: Gelpi R., Boveris A., Poderoso J. (eds) Biochemistry of Oxidative Stress. Advances in Biochemistry in Health and Disease, Vol 16. *Springer, Cham.* 49-77. Online ISBN: 978-3-319-45865-6

https://doi.org/10.1007/978-3-319-45865-6_5.

Ajibade, T, Oyagbemi, A, Omobowale, T, Asenuga, E, Afolabi, J, Adedapo, A. (2016) Mitigation of diazinon-induced cardiovascular and renal dysfunction by gallic acid. *Interdisciplinary Toxicology.* 9(2): 66–77

https://dx.doi.org/10.1515%2Fintox-2016-0008

Akbarzadeh, A, Rezaei-Sadabady, R, Davaran, S, Joo, S, Zarghami, N, Hanifehpour, Y, Samiei, M, Kouhi, M, Nejati-Koshki, K. (2013) Liposome: classification, preparation, and applications. *Nanoscale Research Letters*. 8: 102

https://doi.org/10.1186/1556-276X-8-102

Akomolafe, S, Akinyemi, A, Anadosie, S. (2014) Phenolic acids (Gallic and tannic Acids) modulate antioxidant status and cisplatin induced nephrotoxicity in rats. *International Scholarly Research Notices.* 2014: 8

https://doi.org/10.1155/2014/984709

Alawam, K. (2014). Application of proteomics in diagnosis of ADHD, schizophrenia, major depression, and suicidal behavior. In: Donev, R. (eds) Advances in protein chemistry and structural biology. *Academic Press*. 283-315. Online ISBN: 9780128004531

https://doi.org/10.1016/B978-0-12-800453-1.00009-9

Alexis. F, Pridgen, E, Molnar, L, Farokhzad, O. (2008) Factors affecting the clearance and biodistribution of polymeric nanoparticles. *Molecular Pharmaceutics*. 5(4): 505–515

https://doi.org/10.1021/mp800051m

Alhusaini, A, Fadda, L, Hassan, I, Ali, M, Alsaadan, N, Aldowsari, N, Alharbi, B., 2018. Liposomal curcumin attenuates the incidence of oxidative stress, inflammation, and DNA damage induced by copper sulfate in rat liver. *Dose-Response*. 16(3): 1559325818790869

https://doi.org/10.1177/1559325818790869

Alidori,S Akhavein, N, Thorek, D, Behling, K, Romin, Y, Queen, D, Beattie, B, Manova-Todorova, K, Bergkvist, M, Scheiberg, D, McDevitt, M. (2016) Targeted fibrillar nanocarbon RNAi treatment of acute kidney injury. *Science translational medicine*. 8(331): 331-339

https://dx.doi.org/10.1126%2Fscitranslmed.aac9647

Alqahtani, S, Simon, L, Astete, C, Alayoubi, A, Sylvester, P, Nazzal, S, Shen, Y, Kaddoumi, A, Sabliov, C. (2015) Cellular uptake, antioxidant and antiproliferative activity of entrapped α-tocopherol and γ-tocotrienol in poly (lactic-co-glycolic) acid (PLGA) and chitosan covered PLGA nanoparticles (PLGA-Chi). *Journal of Colloid and Interface Science.* 445: 243-251

https://doi.org/10.1016/j.jcis.2014.12.083

Anais, J, Razzouq, N, Carvalho, M, Fernandez, C, Astier, A, Paul, M, Asteir, A, Fessi, H, Lorino, A. (2009) Development of α-tocopherol acetate nanoparticles: influence of preparative processes. *Drug Development and Industrial Pharmacy*. 35(2): 216-223

https://doi.org/10.1080/03639040802248798

Anderson, M, Omri, A. (2008) The Effect of different lipid components on the *in vitro* stability and release kinetics of liposome formulations. *Drug Delivery*. 11(1): 33-39

https://doi.org/10.1080/10717540490265243

Ansari, M. (2017) Sinapic acid modulates Nrf2/HO-1 signaling pathway in cisplatin-induced nephrotoxicity in rats. *Biomedicine & Pharmacotherapy*. 93: 646-653

https://doi.org/10.1016/j.biopha.2017.06.085

Anson, U, Berg, R, Havenaar, R, Bast, A, Haenen, C., 2009. Bioavailability of ferulic acid is determined by its bioaccessibility. *Journal of Cereal Science*. 49(2): 296-300

https://doi.org/10.1016/j.jcs.2008.12.001

Apak, R, Güçlü, K, Demirata, B, Özyürek, M, Çelik, S, Bektaşoğlu, B, Berker, I, Özyurt, D. (2007) Comparative evaluation of various total antioxidant capacity assays applied to phenolic compounds with the CUPRAC assay. *Molecules*. 12: 1496-1547

https://doi.org/10.3390/12071496

Asci, H, Ozmen, O, Ellidag, H, Aydin, B, Bas, E, Yilmaz, N. (2017) The impact of gallic acid on the methotrexate-induced kidney damage in rats. *Journal of Food and Drug Analysis.* 25(4): 890-897

https://doi.org/10.1016/j.jfda.2017.05.001

Augusti, P, Conterato, G, Somacal, S, Sobieski, R, Spohr, P, Torres, J, Charão, M, Moro, A, Rocha, M, Garcia, S, Emanuelli, T. (2008) Effect of astaxanthin on kidney function impairment and oxidative stress induced by mercuric chloride in rats. *Food and Chemical Toxicology.* 46(1): 212-219

https://doi.org/10.1016/j.fct.2007.08.001

Autio, K, Dreicer, R, Anderson, J, Garcia, J, Alva, A, Hart, L, ilowsky, M, Posadas, E, Ryan, C, Graf, R, Morris M, Scher, H. (2018) Safety and efficacy of BIND-014, a docetaxel nanoparticle targeting prostate-specific membrane antigen for patients with metastatic castration-resistant prostate cancer. A Phase 2 clinical trial. *JAMA Oncology*. 4(10): 1344–1351

https://doi.10.1001/jamaoncol.2018.2168

Ayala, T, Andérica-Romero, A, Chaverri, J. (2014) New insights into antioxidant strategies against paraquat toxicity. *Free Radical Research*. 48(6): 623-640

http://dx.doi.org/10.3109/10715762.2014.899694

Aytekin, A, Tanriverddi, S, Kose, F, Kart, D, Eroglu, I, Ozer. (2020) Propolis loaded liposomes: Evaluation of antimicrobial and antioxidant activities. *Journal of liposomal Research*. 30(2): 107-116

https://doi.org/10.1080/08982104.2019.1599012

Bagchi, D, Bagchi, M, Stohs, S, Das, D, Ray, S, Kuszynski, C, Joshi, S, Pruess, H. (2000) Free radicals and grape seed proanthocyanidin extract: Importance in human health and disease prevention. *Toxicology.* 148(2-3): 187-197

https://doi.org/10.1016/s0300-483x(00)00210-9

Bairagi, U, Mittal, P, Singh, J, Mishra, B. (2018) Preparation, characterization, and *in vivo* evaluation of nano formulations of ferulic acid in diabetic wound healing. *Drug Development and Industrial Pharmacy*. 44(11): 1783-1796

https://doi.org/10.1080/03639045.2018.1496448

Balagangadharan, K, Trivedi, R, Vairamani, M, Selvamurugan, N. (2019) Sinapic acid-loaded chitosan nanoparticles in polycaprolactone electrospun fibers for bone regeneration *in vitro* and *in vivo. Carbohydrate Polymers.* 216: 1-16

https://doi.org/10.1016/j.carbpol.2019.04.002

Baliga, R, Zhang, Z, Baliga, M, Ueda, N, Shah, V. (1998) *In vitro* and *in vivo* evidence suggesting a role for iron in cisplatin-induced nephrotoxicity. *Kidney International.* 53(2): 394-401

https://doi.org/10.1046/j.1523-1755.1998.00767.x

Banerjee, A, Kunwar, A, Mishra, B, Priyadarsini, K. (2008) Concentration dependent antioxidant/pro-oxidant activity of curcumin: Studies from AAPH induced hemolysis of RBCs. *Chemico-Biological Interactions*. 174(2): 134-139

https://doi.org/10.1016/j.cbi.2008.05.009

Banerjee, R. (2001) Liposomes: Application in medicine. *Journal of Biomaterials Applications.* 16(1): 3-21

https://doi.org/10.1106/RA7U-1V9C-RV7C-8QXL

Barnett, F, Moreno-Ulloa, A, Sheva, S. Ramirez-Sanchez, I, R, Pam. Su, Y, Ceballos, G, Dugar, S, Schreiner, G, Villarreal. (2015) Pharmacokinetic, partial pharmacodynamic and initial safety analysis of (−)-epicatechin in healthy volunteers. *Food and Function. 6: 824-833*

https://doi.org/10.1039/c4fo00596a

Bartesaghi, S, Radi, R (2018) Fundamentals on the biochemistry of peroxynitrite and protein tyrosine nitration. *Redox Biology.* 14: 618-625

https://doi.org/10.1016/j.redox.2017.09.009

Barzilia, A, Yamamato, K. (2005) DNA damage responses to oxidative stress. *DNA Repair.* 3(8-9): 1109-1115

https://doi.org/10.1016/j.dnarep.2004.03.002

Basile, D, Anderson, M, Sutton, T. (2012) Pathophysiology of acute kidney injury. *Comprehensive Physiology. 2(2): 1303–1353*

https://dx.doi.org/10.1002%2Fcphy.c110041

Basile, P, Donohoe, L, Roethe, K, Mattson, L. (2003) Chronic renal hypoxia after acute ischemic injury: effects of L-arginine on hypoxia and secondary damage. *American Journal of Physiology. Renal Physiology.*284(2): 338-348

https://doi.org/10.1152/ajprenal.00169.2002

Basiri, L, Rajabzadeh, G, Bostan, A. (2017) Physicochemical properties and release behaviour of span 60/tween 60 niosomes as vehicle for α-tocopherol delivery. *LWT-Food Science and Technology*. 84: 471-478

https://doi.org/10.1016/j.lwt.2017.06.009

Baskin, S, Salem, H. (Eds.) (2020) Oxidants, antioxidants, and free radicals. *CRC Press. 41- 107.* Online ISBN*: 9780203744673*

https://doi.org/10.1201/9780203744673

Batool, S, Asad, J, Arshad, M, Ahmed, W, Sohail, M, Abbasi, S, Ahmad, S, Saleem, R, Ahmed, M. (2021) *In Silico* validation, fabrication and evaluation of nano-liposomes of *Bistorta amplexicaulis* extract for improved anticancer activity against hepatoma cell line (HepG2). *Current Drug Delivery*. 18: 1

https://doi.org/10.2174/1567201818666210316113640

Beek, M, Chun, H, Yu, J, Lee, J, Kim, T, Oh, J, Lee, W, Paek, S, Lee, J, Jeong, J, Choy, J, Choi, S. (2012) Pharmacokinetics, tissue distribution, and excretion of zinc oxide nanoparticles. *International Journal of Nanomedicine*. 7: 3081–3097

https://dx.doi.org/10.2147%2FIJN.S32593

Berg, R, Haeen, G, Berg, H, Bast, A. (1999) Applicability of an improved trolox equivalent antioxidant capacity (TEAC) assay for evaluation of antioxidant capacity measurements of mixtures. *Food Chemistry*. 66(4): 511-517

https://doi.org/10.1016/S0308-8146(99)00089-8

Bergin, I, Witzmann, F. (2013) Nanoparticle toxicity by the gastrointestinal route: evidence and knowledge gaps. *International Journal of Biomedical Nanoscience and Nanotechnology*. 3(1-2): 163-210

https://doi.org/10.1504/ijbnn.2013.054515

Berlett, B, Stadtman, E. (1997) Protein oxidation in aging, disease, and oxidative stress. *The Journal of Biological Chemistry. 272: 20313-20316*

https://doi.org/10.1074/jbc.272.33.20313

Bellomo, R, Kellum, J, Ronco, C. (2012) Acute kidney injury. *The Lancet.* 380 (9843): 756-766

https://doi.org/10.1016/S0140-6736(11)61454-2

Bolhassani, A, Javanzad, S, Saleh, T, Hashemi, M, Aghasadeghi, M, Sadat, S. (2013) Polymeric nanoparticles. Potent vectors for vaccine delivery targeting cancer and infectious diseases. *Human Vaccines & Immunotherapeutics*. 10(2): 321–332

https://doi.org/10.4161/hv.26796

Bonechi, C, Martini, S, Ciani, L, Lamponi, S, Rebmann, H, Rossi, C, Ristori, S. (2012) Using liposomes as carriers for polyphenolic compounds: the case of trans-resveratrol. *PLoS One*. 7(8): e41438

https://doi.org/10.1371/journal.pone.0041438

Bonventre, J, Yang, L. (2011) Cellular pathophysiology of ischemic acute kidney injury. *The Journal of Clinical Investigation.* 121(11): 4210–4221

https://dx.doi.org/10.1172%2FJCI45161

Boozari, M, Hosseinzadeh, H. (2017) Natural medicines for acute renal failure: A review. *Phytotherapy Research.* 31(12): 1824-1835

https://doi.org/10.1002/ptr.5943

Brand, M. (2016) Mitochondrial generation of superoxide and hydrogen peroxide as the source of mitochondrial redox signalling. *Free Radical Biology and Medicine. 100:* 14-31

https://doi.org/10.1016/j.freeradbiomed.2016.04.001

Brueck, M, Cengiz, H, Hoeltgen, R, Wieczorek, M, Boedeker, R, Scheibelhut, C, Boening, A. (2013) Usefulness of N-acetylcysteine or ascorbic acid versus placebo to prevent contrast-induced acute kidney injury in patients undergoing elective cardiac catheterization: a single-centre, prospective, randomised, double-blind, placebo-controlled trial. *Journal of Invasive Cardiology* 25(6): 276-228

Bulbake, U, Doppalapudi, S, Kommineni, N, Khan, W. (2017) Liposomal formulations in clinical use: An updated review. *Pharmaceutics. 9(2): 12*

https://doi.org/10.3390/pharmaceutics9020012

Buhecha, M, Lansley, B, Somavarapu, S, Pannala, S. (2019) Development and characterization of PLA nanoparticles for pulmonary drug delivery: Co-encapsulation of theophylline and budesonide, a hydrophilic and lipophilic drug. *Journal of Drug Delivery Science and Technology*. 53: 101128

https://doi.org/10.1016/j.jddst.2019.101128

Bus, J, Aust, S, Gibson, J. (1976) Paraquat toxicity: proposed mechanism of action involving lipid peroxidation. *Environmental Health Perspectives*. 16: 139-146

https://doi.org/10.1289/ehp.7616139

Cadenas, E, Davies, K. (2000) Mitochondrial free radical generation, oxidative stress, and aging. *Free Radical Biology & Medicine*. 29: 222–230

https://doi.org/10.1016/s0891-5849(00)00317-8

Cagdas, M, Sezer,A, Bucak, S. (2014) Liposomes as potential drug carrier systems for drug delivery. In: Sezar, A. (eds) Application of nanotechnology in drug delivery. *IntechOpen*.

DOI: 10.5772/58459

Callaghan, C. (2017) The Renal system at a glance. 4th edition. *John Wiley & Sons, Ltd.* 3-4. ISBN: 9781118393871.

Campani, V, Scotti, L, Silvestri, T, Biondi, M, De Rosa, G. (2020) Skin permeation and thermodynamic features of curcumin-loaded liposomes. *Journal of Materials Science: Materials in Medicine*. 31:18

https://doi.org/10.1007/s10856-019-6351-6

Campbell, R, Balasubramanian, S, Straubinger, R. (2000) Influence of cationic lipids on the stability and membrane properties of paclitaxel-containing liposomes. *Journal of Pharmaceutical Sciences*. 90: 1091-1105

Canbek, M, Ustuner, M, Kabay, S, Uysal, O, Ozden, H, Bayramoglu, G, Senturk, H, Ozbayar, C, Bayramoglu, A, Ustuner, D, Degirmenci, I. (2011) The effect of gallic acid on kidney and liver after experimental renal ischemia/reperfusion injury in the rats. *African Journal of Pharmacy and Pharmacology*. 5(8): 1027-1033

https://doi.org/10.5897/AJPP11.026

Carmines, E, Carchman, R, Borzelleca, J. (1981) Investigations into the mechanism of paraquat toxicity utilizing a cell culture system. *Toxicology and Applied Pharmacology*. 58(3): 353-362

https://doi.org/10.1016/0041-008X(81)90087-9

Caruso, F, Hyeon, T, Rotello, V. (2012) Targeted polymeric therapeutic nanoparticles: design, development and clinical translation. *Chemical Society Review*. 41: 2971–3010

https://doi.org/10.1039/C2CS15344K

Chakravarty, P, Famili, A, Nagapudi, K, Al-Sayah, M. (2019) Using supercritical fluid technology as a green alternative during the preparation of drug delivery systems. *Pharmaceutics.* 11(12): 629

https://doi.org/10.3390/pharmaceutics11120629

Chang, P, Peng, S, Lee, C, Lu, C, Tsai, S, Shieh, T, Wu, T, Tu, M, Chen, M, Yang, J. (2013) Curcumin-loaded nanoparticles induce apoptotic cell death through regulation of the function of MDR1 and reactive oxygen species in cisplatin-resistant CAR human oral cancer cells. *International Journal of Oncology*. 43(4): 1141- 1150

https://doi.org/10.3892/ijo.2013.2050

Chandrasekaran, A, Idelchik, M, Melendez, A. (2016) Redox control of senescence and age-related disease. *Redox Biology.* 11: 91-102

https://doi.org/10.1016/j.redox.2016.11.005

Chauhan, A (2015) Dendrimer nanotechnology for enhanced formulation and controlled delivery of resveratrol. *The New York Academy of Sciences.* 1384(1): 134-140

https://doi.org/10.1111/nyas.12816

Chatterjee P, Chatterjee B, Pedersen H, Sivarajah A, McDonald M, Mota-Filipe H, Brown P, Stewart K, Cuzzocrea S, Threadgill M, Thiemermann C. (2004) 5-Aminoisoquinolinone reduces renal injury and dysfunction caused by experimental ischemia/reperfusion. *Kidney International*. 65(2): 499-509

https://doi.org/10.1111/j.1523-1755.2004.00415.x

Chatterjee P, Cuzzocrea S, Brown P, Zacharowski K, Stewart K, Mota-Filipe H, Thiemermann C. (2000) Tempol, a membrane-permeable radical scavenger, reduces oxidant stress-mediated renal dysfunction and injury in the rat. *Kidney International.* 58(2): 658-673

https://doi.org/10.1046/j.1523-1755.2000.00212.x

Chatterjee P, Zacharowski K, Cuzzocrea S, Otto M, Thiemermann C. (2000) Inhibitors of poly (ADP-ribose) synthetase reduce renal ischemia-reperfusion injury in the anesthetized rat *in vivo*. *Federation of American Societies for Experimental Biology*. 14(5): 641-651

https://doi.org/10.1096/fasebj.14.5.641

Chatterjee, S, Banerjee, K. (2002) preparation, isolation, and characterization of liposomes containing natural and synthetic lipids. In: Basu, C, Basu, M. (eds) Liposome methods and protocols. Methods in Molecular Biology. Vol 199. *Humana Press.* Online ISBN: 978-1-59259-175-6

https://doi.org/10.1385/1-59259-175-2:03

Chen, C. (2015) Sinapic acid and its derivatives as medicine in oxidative stress-induced diseases and aging. *Oxidative Medicine and Cellular Longevity.* 2016: 3571614

https://doi.org/10.1155/2016/3571614

Chen, H, Busse, L. (2017) Novel therapies for acute kidney injury. *Kidney International Reports*. 2: 758-799

https://dx.doi.org/10.1016%2Fj.ekir.2017.06.020

Chen, L, Yang, S, Zumbrun, E, Guan, H, Nagarkatti, S, Nagarkatti, M. (2015) Resveratrol attenuates lipopolysaccharide-induced acute kidney injury by suppressing inflammation driven by macrophages. *Molecular Nutrition & Food Research* 59(5): 853-864

https://doi.org/10.1002/mnfr.201400819

Chen, X, Sun, J, Li H, Wang, H, Lin, Y, Hu, Y, Zheng, D. (2017) Curcumin-loaded nanoparticles protect against rhabdomyolysis-induced acute kidney injury. *Cellular Physiology and Biochemistry.* 43: 2143–2154

https://doi.org/10.1159/000484233

Chen, X, Zou, L, Niu, J, Liu, W, Peng, S, Liu, C. (2015) The stability, sustained release and cellular antioxidant activity of curcumin nanoliposomes. *Molecules*. 20(8): 14293–14311

https://dx.doi.org/10.3390%2Fmolecules200814293

Chen, Y, Hsu, K.Y. (2009) Pharmacokinetics of (-)-epicatechin in rabbits. *Archives of Pharmaceutical Research*. 32(1): 149-154

https://doi.org/10.1007/s12272-009-1129-x

Chenthamara, D, Subramaniam, S, Ramakrishnan, S, Krishnaswamy, S, Essa, M, Lin, F, Qoronfleh. (2019) Therapeutic efficacy of nanoparticles and routes of administration. *Biomaterial Research*. 23: 20

https://doi.org/10.1186/s40824-019-0166-x

Chepda, M, Cadau, A, Chamson, C, Alexandre, C, Frey, J. (1999) Alpha-tocopherol as a protective agent in cell culture. *In vitro Cellular & Developmental Biology - Animal*. 35(9): 491-2

https://doi.org/10.1007/s11626-999-0058-9

Chertow, G, Burdick, E, Honour, M, Bonventre, J, Bates. (2005) Acute kidney injury, mortality, length of stay, and costs in hospitalized patients. *Journal of the American Society of Nephrology.* 16 (11): 3365-3370

https://doi.org/10.1681/ASN.2004090740

Chibowski, E, Szczes, A. (2016) Zeta potential and surface charge of DPPC and DOPC liposomes in the presence of PLC enzyme. *Adsorption*. 22: 755–765

https://doi.org/10.1007/s10450-016-9767-z

Chirino, Y, Hernández-Pando, R, Pedraza-Chaverrí, J. (2004) Peroxynitrite decomposition catalyst ameliorates renal damage and protein nitration in cisplatin-induced nephrotoxicity in rats. *BMC Pharmacology.* 4: 20

https://doi.org/10.1186/1471-2210-4-20

Cho, M, Kim, S, Park, H, Chung, S, Kim, K. (2017) Could vitamin E prevent contrast-induced acute kidney injury? A systematic review and meta-analysis. *Journal of Korean Medical Science.* 32(9): 1468–1473.

https://doi.org/10.3346/jkms.2017.32.9.1468

Choe, E. (2020) Roles and action mechanisms of herbs added to the emulsion on its lipid oxidation. *Food Science and Biotechnology*. 29: 1165–1179

https://doi.org/10.1007/s10068-020-00800-z

Choi, C, Zuckerman, J, Webster, P, Davis, M. (2011) Targeting kidney mesangium by nanoparticles of defined size. *Proceedings of the National Academy of Sciences of the United States of America*. 108(16): 6656-6661

https://doi.org/10.1073/pnas.1103573108

Chung, I, Subramanian, U, Thirupathi, P, Venkidasamy, B, Samynathan, R, Gangadhar, B, Rajakumar, G, Thiruvengadam, M. (2020) Resveratrol nanoparticles: A promising therapeutic advancement over native resveratrol. *Processes*. 8(4): 458

http://dx.doi.org/10.3390/pr8040458

Clogston, J, Patri, A. (2011) Zeta potential measurement. In: McNeil, S. Characterization of nanoparticles intended for drug delivery. Methods in Molecular

Biology (Methods and Protocols). *Humana Press*. Vol. 697: 63-70. Online ISBN: 978-1-60327-198-1

https://doi.org/10.1007/978-1-60327-198-1_6

Coca, S, Singanamala, S, Parikh, C. (2012) Chronic kidney disease after acute kidney injury: A systematic review and meta-analysis. *Kidney International.* 81(5): 442-448

https://doi.org/10.1038/ki.2011.379

Cohen-Sela, E, Chorny, M, Koroukhov, N, Danenberg, H, Golomb, G. A new double emulsion solvent diffusion technique for encapsulating hydrophilic molecules in PLGA nanoparticles. *Journal of Controlled Release*. 133(2): 90-95

https://doi.org/10.1016/j.jconrel.2008.09.073

Crowell, J, Korytko, P, Morrissey, R, Booth, T, Levine, B. (2004) Resveratrol-associated renal toxicity. *Toxicological Science.* 82(2): 614-619

https://doi.org/10.1093/toxsci/kfh263

Crucho, C, Barros, M. (2017) Polymeric nanoparticles: A study on the preparation variables and characterization methods. *Materials Science and Engineering: C.* 80(1):771-784

https://doi.org/10.1016/j.msec.2017.06.004

Cruz, D, Fardilha, M. (2016) Relevance of peroxynitrite formation and 3-nitrotyrosine on spermatozoa physiology. *Porto Biomedical Journal*. 1(4): 129-135

https://doi.org/10.1016/j.pbj.2016.07.004

Csiszár, A, Csiszar, A, Pinto, T, Gautam, T, Kleusch, C, Hoffmann, B, Ungvari, Z. (2015) Resveratrol encapsulated in novel fusogenic liposomes activates Nrf2 and attenuates oxidative stress in cerebromicrovascular endothelial cells from aged rats. *The journals of gerontology. Series A, Biological sciences and medical sciences*. 70(3): 303–313

https://doi.org/10.1093/gerona/glu029

Danaei, M, Dehghankhold, M, Ataei, S, Davarani, F, Javanmard, R, Dokhani, A, Khorasani, S, Mozafari, M. (2108) Impact of particle size and polydispersity index on the clinical applications of lipidic nanocarrier systems. *Pharmaceutics*. 10(2): 57

https://doi.org/10.3390/pharmaceutics10020057

Degim, Z, Agardan, N, Nacar, A, Yilmaz, S. (2010) Investigation of liposome formulation effects on rivastigmine transport through human colonic adenocarcinoma cell line (CACO-2). *Die Pharmazie - An International Journal of Pharmaceutical Sciences.* 65(1): 32-40

https://doi.org/10.1691/ph.2010.9179

Dennis, J, Witting, P. (2017) Protective role for antioxidants in acute kidney disease*. Nutrients*. *9*(7): 718.

https://dx.doi.org/10.3390%2Fnu9070718

Devalaraja-Narashimhaa, K, Singaravelua, K, Padanilam, B. (2005) Poly (ADP-ribose) polymerase-mediated cell injury in acute renal failure. *Pharmacological Research.* 52(1): 44-59

https://doi.org/10.1016/j.phrs.2005.02.022

Dichello, G, Fukuda, T, Maekawa, T, Whitby, R, Mikhalovsky, S, Alavijeh, M, Pannala, A, Sarker, D. (2017) Preparation of liposomes containing small gold nanoparticles using electrostatic interactions. *European Journal of Pharmaceutical Sciences.* 105: 55-63

https://doi.org/10.1016/j.ejps.2017.05.001

Dinis-Oliveira, J, Duarte, A, Sánchez-Navarro, A, Remião, F, Bastos, L, Carvalho, F. (2008) Paraquat poisonings: mechanisms of lung toxicity, clinical features, and treatment. *Critical Reviews in Toxicology.* 38(1): 13-71

https://doi.org/10.1080/10408440701669959

Dixit, G, Kelley, J, Houser, J, Elston, T, Dohlman, H. (2014) Cellular noise suppression by the regulator of G protein signalling Sst2. *Molecular Cell*. 55(1): 85-96

https://doi.org/10.1016/j.molcel.2014.05.019

Dobashi K, Ghosh B, Orak JK, Singh I, Singh AK. (2000) Kidney ischemia-reperfusion: Modulation of antioxidant defences. *Molecular Cell Biochemistry.* 205(1-2): 1-11

https://doi.org/10.1023/a:1007047505107

Du, C, Guan, Q, Diao, H, Yin, Z, Jevnikar, AM. (2006) Nitric oxide induces apoptosis in renal tubular epithelial cells through activation of caspase-8. *American Journal of Physiology. Renal Physiology.* 290(5): 1044-1054

https://doi.org/10.1152/ajprenal.00341.2005

Du, C, Guan, Q, Yin Z, Zhong, R, Jevnikar, M. (2005) IL-2-mediated apoptosis of kidney tubular epithelial cells is regulated by the caspase-8 inhibitor c-FLIP. *Kidney International.* 67(4): 1397-1409

https://doi.org/10.1111/j.1523-1755.2005.00217.x

El-Naggar, M, Al-Joufi, F, Anwar, M, Attia, M, El-bana, M. (2019) Curcumin-loaded PLA-PEG copolymer nanoparticles for treatment of liver inflammation in streptozotocin-induced diabetic rats. *Colloids and Surfaces B: Biointerfaces.* 177: 389-398

https://doi.org/10.1016/j.colsurfb.2019.02.024

Elisha-Lambert, B. (2017) The Role of dietary antioxidants against oxidant-induced acute kidney injury. *PhD thesis*. University of Brighton.

Esatbeyoglu, T, Huebbe, P, Ernst, I, Chin, D, Wagner, A, Rimbach, G. (2012) Curcumin—from molecule to biological function. *Angewandte Chemie International Edition*. 51(22): 5308-5332

https://doi-org.ezproxy.brighton.ac.uk/10.1002/anie.201107724

Fahim, M, Howarth, F, Nemmar, A, Qureshi, M, Shafiullah, M, Jayaprakash, P, Hasan, M. (2013) Vitamin E ameliorates the decremental effect of paraquat on cardiomyocyte contractility in rats. *Plos One*. 8(3): e57651

https://doi.org/10.1371/journal.pone.0057651

Fan, S, Zhang, Z, Zheng, Y, Lu, J, Wu, D, Shan, Q, Hu, B, Wang, Y. (2008) Troxerutin protects the mouse kidney from d-galactose-caused injury through anti-inflammation and anti-oxidation. *International Immunopharmacology.* 9(1): 91-96

https://doi.org/10.1016/j.intimp.2008.10.008

Fan, Y, Chen, H, Peng, H, Haung, F, Zhong, J, Zhou, J. (2017) Molecular mechanisms of curcumin renoprotection in experimental acute renal injury. *Frontiers in Pharmacology*. 8: 912

https://doi.org/10.3389/fphar.2017.00912

Fang, J, Hung, C, Hwang, T, Huang, Y., 2005. Physicochemical characteristics and *in-vivo* deposition of liposome-encapsulated tea catechins by topical and intratumor administrations. *Journal of Drug Targeting*. 13(1): 19-27

https://doi.org/10.1080/10611860400015977

Fang, J, Lee, W, Shen, S, Huang, Y., 2006. Effect of liposome encapsulation of tea catechins on their accumulation in basal cell carcinomas. *Journal of Dermatological Science*. 42: 101-109

https://doi.org/10.1016/j.jdermsci.2005.12.010

Faraji, AH, Wipf, P. (2009) Nanoparticles in cellular drug delivery. *Bioorganic & Medicinal Chemistry* 17(8): 2950-2962

https://doi.org/10.1016/j.bmc.2009.02.043

Feng, T, Wei, Y, Lee, R, Zhao, L. (2017) Liposomal curcumin and its application in cancer. *International Journal of Nanomedicine*. 12: 6027–6044

https://dx.doi.org/10.2147%2FIJN.S132434

Field, A. (2009) Discovering statistics using SPSS. 3rd edition. *SAGE Publications Ltd, Oriental Press*, Dubai. 372 – 375. ISBN: 978-1-84787-906-6

Field, M, Pollock, C, Harris, D. (2001) The renal system. Basic science and clinical conditions. Second edition. *Churchill Livingstone, Elsevier. 2,3.* ISBN: 978-0-7020-3371-1

Finlay, S, Jones, M. (2017) Acute Kidney Injury. *Medicine.* 45(3): 173-176

https://doi.org/10.1016/j.mpmed.2016.12.010

Florence, A. (2005) Nanoparticle uptake by the oral route: Fulfilling its potential? *Drug Discovery Today: Technologies*. 2(1): 75-81

https://doi.org/10.1016/j.ddtec.2005.05.019

Fotakis, G, Timbrell, J. (2006) *In vitro* cytotoxicity assays: Comparison of LDH, neutral red, MTT and protein assay in hepatoma cell lines following exposure to cadmium chloride. *Toxicology Letters*. 160(2): 171-177

https://doi.org/10.1016/j.toxlet.2005.07.001

Frederiksen, L, Anton, K, Hoogevest, N, Keller, P, Leuenberger, H. (1997) Preparation of liposomes encapsulating water-soluble compounds using supercritical carbon dioxide. *Journal of Pharmaceutical Science*. 86: 921-928

http://doi.org/10.1021/js960403q

Frei, B, England, L, Ames, B. (1989) Ascorbate is an outstanding antioxidant in human blood plasma. *Proceedings of the National Academy of Sciences of the United States of America.* 86 (16): 6377-6381

https://dx.doi.org/10.1073%2Fpnas.86.16.6377

Funamoto, M, Masumoto, H, Takaori, K, Taki, T, Setozaki, S, Yamazaki, K, Minakata, K, Ikeda, T, Hyon, S, Sakata, R. (2015) Green tea polyphenol prevents diabetic rats from acute kidney injury after cardiopulmonary bypass. *The Annals of Thoracic Surgery.* 101(4): 1507-1513

https://doi.org/10.1016/j.athoracsur.2015.09.080

Fugita, R, Galico, D, Guerra, G, Perpetuo, G, Treu-Filho, O, Galhiane, M, Mendes, R, Bannach, G. (2012) Thermal behaviour of curcumin. *Brazilian Journal of Thermal Analysis.* 1(1)

Funk, J, Odejinmi, S, Schnellmann, R. (2010) SRT1720 Induces mitochondrial biogenesis and rescues mitochondrial function after oxidant injury in renal proximal tubule cells. *The Journal Pharmacology and Experimental Therapeutics.* 333(2): 593–601

https://doi.org/10.1124/jpet.109.161992

Gagliardi, A, Giuliano, E, Venkateswararao, E, Fresta, M, Bulotta, A, Awasthi, V, Cosco, D. (2021) Biodegradable polymeric nanoparticles for drug delivery to solid tumours. *Frontiers in Pharmacology*. 12:17

https://doi.org/10.3389/fphar.2021.601626

Galanakis C, Goulas, V, Tsakona, S, Manganaris, G, Gekas, V. (2013) A knowledge base for the recovery of natural phenols with different solvents. *International Journal of Food Properties*. 16: 382–396

https://doi.org/10.1080/10942912.2010.522750

Galvão, A, Galvão, J, Pereira, M, Cadena, P, Santos, M, Fink, M, Andrade, A, Castro, C, Maia, M. (2016) Cationic liposomes containing antioxidants reduces

pulmonary injury in experimental model of sepsis: Liposomes antioxidants reduces pulmonary damage. *Respiratory Physiology & Neurobiology*. 231: 55-62

https://doi.org/10.1016/j.resp.2016.06.001

Gan, Y, Tao, S, Cao, D, Xie, H, Zeng, Q. (2017) Protection of resveratrol on acute kidney injury in septic rats. *Human and Experimental Toxicology.* 36(10): 1015-1022

https://doi.org/10.1177/0960327116678298

Gao, D, Li, W. (2018) Research progress of astaxanthin on contrast agent induced acute kidney injury. *Journal of Cardiology and Cardiovascular Science.* 2(3): 6-9

https://doi.org/10.29245/2578-3025/2018/3.1123

Garcia-Criado, J, Eleno, N, Santos-Benito, F, Valdunciel, J, Reverte, M, Lozano-Sánchez, S, Ludeña, D, Gomez-Alonso, A, López-Novoa, M. (1995) Protective effect of exogenous nitric oxide on the renal function and inflammatory response in a model of ischemia-reperfusion. *Transplantation.* 66(8): 982-90

https://doi.org/10.1097/00007890-199810270-00003

Garg, A, Devereaux, P, Hill, A, Sood, M, Aggarwal, B, Dubois, L, Hiremath, S, Guzman, R, Iyer, V, James, M, McArthur, E, Moist, L, Ouellet, G, Parikh, C, Schumann, V, Sharan, S, Thiessen-Philbrook, H, Tobe, S, Wald, R, Walsh, M, Weir, M, Pannu, N, and Curcumin AAA AKI Investigators. (2018) Oral curcumin in elective abdominal aortic aneurysm repair: A multicentre randomized controlled trial. *Canadian Medical Association Journal*. 190 (48): E1425

https://doi.org/10.1503/cmaj.180510

Geng, T, Zhao, X, Ma, M, Zhu, G, Yin, L. (2017) Resveratrol-loaded albumin nanoparticles with prolonged blood circulation and improved biocompatibility for highly effective targeted pancreatic tumour therapy. *Nanoscale Research Letters.* 437

https://doi.org/10.1186/s11671-017-2206-6

Ghaznavi, H, Fatemi, I, Kalantari, H, Tabatabaei, S, Mehrabani, M, Gholamine, B. (2017) Ameliorative effects of gallic acid on gentamicin-induced nephrotoxicity in rats. *Journal of Asian Natural Products Research.* 20(12): 1182-1193

https://doi.org/10.1080/10286020.2017.1384819

Ghosh, P, Bag, S, Roy, A, Sabramani, E, Chaudhury, K, Dasgupta, S. (2016) Solubility enhancement of morin and epicatechin through encapsulation in an albumin based nanoparticulate system and their anticancer activity against the MDA-MB-468 breast cancer cell line. *Royal Society of Chemistry Advances*. 103(6): 101415-101429

https://doi.org/10.1039/C6RA20441D

Gloire, G, Legrand-poels, S, Piette, J. (2006) NF-κB activation by reactive oxygen species: Fifteen years later. *Biochemical Pharmacology*. 72(11): 1493-1505

https://doi.org/10.1016/j.bcp.2006.04.011

Goldstein, J, Newbury, D, Michael, J, Ritchie, J, Joy, D. (2018) Scanning Electron Microscopy and X-Ray Microanalysis. 4th edition. *Springer*. 65-89. Online ISBN: 978-1-4939-6676-9

https://doi.org/10.1007/978-1-4939-6676-9

González-Flecha, B, Boveris, A. (1995) Mitochondrial sites of hydrogen peroxide production in reperfused rat kidney cortex. *Biochimica et Biophysica Acta. (BBA)-General Subjects*. 1243(3): 361-366

https://doi.org/10.1016/0304-4165(94)00160-y

Gottumukkala, R, Nadimpalli, N, Sukala, K, and Subbaraju, G. (2014) Determination of catechin and epicatechin content in chocolates by high-performance liquid chromatography. *International scholarly research notices*. 2014: 628196

https://dx.doi.org/10.1155%2F2014%2F628196

Guangping, Li, Yin, L, Liu, T, Zheng, X, Xu, G, Xu, Y, Yuan, R, Che, J, Liu, H, Zhou, L, Chen, X, He, M, LI, Y, Wu, L, Liu, E. (2009) Role of probucol in preventing contrast-induced acute kidney injury after coronary interventional procedure. *The American Journal of Cardiology*. 103(4): 512-514

https://doi.org/10.1016/j.amjcard.2008.10.009

Gumustas, M, Sengel-Turk, C, Gumustas, A, Ozkan, S, Uslu, B. (2017) Effect of polymer-based nanoparticles on the assay of antimicrobial drug delivery systems. In: Grumezescu, A. Multifunctional systems for combined delivery. *Biosensing and Diagnostics. Elsevier.* 67-108. Online ISBN 9780323527255

https://doi.org/10.1016/B978-0-323-52725-5.00005-8

Guo, S, Zhou, H, Huang, C, You, C, Fang, Q, Wu, P, Wang, X, Han, C. (2015) Astaxanthin attenuates early acute kidney injury following severe burns in rats by ameliorating oxidative stress and mitochondrial-related apoptosis. *Marine Drugs.* 13(4): 2105–2123

https://doi.org/10.3390/md13042105

Gupta, A, Devaraju, K. (2014) Spectrophotometric estimation of nitro tyrosine by azo-coupling reaction. *International Journal of Pharma and Bio Sciences.* 5(1): 269-277

Gupta, K, Das, S, Chow, P, Macbeath, C. (2020) Encapsulation of ferulic acid in lipid nanoparticles as antioxidant for skin: mechanistic understanding through experiment and molecular simulation. *American Chemical Society*. *Applied Nano Materials*. 3(6): 5351–5361

https://doi.org/10.1021/acsanm.0c00717

Gutteridge, J, Halliwell, B. (1996) Antioxidants in nutrition, health, and disease. *Oxford University Press.* 7-16. ISBN: 0 19 854902 4

https://doi.org/10.1146/annurev.nu.16.070196.000341

Hagens, W, Oomen, A, Jong, W, Cassee, F, Sips, A. (2007) What do we (need to) know about the kinetic properties of nanoparticles in the body? *Regulatory Toxicology and Pharmacology.* 49(3): 217-229

https://doi.org/10.1016/j.yrtph.2007.07.006

Halliwell, B. (2008) Are polyphenols antioxidants or pro-oxidants? What do we learn from cell culture and *in vivo* studies? *Archives of Biochemistry and Biophysics*. 476(2): 107-112

https://doi.org/10.1016/j.abb.2008.01.028

Halliwell, B, Gutteridge, J. (2007) Free radicals in biology and medicine, fourth edition. *Oxford University Press.* 19, 22, 176-183. ISBN: 978-0-19-856868-1

Hamdi, S, Selmi, W, Hraiech, A, Jomaa, W, Hamda K, Maatouk, F. (2012) CRT-66 Prevention of contrast induced nephropathy in patients undergoing coronarography with ascorbic acid. *Journal of American College of Cardiology: Cardiovascular Interventions.* 6(2): S22

https://doi.org/10.1016/j.jcin.2012.12.084

Hammad, F, Salam, S, Lubbad, L. (2012) Curcumin provides incomplete protection of the kidney in ischemia reperfusion injury. *Physiological Research.* 61: 503-511

https://doi.org/10.33549/physiolres.932376

Hao, Q, Xiao, X, Zheng, J, Feng, J, Song, C, Jiang, B, HU, Z. (2016) Resveratrol attenuates acute kidney injury by inhibiting death receptor-mediated apoptotic pathways in a cisplatin-induced rat model. *Molecular Medicine Reports.* 14(4): 3683-3689

https://doi.org/10.3892/mmr.2016.5714

Havasi, A, Borkan, S. (2011) Apoptosis and acute kidney injury. *Kidney International.* 80(1): 29-40

https://doi.org/10.1038/ki.2011.120

Hasan, H, Edrees, G, El-Gamel, E, El-Sayed, E. (2014) Amelioration of cisplatin-induced nephrotoxicity by grape seed extract and fish oil is mediated by lowering oxidative stress and DNA damage. *Cytotechnology.* 66(3): 419–429

https://doi.org/10.1007/s10616-013-9589-8

He, L, Peng, X, Zhu, J, Liu, G, Chen, X, Tang, C, Liu, H, Liu, F, Peng, Y. (2015) Protective effects of curcumin on acute gentamicin-induced nephrotoxicity in rats. *Canadian Journal of Physiology and Pharmacology.* 93(4): 275-282

https://doi.org/10.1139/cjpp-2014-0459

He, L, Zeng, Y, Qin, X, Pan, T, Chen, T, Wang, Q, Ma, Y, Fang, J. (2021) Delivery of ferulic acid with pegylated diphenylalanine nanoparticles for pre-arthritis therapy. *Research square*. (Preprint)

https://doi.org/10.21203/rs.3.rs-140007/v2

He, X, Wang, L, Szclarz, G, Bi, Y, Ma, Q. (2012) Resveratrol inhibits paraquat-induced oxidative stress and fibrogenic response by activating the nuclear factor erythroid 2-related factor 2 pathway. The *Journal of Pharmacology and Experimental Therapeutics*. 342(1): 81-90

https://doi.org/10.1124/jpet.112.194142

Hegarty, J, Young, S, Kirwan, N, O'Neill, J, Bouchier-Hayes, M, Sweeney, P, Watson, W, Fitzpatrick, M. (2001) Nitric oxide in unilateral ureteral obstruction: effect on regional renal blood flow. *Kidney International.* 59(3): 1059-1065

https://doi.org/10.1046/j.1523-1755.2001.0590031059.x

Herrmann, M, Weaver, M. (1999) "The Shikimate pathway". *Annual Review of Plant Physiology and Plant Molecular Biology*. 50: 473–503

https://doi.org/10.1146/annurev.arplant.50.1.473

Hillaireau, H, Couvreur, P. (2009) Nanocarriers' entry into the cell: Relevance to drug delivery. *Cellular and Molecular Life Sciences*. 66: 2873–2896

https://doi.org/10.1007/s00018-009-0053-z

Hismiogullari, A, Hismiogullari, S, Karaca, O, Sunay, F, Paksoy, S, Can, M, Kus, I, Serek, K, Yuvuz, O. (2015) The protective effect of curcumin administration on carbon tetrachloride (CCl4)-induced nephrotoxicity in rats. *Pharmacological Reports.* 67(3): 410-416

https://doi.org/10.1016/j.pharep.2014.10.021

Hoenig, M, Zeidel, L. (2014) Homeostasis, the milieu intérieur, and the wisdom of the nephron. *Clinical Journal of American Society of Nephrology*. 9(7): 1272-1281

https://doi.org/10.2215/CJN.08860813

Hohne, G, Hemminger, W, Flammersheim, H. (2003) Differential scanning calorimetry. *Springer-Verlag Berlin Heidelberg New York*. 1-27. ISBN: 978-3-662-06710-9

Holthoff, J, Wang, Z, Seely, K, Gokden, N, Mayeux, P. (2012) Resveratrol improves renal microcirculation, protects the tubular epithelium, and prolongs survival in a mouse model of sepsis-induced acute kidney injury. *Kidney International.* 81(4): 370-378

https://doi.org/10.1038/ki.2011.347

Hope, M, Nayar, R, Mayer, L, Cullis, P. (1993) Reduction of liposome size and preparation of unilamellar vesicles by extrusion techniques. In: Gregoriadis, G (eds). Liposome technology. *CRC Press*. 123-126

Hoste, E, Clermont, G, Kersten, A, Venkataraman, R, Angus, D, Bacquer, D, Kellum, J. (2006) RIFLE criteria for acute kidney injury are associated with hospital mortality in critically ill patients: A cohort analysis. *Critical Care*. 10: R73

https://dx.doi.org/10.1186%2Fcc4915

Huang, D, Qu, B, Prior, R. (2005) The chemistry behind antioxidant capacity assays. *Journal of Agriculture and Food Chemistry*. 53(6): 1841–1856

https://doi.org/10.1021/jf030723c

Huyut, Z, Beydemir, S, Gulcin, I. (2017) Antioxidant and antiradical properties of selected flavonoids and phenolic compounds. *Biochemistry Research International*. Article ID: 7616791

https://doi.org/10.1155/2017/7616791

ICH Topic Q2 (R1): Notes for guidance validation of analytical procedures: Text and methodology. (1995) *European Medicines Agency*. (CPMP/ICH/381/95).

Ichikawa, I, Kiyama, S, Yoshioka, T. (1994) Renal antioxidant enzymes: Their regulation and function. *Kidney International.* 45: 1-9

https://doi.org/10.1038/ki.1994.1

Isailović, B, Kostić, I, Zvonar, A, Đorđević, V, Gašperlin, M, Nedović, N, Bugarski, B. (2013) Resveratrol loaded liposomes produced by different techniques. *Innovative Food Science & Emerging Technologies*. 19: 181-189

Ishimoto, Y, Inagi, R. (2016) Mitochondria: A therapeutic target in acute kidney injury. *Nephrology Dialysis Transplantation.* 31(7): 1062-1069

https://doi.org/10.1093/ndt/gfv317

Jadhav, B, Mahadik, K, Paradkar, A. (2007) Development and validation of improved reversed phase-HPLC method for simultaneous determination of curcumin, demethoxycurcumin and bis-demethoxycurcumin. *Chromatographia*. 65(7): 483-488

https://doi.org/10.1365/s10337-006-0164-8

Jangle, R, Thorat, B. (2013) Reserved-phase high-performance liquid chromatography method for analysis of curcuminoids and curcuminoid-loaded liposome formulation. *Indian Journal of Pharmaceutical Sciences.* 75(1): 60-66

https://doi.org/10.4103/0250-474X.113555

Jawahar, N, Meyyanathan, SN. (2012) Polymeric nanoparticles for drug delivery and targeting: A comprehensive review. *International Journal of Health and Allied Sciences*. 1(4): 217-223

https://www.ijhas.in/text.asp?2012/1/4/217/107832

Jeon, Y, Lee, J, Lee, H. (2016) Improving solubility, stability, and cellular uptake of resveratrol by nanoencapsulation with chitosan and γ-poly (glutamic acid). *Colloids and Surfaces B: Biointerfaces*. 147: 224- 233

https://doi.org/10.1016/j.colsurfb.2016.07.062

Kadian, R. (2018) Nanoparticles: A promising drug delivery approach. *Asian Journal of Pharmaceutical and Clinical Research*. 11(1): 30-35

http://dx.doi.org/10.22159/ajpcr.2017.v11i1.22035

Karlberg, L, Norlén, J, Ojteg, G, Wolgast, M. (1983) Impaired medullary circulation in postischemic acute renal failure. *Acta Physiologica.* 118(1): 11-7

https://doi.org/10.1111/j.1748-1716.1983.tb07234.x

Katerji, M, Filippova, M, Duerksen-Hughes, P. (2019) Approaches and methods to measure oxidative stress in clinical samples: Research applications in the cancer field. *Oxidative Medicine and Cellular Longevity.* Article ID 1279250, 29 pages

https://doi.org/10.1155/2019/1279250

Katragadda, A, Singh, M, Betageri, G. (1999) Encapsulation, stability, and *in vitro* release characteristics of liposomal formulations of stavudine (D4T). *Drug Delivery*. 6(1): 31-37

https://doi.org/10.1080/107175499267138

Katuwavila, N, Perera, A, Karunaratne, V, Amaratuga, G, Karunaratne, N. (2016) Improved delivery of caffeic acid through liposomal encapsulation. *Journal of Nanomaterial*. Article ID 9701870

https://doi.org/10.1155/2016/9701870

Kaur, A, Kaur, T, Singh, B, Pathak, Buttar, H, Singh, A. (2016) Curcumin alleviates ischemia reperfusion-induced acute kidney injury through NMDA receptor antagonism in rats. *Renal Failure.* 38(9): 1462-1467

https://doi.org/10.1080/0886022X.2016.1214892

Kaur, G, Dufour, J. (2012) Cell lines. Valuable tools or useless artefacts. *Spermatogenesis*. 2(1): 1-5

https://dx.doi.org/10.4161%2Fspmg.19885

Kellum, J, Ronco, C, Vincent, J. (2011) Controversies in acute kidney injury. In: Ronco, C. (eds) Contributions to Nephrology. Vol. *174. Basel, Karger.* 1, 2, 57-59. Online ISBN: 978-3-8055-9811-8

DOI: 10.1159/isbn.978-3-8055-9811-8

Kern, S, Bennett, R, Mellon, F, Kroon, P, Garcia-Conesa, M. (2003) Absorption of hydroxycinnamates in humans after high-bran cereal consumption. *Journal of Agricultural and Food Chemistry*. 51(20): 6050-6055

https://doi.org/10.1021/jf0302299

Khan, R ,Siddiqui, S , Parveen, K , Javed, S , Diwakar, S , Siddiqui, A. (2010) Nephroprotective action of tocotrienol-rich fraction (TRF) from palm oil against potassium dichromate ($K_2Cr_2O_7$)-induced acute renal injury in rats. *Chemico-Biological Interactions*. 186(2): 228-238

https://doi.org/10.1016/j.cbi.2010.04.025

Ki, C, Cho, N. (1995) Scavenging effects of flavonoids on paraquat induced pulmonary toxicity. *The Korean Society of Environmental Toxicology*. 10(3∽4): 29-40

Kim, B, Eun, H, Lee, H, Chung, J. (1998) A study of a selection of antidotes for paraquat-induced skin damage. *Annals of Dermatology*. 10(1): 13-19

Kim, B, Shanu, A, Wood, S, Parry, N, Collet, M, McMahon, A, Witting, K. (2011) Phenolic antioxidants tert-butyl-bisphenol and vitamin E decrease oxidative stress and enhance vascular function in an animal model of rhabdomyolysis yet do not improve acute renal dysfunction. *Free Radical Research.* 45(9): 1000-1012

https://doi.org/10.3109/10715762.2011.590137

Kim, H, Park, B, oh, Y, Lee, Y, Lee, D, Kim, H, Kim, J, Shim, T, Lee, S. (2006) Green tea extract inhibits paraquat-induced pulmonary fibrosis by suppression of oxidative stress and endothelin-l expression. *Interstitial Lung Disease*. 184: 287–295

https://doi.org/10.1007/s00408-005-2592-x

Kim, J, Park, E, Ha, H, Jo, C, Lee, W, Lee, S, Kim, J. (2016) Resveratrol loaded nanoparticles induce antioxidant activity against oxidative stress. *The Asian-Australasian Association of Animal Production Societies*. 29(2): 288-298

http://doi.org/10.5713/ ajas 1 5 .0 774

Kim, S, He, L, Lemasters, J. (2003) Mitochondrial permeability transition: A common pathway to necrosis and apoptosis. *Biochemical and Biophysical Research Community.* 304(3): 463-470

https://doi.org/10.1016/s0006-291x(03)00618-1

Kim, S, Jin, Y, Lemasters, J. (2006) Reactive oxygen species, but not Ca_2+ overloading, trigger pH- and mitochondrial permeability transition-dependent death of adult rat myocytes after ischemia-reperfusion. *American Journal of Physiology. Heart and Circulatory Physiology.* 290(5): 2024-2034

https://doi.org/10.1152/ajpheart.00683.2005

Kimbrough, R. (1974) Toxic Effects of the Herbicide Paraquat. *Chest Journal*. 65(4): 65S–67S

https://doi.org/10.1378/chest.65.4_Supplement.65S

Kreuter, J. (1991) Nanoparticle based drug delivery systems. *Journal of Controlled Release*. 16: 169-176

https://doi.org/10.1016/0168-3659(91)90040-K

Kristl, J, Teskac, K, Caddeo, C, Abramovic, Z, Sentjurc, M. (2009) Improvements of cellular stress response on resveratrol in liposomes. *European Journal of Pharmaceutics and Biopharmaceutics.* 73(2): 253-259.

https://doi.org/10.1016/j.ejpb.2009.06.006

Kruidering, M, Van de Water, B, de Heer, E, Mulder, J, Nagelkerke, F. (1997) Cisplatin-induced nephrotoxicity in porcine proximal tubular cells: Mitochondrial dysfunction by inhibition of complexes I to IV of the respiratory chain. *The Journal of Pharmacology and Experimental Therapeutics.* 280(2): 638-49

PMID: 9023274

Kulkarni, S, Betageri, G, Singh, M. (1995) Factors affecting microencapsulation of drugs in liposomes. *Journal of Microencapsulation.* 12(3): 229-46

https://doi.org/10.3109/02652049509010292

Kumar, A, Dixit, C. (2017) Methods for characterization of nanoparticles. *Advances in Nanomedicine for the Delivery of Therapeutic Nucleic Acids.* 43-58

https://doi.org/10.1016/B978-0-08-100557-6.00003-1

Kumar, K, Naidu, M, Shifow, A, Ratnakar, A. (2000) Probucol protects against gentamicin-induced nephrotoxicity in rats. *Indian Journal of Pharmacology.* 32:108-113

Kumari, A, Kumar, V, Yadav, S. (2012) Plant extract synthesized PLA nanoparticles for controlled and sustained release of quercetin: A green approach. *PLoS One*. 7(7) :e41230

10.1371/journal.pone.0041230

Kyung Jo, S, Rosner, M, Okuso, M. (2007) Pharmacologic treatment of acute kidney injury: Why drugs haven't worked and what is on the horizon. *Clinical Journal of the American Society of Nephrology.* 2: 356-365

https://doi.org/10.2215/CJN.03280906

Laouini, A, Jaafar-Maalej, C, Limayem-Blouza, I, Sfar, S, Charcosset, C, Fessi, H. (2012) Preparation, characterization and applications of liposomes: State of the art. *Journal of Colloid Science and Biotechnology.* 1: 147-168

http://doi.org/10.1166/jcsb.2012.1020

Leach, M, Frank, S, Olbrich, A, Pfeilschifter, J, Thiemermann, C. (1998) Decline in the expression of copper/zinc superoxide dismutase in the kidney of rats with endotoxic shock: Effects of the superoxide anion radical scavenger, tempol, on organ injury. *British Journal of Pharmacology.* 125(4): 817–825

https://doi.org/10.1038/sj.bjp.0702123

Lee, B, Yun, Y, Park, K. (2016) PLA micro- and nano-particles. *Advanced Drug Delivery Reviews*. 107: 176-191

https://doi.org/10.1016/j.addr.2016.05.020

Lee, J, Yeo, Y. (2014) Controlled drug release from pharmaceutical nanocarriers. *Chemical Engineering Science.* 125: 75-84

https://doi.org/10.1016/j.ces.2014.08.046

Lee, S, Kim, Y, Cho, C, Kim, Y, Kim, S, Hur, S, Kim, J, Kim, B, Kim, S, Ryu, H, Kang, S. (2018) An open-label, randomized, parallel, phase II trial to evaluate the efficacy and safety of a cremophor-free polymeric micelle formulation of paclitaxel as first-line treatment for ovarian cancer: A Korean gynecologic oncology group study (KGOG-3021). *Cancer Research and Treatment*. 50(1): 195-203

https://doi.org/10.4143/crt.2016.376

Lee, S, Munerol, B, Pollard, S, Youdim, K, Pannala, A, Kuhnle, G, Debnam, E, Rice-Evans, C, Spencer, G. (2006) The reaction of flavanols with nitrous acid protects against *N*-nitrosamine formation and leads to the formation of nitroso derivatives which inhibit cancer cell growth. *Radical Biology and Medicine.* 40 (2): 323-334

https://doi.org/10.1016/j.freeradbiomed.2005.08.031

Lemasters, J, Nieminen, A, Qian, T, Trost, L, Elmore, S, Nishimura, Y, Crowe, R, Cascio ,W, Bradham, C, Brenner, D, Herman, B. (1998) The mitochondrial permeability transition in cell death: A common mechanism in necrosis, apoptosis and autophagy. *Biochimica et Biophysica Acta (BBA) - Bioenergetics.* 1366(1–2): 177-196

https://doi.org/10.1016/s0005-2728(98)00112-1

Levine, G, Frei, B, Koulouris, S, Gerhard, M, KeaneyJr, J, Vita, J. (1996) Ascorbic acid reverses endothelial vasomotor dysfunction in patients with coronary artery disease. *Circulation*. 93: 1107–1113

https://doi.org/10.1161/01.CIR.93.6.1107

Lewington, A, Cedra, J, Meht, R. (2013) Raising awareness of acute kidney injury: A global perspective of a silent killer. *Kidney International*. 84(3): 457-467

https://doi.org/10.1038/ki.2013.153

Li, J, Li, L, Wang, S, Zhang, C, Zheng, L, Jia, Y, Xu, M, Zhu, T, Zhang, Y, Rong, R. (2018) resveratrol alleviates inflammatory responses and oxidative stress in rat kidney ischemia-reperfusion injury and H_2O_2-induced NRK-52E Cells *via* the Nrf2/TLR4/NF-κB pathway. *Cellular Physiology and Chemistry.* 45(4): 1677-1689

https://doi.org/10.1159/000487735

Li, J, Wang, X, Zhang, T, Wang, C, Huang, Z, Luo, X, Deng, Y. (2015) A review on phospholipids and their main applications in drug delivery systems. *Asian Journal of Pharmaceutical Sciences*. 10(2): 81-98

https://doi.org/10.1016/j.ajps.2014.09.004

Li, R, Chen, H. (2012) Prevention of contrast-induced nephropathy with ascorbic acid. *Cardiovascular Disease Clinical Research*. 98(2): 211

https://doi.org/10.2169/internalmedicine.51.6260

Li, Y, Guangping, L, Liu, T, Yuan, R, Zheng, X, Xu, G, Xu, Y, Che, J, Liu, X, Ma, X, LI, F, Liu, E, Chen, X, Wu, L, Fan, Z, Ruan, Y, He, M, Li, Y. (2013) Probucol for the prevention of cystatin C-based contrast-induced acute kidney injury following primary or urgent angioplasty: A randomized, controlled trial. *International Journal of Cardiology.* 167(2): 426-429

https://doi.org/10.1016/j.ijcard.2012.01.017

Liang, H, Friedman, J, Nacharaju, P. (2016) Fabrication of biodegradable PEG–PLA nanospheres for solubility, stabilization, and delivery of curcumin. *Artificial Cells, Nanomedicine, and Biotechnology*. 45(2)

https://doi.org/10.3109/21691401.2016.1146736

Lima, I, Khalil, N, Tominaga, T, Lechanteur, A, Sarmento, B, Mainardes, R. (2018) Mucoadhesive chitosan-coated PLGA nanoparticles for oral delivery of ferulic acid. *Artificial Cells, Nanomedicines, and Biotechnology*. 46: 993-1002

https://doi.org/10.1080/21691401.2018.1477788

Lindner, G, Khalil, N, Mainardes, R. (2013) Resveratrol-loaded polymeric nanoparticles: Validation of an HPLC-PDA method to determine the drug entrapment and evaluation of its antioxidant activity. *The Scientific World Journal.* 2013: 506083

https://doi.org/10.1155/2013/506083

Linkerann, A, Zen, F, Weinberg, J, Kunzendorf, U, Krautwald. (2012) Programmed necrosis in acute kidney injury. *Nephrology Dialysis Transplantation.* 27(9): 3412-3419

https://doi.org/10.1093/ndt/gfs373

Liu, B, Hu, X. (2020) Hollow micro- and nanomaterials: Synthesis and applications. In: Zhao, Q. (eds) Micro and Nano Technologies. Advanced Nanomaterials for Pollutant Sensing and Environmental Catalysis. *Elsevier.* 1-38. ISBN: 9780128147962

https://doi.org/10.1016/B978-0-12-814796-2.00001-0

Liu, C, Ma, J, Lou, Y. (2010) Chronic administration of troxerutin protects mouse kidney against d-galactose-induced oxidative DNA damage. *Food and Chemical Toxicology.* 48(10): 2809-2817

https://doi.org/10.1016/j.fct.2010.07.011

Liu, F, Ni, W, Zhang, J, Wang, G, Li, F. Ren, W. (2017) Administration of curcumin protects kidney tubules against renal ischemia-reperfusion injury (RIRI) by modulating nitric oxide (NO) signalling pathway. *Cellular Physiology and Biochemistry.* 44: 401–411

https://doi.org/10.1159/000484920

Liu, N, Chen, J, Gao, D, Li, W, Zheng, D. (2018) Astaxanthin attenuates contrast agent-induced acute kidney injury *in vitro* and *in vivo via* the regulation of SIRT1/FOXO3a expression. *International Urology and Nephrology.* 50(6): 1171–1180

https://doi.org/10.1007/s11255-018-1788-y

Liu, P, Feng, Y, Wang, Y, Zhou, Y, Zhao, L. (2015) Protective effect of vitamin E against acute kidney injury. *Bio-Medical Materials and Engineering*. 26: 2133–2144

https://doi.org/10.3233/BME-151519

Lopes, J, Jorge, S. (2013) The RIFLE and AKIN classifications for acute kidney injury: A critical and comprehensive review**.** *Clinical Kidney Journal*. 6(1): 8–14

https://doi.org/10.1093/ckj/sfs160

Lu, D, Yang, L, Zhou, T, Lei, z. (2008) Synthesis, characterization and properties of biodegradable polylactic acid-β-cyclodextrin cross-linked copolymer microgels. *European Polymer Journal.* 44(7): 2140-2145

https://doi.org/10.1016/j.eurpolymj.2008.04.014

Lushchak, V. (2014) Classification of oxidative stress based on its intensity. *Experimental and clinical sciences journal*. 13: 922–937

https://www.ncbi.nlm.nih.gov/pubmed/26417312

Ma, H, Kuang, Z, Hao, Z, Gu, N. (2009) Preparation and characterization of tea polyphenols and vitamin E loaded nanoscale complex liposome. *Journal of Nanoscience and Nanotechnology*. 9(2): 1379-1383(5)

https://doi.org/10.1166/jnn.2009.C161

Ma, P, Mumper, R. (2013) Paclitaxel nano-delivery systems: A comprehensive review. *Journal of Nanomedicine and Nanotechnology.* 4(2): 1000164

hhtps://doi,org/10.4172/2157-7439.1000164

Makris, K, Spanou, L. (2016) Acute kidney injury: Definition, pathophysiology and clinical phenotypes. *The Clinical Biochemical Reviews*. 37(2): 85–98

http://www.ncbi.nlm.nih.gov/pmc/articles/pmc5198510/

Malik, S, Suchal, K, Bhatia, J, Gamad, N, Dinda, A, Gupta, Y, Arya, D. (2016) Molecular mechanisms underlying attenuation of cisplatin-induced acute kidney injury by epicatechin gallate. *Genitourinary and Reproductive Systems*. 96: 853-861

https://doi.org/10.1038/labinvest.2016.60

Mandade, R, Sreenivas, S, Sakarkar, D, Choudhury, A. (2011) Radical scavenging and antioxidant activity of *Hibiscus rosasinensis* extract. *African Journal of Pharmacy and Pharmacology*. 5(17): 2027-2034

https://doi.org/10.5897/AJPP11.522

Manosroi, A, Thathang, K, Werner, R, Schubert, R, Manosroi, J. (2008) Stability of luciferase plasmid entrapped in cationic bilayer vesicles. *International Journal of Pharmaceutics*. 356(1-2): 291-299

https://doi.org/10.1016/j.ijpharm.2008.01.001

Manzanares, D, Cena, V. (2020) Endocytosis: The nanoparticle and submicron nanocompounds gateway into the cell. *Pharmaceutics*. 12:371

https://doi.org/10.3390/pharmaceutics12040371

Martin, C, Sousa, F, Araujo, F, Sarmento, B. (2018) Functionalizing PLGA and PLGA derivatives for drug delivery and tissue regeneration applications. *Advanced Healthcare Materials*. 7: 1701035

https://doi.org/10.1002/adhm.201701035

Matteis, V. (2017) Exposure to inorganic nanoparticles: routes of entry, immune response, biodistribution and *in vitro/in vivo* toxicity evaluation. *Toxics*. 5(4): 29

https://doi.org/10.3390/toxics5040029

Mayer, B. (2015) Encyclopedia of nephrology and acute kidney injury. *Foster Academics.* 147,161,163. ISBN 978-1-63242-166-1

McCormick, C, Parker, R. (2004) The cytotoxicity of vitamin E is both vitamer- and cell-specific and involves a selectable trait. *The Journal of Nutrition*. 134(12): 3335-3342

https://doi.org/10.1093/jn/134.12.3335

Meydani, M. (2001) Vitamin E and atherosclerosis: Beyond prevention of LDL oxidation. *The Journal of Nutrition.* 131(2): 366S-368S

https://doi.org/10.1093/jn/131.2.366S

Mehta, R, *Kellum, J, Shah, S, Molitoris, B, Ronco, C, Warnock, D, Levin, A.* (2007) Acute kidney injury network: Report of an initiative to improve outcomes in acute kidney injury. *Critical Care*. 11: R31

https://doi.org/10.1186/cc5713

Mehta, R, *Cerda, J, Burdmann, E, Tonelli, E.* (2015) International society of nephrology's 0by25 initiative for acute kidney injury (zero preventable deaths by 2025): A human rights case for nephrology. *The Lancet Commissions.* 385(9987): 2616-2643

https://doi.org/10.1016/S0140-6736(15)60126-X

Mendoza, J. (2011) Acute kidney injury: Causes, diagnosis, and treatments. *Nova Science Publishers*, ISBN 987-1-61209-790-9.

Mercantepe, F, Mercantepe, T, Topcu, A, Yilmaz, A, Tumkaya, A. (2018) Protective effects of amifostine, curcumin, and melatonin against cisplatin-induced

acute kidney injury. *Naunyn-Schmiedeberg's Archives of Pharmacology*. 391(9): 915–931

https://doi.org/10.1007/s00210-018-1514-4

Merlin, J, Prasad, N, Shibli, S, Sebeela, M. (2012) Ferulic acid loaded Poly-d,l-lactide-co-glycolide nanoparticles: Systematic study of particle size, drug encapsulation efficiency and anticancer effect in non-small cell lung carcinoma cell line *in vitro*. *Biomedicine & Preventive Nutrition.* 2(1): 69-76

https://doi.org/10.1016/j.bionut.2011.12.007

Miele, D, Catenacci, L, Sorrenti, M, Rossi, S, Sandri, G, Malavasi, L, Dacarro, G, Ferrari, F, Bonferoni, M. (2019) Chitosan oleate coated poly lactic-glycolic acid (PLGA) nanoparticles versus chitosan oleate self-assembled polymeric micelles, loaded with resveratrol. *Marine Drugs*. 17(9): 515

https://doi.org/10.3390/md17090515

Min, J, Kim, E, Lee, J, Lee, H. (2018) Preparation, characterization, and cellular uptake of resveratrol-loaded trimethyl chitosan nanoparticles. *Food Science and Biotechnology*. 27(2): 441–450

https://dx.doi.org/10.1007%2Fs10068-017-0272-2

Modi, K, Morrisey, J, Shah, S, Schreiner, G, Klahr, S. (1990) Effects of probucol on renal function in rats with bilateral ureteral obstruction. *Kidney International.* 38: 835-850

https://doi.org/10.1038/ki.1990.280

Mohammed, M, Abdoulhoda, B, Mahmoud, R. (2018) Vitamin D attenuates gentamicin-induced acute renal damage *via* prevention of oxidative stress and DNA damage. *Human & Experimental Toxicology*. 38(3): 321-335

https://doi.org/10.1177/0960327118812166

Molinari, M, Watt, K, Kruszyna, T, Nelson, R, Walsh, M, Nashan, H, Peltekian, K. (2006) Acute liver failure induced by green tea extracts: Case report and review of the literature. *Liver Transplantation.* 12(12): 1892-1895

https://doi.org/10.1002/lt.21021

Moon, J, Shibamoto, T. (2009) Antioxidant assays for plant and food components. *Journal of Agricultural and Food Chemistry*. 57(5): 1655–1666

https://doi.org/10.1021/jf803537k

Moorkoth, D, Nampoothiri, K. (2014) Synthesis, colloidal properties and cytotoxicity of biopolymer nanoparticles. *Applied Biochemistry and Biotechnology.* 174(6)

10.1007/s12010-014-1172-z

Moosavi, S, Ghassabian, S. (2018) Linearity of calibration curves for analytical methods: a review of criteria for assessment of method reliability. In: Stauffer, M. Calibration and validation of analytical methods - A sampling of current approaches. *IntechOpen*.

https://doi.org/10.5772/INTECHOPEN.72932

Mossmann, T. (1983) Rapid colorimetric assay for cellular growth and survival: Application to proliferation and cytotoxicity assays. *Journal of Immunological Methods*. 65: 55-63

https://doi.org/10.1016/0022-1759(83)90303-4

Moustapha, A, Peretout, P, Rainey, N, Sureau, F, Geze, M, Petit, J, Dewailly, E, Slomianny, C, Petit, P. (2015) Curcumin induces crosstalk between autophagy and apoptosis mediated by calcium release from the endoplasmic reticulum, lysosomal destabilization and mitochondrial events. *Cell Death Discovery*. 1: 15017

doi:10.1038/cddiscovery.2015.17

Nabavi, S, Habtemariam, S, Nabavi, F, Sureda, A, Daglia, M, Moghaddam, A, Amani, M. (2013) Protective effect of gallic acid isolated from Peltiphyllum peltatum against sodium fluoride-induced oxidative stress in rat's kidney. *Molecular and Cellular Biochemistry.* 372(1-2): 233-239

Nabavi, S, Moghaddam, A, Eslami, S, Nabavi, M. (2011) Protective effects of curcumin against sodium fluoride-induced toxicity in rat kidneys. *Biological Trace Element Research*. 145(3): 369-374

https://doi.org/10.1007/s12011-011-9194-7

Nadal, J, Gomes, M, Borsata, D, Almeida, M, Barboza, F, Zawadzki, S, Farago, P, Zanin, S. Spray-dried solid dispersions containing ferulic acid: Comparative analysis of three carriers, *in vitro* dissolution, antioxidant potential and *in vivo* anti-platelet effect. *Drug Development and Industrial Pharmacy*. 42(11): 1813-1824

https://doi.org/10.3109/03639045.2016.1173055

Nagavarma, N, Yadav, H, Vasudha, A, Shivakumar, G. (2012) Different techniques for preparation of polymeric nanoparticles- A review. *Asian Journal of Pharmaceutical and Clinical Research.* 5(3): 16-23

https://doi.org/10.1007/s13346-013-0150-2

Nagesh, G, Charitra, Venkatapurwar, P, Lamprou, Dimitrios, Kumar, R. (2013) Towards scale-up and regulatory shelf-stability testing of curcumin encapsulated polyester nanoparticles. *Drug Delivery and Translational Research*. 3(3): 286-293

https://doi.org/10.1007/s13346-013-0150-2

Najafi, H, Ashtiyani, S, Sayedzadeh, S, Yarijani, Z, Fakhri, S. (2015) Therapeutic effects of curcumin on the functional disturbances and oxidative stress induced by renal ischemia/reperfusion in rats. *Aicenna Journal of Phytomedicine.* 5(6): 576–586

https://www.ncbi.nlm.nih.gov/pubmed/26693415

Narayanan, N, Nargi, D, Randolph, C, Naryanan, B. (2009) Liposome encapsulation of curcumin and resveratrol in combination reduces prostate cancer incidence in PTEN knockout mice. *International Journal of Cancer.* 125(1): 1-8

https://doi.org/10.1002/ijc.24336

Nasri, H, Adedi-Gheshlaghi, Z, Rafieian-Kopaei, M. (2016) Curcumin and kidney protection; current findings and new concepts. *Acta Persica Pathophysiologica.* 1(1): e01

Nasri, H, Ahmadi, A, Baradaran, A, Nasri, P, Hajian, S, Pour-Arian, A, Kohi, G, Rafieian-Kopaei, M. (2014) A biochemical study on ameliorative effect of green tea (*Camellia sinensis*) extract against contrast media induced acute kidney injury. *Journal of Renal Injury Prevention.* 3(2): 47–49

https://doi.org/10.12861/jrip.2014.16

Nechipadappu, S, Trivedi, D. (2018) Cocrystal of nutraceutical sinapic acid with active pharmaceutical ingredients ethenzamide and 2-chloro-4-nitrobenzoic acid: Equilibrium solubility and stability study. *Journal of Molecular Structure.* 1171: 898-905

https://doi.org/10.1016/j.molstruc.2018.06.074

Nelson, K, Dahlin, J, Bisson, J, Graham, J, Pauli, G, Walters, M. (2017) The essential medicinal chemistry of curcumin. *American Chemical Society Publications*. 60(5): 1620–1637

https://doi.org/10.1021/acs.jmedchem.6b00975

Newsholme, P, Fernades Cruzat, V, Keane, K, Carlessi, R, Bitterencourt Jr, P. (2016) Molecular mechanisms of ROS production and oxidative stress in diabetes. *Biochemical Journal.* 473 (24): 4527-4550

https://doi.org/10.1042/BCJ20160503C

Nguyen, T, Tang, Q, Daun, D, Dang, M. (2016) Micro and nano liposome vesicles containing curcumin for a drug delivery system. *Advances in Natural Sciences: Nanoscience and nanotechnology.* 7: 035003

https://doi.org/10.1088/2043-6262/7/3/035003

Nikdad, S, Ghasemi, H, Khiripour, N, Ranjbar, A. (2020) Antioxidative effects of nano-curcumin on liver mitochondria function in paraquat-induced oxidative stress. *Research in Molecular Medicine*. 8(1): 37-42

https://doi.org/10.32598/rmm.8.1.37

Niki, E, Abe, K. (2019) Vitamin E: Structure, properties and functions. In: Niki, E. (eds) Vitamin E: Chemistry and nutritional benefits. *Royal Society of Chemistry*. 1-11. ISBN: 978-1-78801-733-6

https://doi.org/10.1039/9781788016216

Nikiforovic, N, Abramovic, H. (2013) Sinapic acid and its derivatives: Natural sources and bioactivity. *Comprehensive Reviews in Food Science and Food Safety*. 13(1)

https://doi.org/10.1111/1541-4337.12041

Nisini, r, Poerio, N, Mariotti, S, DE Santis, F, Fraziano, M. (2018) The multirole of liposomes in therapy and prevention of infectious diseases. *Frontiers in Immunology*. 9:155

https://doi.org/10.3389/fimmu.2018.00155

Nithya, R. (2017) Antioxidant properties of sinapic acid: *In vitro* and *in vivo* approach*. Asian Journal of Pharmaceutical and Clinical Research*. 10(6): 255-262

https://doi.org/10.22159/ajpcr.2017.v10i6.18263

Noiri, E, Nakao, A, Uchida, K, Tsukahara, H, Ohno, M. (2001) Oxidative and nitrosative stress in acute renal ischemia. *The American Physiological Society*. 281(5): 948-957

https://doi.org/10.1152/ajprenal.2001.281.5.F948

Nowak, G, Aleo, D, Morgan, A, Schnellmann, G. (1998) Recovery of cellular functions following oxidant injury. *The American Journal of Physiology.* 274: 509-515

https://doi.org/10.1152/ajprenal.1998.274.3.F509

Okumura, H, Ikeda, Y, Ichitani, M, Takihara, T, Kuriyama, N, Nakajima, T, Shoji, N, Kunimoto, K. (2009) HPLC behaviour of tea catechins on cyclodextrin-bonded silica column. *Japanese Journal of Food Chemistry and Safety*. 16(3): 152-156

Olayinka, E, Ore, A, Ola, A, Adeyemo, O. (2015) Ameliorative effect of gallic acid on cyclophosphamide-induced oxidative injury and hepatic dysfunction in rats. *Medical Sciences.* 3(3): 78-92

https://dx.doi.org/10.3390%2Fmedsci3030078

Oliveira, A, Jager, E, Stepanek, P, Giacomelli, F. (2013) Physicochemical aspects behind the size of biodegradable polymeric nanoparticles: A step forward. *Colloids and Surfaces A: Physicochemical and Engineering Aspects.* 436: 1092-1102

https://doi.org/10.1016/j.colsurfa.2013.08.056

Ong, S, Chitneni. M, Lee, K, Ming, L, Yuen, K. (2016) Evaluation of extrusion technique for nanosizing liposomes. *Pharmaceutics*. 8(4): 36

https://dx.doi.org/10.3390%2Fpharmaceutics8040036

Ortiz-Ortiz, M, Moran, J, Bravosanpedro, J, González-Polo, B, Niso-Santano, M, Anantharam, V, Kanthasamy, A, Soler, G, Fuentes, J. curcumin enhances paraquat-induced apoptosis of N27 mesencephalic cells *via* the generation of reactive oxygen species. *Neurotoxicology*. 30(6): 1008–1018

https://dx.doi.org/10.1016%2Fj.neuro.2009.07.016

Ostro, M, Cullis, P. (1989) Use of Liposomes as Injectable-Drug Delivery Systems. *American Journal of Hospital Pharmacy.* 46(8): 1576-87

Ozkan, G, Ulusoy, S, Orem, A, Alkanat, M, Yucesan, B, Kaynar, K, Al, S. (2012) Protective effect of the grape seed proanthocyanidin extract in a rat model of contrast-induced nephropathy. *Kidney and Blood Pressure Research.* 35: 445–453

https://doi.org/10.1159/000337926

Padma, V, Sowmya, P, Felix, T, Baskaran, R, Poornima, P. (2011) Protective effect of gallic acid against lindane induced toxicity in experimental rats. *Food and Chemical Toxicology.* 49(4): 991-998

https://doi.org/10.1016/j.fct.2011.01.005

Paka, G, Ramassamy, C. (2017) Optimization of curcumin-loaded PEG-PLGA nanoparticles by GSH functionalization: Investigation of the internalization pathway in neuronal cells. *Molecular Pharmaceutics*. 14(1): 93–106

https://doi.org/10.1021/acs.molpharmaceut.6b00738

Palamoor, M, Jablonski, M. (2014) Comparative study on diffusion and evaporation emulsion methods used to load hydrophilic drugs in poly (ortho ester) nanoparticle emulsions. *Powder Technology.* 253: 53-62

https://doi.org/10.1016/j.powtec.2013.11.014

Palipoch, S. (2013) A Review of oxidative stress in acute kidney injury: Protective role of medicinal plants-derived antioxidants. *African Journal of Traditional, Complementary and Alternative Medicine.* 10(4): 88–93

https://doi.org/10.4314/ajtcam.v10i4.15

Paller, M, Hoidal, J, Ferris, T. (1984) Oxygen free radicals in ischemic acute renal failure in the rat. *Journal of Clinical Investigations.* 74(4): 1156–1164

https://dx.doi.org/10.1172%2FJCI111524

Palozza, P. (2004) Evidence for pro-oxidant effects of carotenoids *in vitro* and *in vivo*: Implications in health and disease. In: Krinsky, N, Mayne, S, Sies, H. (eds) Carotenoids in health and disease. *CRC Press*. ISBN: 1135534810, 9781135534813

Pamunuwa, G, Karunaratne, V, N, Karunaratne. (2015) Effect of lipid composition and preparation method on properties of ferulic acid encapsulated liposomes. *Third International Conference on Advances in Applied Science and Environmental Technology. ASET 2015.*

10.15224/978-1-63248-084-2-48

Pandita, D, Kumar, S, Poonia, N, Lather, V. (2014) Solid lipid nanoparticles enhance oral bioavailability of resveratrol, a natural polyphenol. *Food Research International.* 62: 1165-1174

https://doi.org/10.1016/j.foodres.2014.05.059

Pangeni, R, Pharm, B, Sahni, J, Ali, J, Sharma, S, Baboota, S. (2014) Resveratrol: Review on therapeutic potential and recent advances in drug delivery. *Expert Opinion on Drug Delivery.* 11(8): 1285-1298

https://doi.org/10.1517/17425247.2014.919253

Pannala, A, Chan, T, O'Brien, P, Rice-Evans, C. (2001) Flavonoid B-ring chemistry and antioxidant activity: Fast reaction kinetics. *Biochemical and Biophysical Research Communications*. 282: 1161–1168

https://doi:10.1006/bbrc.2001.4705

Pannala, A, Razaq, R, Halliwell, B, Singh, S, Rice-Evans, C. (1998) Inhibition of peroxynitrite- mediated tyrosine nitration by hydroxycinnamates: Nitration or electron donation? *Free Radical Biology & Medicine. 24(4): 594-60.*

https://doi.org/10.1016/S0891-5849(97)00321-3

Pannala, A, Rice-Evans, C, Halliwell, B, Singh, S. (1997) Inhibition of peroxynitrite-mediated tyrosine nitration by catechin polyphenols. *Biomedical and Biophysical Research Communications* 232: 164-168

https://doi.org/10.1006/bbrc.1997.6254

Pannala, A, Rice-Evans, C, Sampson, J, Singh, S. (1998) Interaction of peroxynitrite with carotenoids and tocopherols within low density lipoprotein. *Federation of European Biochemical Societies Letters.* 423. 297-301

https://doi.org/10.1016/S0014-5793(98)00108-2

Panwar, R, Pemmaraju, S, Sharma, A, Pruthi, V. (2016) Efficacy of ferulic acid encapsulated chitosan nanoparticles against *Candida albicans* biofilm. *Microbial Pathogenesis*. 95 (2016): 21-31

10.1016/j.micpath.2016.02.007

Park, S, Jo, N, Jeon, S. (2014) Chitosan-coated liposomes for enhanced skin permeation of resveratrol. *Journal of Industrial and Engineering Chemistry*. 20(4): 1481-1485

https://doi.org/10.1016/j.jiec.2013.07.035

Park, K, Park, J, Lee, H, Choi, J, Yu, W, Lee, J. (2018) Toxicity and tissue distribution of cerium oxide nanoparticles in rats by two different routes: single intravenous injection and single oral administration. *Archives of Pharmacal Research*. 41: 1108–1116

https://doi.org/10.1007/s12272-018-1074-7

Parveen, S, Misra, R, Sahoo, SK. (2012) Nanoparticles: A boon to drug delivery, therapeutics, diagnostics and imaging. *Nanomedicine: Nanotechnology, Biology and Medicine* 8(2):147

https://doi.org/10.1016/j.nano.2011.05.016

Patel, S, Beer, S, Kearney, D, Philips, G, Carter, B. (2013) Green tea extract: A potential cause of acute liver failure. *World Journal of Gastroenterology*. 19(31): 5174–5177

https://doi.org/10.3748/wjg.v19.i31.5174

Pavlakou, P, Zhang, H, O'Connor, Z, Chertow, M, Crowley, T, Choudhury, D, Finkel, K, Kellum, A, Paganini, E, Schein, M, Smith, W, Swanson, M, Thompson, T, Vijayan, A, Watnick, S, Star, A, Peduzzi, P. (2008) Intensity of renal support in critically ill patients with acute renal injury. *The New England Journal of Medicine*.359: 7-20

https://doi.org/10.1056/NEJMoa0802639

Pavlakou, P, Liakopoulos, V, Elftheriadis, T, Mitsis, M, Dounousi, E. (2017) Oxidative stress and acute kidney injury in critical illness: Pathophysiologic mechanisms-biomarkers-interventions, and future perspectives. *Oxidative Stress Cell Longevity*. 2017: 11

https://doi.org/10.1155/2017/6193694

Pearson, P, Lewis, S, Britton, J, Young, I, Fogarty, A. (2006) The pro-oxidant activity of high-dose vitamin E supplements *in vivo. BioDrugs*. 20: 271–273

https://doi.org/10.2165/00063030-200620050-00002

Penalva, R, Morales, J, Gonzalez-Navarro, J, Larrañeta , E, Quincoces, G, Penuelas, I, Irache, M. (2018). Increased oral bioavailability of resveratrol by its encapsulation in casein nanoparticles. *International Journal of Molecular Sciences*. 19(9): 2816

https://doi.org/10.3390/ijms19092816

Pentek, T, Newenhouse, E, O'Brien, B, Chauhan, A. (2017) Development of a topical resveratrol formulation for commercial applications using dendrimer nanotechnology. *Molecules.* 22(1): 137

https://doi.org/10.3390/molecules22010137

Perez-Ruiz, A, Ganem, A, Olivares-Corichi, I, Garcia-Sanchez, J. (2018) Lecithin–chitosan–TPGS nanoparticles as nanocarriers of (−)-epicatechin enhanced its anticancer activity in breast cancer cells. *Royal Society of Chemistry*. 8: 34773-34782

https://doi.org/10.1039/C8RA06327C

Picone, P, Bondi, M, Montana, G, Bruno, A, Pitarresi, G, Giammona, G, Carlo, M. (2009) Ferulic acid inhibits oxidative stress and cell death induced by Ab oligomers: improved delivery by solid lipid nanoparticles. *Free Radical Research*. 43(11): 1133-1145

10.1080/10715760903214454

Pillai, O, Panchagnula, R. (2001) Polymers in drug delivery. *Current Opinions in Chemical Biology*. 5(4): 447-451

https://doi.org/10.1016/s1367-5931(00)00227-1

Pinto Reis, C, Neufeld, RJ, Ribeiro, AJ, Veiga, F. (2006) Nanoencapsulation I. Methods for preparation of drug-loaded polymeric nanoparticles. *Nanomedicine: Nanotechnology, Biology, and Medicine* 2(1): 8-21

https://doi.org/10.1016/j.nano.2005.12.003

Poljsak, B, Raspor, P. (2004) The antioxidant and pro-oxidant activity of vitamin C and trolox *in vitro*: A comparative study. *Journal of Applied Toxicology*. 28(2): 183-188

https://doi.org/10.1002/jat.1264

Punfa, W, Yodkeeree, S, Pitchakarn, P, Ampasavate, C, Limtrakul, P. (2012) Enhancement of cellular uptake and cytotoxicity of curcumin-loaded PLGA nanoparticles by conjugation with anti-P-glycoprotein in drug resistance cancer cells. *Acta Pharmacologica Sinica*. 33(6): 823- 831

https://dx.doi.org/10.1038%2Faps.2012.34

Purohit, R, Mittal, A, Dalela, S, Warudkar, V, Purohit, S. (2017) Social, environmental and ethical impacts of nanotechnology. *Materials today: Proceedings.* 4(4)D: 5461-5467

https://doi.org/10.1016/j.matpr.2017.05.058

Puskas, I, Csempesz, F. (2007) Influence of cyclodextrins on the physical stability of DPPC-liposomes. *Colloids and Surfaces B: Biointerfaces.* 58(2): 218-224

10.1016/j.colsurfb.2007.03.011

Prado-Audelo, M, Caballero-Floran, I, Meza-Toledo, J, Mendoz-Munoz, N, Gonalez-Torres, M, Floran, B, Cortes, H, Leyva-Gomez, G. (2019) Formulations of curcumin nanoparticles for brain diseases. *Biomolecules.* 9(56)

https://doi.org/10.3390/biom9020056

Preedy, V. (2014) Aging: Oxidative stress and dietary antioxidants. *Academic Press. Elsevier.* 7.9. ISBN 978-0-12-405933-7.

Prince, P, Fischerman, L, Toblli, J, Fraga, C, Galleano, M. (2017) LPS-induced renal inflammation is prevented by (−)-epicatechin in rats. *Redox Biology.* 11: 342-349

https://dx.doi.org/10.1016%2Fj.redox.2016.12.023

Prior, R, Wu, X, Schaich, K. (2005) Standardized methods for the determination of antioxidant capacity and phenolics in foods and dietary supplements. *Journal of Agricultural and Food Chemistry*. 53(10): 4290–4302

https://doi.org/10.1021/jf0502698

Priyadarsini, K. (2014) The Chemistry of curcumin: From extraction to therapeutic agent. *Molecules*. 19: 20091-20112

https://doi.org/10.3390/molecules191220091

Qian, J, Deng, P, Liang, Y, Pang, L, Wu, L, Yang, L, Zhou, Z, Yu, Z. (2019) 8-Formylophiopogonanone B antagonizes paraquat-induced hepatotoxicity by suppressing oxidative stress. *Frontiers in Pharmacology*. 10: 1283

https://doi.org/10.3389/fphar.2019.01283

Qin, J, Chen, D, Lu, W, Xu, H, Yan, C, Hu, H, Chen, B, Qiao, M, Zhao, X. (2008) Preparation, characterization, and evaluation of liposomal ferulic acid *in vitro* and *in vivo*. *Drug Development and Industrial Pharmacy*. 34(6): 602-608

Qin, X, Zhang, S, Zarkovic, H, Nakatsuru, Y, Ishikawa, T, Ishikawa, T. (1995) Inhibitory effect of probucol on nephrotoxicity induced by ferric nitrilotriacetate (Fe-NTA) in rats. *Carcinogenesis.* 16(10): 2549–2552

https://doi.org/10.1093/carcin/16.10.2549

Rachmawati, H, Yanda, Y, Rahma, A, Mase, N. (2016) Curcumin-loaded PLA nanoparticles: Formulation and physical evaluation. *Scientia Pharmaceutica.* 84(1): 191–202

https://dx.doi.org/10.3797%2Fscipharm.ISP.2015.10

Radi, R, Beckman, J S, Bush, K M. (1991) Peroxynitrite-induced membrane lipid peroxidation: The cytotoxic potential of superoxide and nitric oxide. *Archives of Biochemistry and Biophysics.* 288.2

https://doi.org/10.1016/0003-9861(91)90224-7

Rah, D, Han, D, Baek, H, Hyon, S, Park, B, Park, J. (2007) Protection of rabbit kidney from ischemia/reperfusion injury by green tea polyphenol pre-treatment. *Archives of Pharmaceutical Research.* 30(11): 1447-1454

https://doi.org/10.1007/BF02977370

Rahman, M, Shad, F, Michael, C. (2012) Acute kidney injury: A guide to diagnosis and management. *American Family Physician.* 86(7): 631-639

Rai, M, Kon, K. (2015) Nanotechnology in diagnosis, treatment and prophylaxis of infectious diseases. 133-149. *Academic Press*. ISBN 9780128013175

Rangaswamy, D, Sud, K. (2018) Acute kidney injury and disease: Long-term consequences and management. *Nephrology*. 23: 969–980

https://doi.org/10.1111/nep.13408

Rao, JP, Geckeler, KE. (2011) Polymer nanoparticles: Preparation techniques and size-control parameters. *Progress in Polymer Science* 36(7): 887-913h

https://doi.org/10.1016/j.progpolymsci.2011.01.001

Ray, P, Haung, B, Tisuji, Y. (2012) Reactive oxygen species (ROS) homeostasis and redox regulation in cellular signalling. *Cell Signal.* 24(5): 981-990

https://doi.org/10.1016/j.cellsig.2012.01.008

Ratnam, D, Ankola, D, Bhardwaj, V, Sahana, D, Ravi Kumar, M. (2006) Role of antioxidants in prophylaxis and therapy: A pharmaceutical perspective. *Journal of Controlled Release.* 113(3): 189-207

https://doi.org/10.1016/j.jconrel.2006.04.015

Re, R, Pellegrini, N, Proteggente, A, Pannala, A, Yang, M, Rive-Evans, C. (1999) Antioxidant activity applying an improved ABTS radical cation assay. *Free Radical Biology and Medicine*. 26(9-10)

https//doi.org/10.1016/S0891-5849(98)00315-3

Rebholz, C, Crews, D, Grams, M, Steffen, L, Levey, A, Miller III, E, L, Coresh, J. (2016) DASH (Dietary Approaches to Stop Hypertension) Diet and risk of subsequent kidney disease. *American Journal of Kidney Diseases.* 68 (6): 853–861

https://doi.org/10.1053/j.ajkd.2016.05.019

Rees, O. (2010) Fourier transform infrared spectroscopy: Developments, techniques and applications. *Nova Science Publishers, Incorporated.* 1-4. ISBN: 9781613243831

Rehman, H, Krishnasamy, Y, Haque, K, Thurman, G, Lemasters, J, Schnellmann, G. (2013) Green tea polyphenols stimulate mitochondrial biogenesis and improve renal function after chronic cyclosporin a treatment in rats. *PLOS One.* 8: 1–12

https://doi.org/10.1371/journal.pone.0065029

Reis, C, Neufeld, R, Ribeiro, A, Veiga, F. (2006) Nanoencapsulation I. Methods for preparation of drug-loaded polymeric nanoparticles. *Nanomedicine: Nanotechnology, Biology and Medicine.* 2(1): 8-21

https://doi.org/10.1016/j.nano.2005.12.003

Rezaei, Y, Hemila, H. (2017) Vitamins E and C may differ in their effect on contrast-induced acute kidney injury. *American Journal of Kidney Disease.* 69(5): 708–709

https://doi.org/10.1053/j.ajkd.2016.12.022

Rivas, C, Tarhini, M, Badri, W, Miladi, K, Greige-Gerger, H, Nazari, Q, Rodriguez, S, Roman, R, Fessi, H, Elaissari, A. (2017) Nanoprecipitation process: From encapsulation to drug delivery. *International Journal of Pharmaceutics.* 532(1): 66-81

https://doi.org/10.1016/j.ijpharm.2017.08.064

Robson, A, Dastoor, P, Flynn, J, Palmer, W, Martin, A, Smith, D, Woldu, A, Hua, S. (2018) Advantages and limitations of current imaging techniques for characterizing liposome morphology. *Frontiers in Pharmacology*. 9: 80

https://doi.org/10.3389/fphar.2018.00080

Rodrigo, R. (2009) Oxidative stress and antioxidants: Their role in human diseases. *Nova Biomedical publishers, Inc.* 111-127. ISBN: 978-1-60741-554-1

Rogers, M, Stephenson, M, Kitching, A, Horowitz, J, Coates, P. (2011) Amelioration of renal ischaemia–reperfusion injury by liposomal delivery of curcumin to renal tubular epithelial and antigen-presenting cells. *British Journal of Pharmacology.* 166: 194–209

https://doi.org/10.1111/j.1476-5381.2011.01590.x

Ronco, C, Bellomo, R, Kellum, J. (2007) Acute kidney injury. *Contributions to Nephrology.* 156: 3-43. ISSN 0302-5144.156.

Roob, J, Khoschssorur, G, Tiran, A, Horina, J, Holzer, H, Winklhofer-Roob, B. (2000) Vitamin E attenuates oxidative stress induced by intravenous iron in patients on hemodialysis. *Journal of the American Society of Nephrology* 11: 539–549

Rotches-Ribalta, M, Andres-Lacueva, C, Estruch, R, Escribano, E, Urpi-Sarda. (2012) Pharmacokinetics of resveratrol metabolic profile in healthy humans after moderate consumption of red wine and grape extract tablets. *Pharmacological Research*. 66(5): 375-382

https://doi.org/10.1016/j.phrs.2012.08.001

Ruysschaert, T, Marque, A, Duteyrat, J, Lesieur, S, Winterhalter, M, Fournier, D. (2005) Liposome retention in size exclusion chromatography. *BMC Biotechnology*. 5:11

https://dx.doi.org/10.1186%2F1472-6750-5-11

Ryu, H, Kim, L, Chung, H, Lee, R, Kim, H, Shin, C. (2011) Renoprotective effects of green tea extract on renin-angiotensin-aldosterone system in chronic cyclosporine-treated rats. *Nephrology Dialysis Transplantation.* 26: 1188–1193

https://doi.org/10.1093/ndt/gfq616

Saad, A, Youssef, M, Shenaaway, L. (2009) Cisplatin induced damage in kidney genomic DNA and nephrotoxicity in male rats: The protective effect of grape seed proanthocyanidin extract. *Food and Chemical Toxicology.* 47(7):1499-1506

https://doi.org/10.1016/j.fct.2009.03.043

Sadat, U, Usman, A, Gillard, J, Boyle, J. (2013) Does Ascorbic acid protect against contrast-induced acute kidney injury in patients undergoing coronary angiography. A systematic review with meta-analysis of randomized, controlled trials. *Journal of the American College of Cardiology.* 62(23): 167-175

https://doi.org/10.1016/j.jacc.2013.07.065

Sadeghi, F, Nematbakhsh, M, Noori-Diziche, A, Eshraghi-Jazi, F, Talebi, A, Nasri, H, Mansuri, A, Dehghani, A, Saberi, S, Shirdavani, S, Ashrafi, F. (2015) Protective effect of pomegranate flower extract against gentamicin-induced renal toxicity in male rats. *Journal of Renal Injury Prevention.* 4(2): 45–50

https://dx.doi.org/10.12861%2Fjrip.2015.10

Safa, J, Argani, H, Bastani, B, Nezami, N, Ardebili, B, Ghorbanihaghjo, A, Kalagheichi, H, Amirfirouzi, A, Mesgari, M, Rad, G. (2010) Protective effect of grape seed extract on gentamicin induced acute kidney injury. *Iranian Journal of Kidney Diseases.* 4(4): 285-291

Sahu, B, Kumar, J, Sistla, R. (2015) Baicalein, a bioflavonoid, prevents cisplatin-induced acute kidney injury by up-regulating antioxidant defences and down-regulating the MAPKs and NF-κB pathways. *Peer-Reviewed Open Access Scientific Journal.* 10(7): e0134139

https://doi.org/10.1371/journal.pone.0134139

Salmonowicz, B, Krzystek-Korpacka, M, Noczynska, A. (2014) Trace elements, magnesium, and the efficacy of antioxidant systems in children with type 1 diabetes mellitus and in their siblings. *Advances in Clinical and Experimental Medicine.* 23(2): 259-68

https://doi.org/10.17219/acem/37074

Sayed, A. (2009) Proanthocyanidin protects against cisplatin-induced nephrotoxicity. *Phytotherapy Research.* 23(12): *1738-1741*

https://doi.org/10.1002/ptr.2833

Seely, R, Van Putte, C, Regan, J, Russo, A. (2011) Seely's anatomy and physiology, ninth edition. *McGraw-Hill*. ISBN: 978-0-07-352561-7

Sehwag, S, Das, M. (2013) Antioxidant activity: An overview. *Research & Reviews: Journal of Food Science & Technology*. 2(3): 1-10. ISSN: 2278 –2249

Selby, L, Cortez-Jugo, C, Such, G, Johnston, A. (2017) Nanoescapology: progress toward understanding the endosomal escape of polymeric nanoparticles. *WIREs Nanomedicine and Nanobiotechnology*. 9(5): e1452

https://doi-org.ezproxy.brighton.ac.uk/10.1002/wnan.1452

Semba, RD, Ferrucci, L, Bartali, B., 2014. Resveratrol levels and all-cause mortality in older community-dwelling adults. *JAMA Internal Medicine*. 174(7): 1077–1084

https://doi.org/10.1001/jamainternmed.2014.1582

Sercombe, L, Veerati, T, Moheimani, F, Wu, S, Sood, A, Hua, S. (2015) Advances and challenges of liposome assisted drug delivery. *Frontiers in Pharmacology.* 6:286

https://doi.org/10.3389/fphar.2015.00286

Schmuck, G, Rohrdanz, E, Tran-Thi, Q, Kahl, R, Schluter, G. (2002) Oxidative stress in rat cortical neurons and astrocytes induced by paraquat *in vitro*. *Neurotoxicity Research*. 4(1): 1-13

https://doi.org/10.1080/10298420290007574

Schwedhelm, E, Maas, R, Troost, R, Bogar, R. (2003) Clinical pharmacokinetics of antioxidants and their impact on systemic oxidative stress. *Clinical Pharmacokinetics.* 42(5): 437

https://doi.org/10.2165/00003088-200342050-00003

Shaito, A, Posadino, A, Younes, N, Hasan, H, Halabi, S, Alhababi, D, Al-Mohannadi, A, Abdel-Rahman, W, Eid, A, Nasrallah, G, Pintus, G. (2020) Potential adverse effects of resveratrol: A literature review. *International Journal of Molecular Sciences*. 21(6): 2084

https://doi.org/10.3390/ijms21062084

Shakeel, F, Raish, M, Anwar, K, Al-Shdefat, R. (2016) Self-nanoemulsifying drug delivery system of sinapic acid: *In vitro* and *in vivo* evaluation. *Journal of Molecular Lipids*. 224(A): 351-358

https://doi.org/10.1016/j.molliq.2016.10.017

Sharma, K, Steward, W, Gescher, A. (2007) Pharmacokinetic and pharmacodynamics of curcumin. *Advances in Experimental Medicine and Biology.* 595: 453-570

https://doi.org/10.1007/978-0-387-46401-5_20

Shi, Q, Wang, X, Tang, X, Zhen, N, Wang, Y, Luo, Zhang, H, Liu, J, Zhou, D, Huang, K. (2021) *In vitro* antioxidant and antitumor study of zein/SHA nanoparticles loaded with resveratrol. *Food Science and Nutrition*. 00: 1– 8

https://doi.org/10.1002/fsn3.2302

Shi, Y, Hua, Q, Li, N, Zhao, M, Cui, Y. (2019) Protective effects of evodiamine against LPS-induced acute kidney injury through regulation of ROS-NF-κB-mediated inflammation. *Evidence-Based Complementary and Alternative Medicine.* Article ID 2190847

https://doi.org/10.1155/2019/2190847

Shin, C, Kwon, E, Chung, H, Kim, L. (2012) The antiproteinuric effects of green tea extract on acute cyclosporine-induced nephrotoxicity in rats. *Transplantation Proceeding.* 44(4): 1080-1082

https://doi.org/10.1016/j.transproceed.2012.03.047

Song, N, Thaiss, F, Guo, L. (2019) NFκB and kidney injury. *Frontiers in Immunology*. 10: 815

https://doi.org/10.3389/fimmu.2019.00815

Sonntag, C. (2006) Free Radical-Induced DNA Damage and Its Repair: A Chemical perspective. *Springer Science & Business Media.* ISBN 3540305920, 9783540305927.

Silva, D, Kaduri, M, Poley, M, Adir, O, Krinsky, N, Shainsky-Roitman, J, Schroeder, A. (2018) Biocompatibility, biodegradation and excretion of polylactic acid (PLA) in medical implants and theranostic systems. *Chemical Engineering Journal. 340: 9-14*

https://doi.org/10.1016/j.cej.2018.01.010

Soo, E, Thakur, S, Qu, Z, Jambhrunkar, S, Parekh, H, Popat, A. (2015) Enhancing delivery and cytotoxicity of resveratrol through a dual nanoencapsulation approach. *Journal of Colloid and Interface Science*. S0021-9797(15)30267-8

http://dx.doi.org/10.1016/j.jcis.2015.10.022

Soppimath, K, Aminabhavi, T, Kulkarni, A, Rudzinski, W. (2001) Biodegradable polymeric nanoparticles as drug delivery devices. *Journal of Controlled Release.* 70(1–2): 1-20

https://doi.org/10.1016/S0168-3659(00)00339-4

Sotler, R, Poljsak, B, Dahmane, R, Jukic, T, Jukic, D, Rotim, C, Trese, Starc, A. (2019) Prooxidant activities of antioxidants and their impact on health. *Acta Clinica Croatica*. 58(4): 726–736

https://dx.doi.org/10.20471%2Facc.2019.58.04.20

Spickett, C, Forma, H. (2015) Lipid Oxidation in Health and Disease. *CRC Press, Taylor & Francis Group.* ISBN: 978-1-4822-0286-1

Stanic, Z., 2017. Curcumin, a compound from natural sources, a true scientific challenge - A Review. *Plant Foods for Human Nutrition*. 72(1): 1-12

https://doi.org/10.1007/s11130-016-0590-1

Stojiljkovic, N, Ilic, S, Veljkovic, Todorovic, J, Mladenovic, M. (2018) α-Tocopherol reduces morphological changes and oxidative stress during gentamicin-induced acute renal failure. *Bulletin of Experimental Biology and Medicine.* 164: 442–445

https://doi.org/10.1007/s10517-018-4008-y

Stoller, M, Berger, A. (2009) Laparoscopic renal surgery.

http://health-fts.blogspot.com/2012/04/laparoscopic-renal-surgery.html. Accessed on 25/10/2018.

Storka, A, Vcelar, B, Klickovic, U, Gouya, G, Wesshaar, S, Aschaur, S, Helson, L, Wolzt, M. (2013) Effect of liposomal curcumin on red blood cells *in vitro. Anticancer Research*. 33(9): 3629-3634

Surh, Y. (2005) Oxidative Stress, Inflammation, and Health. *CRC Press. Taylor & Francis Group. 2-4.* ISBN 978-0-8247-2733-8.

Suntres Z. (2002) Role of antioxidants in paraquat toxicity. *Toxicology.* 180(1) 30: 65-77

https://doi.org/10.1016/S0300-483X(02)00382-7

Suntres, Z, Hepworth, S, Shek, P. (1993) Pulmonary uptake of liposome-associated α-tocopherol following intratracheal instillation in rats. *Journal of Pharmacy and Pharmacology*. 45(6): 514-520

https://doi.org/10.1111/j.2042-7158.1993.tb05590.x

Suntres, Z, Shek, P. (2008) Liposomal α-tocopherol alleviates the progression of paraquat-induced lung damage. *Journal of Drug Targeting*. 2(6): 493-500

https://doi.org/10.3109/10611869509015919

Sutton, T. (2009) Alteration of microvascular permeability in acute kidney injury. *Microvascular Research.* 77(1): 4–7

https://dx.doi.org/10.1016%2Fj.mvr.2008.09.004

Takeyama, N, Miki, S, Hirakawa, A, Tanaka, T. (2002) Role of the mitochondrial permeability transition and cytochrome C release in hydrogen peroxide-induced apoptosis. *Experimental Cell Research.* 274(1): 16-24

https://doi.org/10.1006/excr.2001.5447

Tan, Y, Ho, H. (2018) Navigating albumin-based nanoparticles through various drug delivery routes. *Drug Discovery Today*. 23(5): 1108-1114

https://doi.org/10.1016/j.drudis.2018.01.051

Tanabe, K, Tamura, Y, Lanaspa, M, Miayzaki, M. (2012) Epicatechin limits renal injury by mitochondrial protection in cisplatin nephropathy. *American Journal of Physiology. Renal Physiology*. 303(9): 1264-1274

https://doi.org/10.1152/ajprenal.00227.2012

Tang, D, Yu, S, Ho, Y, Huang, B, Tsai, G, Hsieh, H, Sung, H, Mi, F. (2012) Characterization of tea catechins-loaded nanoparticles prepared from chitosan and an edible polypeptide. *Food Hydrocolloids*. 30(1): 33-41

https://doi.org/10.1016/j.foodhyd.2012.04.014

Taouzinet, L, Fatmi, S, Khellouf, A, Skiba, M, Iguer-ouada, M. (2020) Alpha tocopherol loaded in liposome: Preparation, optimization, characterization and sperm motility protection. *Drug Delivery Letters*. 10(3): 228-236

https://doi.org/10.2174/2210303110666200302113209

Tapia, E, Sanchez-Lozada, L, Garcia-Nino, W, Garcia, E, Cerecedo, A, Garcia-Arroyo, E. (2014) Curcumin prevents maleate-induced nephrotoxicity: Relation to hemodynamic alterations, oxidative stress, mitochondrial oxygen consumption and activity of respiratory complex I. *Free Radical Research.* 48(11): 1342-1354

https://doi.org/10.3109/10715762.2014.954109

Tasanarong, A, Kongkham, S, Itharat, A. (2014) Antioxidant effect of *Phyllanthus emblica* extract prevents contrast-induced acute kidney injury. *Biomedcentral, Complementary and Alternative Medicine.* 14:138

https://doi.org/10.1186/1472-6882-14-138

Tasanarong, A, Vohakiat, A, Hutayanon, P, Piyayotai, D. (2013) New strategy of α- and γ-tocopherol to prevent contrast-induced acute kidney injury in chronic kidney disease patients undergoing elective coronary procedures. *Nephrology Dialysis Transplantation*. 28(2): 337–344

https://doi.org/10.1093/ndt/gfs525

Thaker, C. (2013) Perioperative acute kidney injury. *Advances in chronic kidney disease.* 20(1): 67

https://doi.org/10.1053/j.ackd.2012.10.003

Thaker, C, Chrisianson, A, Freyberg, R, Almenoff, P, Render, L. (2009) Incidence and outcomes of acute kidney injury in intensive care units: A veterans administration study. *Critical Care Medicine*. 37(9): 2552

https://doi.org/10.1097/CCM.0b013e3181a5906f

Thong, P, Nam, N, Phuc, N, Manh, D, Thu, H. (2014) Impact of PLA/PEG ratios on curcumin solubility and encapsulation efficiency, size and release behavior of curcumin loaded poly(lactide)-poly(ethylenglycol) polymeric micelles. *International Journal of Drug Delivery.* 6: 279-285

Topcu-Tarladacalisir, Y, Sapmaz-Metin, M, Karaca, T. (2016) Curcumin counteracts cisplatin-induced nephrotoxicity by preventing renal tubular cell apoptosis. *Renal Failure.* 38(10): 1741-1748

https://doi.org/10.1080/0886022X.2016.1229996

Ugur, S, Ulu, R, Dogukan, D, Gurel, A, Pembegul, Y, Gozel, N. (2014) The renoprotective effect of curcumin in cisplatin-induced nephrotoxicity. *Renal Failure.* 37(2): 332-336

https://doi.org/10.3109/0886022X.2014.986005

Ulusoy, S, Ozkan, G, Alkanat, M, Mungan, S, Yulug, E, Orem, A. (2013) Perspective on rhabdomyolysis-induced acute kidney injury and new treatment options. *American Journal of Nephrology.* 38: 368-378

https://doi.org/10.1159/000355537

Ulusoy, S, Ozkan, G, Yucesan, F, Eroz, S, Orem, A, Alkanat, M, Yulug, E, Kaynar, K, Al, S. (2012) Anti-apoptotic and antioxidant effects of grape seed

proanthocyanidin extract in preventing cyclosporine A-induced nephropathy. *Nephrology.* 17(4): 372-379

https://doi.org/10.1111/j.1440-1797.2012.01565.x

Vagra. N, Turcsanyi, A, Hornok, V, Csapo, E. (2019) Vitamin E-loaded PLA- and PLGA-based core-shell nanoparticles: Synthesis, structure optimization and controlled drug release. *Pharmaceutics*. 11(7): 357

https://doi.org/10.3390/pharmaceutics11070357

Vakifahmetoglu-Norberg, H, Ouchida, A, Norberg, E. (2016) The Role of mitochondria in metabolism and cell death. *Biochemical and Biophysical Research Communications.* 482(3): 426-431

https://doi.org/10.1016/j.bbrc.2016.11.088

Valavanidis, A, Vlachogianni, T, Fiotakis, C. (2009) 8-hydroxy-2-deoxyguanosine (8-OHdG): A critical biomarker of oxidative stress and carcinogenesis. *Journal of Environmental Science and Health Part C*. 27: 120–139.

https://doi.org/10.1080/10590500902885684

Vance, M, Kuiken, T, Vejerano, E, McGinnis, S, Hochella Jr, M, Rejeski, D, Hull, M. (2015) Nanotechnology in the real world: Redeveloping the nanomaterial consumer products inventory. *Beilstein Journal of Nanotechnology*. 6: 1769–1780

https://doi.org/10.3762/bjnano.6.181

Vauthier, C, Bouchemal, K. (2009) Methods for the preparation and manufacture of polymeric nanoparticles. *Pharmaceutical Research*. 26(5): 1025-58

https://doi.org/10.1007/s11095-008-9800-3

Veljkovic, M, Pavlovic, D, Stojiljkovic, N, Ilic, S, Petrovic, A, Jovanovic, I, Radenkovic, M. (2016) Morphological and morphometric study of protective effect of green tea in gentamicin-induced nephrotoxicity in rats. *Life Sciences.* 147(15): 85-91

https://doi.org/10.1016/j.lfs.2016.01.035

Vijayakumar, S. (2019) Stability Studies on Nanomaterials Used in Drugs. Characterization and biology of nanomaterials for drug delivery. *Micro and Nano Technologies.* 15: 425-444. ISBN 9780128140314

https://doi.org/10.1016/B978-0-12-814031-4.00015-5

Vlahovic, P, Cvetkovic, T, Savic, V, Stefanovic, V. (2007) Dietary curcumin does not protect kidney in glycerol-induced acute renal failure. *Food and Chemical Toxicology. 45(9): 1777-1782*

https://doi.org/10.1016/j.fct.2007.04.004

Waikar, S, Bonventre, J. (2008) Creatinine kinetics and the definition of acute kidney injury. *Journal of the American Society of Nephrology.* 20(3): 672-679

https://doi.org/10.1681/ASN.2008070669

Wald, R, Quinn, R, Luo, J, Li, P, Scales, C, Mamdani, M, Ray, G. (2009) Chronic dialysis and death among survivors of acute kidney injury requiring dialysis. *The Journal of the American Medical Association*. 302(11): 1179-1185

https://doi.org/10.1001/jama.2009.1322

Walle, T. (2011) Bioavailability of resveratrol. *Annals of the New York Academy of Sciences.* 1215(1): 9-15

https://doi.org/10.1111/j.1749-6632.2010.05842.x

Wang, L, Rao, Y, Liu, X, Sun, L, Gong, J, Zhang, H, Shen, L, Bao, A, Yang, H. (2021) Administration route governs the therapeutic efficacy, biodistribution and macrophage targeting of anti-inflammatory nanoparticles in the lung. *Journal of Biotechnology*. 19: 56

https://doi.org/10.1186/s12951-021-00803-w

Wang, N, Mao, L, Yang, L, Zou, J, Liu, K, Liu, M, Zhang, H, Xiao, X, Wang, K. (2017) Resveratrol protects against early polymicrobial sepsis-induced acute kidney injury through inhibiting endoplasmic reticulum stress-activated NF-κB pathway. *Oncotarget.* 8(22): 36449–36461

https://doi.org/10.18632/oncotarget.16860

Wang, N, Wei, R, Li, Q, Yang X, LI, P, Huang, M, Wang, R, Cia, G, Chen, X. (2015) Renal protective effect of probucol in rats with contrast-induced nephropathy and its underlying mechanism. *Medical Science Monitor.* 21: 2886–2892

https://dx.doi.org/10.12659%2FMSM.895543

Wang, Q, Rojas, E, Papadopoulosa, K. (2012) Cationic liposomes in double emulsions for controlled release. *Journal of Colloid and Interface Science*. 383(1): 89-95

https://doi.org/10.1016/j.jcis.2012.06.036

Wang, W, Jittikanont, S, Falk, S, Shrir, R. (2003) Interaction among nitric oxide, reactive oxygen species, and antioxidants during endotoxemia-related acute renal failure. *Renal Physiology*. 284(3): 532-537

https://doi.org/10.1152/ajprenal.00323.2002

Wenzel, E, Somoza, V. (2005) Metabolism and bioavailability of trans-resveratrol. *Molecular Nutrition and Food Research.* 49(5): 472-81

https://doi.org/10.1002/mnfr.200500010

Williams, R, Shah, J, Brandon, Ng, Minton, D, Gudas, L, Park, C, Heller, D. (2015) Mesoscale nanoparticles selectively target the renal proximal tubule epithelium. *Nano Letters*. 15(4): 2358–2364

https://dx.doi.org/10.1021%2Fnl504610d

Williams, R, Shah, J, Tian, H, Chen, X, Geissmann, F, Jaimes, E, Heller, D. (2018) Selective nanoparticle targeting of the renal tubules. *Hypertension*. 71(1): 87–94.

https://dx.doi.org/10.1161%2FHYPERTENSIONAHA.117.09843

Wu, J, Pan, X, Fu, H, Zheng, Y, Dai, Y, Yin, Y, Chen, Q, Hao, Q, Bao, D, Hou, D. (2017) Effect of curcumin on glycerol-induced acute kidney injury in rats. *Scientific Reports.* 7: 10114

Wu, Y, Wang, D, Li, Y. (2014) Nanocrystals from solutions: Catalysts. *Chemical Society Reviews*. 43: 2112-2124

https://doi-org.ezproxy.brighton.ac.uk/10.1039/C3CS60221D

Xiao, F, Xu, T, Lu, B, Liu, R. (2020) Guidelines for antioxidant assays for food components. *Food Frontiers*. 1(1): 60-69

https://doi.org/10.1002/fft2.10

Xiao, XF, Gao, MY, Zhu, QH, Mo, F, Liu, HL, Gao, S. (2009) Studies on pharmacokinetics and metabolism of ferulic acid. *Asian Journal of Pharmacodynamics and Pharmacokinetics* 9(2): 135-143

Xu, S, Gao, Y, Zhang, Q, Wei, S, Chen, Z, Dia, X, Zeng, Z, Zhao, K. (2016) SIRT1/3 Activation by resveratrol attenuates acute kidney injury in a septic rat model. *Oxidative Medicine and Cellular Longevity.* 2016: 12

https://doi.org/10.1155/2016/7296092

Xu, S, Wang, G, Liu, H, Wang, L, Wang, H. (2007) A DMol^3 study on the reaction between trans-resveratrol and hydroperoxyl radical: Dissimilarity of antioxidant activity among O–H groups of trans-resveratrol. *Journal of Molecular Structure: THEOCHEM*. 806(1-3): 79-85

https://doi.org/10.1016/j.theochem.2007.01.036

Xu, Y, Zhang, B, Xie, D, Hu, Y, Li, H, Zhong, L, Wang, H, Jiang, W, Ke, Z, Zheng, D. (2017) Nanoparticle-mediated dual delivery of resveratrol and DAP5 ameliorates kidney ischemia/reperfusion injury by inhibiting cell apoptosis and inflammation. *Oncotarget.* 8(24): 39547–39558

https://doi.org/10.18632/oncotarget.17135

Yadav, R, Kumar, D, Kumari, A, Yadaf, S. (2014) Encapsulation of catechin and epicatechin on BSA NPS improved their stability and antioxidant potential. *Experimental and Clinical Science.* 13: 331–346

https://www.ncbi.nlm.nih.gov/pubmed/26417264

Yamanobe, T, Okada, F, Iuchi, Y, Onuma, K, Tomita, Y, Fujii, J. Deterioration of ischemia/reperfusion-induced acute renal failure in SOD1-deficient mice. *Free Radical Research.* 41(2): 200-207

https://doi.org/10.1080/10715760601038791

Yan, H, Wang, H, Zhang, X, Li, X, Yu, J. (2015) Ascorbic acid ameliorates oxidative stress and inflammation in dextran sulphate sodium-induced ulcerative colitis in mice. *International Journal of Clinical and Experimental Medicine*. 8(11): 20245–20253

http://www.ncbi.nlm.nih.gov/pmc/articles/pmc4723782/

Yan, X, Cao, Li, Y, Xiao, P, Huang, Z, Li, H, Ma, Y. (2019) Internalization and subcellular transport mechanisms of different curcumin loaded nanocarriers across Caco-2 cell model. *Journal of Drug Delivery Science and Technology*. 52: 660-669

https://doi.org/10.1016/j.jddst.2019.05.040

Yang, D, Wang, F, Zhang, L, Gong, N, Lv, Y. (2015) Development of a new ferulic acid certified reference material for use in clinical chemistry and pharmaceutical analysis. *Acta Pharmaceutica Sinica B.* 5(3): 231-237

https://doi.org/10.1016/j.apsb.2015.03.009

Yang J, Lu C, Yan L, Tang X, Li W, Yang Y, Hu D. (2013) The association between atherosclerotic renal artery stenosis and acute kidney injury in patients undergoing cardiac surgery. *Peer-Reviewed Open Access Scientific Journal.* 8(5): 64104

https://doi.org/10.1371/journal.pone.0064104

Yang, Y, Liu, H, Shi, A, Liu, L, Hu, H, Wang, Q. (2017) *In vitro* bioavailability of resveratrol encapsulated in liposomes: Influence of chitosan coating and liposome compositions. *Journal of Controlled Release*. 259: 172-173

https://doi.org/10.1016/j.jconrel.2017.03.342

Yasmin, H, Murugesan, R, Girigoswami, A. (2014) Gene Expression profile induced by liposomal nanoformulation of anticancer agents: Insight into cell death mechanism. *Advanced Science Engineering and Medicine*. 6(2): 159-165

10.1166/asem.2014.1476

Yin, L, Li GP, Liu T, Liu M, Chen X, He M, Zheng X, Liu E, Zhou L. (2009) Role of probucol in preventing contrast induced acute kidney injury after coronary interventional procedure: a randomized trial. *Zhonghua Xin Xue Guan Bing Za Zhi*. 37(5): 385-388

Yu, M, Xue, J, LI, Y, Zhang, W, Ma, D, Liu, L, Zhang, Z. (2013) Resveratrol protects against arsenic trioxide-induced nephrotoxicity by facilitating arsenic metabolism and decreasing oxidative stress. *Achieves of Toxicology.* 87(6): 1025-1035

https://doi.org/10.1007/s00204-013-1026-4

Yucel, C, Seker-Karatoprak, G. (2017) Development and evaluation of the antioxidant activity of liposomes and nanospheres containing rosmarinic acid. *Farmacia*. 65:1

Zaborova, O, Filippov, S, Chytil, P, Kovacik, L, Ulbrich, K, Yaroslavov, A, Etrych, T. (2018) A novel approach to increase the stability of liposomal containers *via* in

prep coating by Poly[N-(2-hydroxypropyl)methacrylamide] with covalently attached cholesterol groups. *Macro-Molecular Chemistry and Physics.* 219(7): 1700508

https://doi.org/10.1002/macp.201700508

Zdunska, K, Dana, A, Kolodziejczak, A, Rotsztejn, H. (2018) Antioxidant properties of ferulic acid and its possible application. *Skin Pharmacology and Physiology*. 31: 332–336

DOI: 10.1159/000491755

Zhang, H, Sun, S. (2015) NF-κB in inflammation and renal diseases. *Cell & Bioscience*. 5: 63

https://doi.org/10.1186/s13578-015-0056-4

Zhang, H, Sun, X, Cao, J, Zhou, H, Guo, X, Wang, Y. (2014) Protective effect of epimedium combined with oligomeric proanthocyanidins on exercise-induced renal ischemia-reperfusion injury of rats. *International Journal of Clinical and Experimental Medicine.* 7(12): 5730–5736

PMCID: PMC4307546

Zhao, H, Zhao, M, Wang, Y, Li, F, Zhang, Z. (2016) Glycyrrhizic acid attenuates sepsis-induced acute kidney injury by inhibiting NF-κB Signaling pathway. *Evidence-Based Complementary and Alternative Medicine.* Article ID 8219287

https://doi.org/10.1155/2016/8219287

Zhao, J, Stenzel, M. (2018) Entry of nanoparticles into cells: the importance of nanoparticle properties. *Polymer Chemistry*. 9: 259-272

https://doi.org/10.1039/C7PY01603D

Zigoneanu, I, Astete, C, Sabliov, C. (2008) Nanoparticles with entrapped α-tocopherol: Synthesis, characterization, and controlled release. *Nanotechnology.* 19(10): 105606

https://doi.org/10.1088/0957-4484/19/10/105606

Appendices

(Due to the large number of data produced, only selected reports are displayed)

Appendix I: particle size reports

a. Particle size analysis report for sample 9-TL (α-Tocopherol-loaded liposomes) produced by the Zetasizer software

Size Distribution Modal Analysis
v2.1

Malvern

Sample Details

Sample Name:	a-Tocopherol LP size 1		
SOP Name:	mansettings.nano		
General Notes:			
File Name:	alpha-tocopherol LP.dts	**Dispersant Name:**	Water
Record Number:	1	**Dispersant RI:**	1.330
Material RI:	1.59	**Viscosity (cP):**	0.8872
Material Absorbtion:	0.010	**Measurement Date and Time:**	05 November 2019 14:02:43

System

Temperature (°C):	24.9	**Duration Used (s):**	60
Count Rate (kcps):	282.1	**Measurement Position (mm):**	4.65
Cell Description:	Disposable sizing cuvette	**Attenuator:**	9

Results

		Size (d.n...	Width (d.n...	% Intensity	: Volume	: Num...
Z-Average (d.nm):	177.2	**Peak 1:** 184.2	39.85	100.0	100.0	100.0
PdI:	0.006	**Peak 2:** 0.000	0.000	0.0	0.0	0.0
Intercept:	0.882	**Peak...** 0.000	0.000	0.0	0.0	0.0
Result quality	Good					

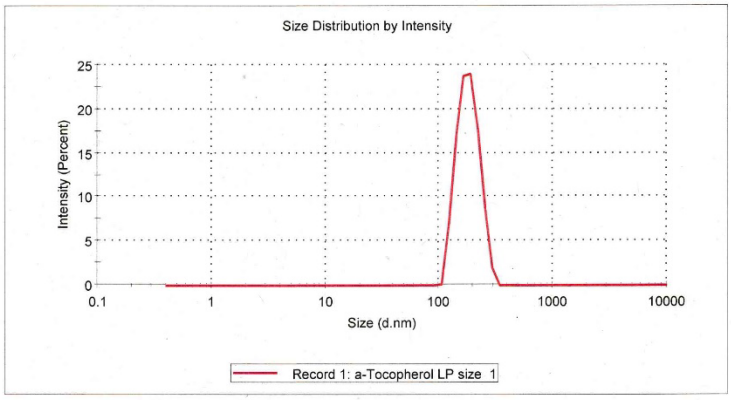

Malvern Instruments Ltd
www.malvern.com

Zetasizer Ver. 7.11
Serial Number : MAL1057082

File name: alpha-tocopherol LP.dts
Record Number: 1
05 Nov 2019 14:09:37

b. Particle size analysis report for sample 9-CL (curcumin liposomes) on the first day of preparation

Size Distribution Report by Volume

v2.2

Malvern

Sample Details

Sample Name: Curcumin LP size day1 3
SOP Name: mansettings.nano
General Notes:

File Name:	curcumin stability.dts	**Dispersant Name:**	Water
Record Number:	3	**Dispersant RI:**	1.330
Material RI:	1.59	**Viscosity (cP):**	0.8872
Material Absorbtion:	0.010	**Measurement Date and Time:**	16 September 2019 15:4...

System

Temperature (°C):	25.0	**Duration Used (s):**	60
Count Rate (kcps):	269.3	**Measurement Position (mm):**	4.65
Cell Description:	Disposable sizing cuvette	**Attenuator:**	9

Results

			Size (d.nm):	% Volume:	St Dev (d.nm):
Z-Average (d.nm):	148.5	**Peak 1:**	132.8	100.0	79.18
PdI:	0.160	**Peak 2:**	0.000	0.0	0.000
Intercept:	0.962	**Peak 3:**	0.000	0.0	0.000
Result quality	Good				

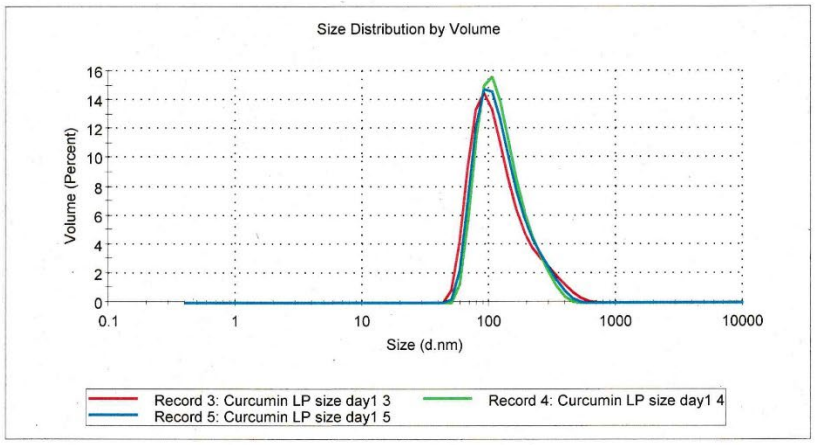

c. Particle size analysis report for sample 9-CL (curcumin liposomes) on the tenth day after preparation

Size Distribution Report by Intensity

v2.2

Malvern

Sample Details

Sample Name: curcumin LP size day10 3
SOP Name: mansettings.nano
General Notes:

File Name: curcumin stability.dts
Record Number: 38
Material RI: 1.59
Material Absorbtion: 0.010
Dispersant Name: Water
Dispersant RI: 1.330
Viscosity (cP): 0.8872
Measurement Date and Time: 25 September 2019 14:36:02

System

Temperature (°C): 25.1
Count Rate (kcps): 242.9
Cell Description: Disposable sizing cuvette
Duration Used (s): 70
Measurement Position (mm): 4.65
Attenuator: 9

Results

			Size (d.n...	% Intensity:	St Dev (d.n...
Z-Average (d.nm):	182.5	Peak 1:	189.1	95.2	67.76
PdI:	0.227	Peak 2:	4640	4.8	810.1
Intercept:	0.959	Peak 3:	0.000	0.0	0.000

Result quality Good

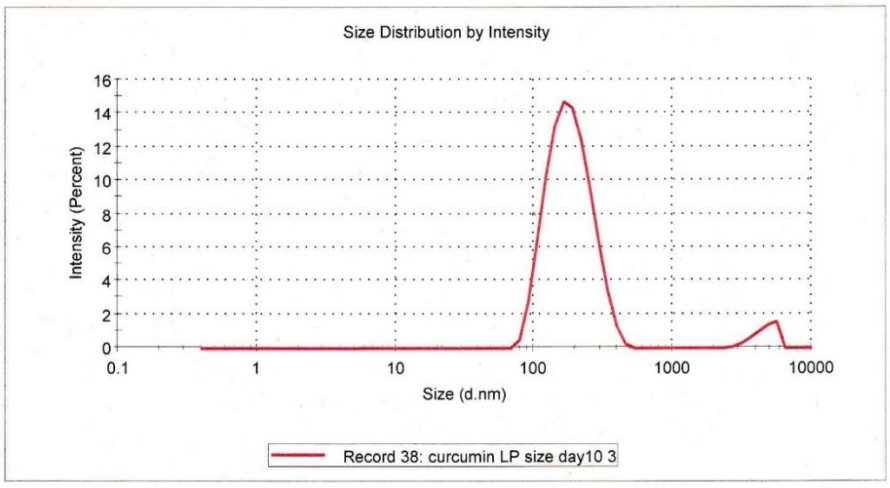

Malvern Instruments Ltd
www.malvern.com

Zetasizer Ver. 7.11
Serial Number : MAL1057082

File name: curcumin stability
Record Number: 38
25 Sep 2019 14:39:34

Appendix II: zeta-potential reports

A zeta-potential report for α-tocopherol-loaded liposomes produced by the Zetasizer software

Zeta Potential Report

v2.3

Malvern

Sample Details

Sample Name: a-tocopherol LP Zeta potential 1
SOP Name: mansettings.nano
General Notes:

File Name: alpha-tocopherol LP.dts
Record Number: 4
Date and Time: 05 November 2019 14:14:38
Dispersant Name: Water
Dispersant RI: 1.330
Viscosity (cP): 0.8872
Dispersant Dielectric Constant: 78.5

System

Temperature (°C): 24.9
Count Rate (kcps): 148.3
Cell Description: Clear disposable zeta c...
Zeta Runs: 12
Measurement Position (mm): 2.00
Attenuator: 6

Results

		Mean (mV)	Area (%)	St Dev (mV)
Zeta Potential (mV): 19.1	**Peak 1:**	19.1	100.0	4.36
Zeta Deviation (mV): 4.36	**Peak 2:**	0.00	0.0	0.00
Conductivity (mS/cm): 0.00943	**Peak 3:**	0.00	0.0	0.00

Result quality Good

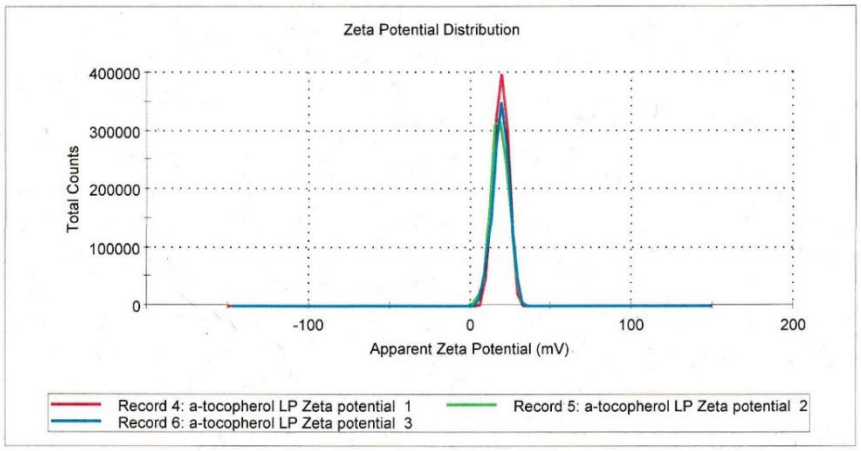

Appendix III: FT-IR reports

a. FT-IR report for α-tocopherol PLA nanoparticles (sample 2-TP)

PerkinElmer Spectrum Version 10.03.07
Wednesday, November 20, 2019, 2:34 PM

Sample Details

Sample Name	a-tocopherol NP
Sample Description	Date Tuesday, March 05, 2019
Analyst	pharmacy
Creation Date	3/5/2019 12:21:24 PM
X-Axis Units	cm-1
Y-Axis Units	%T

Spectrum Graph

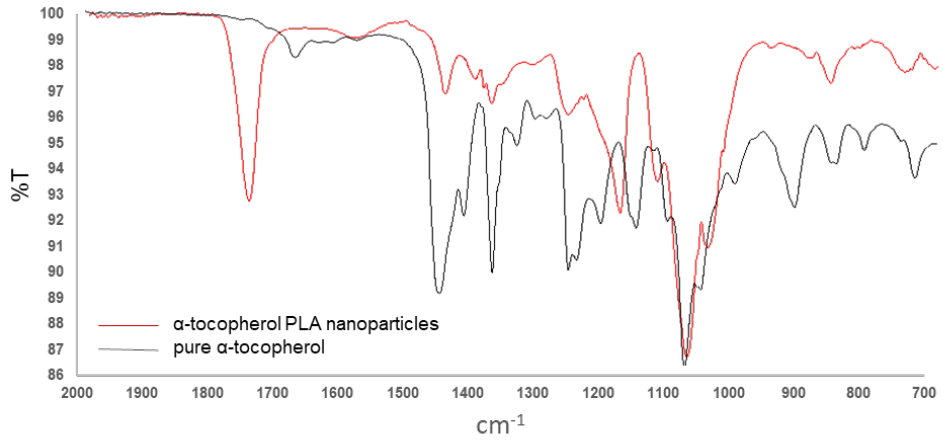

Name	Description
a-tochopherol NP	Date Tuesday, March 05 2019

Compare Result Graph

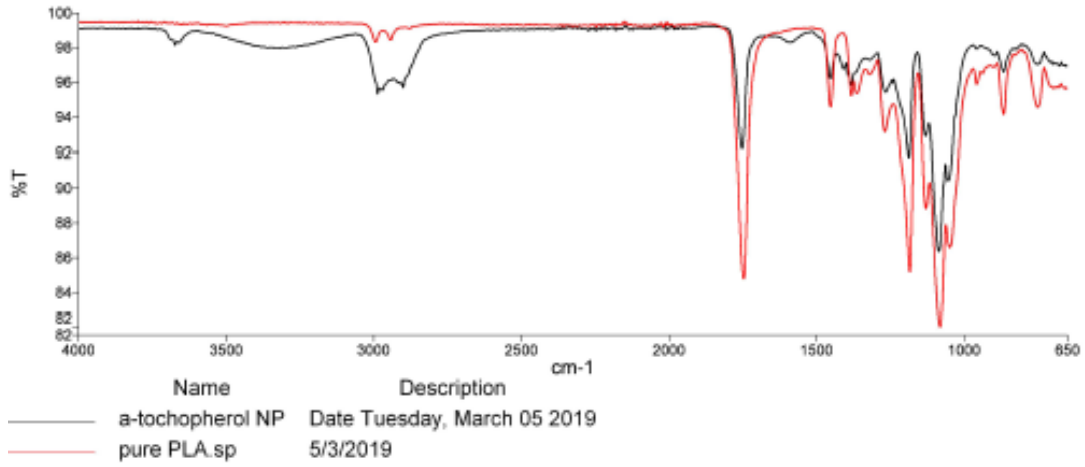

b. FT-IR report for curcumin PLA nanoparticles (sample 3-CP)

PerkinElmer Spectrum Version 10.03.07
Wednesday, November 20, 2019, 2:38 PM

Sample Details

Sample Name	curcumin NP
Sample Description	Sample 036 By pharmacy Date Tuesday, March 05, 2019
Analyst	pharmacy
Creation Date	3/5/2019 12:42:47 PM
X-Axis Units	cm-1
Y-Axis Units	%T

Spectrum Graph

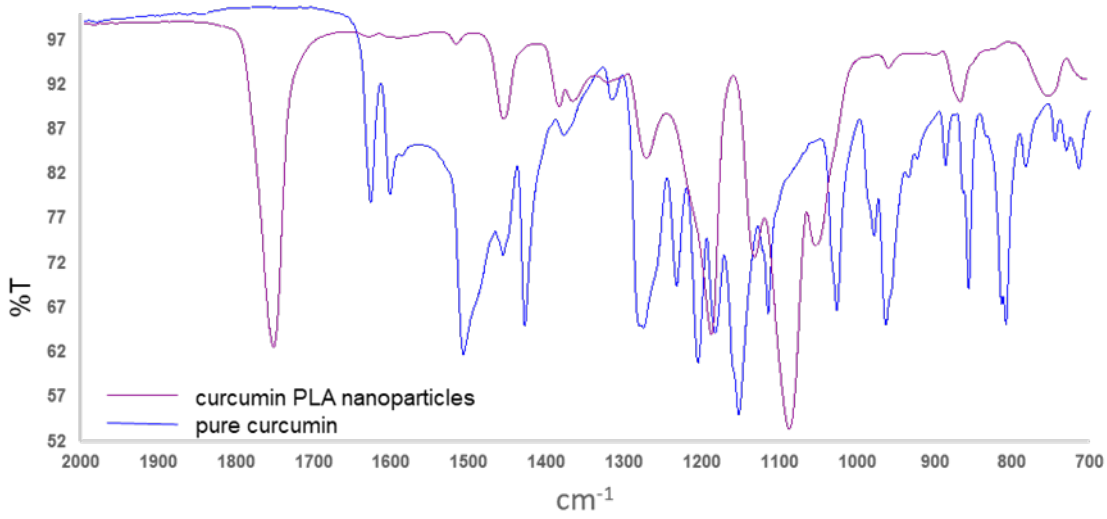

Name	Description
curcumin NP	Sample 036 By pharmacy Date Tuesday, March 05 2019

Compare Result Graph

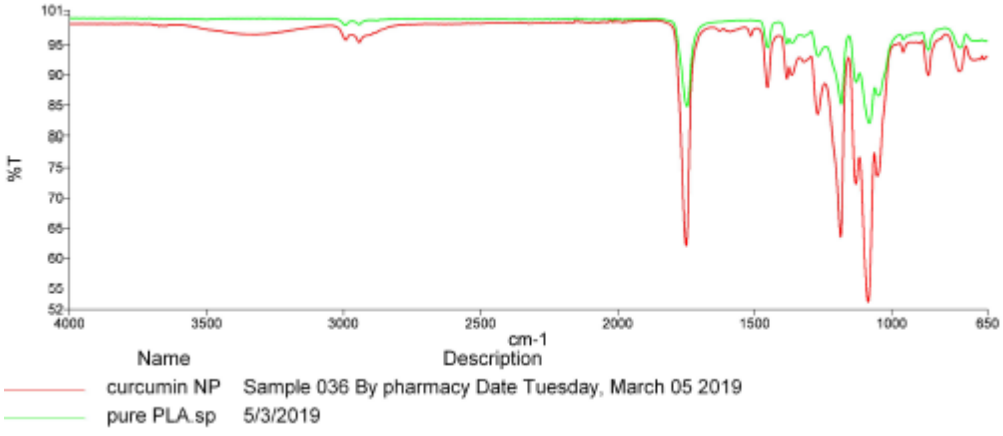

c. FT-IR report for resveratrol PLA nanoparticles (sample 4-RP)

PerkinElmer Spectrum Version 10.03.07
Wednesday, November 20, 2019, 2:43 PM

Sample Details

Sample Name	resveratrol NP
Sample Description	Sample 044 By pharmacy Date Tuesday, March 05, 2019
Analyst	pharmacy
Creation Date	3/5/2019 1:33:23 PM
X-Axis Units	cm-1
Y-Axis Units	%T

Spectrum Graph

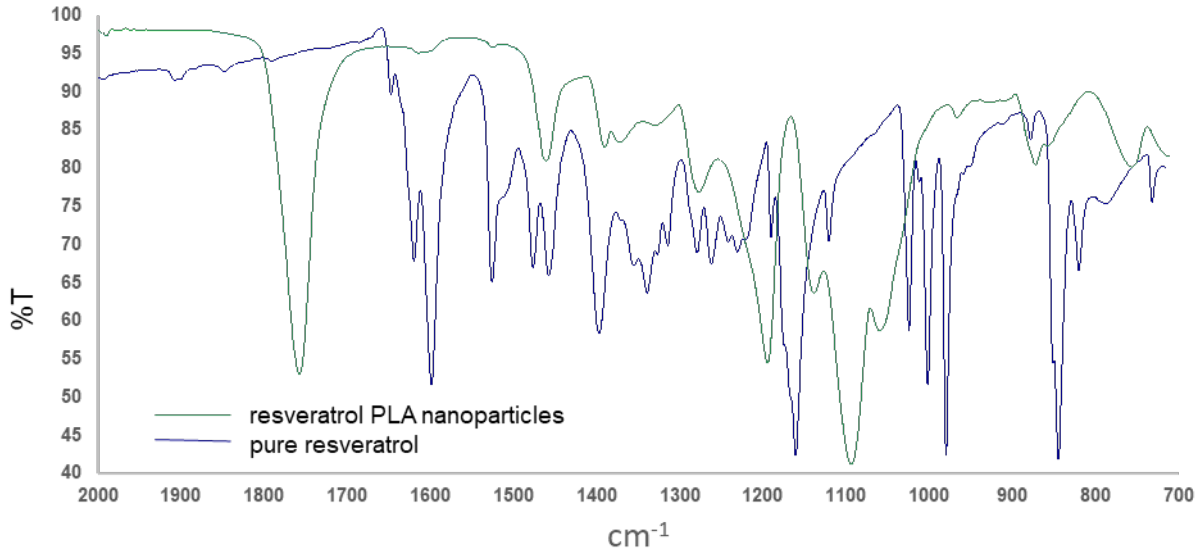

Name	Description
resveratrol NP	Sample 044 By pharmacy Date Tuesday, March 05 2019

Compare Result Graph

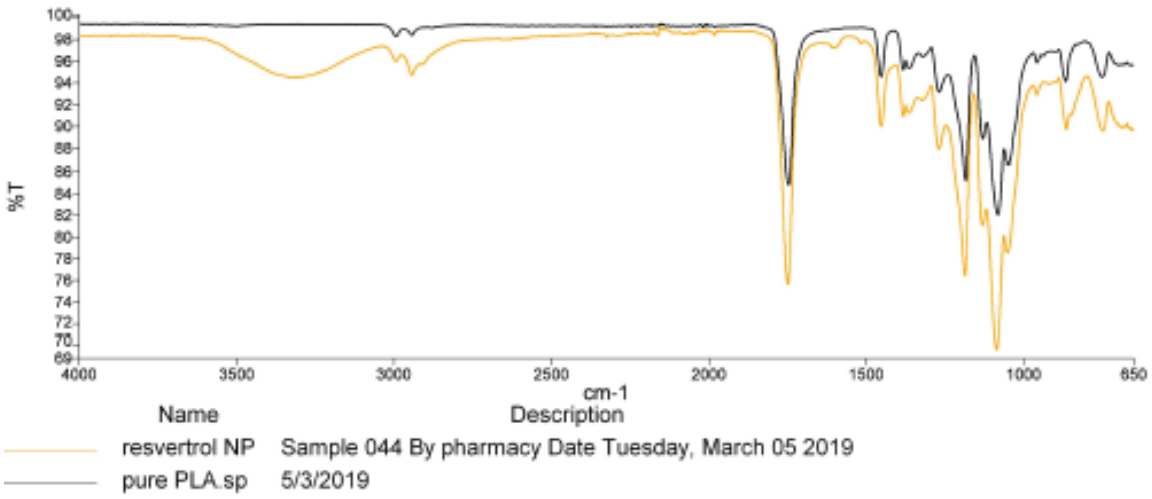

Name	Description
resvertrol NP	Sample 044 By pharmacy Date Tuesday, March 05 2019
pure PLA.sp	5/3/2019

d. FT-IR report for ferulic acid PLA nanoparticles (sample 5-FP)

PerkinElmer Spectrum Version 10.03.07
Wednesday, November 20, 2019, 2:41 PM

Sample Details

Sample Name	ferulic acid NP
Sample Description	Sample 042 By pharmacy Date Tuesday, March 05, 2019
Analyst	pharmacy
Creation Date	3/5/2019 1:18:47 PM
X-Axis Units	cm-1
Y-Axis Units	%T

Spectrum Graph

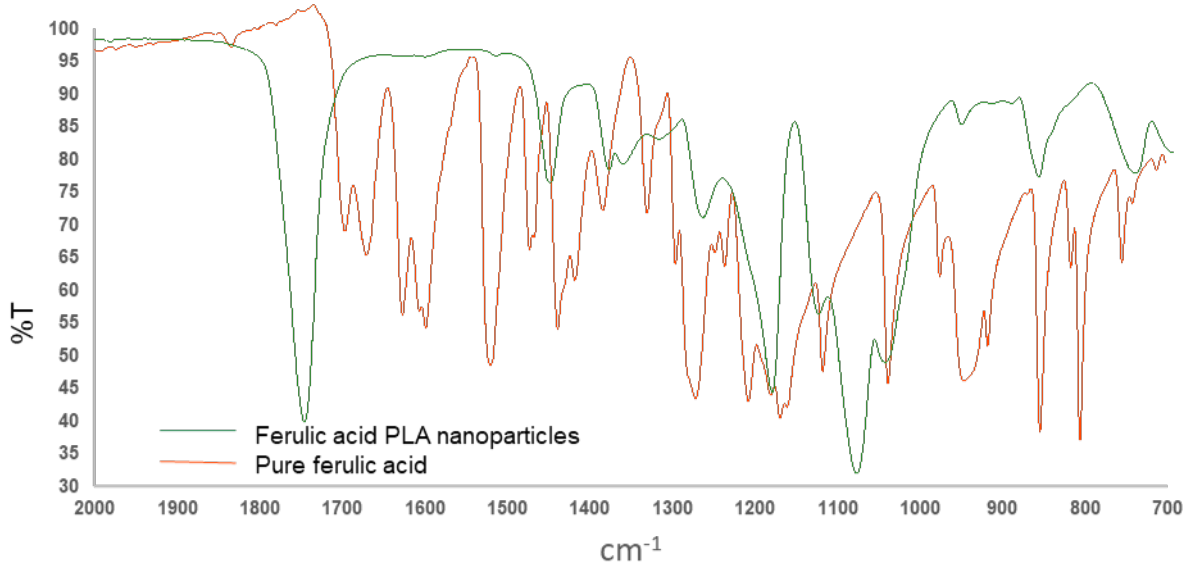

Name	Description
ferulic acid NP	Sample 042 By pharmacy Date Tuesday, March 05 2019

Compare Result Graph

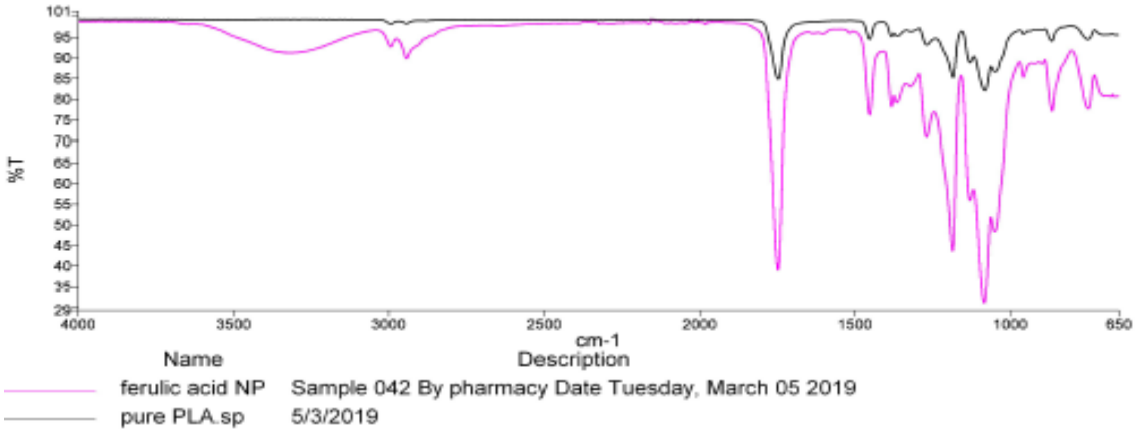

e. FT-IR report for sinapic acid PLA nanoparticles (sample 6-FP)

PerkinElmer Spectrum Version 10.03.07
Wednesday, November 20, 2019, 2:42 PM

Sample Details

Sample Name	sinapic acid NP
Sample Description	Sample 040 By pharmacy Date Tuesday, March 05, 2019
Analyst	pharmacy
Creation Date	3/5/2019 1:08:46 PM
X-Axis Units	cm-1
Y-Axis Units	%T

Spectrum Graph

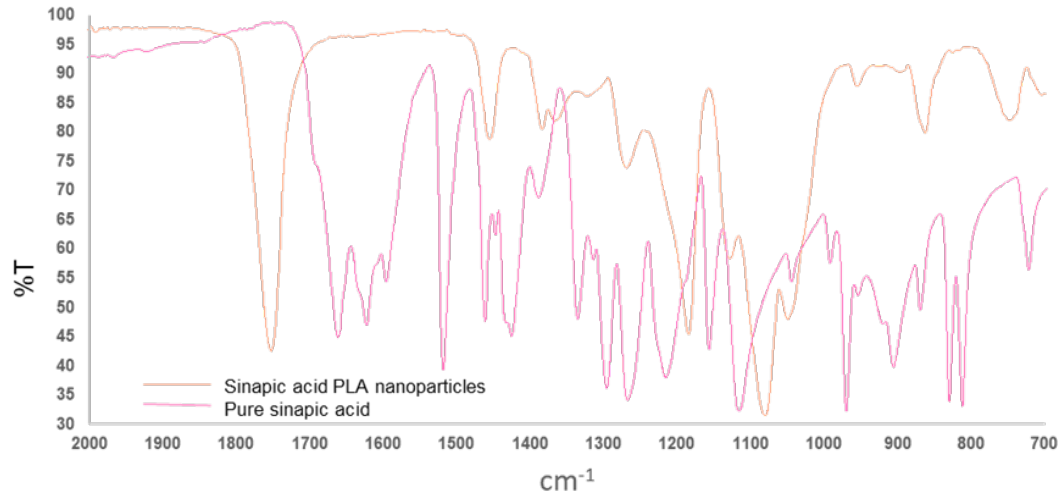

Name	Description
sinapic acid NP	Sample 040 By pharmacy Date Tuesday, March 05 2019

Compare Result Graph

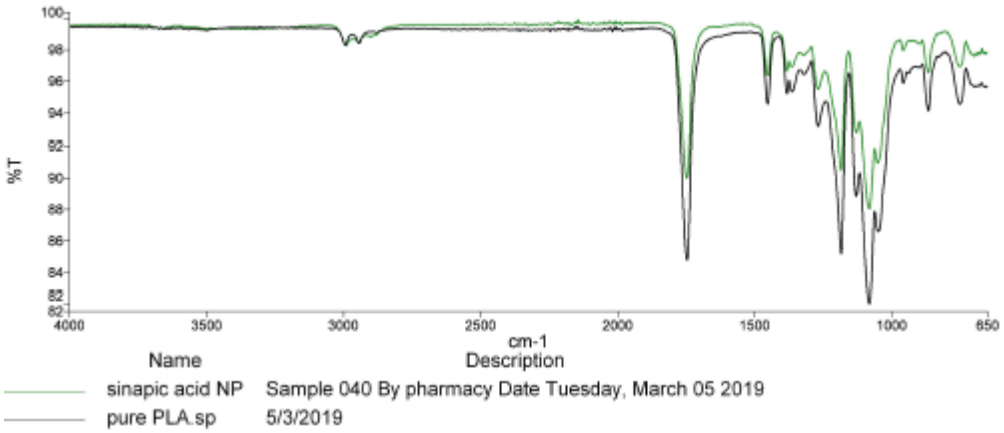

f. FT-IR report for epicatechin PLA nanoparticles (sample 7-EP)

PerkinElmer Spectrum Version 10.03.07
Wednesday, November 20, 2019, 2:40 PM

Sample Details

Sample Name	epicatechin NP
Sample Description	Sample 038 By pharmacy Date Tuesday, March 05, 2019
Analyst	pharmacy
Creation Date	3/5/2019 12:56:06 PM
X-Axis Units	cm-1
Y-Axis Units	%T

Spectrum Graph

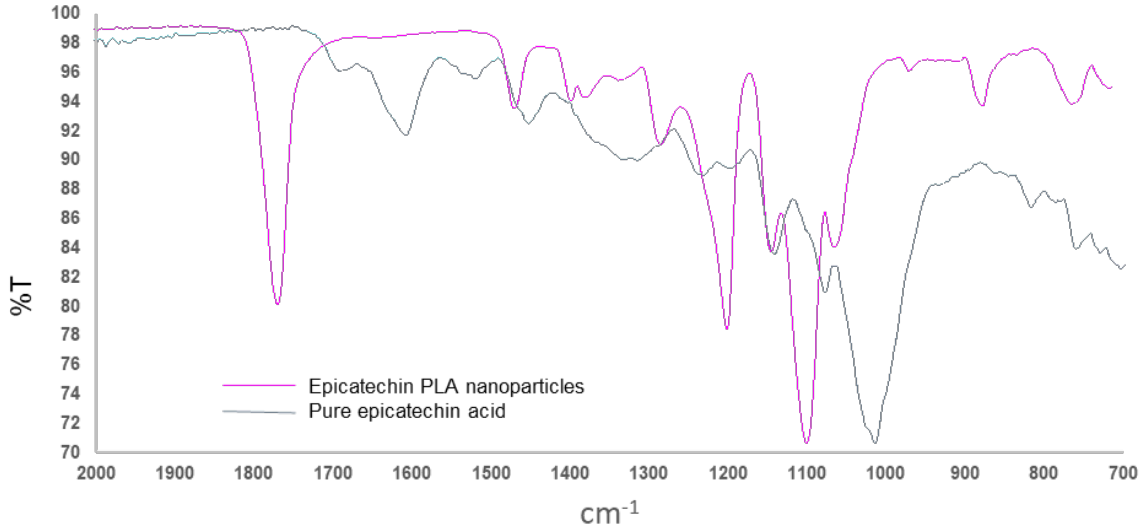

Name	Description
epicatechin NP	Sample 038 By pharmacy Date Tuesday, March 05 2019

Compare Result Graph

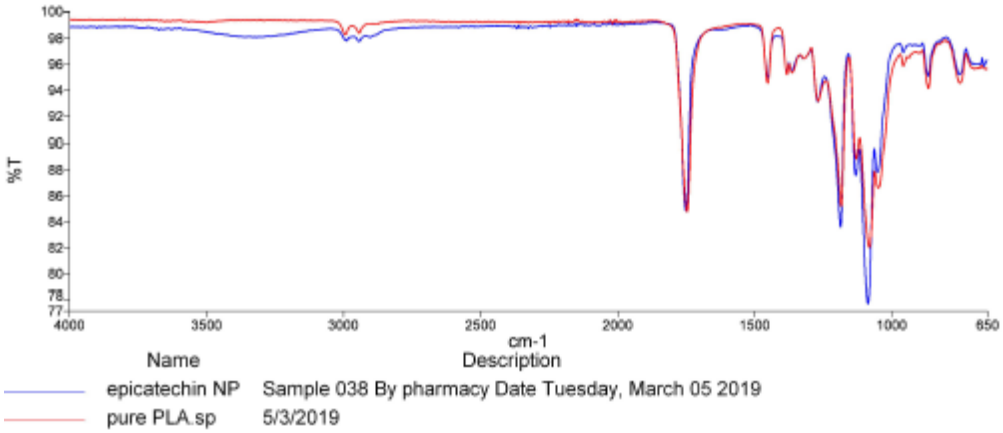

Name	Description
epicatechin NP	Sample 038 By pharmacy Date Tuesday, March 05 2019
pure PLA.sp	5/3/2019

Appendix IV: HPLC chromatographs

a. HPLC chromatograph for 100 µg/mL α-tocopherol standard solution

20/11/2020 14:45 Chromatogram C:\Clarity\DataFiles\WORK1\Data\a-tocopherol 100ug_ml28_01_202012_42.prm Page 1 of 1

Clarity - Chromatography SW
DataApex
www.dataapex.com

Chromatogram Info:

File Name	: C:\Clarity\DataFiles\WORK1\Data\a-tocopherol 100ug_ml28_01_202012_42.prm	File Created	: 28/01/2020 12:42:28
Origin	: Acquired, Acquisition started 28/01/2020 12:32:28	Acquired Date	: 28/01/2020 12:42:28
Project	: WORK1	By	: pharmacy

Printed Version Info:

Printed Version	: 28/01/2020 12:42:28, IA: 8.0 Rev.0	Printed Date	: 20/11/2020 14:45:18
Report Style	: C:\Clarity\DataFiles\Common\Chromatogram.sty	By	: pharmacy
Calibration File	: None		

Sample Description:

Sample ID	: standards and sample
Sample	: a-tocopherol 100ug/ml

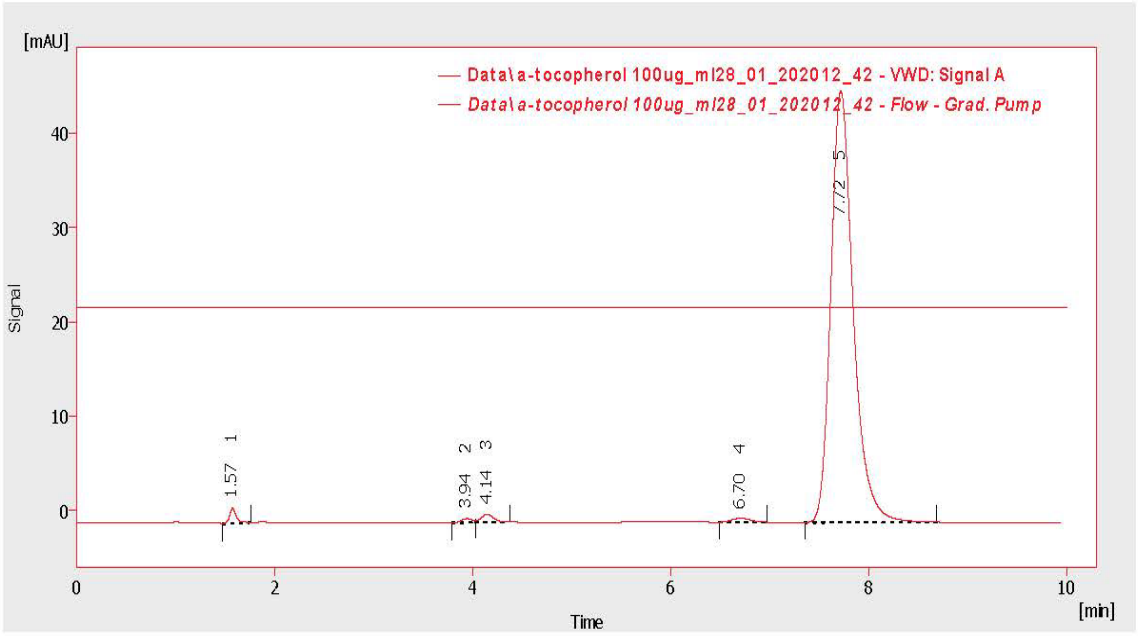

Result Table (Uncal - Data\a-tocopherol 100ug_ml28_01_202012_42 - VWD: Signal A)

	Reten. Time [min]	Area [mAU.s]	Height [mAU]	Area [%]	Height [%]	W05 [min]	Compound Name
1	1.570	7.457	1.619	1.0	3.3	0.07	
2	3.940	3.112	0.411	0.4	0.8	0.15	
3	4.143	7.209	0.834	1.0	1.7	0.13	
4	6.703	5.582	0.422	0.8	0.9	0.21	
5	7.717	716.679	45.765	96.8	93.3	0.23	
	Total	740.038	49.051	100.0	100.0		

b. HPLC chromatograph for 25 µg/mL curcumin standard solution

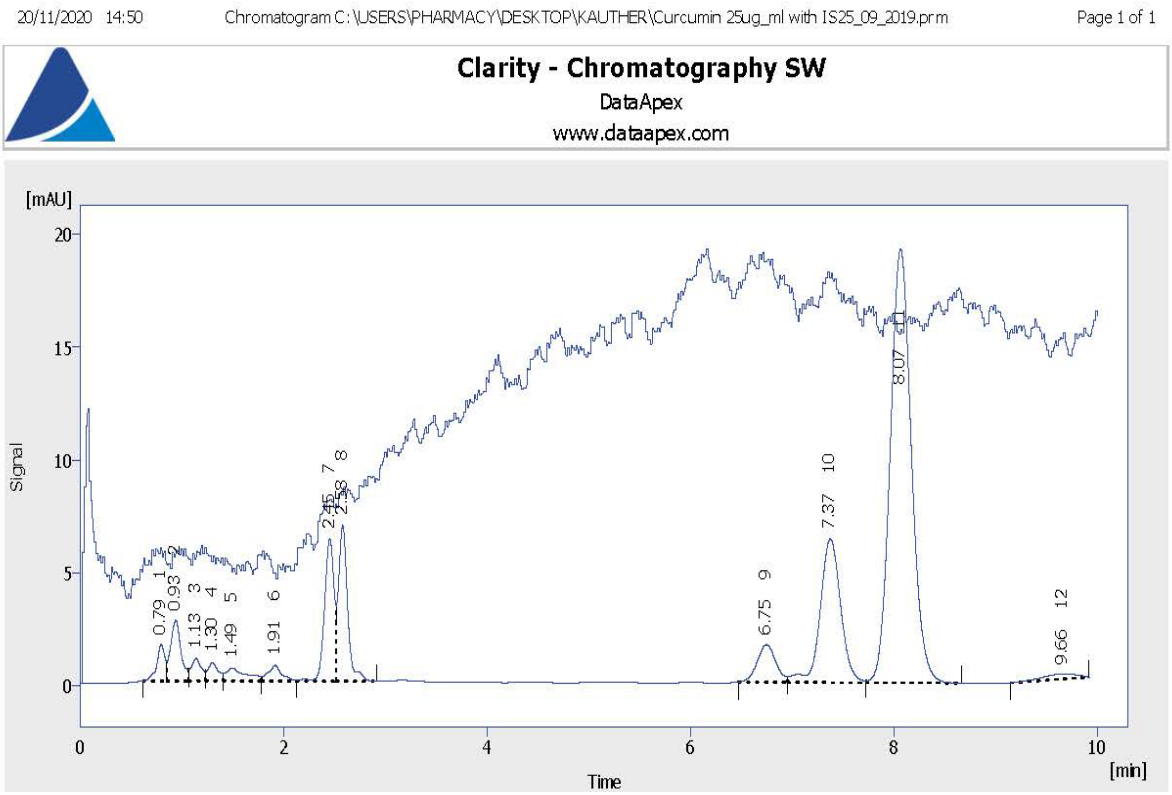

Result Table (Uncal - C:\USERS\PHARMACY\DESKTOP\KAUTHER\Curcumin 25ug_ml with IS25_09_2019 - VWD: Signal A)

	Reten. Time [min]	Area [mAU.s]	Height [mAU]	Area [%]	Height [%]	W05 [min]	Compound Name
1	0.790	8.814	1.611	1.7	3.4	0.09	
2	0.933	19.100	2.675	3.6	5.6	0.11	
3	1.133	6.968	0.993	1.3	2.1	0.14	
4	1.297	5.863	0.826	1.1	1.7	0.13	
5	1.493	7.899	0.579	1.5	1.2	0.23	
6	1.913	6.493	0.694	1.2	1.4	0.14	
7	2.450	40.549	6.314	7.6	13.1	0.12	
8	2.577	43.528	6.900	8.2	14.4	0.11	
9	6.747	21.178	1.661	4.0	3.5	0.20	
10	7.373	89.508	6.363	16.8	13.2	0.21	
11	8.067	276.698	19.203	52.0	40.0	0.22	
12	9.663	5.424	0.216	1.0	0.5	0.40	
	Total	532.022	48.035	100.0	100.0		

c. HPLC chromatograph for 4 µg/mL resveratrol standard solution

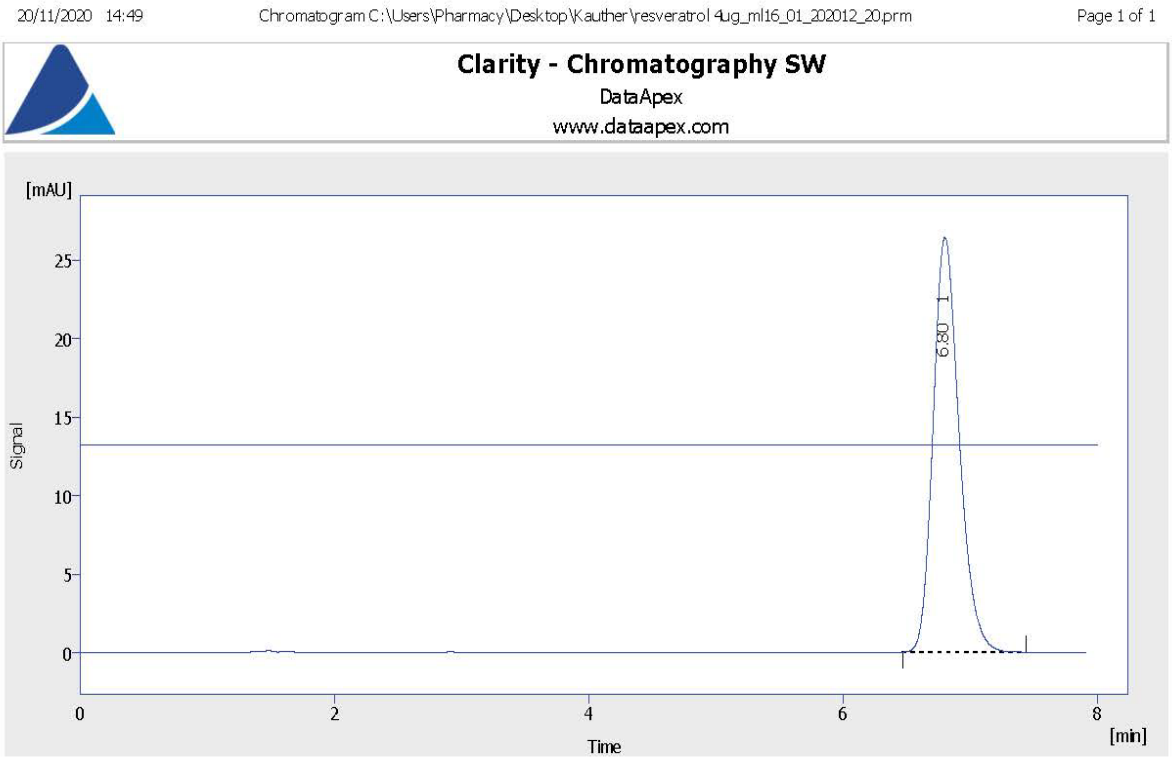

Result Table (Uncal - C:\Users\Pharmacy\Desktop\Kauther\resveratrol 4ug_ml16_01_202012_20 - VWD: Signal A)

	Reten. Time [min]	Area [mAU.s]	Height [mAU]	Area [%]	Height [%]	W05 [min]	Compound Name
1	6.800	376.089	26.411	100.0	100.0	0.22	
	Total	376.089	26.411	100.0	100.0		

d. HPLC chromatograph for 4 µg/mL ferulic acid standard solution

22/01/2020 11:48 Chromatogram C:\Users\pharmacy\Desktop\kauther\Ferulic acid 4ug_ml22_01_202011_47.prm Page 1 of 1

Clarity - Chromatography SW
DataApex
www.dataapex.com

Chromatogram Info:

File Name	: C:\Users\pharmacy\Desktop\kauther\Ferulic acid 4ug_ml22_01_202011_47.prm	File Created	: 22/01/2020 11:47:22
Origin	: Acquired, Acquisition started 22/01/2020 11:43:22	Acquired Date	: 22/01/2020 11:47:22
Project	: WORK1	By	: pharmacy

Printed Version Info:

Printed Version	: 22/01/2020 11:47:22, IA: 8.0 Rev.0	Printed Date	: 22/01/2020 11:48:46
Report Style	: C:\Clarity\DataFiles\Common\Chromatogram.sty	By	: pharmacy
Calibration File	: None		

Sample Description:

Sample ID	: standards and sample
Sample	: Ferulic acid 4ug/ml

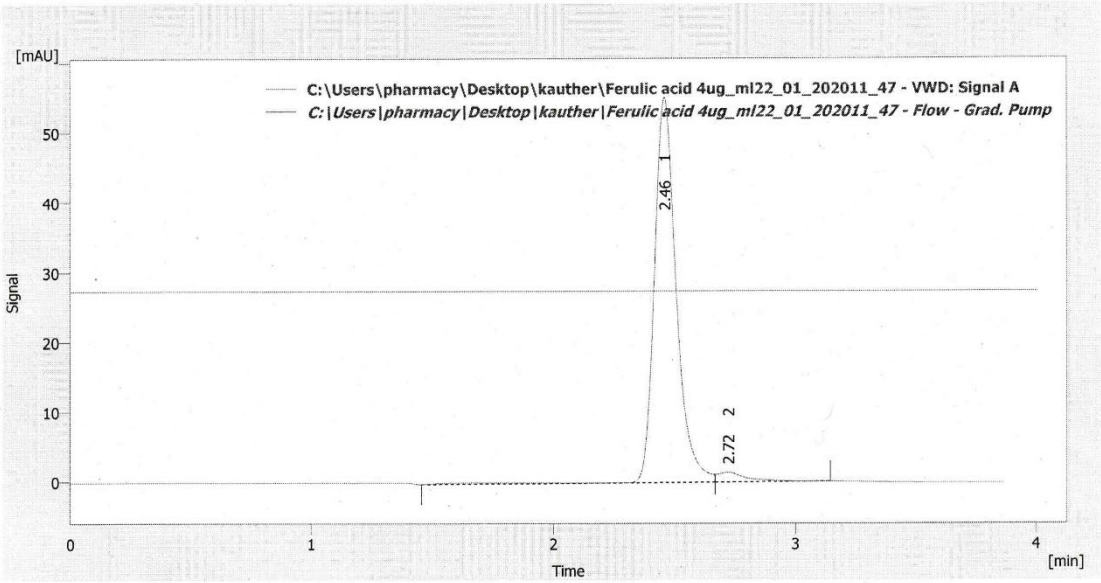

Result Table (Uncal - C:\Users\pharmacy\Desktop\kauther\Ferulic acid 4ug_ml22_01_202011_47 - VWD: Signal A)

	Reten. Time [min]	Area [mAU.s]	Height [mAU]	Area [%]	Height [%]	W05 [min]	Compound Name
1	2.460	351.683	55.141	96.8	97.6	0.10	
2	2.723	11.742	1.375	3.2	2.4	0.12	
	Total	363.425	56.516	100.0	100.0		

e. HPLC chromatograph for 10 µg/mL sinapic acid standard solution

20/11/2020 14:45 Chromatogram C:\Clarity\DataFiles\WORK1\Data\sinapic acid 10ug_ml16_01_202011_42.prm Page 1 of 1

Clarity - Chromatography SW
DataApex
www.dataapex.com

Chromatogram Info:

File Name	: C:\Clarity\DataFiles\WORK1\Data\sinapic acid 10ug_ml16_01_202011_42.prm	File Created	: 16/01/2020 11:42:16
Origin	: Acquired, Acquisition started 16/01/2020 11:32:15	Acquired Date	: 16/01/2020 11:42:15
Project	: WORK1	By	: pharmacy

Printed Version Info:

Printed Version	: 16/01/2020 11:42:16, IA: 8.0 Rev.0	Printed Date	: 20/11/2020 14:45:58
Report Style	: C:\Clarity\DataFiles\Common\Chromatogram.sty	By	: pharmacy
Calibration File	: None		

Sample Description:

Sample ID	: standards and sample
Sample	: sinapic acid 10ug/ml

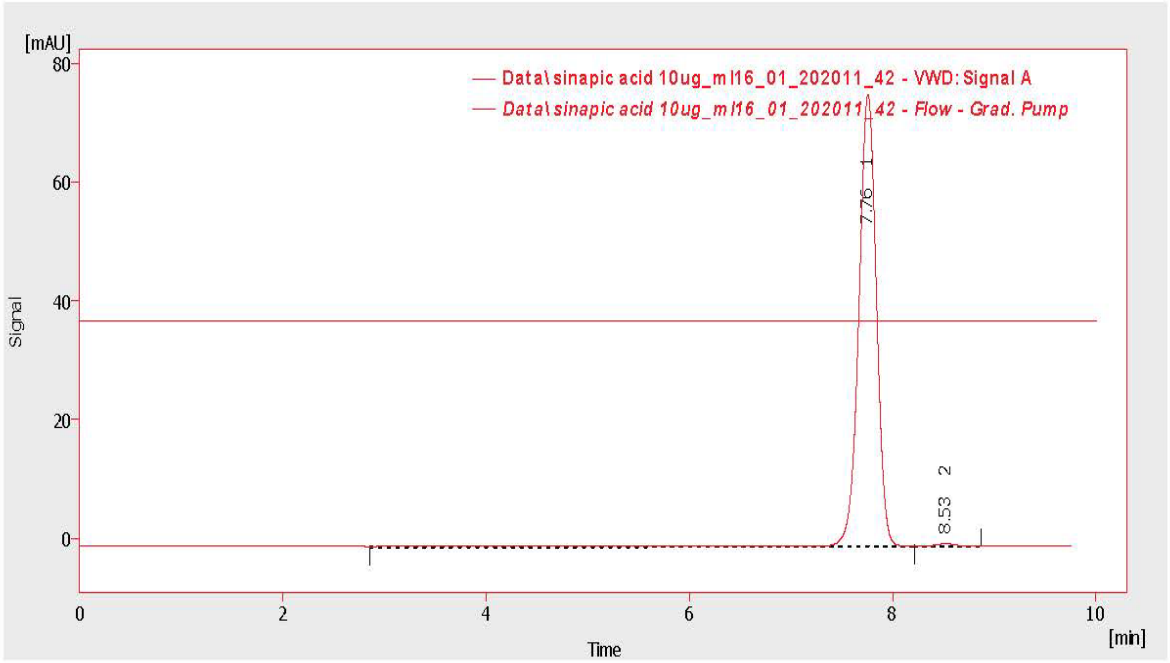

Result Table (Uncal - Data\sinapic acid 10ug_ml16_01_202011_42 - VWD: Signal A)

	Reten. Time [min]	Area [mAU.s]	Height [mAU]	Area [%]	Height [%]	W05 [min]	Compound Name
1	7.757	937.929	76.080	99.3	99.4	0.19	
2	8.527	6.644	0.461	0.7	0.6	0.21	
	Total	944.572	76.541	100.0	100.0		

f. HPLC chromatograph for 200µg/mL epicatechin standard solution

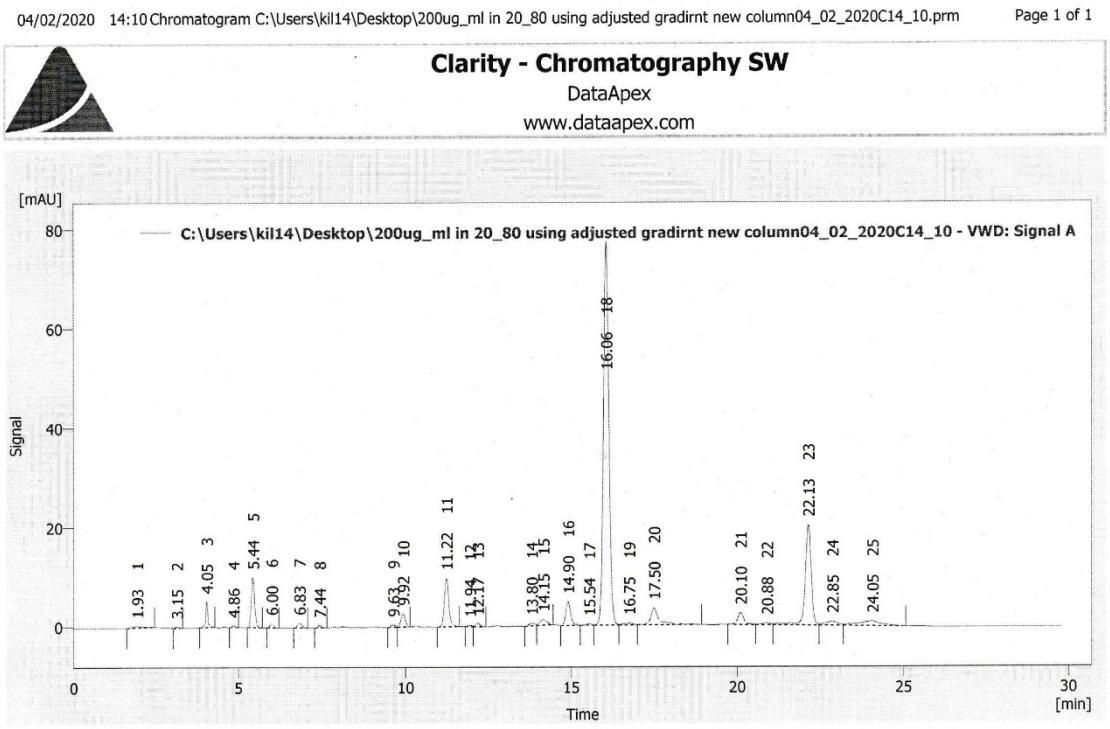

Result Table (Uncal - C:\Users\kil14\Desktop\200ug_ml in 20_80 using adjusted gradirnt new column04_02_2020C14_10 - VWD: Signal A)

	Reten. Time [min]	Area [mAU.s]	Height [mAU]	Area [%]	Height [%]	W05 [min]	Compound Name
1	1.927	7.650	0.286	0.5	0.2	0.70	
2	3.147	2.465	0.327	0.1	0.2	0.12	
3	4.047	23.254	5.182	1.4	3.6	0.06	
4	4.857	2.577	0.378	0.2	0.3	0.11	
5	5.437	73.124	10.083	4.4	6.9	0.12	
6	6.003	5.983	0.858	0.4	0.6	0.11	
7	6.830	8.131	0.907	0.5	0.6	0.14	
8	7.437	3.452	0.417	0.2	0.3	0.13	
9	9.630	4.467	0.496	0.3	0.3	0.15	
10	9.923	24.373	2.719	1.5	1.9	0.14	
11	11.223	90.979	9.760	5.5	6.7	0.14	
12	11.937	2.498	0.285	0.2	0.2	0.16	
13	12.170	6.951	0.671	0.4	0.5	0.17	
14	13.800	6.264	0.535	0.4	0.4	0.23	
15	14.147	17.111	1.140	1.0	0.8	0.24	
16	14.903	51.360	4.770	3.1	3.3	0.16	
17	15.543	3.914	0.330	0.2	0.2	0.16	
18	16.060	873.749	77.306	53.1	53.2	0.17	
19	16.747	8.475	0.410	0.5	0.3	0.35	
20	17.500	61.765	3.430	3.8	2.4	0.20	
21	20.100	31.962	2.417	1.9	1.7	0.18	
22	20.883	6.938	0.384	0.4	0.3	0.28	
23	22.133	257.189	20.193	15.6	13.9	0.19	
24	22.850	22.043	0.868	1.3	0.6	0.40	
25	24.053	48.669	1.032	3.0	0.7	0.62	
	Total	1645.343	145.186	100.0	100.0		